frontiers | Research Topics

CD4 T cells in HIV: A friend or foe?

Edited by
Sunil Kannanganat Sidharthan, Constantinos Petrovas, Monica Vaccari and Vijayakumar Velu

Published in
Frontiers in Immunology

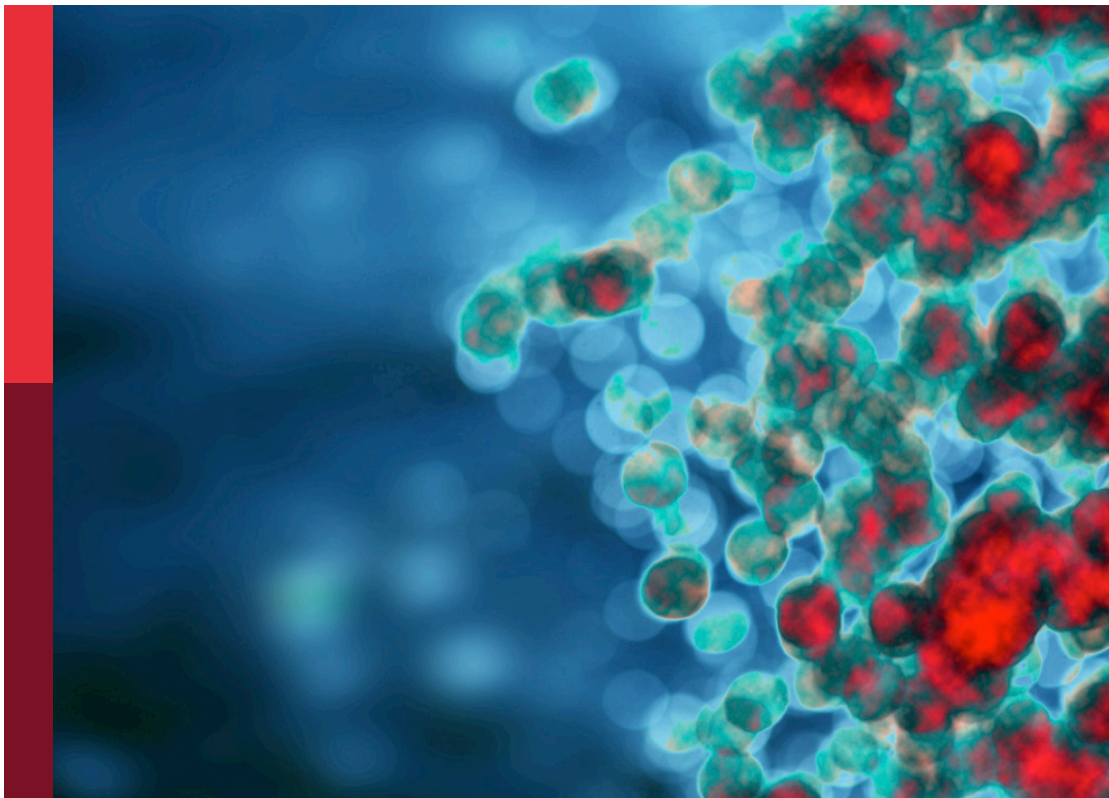

ISSN 1664-8714
ISBN 978-2-8325-3076-4
DOI 10.3389/978-2-8325-3076-4

About Frontiers

Frontiers is more than just an open access publisher of scholarly articles: it is a pioneering approach to the world of academia, radically improving the way scholarly research is managed. The grand vision of Frontiers is a world where all people have an equal opportunity to seek, share and generate knowledge. Frontiers provides immediate and permanent online open access to all its publications, but this alone is not enough to realize our grand goals.

Frontiers journal series

The Frontiers journal series is a multi-tier and interdisciplinary set of open-access, online journals, promising a paradigm shift from the current review, selection and dissemination processes in academic publishing. All Frontiers journals are driven by researchers for researchers; therefore, they constitute a service to the scholarly community. At the same time, the *Frontiers journal series* operates on a revolutionary invention, the tiered publishing system, initially addressing specific communities of scholars, and gradually climbing up to broader public understanding, thus serving the interests of the lay society, too.

Dedication to quality

Each Frontiers article is a landmark of the highest quality, thanks to genuinely collaborative interactions between authors and review editors, who include some of the world's best academicians. Research must be certified by peers before entering a stream of knowledge that may eventually reach the public - and shape society; therefore, Frontiers only applies the most rigorous and unbiased reviews. Frontiers revolutionizes research publishing by freely delivering the most outstanding research, evaluated with no bias from both the academic and social point of view. By applying the most advanced information technologies, Frontiers is catapulting scholarly publishing into a new generation.

What are Frontiers Research Topics?

Frontiers Research Topics are very popular trademarks of the *Frontiers journals series*: they are collections of at least ten articles, all centered on a particular subject. With their unique mix of varied contributions from Original Research to Review Articles, Frontiers Research Topics unify the most influential researchers, the latest key findings and historical advances in a hot research area.

Find out more on how to host your own Frontiers Research Topic or contribute to one as an author by contacting the Frontiers editorial office: frontiersin.org/about/contact

CD4 T cells in HIV: A friend or foe?

Topic editors

Sunil Kannanganat Sidharthan — Baylor College of Medicine, United States

Constantinos Petrovas — Centre Hospitalier Universitaire Vaudois (CHUV), Switzerland

Monica Vaccari — Tulane University, United States

Vijayakumar Velu — Emory University, United States

Citation

Sidharthan, S. K., Petrovas, C., Vaccari, M., Velu, V., eds. (2023). *CD4 T cells in HIV: A friend or foe?* Lausanne: Frontiers Media SA. doi: 10.3389/978-2-8325-3076-4

The authors declare that the research was conducted in the absence of any commercial or financial relationships that could be construed as a potential conflict of interest.

Table of contents

frontiers | Frontiers in Immunology

TYPE Editorial
PUBLISHED 11 July 2023
DOI 10.3389/fimmu.2023.1203531

OPEN ACCESS

EDITED AND REVIEWED BY
Mariolina Salio,
Immunocore, United Kingdom

*CORRESPONDENCE
Vijayakumar Velu
vvelu@emory.edu

RECEIVED 10 April 2023
ACCEPTED 26 June 2023
PUBLISHED 11 July 2023

CITATION
Govindaraj S, Babu H, Kannanganat S, Vaccari M, Petrovas C and Velu V (2023) Editorial: CD4+ T cells in HIV: A Friend or a Foe?
Front. Immunol. 14:1203531.
doi: 10.3389/fimmu.2023.1203531

Editorial: CD4+ T cells in HIV: A Friend or a Foe?

Sakthivel Govindaraj[1,2], Hemalatha Babu[1,2], Sunil Kannanganat[3], Monica Vaccari[4,5], Constantinos Petrovas[6] and Vijayakumar Velu[1,2]*

[1]Department of Pathology and Laboratory Medicine, Emory University School of Medicine, Atlanta, GA, United States, [2]Division of Microbiology and Immunology, Emory Vaccine Center, Emory University, Atlanta, GA, United States, [3]Department of Pathology and Genomic Medicine, Houston Methodist Hospital Research Institute, Houston, TX, United States, [4]Division of Immunology, Tulane National Primate Research Center, Covington, LA, United States, [5]Department of Microbiology and Immunology, Tulane School of Medicine, New Orleans, LA, United States, [6]Department of Laboratory Medicine and Pathology, Institute of Pathology, Lausanne University Hospital, University of Lausanne, Lausanne, Switzerland

KEYWORDS

HIV, CD4+ T cells, reservoirs, HIV cure, follicular T helper cells

Editorial on the Research Topic
CD4+ T cells in HIV: a friend or a foe?

Currently, there are approximately 38.4 million individuals living with the Human Immunodeficiency Virus (HIV), of which 36.7 million adults, 1.7 million children (<15 years old), with 54% of cases being females. Since the start of the HIV epidemic, an estimated 84.2 million individuals have been infected with the virus. Tragically, this global health crisis has resulted in the loss of approximately 40 million lives. In 2021 the World Health Organization (WHO) estimated 1.5 million new infections (1). In the early stages of HIV infection, several important events occur within CD4+ T cells, which are a primary target of the virus. CD4+ T cell depletion: HIV infects and destroys CD4+ T cells during the replication process. If left untreated, HIV is the virus kills infected cells directly and indirectly through immune responses that cause cell death. This progressive loss of CD4+ T cells weakens the immune system over time even following antiretroviral treatment (cART) in HIV infected individuals (2). HIV-infected individuals often experience imbalances in CD4+ T cell levels and function. While cART is highly effective in suppressing viral replication and restoring immune function, it may not completely normalize CD4+ T cell counts or fully restore immune balance in all individuals. Some HIV reservoirs, such as latently infected CD4+ T cells or tissues with lower drug penetration, may continue to harbor the virus, and chronic immune activation and inflammation associated with HIV infection can lead to immune exhaustion, where immune cells, including CD4+ T cells, become functionally impaired and less responsive. Despite extensive research, the mechanisms underlying CD4+ T cell loss and dysfunction in HIV infection are not fully understood (3). This edited topic is aimed at shedding lights on the effects of HIV infection on CD4+ T cells, considering their complexity in terms of heterogeneity and tissue distribution (4–7).

The relationship between HIV infection and CD4+ T cell population is intricate, partly because of their important functions and heterogenous nature. $CD4^+$ T cell responses are central in orchestrating the adaptive immune responses to pathogens (8). Moreover, they are critical in inducing long-lasting vaccine-mediated protection (9). Their main function is to provide help adaptive immune cells; they support antibody production by B cells, affinity maturation, and the selection and they support the generation of long-lasting effective CD8+ T cells, and their antiviral functions. In the last decade, however, our understanding of CD4+ T cell immunology has grown, and it has become clear that CD4+ T cells function extends well beyond the simplistic view of B and T cell help. Many new CD4+ T cell subsets have been discovered (10) with highly specialized and distinct functions and tissue distribution; these subsets include negative regulators of the immune system, T regulatory cells (T-regs), preferentially mucosal CD4+ T cells Th17 and Th9 cells, and B zone resident T follicular helper (Tfh) cells and T follicular regulatory cells (11, 12). All subsets can be defined by specific surface and intracellular markers, including their own unique transcription factor and cytokine profiles. However, many questions remain elusive about their specific role in HIV infection. These subsets are not equally susceptible and each of them may play a unique yet significant role in establishing and maintaining virus reservoirs. Moreover, difference in HIV susceptibility of various CD4 T cells and the loss of CD4+ T cells very early in infection and the imbalance between these subsets is likely to affect the effectiveness of prophylactics vaccines and therapeutic approaches for HIV.

Activated CD4+ T cells located at mucosal sites are the main targets for HIV infection. Therefore, interventions aimed at reducing the vulnerability of these mucosal targets, particularly in the genital tract which serves as the portal of entry for HIV, could potentially lower the risk of HIV acquisition. Lajoie et al. investigated the effect of acetylsalicylic acid (ASA), a well-known and safe systemic anti-inflammatory drug, on T cell activation of the vaginal tract. The study was conducted in a cohort of HIV-uninfected women from Kenya who were given oral ASA at a low dose of 81mg daily for six weeks. Participants were followed for one month to establish a baseline immune activation in the blood and the female genital tract (FGT). Changes to T cell immune activation were measured both systemically and in the mucosal compartment, relative to baseline levels. The authors found that while concentration of ASA in the blood was 58% higher than the level measured in the FGT changes where noticeable in both sites. The blood level of ASA was correlated with lower levels of Th17 cells, CCR5 expressing target CD4+ T cells, and a specialized subset of CD8+ cells called Tc17. Importantly, in the FGT, low- dose ASA resulted in decreased levels of activated CD4+ T cells. Activation was measured by expression of the CCR5, CD95, and CD161+, all of which are markers associate with increased HIV replication (13, 14). This study suggests that ASA may be used to decrease activated FGT CD4+ T cells, thereby potentially reducing the risk of HIV vaginal transmission.

Recent studies showed that CD4+ T cells expressing the surface receptor glycoprotein CD32 are more susceptible to infection, and virological analyses revealed that CD32+ CD4+ T cells express high levels of inflammatory markers (HIV co-receptor CCR5, and PD-1, CXCR3) and confirming their heightened susceptibility to HIV infection and serve as a HIV reservoir. Overall, the study characterized a new susceptible CD4+ T cell subset in monkeys that exhibits an activated profile and higher expression of markers associated with HIV-infected and/or reservoir cells, and thus may represent a novel therapeutic target (Huot et al.).

Olwenyi et al. examined a subset of cytotoxic (CTLs) CD4+ T cells and investigated their contribution to HIV persistence. CD4+ CTLs T cells can reduce viral replication and have been shown to kill infected macrophages, by secreting granzyme B and perforin and to kill the target cells in an MHC class II-restricted fashion. While they may play important roles in antiviral immunity, the lack of robust markers in various animal models limits understanding of their role in HIV immunopathology. The group found that CD4+ T cells expressing high levels of the integrin beta CD29 are highly cytotoxic *in vitro*, and they corroborated the use of CD29 as a marker to detect CD4+ CTLs T cells *ex vivo*, using PBMCs obtained from SIV infected macaques. Interestingly, CD29+ CD4+ T cells are depleted during untreated SIV infection and reconstituted after early initiation of ART. Moreover, functional characterization of these cells showed that they produce IL-21 and granzyme B and that their ability to secrete anti-viral cytokines is reduced by morphine, an opioid drug. These findings are relevant because they suggest that CD4+ CTLs play a crucial role in limiting HIV pathogenesis and persistence (15).

Despite the remarkable effectiveness of combination antiretroviral therapy (cART) in suppressing HIV replication in the bloodstream over long periods of time, achieving sustained virologic remission in HIV-infected individuals continues to be a formidable challenge. One of the primary reasons for the challenge in achieving sustained virologic remission is the presence of latent HIV reservoirs. These reservoirs consist of HIV-infected cells that are in a dormant or inactive state, allowing them to evade the effects of antiretroviral therapy. While cART effectively suppresses active viral replication, it is unable to eliminate these latent reservoirs. As a result, even with long-term treatment, the potential for viral rebound and the need for ongoing therapy persist. Efforts to target and eliminate these latent reservoirs are a critical focus of HIV cure research. Several attempts have been made to clear viral reservoirs including cART (16), latency-reversing agents (LRA) (17), immune based therapies (15), gene editing and gene therapy (18), stem cell transplantation (19) and combination therapies (20). In the study by de Armas et al., FDA-approved JAK1/2 inhibitors, ruxolitinib, and baricitinib, were tested as a potential therapeutic strategy to target latent reservoirs. The study used the dual reporter virus HIVGKO to investigate latency establishment and maintenance in lymphoid-derived CD4+ T cells. Single-cell technologies were integrated to evaluate protein expression, host gene expression, and HIV transcript expression, and identify and analyze latently infected cells. The latency establishment and maintenance were validated using the tonsillar CD4+ T cells *in vitro* method. The results from this study show that CD4+ T cells with latent infection exhibit similar activation profiles as productively infected cells. Single-cell RNAseq analysis revealed

that Sirtuin signaling, Oxidative Phosphorylation, Mitochondrial Dysfunction, and EIF2 Signaling were enriched when comparing latent cells versus productively infected cells. In addition, molecular JAK1/2 inhibition resulted in dose-dependent downregulation of activation markers on CD4+ T cells. Moreover, the expression of activation markers such as CD25 and CD69 was affected by both drugs. Finally, HIV reactivation above the level of spontaneous reactivation was observed in the presence of a LRA, but pretreatment of cells with baricitinib abrogated the response, with the greatest effect occurring at the highest concentration of the drug. It is therefore, plausible that JAK1/2 inhibition may block HIV-induced IFN and thus lead to a reduction in viral reservoirs.

The crucial involvement of T follicular helper (Tfh) cells in B cell responses, including against HIV is widely recognized (10, 21, 22). However, while harnessing Tfh may be desirable, they also harbor the virus (23). Moreover, there remains uncertainty regarding which specific subset of Tfh cells, either from lymph nodes or circulating in the blood, harbors a higher reservoir burden.

TABLE 1 Highlights of the articles presented in the Research Topic *CD4+ T cells in HIV: A Friend or a Foe*?

Article Description	Citation
Acetylsalicylic acid (ASA) use was associated with a decrease in activated CD4+ T cells CD4+CCR5+CD161+ and CD4+CCR5+CD95+ cells, both at the systemic and female genital tract.	Lajoie et al.
The CXCR5+ and CXCR4+ CD4 T cell subsets are preferentially killed during HIV infection, while those that are preferentially infected exhibit an activated and exhausted effector memory cell phenotype. Single-cell RNA-seq analysis showed that the preferentially killed subsets express genes that favor abortive infection and pyroptosis, and exhibits increased mRNA expression of inflammatory caspases (caspase 1 and caspase 4) as well as the pyroptotic executioner, gasdermin D.	Luo et al.
The CD32+CD4+ T cells exhibit an activated profile and higher expression of markers associated with HIV-infected and/or reservoir cells.	Huot et al.
The CD29hi CD4 T cells can serve as a reliable marker to identify CD4+ cytotoxic T lymphocytes (CTLs) in rhesus macaques. These CTLs secrete higher levels of cytotoxic and proinflammatory cytokines, and elevated expression of either IL-21 or granzyme B hi T Bet+ upon antigen stimulation. CD4+ CTLs play a crucial role in limiting SIV pathogenesis and persistence. However, their expression is reduced following morphine exposure.	Olwenyi et al.
JAK1/2 inhibition by baricitinib may block HIV-induced IFN and lead to a reduction in the HIV reservoir.	de Armas et al.
This study optimized eight multispectral confocal microscopy immunofluorescence panels for a comprehensive characterization and immune-profiling of relevant immune cells in formalin-fixed paraffin-embedded human lymphoid tissue samples. To characterize cells harboring actively transcribed virus, authors were employed an *in-situ* hybridization assay in combination with additional protein markers (multispectral RNAscope). This type of analysis can increase the dimensionality and predictive power of flow-cytometry and single-cell RNA expression analyses, thus accelerating biomarker discovery in the context of infection and vaccination.	Moysi et al.
The GAS5 regulates TCR-mediated activation and apoptosis in CD4 T cells during HIV infection through miR-21-mediated signaling, results in prolonged survival of CD4 T cells during HIV.	Nguyen et al.
The composition of circulating innate and adaptive immune cells is altered in a large group of PLHIV receiving cART for more than six months. Specifically, certain adaptive immune responses (Th17) are preserved while IFN-g responses are compromised. The study suggests that the changes in the immune cell architecture and functional immunity in treated HIV highlight associations with the HIV reservoir, thereby emphasizing the importance of early cART initiation.	Van de Wijer et al.
This study demonstrates a direct causal relationship between the presence of HIV in platelets and T-cell dysfunctions in immunological non-responders (InRs), thereby providing valuable insights for the development of a targeted platelet therapy for improving immune reconstitution in these individuals.	Zhu et al.
This study documented the elevated levels of CD4+ Tfh and CD4+ Tscm cells, as well as an abundance of memory and effector T cells in HIV-2 infected individuals. Additionally, they found increased frequencies of CXCR5+ CD8+ T cells and CD8+ Tscm cells as well as memory B cells responsible for NAb development in HIV-2 infected persons.	Ponnan et al.
This systematic review on the dynamics of CD4+ T cells in SIV and HIV infection described the mechanism of CD4+ depletion, disease progression, and the influence of early ART on restoration.	Le Hingrat et al.
This review discussed the impact of HIV infection on Tfh cells and mucosal IgA responses in the GIT, as well as the implications these effects have on gut dysbiosis and mucosal immunopathogenesis.	Onabajo and Mattapallil
In this systematic review, authors performed a pooled data-analysis comparing the transcriptome profiles of latently- and reactivated HIV-1 infected cells of 5 *in vitro* primary CD4+ T cell models of HIV-1 latency and 2 *ex vivo* studies of reactivated HIV-1 infected primary CD4+ T cells from HIV-1 infected individuals. They observed 5 differentially expressed genes FRY, GCSAM, GNLY, GPR15 and MSRB2 and natural ligands (CCL4 & CCL5) and coreceptors (CXCR6) were predominantly downregulated that co-occurred in latently- and reactivated HIV-1 infected primary CD4+ T cells	Inderbitzin et al.
This study provided the overview of host characteristics and hyper-inflammatory response in COVID-19 and HIV infection to better understand the mechanisms of T cell dysfunction. The study summarized that both HIV-1 and SARS-CoV-2 infections are associated with CD4+ T cell loss and immunodeficiency. The study suggests that a better understanding of mechanism of T cell dysfunction will contribute to the development of targeted therapy against severe COVID-19 and will help to rationally design vaccine involving T cell response for the long-term control of viral infection	Peng et al.
In this study, reviewed the current literature on the pathogenesis of HIV/HCV coinfection, the impact of HCV coinfection on HIV disease progression in the presence of ART, the effects of HIV on HCV-associated liver morbidity, and the consequences of DAA-mediated HCV cure on immune reconstitution and HIV reservoir persistence in coinfected patients. The study also found that HIV reservoirs are higher in HCV/HIV coinfected individuals than in those with HIV mono-infection, and DAA-mediated HCV cure does not reduce HIV persistence or protect against HCV reinfection.	Gobran et al.

This is due to the heterogeneity within the Tfh cell population, it is challenging to determine their unique and complex role in HIV pathogenesis and their potential in HIV prevention. Therefore, a better understanding of the mechanisms underlying Tfh cell differentiation and function in lymphoid tissues and immune contexts is essential for developing effective treatment strategies for HIV.

Moysi et al. conducted a study in which they developed and optimized eight multispectral confocal microscopy immunofluorescence panels for a comprehensive characterization of Tfh and other important cells (Tregs, CD8 and macrophages) using formalin-fixed paraffin embedded human lymphoid tissue samples. Here the authors discuss how the resulting multispectral confocal datasets can be analyzed quantitatively using a pipeline named HistoCytometry to gather information about relative frequencies and spatial distributions of immune cells. To characterize cells harboring the actively transcribed virus, the study used an *in-situ* hybridization assay in combination with additional protein markers (multispectral RNAscope). By increasing the dimensionality and predictive power of flow cytometry and single-cell RNA expression analyses. Applying this methodology to lymphoid tissues may provide an opportunity to investigate multiple immune cell targets of interest simultaneously, with improved resolution and reproducibility. This approach may therefore serve as a valuable tool to guide studies on CD4+ T-cells in the context of infection and vaccination, offering deeper insights into their dynamics and responses (24).

Studying HIV-2 in comparison to HIV-1 provides several important insights and contributions to our understanding of HIV infection disease progression and clinical outcomes: HIV-2 infection typically progresses more slowly compared to HIV-1, leading to a milder disease course. Thus, studying CD4 T cells in HIV-2 may allow to investigate factors related to this slower progression. Ponnan et al. evaluated the different subsets of CD4+ T cells, including Tfhs, in HIV-2 infected individuals to understand their role in controlling virus replication and delaying disease progression. The authors observed elevated levels of CD4+ Tfh and Stem cell memory Tscm CD4+ cells, as well as an abundance of memory and effector T cells in HIV-2-infected individuals. Additionally, they found increased frequencies of CXCR5+ CD8+ T cells and CD8+ Tscm cells, as well as memory B cells responsible for NAb development in HIV-2 infected persons. Interestingly, the frequency of memory CD4+ T cells and memory B cells significantly correlated with neutralizing antibody titers in HIV-2-infected individuals. Overall, this study suggests that a more robust CD4+ T cell response that supports B cell differentiation, antibody production, and CD8+ T cell development in HIV-2 infected individuals contributes to better control of the virus and slower disease progression.

Luo et al. conducted a study to explore the diversity of CD4+ T cell subsets in terms of their susceptibility or resistance to HIV-associated killing to understand the pathogenesis of disease progression in CD4+ T cells. The authors used lymphoid cells obtained from human tonsils and employed mass cytometry and single-cell RNA-seq techniques to test their hypothesis. Their results indicated that subsets of CD4+ T cells that are preferentially killed express CXCR4 and CXCR5, a marker used to identify Tfh and the receptor allowing CD4 T cells to migrate to the B cell zone. Further analysis using single-cell RNA-seq showed that the preferentially killed subsets express genes that favor abortive infection and pyroptosis. These findings highlight the complex interplay between HIV and distinct tissue based CD4+ T cell subsets, including Thfs. The study also found that bystander death is more likely to happen when infection involves X4-tropic viruses and is associated with higher expression levels of CXCR4. Additionally, susceptible bystander cells appear to be primed for death by pyroptosis, as indicated by increased mRNA expression of inflammatory caspases (caspase 1 and caspase 4) as well as the pyroptotic executioner, gasdermin D (25).

The review by Onabajo and Mattapallil discusses the effect of HIV infection on Tfh cells and mucosal antibody responses in the gastrointestinal tract (GIT). They highlighted the consequences of such immune deregulations on gut dysbiosis and pathogenesis during chronic HIV infection. Mucosal immunoglobulins A (IgA) play a critical role in protecting the GIT from invasive bacteria. The study also suggests that the dysregulation of Tfh cells leads to compromise B cell responses, especially the secretion of microbe-specific IgA, and it is likely to drive gut microbial dysbiosis during chronic HIV infection. Hence, preserving and maintaining Tfh cell responses in the mucosa could potentially restore high-affinity mucosal IgA, aiding in protecting the mucosal epithelial barrier from invasive dysbiotic bacteria (26).

T cell responses are intricately regulated by a complex network of non-coding RNAs, which includes microRNAs (miRNAs) and long non-coding RNAs (lncRNAs) (27, 28). These non-coding RNAs play crucial roles in modulating gene expression, influencing various aspects of T cell development, activation, differentiation, and effector functions. MicroRNAs are small RNA molecules that can bind to target messenger RNAs (mRNAs), leading to their degradation or inhibition of translation, thereby regulating the expression of specific genes. On the other hand, long non-coding RNAs are larger RNA molecules that can interact with chromatin, proteins, and other RNA molecules to regulate gene expression at multiple levels (24, 29, 30). Together, these non-coding RNAs contribute to the fine-tuning and coordination of T cell responses in both health and disease. Further research into the functions and mechanisms of non-coding RNAs in T cells continues to expand our understanding of immune regulation and may provide insights into HIV pathogenesis. The study conducted by Nguyen et al. aimed to investigate the role of long non-coding RNAs in the development of CD4+ T cell dysfunction and apoptosis in people living with HIV (PLHIV). The results revealed that the growth arrest-specific transcript 5 (GAS5) negatively regulates miR-21 expression, which controls critical signaling pathways involved in DNA damage and cellular response. Prolonged T cell stimulation reduced GAS5 and increased miR-21, leading to dysfunction and apoptosis in CD4+ T cells. These findings suggest that GAS5 regulates TCR-mediated activation and apoptosis in CD4 T cells during HIV infection through miR-21-mediated signaling pathway (37).

Van de Wijer et al. conducted a study aimed to investigate long-term changes in the immune system of people living with HIV

(PLWH) who have successfully undergone treatment. Samples obtained from a cohort of 211 PLWH on stable antiretroviral therapy and 56 HIV-uninfected controls were assessed using flow cytometry to analyze 108 white blood cell (WBC) populations. The results indicated significant differences in T cell maturation and differentiation between PLWH and HIV-uninfected controls, with the PLWH exhibiting reduced percentages of CD4+ T cells and naive T cells, and increased percentages of CD8+ T cells, effector T cells, and T helper 17 (Th17) cells. In addition, the Th17/regulatory T cell (T-reg) ratios were found to be increased. PLWH also had altered B cell maturation, with reduced percentages of memory B cells and increased numbers of plasma blasts. Overall, this study suggests that the composition of circulating innate and adaptive immune cells is altered in PLHIV receiving cART for more than six months. The findings further suggest that while some adaptive immune responses such as Th17 are preserved, IFN-g responses are compromised in PLHIV (Van de Wijer et al.).

The manuscript by Zhu et al. conducted a study to investigate the immunological failure seen in immunological non-responders (InRs), HIV-infected individuals treated with ART, although successful in suppressing viral replication, they cannot properly reconstitute circulating CD4+ T-cell numbers to immunocompetent levels. The study found that InRs had platelets containing infectious HIV, which presence was linked to T-cell dysfunctions. The authors showed that platelet-T cell conjugates were more frequent among CD4+ T cells in InRs with HIV-containing platelets (<350 CD4+ T cells/ml blood for >1 year) compared to healthy donors or IRs (>350 CD4+ T cells/ml). Based on these findings, the authors suggest that targeted therapy aimed at platelets may improve immune reconstitution in InRs (39).

The systematic review by Le Hingrat et al. focused on the dynamics of CD4+ T cells in SIV and HIV. The reviewed literature includes studies on the possible mechanism of CD4+ T cell depletion and restoration in disease progression, and during early ART, respectively. The role of cell death and loss of CD4+ cell subsets in gut health are discussed. Reviewed studies suggest that the loss of CD4+ T cells contributes to mucosal inflammation and enteropathy, which weakens the mucosal barrier, leading to microbial translocation, a major driver of immune activation/inflammation. Studies also suggest that the loss of CD4+ T cells drives opportunistic infections, cancers, and comorbidities. Additionally, the authors discussed the crucial role of Th17 cells in maintaining gut integrity and protecting against bacterial and fungal infections (40).

In their systematic review, Inderbitzin et al. utilized primary CD4+ T cell models to investigate HIV-1 latency and potential cure strategies. The authors performed a pooled data analysis, comparing transcriptome profiles of latently and reactivated HIV-1 infected cells from five *in vitro* primary CD4+ T cell models and two *ex-vivo* studies of reactivated HIV-1 infected primary CD4+ T cells from HIV-1 infected individuals. The authors found that natural ligands CCL4, CCL5 and chemokine receptor CXCR6 were predominantly downregulated in latently infected cells, while genes associated with apoptosis, cell cycle, and HLA class II were upregulated in reactivated infected cells. Furthermore, they identified 5 genes FRY, GCSAM, GNLY, GPR15 and MSRB2 that co-occurred in both latently- and reactivated HIV-1 infected primary CD4+ T cells. The upregulation of MSRB2 in latently HIV-1 infected primary CD4+ T cells could inhibit apoptosis, while downregulation in reactivated HIV-1 infected genes leads to apoptosis due to the cytotoxic response of LRA or infectious virus particle release. This study sheds light on the differentially expressed genes that may contribute to the HIV-1 latency (41).

Both SARS-CoV-2 and HIV can dysregulate the immune system, leading to acute and long lasting inflammation, albeit through different mechanisms. By comparing the immune dysregulation caused by these viruses, we can identify commonalities and differences, which may inform the development of immunomodulatory therapies and approaches to mitigate immune-mediated damage in COVID-19. Peng et al. provided an overview of host characteristics and hyper-inflammatory responses in COVID-19 and HIV infection to understand the mechanisms of T-cell dysfunction better. The study summarized that both HIV-1 and SARS-CoV-2 infections are associated with CD4+ T cell loss and immunodeficiency. Direct attacks on CD4+ T cells, immune activation, and redistribution of CD4+ T cells contribute to CD4+ T cell lymphopenia in both diseases, but in different proportions. During the period of immunodeficiency, systemic inflammation may be fueled by a leaky gut and lead to severe complications. However, the co-occurrence of HIV and COVID-19 does not seem to increase the occurrence of COVID-19 or cause excess morbidity and mortality among people living with HIV with symptomatic COVID-19. Overall, the experience in HIV clinical management and past clinical trials represents a special use case for innovative studies aimed at increasing CD4+ T cell function and reducing COVID-19 severity (42).

The review by Gobran et al. discuss the current literature on the pathogenesis of HIV/HCV coinfection, the impact of HCV coinfection on HIV disease progression in the presence of ART, the effects of HIV on HCV-associated liver morbidity. Globally, approximately 2.3 million individuals are affected by a co-infection of the HIV and hepatitis C virus (HCV), with about 6.2% of people living with HIV (PLWH) also co-infected with HCV. PLWH have a six times higher incidence of being infected with HCV compared to those who are HIV-negative. The prevalence of co-infection is highest among individuals who inject drugs (PWID) and men who have sex with men (MSM). When HIV and HCV coexist, HCV's natural history is negatively affected, leading to higher rates of HCV persistence following acute infection, higher viral loads, accelerated progression of liver fibrosis, and development of end-stage liver disease compared to HCV infection alone. Similarly, HCV coinfection harms the homeostasis of CD4+ T cell counts and facilitates HIV replication and viral reservoir persistence in PLWH receiving antiretroviral therapies (ART). Moreover, the consequences of Direct Acting antiviral (DAA)-mediated HCV cure on immune reconstitution and HIV reservoir persistence in coinfected patients is also discussed. The author comment on studies where it was shown that HIV reservoir is higher in HCV/HIV coinfected individuals than in those with HIV mono-infection, and DAA-mediated HCV cure does not reduce HIV persistence or protect against HCV reinfection. Therefore, developing effective

treatment and prophylactic anti-HCV and anti-HIV vaccines remains a priority to achieve HCV/HIV elimination (43).

HIV vaccine and cure strategies aim to enhance immune responses to achieve long-lasting and, ideally, sterilizing immunity against the virus. The presence of antibodies (preferably broadly neutralizing) and cytotoxic T cells at the site of viral entry is crucial in stopping infection and virus dissemination. In contrast, CD4+ T cells are necessary for mounting a robust vaccine response. However, inducing a strong CD4+ T cell response in HIV infection is a double-edged sword. This is because CD4+ T cells also serve as primary targets of HIV infection and activated CD4+ T cells can be preferentially infected during the early stages of infection. High frequencies of vaccine-elicited CD4+ T cells may also limit vaccine-mediated protection. The specific lineages of CD4+ T cells have been reported to act as HIV reservoirs during chronic HIV infection (10, 25, 31). Furthermore, accumulating evidence suggests that some forms of vaccine specific CD4+ T cell responses may increase susceptibility to HIV infection.

While CD4 T cells are important to generate and maintain effective B and CD8 T cells responses, CD4 T cell induction trough vaccination may be a double edge sword. Evidence is mounting that some of vaccine induced CD4+ T cell responses may increase susceptibility to HIV infection. Results from the STEP HIV vaccine trial highlighted a potential role for total activated vaccine induced CD4+ T cells in promoting HIV acquisition (26, 32, 33). The trial also revealed that preexisting adenoviral immunity triggered a recall response, leading to the activation of adenovirus specific CD4+ T cells. These activated CD4+ T cells could potentially become additional target cells and may have increased the susceptibility to HIV infection in the vaccine arm of the study (34). Interestingly recent studies in macaques showed that the DNA prime/modified vaccinia Ankara boost vaccine induced interferon-γ (IFN-γ^+) CD4+ T cells (Th1 cells), which rapidly migrate to multiple tissues including colon, cervix, and vaginal mucosa. These mucosal Th1 cells persisted at higher frequencies and expressed higher density of CCR5, a viral coreceptor, compared to cells in blood. After intravaginal or intrarectal simian immunodeficiency virus (SIV)/simian-human immunodeficiency virus (SHIV) challenges, strong vaccine protection was evident only in animals that had lower frequencies of vaccine-specific Th1 cells but not in animals that had higher frequencies of Th1 cells, despite comparable vaccine-induced humoral and CD8+ T cell immunity in both groups (35). These results corroborate the notion that high and persisting frequencies of HIV vaccine-induced Th1-biased CD4+ T cells in the intestinal and genital mucosa can mitigate beneficial effects of protective antibodies and CD8+ T cells, highlighting the critical need to better understand how to harness protective responses without increasing HIV susceptibility (36). Given the paradoxical role of CD4+ T cells in HIV infection, understanding the interplay between vaccine-induced CD4+ T cells and vaccine-mediated protection is paramount. To tip the balance in favor of vaccine-mediated protection, a rational design and delivery of vaccines in combination with newer immunotherapeutic strategies like engineered T cells (such as CAR/TCR-T cells) are required. This Research Topic is expected to bring together the current knowledge of CD4+ T cells as important central mediators of adaptive immunity while also being the cellular reservoir and targets for the multiplication and persistence of HIV. Recent research has provided valuable insights into the mechanisms underlying CD4+ T cell depletion and dysfunction in HIV infection, as well as the factors contributing to the natural control of the virus. This Research Topic presents a comprehensive overview (Highlights summarized in Table 1) of these recent advances, focusing on CD4+ T cell dynamics in HIV immunology and pathogenesis. By summarizing the latest findings and highlighting key knowledge gaps, this Research Topic aims to provide a useful resource for researchers and clinicians working on HIV/AIDS, as well as to inspire further research into the discovery of novel therapeutic targets.

Author contributions

VV, CP, MV and SKS edited this topic; SG and VV wrote the original draft; MV, CP, HB and SKS reviewed and edited the final manuscript. All authors contributed to the article and approved the submitted version.

Funding

This research was supported by the Office of Research Infrastructure Programs (ORIP/NIH) base grant P51 OD011132 to ENPRC. This work was partly supported by National Institutes of Health Grants CFAR ERASE AIDS-R03, R01 HD095741-01, 1R01AI148377-01A1 (to VV), Emory University CFAR grant P30 AI050409, P51 OD011104/OD/NIH HHS/United States.

Acknowledgments

We are grateful to all the authors who have contributed to this Research Topic by submitting their valuable work.

Conflict of interest

The authors declare that the research was conducted in the absence of any commercial or financial relationships that could be construed as a potential conflict of interest.

Publisher's note

References

1. Organization WH. Summary of the global HIV epidemic 2021. In: *Summary of the global HIV epidemic* (2021) WHO. Available at: https://www.who.int/data/gho/data/themes/hiv-aids.

2. Vidya Vijayan KK, Karthigeyan KP, Tripathi SP, Hanna LE. Pathophysiology of CD4+ T-cell depletion in HIV-1 and HIV-2 infections. *Front Immunol* (2017) 8:580. doi: 10.3389/fimmu.2017.00580

3. Okoye AA, Picker LJ. CD4(+) T-cell depletion in HIV infection: mechanisms of immunological failure. *Immunol Rev* (2013) 254(1):54–64. doi: 10.1111/imr.12066

4. Kaech SM, Wherry EJ, Ahmed R. Effector and memory T-cell differentiation: implications for vaccine development. *Nat Rev Immunol* (2002) 2(4):251–62. doi: 10.1038/nri778

5. Arck PC, Sallusto F. Heterogeneity of tissue-resident immunity across organs and in health and disease. *Semin Immunopathol* (2022) 44(6):745–6. doi: 10.1007/s00281-022-00967-z

6. Sallusto F, Cassotta A, Hoces D, Foglierini M, Lanzavecchia A. Do memory CD4 T cells keep their cell-type programming: plasticity versus fate commitment? T-cell heterogeneity, plasticity, and selection in humans. *Cold Spring Harb Perspect Biol* (2018) 10(3). doi: 10.1101/cshperspect.a029421

7. Sallusto F. Heterogeneity of human CD4(+) T cells against microbes. *Annu Rev Immunol* (2016) 34:317–34. doi: 10.1146/annurev-immunol-032414-112056

8. Swain SL, McKinstry KK, Strutt TM. Expanding roles for CD4(+) T cells in immunity to viruses. *Nat Rev Immunol* (2012) 12(2):136–48. doi: 10.1038/nri3152

9. Streeck H, D'Souza MP, Littman DR, Crotty S. Harnessing CD4(+) T cell responses in HIV vaccine development. *Nat Med* (2013) 19(2):143–9. doi: 10.1038/nm.3054

10. Velu V, Mylvaganam GH, Gangadhara S, Hong JJ, Iyer SS, Gumber S, et al. Induction of Th1-biased T follicular helper (Tfh) cells in lymphoid tissues during chronic simian immunodeficiency virus infection defines functionally distinct germinal center tfh cells. *J Immunol* (2016) 197(5):1832–42. doi: 10.4049/jimmunol.1600143

11. Crotty S. T Follicular helper cell biology: a decade of discovery and diseases. *Immunity* (2019) 50(5):1132–48. doi: 10.1016/j.immuni.2019.04.011

12. Crotty S. T Follicular helper cell differentiation, function, and roles in disease. *Immunity* (2014) 41(4):529–42. doi: 10.1016/j.immuni.2014.10.004

13. McGary CS, Alvarez X, Harrington S, Cervasi B, Ryan ES, Iriele RI, et al. The loss of CCR6(+) and CD161(+) CD4(+) T-cell homeostasis contributes to disease progression in SIV-infected rhesus macaques. *Mucosal Immunol* (2017) 10(4):1082–96. doi: 10.1038/mi.2016.116

14. Paiardini M, Cervasi B, Reyes-Aviles E, Micci L, Ortiz AM, Chahroudi A, et al. Low levels of SIV infection in sooty mangabey central memory CD(4)(+) T cells are associated with limited CCR5 expression. *Nat Med* (2011) 17(7):830–6. doi: 10.1038/nm.2395

15. Ward AR, Mota TM, Jones RB. Immunological approaches to HIV cure. *Semin Immunol* (2021) 51:101412. doi: 10.1016/j.smim.2020.101412

16. Chun TW, Davey RTJr., Ostrowski M, Shawn Justement J, Engel D, Mullins JI, et al. Relationship between pre-existing viral reservoirs and the re-emergence of plasma viremia after discontinuation of highly active anti-retroviral therapy. *Nat Med* (2000) 6(7):757–61. doi: 10.1038/77481

17. Chomont N, Okoye AA, Favre D, Trautmann L. Wake me up before you go: a strategy to reduce the latent HIV reservoir. *AIDS* (2018) 32(3):293–8. doi: 10.1097/QAD.0000000000001695

18. Dash PK, Chen C, Kaminski R, Su H, Mancuso P, Sillman B, et al. CRISPR editing of CCR5 and HIV-1 facilitates viral elimination in antiretroviral drug-suppressed virus-infected humanized mice. *Proc Natl Acad Sci U S A.* (2023) 120(19):e2217887120. doi: 10.1073/pnas.2217887120

19. Jensen BO, Knops E, Cords L, Lubke N, Salgado M, Busman-Sahay K, et al. In-depth virological and immunological characterization of HIV-1 cure after CCR5Delta32/Delta32 allogeneic hematopoietic stem cell transplantation. *Nat Med* (2023) 29(3):583–7. doi: 10.1038/s41591-023-02213-x

20. Kim JT, Zhang TH, Carmona C, Lee B, Seet CS, Kostelny M, et al. Latency reversal plus natural killer cells diminish HIV reservoir *in vivo*. *Nat Commun* (2022) 13(1):121. doi: 10.1038/s41467-021-27647-0

21. Cubas RA, Mudd JC, Savoye AL, Perreau M, van Grevenynghe J, Metcalf T, et al. Inadequate T follicular cell help impairs B cell immunity during HIV infection. *Nat Med* (2013) 19(4):494–9. doi: 10.1038/nm.3109

22. Locci M, Havenar-Daughton C, Landais E, Wu J, Kroenke MA, Arlehamn CL, et al. Human circulating PD-1+CXCR3-CXCR5+ memory tfh cells are highly functional and correlate with broadly neutralizing HIV antibody responses. *Immunity* (2013) 39(4):758–69. doi: 10.1016/j.immuni.2013.08.031

23. Perreau M, Savoye AL, De Crignis E, Corpataux JM, Cubas R, Haddad EK, et al. Follicular helper T cells serve as the major CD4 T cell compartment for HIV-1 infection, replication, and production. *J Exp Med* (2013) 210(1):143–56. doi: 10.1084/jem.20121932

24. Statello L, Guo CJ, Chen LL, Huarte M. Gene regulation by long non-coding RNAs and its biological functions. *Nat Rev Mol Cell Biol* (2021) 22(2):96–118. doi: 10.1038/s41580-020-00315-9

25. Petrovas C, Velu V. Editorial: lymph node T cell dynamics and novel strategies for HIV cure. *Front Immunol* (2018) 9:2950. doi: 10.3389/fimmu.2018.02950

26. McElrath MJ, De Rosa SC, Moodie Z, Dubey S, Kierstead L, Janes H, et al. HIV-1 vaccine-induced immunity in the test-of-concept step study: a case-cohort analysis. *Lancet* (2008) 372(9653):1894–905. doi: 10.1016/S0140-6736(08)61592-5

27. Liu X, Xu M, Li P, Zhang W, Zeng LH, Yang Y, et al. Roles of lncRNAs in the transcription regulation of HIV-1. *BioMed J* (2022) 45(4):580–93. doi: 10.1016/j.bj.2022.03.012

28. Taheri M, Barth DA, Kargl J, Rezaei O, Ghafouri-Fard S , Pichler M. Emerging role of non-coding RNAs in regulation of T-lymphocyte function. *Front Immunol* (2021) 12:756042. doi: 10.3389/fimmu.2021.756042

29. Zhang X, Wang W, Zhu W, Dong J, Cheng Y, Yin Z, et al. Mechanisms and functions of long non-coding RNAs at multiple regulatory levels. *Int J Mol Sci* (2019) 20(22). doi: 10.3390/ijms20225573

30. Mattick JS, Amaral PP, Carninci P, Carpenter S, Chang HY, Chen LL, et al. Long non-coding RNAs: definitions, functions, challenges and recommendations. *Nat Rev Mol Cell Biol* (2023) 24(6):430–47. doi: 10.1038/s41580-022-00566-8

31. Velu V, Mylvaganam G, Ibegbu C , Amara RR. Tfh1 cells in germinal centers during chronic HIV/SIV infection. *Front Immunol* (2018) 9:1272. doi: 10.3389/fimmu.2018.01272

32. Buchbinder SP, Mehrotra DV, Duerr A, Fitzgerald DW, Mogg R, Li D, et al. Efficacy assessment of a cell-mediated immunity HIV-1 vaccine (the step study): a double-blind, randomised, placebo-controlled, test-of-concept trial. *Lancet* (2008) 372(9653):1881–93. doi: 10.1016/S0140-6736(08)61591-3

33. Petrovas C, Yamamoto T, Gerner MY, Boswell KL, Wloka K, Smith EC, et al. CD4 T follicular helper cell dynamics during SIV infection. *J Clin Invest.* (2012) 122(9):3281–94. doi: 10.1172/JCI63039

34. Koblin BA, Mayer KH, Noonan E, Wang CY, Marmor M, Sanchez J, et al. Sexual risk behaviors, circumcision status, and preexisting immunity to adenovirus type 5 among men who have sex with men participating in a randomized HIV-1 vaccine efficacy trial: step study. *J Acquir Immune Defic Syndr* (2012) 60(4):405–13. doi: 10.1097/QAI.0b013e31825325aa

35. Chamcha V, Reddy PBJ, Kannanganat S, Wilkins C, Gangadhara S, Velu V, et al. Strong T(H)1-biased CD4 T cell responses are associated with diminished SIV vaccine efficacy. *Sci Transl Med* (2019) 11(519). doi: 10.1126/scitranslmed.aav1800

36. Lewis GK, DeVico AL, Gallo RC. Antibody persistence and T-cell balance: two key factors confronting HIV vaccine development. *Proc Natl Acad Sci U S A.* (2014) 111(44):15614–21. doi: 10.1073/pnas.1413550111

frontiers in Immunology

REVIEW
published: 15 December 2020
doi: 10.3389/fimmu.2020.596631

Sharing CD4+ T Cell Loss: When COVID-19 and HIV Collide on Immune System

Xiaorong Peng[1,2,3], *Jing Ouyang*[4], *Stéphane Isnard*[1,2,5], *John Lin*[1,2], *Brandon Fombuena*[1,2], *Biao Zhu*[3] *and Jean-Pierre Routy*[1,2,6*]

[1] *Infectious Diseases and Immunity in Global Health Program, Research Institute, McGill University Health Centre, Montréal, QC, Canada,* [2] *Chronic Viral Illness Service, McGill University Health Centre, Montréal, QC, Canada,* [3] *State Key Laboratory for Diagnosis and Treatment of Infectious Diseases, National Clinical Research Center for Infectious Diseases, Collaborative Innovation Center for Diagnosis and Treatment of Infectious Diseases, The First Affiliated Hospital, College of Medicine, Zhejiang University, Hangzhou, China,* [4] *Chongqing Public Health Medical Center, Chongqing, China,* [5] *CIHR Canadian HIV Trials Network, Vancouver, BC, Canada,* [6] *Division of Hematology, McGill University Health Centre, Montréal, QC, Canada*

COVID-19 is a distinctive infection characterized by elevated inter-human transmission and presenting from absence of symptoms to severe cytokine storm that can lead to dismal prognosis. Like for HIV, lymphopenia and drastic reduction of CD4+ T cell counts in COVID-19 patients have been linked with poor clinical outcome. As CD4+ T cells play a critical role in orchestrating responses against viral infections, important lessons can be drawn by comparing T cell response in COVID-19 and in HIV infection and by studying HIV-infected patients who became infected by SARS-CoV-2. We critically reviewed host characteristics and hyper-inflammatory response in these two viral infections to have a better insight on the large difference in clinical outcome in persons being infected by SARS-CoV-2. The better understanding of mechanism of T cell dysfunction will contribute to the development of targeted therapy against severe COVID-19 and will help to rationally design vaccine involving T cell response for the long-term control of viral infection.

Keywords: COVID-19, HIV, CD4 exhaustion, cytokine storm, leaky gut

OPEN ACCESS

Edited by:
Monica Vaccari,
Tulane University, United States

Reviewed by:
Francesca Caccuri,
University of Brescia, Italy
Nicholas Maness,
Tulane University, United States

***Correspondence:**
Jean-Pierre Routy
jean-pierre.routy@mcgill.ca

Specialty section:
This article was submitted to Viral Immunology, a section of the journal Frontiers in Immunology

Received: *19 August 2020*
Accepted: *17 November 2020*
Published: *15 December 2020*

Citation:
Peng X, Ouyang J, Isnard S, Lin J, Fombuena B, Zhu B and Routy J-P (2020) Sharing CD4+ T Cell Loss: When COVID-19 and HIV Collide on Immune System. Front. Immunol. 11:596631. doi: 10.3389/fimmu.2020.596631

INTRODUCTION

An outbreak of an unknown infectious pneumonia occurred in Wuhan, China, in December 2019 (1). The pathogen of the disease was quickly identified as a novel coronavirus coined severe acute respiratory syndrome coronavirus 2 (SARS-CoV-2), and the disease was named coronavirus disease-19 (COVID-19) by the WHO (2–4). The virus has since caused more than 48 million confirmed cases and over 1.2 million deaths worldwide by November, 2020 (5). The majority of individuals with COVID-19 have mild clinical presentation with or without flu-like symptoms including dry cough, fever, a runny nose, fatigue, muscle pain and diarrhea. Some cases can evolve into acute respiratory distress syndrome, septic shock, coagulation dysfunction, and multiorgan failure (1, 6, 7). The severity of the disease is influenced by factors such as older age, obesity and metabolic syndrome (8, 9). Acute infection with SARS-CoV-2 is associated with lymphopenia in approximately 80% of patients (6, 10–21). Furthermore, lymphopenia with the suppression of B, helper (CD4+) and cytotoxic (CD8+) T cell function, is an indicator of a poor clinical outcome

(10–15, 17–19, 21–27). It is likely that lymphopenia delays viral clearance, favoring macrophage stimulation and the accompanying cytokine storm, leading to organ dysfunction (7, 15, 18, 19, 21, 23, 24, 26, 28, 29).

Apart from SARS-CoV-2, other viruses—including SARS coronavirus, measles virus, avian influenza virus H5N1, swine foot-and-mouth disease virus, respiratory syncytial virus and human immunodeficiency virus (HIV)—are associated with lymphopenia (30). Among them, HIV can cause an well-known lymphopenia-associated disease acquired immune deficiency syndrome (AIDS) (31). The acute phase of HIV infection is characterized by a substantial drop in peripheral CD4+ T cell counts, while during the chronic phase, a slower and persistent decline of these CD4+ T cells is associated with the development of AIDS. Antiretroviral therapy (ART) rapidly suppresses HIV replication, and the number of CD4+ T cell counts recovers, preventing AIDS. However, systemic immune activation persists in those people even after years of ART (32), and is characterized by increased proinflammatory mediators and low CD4/CD8 ratio (33), combined with exhausted and senescent T cells. Systemic immune activation is also associated with non-infectious comorbidities, such as cardiovascular diseases, neurocognitive disorders and cancers.

CD4+ T cells orchestrate the response to acute and chronic viral infections by coordinating the immune system. These cells activate multiple cells of the innate immune system, as well as B cells, cytotoxic CD8+ T cells, and non-immune cells. CD4+ T cells also play a key role for the establishment of long-term cellular and humoral antigen specific immunity, which is the basis of life-long protection for many viral infections and vaccines (34, 35).

Both HIV-1 and SARS-CoV-2 have distinct virological characteristics while sharing CD4+ T cell lymphopenia. In this review, we critically assessed the possible mechanisms and the potential influence of CD4+ T cell lymphopenia in acute and chronic viral infections. We also discuss host characteristics and hyper-inflammatory response in these two dramatic viral infections and the impact of COVID-19 infection in people living with HIV (PLWH).

THE T CELL DYSREGULATION IN PLWH AND COVID-19

The acute phase of HIV infection is characterized by a substantial drop in peripheral CD4+ T cell counts while in the chronic phase, a continued decline of CD4+ T cells is associated with the development of AIDS (**Figure 1**). In contrast, expansion of CD8+ T cells is observed which is driven mainly by an exhausted cytotoxic response toward HIV, leading to an inversed CD4/CD8 ratio. Despite ART, PLWH still present persistent immune activation and inflammation. The expressions of CD38 and HLA-DR as well as programmed death -1 (PD-1) are biomarkers of activated T cells, contributing to T cell exhaustion (36). Exhausted virus-specific CD4+ T cells express PD-1 at elevated levels correlating with disease progression, viral loads and reduced CD4+ T cell count (37).

Compared to healthy controls, in both acutely and chronically PLWH, the absolute number of regulatory T cells (Tregs) in the circulating blood is decreased, however the percentage of Tregs in chronic infection is increased (38, 39), further contributing to T cell dysfunction. Gut CD4+ T cells with a mucosa protective Th17 function are rapidly depleted (40) contributing to mucosal barrier dysfunction, leading to increase microbial translocation and systemic immune activation (41). Despite the decreased CD4+ T cell subgroup, both cell number and relative percentage of circulating T follicular helper (Tfh) cells increased in the blood during the chronic phase of HIV infection (42, 43). Tfh cells provide help to B cells in germinal center of secondary lymphoid organs and are central to the generation of efficient neutralizing and non-neutralizing antibody responses in HIV infection and will be essential in generating an effective vaccine (44). Expansion and altered features of HIV-specific and non-HIV specific circulating Tfh cells do not improve during ART and may be driven by persistent HIV antigen expression (45). Viral suppression by ART resulted with a reduction in the expression of genes associated with Tfh cells compared to viremic phase, which is accompanied by persistently low expression of genes associated with Th17 cells compared to persons who spontaneously control viremia (46).

Lymphocytopenia is a hallmark of patients with severe COVID-19 (6, 10–15, 17–19, 21) and is associated with poor clinical outcomes. The CD4+ lymphocyte count dynamic during mild and severe COVID-19 is shown in **Figure 1**. Helper CD4+ T cells are important in mediating protective humoral immunity by stimulating B cells to produce virus-specific antibodies. On the other hand, CD8+ T cells are responsible for the elimination of infected cells, mainly through the production of perforin and granzyme, and are key players in controlling different types of viruses through the secretion of cytokines. Both CD4+ and CD8+ T cell counts are reduced in severe COVID-19 (10–15, 17–19, 21–27). Similarly, reduced B cell counts are also observed in severe COVID-19 (14, 23). Moreover, within the CD4+ T cell subset, decreased numbers of effector memory T cells (CD45RO+) and Tregs (CD25+CD127low) were noted, while the proportion of naive T cells (CD45RA+) increased (16). The frequency of Tregs, which are responsible for the maintenance of immune homeostasis by suppressing activation and pro-inflammatory functions, was very low in severe cases. In addition, relative increased recirculation of activated CXCR5 +PD-1^{high} CD4+ Tfh cells is observed in severe COVID-19.

CD4+ T cells in COVID-19 are activated as characterized by expression of cellular markers like HLA-DR, CD25, CD38 and Ki-67 (47). T cell exhaustion based on increased inhibitory markers such as PD-1 and TIM-3 receptor on peripheral T cells has also been reported (47–49). Studies have demonstrated that decreases in polyfunctionality (multiple cytokine secretion) and cytotoxicity of T cells were correlated with disease progression (21, 49). Conversely to HIV, a study demonstrated an increase in the number of Th17 cells in the peripheral blood in COVID-19 patients (50). In hospitalized patients compared to non-

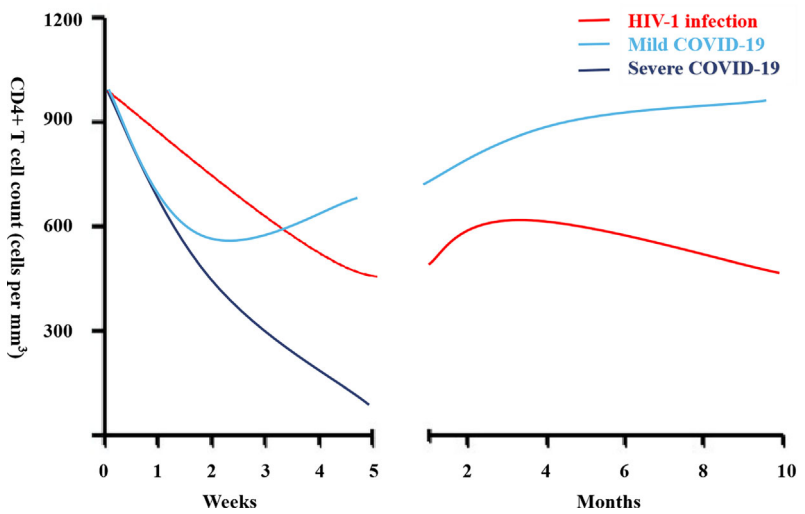

FIGURE 1 | CD4+ lymphocyte count during acute infection in people living with HIV (PLWH) and coronavirus disease-19 (COVID-19).

hospitalized patients, Mathew *et al.* found increased proportion of cytotoxic follicular helper cells and cytotoxic T helper cells responding to SARS-CoV-2 and reduced proportion of SARS-CoV-2-reactive Treg cells (47). Elevated SARS-CoV-2-specific CD4+ and CD8+ T cells were each associated with milder disease, fostering important roles for both CD4+ and CD8+ T cells in protective immunity in COVID-19 (51). Furthermore, absence of these virus-specific cells leads to uncoordinated antigen-specific immune responses and failure to control COVID-19, predominantly in older individuals with low naïve CD4+ T cells. Similarly, PLWH are not able to mount an effective HIV-specific CD4+ and CD8+ T cell responses with the exception of HIV controllers who can maintain undetectable or low levels of viremia despite not being on ART (46, 52, 53). Features of different peripheral blood cell types in PLWH and severe COVID-19 are shown in **Figure 2**.

LEAKY GUT

Depletion of gut CD4+ T cells will be followed by disruption of the tight junctions, and cell death of intestinal epithelium. Epithelial gut damage leads to both an imbalance of the intestinal microbiota composition (dysbiosis) and the release of

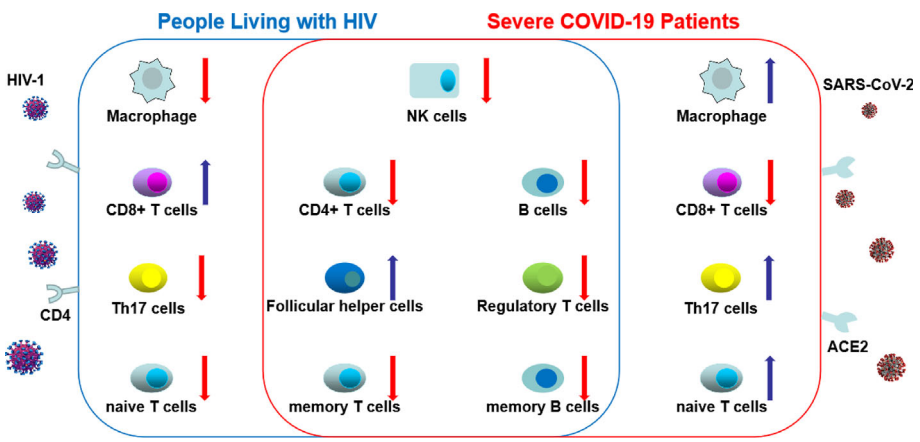

FIGURE 2 | The changes of different peripheral blood cell types in HIV and severe coronavirus disease-19 (COVID-19). In COVID-19 and HIV infection, total count of natural killer cells, B cells, CD4+ T cells, regulatory T cells, memory T and B cells decrease, whereas the count of follicular helper cells increase. These common changes between HIV and COVID-19 were shown in the central circle. However, distinct changes were shown in total count of macrophage, CD8+ T cells, Th17 cells and naive T cells between people living with HIV (PLWH) and severe COVID-19. (The red arrow indicates a decrease in the number of cells; the blue arrow indicates an increase in the number of cells).

bacterial products in the circulation (microbial translocation), participating in chronic immune activation and inflammation (54, 55).

Apart from relevant metabolic functions for the host homeostasis, the gut microbiota exerts protective actions against pathogenic colonization of bacteria and viruses, which could be at least partially attributed to their role in educating and strengthening the immune system (56). The triad gut microbiota dysbiosis–immune hyper-response–inflammation is involved in both HIV and COVID-19 pathogenesis (57).

Within a few weeks of HIV infection, the virus begins a massive assault on the gut, which undergoes a significant depletion of CD4+ T cells with Th17 function (58). PLWH have an altered microbiota composition with an increase of pro-inflammatory and potentially pathogenic bacteria as well as a decrease of beneficial bacteria (59, 60). Gut damage allows microbial translocation, a cause of systemic immune activation in chronic HIV which is usually determined by measuring plasma levels of markers of microbial translocation such as lipopolysaccharide (LPS) and (1→3)-β-D-Glucan (BDG), all of which are elevated in PLWH, even those on ART (61, 62). Previous studies have shown that LPS and BDG were associated with disease progression, lower CD4+ T cell count, and induce immune activation (61–63).

Over 60% of patients with COVID-19 report evidence of gastrointestinal symptoms, such as diarrhea, nausea and vomiting (64). There is direct evidence that SARS-CoV-2 can replicate in intestinal cells (65). Moreover, many viral infections, including influenza, drive changes in the gut and lung microbiota with viral-mediated changes in the gut including dysbiosis and increased permeability (66). Indeed, recent studies found some differences in gut microbial features and related metabolites in SARS-CoV-2 infection (67). More attention should be directed to gut dysbiosis and microbial translocation in the contribution to severe COVID-19.

HYPER-INFLAMMATION IN HIV INFECTION AND COVID-19

Examination of plasma cytokines of acute HIV infection revealed that interferon (IFN)-α was the first cytokine to be increased within a few days after detection of viremia, followed by tumor necrosis factor α (TNF-α), IFN-γ, and interleukin (IL)-12 (68). Initiation of ART during Fiebig stages I-II can abrogate the HIV-induced cytokine storm (69). Elevation of IFN-α, IFN-γ, monocyte chemoattractant protein (MCP)-1, soluble IL-2 receptor (sCD25), IL-6 and IL-8 was seen in chronically-infected untreated individuals (63, 70, 71). Initiation of ART significantly reduces plasma levels of inflammatory cytokines, markers of inflammation and monocyte activation, without normalization compared to HIV-uninfected individuals (72).

Similarly, in COVID-19 patients, elevation of inflammatory cytokines was also observed. In severe cases, elevations of TNF-α, IFN-γ, IL-2R, IL-6, IL-8, and IL-10 were detected (7, 15, 18, 19, 21, 23, 24, 26, 28, 29). However, a highly impaired interferon (IFN) type I response was observed, characterized by no IFN-β and low IFN-α production and activity (73). Furthermore, studies have found increased production of proinflammatory cytokines and chemokines, IL-2, IL-7, IL-10, granulocyte colony-stimulating factor (G-CSF), CXCL-10/IP-10, TNF-α and macrophage inflammatory protein (MIP)-1α in intensive care unit (ICU) patients compared with non-ICU patients (7). In addition, IL-6 levels were considered as a biomarker of disease severity and mortality (28, 29) and ongoing clinical trials are assessing IL-6 blockade to improve outcome in COVID-19 patients (74).

A pre-existed low-level inflammation and leaky gut in type 2 diabetes mellitus (T2DM) may be associated with higher COVID-19 mortality (75, 76). Retrospective studies have shown a reduction in mortality in metformin users compared with non-users among patients with T2DM hospitalized for COVID-19 (77). The potential effects of metformin in COVID-19 could be through inhibition of the mTOR pathway and prevention of immune hyperactivation (78). Reduced production of cytokines such as TNF-α and IL-6 was seen in metformin-treated patients (79). Furthermore, metformin may also reduce inflammation by altering the composition of gut microbiota (80, 81). A retrospective cohort study on PLWH with diabetes mellitus showed that Metformin use was associated with improved CD4 recovery (82). Whether metformin could be a potential treatment strategy for CD4+ T cells lymphopenia in COVID-19 need further investigation.

COMORBIDITIES IN PLWH AND COVID-19

Although ART reduced the risk of developing AIDS (83), it does not normalize inflammation that is associated with risk of non-AIDS comorbidities, including cardiovascular and metabolic diseases and neurocognitive dysfunctions (84–86).

In COVID-19, direct viral attack and systemic hyper-inflammation can cause dysfunction of several organs. Postmortem analyses showed that the main damage occurred in the lungs, to the alveolar epithelial cells, hyaline membrane formation, and hyperplasia of type II pneumocytes, all components of diffuse alveolar damage (87, 88). Nearly 20% of patients hospitalized for COVID-19 in Wuhan, China showed evidence of cardiac injury (89, 90). More than half of COVID-19 patients hospitalized had elevated levels of enzymes indicating injury to the liver (91). In a case series of 214 patients with COVID-19, neurologic symptoms were seen in 36.4% of patients which included acute cerebrovascular events, impaired consciousness, and muscle injury (92).

MECHANISMS OF CD4+ T CELL LYMPHOPENIA

The thymus supports T cell differentiation from T progenitor cells, which differentiate from hematopoietic stem cells in bone marrow, and selects mature CD3+ CD4+ and CD3+ CD8+ thymocytes (41). Quantitative estimates indicate that healthy

young (<30 year old) adults harbor about 2.2×10^{11} mature CD4+ T cells (93). Most CD3+CD4+ and CD3+CD8+ T cells reside in peripheral lymphoid organs where T and B cell responses are coordinated by antigen-presenting cells (APC). CD4+ T cell numbers are kept constant in the human body by homeostatic mechanisms including IL-7 (41). Total CD4+ T cells may be depleted due to cell death, shortened half-life or impaired production. In addition, the proportion of circulating CD4+ cells may decrease through lymphoid tissue redistribution at sites of inflammation. A number of dynamic models have been put forth explaining HIV-mediated depletion of CD4+ T cells (94, 95). However, CD4+ lymphopenia is poorly understood in COVID-19. Potential mechanisms and consequences of CD4+ lymphopenia in PLWH and COVID-19 are shown in **Figure 3**.

Direct Attacks on CD4+ T Cells

Early experiments done with laboratory-adapted HIV isolates in tissue culture revealed a cytopathic virus with high tropism for CD4+ T cells (96). There is a homeostatic response by which the loss of CD4+ T cells due to HIV infection is counteracted by production of T cells; however, this balance is ultimately disrupted once the production of T cells in response to homeostasis is exhausted. This has been substantiated by quantitative image analysis of decreased numbers of CD4+ T cells and increased levels of cellular proliferation and apoptosis in PLWH (97, 98). However, evidence showed that HIV pathogenesis cannot be solely explained by the direct viral killing hypothesis as uninfected CD4+ T cells have a shortened half-life by cellular viral contact affecting IL-7 signalization (99). Another explanation is phospholipase A2 group IB (PLA2G1B) which synergizes with the HIV gp41 envelope protein and targets the CD4+ T cell surface, leading to CD4+ T cell unresponsiveness (anergy) (100).

The question arises whether SARS-CoV-2, like HIV, can directly decrease CD4+ T cell count. ACE2 (angiotensin-converting enzyme 2) is the SARS-CoV-2 internalization receptor (101), in concert with the host's TMPRSS2 (transmembrane protease serine 2) membrane protease that primes the coronavirus spike S protein to facilitate its cell entry (102). ACE2 and TMPRSS2 are co-expressed in lung, heart, liver, kidney, neurons and immune cells (103). Immune cells could potentially be infected by SARS-CoV-2, as in the case of SARS-CoV (104), with both viruses sharing the same receptor ACE2 (102). Studies showed that SARS-CoV can infect 50% of lymphocytes in the circulation (105), resulting in cell death by apoptosis, necrosis, or pyroptosis (106, 107). Furthermore, under the influence of SARS-CoV, the germinal center regressed, and both T and B lymphocytes are depleted (108). Extensive cell death of lymphocytes was observed in an autopsy study of spleens and hilar lymph nodes of six patients with COVID-19. However, the direct evidence of whether SARS-CoV-2 infects T cells is still lacking.

Immune Activation and T Cell Death

Previous studies proposed that activated CD4+ T cells have a very short life span due to activation-induced cell death or apoptosis (109). In HIV infection, the activation of CD4+ T cells is driven by the antigenic stimulus by HIV proteins (110) and in part by antigen-independent mechanisms through the production of inflammatory cytokines. Continuous hyperactivation of T cells may lead to accelerated consumption of naïve T cells through apoptosis or differentiation toward a memory phenotype.

Elevation of inflammatory cytokines and cytokine storm was observed in COVID-19 patients. Previous studies showed that a number of inhibitory cytokines are released by infected lung macrophages or epithelial cells. These cytokines include TNF-α which causes T cell apoptosis (111), IL-10 which is known to prevent T cell proliferation (112), and type-I IFN which regulates lymphocyte recirculation (113). Whether these inflammatory cytokines contribute to the loss of CD4+ T cell needs further investigation.

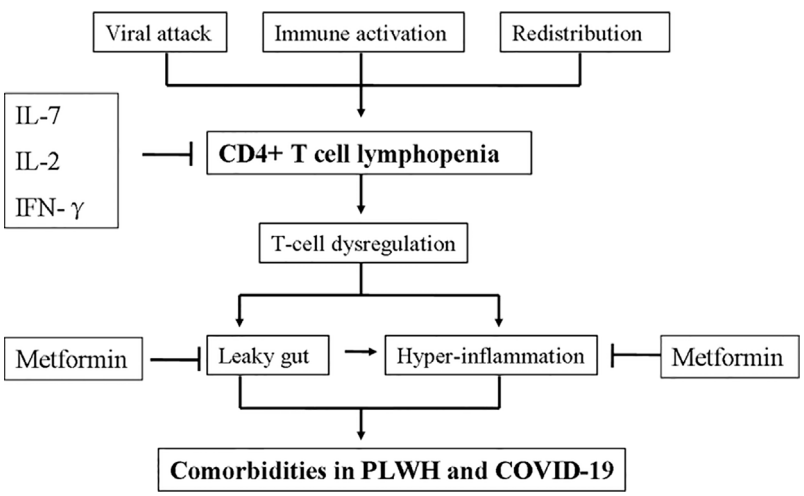

FIGURE 3 | Potential mechanism and consequence of CD4+ lymphopenia in people living with HIV (PLWH) and coronavirus disease-19 (COVID-19).

Redistribution of CD4+ T Cells

Circulating CD4+ T cell counts are most studied due to their ease of access. However, CD4+ T cell in the blood compartment does not always reflect the composition of lymphoid organs or infected sites where CD4+ T cells are recruited. Hence, CD4+ T cell lymphopenia could be a reflection of CD4+ T cell redistribution throughout the body.

Some evidence from simian immunodeficiency virus (SIV) macaque models indicates CD4+ T cell redistribution from the peripheral blood to lymph nodes and the gut (114). When blood levels of CD4+ lymphocytes begin to drop significantly, these cells often increase in number in the lymph nodes (115). This suggests that the loss of CD4+ T cells in the blood can in part be explained by an enhanced homing of CD4+ lymphocytes into the lymph nodes. Furthermore, CD62L, the receptor for lymph node homing, could be unregulated after infection with HIV (116). After the initiation of effective antiretroviral therapy, decreased levels of adhesion molecules like VCAM-1 and ICAM-1, which mediate lymphocyte sequestration into lymphoid tissue, were associated a rapid increased of CD4 T cells and decreased LN size (117).

SARS-CoV-2 prefentially infects and destroys alveolar epithelial cells that may in turn trigger the production or the overproduction by macrophages of pro-inflammatory cytokines and chemokines (including interleukin-6 (IL-6), IL-8, CXCL10/IP-10, CCL3/MIP1α, CCL4/MIP1β) (118). Secretion of such cytokines and chemokines attracts immune cells, notably monocytes and T lymphocytes, from the blood into the infected site, which may explain the circulating lymphopenia. Additionally, the first autopsy of a patient with COVID-19 revealed an accumulation of mononuclear cells (monocytes and T cells) in the lungs, coupled with low levels of hyperactive T cells in the peripheral blood (88). Furthermore, anti-IL-6 immediately reversed lymphopenia favoring tissue redistribution in patients having multicentric Castleman disease, a condition characterized by an enhanced level of IL-6 (119). Animal models and future clinical trials will help decipher the mechanism responsible for SARS-CoV-2 associated lymphopenia.

WHEN HIV MEETS COVID-19

Several case reports assessed the influence of COVID-19 in PLWH (120–123). In a case series of 33 PLWH patients with COVID-19, three out of 32 patients with documented outcome died (9%). However, 91% of the patients recovered and 76% have been classified as mild cases, indicating that there is no excess morbidity and mortality among PLWH with symptomatic COVID-19 compared to COVID-19 HIV-negative patients (123). In a study in Wuhan, there were 8 COVID-19 out of 1174 investigated HIV/AIDS patients. The authors reported absence of influence of sex, CD4+ T cells counts, HIV viral load, or ART regimen associated with the occurrence of COVID-19, only older age was associated with COVID-19 infection (124).

HYPOTHESES FOR THE NON-INFLUENCE OF HIV INFECTION IN COVID-19 DISEASE

A compromised immune system with a lower CD4+ T cells counts and elevated interferon levels in HIV infection might reduce clinical symptoms of COVID-19. There is a hypothesis that a lower active immune status might protect the human body from a virus-induced cytokine storm, such as SARS and MERS (125).

Some ART medications (lopinavir/ritonavir, ritonavir, darunavir, and dolutegravir), were screened for anti-SARS-CoV-2 replication activity and were initially used to treat COVID-19 (126). However, clinical trials using lopinavir/ritonavir, a protease inhibitor that could suppress SARS-CoV-2 replication *in vitro*, had no impact on COVID-19 outcome (127). Another drug is tenofovir (TDF), a nucleoside analog of remdesivir, which can inhibit SARS-CoV-2 RNA-dependent RNA polymerase (RdRp) activity *in vitro* and shorten the time to recovery in adults who were hospitalized with COVID-19 and had evidence of lower respiratory tract infection (128).

In a cohort study with 77 590 HIV-positive persons receiving ART, the result showed that HIV-positive patients receiving TDF/Emtricitabine (FTC) had a lower risk for COVID-19 and related hospitalization than those receiving other therapies (129). These findings warrant further investigation in healthy individuals taking these two drugs for HIV preexposure prophylaxis studies and randomized trials in persons with and without HIV.

POTENTIAL TREATMENT OF CD4+ T CELLS LYMPHOPENIA

IL-7

IL-7 levels are known to be inversely correlated with CD4+ T cell counts in patients with HIV/AIDS, and is likely associated with a homeostatic response (130). IL-7 is essential to B and T cell lymphopoiesis in the bone marrow. Clinical studies showed that recombinant IL-7 treatment increased the number of naive and memory CD4+ and CD8+ T cells while conserving T cell functions (131, 132). Several clinical trials are currently under way to evaluate the efficacy of IL-7 to improve clinical outcomes in lymphopenic patients with COVID-19 (NCT04407689, NCT04379076, NCT04442178 and NCT04442178).

IL-2 and IFN-γ

IL-2 is a potent mitogen and growth factor in antigen-stimulated CD4+ T cells (133). IL-2 has been studied in HIV and has been shown to increase CD4+ T cells counts (134, 135). IL-2 levels in the peripheral blood were increased in severe COVID-19 cases compared to mild cases (7, 15, 18, 19, 21, 23, 24, 26, 28, 29). Whether IL-2 can be used to improve CD4+ T cell lymphopenia in COVID-19 patients should be carefully considered. The efficacy of low-dose IL-2 administration is under evaluation in patients with SARS-CoV2-related acute respiratory distress syndrome in a randomized controlled trial (NCT04357444).

LIMITATIONS

There are still some knowledge gaps about CD4+ T cell loss in PLWH and COVID-19. Firstly, the dynamic of change in CD4+ T cell is difficult to be compared, especially as HIV induces both an acute and chronic disease state. Secondly, the data in COVID-19 are limited. New studies need to be conducted to learn more about this new disease, and lessons from studies on HIV infection and care of PLWH could definitely help designing new therapeutic tools.

CONCLUSION

Both HIV-1 and SARS-CoV-2 infection share CD4+ T cell loss in association with disease outcome and immunodeficiency. Direct attacks on CD4+ T cells, immune activation and redistribution of CD4+ T cell are contributing mechanisms in very different proportion for CD4+ T cell lymphopenia in both diseases. During the period of immunodeficiency, systemic inflammation could be fueled by leaky gut and lead to severe complications. However, when HIV meets COVID-19, no increase in the occurrence of COVID-19 and no excess morbidity and mortality among PLWH with symptomatic COVID-19 has been reported. IL-7 and IL-2 were previously used to increase CD4+ T cell counts in HIV-1 infection, however, no improvement in their function were reported. Despite this, the short-term effect for COVID-19 is under investigation. As CD4+ T cells orchestrate immune responses, proper CD4+ T cell function is required for effective vaccine responses. Hence, anti-SARS-CoV-2 antibodies and CD4 responses should be studied in order to develop long-term efficiency vaccine formulation. Overall, experience in HIV clinical management and past clinical trials represent a special use case for innovative studies aiming at increasing CD4+ T cell function and reducing COVID-19 morbidity.

AUTHOR CONTRIBUTIONS

XP wrote the first draft of the manuscript. JO, SI, JL, BF, and BZ provided critical revision of the manuscript. J-PR conceived and designed the manuscript. All authors contributed to the article and approved the submitted version.

FUNDING

This work was funded by the China Scholarship Council (No.201906325018), the Canadian Institutes of Health Research (CIHR; grants MOP 103230 and PTJ 166049), the Vaccines & Immunotherapy Core of the CIHR Canadian HIV Trials Network (CTN, grant CTN 257), the CIHR-funded Canadian HIV Cure Enterprise (CanCURE) Team Grant HB2-164064, This work was also supported by the Fonds de la Recherche Québec-Santé (FRQ-S): Réseau SIDA/Maladies infectieuses and Thérapie cellulaire. JO is supported by the Chinese National Science and Technology Major Project during the 13th Five-Year Plan (No. 2018ZX10302104). SI is supported by a Fond de Recherche Québec Santé fellowship and a CIHR/CTN Postdoctoral Fellowship Award. JP-R is the holder of the Louis Lowenstein Chair in Hematology and Oncology, McGill University and William Turner award holder from the McGill University Health Centre.

ACKNOWLEDGMENTS

We are highly grateful to Angie Massicotte, Josée Girouard, and Cezar Iovi for coordination and assistance.

REFERENCES

1. Chen N, Zhou M, Dong X, Qu J, Gong F, Han Y, et al. Epidemiological and clinical characteristics of 99 cases of 2019 novel coronavirus pneumonia in Wuhan, China: a descriptive study. *Lancet* (2020) 395(10223):507–13. doi: 10.1016/S0140-6736(20)30211-7
2. Coronaviridae Study Group of the International Committee on Taxonomy of V. The species Severe acute respiratory syndrome-related coronavirus: classifying 2019-nCoV and naming it SARS-CoV-2. *Nat Microbiol* (2020) 5 (4):536–44. doi: 10.1038/s41564-020-0695-z
3. Zhou P, Yang XL, Wang XG, Hu B, Zhang L, Zhang W, et al. A pneumonia outbreak associated with a new coronavirus of probable bat origin. *Nature* (2020) 579(7798):270–3. doi: 10.1038/s41586-020-2012-7
4. Zhu N, Zhang D, Wang W, Li X, Yang B, Song J, et al. A Novel Coronavirus from Patients with Pneumonia in China, 2019. *New Engl J Med* (2020) 382 (8):727–33. doi: 10.1056/NEJMoa2001017
5. Dong E, Du H, Gardner L. An interactive web-based dashboard to track COVID-19 in real time. *Lancet Infect Diseases* (2020) 20(5):533–4. doi: 10.1016/S1473-3099(20)30120-1
6. Wang D, Hu B, Hu C, Zhu F, Liu X, Zhang J, et al. Clinical Characteristics of 138 Hospitalized Patients With 2019 Novel Coronavirus-Infected Pneumonia in Wuhan, China. *Jama* (2020) 323(11):1061–9. doi: 10.1001/jama.2020.1585
7. Huang C, Wang Y, Li X, Ren L, Zhao J, Hu Y, et al. Clinical features of patients infected with 2019 novel coronavirus in Wuhan, China. *Lancet* (2020) 395(10223):497–506. doi: 10.1016/S0140-6736(20)30183-5
8. Wu C, Chen X, Cai Y, Xia J, Zhou X, Xu S, et al. Risk Factors Associated With Acute Respiratory Distress Syndrome and Death in Patients With Coronavirus Disease 2019 Pneumonia in Wuhan, China. *JAMA Internal Med* (2020) 180(7):934–43. doi: 10.1001/jamainternmed.2020.0994
9. Vardavas CI, Nikitara K. COVID-19 and smoking: A systematic review of the evidence. *Tobacco Induced Diseases* (2020) 18:20. doi: 10.18332/tid/119324
10. Zhou Y, Zhang Z, Tian J, Xiong S. Risk factors associated with disease progression in a cohort of patients infected with the 2019 novel coronavirus. *Ann Palliative Med* (2020) 9(2):428–36. doi: 10.21037/apm.2020.03.26
11. Zheng Y, Xu H, Yang M, Zeng Y, Chen H, Liu R, et al. Epidemiological characteristics and clinical features of 32 critical and 67 noncritical cases of COVID-19 in Chengdu. Journal of clinical virology : the official publication of the Pan American Society for. *Clin Virol* (2020) 127:104366. doi: 10.1016/j.jcv.2020.104366
12. Xu B, Fan CY, Wang AL, Zou YL, Yu YH, He C, et al. Suppressed T cell-mediated immunity in patients with COVID-19: A clinical retrospective study in Wuhan, China. *J Infect* (2020) 81(1):e51–60. doi: 10.2139/ssrn.3558005
13. Xia XY, Wu J, Liu HL, Xia H, Jia B, Huang WX. Epidemiological and initial clinical characteristics of patients with family aggregation of COVID-19. *J Clin Virol Off Publ Pan Am Soc Clin Virol* (2020) 127:104360. doi: 10.1016/j.jcv.2020.104360
14. Wang F, Nie J, Wang H, Zhao Q, Xiong Y, Deng L, et al. Characteristics of peripheral lymphocyte subset alteration in COVID-19 pneumonia. *J Infect Diseases* (2020) 221(11):1762–9. doi: 10.1093/infdis/jiaa150

15. Wan S, Yi Q, Fan S, Lv J, Zhang X, Guo L, et al. Relationships among lymphocyte subsets, cytokines, and the pulmonary inflammation index in coronavirus (COVID-19) infected patients. *Br J Haematol* (2020) 189 (3):428–37. doi: 10.1111/bjh.16659
16. Qin C, Zhou L, Hu Z, Zhang S, Yang S, Tao Y, et al. Dysregulation of immune response in patients with COVID-19 in Wuhan, China. *Clin Infect Dis an Off Publ Infect Dis Soc America* (2020) 71(15):762–8. doi: 10.1093/cid/ciaa248
17. Liu Z, Long W, Tu M, Chen S, Huang Y, Wang S, et al. Lymphocyte subset (CD4+, CD8+) counts reflect the severity of infection and predict the clinical outcomes in patients with COVID-19. *J Infect* (2020) 81(2):318–56. doi: 10.1016/j.jinf.2020.03.054
18. Liu Y, Liao W, Wan L, Xiang T, Zhang W. Correlation Between Relative Nasopharyngeal Virus RNA Load and Lymphocyte Count Disease Severity in Patients with COVID-19. *Viral Immunol* (2020). doi: 10.1089/vim.2020.0062
19. Giamarellos-Bourboulis EJ, Netea MG, Rovina N, Akinosoglou K, Antoniadou A, Antonakos N, et al. Complex Immune Dysregulation in COVID-19 Patients with Severe Respiratory Failure. *Cell Host Microbe* (2020) 27(6):992–1000 e3. doi: 10.1016/j.chom.2020.04.009
20. Ganji A, Farahani I, Khansarinejad B, Ghazavi A, Mosayebi G. Increased expression of CD8 marker on T-cells in COVID-19 patients. *Blood Cells Molecules Diseases* (2020) 83:102437. doi: 10.1016/j.bcmd.2020.102437
21. Chen G, Wu D, Guo W, Cao Y, Huang D, Wang H, et al. Clinical and immunological features of severe and moderate coronavirus disease 2019. *J Clin Invest* (2020) 130(5):2620–9. doi: 10.1101/2020.02.16.20023903
22. Wang M, Luo L, Bu H, Xia H. Case Report: One Case of Coronavirus Desease 2019(COVID-19) in Patient Co-nfected by HIV With a Low CD4+ T Cell Count. *Int J Infect Dis IJID Off Publ Int Soc Infect Diseases* (2020) 96:148–50. doi: 10.1016/j.ijid.2020.04.060
23. Wang F, Hou H, Luo Y, Tang G, Wu S, Huang M, et al. The laboratory tests and host immunity of COVID-19 patients with different severity of illness. *JCI Insight* (2020) 5(10). doi: 10.1172/jci.insight.137799
24. Sun D, Li H, Lu XX, Xiao H, Ren J, Zhang FR, et al. Clinical features of severe pediatric patients with coronavirus disease 2019 in Wuhan: a single center's observational study. *World J Pediatr WJP* (2020) 16(3):251–9. doi: 10.1007/s12519-020-00354-4
25. Ouyang Y, Yin J, Wang W, Shi H, Shi Y, Xu B, et al. Down-regulated gene expression spectrum and immune responses changed during the disease progression in COVID-19 patients. *Clin Infect Dis an Off Publ Infect Dis Soc America* (2020) 71(16):2052–60. doi: 10.1093/cid/ciaa462
26. Conti P, Younes A. Coronavirus COV-19/SARS-CoV-2 affects women less than men: clinical response to viral infection. *J Biol Regul Homeost Agents* (2020) 34(2):339–43. doi: 10.23812/Editorial-Conti-3
27. Chen J, Qi T, Liu L, Ling Y, Qian Z, Li T, et al. Clinical progression of patients with COVID-19 in Shanghai, China. *J Infect* (2020) 80(5):e1–6. doi: 10.1016/j.jinf.2020.03.004
28. Gao Y, Li T, Han M, Li X, Wu D, Xu Y, et al. Diagnostic utility of clinical laboratory data determinations for patients with the severe COVID-19. *J Med Virol* (2020) 92(7):791–6. doi: 10.1002/jmv.25770
29. Henry BM, de Oliveira MHS, Benoit S, Plebani M, Lippi G. Hematologic, biochemical and immune biomarker abnormalities associated with severe illness and mortality in coronavirus disease 2019 (COVID-19): a meta-analysis. *Clin Chem Lab Med* (2020) 58(7):1021–8. doi: 10.1515/cclm-2020-0369
30. Li T, Qiu Z, Zhang L, Han Y, He W, Liu Z, et al. Significant changes of peripheral T lymphocyte subsets in patients with severe acute respiratory syndrome. *J Infect Diseases* (2004) 189(4):648–51. doi: 10.1086/381535
31. Ghosn J, Taiwo B, Seedat S, Autran B, Katlama C. Hiv. *Lancet* (2018) 392 (10148):685–97. doi: 10.1016/S0140-6736(18)31311-4
32. Sereti I, Krebs SJ, Phanuphak N, Fletcher JL, Slike B, Pinyakorn S, et al. Persistent, Albeit Reduced, Chronic Inflammation in Persons Starting Antiretroviral Therapy in Acute HIV Infection. *Clin Infect Dis an Off Publ Infect Dis Soc America* (2017) 64(2):124–31. doi: 10.1093/cid/ciw683
33. Caby F, Guihot A, Lambert-Niclot S, Guiguet M, Boutolleau D, Agher R, et al. Determinants of a Low CD4/CD8 Ratio in HIV-1-Infected Individuals Despite Long-term Viral Suppression. *Clin Infect Dis an Off Publ Infect Dis Soc America* (2016) 62(10):1297–303. doi: 10.1093/cid/ciw076
34. Davis CW, Jackson KJL, McCausland MM, Darce J, Chang C, Linderman SL, et al. Influenza vaccine-induced human bone marrow plasma cells decline within a year after vaccination. *Science* (2020) 370(6513):237–41. doi: 10.1126/science.aaz8432
35. Kaech SM, Wherry EJ, Ahmed R. Effector and memory T-cell differentiation: implications for vaccine development. *Nat Rev Immunol* (2002) 2(4):251–62. doi: 10.1038/nri778
36. Papagno L, Spina CA, Marchant A, Salio M, Rufer N, Little S, et al. Immune activation and CD8+ T-cell differentiation towards senescence in HIV-1 infection. *PloS Biol* (2004) 2(2):E20. doi: 10.1371/journal.pbio.0020020
37. Trautmann L, Janbazian L, Chomont N, Said EA, Gimmig S, Bessette B, et al. Upregulation of PD-1 expression on HIV-specific CD8+ T cells leads to reversible immune dysfunction. *Nat Med* (2006) 12(10):1198–202. doi: 10.1038/nm1482
38. Moreno-Fernandez ME, Presicce P, Chougnet CA. Homeostasis and function of regulatory T cells in HIV/SIV infection. *J Virol* (2012) 86 (19):10262–9. doi: 10.1128/JVI.00993-12
39. Jenabian MA, Ancuta P, Gilmore N, Routy JP. Regulatory T cells in HIV infection: can immunotherapy regulate the regulator? *Clin Dev Immunol* (2012) 2012:908314. doi: 10.1155/2012/908314
40. Bixler SL, Mattapallil JJ. Loss and dysregulation of Th17 cells during HIV infection. *Clin Dev Immunol* (2013) 2013:852418. doi: 10.1155/2013/852418
41. McCune JM. The dynamics of CD4+ T-cell depletion in HIV disease. *Nature* (2001) 410(6831):974–9. doi: 10.1038/35073648
42. Lindqvist M, van Lunzen J, Soghoian DZ, Kuhl BD, Ranasinghe S, Kranias G, et al. Expansion of HIV-specific T follicular helper cells in chronic HIV infection. *J Clin Invest* (2012) 122(9):3271–80. doi: 10.1172/JCI64314
43. Phetsouphanh C, Xu Y, Zaunders J. CD4 T Cells Mediate Both Positive and Negative Regulation of the Immune Response to HIV Infection: Complex Role of T Follicular Helper Cells and Regulatory T Cells in Pathogenesis. *Front Immunol* (2014) 5:681. doi: 10.3389/fimmu.2014.00681
44. Pissani F, Streeck H. Emerging concepts on T follicular helper cell dynamics in HIV infection. *Trends Immunol* (2014) 35(6):278–86. doi: 10.1016/j.it.2014.02.010
45. Niessl J, Baxter AE, Morou A, Brunet-Ratnasingham E, Sannier G, Gendron-Lepage G, et al. Persistent expansion and Th1-like skewing of HIV-specific circulating T follicular helper cells during antiretroviral therapy. *EBioMedicine* (2020) 54:102727. doi: 10.1016/j.ebiom.2020.102727
46. Morou A, Brunet-Ratnasingham E, Dube M, Charlebois R, Mercier E, Darko S, et al. Altered differentiation is central to HIV-specific CD4(+) T cell dysfunction in progressive disease. *Nat Immunol* (2019) 20(8):1059–70. doi: 10.1038/s41590-019-0418-x
47. Mathew D, Giles JR, Baxter AE, Oldridge DA, Greenplate AR, Wu JE, et al. Deep immune profiling of COVID-19 patients reveals distinct immunotypes with therapeutic implications. *Science* (2020) 369(6508). doi: 10.1126/science.abc8511
48. Zheng HY, Zhang M, Yang CX, Zhang N, Wang XC, Yang XP, et al. Elevated exhaustion levels and reduced functional diversity of T cells in peripheral blood may predict severe progression in COVID-19 patients. *Cell Mol Immunol* (2020) 17(5):541–3. doi: 10.1038/s41423-020-0401-3
49. Zheng M, Gao Y, Wang G, Song G, Liu S, Sun D, et al. Functional exhaustion of antiviral lymphocytes in COVID-19 patients. *Cell Mol Immunol* (2020) 17 (5):533–5. doi: 10.1038/s41423-020-0402-2
50. He R, Lu Z, Zhang L, Fan T, Xiong R, Shen X, et al. The clinical course and its correlated immune status in COVID-19 pneumonia. *J Clin Virol Off Publ Pan Am Soc Clin Virol* (2020) 127:104361. doi: 10.1016/j.jcv.2020.104361
51. Rydyznski Moderbacher C, Ramirez SI, Dan JM, Grifoni A, Hastie KM, Weiskopf D, et al. Antigen-Specific Adaptive Immunity to SARS-CoV-2 in Acute COVID-19 and Associations with Age and Disease Severity. *Cell* (2020) 183(4):996–1012.e19. doi: 10.1016/j.cell.2020.09.038
52. Vingert B, Benati D, Lambotte O, de Truchis P, Slama L, Jeannin P, et al. HIV controllers maintain a population of highly efficient Th1 effector cells in contrast to patients treated in the long term. *J Virol* (2012) 86(19):10661–74. doi: 10.1128/JVI.00056-12
53. Macatangay BJ, Rinaldo CR. Preserving HIV-specific T cell responses: does timing of antiretroviral therapy help? *Curr Opin HIV AIDS* (2015) 10(1):55–60. doi: 10.1097/COH.0000000000000124

54. Ramendra R, Isnard S, Mehraj V, Chen J, Zhang Y, Finkelman M, et al. Circulating LPS and (1–>3)-beta-D-Glucan: A Folie a Deux Contributing to HIV-Associated Immune Activation. *Front Immunol* (2019) 10:465. doi: 10.3389/fimmu.2019.00465
55. Lu W, Feng Y, Jing F, Han Y, Lyu N, Liu F, et al. Association Between Gut Microbiota and CD4 Recovery in HIV-1 Infected Patients. *Front Microbiol* (2018) 9:1451. doi: 10.3389/fmicb.2018.01451
56. Geuking MB, Koller Y, Rupp S, McCoy KD. The interplay between the gut microbiota and the immune system. *Gut Microbes* (2014) 5(3):411–8. doi: 10.4161/gmic.29330
57. Penninger JM, Grant MB, Sung JJY. The Role of Angiotensin Converting Enzyme 2 (ACE2) in Modulating Gut Microbiota, Intestinal Inflammation, and Coronavirus Infection. *Gastroenterology* (2020). doi: 10.1053/j.gastro.2020.07.067
58. Planas D, Zhang Y, Monteiro P, Goulet JP, Gosselin A, Grandvaux N, et al. HIV-1 selectively targets gut-homing CCR6+CD4+ T cells via mTOR-dependent mechanisms. *JCI Insight* (2017) 2(15):e93230. doi: 10.1172/jci.insight.93230
59. Vujkovic-Cvijin I, Dunham RM, Iwai S, Maher MC, Albright RG, Broadhurst MJ, et al. Dysbiosis of the gut microbiota is associated with HIV disease progression and tryptophan catabolism. *Sci Trans Med* (2013) 5 (193):193ra91. doi: 10.1126/scitranslmed.3006438
60. Mutlu EA, Keshavarzian A, Losurdo J, Swanson G, Siewe B, Forsyth C, et al. A compositional look at the human gastrointestinal microbiome and immune activation parameters in HIV infected subjects. *PloS Pathog* (2014) 10(2):e1003829. doi: 10.1371/journal.ppat.1003829
61. Mehraj V, Ramendra R, Isnard S, Dupuy FP, Ponte R, Chen J, et al. Circulating (1–>3)-beta-D-glucan Is Associated With Immune Activation During Human Immunodeficiency Virus Infection. *Clin Infect Dis an Off Publ Infect Dis Soc America* (2020) 70(2):232–41. doi: 10.3389/fimmu.2019.00465
62. Brenchley JM, Price DA, Schacker TW, Asher TE, Silvestri G, Rao S, et al. Microbial translocation is a cause of systemic immune activation in chronic HIV infection. *Nat Med* (2006) 12(12):1365–71. doi: 10.1038/nm1511
63. Mehraj V, Ramendra R, Isnard S, Dupuy FP, Lebouche B, Costiniuk C, et al. CXCL13 as a Biomarker of Immune Activation During Early and Chronic HIV Infection. *Front Immunol* (2019) 10:289. doi: 10.3389/fimmu.2019.00289
64. Song Y, Liu P, Shi XL, Chu YL, Zhang J, Xia J, et al. SARS-CoV-2 induced diarrhoea as onset symptom in patient with COVID-19. *Gut* (2020) 69 (6):1143–4. doi: 10.1136/gutjnl-2020-320891
65. Lamers MM, Beumer J, van der Vaart J, Knoops K, Puschhof J, Breugem TI, et al. SARS-CoV-2 productively infects human gut enterocytes. *Science* (2020) 369(6499):50–4. doi: 10.1101/2020.04.25.060350
66. Hanada S, Pirzadeh M, Carver KY, Deng JC. Respiratory Viral Infection-Induced Microbiome Alterations and Secondary Bacterial Pneumonia. *Front Immunol* (2018) 9:2640. doi: 10.3389/fimmu.2018.02640
67. Ferreira C, Viana SD, Reis F. Gut Microbiota Dysbiosis-Immune Hyperresponse-Inflammation Triad in Coronavirus Disease 2019 (COVID-19): Impact of Pharmacological and Nutraceutical Approaches. *Microorganisms* (2020) 8(10):1514. doi: 10.3390/microorganisms8101514
68. Stacey AR, Norris PJ, Qin L, Haygreen EA, Taylor E, Heitman J, et al. Induction of a striking systemic cytokine cascade prior to peak viremia in acute human immunodeficiency virus type 1 infection, in contrast to more modest and delayed responses in acute hepatitis B and C virus infections. *J Virol* (2009) 83(8):3719–33. doi: 10.1128/JVI.01844-08
69. Muema DM, Akilimali NA, Ndumnego OC, Rasehlo SS, Durgiah R, Ojwach DBA, et al. Association between the cytokine storm, immune cell dynamics, and viral replicative capacity in hyperacute HIV infection. *BMC Med* (2020) 18(1):81. doi: 10.1186/s12916-020-01529-6
70. Kelesidis T, Tran TT, Stein JH, Brown TT, Moser C, Ribaudo HJ, et al. Changes in Inflammation and Immune Activation With Atazanavir-, Raltegravir-, Darunavir-Based Initial Antiviral Therapy: ACTG 5260s. *Clin Infect Dis an Off Publ Infect Dis Soc America* (2015) 61(4):651–60. doi: 10.1093/cid/civ327
71. Funderburg NT, Andrade A, Chan ES, Rosenkranz SL, Lu D, Clagett B, et al. Dynamics of immune reconstitution and activation markers in HIV+ treatment-naive patients treated with raltegravir, tenofovir disoproxil fumarate and emtricitabine. *PloS One* (2013) 8(12):e83514. doi: 10.1371/journal.pone.0083514
72. Nou E, Lo J, Grinspoon SK. Inflammation, immune activation, and cardiovascular disease in HIV. *Aids* (2016) 30(10):1495–509. doi: 10.1097/QAD.0000000000001109
73. Hadjadj J, Yatim N, Barnabei L, Corneau A, Boussier J, Smith N, et al. Impaired type I interferon activity and inflammatory responses in severe COVID-19 patients. *Science* (2020) 369(6504):718–24. doi: 10.1126/science.abc6027
74. Guaraldi G, Meschiari M, Cozzi-Lepri A, Milic J, Tonelli R, Menozzi M, et al. Tocilizumab in patients with severe COVID-19: a retrospective cohort study. *Lancet Rheumatol* (2020) 2(8):e474–84. doi: 10.1016/S2665-9913(20)30173-9
75. Lisco G, De Tullio A, Giagulli VA, Guastamacchia E, De Pergola G, Triggiani V. Hypothesized mechanisms explaining poor prognosis in type 2 diabetes patients with COVID-19: a review. *Endocrine* (2020) 70(3):441–53. doi: 10.1007/s12020-020-02444-9
76. Azar WS, Njeim R, Fares AH, Azar NS, Azar ST, El Sayed M, et al. COVID-19 and diabetes mellitus: how one pandemic worsens the other. *Rev Endocr Metab Disord* (2020) 21(4):451–63. doi: 10.1007/s11154-020-09573-6
77. Scheen AJ. Metformin and COVID-19: From cellular mechanisms to reduced mortality. *Diabetes Metab* (2020) 46(6):423–6. doi: 10.1016/j.diabet.2020.07.006
78. Singh AK, Singh R. Is metformin ahead in the race as a repurposed host-directed therapy for patients with diabetes and COVID-19? *Diabetes Res Clin Pract* (2020) 165:108268. doi: 10.1016/j.diabres.2020.108268
79. Chen Y, Yang D, Cheng B, Chen J, Peng A, Yang C, et al. Clinical Characteristics and Outcomes of Patients With Diabetes and COVID-19 in Association With Glucose-Lowering Medication. *Diabetes Care* (2020) 43 (7):1399–407. doi: 10.2337/dc20-0660
80. Ouyang J, Isnard S, Lin J, Fombuena B, Marette A, Routy B, et al. Metformin effect on gut microbiota: insights for HIV-related inflammation. *AIDS Res Ther* (2020) 17(1):10. doi: 10.1186/s12981-020-00267-2
81. Isnard S, Lin J, Fombuena B, Ouyang J, Varin TV, Richard C, et al. Repurposing metformin in non-diabetic people living with HIV: Influence on weight and gut microbiota. *Open Forum Infect Diseases* (2020) 7(9): ofaa338. doi: 10.1093/ofid/ofaa338
82. Moyo D, Tanthuma G, Cary MS, Mushisha O, Kwadiba G, Chikuse F, et al. Cohort study of diabetes in HIV-infected adult patients: evaluating the effect of diabetes mellitus on immune reconstitution. *Diabetes Res Clin Pract* (2014) 103(3):e34–6. doi: 10.1016/j.diabres.2013.12.042
83. Appay V, Sauce D. Immune activation and inflammation in HIV-1 infection: causes and consequences. *J Pathol* (2008) 214(2):231–41. doi: 10.1002/path.2276
84. Kaplan RC, Sinclair E, Landay AL, Lurain N, Sharrett AR, Gange SJ, et al. T cell activation and senescence predict subclinical carotid artery disease in HIV-infected women. *J Infect Diseases* (2011) 203(4):452–63. doi: 10.1093/infdis/jiq071
85. Triant VA, Brown TT, Lee H, Grinspoon SK. Fracture prevalence among human immunodeficiency virus (HIV)-infected versus non-HIV-infected patients in a large U.S. healthcare system. *J Clin Endocrinol Metab* (2008) 93 (9):3499–504. doi: 10.1210/jc.2008-0828
86. Deeken JF, Tjen ALA, Rudek MA, Okuliar C, Young M, Little RF, et al. The rising challenge of non-AIDS-defining cancers in HIV-infected patients. *Clin Infect Dis an Off Publ Infect Dis Soc America* (2012) 55(9):1228–35. doi: 10.1093/cid/cis613
87. Tian S, Xiong Y, Liu H, Niu L, Guo J, Liao M, et al. Pathological study of the 2019 novel coronavirus disease (COVID-19) through postmortem core biopsies. *Modern Pathol an Off J U States Can Acad Pathol Inc* (2020) 33 (6):1007–14. doi: 10.20944/preprints202003.0311.v1
88. Xu Z, Shi L, Wang Y, Zhang J, Huang L, Zhang C, et al. Pathological findings of COVID-19 associated with acute respiratory distress syndrome. *Lancet Respir Med* (2020) 8(4):420–2. doi: 10.1016/S2213-2600(20)30076-X
89. Shi S, Qin M, Shen B, Cai Y, Liu T, Yang F, et al. Association of Cardiac Injury With Mortality in Hospitalized Patients With COVID-19 in Wuhan, China. *JAMA Cardiol* (2020) 5(7):802–10. doi: 10.1001/jamacardio.2020.0950
90. Wu P, Duan F, Luo C, Liu Q, Qu X, Liang L, et al. Characteristics of Ocular Findings of Patients With Coronavirus Disease 2019 (COVID-19) in Hubei

Province, China. *JAMA Ophthalmol* (2020) 138(5):575–8. doi: 10.1001/jamaophthalmol.2020.1291
91. Zhang C, Shi L, Wang FS. Liver injury in COVID-19: management and challenges. *Lancet Gastroenterol Hepatol* (2020) 5(5):428–30. doi: 10.1016/S2468-1253(20)30057-1
92. Mao L, Jin H, Wang M, Hu Y, Chen S, He Q, et al. Neurologic Manifestations of Hospitalized Patients With Coronavirus Disease 2019 in Wuhan, China. *JAMA Neurol* (2020) 77(6):683–90. doi: 10.1001/jamaneurol.2020.1127
93. Haase AT. Population biology of HIV-1 infection: viral and CD4+ T cell demographics and dynamics in lymphatic tissues. *Annu Rev Immunol* (1999) 17:625–56. doi: 10.1146/annurev.immunol.17.1.625
94. Ho DD, Neumann AU, Perelson AS, Chen W, Leonard JM, Markowitz M. Rapid turnover of plasma virions and CD4 lymphocytes in HIV-1 infection. *Nature* (1995) 373(6510):123–6. doi: 10.1038/373123a0
95. Deeks SG, Kitchen CM, Liu L, Guo H, Gascon R, Narvaez AB, et al. Immune activation set point during early HIV infection predicts subsequent CD4+ T-cell changes independent of viral load. *Blood* (2004) 104(4):942–7. doi: 10.1182/blood-2003-09-3333
96. Wei X, Ghosh SK, Taylor ME, Johnson VA, Emini EA, Deutsch P, et al. Viral dynamics in human immunodeficiency virus type 1 infection. *Nature* (1995) 373(6510):117–22. doi: 10.1038/373117a0
97. Hazenberg MD, Hamann D, Schuitemaker H, Miedema F. T cell depletion in HIV-1 infection: how CD4+ T cells go out of stock. *Nat Immunol* (2000) 1 (4):285–9. doi: 10.1038/79724
98. Cooper A, Garcia M, Petrovas C, Yamamoto T, Koup RA, Nabel GJ. HIV-1 causes CD4 cell death through DNA-dependent protein kinase during viral integration. *Nature* (2013) 498(7454):376–9. doi: 10.1038/nature12274
99. Fleury S, Rizzardi GP, Chapuis A, Tambussi G, Knabenhans C, Simeoni E, et al. Long-term kinetics of T cell production in HIV-infected subjects treated with highly active antiretroviral therapy. *Proc Natl Acad Sci U States America* (2000) 97(10):5393–8. doi: 10.1073/pnas.97.10.5393
100. Pothlichet J, Rose T, Bugault F, Jeammet L, Meola A, Haouz A, et al. PLA2G1B is involved in CD4 anergy and CD4 lymphopenia in HIV-infected patients. *J Clin Invest* (2020) 130(6):2872–87. doi: 10.1172/JCI131842
101. Walls AC, Park YJ, Tortorici MA, Wall A, McGuire AT, Veesler D. Structure, Function, and Antigenicity of the SARS-CoV-2 Spike Glycoprotein. *Cell* (2020) 181(2):281–92 e6. doi: 10.1016/j.cell.2020.02.058
102. Hoffmann M, Kleine-Weber H, Schroeder S, Kruger N, Herrler T, Erichsen S, et al. SARS-CoV-2 Cell Entry Depends on ACE2 and TMPRSS2 and Is Blocked by a Clinically Proven Protease Inhibitor. *Cell* (2020) 181(2):271–80 e8. doi: 10.1016/j.cell.2020.02.052
103. Bertram S, Heurich A, Lavender H, Gierer S, Danisch S, Perin P, et al. Influenza and SARS-coronavirus activating proteases TMPRSS2 and HAT are expressed at multiple sites in human respiratory and gastrointestinal tracts. *PloS One* (2012) 7(4):e35876. doi: 10.1371/journal.pone.0035876
104. Gu J, Gong E, Zhang B, Zheng J, Gao Z, Zhong Y, et al. Multiple organ infection and the pathogenesis of SARS. *J Exp Med* (2005) 202(3):415–24. doi: 10.1084/jem.20050828
105. Xu X, Gao X. Immunological responses against SARS-coronavirus infection in humans. *Cell Mol Immunol* (2004) 1(2):119–22.
106. Yue Y, Nabar NR, Shi CS, Kamenyeva O, Xiao X, Hwang IY, et al. SARS-Coronavirus Open Reading Frame-3a drives multimodal necrotic cell death. *Cell Death Disease* (2018) 9(9):904. doi: 10.1038/s41419-018-0917-y
107. Tan YX, Tan TH, Lee MJ, Tham PY, Gunalan V, Druce J, et al. Induction of apoptosis by the severe acute respiratory syndrome coronavirus 7a protein is dependent on its interaction with the Bcl-XL protein. *J Virol* (2007) 81 (12):6346–55. doi: 10.1128/JVI.00090-07
108. Shi X, Gong E, Gao D, Zhang B, Zheng J, Gao Z, et al. Severe acute respiratory syndrome associated coronavirus is detected in intestinal tissues of fatal cases. *Am J Gastroenterol* (2005) 100(1):169–76. doi: 10.1111/j.1572-0241.2005.40377.x
109. Yates A, Stark J, Klein N, Antia R, Callard R. Understanding the slow depletion of memory CD4+ T cells in HIV infection. *PloS Med* (2007) 4(5): e177. doi: 10.1371/journal.pmed.0040177
110. Swingler S, Mann A, Jacque J, Brichacek B, Sasseville VG, Williams K, et al. HIV-1 Nef mediates lymphocyte chemotaxis and activation by infected macrophages. *Nat Med* (1999) 5(9):997–103. doi: 10.1038/12433
111. Mehta AK, Gracias DT, Croft M. TNF activity and T cells. *Cytokine* (2018) 101:14–8. doi: 10.1016/j.cyto.2016.08.003
112. Brooks DG, Trifilo MJ, Edelmann KH, Teyton L, McGavern DB, Oldstone MB. Interleukin-10 determines viral clearance or persistence in vivo. *Nat Med* (2006) 12(11):1301–9. doi: 10.1038/nm1492
113. Kamphuis E, Junt T, Waibler Z, Forster R, Kalinke U. Type I interferons directly regulate lymphocyte recirculation and cause transient blood lymphopenia. *Blood* (2006) 108(10):3253–61. doi: 10.1182/blood-2006-06-027599
114. Ponte R, Rancez M, Figueiredo-Morgado S, Dutrieux J, Fabre-Mersseman V, Charmeteau-de-Muylder B, et al. Acute Simian Immunodeficiency Virus Infection Triggers Early and Transient Interleukin-7 Production in the Gut, Leading to Enhanced Local Chemokine Expression and Intestinal Immune Cell Homing. *Front Immunol* (2017) 8:588. doi: 10.3389/fimmu.2017.00588
115. Janossy G, Pinching AJ, Bofill M, Weber J, McLaughlin JE, Ornstein M, et al. An immunohistological approach to persistent lymphadenopathy and its relevance to AIDS. *Clin Exp Immunol* (1985) 59(2):257–66.
116. Wang L, Robb CW, Cloyd MW. HIV induces homing of resting T lymphocytes to lymph nodes. *Virology* (1997) 228(2):141–52. doi: 10.1006/viro.1996.8397
117. Bucy RP, Hockett RD, Derdeyn CA, Saag MS, Squires K, Sillers M, et al. Initial increase in blood CD4(+) lymphocytes after HIV antiretroviral therapy reflects redistribution from lymphoid tissues. *J Clin Invest* (1999) 103(10):1391–8. doi: 10.1172/JCI5863
118. Tay MZ, Poh CM, Renia L, MacAry PA, Ng LFP. The trinity of COVID-19: immunity, inflammation and intervention. *Nat Rev Immunol* (2020) 20 (6):363–74. doi: 10.1038/s41577-020-0311-8
119. Nishimoto N, Sasai M, Shima Y, Nakagawa M, Matsumoto T, Shirai T, et al. Improvement in Castleman's disease by humanized anti-interleukin-6 receptor antibody therapy. *Blood* (2000) 95(1):56–61. doi: 10.1182/blood.V95.1.56.001k13_56_61
120. Blanco JL, Ambrosioni J, Garcia F, Martinez E, Soriano A, Mallolas J, et al. COVID-19 in patients with HIV: clinical case series. *Lancet HIV* (2020) 7(5): e314–e6. doi: 10.1016/S2352-3018(20)30111-9
121. Zhao J, Liao X, Wang H, Wei L, Xing M, Liu L, et al. Early virus clearance and delayed antibody response in a case of COVID-19 with a history of co-infection with HIV-1 and HCV. *Clin Infect Dis an Off Publ Infect Dis Soc America* (2020) 71(16):2233–5. doi: 10.1093/cid/ciaa408
122. Zhu F, Cao Y, Xu S, Zhou M. Co-infection of SARS-CoV-2 and HIV in a patient in Wuhan city, China. *J Med Virol* (2020) 92(6):529–30. doi: 10.1002/jmv.25732
123. Harter G, Spinner CD, Roider J, Bickel M, Krznaric I, Grunwald S, et al. COVID-19 in people living with human immunodeficiency virus: a case series of 33 patients. *Infection* (2020) 48(5):681–6. doi: 10.1007/s15010-020-01438-z
124. Guo W, Ming F, Dong Y, Zhang Q, Zhang X, Mo P, et al. A Survey for COVID-19 Among HIV/AIDS Patients in Two Districts of Wuhan, China. *Lancet* (2020). Preprint research paper. doi: 10.2139/ssrn.3550029
125. Laurence J. Why Aren't People Living with HIV at Higher Risk for Developing Severe Coronavirus Disease 2019 (COVID-19)? *AIDS patient Care STDs* (2020) 34(6):247–8. doi: 10.1089/apc.2020.29005.com
126. Beck BR, Shin B, Choi Y, Park S, Kang K. Predicting commercially available antiviral drugs that may act on the novel coronavirus (SARS-CoV-2) through a drug-target interaction deep learning model. *Comput Struct Biotechnol J* (2020) 18:784–90. doi: 10.1016/j.csbj.2020.03.025
127. Cao B, Wang Y, Wen D, Liu W, Wang J, Fan G, et al. A Trial of Lopinavir-Ritonavir in Adults Hospitalized with Severe Covid-19. *New Engl J Med* (2020) 382(19):1787–99. doi: 10.1056/NEJMoa2001282
128. Beigel JH, Tomashek KM, Dodd LE, Mehta AK, Zingman BS, Kalil AC, et al. Remdesivir for the Treatment of Covid-19 - Final Report. *New Engl J Med* (2020) 383(19):1813–26. doi: 10.1056/NEJMoa2007764
129. Del Amo J, Polo R, Moreno S, Diaz A, Martinez E, Arribas JR, et al. Incidence and Severity of COVID-19 in HIV-Positive Persons Receiving Antiretroviral Therapy : A Cohort Study. *Ann Internal Med* (2020) 173(7):536–41. doi: 10.7326/M20-3689
130. Puronen CE, Thompson WL, Imamichi H, Beq S, Hodge JN, Rehm C, et al. Decreased interleukin 7 responsiveness of T lymphocytes in patients with idiopathic CD4 lymphopenia. *J Infect Diseases* (2012) 205(9):1382–90. doi: 10.1093/infdis/jis219

131. Thiebaut R, Jarne A, Routy JP, Sereti I, Fischl M, Ive P, et al. Repeated Cycles of Recombinant Human Interleukin 7 in HIV-Infected Patients With Low CD4 T-Cell Reconstitution on Antiretroviral Therapy: Results of 2 Phase II Multicenter Studies. *Clin Infect Dis an Off Publ Infect Dis Soc America* (2016) 62(9):1178–85. doi: 10.1093/cid/ciw065
132. Levy Y, Sereti I, Tambussi G, Routy JP, Lelievre JD, Delfraissy JF, et al. Effects of recombinant human interleukin 7 on T-cell recovery and thymic output in HIV-infected patients receiving antiretroviral therapy: results of a phase I/IIa randomized, placebo-controlled, multicenter study. *Clin Infect Dis an Off Publ Infect Dis Soc America* (2012) 55(2):291–300. doi: 10.1093/cid/cis383
133. Ross SH, Cantrell DA. Signaling and Function of Interleukin-2 in T Lymphocytes. *Annu Rev Immunol* (2018) 36:411–33. doi: 10.1146/annurev-immunol-042617-053352
134. Group I-ES, Committee SS, Abrams D, Levy Y, Losso MH, Babiker A, et al. Interleukin-2 therapy in patients with HIV infection. *New Engl J Med* (2009) 361(16):1548–59. doi: 10.1056/NEJMoa0903175
135. De Paoli P. Immunological effects of interleukin-2 therapy in human immunodeficiency virus-positive subjects. *Clin Diagn Lab Immunol* (2001) 8(4):671–7. doi: 10.1128/CDLI.8.4.671-677.2001

Conflict of Interest: The authors declare that the research was conducted in the absence of any commercial or financial relationships that could be construed as a potential conflict of interest.

frontiers in Immunology

ORIGINAL RESEARCH
published: 12 March 2021
doi: 10.3389/fimmu.2021.601298

Long Non-coding RNA GAS5 Regulates T Cell Functions via miR21-Mediated Signaling in People Living With HIV

Lam Ngoc Thao Nguyen[1,2], *Lam Nhat Nguyen*[1,2], *Juan Zhao*[1,2], *Madison Schank*[1,2], *Xindi Dang*[1,2], *Dechao Cao*[1,2], *Sushant Khanal*[1,2], *Bal Krishna Chand Thakuri*[1,2], *Zeyuan Lu*[1,2], *Jinyu Zhang*[1,2], *Zhengke Li*[1,2], *Zheng D. Morrison*[1,2], *Xiao Y. Wu*[1,2], *Mohamed El Gazzar*[1,2], *Shunbin Ning*[1,2], *Ling Wang*[1,2], *Jonathan P. Moorman*[1,2,3] *and Zhi Q. Yao*[1,2,3]*

[1] Center of Excellence in Inflammation, Infectious Disease and Immunity, James H. Quillen College of Medicine, East Tennessee State University, Johnson City, TN, United States, [2] Division of Infectious, Inflammatory and Immunologic Diseases, Department of Internal Medicine, Quillen College of Medicine, East Tennessee State University (ETSU), Johnson City, TN, United States, [3] Hepatitis C Virus/Hepatitis B Virus/Human Immunodeficiency Virus (HCV/HBV/HIV) Program, Department of Veterans Affairs, James H. Quillen VA Medical Center, Johnson City, TN, United States

OPEN ACCESS

Edited by:
Constantinos Petrovas, Centre Hospitalier Universitaire Vaudois (CHUV), Switzerland

Reviewed by:
Vincenzo Barnaba, Sapienza University of Rome, Italy
Giulia Fabozzi, National Institute of Allergy and Infectious Diseases (NIH), United States

***Correspondence:**
Zhi Q. Yao
yao@etsu.edu

Specialty section:
This article was submitted to T Cell Biology, a section of the journal Frontiers in Immunology

Received: *31 August 2020*
Accepted: *18 February 2021*
Published: *12 March 2021*

Citation:
Nguyen LNT, Nguyen LN, Zhao J, Schank M, Dang X, Cao D, Khanal S, Chand Thakuri BK, Lu Z, Zhang J, Li Z, Morrison ZD, Wu XY, El Gazzar M, Ning S, Wang L, Moorman JP and Yao ZQ (2021) Long Non-coding RNA GAS5 Regulates T Cell Functions via miR21-Mediated Signaling in People Living With HIV. Front. Immunol. 12:601298. doi: 10.3389/fimmu.2021.601298

T cells are critical for the control of viral infections and T cell responses are regulated by a dynamic network of non-coding RNAs, including microRNAs (miR) and long non-coding RNAs (lncRNA). Here we show that an activation-induced decline of lncRNA growth arrest-specific transcript 5 (GAS5) activates DNA damage response (DDR), and regulates cellular functions and apoptosis in CD4 T cells derived from people living with HIV (PLHIV) via upregulation of miR-21. Notably, GAS5-miR21-mediated DDR and T cell dysfunction are observed in PLHIV on antiretroviral therapy (ART), who often exhibit immune activation due to low-grade inflammation despite robust virologic control. We found that GAS5 negatively regulates miR-21 expression, which in turn controls critical signaling pathways involved in DNA damage and cellular response. The sustained stimulation of T cells decreased GAS5, increased miR-21 and, as a result, caused dysfunction and apoptosis in CD4 T cells. Importantly, this inflammation-driven T cell over-activation and aberrant apoptosis in ART-controlled PLHIV and healthy subjects (HS) could be reversed by antagonizing the GAS5-miR-21 axis. Also, mutation of the miR-21 binding site on exon 4 of GAS5 gene to generate a GAS5 mutant abolished its ability to regulate miR-21 expression as well as T cell activation and apoptosis markers compared to the wild-type GAS5 transcript. Our data suggest that GAS5 regulates TCR-mediated activation and apoptosis in CD4 T cells during HIV infection through miR-21-mediated signaling. However, GAS5 effects on T cell exhaustion during HIV infection may be mediated by a mechanism beyond the GAS5-miR-21-mediated signaling. These results indicate that targeting the GAS5-miR-21 axis may improve activity and longevity of CD4 T cells in ART-treated PLHIV. This approach may also be useful for targeting other infectious or inflammatory diseases associated with T cell over-activation, exhaustion, and premature immune aging.

Keywords: Gas5, HIV, lncRNA, miR-21, T cell dysregulation

INTRODUCTION

HIV/AIDS pandemic affects 1.1 million individuals in the United States and more than 36 million people worldwide (1, 2). The hallmark of HIV/AIDS is a gradual depletion of CD4 T cells, with progressive decline of host immunity, leading to an increased susceptibility to opportunistic infections, malignancies, and ultimately death (3, 4). While combined antiretroviral therapy (ART) can effectively control viral replication in the majority of people living with HIV (PLHIV), ART does not always result in complete recovery of CD4 T cells (5, 6). Even with satisfactory salvage of CD4 T cell numbers, ART-controlled PLHIV often exhibit immunologic scarring and residual inflammation, inducing an inflammaging phenotype that is characterized by shortened telomeres, poor proliferative capacity, and blunted vaccine responses (7–10). The inflammaging imposed by latent HIV infection exposes the immune system to unique challenges that lead to profound T cell exhaustion and senescence, a major driver of increased infections, cancers, cardiovascular diseases, and neurodegeneration, and similar to what is observed in the elderly (11, 12). Therefore, it is fundamentally important to elucidate the mechanisms underlying T cell aging in PLHIV with ART-controlled latent infection.

In addition to protein-coding genes, the human genome expresses different classes of non-coding RNAs, including microRNAs (miRNA) and long non-coding RNAs (lncRNA) (13–16). Overall, protein-coding genes account for only 2% of the human genome, whereas the vast majority of gene transcripts are non-coding RNAs. MiRNAs (∼20 nucleotides) and lncRNAs (>200 nucleotides) are RNA transcripts that do not encode proteins but possess regulatory functions. Using RNA sequencing and annotation of the GENECODE project (17), recent studies revealed over 30,000 lncRNAs (listed at www.noncode.org and www.lncipedia.org), and this number continues to grow, but the functions of these lncRNAs remain largely elusive.

The growth arrest-specific transcript 5 (GAS5) is a lncRNA originally isolated from murine NIH 3T3 cells, and later identified in human cells (NR_002578 and AF141346) (18). GAS5 is induced under stress conditions such as serum starvation and cell-cell contact inhibition and has been reported to possess tumor-suppressive functions in humans (19–24). GAS5 has also been shown to inhibit tumor growth by regulating miR-21 (19, 24), a miRNA that regulates inflammation and immune response (25–28). Of note, the expressions and functions of lncRNAs, as well as miRNAs, are species-, cell-, and disease-specific. In addition to suppressing cancer development and metastasis in humans, GAS5 has been shown to control HIV replication through interaction with miR-873 (29), but its role in regulating T cell functions in ART-controlled HIV infection remains unclear.

We have previously shown that PLHIV exhibit CD4 T cell exhaustion, senescence, apoptosis, and dysfunction, despite ostensibly complete control of viral replication by ART (30–36). How T cell functions are dysregulated in ART-controlled PLHIV is incompletely understood. In this study, we observed differential regulation of GAS5 and miR-21 expressions in CD4 T cells derived from ART-controlled PLHIV and age-matched healthy subjects (HS). Notably, GAS5 controlled miR-21 expression and regulated signaling molecules involved in DNA damage and cellular responses following T cell receptor (TCR) stimulation. Importantly, interrupting this GAS5-miR-21 axis during TCR activation reversed T cell dysfunction and rescued apoptosis in CD4 T cells derived from ART-treated PLHIV. Our data suggest that GAS5 regulates TCR-induced activation and apoptosis of CD4 T cells during HIV infection through a miR-21-mediated signaling. However, T cell exhaustion during HIV infection may be mediated by a mechanism beyond the GAS5-miR-21-mediated signaling. This study provides a novel strategy to improve immunotherapies and vaccine responses in the setting of latent HIV infection.

MATERIALS AND METHODS

Subjects

The study protocol was approved by the institutional review board (IRB) of East Tennessee State University and James H. Quillen VA Medical Center (ETSU/VA IRB; Johnson City, Tennessee). All participants were adults and signed informed consent forms. Participants included 142 people living with HIV (PLHIV) and 58 age-matched HS. All PLHIV participants were on ART, virologically suppressed as evidenced by undetectable (<20 copies/ml) viral RNAs. Blood from HS was supplied by Physicians Plasma Alliance (PPA, Gray, TN) and was negative for HBV, HCV, and HIV infections. The demographic information of all participants is listed in **Table 1**.

Cell Isolation and Culture

PBMCs were isolated from whole blood of HS and PLHIV using Ficoll-Paque solution (GE Healthcare; Piscataway, NJ) and density gradient centrifugation separation. CD4 T cells were purified from PBMCs using CD4 T cell negative selection kit (Miltenyi Biotec; Auburn, CA). The cells were cultured for 24 h in RPMI-1640 media (Fisher Scientific; Pittsburgh, PA) supplemented with 10% heat-inactivated fetal bovine serum (Atlanta Biologicals; Flowery Branch, GA), 100 IU/ml penicillin, and 2 mM L-glutamine (Thermo Scientific; Logan, Utah) at 37°C and 5% CO_2 atmosphere. For TCR stimulation, CD4 T cells were cultured in media containing Dynabeads coated with human T-activator CD3/CD28 (Fisher Scientific).

TABLE 1 | Demographic information of the study participants.

	Total	Gender male/female	Age mean (SD/range)	CD4 count mean (SD/range)
HS	58	46/12	43 (9/34)	N/A
PLHIV	142	122/20	48 (9/47)	987 (389/2,245)

This table consists of demographic information of the participants in this study, including the total number of subjects, gender (M/F), age (SD/Range), and CD4 number (SD/Range) of each group, either HS or PLHIV.

For knockdown and overexpression experiments, the cells were stimulated with soluble CD3/CD28 (BD biosciences; San Jose, CA) and recombinant human IL-2 (PeproTech; Rocky Hill, NJ) for 2 days prior to lentivirus infections and for another 3 days post transfection. For anti-PD-1 treatment and IL-2 administration experiment, CD4 T cells isolated from HS were cultured for 24 h in the presence of Dynabeads coated with human T cell activator anti-CD3/CD28, anti-PD-1 (nivolumab, 20 μg/ml; Selleckchem, TX), human IgG4 isotype control antibody antibodies (Biolegend), or IL-2 (100 units/ml; Biolegend).

Lentiviral-Mediated shRNA Knockdown or Overexpression

The following constructs were used in this study: GreenPuro Scramble Hairpin Control (System Biosciences; Palo Alto, CA), miRZip-21 anti-miR-21 (System Biosciences), and control vector and GAS5 constructs as described previously (24). Gas5-mutant construct was generated using Q5 Site-Directed Mutagenesis Kit (New England BioLab, E0554S) according to manufacturer's protocol. Briefly, GAS5 WT vector was used as the template for site-directed mutagenesis PCR with primers (sequences shown in **Table 1**) that target exon 4 of GAS5 WT transcript, abolishing the miR-21 binding site on GAS5. The primers were generated using NEBaseChanger site (New England Biolab). DNA plasmid was transfected into Stbl3™ chemically competent *E. Coli* (Introvigen). The transformed cells were cultured on agar plates, positive colonies were selected for plasmid DNA isolation. The plasmid DNA was then subjected for DNA sequencing to confirm the mutation.

The control, GAS5-WT, and GAS5-mutant vectors were transfected into HEK 293T cells (ATCC) together with psPAX2 and PMD2G vectors to generate the respective lentiviruses using the FuGENE® HD Transduction Reagent (System Bioscience). HEK 293T cells were cultured in DMEM media (Fisher Scientific) containing 10% fetal bovine serum, 100 IU/ml penicillin, and 2 mM L-glutamine at 37°C and 5% CO_2 atmosphere. The supernatants were collected and the virus particles were concentrated using PEG-it Virus Precipitation Solution (System Bioscience) according to the manufacturer's instructions.

Isolated CD4 T cells from HS or PLHIV were stimulated with soluble anti-CD3 and anti-CD28 for 2 days before lentiviral infection. The transdux max (System Bioscience) reagent was used followed the manufacturer protocol to enhance the infection efficiency. CD4 T cells were harvested 3 days post infection and subjected for further experiments.

RNA Extraction, cDNA Synthesis, and Real-Time RT-PCR

Total RNA was extracted from ∼1 × 10^6 CD4 T cells isolated from each subject using the RNeasy Mini Kit (Qiagen; Germantown, MD). Approximately 100 ng of RNA was reverse transcribed using the High Capacity cDNA Reverse Transcription Kit (Applied Biosystems; Foster City, CA). For miRNA measurements, miRNA was extracted using the miRNeasy Micro kit (Qiagen) and cDNA was synthesized using the TaqMan Advanced miRNA cDNA Synthesis Kit (Qiagen) following the manufacturer's instructions.

Quantitative real-time PCR was performed using iTag Universal SYBR Green Supermix (Bio-Rad; Hercules, CA). Gene expression was determined using the $2^{-\Delta\Delta ct}$ method and normalized to GAPDH (for mRNA and lncRNA expressions) and miR-191-5p (for miRNA expression), and the results are presented as relative fold changes. The PCR primers are listed in **Table 2**.

Flow Cytometry

Sample preparation and surface and intracellular marker staining were performed using the following antibodies, according to the manufacturer's protocols: anti-human CD279 (PD-1)/PE [NAT105] (35), H2A.X Phospho (Ser139)/PE [2F3], CD69/FITC [FN50], IL-2/PE [MQ1-17H12], IFN-γ /PE [4S.B3], TNF-α /APC [MAb11], CD366 (Tim-3)/APC [F38-2E2], Phospho-AKT/ APC (Ser473) [SDRNR], MAPK/Alexa Fluor 488 [pT180/pY182], Bcl-2/Alexa Fluor 647 [C-2], and TGF-β1/PE [TW4-2F8] (all from Biolegend; San Diego, CA). The cells were stimulated with PMA/ionomycin (Sigma-Aldrich; St. Louis, MO) for 4–6 h before the detection of IL-2, IFN-γ, TNF-α, and TGF-β1. For apoptosis analysis, cells were stained with Annexin V and 7-AAD from the PE Annexin V apoptosis detection kit (BD

TABLE 2 | Primer sequences used for RT-qPCR experiments in the paper.

Primer sequences	Supplier	Catalog number
Gapdh forward, GGATTTGGTCGTATTGGG	Thermo Fisher	N/A
Gapdh reverse, GGAAGATGGTGATGGGATT	Thermo Fisher	N/A
Gas5 forward, GGACCGGGAGATAGGAGTG	Thermo Fisher	N/A
Gas5 reverse, CACGGACTCCAGGTGATGAG	Thermo Fisher	N/A
Gas5-mutant forward, ACAGATCAAGGTGAAGTTGAAATGGTGGAGTC	Thermo Fisher	N/A
Gas5-mutant reverse, AATTCATTTGTGTGCCAATGGCTTGAGTT	Thermo Fisher	N/A
hsa-miR-21-5p	Fisher Scientific	477975_A26676
hsa-miR-191-5p	Fisher Scientific	477952_A26676

This table provides the primer sequences, the supplier information and catalog number of each primer used for RT-qPCR experiments in this study.

Biosciences; San Jose, CA). Active caspase-3 was detected using a cleaved caspase-3 staining kit (FITC or Red) following the manufacturer's instructions (Abcam; Cambridge, MA). For cell cycle progression, TCR-stimulated CD4 T cells from PLHIV and HS were harvested at days 1, 3, and 5 and stained with Propidium Iodide (PI) using PI flow cytometry kit (Abcam) following the manufacturer's protocol. Samples were acquired on a BD Accuri^{TM} C6 flow cytometer and analyzed using Flowjo software.

Western Blot

Western Blot was performed as described previously (33). The primary antibodies used were rabbit PARP-1 Ab (clone 46D11; Cat #9532), rabbit phospho-histone H2A.X Ab (Ser139) (clone 20E3; Cat #9718), rabbit phospho-S6 ribosomal protein (Ser235/236) Ab (clone D57.2.2E; Cat #4858), rabbit phospho-Akt (Ser473) XP Ab (clone D9E; Cat #4060), mouse AGO2 Ab (clone 2E12-1C9; Cat #57113), and rabbit GAPDH XP mAb (clone D16H11; Cat #5174) (all from Cell Signaling Technology; Danvers, MA). After washing, the blots were incubated with appropriate horseradish peroxide-conjugated secondary antibodies (Cell Signaling), and protein bands were developed with the Amersham ECL Prime Western Blotting Detection Reagent (GE Healthcare). The chemiluminescent signal was detected and quantified by Chemi Doc^{TM} MP Imaging System (Bio-Rad) and normalized to GAPDH.

Statistical Analysis

The data were analyzed using Prism 7 software and are presented as mean ± SEM or median with interquartile range. Statistical outliers were removed by the ROUT method ($Q = 1\%$). Based on whether the values passed the D'Agostino-Pearson normality or Kolmogorov-Smirnov test, either paired Student's *t*-test or Wilcoxon matched-pairs signed-rank test was used for the analysis involving knockdown/overexpression experiments. Likewise, independent unpaired Student's *t*-test with Welch's correction or Mann Whitney *U*-test for non-paired experiments. Correlations were analyzed by either Pearson's or Spearman's correlation, depending on the data normal distribution test. $P < 0.05$ and $P < 0.001$ were considered statistically significant and very significant, respectively.

RESULTS

Differential Regulation of GAS5 and miR-21 Expressions in CD4 T Cells Derived From PLHIV and HS

While thousands of lncRNAs have been identified in human cells, only a small number have been experimentally validated and shown to be associated with human diseases, particularly with infectious diseases. Among these lncRNAs, GAS5 has been shown to simultaneously target multiple genes involved in cell growth and apoptosis. As a first step to elucidate the role of GAS5 in T cell regulation during HIV infection, we measured its expression in CD4 T cells isolated from ART-controlled PLHIV and age-matched HS. Because human GAS5 encodes several splicing isoforms (GAS5a and GAS5b, in addition to 5 GAS5 EST sequences) (37), we synthesized a primer set within exon 12, which can amplify all known isoforms of GAS5, and measured expression levels by real-time RT-PCR. As shown in **Figure 1A**, GAS5 transcripts were significantly lower in CD4 T cells from PLHIV compared with HS ($n = 8$ subjects).

In addition to targeting protein-coding genes, lncRNAs can also target miRNAs to regulate cellular responses and tumor progression. Bioinformatics analysis using the RNA22 program revealed that GAS5 has sequences complementary to several miRNAs, including miR-21. We were interested in miR-21 because its expression is dynamically upregulated and regulates T cell responses during T cell activation and differentiation. To determine whether GAS5 plays a role in T cell dysfunctions via regulating miR-21 expression during HIV infection, we measured miR-21 levels in CD4 T cells isolated from ART-controlled PLHIV and HS by RT-qPCR. As shown in **Figure 1B**, miR-21 expression was significantly increased in CD4 T cells derived from PLHIV compared with HS ($n = 8$). Since miR-21 is aberrantly upregulated during T cell activation and differentiation, these results are in line with the overall immune activation driven by chronic inflammation in ART-controlled, latent HIV infection. Next, we compared miR-21 and GAS5 expressions in T cells derived from the same subjects. As shown in **Figure 1C**, the decline in GAS5 levels closely correlated with miR-21 upregulation in CD4 T cells from the same HIV patients and HS ($n = 8$ subjects). Also, the level of GAS5 positively correlated, whereas miR-21 negatively correlated, with the CD4 T cell counts in the peripheral blood of ART-controlled PLHIV (**Figures 1D,E**). Taken together, these results indicate that GAS5 is downregulated, whereas miR-21 is upregulated in CD4 T cells during HIV infection, and that their expressions correlate with CD4 T cell counts in the peripheral blood of ART-controlled PLHIV.

Differential Expression of GAS5 and miR-21 Following TCR Stimulation of CD4 T Cells From PLHIV and HS

Although ART controls viral replication, PLHIV still exhibit low-grade inflammation and immune activation, driving T cell exhaustion and senescence. We thus hypothesized that the differential expression of GAS5 and miR-21 in CD4 T cells is likely due to overall immune activation, as additional TCR stimulation *in vitro* could drive aberrant RNA expressions further, but the response of CD4 T cells from PLHIV may be attenuated due to their exhausted and senescent status. To test this hypothesis, we cultured CD4 T cells from PLHIV and age-matched HS ($n = 6$) with or without Dynabeads-coated with anti-CD3 and anti-CD28 antibodies for 1, 3, and 5 days and measured GAS5 transcripts by RT-qPCR. As shown in **Figure 1F,** TCR stimulation decreased GAS5 levels in CD4 T cells from HS at day 1 ($p = 0.0997$), day 3 ($p = 0.0005$), and day 5 ($p = 0.0756$), but such a decrease was only statistically significant at day 3 compared to the unstimulated cells. Similarly, GAS5 levels in CD4 T cells from PLHIV were also significantly downregulated following TCR stimulation at day 3 ($p = 0.0023$) and day 5 ($p = 0.0006$), but not at day 1 ($p = 0.0756$; **Figure 1G**). These results

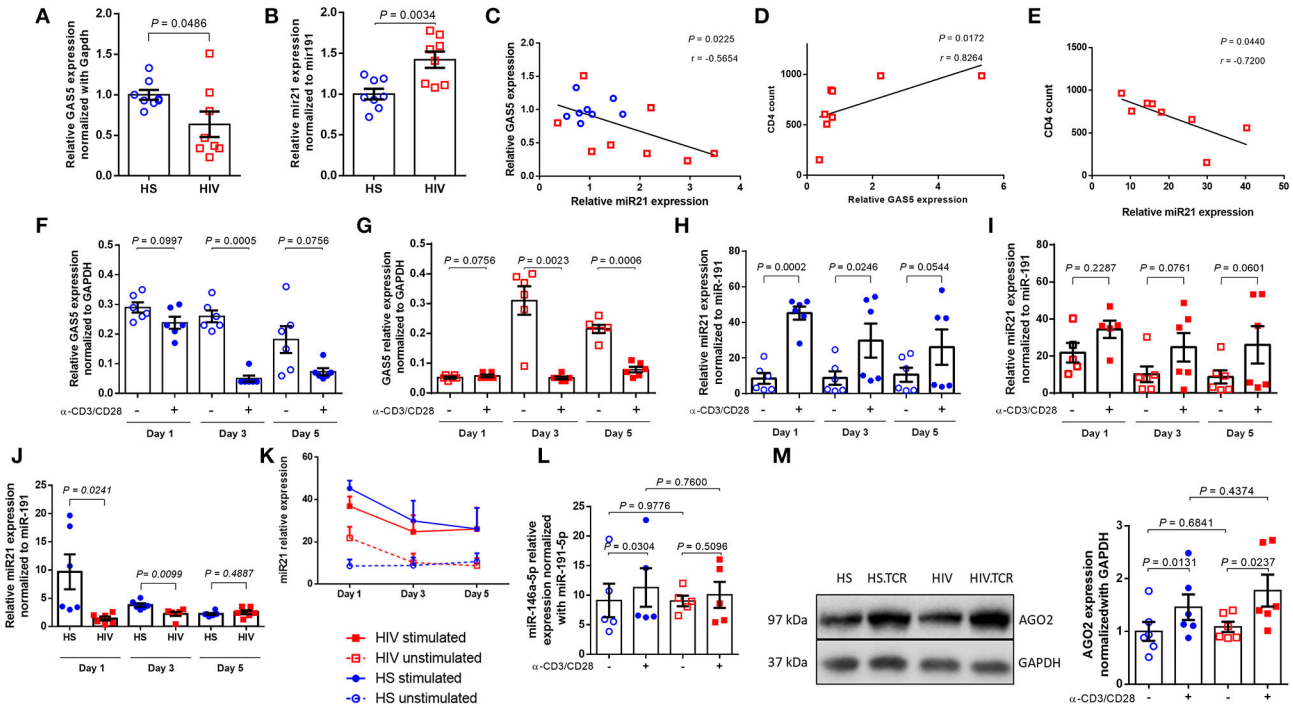

FIGURE 1 | Differential expression of GAS5 and miR-21 in CD4 T cells after TCR stimulation. **(A,B)** Relative expression of GAS5 ($n = 8$) and miR-21 ($n = 8$) in CD4 T cells isolated from HS and PLHIV was determined by RT-qPCR. **(C)** Correlation between GAS5 and miR-21 expressions in CD4 T cells isolated from HS or PLHIV was determined by Pearson correlation analysis. **(D,E)** Correlation between CD4 T cell counts and relative GAS5 ($n = 8$) or miR-21 ($n = 8$) expressions in CD4 T cells from PLHIV was determined by Pearson Correlation analysis. **(F,G)** Relative expression of GAS5 in CD4 T cells from HS and PLHIV in the absence or presence of TCR stimulation for 1, 3, and 5 days ($n = 6$). **(H,I)** Relative expression of miR-21 in HS and PLHIV CD4 T cells with or without TCR stimulation for 1, 3, and 5 days ($n = 6$). **(J)** Relative expression of miR-21 in TCR-stimulated CD4 T cells from HS and PLHIV in 1, 3, and 5 days ($n = 6$). **(K)** Kinetic changes in miR-21 expression in CD4 T cells from both PLHIV and HS following TCR stimulation for 1, 3, and 5 days. **(L)** Relative expression of miR-146a in CD4 T cells from HS and PLHIV with or without TCR stimulation for 24 h ($n = 6$). **(M)** Representative dot blot and relative expression of AGO2 (a major component of RISK complex) in CD4 T cells from HS and PLHIV with or without TCR stimulation for 24 h, determined by Western blotting ($n = 6$).

demonstrate that TCR stimulation reduces GAS5 expression in CD4 T cells derived from both HS and PLHIV.

To determine the effects of T cell activation on miR-21 regulation, we also measured miR-21 levels in CD4 T cells from the same group of PLHIV and age-matched HS ($n = 6$ subjects) after TCR stimulation for 1, 3, and 5 days. Following stimulation with bead-conjugated anti-CD3 and anti-CD28 antibodies, HS CD4 T cells responded robustly and kinetically, with an increasing miR-21 expression, particularly at day 1 (>5-fold increase, $p = 0.0002$) and day 3 (>3-fold increase, $p = 0.0246$; **Figure 1H**). Although HIV CD4 T cells also exhibited increases in miR-21 expression after TCR stimulation, the differences between unstimulated and stimulated cells were not significant (fold-increases between 1 and 2 overtime, all $p > 0.05$; **Figure 1I**). These results indicate that CD4 T cells from PLHIV respond to TCR stimulation poorly compared to those from HS. Notably, miR-21 levels were remarkably higher in CD4 T cells from PLHIV than HS without TCR stimulation *in vitro* (**Figure 1B**), and were significantly lower in TCR-stimulated CD4 T cells from PLHIV after the values were normalized to the unstimulated cells, especially at day 1 (6.85-fold decrease, $p = 0.0241$) and day 3 (1.7-fold decrease, $p = 0.0099$). The day 5 stimulation resulted in a slightly higher miR21 expression in HIV samples (1.13-fold increase, $p = 0.4887$; **Figure 1J**). Also, the changes in miR-21 expressions in CD4 T cells from both PLHIV and HS following TCR stimulation *in vitro* for 1, 3, and 5 days are shown in **Figure 1K** and clearly show that miR-21 was upregulated in CD4 T cells from both PLHIV and HS after TCR stimulation. However, the response of CD4 T cells from PLHIV was attenuated compared to cells from HS, especially at the early phase (day 1–3) of TCR stimulation. Since the day 0 (baseline) data for GAS5 and miR-21 expressions without TCR stimulation are shown in **Figures 1A,B**, we did not include this time point when we set up the TCR stimulation for the kinetic experiments due to limited availability of the cells, which we recognize as a limitation for the analysis of these data (**Figures 1F–K**).

Previous studies have shown that miR-146a is upregulated in TCR-stimulated T cells and in HIV-1-infected individuals (38). Also, the expression of miR-146 was found to be correlated with the expressions of T cell exhaustion and senescence markers, such as PD-1, Tim-3, and LAG-3 (38). Our data in **Figure 1L** show that the levels of miR-146a were increased in CD4 T cells from HS ($p = 0.0304$), but not PLHIV ($p = 0.5096$), following TCR stimulation for 24 h. Also, we found no significant

differences in miR146 levels in CD4 T cells derived from PLHIV and HS, in both unstimulated ($P = 0.9776$) and TCR-stimulated ($P = 0.7600$) conditions (**Figure 1L**).

Argonaute 2 (AGO2) is the catalytic component of RISC that recognizes and cleaves mRNA of complementary sequences. From a duplex, one strand is preferentially loaded into AGO2 to generate a functional miRNA-induced silencing complex (miRISC). We asked whether levels of AGO2 are affected during TCR stimulation. To address it, we measured AGO2 in CD4 T cells from HS and PHLIV with and without TCR stimulation for 24 hours. Although AGO2 expression was increased after TCR stimulation in CD4 T cells from both HS and PHLIV sequence, there were no significant differences in AGO2 levels, between the two groups, in both unstimulated and stimulated (**Figure 1M**). These data indicate that AGO2 expression levels are significantly increased, with no differences between HS and HIV suggesting that TCR stimulation may affect widely miRISC activity.

Effects of IL-2 and Anti-PD1 Treatment on the GAS5-miR-21-Axis

To further define the effect of GAS5-miR-21 on T cell activities, we measured cell cycle progression by PI staining in CD4 T cells from HS and PLHIV, following TCR stimulation for 1, 3, and 5 days. As shown in **Figure 2A** (representative histogram for numbers of CD4 T cells in G0/1, S, and G2/M phases at day 3 and summary data at day 1, 3, and 5), there were significant differences in the percentages of CD4 T cells present in S and G2/M phases of cell cycle with and without TCR stimulation. Notably, the percentages of CD4 T cells from HS and PLHIV in various cell cycle phases were comparable after TCR stimulation for 1 day. We found a significant higher percentage of CD4 T cells from HS were going through cell cycle phases compared to those from PLHIV following TCR stimulation for 3–5 days, particularly at day 3. These data indicate that TCR stimulation induces cellular proliferation and division, but as the expression GAS5 and miR-21 is altered in response to TCR stimulation, CD4 T cells from PLHIV behave differently from HS; in that HS-CD4 T cells respond relatively stronger and ultimately progress to T cell exhaustion and senescence with persistent stimulation.

Attempts have been made to restore dampened T cell functions in PLHIV via manipulating some of the dysregulated signaling pathways. For instance, blockade of the inhibitory PD-1/PD-L1 pathway enhanced viral-specific CD4 T cell response along with a decreased viral replication (39, 40). In addition, administration of IL-2 led to CD4 T cell expansion, and such expansion was coupled with a decreased turnover and improved survival of naive and central memory CD4 T cells, leading to recovery of T cell function and immune response (41, 42). Here, we examined whether PD-1 blockade with IL-2 signaling can impact the GAS5/miR-21 axis during TCR stimulation by determining the levels of GAS5 and miR-21 in TCR-stimulated HIV-CD4 T cells in the presence of PD-1 inhibitor (Nivolumab) and IL-2. As shown in **Figure 2B**, anti-PD1 and IL-2 treatment could not restore the aberrant GAS5/miR-21 expressions following TCR stimulation in CD4 T cells from PLHIV.

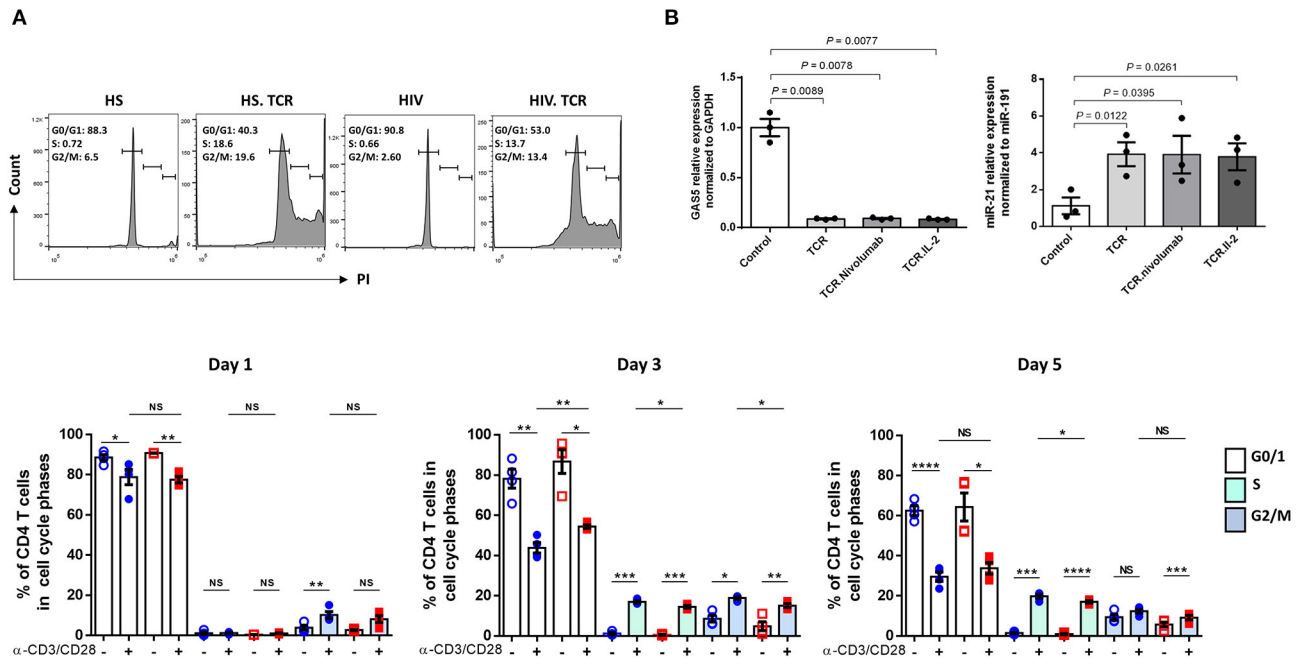

FIGURE 2 | Cell cycle progression, AGO2 expression, and effect of anti-PD1/IL-2 in TCR-stimulated CD4 T cells on GAS5-miR-21 axis. **(A)** Cell cycle progression in CD4 T cells from HS and PLHIV following TCR stimulation at day 1, 3, and 5 measured by PI flow cytometric analysis ($n = 4$). Representative histogram of cell cycle phases of CD4 T cells from HS and PLHIV with and without TCR stimulation at day 3 are shown above and summary data at day 1, 3, 5 are shown below. **(B)** Relative expression of GAS5 and miR-21 in CD4 T cells from HS and PLHIV following anti-PD1 and IL-2 treatments for 24 h, determined by RT-qPCR ($n = 3$). n.s, $P > 0.05$; *$P \leq 0.05$; **$P \leq 0.01$; ***$P \leq 0.001$; ****$P \leq 0.0001$.

PLHIV on ART Exhibit T Cell Dysregulation and Apoptosis due to Aberrant DDR

To determine the possible effects of GAS5/miR-21 on the cellular response during latent HIV infection, we examined the expressions of known protein markers for T cell activation, exhaustion, DNA damage, cellular functions, and apoptosis using flow cytometry and western blotting. As shown in **Figure 3A**, the frequencies of CD69 (an early activation marker) positive cells were significantly increased upon TCR stimulation of CD4 T cells from both PLHIV and HS; however, PLHIV exhibited significantly increased T cell activation at baseline prior to stimulation. Correspondingly, phosphorylation of AKT (pAKT) was upregulated in CD4 T cells from PLHIV after TCR stimulation. Because CD4 T cells are persistently activated during HIV infection, they expressed higher levels of the activation and exhaustion marker programmed death-1 (PD-1) before and after TCR stimulation compared to CD4 T cells from HS (**Figure 3B**). Likewise, CD4 T cells from PLHIV showed relatively lower levels of the survival cytokine interleukine-2 (IL-2) (**Figure 3C**), whereas levels of the pro-inflammatory cytokine TGF-β1 were upregulated after TCR stimulation compared to CD4 T cells from HS.

We have recently reported that chronic inflammation in ART-controlled PLHIV induces telomeric DNA damage and cell apoptosis. Here, we found that phosphorylation of the H2A histone family member γH2AX (a marker of DNA damage) was significantly upregulated by TCR stimulation in CD4 T cells derived from both PLHIV and HS, and was further increased in T cells from PLHIV, with or without TCR stimulation (**Figure 3D**). Correspondingly, PLHIV had a high level of CD4 T cell apoptosis, as evidenced by the significant increase in cleaved caspase-3 and Av/7AAD levels, perhaps due to reduced levels of Bcl-2 expression (an anti-apoptotic molecule), in CD4 T cells under both unstimulated and stimulated conditions compared to HS (**Figure 3E**). The DNA damage-mediated cell apoptosis was confirmed by western blot, which showed increases in the levels of cleaved PARP-1, pAKT, and γH2AX in CD4 T cells from PLHIV compared to HS (**Figure 3F**). These results suggest that CD4 T cells from PLHIV exhibit a phenotype of over-activation, exhaustion, DNA damage, and cell apoptosis.

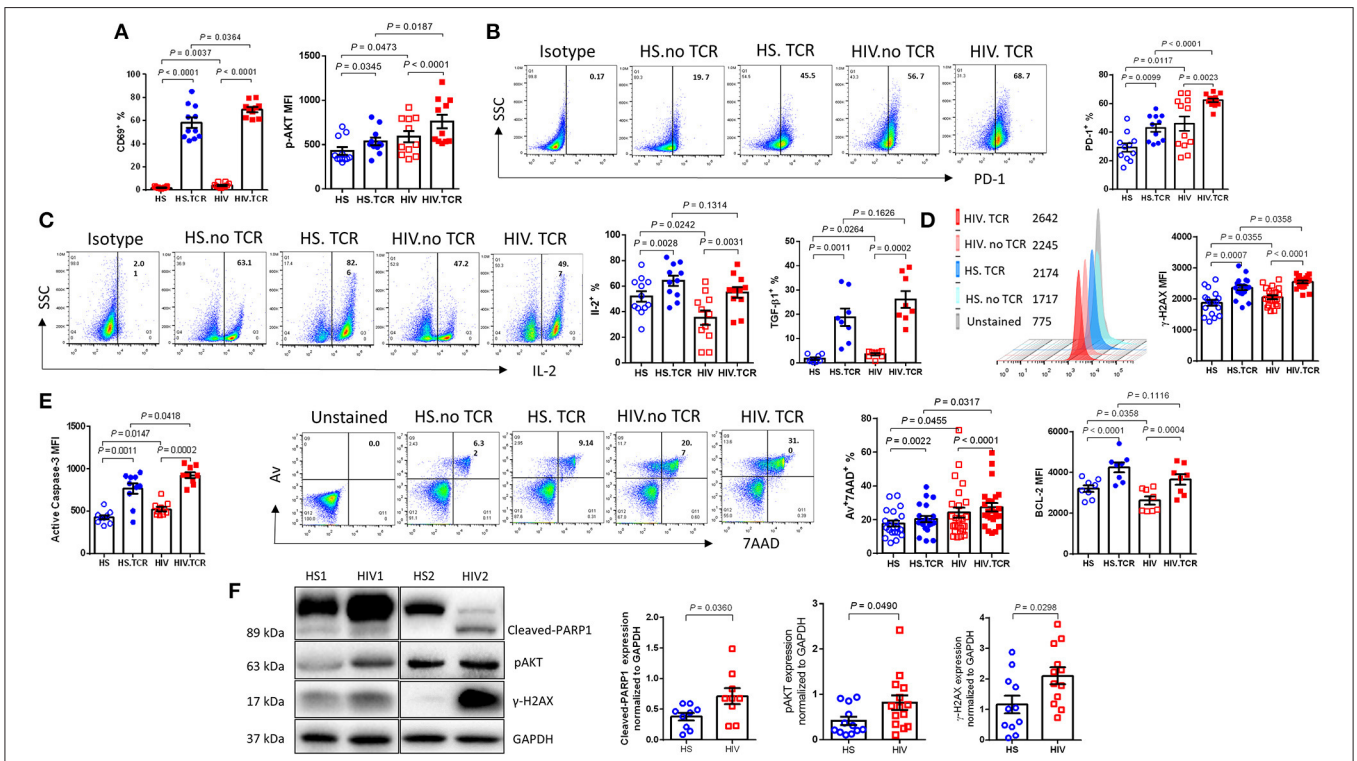

FIGURE 3 | PLHIV on ART exhibit CD4 T cell dysregulation and apoptosis due to aberrant DDR. T cell activation, exhaustion, cytokine production, apoptosis, and DNA damage marker expressions in TCR-stimulated or non-stimulated CD4 T cells isolated from HS or PLHIV were determined by Flow Cytometry and Western Blot. **(A)** Frequency of $CD69^+$ ($n = 11$) and MFI of $pAKT^+$ cells ($n = 11$). **(B)** Representative dot plots and summary data of $PD\text{-}1^+$ cells ($n = 12$). **(C)** Representative dot plots and summary data of IL-2 expression ($n = 12$), expression of TGFβ1 ($n = 8$). **(D)** Representative histogram and summary MFI of γH2AX in CD4 T cells from HS ($n = 18$) and PLHIV ($n = 21$). **(E)** Expression of active caspase-3 ($n = 10$), representative dot plots and summary data of Av^+7AAD^+ CD4 T cells from HS ($n = 21$) and PLHIV ($n = 25$), expression of BCL-2 in CD4 T cells from HS and PLHIV ($n = 8$). **(F)** Representative imaging and summary data of immunoblotting for PARP-1, pAKT, and γH2AX, normalized by GAPDH.

miR-21 Controls CD4 T Cell Response and Apoptosis via Regulating the TCR Signaling Pathways in PLHIV

To examine whether and how miR-21 controls T cell response during HIV infection, we transfected CD4 T cells with lentiviral shRNA against miR-21, and assessed the markers for T cell activation, exhaustion, DNA damage, and cellular apoptosis by flow cytometry and western blotting. **Figure 4A** shows knockdown of miR-21 as determined by a slight decrease in its levels in CD4 T cells transfected with anti-miR21 compared to the control vector. Notably, knockdown of miR-21 did not change the expression of GAS5, indicating that GAS5 expression is not regulated by miR-21. As shown in **Figure 4B**, the frequencies of $pAKT^+$, $pMAPK^+$, PD-1^+, and Tim-3^+ cells were significantly reduced after miR-21 knockdown. Additionally, IL-2 and IFN-γ expressions were increased, whereas the number of TGF-β1 expressing CD4 T cells from PLHIV was significantly decreased (**Figure 4C**), after miR-21 knockdown.

It has been reported that T cell factor-1 (TCF1) critically regulates T cell activation and differentiation through activation of the canonical Wnt signaling pathway during TCR stimulation (43). We thus examined TCF1 expression in PLHIV CD4 T cells following miR-21 knockdown. As shown in **Figure 4C**, the percentage (%) of $TCF1^+$ cells was significantly decreased in PLHIV CD4 T cells transfected with anti-miR-21 siRNA compared to the control. Moreover, the frequencies of $Av^+/7AAD^+$ cells and the MFI of cleaved caspase-3 (**Figure 4D**) and the MFI of DNA damage marker γH2AX (**Figure 4E**) were significantly decreased, in PLHIV CD4 T cells with miR-21 knockdown. To further confirm the changes in the expression of these markers, we measured their levels by Western blotting. As shown in **Figure 4F** (representative blots and summary data), the levels of cleaved PARP-1, pS6, and γ-H2AX were downregulated after miR-21 knockdown. These results indicate that disrupting miR-21-mediated signaling can rescue PLHIV CD4 T cells from over-activation, exhaustion, cytokine inhibition, DNA damage, and cell apoptosis.

GAS5 Negatively Regulates miR-21 Expression in TCR-Activated CD4 T Cells From PLHIV and HS

How GAS5 and miR-21 are differentially regulated by TCR stimulation is poorly understood. As stress-inducible genes, GAS5 and miR-21 are induced in response to cellular stress conditions, such as serum starvation or TCR stimulation. Although previous studies have shown that GAS5 and miR-21 regulate each other's expression in a mutually exclusive way, our results in **Figure 4A** showed that GAS5 expression was not significantly increased after miR-21 knockdown in PLHIV CD4 T cells. In addition, we determined the effect of GAS5 on miR21 expression by overexpressing GAS5 in TCR-activated PLHIV CD4 T cells using the lentivirus expression system, followed by examining GAS5 and miR21 expression. The data in **Figure 5A** confirmed a significant increase in GAS5 levels in TCR-stimulated HIV-CD4 T cells (2 days) transfected with GAS5 ($p = 0.0034$) for additional 3 days. We next determined the levels of miR-21 in CD4 T cells overexpressing GAS5. As shown in **Figure 5A**, the level of miR-21 was downregulated in a dose-dependent manner, depending on the amount of the lentivirus (0, 1.35×10^6 TU/mL, and 2.70×10^6 TU/mL) to overexpress GAS5, indicating that miR-21 level is regulated by GAS5 in TCR-activated PLHIV CD4 T cells. These results demonstrate that GAS5 negatively regulates miR-21 in TCR-activated PLHIV CD4 T cells and provide a further evidence of an endogenous competitive RNA regulatory network.

GAS5 Controls CD4 T Cell Responses and Apoptosis During HIV Infection by Regulating Pathways Beyond miR-21-Mediated Signaling

GAS5 not only regulates miR-21 expression, but also other miRNAs involved in cellular differentiation and proliferation (44, 45). To investigate the regulatory effect of GAS5 on CD4 T cells during HIV infection, independently from miR-21-mediated signaling, we generated a GAS5 mutant where amino acids at exon 4 of GAS5 transcript were altered (GAS5-mutant), as depicted in **Figure 5B**. This mutation abolishes the binding site of miR-21 on GAS5 and thus restricts the interaction between GAS5 and miR-21. Notably, transfection with GAS5-mutant did not significantly alter miR-21 levels compared to control vector, whereas transfection with GAS5-WT significantly decreased miR-21 level ($p = 0.0293$), suggesting that overexpression of GAS5-mutant with no binding affinity for miR-21 does not affect miR-21 expression. We next determined the effect of overexpressing GAS5-mutant on T cell activation and responses. As shown in **Figure 5C**, the expression of early T cell activation marker CD69, was significantly ($p = 0.0025$) downregulated in CD4 T cells transfected with GAS5-WT compared to the control vector transfection. However, the CD69 expression was partially restored in CD4 T cells overexpressing GAS5-mutant compared to the GAS5-WT, and this change was not statistically significant compared to the control. In addition, we observed a significantly lower apoptosis rate in CD4 cells overexpressing GAS5-WT, but not GAS5-mutant compared, to the control vector (**Figure 5D**). Nevertheless, the frequencies of T cells expressing PD-1 and pAKT were significantly downregulated in CD4 T cells overexpressing GAS5-WT and GAS5-mutant compared to the control vector (**Figure 5E**). These results suggest that while GAS5 regulates HIV-CD4 T cell early activation and apoptosis through miR-21-mediated signaling, other signaling pathways may also be involved in the regulation of T cell activation and exhaustion pathways during HIV infection.

GAS5 Controls CD4 T Cell Response and Apoptosis by Regulating miR-21-Mediated Signaling During HIV Infection

Having demonstrated a negative regulatory effect of GAS5 on miR-21 expression, we next examined the functional role of GAS5 in CD4 T cell regulation. We investigated whether overexpression of GAS5 has any effect on miR-21-mediated functional changes in CD4 T cells from PLHIV. GAS5 was

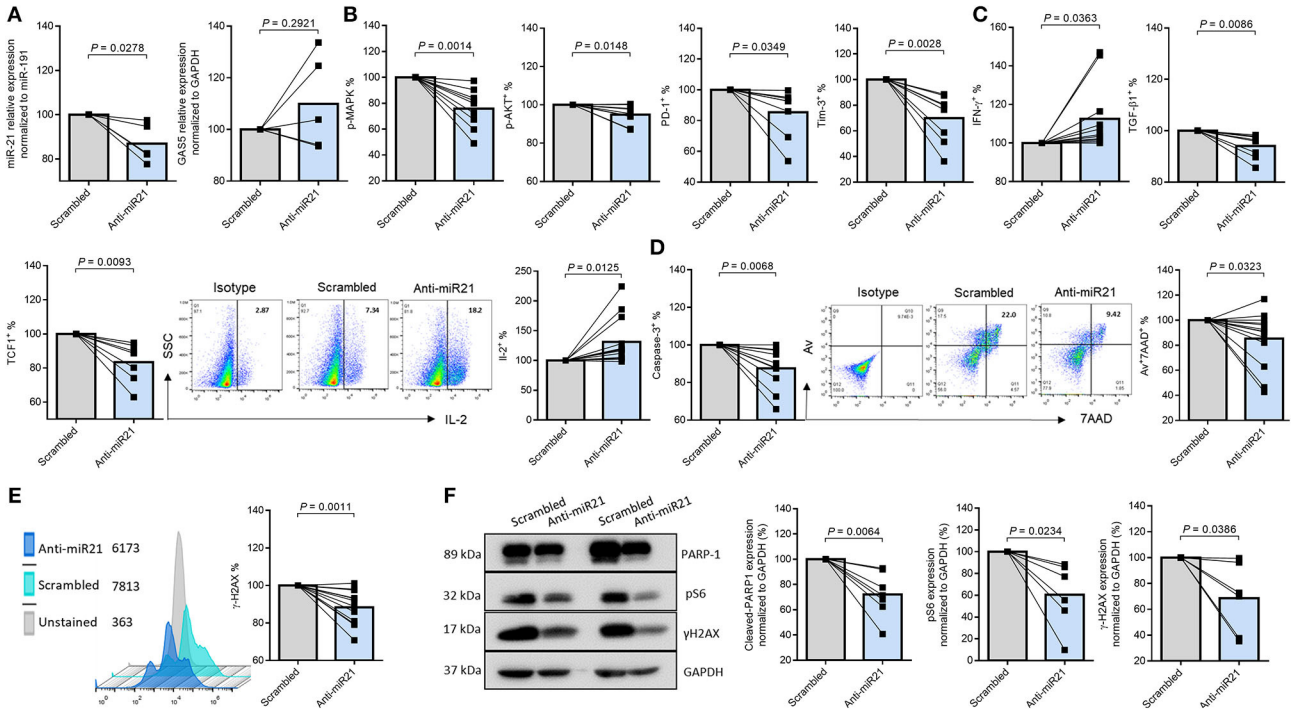

FIGURE 4 | MiR-21 controls CD4 T cell response and apoptosis via regulating the TCR signaling pathways in PLHIV. T cell activation, exhaustion, cytokine production, apoptosis, and DNA damage marker expressions after miR-21 knockdown in CD4 T cells from PLHIV were determined by Flow Cytometry and Western Blot. **(A)** Relative expression of miR-21 and GAS5 following miR-21 knockdown in CD4 T cells from PLHIV determined by RT-qPCR ($n = 5$). **(B)** Frequencies of pMAPK ($n = 9$), pAKT ($n = 9$), PD-1 ($n = 11$), and Tim-3 ($n = 8$). **(C)** Representative dot plot and summary data of IL-2 ($n = 16$), IFN-γ ($n = 16$), TGFβ1 ($n = 8$), and TCF1 ($n = 7$) expressions. **(D)** Representative dot plot and summary data of Av^+ $7AAD^+$ CD4 T cells ($n = 13$), expression of active caspase-3 ($n = 10$). **(E)** Representative histogram and summary data of γH2AX expression ($n = 12$). **(F)** Representative western blots and summary data of cleaved PARP-1 ($n = 8$), pS6 ($n = 6$), and γH2AX ($n = 6$) expressions, normalized to GAPDH.

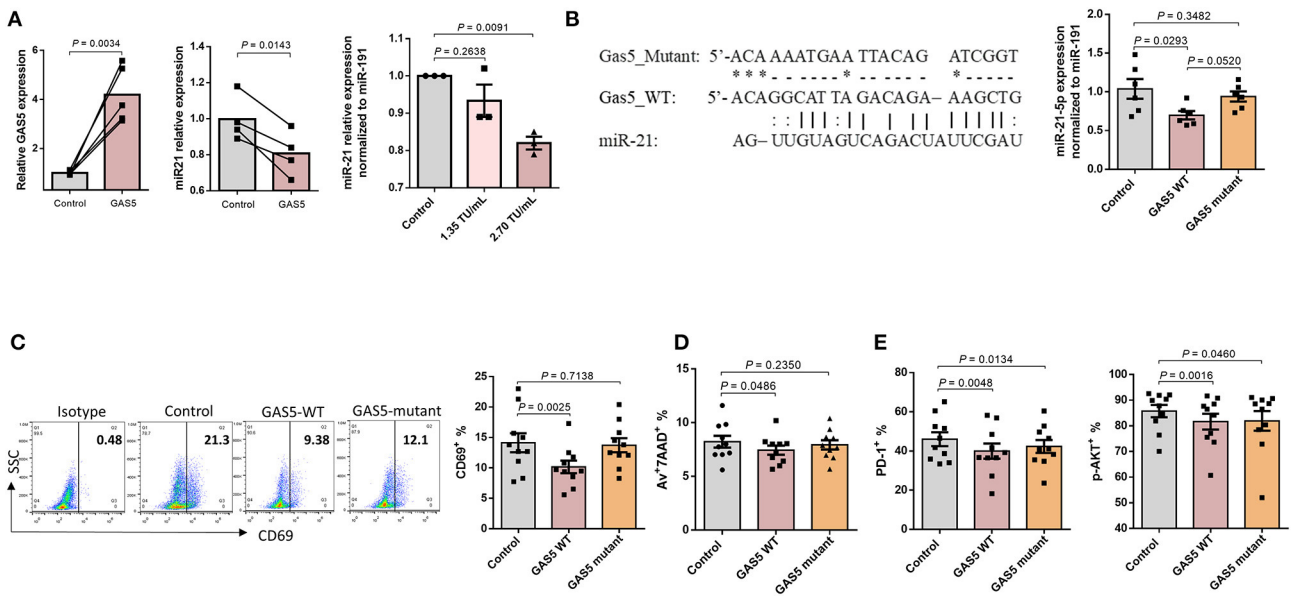

FIGURE 5 | GAS5 controls CD4 T cell response and apoptosis beyond miR-21-mediated signaling pathways. **(A)** Relative expressions of GAS5 ($n = 5$) and miR-21 ($n = 4$) in CD4 T cells from PLHIV, following overexpression of GAS5, determined by RT-qPCR. **(B)** Left panel, sequences of GAS5-mutant and GAS5-WT constructs, and the corresponding miR-21 binding site. Right panel, relative miR-21 expression in CD4 T cells from PLHIV transfected with control, GAS5-WT, or GAS5-mutant constructs ($n = 6$). **(C–E)** Expression of T cell activation, apoptosis, and exhaustion markers in CD4 T cells from PLHIV transfected with control, GAS5-WT, or GAS5-mutant construct, determined by flow cytometry ($n = 10$).

overexpressed using the lentiviral expression system, and the markers for functional T cells were assessed by flow cytometry and western blotting. As shown in **Figure 6A**, the frequencies of pAKT$^+$ and pMAPK$^+$ cells were significantly decreased; PLHIV CD4 T cell exhaustion was reduced, as demonstrated by the downregulation of PD-1$^+$ and Tim-3$^+$ cell frequencies in GAS5-overexpressing CD4 T cells (**Figure 6B**). Additionally, IL-2 and IFN-γ producing CD4 T cells were increased (**Figure 6C**), whereas pro-inflammatory TNF-α producing cells were decreased due to GAS5 overexpression (**Figure 6D**). Moreover, the level of γH2AX was reduced (**Figure 6E**), and the cell apoptosis markers Av/7AAD and cleaved caspase-3 were significantly decreased in GAS5 overexpressing CD4 T cells compared to the control vector expression (**Figure 6F**). To further confirm the changes in the expressions of these markers, we determined their levels by western blotting. As shown in **Figure 6G** (representative blots and summary data), protein levels of cleaved PARP-1, pS6, and γH2AX, were downregulated in GAS5-overexpressing cells compared to the control vector. These results suggest that increasing GAS5 levels in PLHIV CD4 T cells can negatively regulate miR-21 expression, which in turn improves TCR activation, T cell exhaustion, cytokine production, and reduces DNA damage and cell apoptosis.

DISCUSSION

T cells play an essential role in the control of viral infections. However, T cells in PLHIV–despite successful control of viral replication by ART–are aberrantly dysregulated and exhibit an immune aging phenotype, characterized by CD4 T cell over-activation, exhaustion, senescence, accumulated DNA damage, more apoptosis, and impaired cellular functions. While the causes for this immune aging phenotype have been extensively investigated, the molecular mechanisms underlying these cellular alterations remain incompletely understood. In this study, we demonstrated that GAS5 and miR21 are differentially expressed in CD4 T cells derived from ART-controlled PLHIV and that GAS5 controls miR21 expression to regulate signaling molecules involved in DNA damage and cellular responses following T cell receptor (TCR) stimulation. Based on these new findings and our previous studies–showing deficiencies in topoisomerase I/IIα (Top1/2α), ataxia-telangiectasia mutated, human telomerase reverse transcriptase (hTERT), and telomeric repeat-binding factor 2 (TRF2) that can cause telomeric DNA damage–we propose a model (depicted in **Figure 7**) illustrating how the GAS5-miR21 axis controls the function and fate of CD4 T cells in PLHIV. Despite the differential expressions of GAS5 and miR-21, the mechanism of miR21-mediated dysregulation of CD4 T cell

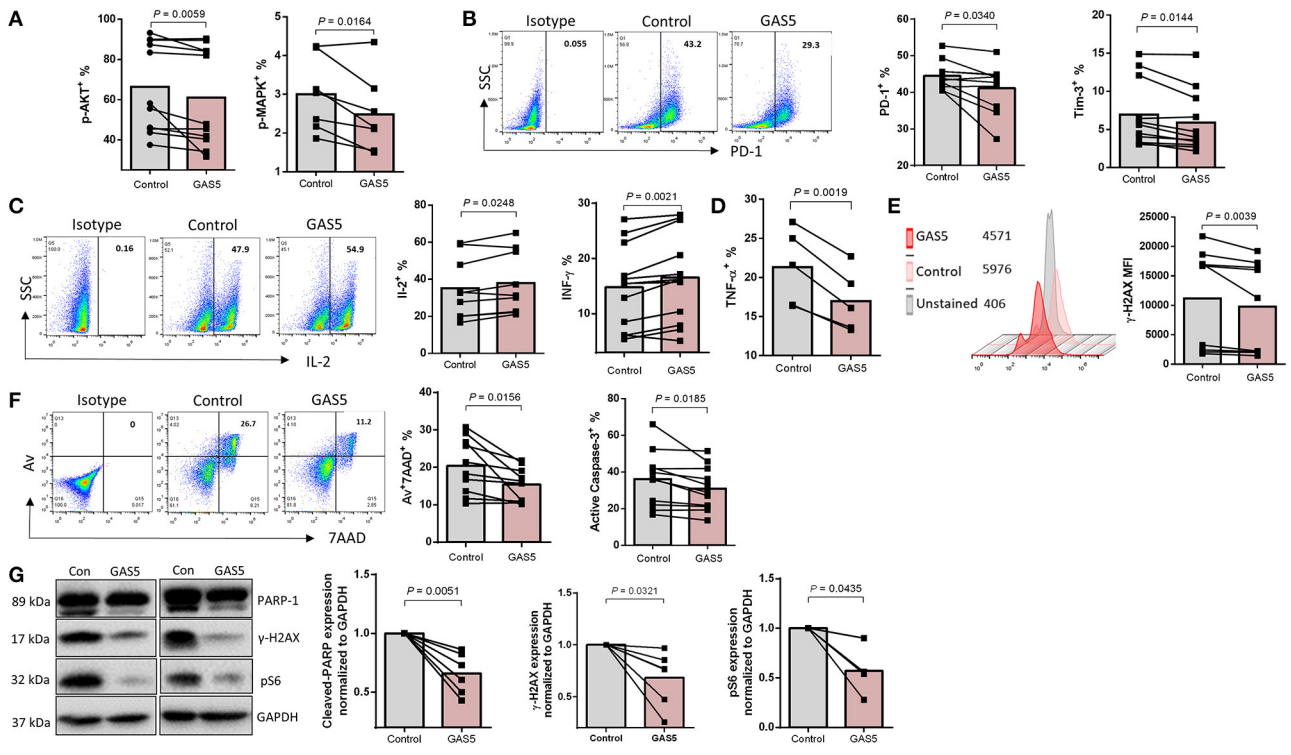

FIGURE 6 | GAS5 controls CD4 T cell response and apoptosis via regulating miR-21-mediated signaling in PLHIV. **(A,B)** Frequencies of pAKT ($n = 11$), pMAPK ($n = 7$), PD-1 ($n = 10$), and Tim-3 ($n = 11$) in control vector or GAS5-transducted CD4 T cells from PLHIV, determined by flow cytometry. **(C,D)** Representative dot plot and summary data of IL-2 expression ($n = 10$), IFN-γ ($n = 12$), and TNF-α ($n = 5$), measured by flow cytometry. **(E)** Representative histogram and summary data of γH2AX expression ($n = 9$). **(F)** Representative dot plot and summary data of Av$^+$7AAD$^+$ CD4 T cells ($n = 10$) and active caspase-3 ($n = 11$). **(G)** Representative western blot imaging and summary data of cleaved PARP-1 ($n = 6$), pS6 ($n = 4$), and γH2AX ($n = 6$) expressions, normalized to GAPDH.

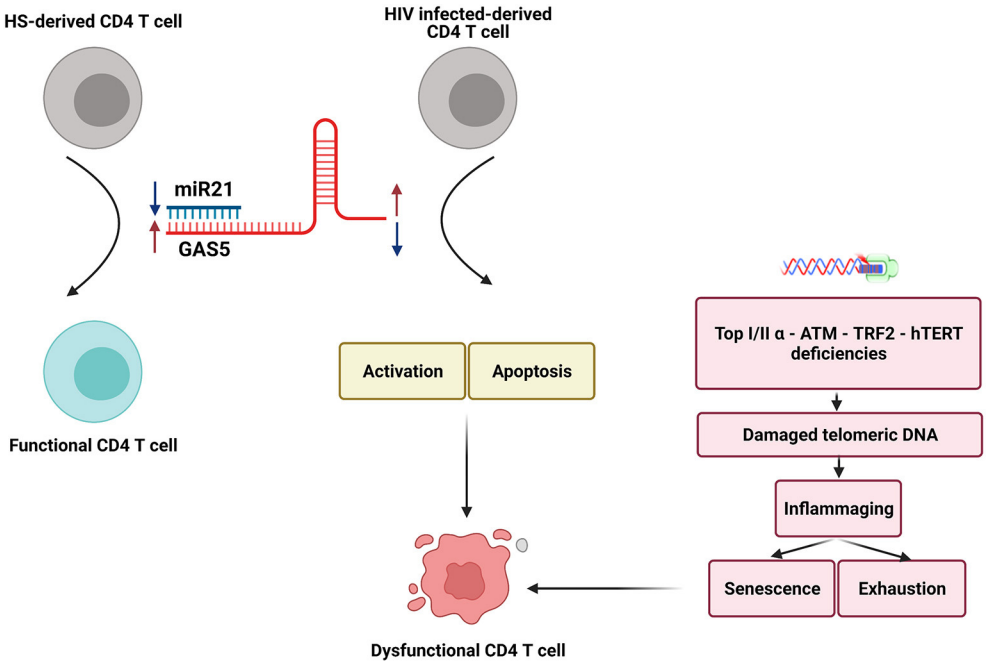

FIGURE 7 | A model depicting how the GAS5-miR-21 axis controls the function and fate of CD4 T cells in PLHIV. Two crucial non-coding RNAs, GAS5 and miR-21 are differentially expressed in CD4 T cells in PLHIV. The decline in GAS5 and increase in miR-21 expressions, along with the deficiencies in crucial enzymatic proteins involved in DNA damage and repair machineries, can cause significant increases in CD4 T cell activation, senescence, apoptosis, DNA damages, and dysregulation of cytokine productions established during latent HIV infection. Importantly, interrupting this GAS5-miR-21 axis may restore T cell homeostasis and competency and resolve premature T cell aging or immune senescence. Notably, GAS5 effects on T cell exhaustion during HIV infection may be mediated by mechanism(s) beyond GAS5-miR21 mediated signaling. Bottom: Deficiencies in Top1/2a, ATM, hTERT, and TRF2 that can cause telomeric DNA damage (30–34, 36) are known to contribute to dysfunctional CD4 T cells in HIV patients.

functions in PLHIV remain unknown. Nevertheless, our data clearly show that the GAS5-miR21 axis can control multiple signaling pathways involved in cell activation, senescence, and apoptosis in PLHIV CD4 T cells. Notably, the decline in GAS5 and the increase in miR21 are associated with the frequencies of CD4 T cells in the peripheral blood of PLHIV. Importantly, GAS5 overexpression or miR21 silencing significantly restored the aberrantly dysregulated T cell activation, DNA damage, apoptosis, and functions of CD4 T cells derived from PLHIV. Additionally, disrupting miR21 binding site in GAS5 transcripts partially restored the GAS5-mediated regulation of CD4 T cell activation and apoptosis but not cell exhaustion, indicating that additional signaling pathways are involved in T cell exhaustion.

Previous studies in cancer have suggested that GAS5 puts a "brake" on cell proliferation, thereby acting as a potential tumor suppressor in various cancers (46). Also, overexpression of GAS5 has been shown to increase apoptosis and reduce cell cycle progression in T cell lines and PBMCs (47). In contrast, low levels of GAS5 are often associated with cell proliferation and cancer metastasis (48). These findings in cancer cells seem to contradict our data showing that decreasing GAS5 in the CD4 T cells of PLHIV resulted in a dampened response in these prematurely aged cells while overexpressing GAS5 restored their dysregulated functions. As a multifunctional lncRNA, GAS5 plays crucial roles in many biological processes, including transcriptional regulation, by acting as a decoy or through promoting histone modifications or competing with endogenous RNA (ceRNA) to regulate various signaling pathways and biological functions (49). Thus, GAS5 expression and functions can be species-, cell-, or disease-specific. In addition, miR-21 is considered a cell activation marker and an oncogene, where its upregulation can cause an overgrowth of many cancers (50). In contrast, it has been shown to be a negative regulator of T cell activation. High expression of miR-21 in T lymphocytes can reduce activation marker (CD69, OX40, CD25, and CD127) and cytokine (IL-2, IFN-γ) gene expressions, and hence, induce T cell over-activation and dysfunction (51). Furthermore, it has been reported that upregulation of miR-21 level in the elderly drives proliferation of naïve T cells to a terminal phenotype instead of a long-lived memory phenotype, thus attenuating T cell responses; this strongly supports our findings, including TCF1 declines upon miR-21 silencing in this study. Previous studies have shown that miR-21 targets several pathways involved in cellular proliferation. The tumor-suppressor pathway–phosphatase and tension homolog (PTEN)/phosphoinositide 3-kinases (PI3K)–is a well-known target of miR-21 (52). Also, miR-21 has been shown to target the programmed cell death 4 (PDCD4)/p21

and Sprouty RTK Signaling Antagonist 1 (SPRY1)/Rapidly Accelerated Fibrosarcoma (RAF) signaling pathways (53, 54). Also, we and others have shown that chronic viral infection-induced inflammaging phenotypes result from deficiencies in Top 1/2α, ATM, hTERT, and TRF2, which correlate closely with the observed, aberrant CD4 T cell apoptosis and depletion. Here, we further demonstrate that a decrease in GAS5 level promotes the upregulation of miR-21 expression and that the GAS5-miR-21 axis may represent a key signaling pathway in controlling persistent activation, exhaustion, senescence, DNA damage, cell apoptosis, and cytokine dysregulation in CD4 T cells derived from PLHIV. Our data showed that GAS5 regulates CD4 T cell responses, not only through miR-21-mediated signaling but also via other undetermined pathways. In support of this notion, we showed that manipulating GAS5/miR-21 expressions or interactions during TCR activation can partially reverse CD4 T cell dysfunctions and apoptosis. These findings provide a novel strategy to improve immunotherapies and vaccine responses in the setting of human viral infection.

PLHIV on ART represent the major HIV-infected population in the era of ART. In this clinical setting, how the differential expression of GAS5 and miR-21 ultimately control CD4 T cell functions remains unknown. Given ART control of HIV replication leads to a very small proportion (one in a million) of PBMCs harboring HIV provirus (55), it is unlikely that HIV itself *per se* can cause GAS5 downregulation and miR-21 upregulation to compromise CD4 T cell functions. While data regarding GAS5 and miR-21 expression at day 0 (baseline level) are included in **Figures 1A,B**, we did not include this time point in the kinetic experiments due to limited cell volumes. However, our TCR kinetic stimulation results (**Figures 1F–K**) clearly indicate that GAS5 and miR-21 expressions are significantly regulated by T cell activation status. Notably, higher amounts of miR-21 and miR-146, along with Ago2, were detected in CD4 T cells from HIV and HS under TCR stimulation conditions, but with no significant differences between HIV and HS, indicating that the altered function of miR-21 in CD4 T cells is driven by GAS5 rather than Ago2. Since miRNAs form a duplex–with one strand preferentially loaded into AGO2 to generate a functional miRNA-induced silencing complex (miRISC)–it is likely that more miRNAs are loaded onto the Ago2-miRISC in CD4 T cells under TCR activation. Indeed, we and others have shown that ART-controlled PLHIV with no detectable viral replication can still exhibit an immune aging phenotype. We thus believe that the observed changes in GAS5 and miR-21 expression and dysregulations of CD4T cell functions in these virus-controlled PLHIV are likely induced by either immunologic scarring during early active viral infection or, perhaps more likely, by low-grade inflammation and persistent T cell activation during latent viral infection, or both. Our interpretation of the cumulative data would include the notion that CD4 T cells in PLHIV on ART exhibit an immune aging phenotype induced by a myriad of viral/host factors, including HIV reservoirs, that may secrete undetectable viral components, pro-inflammatory mediators, increased ROS levels, increased gut permeability and gut microbiota, coinfection with other pathogens (such as HBV, HCV, EBV, and CMV), ART regimens, associated malignancies, and social-related stresses (56–63), all of which may contribute to the failure to restore CD4 T cell homeostasis and/or functionality. These factors can lead to persistent, low-grade inflammation, causing T cell over-activation, exhaustion, senescence, apoptosis, and decreased proliferative potential, as our results suggest. Importantly, such inflammation-driven DNA damage promotes an inflammaging phenotype and exposes the immune system to unique challenges that could lead to CD4 T cell exhaustion, senescence, apoptosis, and homeostasis–a major driver of the increased incidences of infections, cancers, cardiovascular, and neurodegenerative diseases, similar to that observed in the elderly. Therefore, this premature immune aging process puts PLHIV at greater risk of morbidity and mortality.

It should be pointed out that, while the decrease in GAS5 and increase in miR-21 can explain both DNA damage and cell apoptosis, their presence can also result in both overwhelming cell death in acute infection and immune tolerance or immune suppression in chronic infection. Nevertheless, our findings identify, for the first time, the role of the GAS5-miR-21 axis in CD4 T cell dysregulation in PLHIV and shed light on the molecular aspects of immunomodulation during human viral infections. Given the broad regulatory effects of both GAS5 and miR-21, the decline in GAS5 and increase in miR-21 may impair diverse cellular functions during chronic HIV infection. Thus, interrupting this GAS5-miR21 axis may restore CD4 T cell homeostasis and competency during latent HIV infection and prevent premature CD4 T cell aging or immune senescence. This study reveals a novel molecular mechanism underlying CD4 T cell aging and provides a new strategy to develop innovative approaches to correct the aberrant immunopathology, to avoid the untoward consequences of immune senescence and to improve immunotherapy as well as vaccine responses against human viral diseases.

DATA AVAILABILITY STATEMENT

The original contributions presented in the study are included in the article/supplementary material, further inquiries can be directed to the corresponding author/s.

ETHICS STATEMENT

The studies involving human participants were reviewed and approved by East Tennessee State University and James H. Quillen VA Medical Center. The patients/participants provided their written informed consent to participate in this study.

AUTHOR CONTRIBUTIONS

LNTN performed most of the experiments. LNN, JZhao, MS, XD, DC, SK, BC, and ZLu participated in some experiments. XW and ZM provided technical support. SN, ME, LW, JZhang, ZLi, and JM offered intellectual input for troubleshooting and discussion of the findings. ZY supervised the project and wrote the manuscript, with the help of LNTN, LNN, JZhang, MS, XD, DC, SK, BC, ZLu, JZhang, ZLi, ZM, XW, ME, SN, LW,

and JM. All authors contributed to the article and approved the submitted version.

FUNDING

This work was supported by National Institutes of Health grants R01AI114748 and R21AI138598 (to ZY) and R15AI143377 (to JM); VA Merit Review Awards 1I01BX002670 and 1I01BX004281 (to ZY) and S10OD021572 (to JM); DoD Award PR170067 (to ZY). This publication is the result of work supported with resources and the use of facilities at the James H. Quillen Veterans Affairs Medical Center. The contents in this publication do not represent the views of the Department of Veterans Affairs or the United States Government.

REFERENCES

1. Galvani AP, Pandey A, Fitzpatrick MC, Medlock J, Gray GE. Defining control of HIV epidemics. *Lancet HIV.* (2018) 5:e667–e670. doi: 10.1016/S2352-3018(18)30178-4
2. Tyagi M, Bukrinsky M. Human immunodeficiency virus (HIV) latency: the major hurdle in HIV eradication. *Mol Med.* (2012) 18:1096–108. doi: 10.2119/molmed.2012.00194
3. Okoye AA, Picker LJ. CD4(+) T-cell depletion in HIV infection: mechanisms of immunological failure. *Immunol Rev.* (2013) 254:54–64. doi: 10.1111/imr.12066
4. Vidya Vijayan KK, Karthigeyan KP, Tripathi SP, Hanna LE. Pathophysiology of CD4+ T-Cell Depletion in HIV-1 and HIV-2 Infections. *Front Immunol.* (2017) 8:580. doi: 10.3389/fimmu.2017.00580
5. Lederman MM, Calabrese L, Funderburg NT, Clagett B, Medvik K, Bonilla H, et al. Immunologic failure despite suppressive antiretroviral therapy is related to activation and turnover of memory CD4 cells. *J Infect Dis.* (2011) 204:1217–26. doi: 10.1093/infdis/jir507
6. Piconi S, Trabattoni D, Gori A, Parisotto S, Magni C, Meraviglia P, et al. Immune activation, apoptosis, and Treg activity are associated with persistently reduced CD4+ T-cell counts during antiretroviral therapy. *AIDS.* (2010) 24:1991–2000. doi: 10.1097/QAD.0b013e32833c93ce
7. Bestilny LJ, Gill MJ, Mody CH, Riabowol KT. Accelerated replicative senescence of the peripheral immune system induced by HIV infection. *AIDS.* (2000) 14:771–80. doi: 10.1097/00002030-200005050-00002
8. Blanco JR, Jarrin I, Martinez A, Siles E, Larrayoz IM, Canuelo A, et al. Shorter telomere length predicts poorer immunological recovery in virologically suppressed HIV-1-infected patients treated with combined antiretroviral therapy. *J Acquir Immune Defic Syndr.* (2015) 68:21–9. doi: 10.1097/QAI.0000000000000398
9. Leung JM, Fishbane N, Jones M, Morin A, Xu S, Liu JC, et al. Longitudinal study of surrogate aging measures during human immunodeficiency virus seroconversion. *Aging.* (2017) 9:687–705. doi: 10.18632/aging.101184
10. Malaspina A, Moir S, Orsega SM, Vasquez J, Miller NJ, Donoghue ET, et al. Compromised B cell responses to influenza vaccination in HIV-infected individuals. *J Infect Dis.* (2005) 191:1442–50. doi: 10.1086/429298
11. Kirkwood TB. Understanding the odd science of aging. *Cell.* (2005) 120:437–47. doi: 10.1016/j.cell.2005.01.027
12. Tedone E, Huang E, O'Hara R, Batten K, Ludlow AT, Lai TP, et al. Telomere length and telomerase activity in T cells are biomarkers of high-performing centenarians. *Aging Cell.* (2019) 18:e12859. doi: 10.1111/acel.12859
13. Bartel DP. MicroRNAs: genomics, biogenesis, mechanism, and function. *Cell.* (2004) 116:281–97. doi: 10.1016/S0092-8674(04)00045-5
14. Jandura A, Krause HM. The new RNA world: growing evidence for long noncoding RNA functionality. *Trends Genet.* (2017) 33:665–76. doi: 10.1016/j.tig.2017.08.002
15. Morceau F, Chateauvieux S, Gaigneaux A, Dicato M, Diederich M. Long and short non-coding RNAs as regulators of hematopoietic differentiation. *Int J Mol Sci.* (2013) 14:14744–70. doi: 10.3390/ijms140714744
16. Zhang X, Hong R, Chen W, Xu M, Wang L. The role of long noncoding RNA in major human disease. *Bioorg Chem.* (2019) 92:103214. doi: 10.1016/j.bioorg.2019.103214
17. Consortium EP, Birney E, Stamatoyannopoulos JA, Dutta A, Guigo R, Gingeras TR, et al. Identification and analysis of functional elements in 1% of the human genome by the ENCODE pilot project. *Nature.* (2007) 447:799–816. doi: 10.1038/nature05874
18. Schneilder CKR, Phillipson L. Genes specifically expressed at growth arrest of mammalian cells. *Cell.* (1988) 54:787–93. doi: 10.1016/S0092-8674(88)91065-3
19. Lin J, Liu Z, Liao S, Li E, Wu X, Zeng W. Elevation of long non-coding RNA GAS5 and knockdown of microRNA-21 up-regulate RECK expression to enhance esophageal squamous cell carcinoma cell radio-sensitivity after radiotherapy. *Genomics.* (2020) 112:2173–85. doi: 10.1016/j.ygeno.2019.12.013
20. Mourtada-Maarabouni M, Pickard MR, Hedge VL, Farzaneh F, Williams GT. GAS5, a non-protein-coding RNA, controls apoptosis and is downregulated in breast cancer. *Oncogene.* (2009) 28:195–208. doi: 10.1038/onc.2008.373
21. Sun M, Jin FY, Xia R, Kong R, Li JH, Xu TP, et al. Decreased expression of long noncoding RNA GAS5 indicates a poor prognosis and promotes cell proliferation in gastric cancer. *BMC Cancer.* (2014) 14:319. doi: 10.1186/1471-2407-14-319
22. Wang G, Sun J, Zhao H, Li H. Long non-coding RNA (lncRNA) growth arrest specific 5 (GAS5) suppresses esophageal squamous cell carcinoma cell proliferation and migration by inactivating phosphatidylinositol 3-kinase (PI3K)/AKT/mammalian target of rapamycin (mTOR) signaling pathway. *Med Sci Monit.* (2018) 24:7689–96. doi: 10.12659/MSM.910867
23. Wang Y, Wu S, Yang X, Li X, Chen R. Association between polymorphism in the promoter region of lncRNA GAS5 and the risk of colorectal cancer. *Biosci Rep.* (2019) 39:BSR20190091. doi: 10.1042/BSR20190091
24. Zhang Z, Zhu Z, Watabe K, Zhang X, Bai C, Xu M, et al. Negative regulation of lncRNA GAS5 by miR-21. *Cell Death Differ.* (2013) 20:1558–68. doi: 10.1038/cdd.2013.110
25. Kim C, Hu B, Jadhav RR, Jin J, Zhang H, Cavanagh MM, et al. Activation of miR-21-regulated pathways in immune aging selects against signatures characteristic of memory T cells. *Cell Rep.* (2018) 25:2148–62.e2145. doi: 10.1016/j.celrep.2018.10.074
26. Kunze-Schumacher H, Winter SJ, Imelmann E, Krueger A. miRNA miR-21 is largely dispensable for intrathymic T-cell development. *Front Immunol.* (2018) 9:2497. doi: 10.3389/fimmu.2018.02497
27. Lu TX, Hartner J, Lim EJ, Fabry V, Mingler MK, Cole ET, et al. MicroRNA-21 limits in vivo immune response-mediated activation of the IL-12/IFN-gamma pathway, Th1 polarization, and the severity of delayed-type hypersensitivity. *J Immunol.* (2011) 187:3362–73. doi: 10.4049/jimmunol.1101235
28. Sheedy FJ. Turning 21: induction of miR-21 as a key switch in the inflammatory response. *Front Immunol.* (2015) 6:19. doi: 10.3389/fimmu.2015.00019
29. Chen L, Chen L, Zuo L, Gao Z, Shi Y, Yuan P, et al. Short communication: long noncoding RNA GAS5 inhibits HIV-1 replication through interaction with miR-873. *AIDS Res Hum Retroviruses.* (2018) 34:544–9. doi: 10.1089/aid.2017.0177
30. Cao D, Khanal S, Wang L, Li Z, Zhao J, Nguyen LN, et al. A matter of life or death: productively infected and bystander CD4 T cells in early HIV infection. *Front Immunol.* (2021) 11:626431. doi: 10.3389/fimmu.2020.626431
31. Cao D, Zhao J, Nguyan LN, Nguyen LNT, Khanal S, Dang X, et al. Disruption of telomere integrity and DNA repair machineries by KML001 induces T cell senescence, apoptosis, and cellular dysfunctions. *Front Immunol.* (2019) 10:1152. doi: 10.3389/fimmu.2019.01152
32. Dang X, Ogbu SC, Zhao J, Nguyen LNT, Cao D, Nguyen LN, et al. Inhibition of topoisomerase IIA (Top2alpha) induces telomeric DNA damage and T cell dysfunction during chronic viral infection. *Cell Death Dis.* (2020) 11:196. doi: 10.1038/s41419-020-2395-2

33. Ji Y, Dang X, Nguyen LNT, Nguyen LN, Zhao J, Cao D, et al. Topological DNA damage, telomere attrition and T cell senescence during chronic viral infections. *Immun Ageing.* (2019) 16:12. doi: 10.1186/s12979-019-0153-z
34. Khanal S, Tang Q, Cao D, Zhao J, Nguyen LN, Oyedeji OS, et al. Telomere and ATM dynamics in CD4 T-cell depletion in active and virus-suppressed HIV infections. *J Virol.* (2020) 94:e01061–20. doi: 10.1128/JVI.01061-20
35. Schank M, Zhao J, Wang L, Li Z, Cao D, Nguyen LN, et al. Telomeric injury by KML001 in human T cells induces mitochondrial dysfunction through the p53-PGC-1alpha pathway. *Cell Death Dis.* (2020) 11:1030. doi: 10.1038/s41419-020-03238-7
36. Zhao J, Nguyen LNT, Nguyen LN, Dang X, Cao D, Khanal S, et al. ATM deficiency accelerates DNA damage, telomere erosion, and premature T cell aging in HIV-infected individuals on antiretroviral therapy. *Front Immunol.* (2019) 10:2531. doi: 10.3389/fimmu.2019.02531
37. Pickard MR, Williams GT. Molecular and cellular mechanisms of action of tumour suppressor GAS5 LncRNA. *Genes.* (2015) 6:484–99. doi: 10.3390/genes6030484
38. Yu T, Ju Z, Luo M, Hu R, Teng Y, Xie L, et al. Elevated expression of miR-146a correlates with high levels of immune cell exhaustion markers and suppresses cellular immune function in chronic HIV-1-infected patients. *Sci Rep.* (2019) 9:18829. doi: 10.1038/s41598-019-55100-2
39. Palmer BE, Neff CP, Lecureux J, Ehler A, Dsouza M, Remling-Mulder L, et al. In vivo blockade of the PD-1 receptor suppresses HIV-1 viral loads and improves CD4+ T cell levels in humanized mice. *J Immunol.* (2013) 190:211–9. doi: 10.4049/jimmunol.1201108
40. Porichis F, Kaufmann DE. Role of PD-1 in HIV pathogenesis and as target for therapy. *Curr HIV/AIDS Rep.* (2012) 9:81–90. doi: 10.1007/s11904-011-0106-4
41. De Paoli P, Zanussi S, Simonelli C, Bortolin MT, D'Andrea M, Crepaldi C, et al. Effects of subcutaneous interleukin-2 therapy on CD4 subsets and in vitro cytokine production in HIV+ subjects. *J Clin Invest.* (1997) 100:2737–43. doi: 10.1172/JCI119819
42. Sereti I, Sklar P, Ramchandani MS, Read SW, Aggarwal V, Imamichi H, et al. CD4+ T cell responses to interleukin-2 administration in HIV-infected patients are directly related to the baseline level of immune activation. *J Infect Dis.* (2007) 196:677–83. doi: 10.1086/520087
43. Yu Q, Sharma A, Sen JM. TCF1 and beta-catenin regulate T cell development and function. *Immunol Res.* (2010) 47:45–55. doi: 10.1007/s12026-009-8137-2
44. Dong Z, Li S, Wang X, Si L, Ma R, Bao L, et al. lncRNA GAS5 restrains CCl4-induced hepatic fibrosis by targeting miR-23a through the PTEN/PI3K/Akt signaling pathway. *Am J Physiol Gastrointest Liver Physiol.* (2019) 316:G539–G550. doi: 10.1152/ajpgi.00249.2018
45. Zhang XF, Ye Y, Zhao SJ. LncRNA Gas5 acts as a ceRNA to regulate PTEN expression by sponging miR-222-3p in papillary thyroid carcinoma. *Oncotarget.* (2018) 9:11. doi: 10.18632/oncotarget.23336
46. Sharma NS, Gnamlin P, Durden B, Gupta VK, Kesh K, Garrido VT, et al. Long non-coding RNA GAS5 acts as proliferation "brakes" in CD133+ cells responsible for tumor recurrence. *Oncogenesis.* (2019) 8:68. doi: 10.1038/s41389-019-0177-4
47. Mourtada-Maarabouni M, Hedge VL, Kirkham L, Farzaneh F, Williams GT. Growth arrest in human T-cells is controlled by the non-coding RNA growth-arrest-specific transcript 5 (GAS5). *J Cell Sci.* (2008) 121 (Pt. 7):939–46. doi: 10.1242/jcs.024646
48. Yang Y, Shen Z, Yan Y, Wang B, Zhang J, Shen C, et al. Long non-coding RNA GAS5 inhibits cell proliferation, induces G0/G1 arrest and apoptosis, and functions as a prognostic marker in colorectal cancer. *Oncol Lett.* (2017) 13:3151–8. doi: 10.3892/ol.2017.5841
49. Ji J, Dai X, Yeung SJ, He X. The role of long non-coding RNA GAS5 in cancers. *Cancer Manag Res.* (2019) 11:2729–37. doi: 10.2147/CMAR.S189052
50. Bautista-Sanchez D, Arriaga-Canon C, Pedroza-Torres A, De La Rosa-Velazquez IA, Gonzalez-Barrios R, Contreras-Espinosa L, et al. The promising role of miR-21 as a cancer biomarker and its importance in RNA-based therapeutics. *Mol Ther Nucleic Acids.* (2020) 20:409–20. doi: 10.1016/j.omtn.2020.03.003
51. Carissimi C, Carucci N, Colombo T, Piconese S, Azzalin G, Cipolletta E, et al. miR-21 is a negative modulator of T-cell activation. *Biochimie.* (2014) 107 (Pt. B):319–26. doi: 10.1016/j.biochi.2014.09.021
52. Meng F, Henson R, Wehbe-Janek H, Ghoshal K, Jacob ST, Patel T. MicroRNA-21 regulates expression of the PTEN tumor suppressor gene in human hepatocellular cancer. *Gastroenterology.* (2007) 133:647–58. doi: 10.1053/j.gastro.2007.05.022
53. Asangani IA, Rasheed SA, Nikolova DA, Leupold JH, Colburn NH, Post S, et al. MicroRNA-21 (miR-21) post-transcriptionally downregulates tumor suppressor Pdcd4 and stimulates invasion, intravasation and metastasis in colorectal cancer. *Oncogene.* (2008) 27:2128–36. doi: 10.1038/sj.onc.1210856
54. Ma S, Zhang A, Li X, Zhang S, Liu S, Zhao H, et al. MiR-21-5p regulates extracellular matrix degradation and angiogenesis in TMJOA by targeting Spry1. *Arthritis Res Ther.* (2020) 22:99. doi: 10.1186/s13075-020-2145-y
55. Persaud D, Pierson T, Ruff C, Finzi D, Chadwick KR, Margolick JB, et al. A stable latent reservoir for HIV-1 in resting CD4(+) T lymphocytes in infected children. *J Clin Invest.* (2000) 105:995–1003. doi: 10.1172/JCI9006
56. D'Amico R, Yang Y, Mildvan D, Evans SR, Schnizlein-Bick CT, Hafner R, et al. Lower CD4+ T lymphocyte nadirs may indicate limited immune reconstitution in HIV-1 infected individuals on potent antiretroviral therapy: analysis of immunophenotypic marker results of AACTG 5067. *J Clin Immunol.* (2005) 25:106–15. doi: 10.1007/s10875-005-2816-0
57. Desai SN, Landay AL. HIV and aging: role of the microbiome. *Curr Opin HIV AIDS.* (2018) 13:22–7. doi: 10.1097/COH.0000000000000433
58. Engsig FN, Gerstoft J, Kronborg G, Larsen CS, Pedersen G, Roge B, et al. Long-term mortality in HIV patients virally suppressed for more than three years with incomplete CD4 recovery: a cohort study. *BMC Infect Dis.* (2010) 10:318. doi: 10.1186/1471-2334-10-318
59. Greub G, Ledergerber B, Battegay M, Grob P, Perrin L, Furrer H, et al. Clinical progression, survival, and immune recovery during antiretroviral therapy in patients with HIV-1 and hepatitis C virus coinfection: the Swiss HIV cohort study. *Lancet.* (2000) 356:1800–5. doi: 10.1016/S0140-6736(00)03232-3
60. Montejano R, Stella-Ascariz N, Monge S, Bernardino JI, Perez-Valero I, Montes ML, et al. Impact of antiretroviral treatment containing tenofovir difumarate on the telomere length of aviremic HIV-infected patients. *J Acquir Immune Defic Syndr.* (2017) 76:102–9. doi: 10.1097/QAI.0000000000001391
61. Moore RD, Keruly JC. CD4+ cell count 6 years after commencement of highly active antiretroviral therapy in persons with sustained virologic suppression. *Clin Infect Dis.* (2007) 44:441–6. doi: 10.1086/510746
62. Nasi M, De Biasi S, Gibellini L, Bianchini E, Pecorini S, Bacca V, et al. Ageing and inflammation in patients with HIV infection. *Clin Exp Immunol.* (2017) 187:44–52. doi: 10.1111/cei.12814
63. Taddei TH, Lo Re V III, Justice AC. HIV, aging, and viral coinfections: taking the long view. *Curr HIV/AIDS Rep.* (2016) 13:269–78. doi: 10.1007/s11904-016-0327-7

Conflict of Interest: The authors declare that the research was conducted in the absence of any commercial or financial relationships that could be construed as a potential conflict of interest.

frontiers in Immunology

MINI REVIEW
published: 19 March 2021
doi: 10.3389/fimmu.2021.657679

Gut Microbiome Homeostasis and the CD4 T- Follicular Helper Cell IgA Axis in Human Immunodeficiency Virus Infection

Olusegun O. Onabajo[1] *and Joseph J. Mattapallil*[2]*

[1] Laboratory of Translational Genomics, Division of Cancer Epidemiology and Genetics, National Cancer Institute, National Institutes of Health (NIH), Bethesda, MD, United States, [2] F. E. Hebert School of Medicine, Uniformed Services University, Bethesda, MD, United States

Human Immunodeficiency Virus (HIV) and Simian Immunodeficiency Virus (SIV) are associated with severe perturbations in the gut mucosal environment characterized by massive viral replication and depletion of CD4 T cells leading to dysbiosis, breakdown of the epithelial barrier, microbial translocation, immune activation and disease progression. Multiple mechanisms play a role in maintaining homeostasis in the gut mucosa and protecting the integrity of the epithelial barrier. Among these are the secretory IgA (sIgA) that are produced daily in vast quantities throughout the mucosa and play a pivotal role in preventing commensal microbes from breaching the epithelial barrier. These microbe specific, high affinity IgA are produced by IgA+ plasma cells that are present within the Peyer's Patches, mesenteric lymph nodes and the isolated lymphoid follicles that are prevalent in the lamina propria of the gastrointestinal tract (GIT). Differentiation, maturation and class switching to IgA producing plasma cells requires help from T follicular helper (Tfh) cells that are present within these lymphoid tissues. HIV replication and CD4 T cell depletion is accompanied by severe dysregulation of Tfh cell responses that compromises the generation of mucosal IgA that in turn alters barrier integrity leading to commensal bacteria readily breaching the epithelial barrier and causing mucosal pathology. Here we review the effect of HIV infection on Tfh cells and mucosal IgA responses in the GIT and the consequences these have for gut dysbiosis and mucosal immunopathogenesis.

Keywords: HIV, SIV, microbiome, Tfh, IgA, mucosa, GALT, microbial translocation

OPEN ACCESS

Edited by:
Vijayakumar Velu,
Emory University, United States

Reviewed by:
Huanbin Xu,
Tulane University, United States
Suresh Pallikkuth,
University of Miami, United States

***Correspondence:**
Joseph J. Mattapallil
joseph.mattapallil@usuhs.edu

Specialty section:
This article was submitted to Viral Immunology, a section of the journal Frontiers in Immunology

Received: *23 January 2021*
Accepted: *01 March 2021*
Published: *19 March 2021*

Citation:
Onabajo OO and Mattapallil JJ (2021) Gut Microbiome Homeostasis and the CD4 T- Follicular Helper Cell IgA Axis in Human Immunodeficiency Virus Infection. Front. Immunol. 12:657679. doi: 10.3389/fimmu.2021.657679

INTRODUCTION

Human and Simian Immunodeficiency Virus (HIV, SIV) infections are associated with dramatic changes in mucosal tissues such as the gastrointestinal tract (GIT) with massive replication and depletion of CD4 T cells during the acute stages of infection (1–17). Viral replication and associated inflammation persists in these tissues over the course of infection that is accompanied by damage to intestinal epithelial barrier, translocation of microbial products, immune activation and progressive

loss of CD4 T cells (18–22). Though peripheral tissues experience significant levels of restoration after antiretroviral therapy, viral replication in mucosal tissues continues to persist with incomplete restoration of the immune system to a homeostatic state (23–38). As such, the inflammatory microenvironment in the mucosa remains in a state of high activation that is driven by microbial antigens that traverse the leaky epithelial barrier damaged during infection.

The GIT hosts the largest collection of microbes in the human body with bacteria accounting for a majority of the gut microflora. Studies have estimated that there are over 35,000 bacterial species in the human gut (39), a diversity that is only matched by the sheer magnitude of bacteria colonizing the GIT with estimates ranging from 10^{11} – 10^{13} bacteria (40). Within the GIT, the large intestine accounts for over 70% of the microbes that colonize the human body (41).

The resilience of the gastrointestinal mucosa to withstand continuous exposure to foreign antigens alongside the vast magnitude of microbes and their byproducts is exemplified by the homeostatic state that is maintained throughout life that ensures both intestinal and overall health. This homeostatic balance is maintained by a complex interplay between the host immune system and the gut microbiota that is characterized by a combination of tolerant and antigen specific immune responses that is constantly shaped and modulated by the microbes that reside in the GIT. This symbiotic relationship allows for physiological functions to proceed normally in a tightly controlled immunoregulatory environment. This regulation is essential to prevent any immunopathology that may develop due to responses to continuous exposure to both dietary and microbial antigens.

How the mucosal immune system regulates the mucosal microenvironment and at the same time keeps microbes from crossing the intestinal barrier has been an area of extensive research. In addition to innate mechanisms such as the thick mucus lining the mucosal surface, anti-microbial proteins like defensins, and lectins such as RegIIIγ (42–47), numerous studies have delineated the critical role for antibody responses such as microbe specific secretory IgA (sIgA) in preventing invasive microbes from breaching the epithelial barrier and gaining entry into the submucosa and systemic circulation (48–51).

IgA AND ANTIMICROBIAL IMMUNITY

Secretory IgA is the primary immunoglobulin found on mucosal surfaces and exists as a dimer that is bound to each other by the J chain, 15 kD polypeptide (52–55). The J chain binds to cysteine residues in the Fc regions of the heavy chain *via* disulphide bonds (55). Dimeric IgA is transported across the epithelium lining the gut by the polymeric immunoglobulin receptor that binds to IgA on the basolateral side of the epithelium and plays a role in transporting the sIgA across to the apical side and into the gut lumen (56–58). sIgA has significant antimicrobial activity and binds and neutralizes microbes, enhances agglutination of bacteria, and blocks cell adhesion thereby preventing access to the mucosal epithelium (56, 57).

MUCOSAL IgA AND T- FOLLICULAR HELPER CELLS

Secretory IgA is the most abundant antibody (~ 50 mg/Kg/day) found in the lumen of the GIT with the gut associated lymphoid tissue (GALT) hosting ~ 80% of IgA producing plasma cells in the body (59, 60). Microbe specific sIgA are induced in the Peyer's Patches and the lymphoid follicles in the GALT following antigen presentation by mucosal dendritic cells (DC) that sample and present microbial antigens to T and B cells. Following differentiation and class switching sIgA is transcytosed across the gut epithelium into the lumen of the GIT (61). sIgA are primarily generated in the Peyer's patches, isolated lymphoid follicles, and mesenteric lymph nodes that drain the GIT; mice lacking Peyer's patches have little or no IgA+ plasma cells and sIgA in the gut (62, 63). Isolated lymphoid follicles that develop in the lamina propria are significantly influenced by the microbiota colonizing the gut (64); in the absence of microbiota, germ free mice harbor low numbers of IgA producing plasma cells that secrete IgA that have low affinity to antigens and had failed to undergo somatic hypermutation. In contrast, in the presence of gut microbiota, B cells undergo class switch recombination and somatic hypermutation to produce antigen specific high affinity IgA (65, 66).

sIgA is abundant in mucosa associated lymphoid tissues (MALT) found in other mucosal sites such as the female genital tract (67), the LN that drain the upper and lower respiratory tracts (68). Unlike other MALT, however, Peyer's patches are unique and specialized for production of isotype switched IgA, while other MALT produce a mix of both IgA and IgG (68–70).

Unlike the isolated lymphoid follicles in the lamina propria that can generate IgA responses in a T cell independent manner, most of the T cell dependent induction of IgA responses occurs within the Peyer's patches and mesenteric lymph nodes (71–73). T cell dependent induction and differentiation of B cell responses relies on CD4 T cell help (74–78). Though different subsets of CD4 T cells such as Treg (79) and Th-17 (80, 81) have been shown to play a role in the generation of IgA responses in the GIT, T - follicular helper (Tfh) cells are essential for the generation of high affinity IgA responses (82).

Tfh cells are a subset of CD4 T cells that mainly reside in the germinal centers of lymph nodes and provide help to differentiating B cells during the germinal center reaction (83). Tfh cells express CXCR5, PD-1 and ICOS along with BCL6 (83–87), and are a primary source of IL-21, a key cytokine that drives the induction and differentiation of B cell responses (83, 86, 88, 89); mice lacking the IL-21 receptor was found to have defective antibody responses, class-switching, and germinal center (GC) formation (90). A number of other studies have established the central role of Tfh in the induction of high affinity B cell responses (83, 91).

T- FOLLICULAR HELPER CELLS AND HIV INFECTION

HIV and SIV infections are characterized by loss of CD4 T cells that compromises the immune system with viral reservoirs

persisting throughout the life of an infected subject (5, 92–104). Tfh cells residing within the lymph node GC have since been identified as a major source of the persistent latent and productive HIV reservoir (105) due to the inaccessibility of cytotoxic CD8 T cells into B cell follicles within the GC that creates a privileged environment for HIV replication and infection of Tfh cells, the predominant population of CD4 T cells in the follicles (106, 107). Numerous studies have explored the role of lymph nodes in HIV persistence and pathogenesis (108, 109). Perreau et al. (110) reported that HIV infected nonprogressors with low levels of viremia (<1000 HIV RNA copies) harbored high levels of HIV+ Tfh cells as compared to other CD4 T cells subsets. Similarly, SIV infection was associated with significantly high levels of infection in Tfh cells (111–113).

Other studies have reported that HIV specific Tfh significantly expand during chronic HIV infection (114). Similar findings have been reported in a subset of SIV infected macaques where an accumulation of Tfh cells in the lymph nodes that are latently infected is accompanied by higher frequencies of activated GC B cells and SIV specific antibody responses (112, 115–117). Mylvaganam et al. (118) demonstrated that SIV infection was associated with an increase in the frequency of aberrant Tfh in the lymphoid follicles of the rectal mucosa that correlated with lack of viral control. Loss of IL-21+ CD4 T cells was associated with the depletion of other T cell subsets such as Th17 cells and disease progression (119). Numerous studies have documented the depletion of Th17 cells in the mucosa and correlated them with microbial translocation and immune activation (5, 120, 121). A detailed phenotype of Tfh cells that is unique to the GIT is still under investigation. Tfh cells in other specialized lymphoid organs such as the spleen, however express typical Tfh markers, and were shown to decline early during SIV infection (122).

In contrast to the accumulation of Tfh in a subset of infected subjects, numerous studies have reported that HIV and SIV infection were characterized by a depletion of Tfh cells that was associated with altered B cell responses. Mesenteric lymph node Tfh cells were lost very early during SIV infection that was accompanied by a loss of GC and memory B cells (116, 122, 123). Others have reported that the development of both GC reaction and Tfh within these GCs were significantly impaired during HIV and SIV infections that likely contributed to the dysregulation of B cell responses (124–126). Rabezanahary et al. (127) reported a significant decline in Tfh cells in MLN and spleen of SIV infected animals, whereas McGray et al. (128) described a similar decline in the GIT of SIV infected animals during the acute stages of infection. Interestingly, Velu et al. (129) reported that Tfh that expand in the GC during chronic infection harbor a Th-1 bias that differed from conventional Tfh cells raising the possibility that accumulation or depletion of Tfh cells may depend on factors that drive their differentiation.

Despite early antiretroviral therapy, Tfh cells remain major reservoirs in lymphoid tissues and peripheral blood (127, 130, 131). Studies have shown that Tfh were a major source of replication competent HIV and persistent HIV-1 transcription in treated aviremic patients on long term HAART (132). Yu et al. reported that Tfh were enriched for replication competent X4 tropic HIV virus and correlated with progression of disease (133). HIV specific Tfh levels have been shown to significantly correlate with plasma HIV specific antibody levels during HAART (134). Early initiation of HAART maintained HIV-1-reactive memory B cells and Tfh in the gut (135). Rabezanahary et al. (127) reported that Tfh CD4+ T cells in the mesenteric lymph nodes harbor significant levels of viral DNA and RNA in SIV infected rhesus macaques treated with antiretroviral therapy suggesting that Tfh niches that reside in the lymph node GCs were major sites of viral persistence and like other sites are dysregulated during infection. Thornhill et al. (136) demonstrated that CD32 high doublets in the GALT of HIV infected subjects undergoing antiretroviral therapy were primarily composed of Tfh cells that correlated with high levels of rectal HIV DNA.

MUCOSAL B CELL RESPONSES AND HIV INFECTION

Mucosal IgA plays a critical role in protecting the mucosa from invasive bacteria that colonize the GIT (137). IgA are primarily produced in a T- cell dependent manner within the Peyer's Patches and mesenteric lymph node GC with Tfh driving the differentiation, maturation and class switching on B cells (90, 138–142). Chaoul et al. (143) examined T cell dependent IgA responses in the Peyer's Patches and isolated lymphoid follicles in SIV infected rhesus macaques and detected no IgA+ plasma cells in the GC at these sites during acute infection that was accompanied by a significant decrease in the amount of IgA detectable in the duodenum and ileum. Rather surprisingly, both GC and Tfh within the Peyer's Patches and isolated lymphoid follicles were functional and intact. Schäfer et al. (144) reported that the amount of total intestinal IgA decreased and remained low during the first few months after SIV infection. Likewise, numerous studies have reported low levels of IgA in mucosal secretions of HIV infected subjects (145–151) whereas Scamurra et al. (152) showed that low levels of IgA in intestinal secretions during HIV infection was associated with lower frequencies of IgA plasma cells in the GIT. It is highly likely that HIV infection significantly impairs B cell differentiation and IgA class switching in the GALT as reported by Xu et al. (153). Levesque et al. (154) reported that GALT GC display significant levels of apoptosis during HIV infection that do not effectively reconstitute after antiretroviral therapy (155). Given the central role of Tfh cells in this process, the loss or dysregulation of Tfh cells during HIV infection likely contributes to B cell dysfunction in the gut that in turn affects the protective mechanisms at the mucosal epithelial barrier. In line with this argument, Hel et al. (123) demonstrated that HIV infected subjects display lower gut microbiota specific IgA and IgG responses in the GIT that likely contributes to microbial translocation and chronic immune activation. Numerous studies have reported the breakdown of gut epithelial barrier during HIV and SIV infections (25, 121, 156–161).

GUT MICROBIOTA AND T - FOLLICULAR HELPER CELLS

The decrease in intestinal IgA is consequential given its central importance in preventing gut microbes from accessing the intestinal epithelium. Gut commensal bacteria and their metabolites play a role in inducing effector T cells and maintaining immune homeostasis in the GIT (162–167). Hegazy et al. (168) reported that gut microbiota reactive CD4 T cells in intestinal mucosa are readily detectable in healthy humans and were a normal feature of the repertoire of CD4 T cells. Likewise, the development of IgA responses is significantly influenced by the microbiota that colonize the gut (65). Large numbers of Tfh cells reside in the GC of Peyer's patches where gut microbes and their byproducts continuously shape the GC reaction and production of mucosal IgA (169, 170) that in turn regulates gut microbiome interactions with the host. Maruya et al. (171) reported that PD-1 deficiency alters the phenotype of Tfh cells leading to the induction of IgA with reduced capacity to bind gut bacteria that in turn leads to alterations in the composition of the commensal bacteria in the GIT. Loss of PD-1 was also associated with an increase in dysfunctional Tfh cells in the Peyer's patches that is characterized by reduced production of IL-21, increased secretion of IFNγ, and production of IgA with poor affinity maturation (172). Low affinity IgA responses were accompanied by a profound loss of "healthy bacteria" such as Bifidobacterium and Bacteroides, and an increase in *Enterobacteriaceae* (172). Others (173) have shown that Tfh cells within the Peyer's Patches play an essential role in systemic arthritis induced by segmented filamentous bacteria by inhibiting IL-2 signaling with DCs contributing to SFB-mediated Tfh cell induction and IL-2 receptor α (IL-2Rα) suppression. IL-2 signaling pathway has been shown to inhibit Tfh cell differentiation by altering Bcl-6 expression (174, 175). Impairment of Tfh cells, either due to lack of inhibitory co-receptor PD-1 or ATP-gated ionotropic P2RX7 receptors, was found to alter the gut commensal bacteria (172, 176). Micci et al. (119) reported that depletion of IL-21 producing CD4 T cells was associated with progression of SIV disease. Taken together, these findings suggest that compromise of mucosal Tfh cells and high affinity IgA responses probably play a role in altering the composition of gut microbiota during HIV infection.

HIV infection is associated with changes in the composition of the gut microbiota (22, 177, 178) characterized by a decrease in *Bacteroides and Firmicutes* and an increase in the prevalence *Proteobacteria* (179–181). Others have reported alterations in microbial richness (182) and *Prevotella* during chronic HIV infection (181, 183–186). Gut dysbiosis has been reported in SIV infected rhesus macaques that was partially restored with combination antiretroviral therapy (187). SIV infected macaques were found to display an expansion of enteropathogens during advanced stages of disease (188), and macaques with severe disease displayed changes in their bacterial diversity that was characterized by an altered abundance of *Enterobacteriaceae* and *Moraxellaceae* similar to that of HIV infected patients who have low CD4 T cell counts. Lower microbial richness and diversity was associated with poor CD4 T cell reconstitution in HIV infected subjects undergoing treatment with HAART (189, 190). Numerous studies have suggested that some level of gut dysbiosis persists during HAART. Likewise, Tfh cells dysregulated during HIV infection are not fully restored to their healthy state during HART suggesting that B cell dysfunction is likely to persist during therapy that in turn could lead to inadequate protection of the epithelial barrier.

In conclusion, the dysregulation of Tfh cells that compromises B cell responses especially the secretion of microbe specific IgA is one of the likely drivers of gut microbial dysbiosis during HIV infection. This dysregulation that accompanies high levels of HIV replication, loss of mucosal CD4 T cells, breakdown of the integrity of epithelial barrier significantly alters mucosal immune homeostasis leading to microbial translocation, immune activation and progression of disease. Strategies that can preserve and maintain Tfh responses in the mucosa could potentially restore high affinity mucosal IgA that could aid in protecting the mucosal epithelial barrier from invasive dysbiotic bacteria.

AUTHOR CONTRIBUTIONS

OO and JM wrote the manuscript. All authors contributed to the article and approved the submitted version.

ACKNOWLEDGMENTS

The opinions or assertions contained herein are the private ones of the authors and are not to be construed as official or reflecting the views of the Department of the Navy, Department of Defense, the Uniformed Services University of the Health Sciences, National Institutes of Health or any other agency of the U.S. Government.

REFERENCES

1. Allers K, Kunkel D, Hofmann J, Stahl-Hennig C, Moos V, Schneider T. Cell-Associated Simian Immunodeficiency Virus Accelerates Initial Virus Spread and CD4+ T-Cell Depletion in the Intestinal Mucosa. *J Infect Dis* (2018) 217:1421–5. doi: 10.1093/infdis/jiy055
2. Brenchley JM, Douek DC. HIV infection and the gastrointestinal immune system. *Mucosal Immunol* (2008) 1:23–30. doi: 10.1038/mi.2007.1
3. Eberly MD, Kader M, Hassan W, Rogers KA, Zhou J, Mueller YM, et al. Increased IL-15 production is associated with higher susceptibility of memory CD4 T cells to simian immunodeficiency virus during acute infection. *J Immunol* (2009) 182:1439–48. doi: 10.4049/jimmunol.182.3.1439
4. George J, Johnson RC, Mattapallil MJ, Renn L, Rabin R, Merrell DS, et al. Gender differences in innate responses and gene expression profiles in memory CD4 T cells are apparent very early during acute simian immunodeficiency virus infection. *PloS One* (2019) 14:e0221159. doi: 10.1371/journal.pone.0221159

5. Kader M, Wang X, Piatak M, Lifson J, Roederer M, Veazey R, et al. Alpha4 (+)beta7(hi)CD4(+) memory T cells harbor most Th-17 cells and are preferentially infected during acute SIV infection. *Mucosal Immunol* (2009) 2:439–49. doi: 10.1038/mi.2009.90
6. Kovacs SB, Sheikh V, Thompson WL, Morcock DR, Perez-Diez A, Yao MD, et al. T-Cell Depletion in the Colonic Mucosa of Patients With Idiopathic CD4+ Lymphopenia. *J Infect Dis* (2015) 212:1579–87. doi: 10.1093/infdis/jiv282
7. Li Q, Duan L, Estes JD, Ma ZM, Rourke T, Wang Y, et al. Peak SIV replication in resting memory CD4+ T cells depletes gut lamina propria CD4+ T cells. *Nature* (2005) 434:1148–52. doi: 10.1038/nature03513
8. Mattapallil JJ, Douek DC, Hill B, Nishimura Y, Martin M, Roederer M. Massive infection and loss of memory CD4+ T cells in multiple tissues during acute SIV infection. *Nature* (2005) 434:1093–7. doi: 10.1038/nature03501
9. Mattapallil JJ, Letvin NL, Roederer M. T-cell dynamics during acute SIV infection. *AIDS* (2004) 18:13–23. doi: 10.1097/00002030-200401020-00002
10. Mattapallil JJ, Roederer M. Acute HIV infection: it takes more than guts. *Curr Opin HIV AIDS* (2006) 1:10–5. doi: 10.1097/01.COH.0000191896.70685.74
11. Moore AC, Bixler SL, Lewis MG, Verthelyi D, Mattapallil JJ. Mucosal and peripheral Lin- HLA-DR+ CD11c/123- CD13+ CD14- mononuclear cells are preferentially infected during acute simian immunodeficiency virus infection. *J Virol* (2012) 86:1069–78. doi: 10.1128/JVI.06372-11
12. Nishimura Y, Brown CR, Mattapallil JJ, Igarashi T, Buckler-White A, Lafont BA, et al. Resting naive CD4+ T cells are massively infected and eliminated by X4-tropic simian-human immunodeficiency viruses in macaques. *Proc Natl Acad Sci U.S.A.* (2005) 102:8000–5. doi: 10.1073/pnas.0503233102
13. Smit-McBride Z, Mattapallil JJ, McChesney M, Ferrick D, Dandekar S. Gastrointestinal T lymphocytes retain high potential for cytokine responses but have severe CD4(+) T-cell depletion at all stages of simian immunodeficiency virus infection compared to peripheral lymphocytes. *J Virol* (1998) 72:6646–56. doi: 10.1128/JVI.72.8.6646-6656.1998
14. Song K, Rabin RL, Hill BJ, De Rosa SC, Perfetto SP, Zhang HH, et al. Characterization of subsets of CD4+ memory T cells reveals early branched pathways of T cell differentiation in humans. *Proc Natl Acad Sci U.S.A.* (2005) 102:7916–21. doi: 10.1073/pnas.0409720102
15. Tokarev A, McKinnon LR, Pagliuzza A, Sivro A, Omole TE, Kroon E, et al. Preferential Infection of alpha4beta7+ Memory CD4+ T Cells During Early Acute Human Immunodeficiency Virus Type 1 Infection. *Clin Infect Dis* (2020) 71:e735–e43. doi: 10.1093/cid/ciaa497
16. Veazey RS. Intestinal CD4 Depletion in HIV / SIV Infection. *Curr Immunol Rev* (2019) 15:76–91. doi: 10.2174/1573395514666180605083448
17. Veazey RS, DeMaria M, Chalifoux LV, Shvetz DE, Pauley DR, Knight HL, et al. Gastrointestinal tract as a major site of CD4+ T cell depletion and viral replication in SIV infection. *Science* (1998) 280:427–31. doi: 10.1126/science.280.5362.427
18. Brenchley JM, Price DA, Schacker TW, Asher TE, Silvestri G, Rao S, et al. Microbial translocation is a cause of systemic immune activation in chronic HIV infection. *Nat Med* (2006) 12:1365–71. doi: 10.1038/nm1511
19. Epple HJ, Zeitz M. HIV infection and the intestinal mucosal barrier. *Ann N Y Acad Sci* (2012) 1258:19–24. doi: 10.1111/j.1749-6632.2012.06512.x
20. Gordon SN, Cervasi B, Odorizzi P, Silverman R, Aberra F, Ginsberg G, et al. Disruption of intestinal CD4+ T cell homeostasis is a key marker of systemic CD4+ T cell activation in HIV-infected individuals. *J Immunol* (2010) 185:5169–79. doi: 10.4049/jimmunol.1001801
21. Marchetti G, Tincati C, Silvestri G. Microbial translocation in the pathogenesis of HIV infection and AIDS. *Clin Microbiol Rev* (2013) 26:2–18. doi: 10.1128/CMR.00050-12
22. Mudd JC, Brenchley JM. Gut Mucosal Barrier Dysfunction, Microbial Dysbiosis, and Their Role in HIV-1 Disease Progression. *J Infect Dis* (2016) 214 Suppl 2:S58–66. doi: 10.1093/infdis/jiw258
23. Brown D, Mattapallil JJ. Gastrointestinal tract and the mucosal macrophage reservoir in HIV infection. *Clin Vaccine Immunol* (2014) 21:1469–73. doi: 10.1128/CVI.00518-14
24. Cassol E, Malfeld S, Mahasha P, Bond R, Slavik T, Seebregts C, et al. Impaired CD4+ T-cell restoration in the small versus large intestine of HIV-1-positive South Africans receiving combination antiretroviral therapy. *J Infect Dis* (2013) 208:1113–22. doi: 10.1093/infdis/jit249
25. Estes JD, Harris LD, Klatt NR, Tabb B, Pittaluga S, Paiardini M, et al. Damaged intestinal epithelial integrity linked to microbial translocation in pathogenic simian immunodeficiency virus infections. *PloS Pathog* (2010) 6:e1001052. doi: 10.1371/journal.ppat.1001052
26. George J, Wagner W, Lewis MG, Mattapallil JJ. Significant Depletion of CD4 (+) T Cells Occurs in the Oral Mucosa during Simian Immunodeficiency Virus Infection with the Infected CD4(+) T Cell Reservoir Continuing to Persist in the Oral Mucosa during Antiretroviral Therapy. *J Immunol Res* (2015) 2015:673815. doi: 10.1155/2015/673815
27. Kader M, Bixler S, Roederer M, Veazey R, Mattapallil JJ. CD4 T cell subsets in the mucosa are CD28+Ki-67-HLA-DR-CD69+ but show differential infection based on alpha4beta7 receptor expression during acute SIV infection. *J Med Primatol* (2009) 38 Suppl 1:24–31. doi: 10.1111/j.1600-0684.2009.00372.x
28. Kader M, Hassan WM, Eberly M, Piatak M, Lifson JD, Roederer M, et al. Antiretroviral therapy prior to acute viral replication preserves CD4 T cells in the periphery but not in rectal mucosa during acute simian immunodeficiency virus infection. *J Virol* (2008) 82:11467–71. doi: 10.1128/JVI.01143-08
29. Klatt NR, Canary LA, Vanderford TH, Vinton CL, Engram JC, Dunham RM, et al. Dynamics of simian immunodeficiency virus SIVmac239 infection in pigtail macaques. *J Virol* (2012) 86:1203–13. doi: 10.1128/JVI.06033-11
30. Klatt NR, Chomont N, Douek DC, Deeks SG. Immune activation and HIV persistence: implications for curative approaches to HIV infection. *Immunol Rev* (2013) 254:326–42. doi: 10.1111/imr.12065
31. Klatt NR, Funderburg NT, Brenchley JM. Microbial translocation, immune activation, and HIV disease. *Trends Microbiol* (2013) 21:6–13. doi: 10.1016/j.tim.2012.09.001
32. Klatt NR, Vinton CL, Lynch RM, Canary LA, Ho J, Darrah PA, et al. SIV infection of rhesus macaques results in dysfunctional T- and B-cell responses to neo and recall Leishmania major vaccination. *Blood* (2011) 118:5803–12. doi: 10.1182/blood-2011-07-365874
33. Mattapallil JJ, Hill B, Douek DC, Roederer M. Systemic vaccination prevents the total destruction of mucosal CD4 T cells during acute SIV challenge. *J Med Primatol* (2006) 35:217–24. doi: 10.1111/j.1600-0684.2006.00170.x
34. Mattapallil JJ, Reay E, Dandekar S. An early expansion of CD8alphabeta T cells, but depletion of resident CD8alphaalpha T cells, occurs in the intestinal epithelium during primary simian immunodeficiency virus infection. *AIDS* (2000) 14:637–46. doi: 10.1097/00002030-200004140-00002
35. Mavigner M, Cazabat M, Dubois M, L'Faqihi FE, Requena M, Pasquier C, et al. Altered CD4+ T cell homing to the gut impairs mucosal immune reconstitution in treated HIV-infected individuals. *J Clin Invest* (2012) 122:62–9. doi: 10.1172/JCI59011
36. Merriam D, Chen C, Mendez-Lagares G, Rogers KA, Michaels AJ, Yan J, et al. Depletion of Gut-Resident CCR5(+) Cells for HIV Cure Strategies. *AIDS Res Hum Retroviruses* (2017) 33:S70–80. doi: 10.1089/aid.2017.0159
37. Petravic J, Ribeiro RM, Casimiro DR, Mattapallil JJ, Roederer M, Shiver JW, et al. Estimating the impact of vaccination on acute simian-human immunodeficiency virus/simian immunodeficiency virus infections. *J Virol* (2008) 82:11589–98. doi: 10.1128/JVI.01596-08
38. Sainz T, Serrano-Villar S, Mann S, Ma ZM, Utay NS, Thompson CG, et al. Delayed gastrointestinal-associated lymphoid tissue reconstitution in duodenum compared with rectum in HIV-infected patients initiating antiretroviral therapy. *AIDS* (2019) 33:2289–98. doi: 10.1097/QAD.0000000000002361
39. Frank DN, St Amand AL, Feldman RA, Boedeker EC, Harpaz N, Pace NR. Molecular-phylogenetic characterization of microbial community imbalances in human inflammatory bowel diseases. *Proc Natl Acad Sci U.S.A.* (2007) 104:13780–5. doi: 10.1073/pnas.0706625104
40. Sender R, Fuchs S, Milo R. Are We Really Vastly Outnumbered? Revisiting the Ratio of Bacterial to Host Cells in Humans. *Cell* (2016) 164:337–40. doi: 10.1016/j.cell.2016.01.013
41. Jandhyala SM, Talukdar R, Subramanyam C, Vuyyuru H, Sasikala M, Nageshwar Reddy D. Role of the normal gut microbiota. *World J Gastroenterol* (2015) 21:8787–803. doi: 10.3748/wjg.v21.i29.8787

42. Brandl K, Plitas G, Schnabl B, DeMatteo RP, Pamer EG. MyD88-mediated signals induce the bactericidal lectin RegIII gamma and protect mice against intestinal Listeria monocytogenes infection. *J Exp Med* (2007) 204:1891–900. doi: 10.1084/jem.20070563
43. Cash HL, Whitham CV, Behrendt CL, Hooper LV. Symbiotic bacteria direct expression of an intestinal bactericidal lectin. *Science* (2006) 313:1126–30. doi: 10.1126/science.1127119
44. Johansson ME, Larsson JM, Hansson GC. The two mucus layers of colon are organized by the MUC2 mucin, whereas the outer layer is a legislator of host-microbial interactions. *Proc Natl Acad Sci U.S.A.* (2011) 108 Suppl 1:4659–65. doi: 10.1073/pnas.1006451107
45. Johansson ME, Phillipson M, Petersson J, Velcich A, Holm L, Hansson GC. The inner of the two Muc2 mucin-dependent mucus layers in colon is devoid of bacteria. *Proc Natl Acad Sci U.S.A.* (2008) 105:15064–9. doi: 10.1073/pnas.0803124105
46. Vaishnava S, Behrendt CL, Ismail AS, Eckmann L, Hooper LV. Paneth cells directly sense gut commensals and maintain homeostasis at the intestinal host-microbial interface. *Proc Natl Acad Sci U.S.A.* (2008) 105:20858–63. doi: 10.1073/pnas.0808723105
47. Vaishnava S, Yamamoto M, Severson KM, Ruhn KA, Yu X, Koren O, et al. The antibacterial lectin RegIIIgamma promotes the spatial segregation of microbiota and host in the intestine. *Science* (2011) 334:255–8. doi: 10.1126/science.1209791
48. Apter FM, Lencer WI, Finkelstein RA, Mekalanos JJ, Neutra MR. Monoclonal immunoglobulin A antibodies directed against cholera toxin prevent the toxin-induced chloride secretory response and block toxin binding to intestinal epithelial cells in vitro. *Infect Immun* (1993) 61:5271–8. doi: 10.1128/IAI.61.12.5271-5278.1993
49. Hutchings AB, Helander A, Silvey KJ, Chandran K, Lucas WT, Nibert ML, et al. Secretory immunoglobulin A antibodies against the sigma1 outer capsid protein of reovirus type 1 Lang prevent infection of mouse Peyer's patches. *J Virol* (2004) 78:947–57. doi: 10.1128/jvi.78.2.947-957.2004
50. Macpherson AJ, Gatto D, Sainsbury E, Harriman GR, Hengartner H, Zinkernagel RM. A primitive T cell-independent mechanism of intestinal mucosal IgA responses to commensal bacteria. *Science* (2000) 288:2222–6. doi: 10.1126/science.288.5474.2222
51. Macpherson AJ, Uhr T. Induction of protective IgA by intestinal dendritic cells carrying commensal bacteria. *Science* (2004) 303:1662–5. doi: 10.1126/science.1091334
52. Senior BW, Woof JM. The influences of hinge length and composition on the susceptibility of human IgA to cleavage by diverse bacterial IgA1 proteases. *J Immunol* (2005) 174:7792–9. doi: 10.4049/jimmunol.174.12.7792
53. Underdown BJ, Schiff JM. Immunoglobulin A: strategic defense initiative at the mucosal surface. *Annu Rev Immunol* (1986) 4:389–417. doi: 10.1146/annurev.iy.04.040186.002133
54. Woof JM, Mestecky J. Mucosal immunoglobulins. *Immunol Rev* (2005) 206:64–82. doi: 10.1111/j.0105-2896.2005.00290.x
55. Woof JM, Russell MW. Structure and function relationships in IgA. *Mucosal Immunol* (2011) 4:590–7. doi: 10.1038/mi.2011.39
56. Brandtzaeg P. Secretory IgA: Designed for Anti-Microbial Defense. *Front Immunol* (2013) 4:222. doi: 10.3389/fimmu.2013.00222
57. Brandtzaeg P. Gate-keeper function of the intestinal epithelium. *Benef Microbes* (2013) 4:67–82. doi: 10.3920/BM2012.0024
58. Kaetzel CS, Robinson JK, Chintalacharuvu KR, Vaerman JP, Lamm ME. The polymeric immunoglobulin receptor (secretory component) mediates transport of immune complexes across epithelial cells: a local defense function for IgA. *Proc Natl Acad Sci U.S.A.* (1991) 88:8796–800. doi: 10.1073/pnas.88.19.8796
59. Brandtzaeg P, Johansen FE. Mucosal B cells: phenotypic characteristics, transcriptional regulation, and homing properties. *Immunol Rev* (2005) 206:32–63. doi: 10.1111/j.0105-2896.2005.00283.x
60. Fritz JH, Rojas OL, Simard N, McCarthy DD, Hapfelmeier S. Acquisition of a multifunctional IgA+ plasma cell phenotype in the gut. *Nature* (2011) 481:199–203. doi: 10.1038/nature10698
61. Kaetzel CS. The polymeric immunoglobulin receptor: bridging innate and adaptive immune responses at mucosal surfaces. *Immunol Rev* (2005) 206:83–99. doi: 10.1111/j.0105-2896.2005.00278.x
62. Cherrier M, Eberl G. The development of LTi cells. *Curr Opin Immunol* (2012) 24:178–83. doi: 10.1016/j.coi.2012.02.003
63. Kruglov AA, Grivennikov SI, Kuprash DV, Winsauer C, Prepens S, Seleznik GM, et al. Nonredundant function of soluble LTalpha3 produced by innate lymphoid cells in intestinal homeostasis. *Science* (2013) 342:1243–6. doi: 10.1126/science.1243364
64. Pabst O, Herbrand H, Worbs T, Friedrichsen M, Yan S, Hoffmann MW, et al. Cryptopatches and isolated lymphoid follicles: dynamic lymphoid tissues dispensable for the generation of intraepithelial lymphocytes. *Eur J Immunol* (2005) 35:98–107. doi: 10.1002/eji.200425432
65. Hapfelmeier S, Lawson MA, Slack E, Kirundi JK, Stoel M. Reversible microbial colonization of germ-free mice reveals the dynamics of IgA immune responses. *Science* (2010) 328:1705–9. doi: 10.1126/science.1188454
66. Slack E, Balmer ML, Fritz JH, Hapfelmeier S. Functional flexibility of intestinal IgA - broadening the fine line. *Front Immunol* (2012) 3:100:100. doi: 10.3389/fimmu.2012.00100
67. Hickey DK, Patel MV, Fahey JV, Wira CR. Innate and adaptive immunity at mucosal surfaces of the female reproductive tract: stratification and integration of immune protection against the transmission of sexually transmitted infections. *J Reprod Immunol* (2011) 88:185–94. doi: 10.1016/j.jri.2011.01.005
68. Randall TD, Kern JA. Tertiary lymphoid structures target the antitumor immune response to lung cancer. *Am J Respir Crit Care Med* (2014) 189:767–9. doi: 10.1164/rccm.201402-0317ED
69. Craig SW, Cebra JJ. Peyer's patches: an enriched source of precursors for IgA-producing immunocytes in the rabbit. *J Exp Med* (1971) 134:188–200. doi: 10.1084/jem.134.1.188
70. Fagarasan S, Kinoshita K, Muramatsu M, Ikuta K, Honjo T. In situ class switching and differentiation to IgA-producing cells in the gut lamina propria. *Nature* (2001) 413:639–43. doi: 10.1038/35098100
71. Brandtzaeg P. Mucosal immunity: induction, dissemination, and effector functions. *Scand J Immunol* (2009) 70:505–15. doi: 10.1111/j.1365-3083.2009.02319.x
72. Cerutti A, Chen K, Chorny A. Immunoglobulin responses at the mucosal interface. *Annu Rev Immunol* (2011) 29:273–93. doi: 10.1146/annurev-immunol-031210-101317
73. Fagarasan S, Kawamoto S, Kanagawa O, Suzuki K. Adaptive immune regulation in the gut: T cell-dependent and T cell-independent IgA synthesis. *Annu Rev Immunol* (2010) 28:243–73. doi: 10.1146/annurev-immunol-030409-101314
74. Katz DH, Benacerraf B. The regulatory influence of activated T cells on B cell responses to antigen. *Adv Immunol* (1972) 15:1–94. doi: 10.1016/s0065-2776(08)60683-5
75. Miller JF, Mitchell GF. Cell to cell interaction in the immune response. I. Hemolysin-forming cells in neonatally thymectomized mice reconstituted with thymus or thoracic duct lymphocytes. *J Exp Med* (1968) 128:801–20. doi: 10.1084/jem.128.4.801
76. Mitchell GF, Miller JF. Cell to cell interaction in the immune response. II. The source of hemolysin-forming cells in irradiated mice given bone marrow and thymus or thoracic duct lymphocytes. *J Exp Med* (1968) 128:821–37. doi: 10.1084/jem.128.4.821
77. Nossal GJ, Cunningham A, Mitchell GF, Miller JF. Cell to cell interaction in the immune response. 3. Chromosomal marker analysis of single antibody-forming cells in reconstituted, irradiated, or thymectomized mice. *J Exp Med* (1968) 128:839–53. doi: 10.1084/jem.128.4.839
78. Raff MC. Role of thymus-derived lymphocytes in the secondary humoral immune response in mice. *Nature* (1970) 226:1257–8. doi: 10.1038/2261257a0
79. Cong Y, Feng T, Fujihashi K, Schoeb TR, Elson CO. A dominant, coordinated T regulatory cell-IgA response to the intestinal microbiota. *Proc Natl Acad Sci U.S.A.* (2009) 106:19256–61. doi: 10.1073/pnas.0812681106
80. Cao AT, Yao S, Gong B, Elson CO, Cong Y. Th17 cells upregulate polymeric Ig receptor and intestinal IgA and contribute to intestinal homeostasis. *J Immunol* (2012) 189:4666–73. doi: 10.4049/jimmunol.1200955
81. Hirota K, Turner JE, Villa M, Duarte JH, Demengeot J, Steinmetz OM, et al. Plasticity of Th17 cells in Peyer's patches is responsible for the induction of T cell-dependent IgA responses. *Nat Immunol* (2013) 14:372–9. doi: 10.1038/ni.2552

82. Tsuji M, Komatsu N, Kawamoto S, Suzuki K, Kanagawa O. Preferential generation of follicular B helper T cells from Foxp3+ T cells in gut Peyer's patches. *Science* (2009) 323:1488–92. doi: 10.1126/science.1169152
83. Crotty S. Follicular helper CD4 T cells (TFH). *Annu Rev Immunol* (2011) 29:621–63. doi: 10.1146/annurev-immunol-031210-101400
84. Johnston RJ, Poholek AC, DiToro D, Yusuf I, Eto D, Barnett B, et al. Bcl6 and Blimp-1 are reciprocal and antagonistic regulators of T follicular helper cell differentiation. *Science* (2009) 325:1006–10. doi: 10.1126/science.1175870
85. Nurieva RI, Chung Y, Martinez GJ, Yang XO, Tanaka S, Matskevitch TD, et al. Bcl6 mediates the development of T follicular helper cells. *Science* (2009) 325:1001–5. doi: 10.1126/science.1176676
86. Onabajo OO, George J, Lewis MG, Mattapallil JJ. Rhesus macaque lymph node PD-1(hi)CD4+ T cells express high levels of CXCR5 and IL-21 and display a CCR7(lo)ICOS+Bcl6+ T-follicular helper (Tfh) cell phenotype. *PloS One* (2013) 8:e59758. doi: 10.1371/journal.pone.0059758
87. Schaerli P, Willimann K, Lang AB, Lipp M, Loetscher P, Moser B. CXC chemokine receptor 5 expression defines follicular homing T cells with B cell helper function. *J Exp Med* (2000) 192:1553–62. doi: 10.1084/jem.192.11.1553
88. Linterman MA, Beaton L, Yu D, Ramiscal RR, Srivastava M, Hogan JJ, et al. IL-21 acts directly on B cells to regulate Bcl-6 expression and germinal center responses. *J Exp Med* (2010) 207:353–63. doi: 10.1084/jem.20091738
89. Nurieva RI, Chung Y, Hwang D, Yang XO, Kang HS, Ma L, et al. Generation of T follicular helper cells is mediated by interleukin-21 but independent of T helper 1, 2, or 17 cell lineages. *Immunity* (2008) 29:138–49. doi: 10.1016/j.immuni.2008.05.009
90. Ozaki K, Spolski R, Feng CG, Qi CF, Cheng J, Sher A, et al. A critical role for IL-21 in regulating immunoglobulin production. *Science* (2002) 298:1630–4. doi: 10.1126/science.1077002
91. Crotty S. T follicular helper cell differentiation, function, and roles in disease. *Immunity* (2014) 41:529–42. doi: 10.1016/j.immuni.2014.10.004
92. Churchill MJ, Deeks SG, Margolis DM, Siliciano RF, Swanstrom R. HIV reservoirs: what, where and how to target them. *Nat Rev Microbiol* (2016) 14:55–60. doi: 10.1038/nrmicro.2015.5
93. Cohn LB, Chomont N, Deeks SG. The Biology of the HIV-1 Latent Reservoir and Implications for Cure Strategies. *Cell Host Microbe* (2020) 27:519–30. doi: 10.1016/j.chom.2020.03.014
94. George J, Cofano EB, Lybarger E, Louder M, Lafont BA, Mascola JR, et al. Early short-term antiretroviral therapy is associated with a reduced prevalence of CD8(+)FoxP3(+) T cells in simian immunodeficiency virus-infected controller rhesus macaques. *AIDS Res Hum Retroviruses* (2011) 27:763–75. doi: 10.1089/AID.2010.0251
95. George J, Renn L, Verthelyi D, Roederer M, Rabin RL, Mattapallil JJ. Early treatment with reverse transcriptase inhibitors significantly suppresses peak plasma IFNalpha in vivo during acute simian immunodeficiency virus infection. *Cell Immunol* (2016) 310:156–64. doi: 10.1016/j.cellimm.2016.09.003
96. Kuwata T, Dehghani H, Brown CR, Plishka R, Buckler-White A, Igarashi T, et al. Infectious molecular clones from a simian immunodeficiency virus-infected rapid-progressor (RP) macaque: evidence of differential selection of RP-specific envelope mutations in vitro and in vivo. *J Virol* (2006) 80:1463–75. doi: 10.1128/JVI.80.3.1463-1475.2006
97. Mattapallil JJ, Smit-McBride Z, Dailey P, Dandekar S. Activated memory CD4(+) T helper cells repopulate the intestine early following antiretroviral therapy of simian immunodeficiency virus-infected rhesus macaques but exhibit a decreased potential to produce interleukin-2. *J Virol* (1999) 73:6661–9. doi: 10.1128/JVI.73.8.6661-6669.1999
98. Mattapallil JJ, Smit-McBride Z, McChesney M, Dandekar S. Intestinal intraepithelial lymphocytes are primed for gamma interferon and MIP-1beta expression and display antiviral cytotoxic activity despite severe CD4 (+) T-cell depletion in primary simian immunodeficiency virus infection. *J Virol* (1998) 72:6421–9. doi: 10.1128/JVI.72.8.6421-6429.1998
99. Mueller YM, Do DH, Boyer JD, Kader M, Mattapallil JJ, Lewis MG, et al. CD8+ cell depletion of SHIV89.6P-infected macaques induces CD4+ T cell proliferation that contributes to increased viral loads. *J Immunol* (2009) 183:5006–12. doi: 10.4049/jimmunol.0900141
100. Nishimura Y, Sadjadpour R, Mattapallil JJ, Igarashi T, Lee W, Buckler-White A, et al. High frequencies of resting CD4+ T cells containing integrated viral DNA are found in rhesus macaques during acute lentivirus infections. *Proc Natl Acad Sci U.S.A.* (2009) 106:8015–20. doi: 10.1073/pnas.0903022106
101. Petrovas C, Price DA, Mattapallil J, Ambrozak DR, Geldmacher C, Cecchinato V, et al. SIV-specific CD8+ T cells express high levels of PD1 and cytokines but have impaired proliferative capacity in acute and chronic SIVmac251 infection. *Blood* (2007) 110:928–36. doi: 10.1182/blood-2007-01-069112
102. Sengupta S, Siliciano RF. Targeting the Latent Reservoir for HIV-1. *Immunity* (2018) 48:872–95. doi: 10.1016/j.immuni.2018.04.030
103. Vaccari M, Mattapallil J, Song K, Tsai WP, Hryniewicz A, Venzon D, et al. Reduced protection from simian immunodeficiency virus SIVmac251 infection afforded by memory CD8+ T cells induced by vaccination during CD4+ T-cell deficiency. *J Virol* (2008) 82:9629–38. doi: 10.1128/JVI.00893-08
104. Wilson DP, Mattapallil JJ, Lay MD, Zhang L, Roederer M, Davenport MP. Estimating the infectivity of CCR5-tropic simian immunodeficiency virus SIV(mac251) in the gut. *J Virol* (2007) 81:8025–9. doi: 10.1128/JVI.01771-06
105. Fukazawa Y, Lum R, Okoye AA, Park H, Matsuda K, Bae JY, et al. B cell follicle sanctuary permits persistent productive simian immunodeficiency virus infection in elite controllers. *Nat Med* (2015) 21:132–9. doi: 10.1038/nm.3781
106. Connick E, Mattila T, Folkvord JM, Schlichtemeier R, Meditz AL, Ray MG, et al. CTL fail to accumulate at sites of HIV-1 replication in lymphoid tissue. *J Immunol* (2007) 178:6975–83. doi: 10.4049/jimmunol.178.11.6975
107. Sasikala-Appukuttan AK, Kim HO, Kinzel NJ, Hong JJ, Smith AJ, Wagstaff R, et al. Location and dynamics of the immunodominant CD8 T cell response to SIVDeltanef immunization and SIVmac251 vaginal challenge. *PloS One* (2013) 8:e81623. doi: 10.1371/journal.pone.0081623
108. Dimopoulos Y, Moysi E, Petrovas C. The Lymph Node in HIV Pathogenesis. *Curr HIV/AIDS Rep* (2017) 14:133–40. doi: 10.1007/s11904-017-0359-7
109. Hong JJ, Chang KT, Villinger F. The Dynamics of T and B Cells in Lymph Node during Chronic HIV Infection: TFH and HIV, Unhappy Dance Partners? *Front Immunol* (2016) 7:522:522. doi: 10.3389/fimmu.2016.00522
110. Perreau M, Savoye AL, De Crignis E, Corpataux JM, Cubas R, Haddad EK, et al. Follicular helper T cells serve as the major CD4 T cell compartment for HIV-1 infection, replication, and production. *J Exp Med* (2013) 210:143–56. doi: 10.1084/jem.20121932
111. Hong JJ, Amancha PK, Rogers K, Ansari AA, Villinger F. Spatial alterations between CD4(+) T follicular helper, B, and CD8(+) T cells during simian immunodeficiency virus infection: T/B cell homeostasis, activation, and potential mechanism for viral escape. *J Immunol* (2012) 188:3247–56. doi: 10.4049/jimmunol.1103138
112. Petrovas C, Yamamoto T, Gerner MY, Boswell KL, Wloka K, Smith EC, et al. CD4 T follicular helper cell dynamics during SIV infection. *J Clin Invest* (2012) 122:3281–94. doi: 10.1172/JCI63039
113. Xu Y, Weatherall C, Bailey M, Alcantara S, De Rose R, Estaquier J, et al. Simian immunodeficiency virus infects follicular helper CD4 T cells in lymphoid tissues during pathogenic infection of pigtail macaques. *J Virol* (2013) 87:3760–73. doi: 10.1128/JVI.02497-12
114. Lindqvist M, van Lunzen J, Soghoian DZ, Kuhl BD, Ranasinghe S, Kranias G, et al. Expansion of HIV-specific T follicular helper cells in chronic HIV infection. *J Clin Invest* (2012) 122:3271–80. doi: 10.1172/JCI64314
115. Onabajo OO, Lewis MG, Mattapallil JJ. Chronic simian immunodeficiency virus infection is associated with contrasting phenotypes of dysfunctional Bcl6(+) germinal center B cells or Bcl6(-) Bcl2(+) non-germinal center B cells. *J Cell Mol Med* (2018) 22:5682–7. doi: 10.1111/jcmm.13844
116. Onabajo OO, Mattapallil JJ. Expansion or depletion of T follicular helper cells during HIV infection: consequences for B cell responses. *Curr HIV Res* (2013) 11:595–600. doi: 10.2174/1570162x12666140225153552
117. Xu H, Wang X, Malam N, Aye PP, Alvarez X, Lackner AA, et al. Persistent Simian Immunodeficiency Virus Infection Drives Differentiation, Aberrant Accumulation, and Latent Infection of Germinal Center Follicular T Helper Cells. *J Virol* (2016) 90:1578–87. doi: 10.1128/JVI.02471-15
118. Mylvaganam GH, Velu V, Hong JJ, Sadagopal S, Kwa S, Basu R, et al. Diminished viral control during simian immunodeficiency virus infection is associated with aberrant PD-1hi CD4 T cell enrichment in the lymphoid follicles of the rectal mucosa. *J Immunol* (2014) 193:4527–36. doi: 10.4049/jimmunol.1401222

119. Micci L, Cervasi B, Ende ZS, Iriele RI, Reyes-Aviles E, Vinton C, et al. Paucity of IL-21-producing CD4(+) T cells is associated with Th17 cell depletion in SIV infection of rhesus macaques. *Blood* (2012) 120:3925–35. doi: 10.1182/blood-2012-04-420240
120. Bixler SL, Mattapallil JJ. Loss and dysregulation of Th17 cells during HIV infection. *Clin Dev Immunol* (2013) 2013:852418. doi: 10.1155/2013/852418
121. Bixler SL, Sandler NG, Douek DC, Mattapallil JJ. Suppressed Th17 levels correlate with elevated PIAS3, SHP2, and SOCS3 expression in CD4 T cells during acute simian immunodeficiency virus infection. *J Virol* (2013) 87:7093–101. doi: 10.1128/JVI.00600-13
122. Moukambi F, Rabezanahary H, Fortier Y, Rodrigues V, Clain J, Benmadid-Laktout G, et al. Mucosal T follicular helper cells in SIV-infected rhesus macaques: contributing role of IL-27. *Mucosal Immunol* (2019) 12:1038–54. doi: 10.1038/s41385-019-0174-0
123. Hel Z, Xu J, Denning WL, Helton ES, Huijbregts RP, Heath SL, et al. Dysregulation of Systemic and Mucosal Humoral Responses to Microbial and Food Antigens as a Factor Contributing to Microbial Translocation and Chronic Inflammation in HIV-1 Infection. *PloS Pathog* (2017) 13:e1006087. doi: 10.1371/journal.ppat.1006087
124. Cubas RA, Mudd JC, Savoye AL, Perreau M, van Grevenynghe J, Metcalf T, et al. Inadequate T follicular cell help impairs B cell immunity during HIV infection. *Nat Med* (2013) 19:494–9. doi: 10.1038/nm.3109
125. Pallikkuth S, de Armas L, Rinaldi S, Pahwa ST. T Follicular Helper Cells and B Cell Dysfunction in Aging and HIV-1 Infection. *Front Immunol* (2017) 8:1380:1380. doi: 10.3389/fimmu.2017.01380
126. Xu H, Ziani W, Shao J, Doyle-Meyers LA, Russell-Lodrigue KE, Ratterree MS, et al. Impaired Development and Expansion of Germinal Center Follicular Th Cells in Simian Immunodeficiency Virus-Infected Neonatal Macaques. *J Immunol* (2018) 201:1994–2003. doi: 10.4049/jimmunol.1800235
127. Rabezanahary H, Moukambi F, Palesch D, Clain J, Racine G, Andreani G, et al. Despite early antiretroviral therapy effector memory and follicular helper CD4 T cells are major reservoirs in visceral lymphoid tissues of SIV-infected macaques. *Mucosal Immunol* (2020) 13:149–60. doi: 10.1038/s41385-019-0221-x
128. McGary CS, Deleage C, Harper J, Micci L, Ribeiro SP, Paganini S, et al. CTLA-4 (+)PD-1(-) Memory CD4(+) T Cells Critically Contribute to Viral Persistence in Antiretroviral Therapy-Suppressed, SIV-Infected Rhesus Macaques. *Immunity* (2017) 47:776–88 e5. doi: 10.1016/j.immuni.2017.09.018
129. Velu V, Mylvaganam GH, Gangadhara S, Hong JJ, Iyer SS, Gumber S, et al. Induction of Th1-Biased T Follicular Helper (Tfh) Cells in Lymphoid Tissues during Chronic Simian Immunodeficiency Virus Infection Defines Functionally Distinct Germinal Center Tfh Cells. *J Immunol* (2016) 197:1832–42. doi: 10.4049/jimmunol.1600143
130. Morou A, Brunet-Ratnasingham E, Dube M, Charlebois R, Mercier E, Darko S, et al. Altered differentiation is central to HIV-specific CD4(+) T cell dysfunction in progressive disease. *Nat Immunol* (2019) 20:1059–70. doi: 10.1038/s41590-019-0418-x
131. Pallikkuth S, Sharkey M, Babic DZ, Gupta S, Stone GW, Fischl MA, et al. Peripheral T Follicular Helper Cells Are the Major HIV Reservoir within Central Memory CD4 T Cells in Peripheral Blood from Chronically HIV-Infected Individuals on Combination Antiretroviral Therapy. *J Virol* (2015) 90:2718–28. doi: 10.1128/JVI.02883-15
132. Banga R, Procopio FA, Noto A, Pollakis G, Cavassini M, Ohmiti K, et al. PD-1(+) and follicular helper T cells are responsible for persistent HIV-1 transcription in treated aviremic individuals. *Nat Med* (2016) 22:754–61. doi: 10.1038/nm.4113
133. Yu F, Li Q, Chen X, Liu J, Li L, Li B, et al. X4-Tropic Latent HIV-1 Is Enriched in Peripheral Follicular Helper T Cells and Is Correlated with Disease Progression. *J Virol* (2020) 94:e01219–19. doi: 10.1128/JVI.01219-19
134. Niessl J, Baxter AE, Morou A, Brunet-Ratnasingham E, Sannier G, Gendron-Lepage G, et al. Persistent expansion and Th1-like skewing of HIV-specific circulating T follicular helper cells during antiretroviral therapy. *EBioMedicine* (2020) 54:102727. doi: 10.1016/j.ebiom.2020.102727
135. Planchais C, Hocqueloux L, Ibanez C, Gallien S, Copie C, Surenaud M, et al. Early Antiretroviral Therapy Preserves Functional Follicular Helper T and HIV-Specific B Cells in the Gut Mucosa of HIV-1-Infected Individuals. *J Immunol* (2018) 200:3519–29. doi: 10.4049/jimmunol.1701615
136. Thornhill JP, Pace M, Martin GE, Hoare J, Peake S, Herrera C, et al. CD32 expressing doublets in HIV-infected gut-associated lymphoid tissue are associated with a T follicular helper cell phenotype. *Mucosal Immunol* (2019) 12:1212–9. doi: 10.1038/s41385-019-0180-2
137. Suzuki K, Fagarasan S. How host-bacterial interactions lead to IgA synthesis in the gut. *Trends Immunol* (2008) 29:523–31. doi: 10.1016/j.it.2008.08.001
138. Cazac BB, Roes J. TGF-beta receptor controls B cell responsiveness and induction of IgA in vivo. *Immunity* (2000) 13:443–51. doi: 10.1016/s1074-7613(00)00044-3
139. Cerutti A. The regulation of IgA class switching. *Nat Rev Immunol* (2008) 8:421–34. doi: 10.1038/nri2322
140. Cerutti A, Rescigno M. The biology of intestinal immunoglobulin A responses. *Immunity* (2008) 28:740–50. doi: 10.1016/j.immuni.2008.05.001
141. Fagarasan S, Honjo T. Intestinal IgA synthesis: regulation of front-line body defences. *Nat Rev Immunol* (2003) 3:63–72. doi: 10.1038/nri982
142. Macpherson AJ, McCoy KD, Johansen FE, Brandtzaeg P. The immune geography of IgA induction and function. *Mucosal Immunol* (2008) 1:11–22. doi: 10.1038/mi.2007.6
143. Chaoul N, Burelout C, Peruchon S, van Buu BN, Laurent P, Proust A, et al. Default in plasma and intestinal IgA responses during acute infection by simian immunodeficiency virus. *Retrovirology* (2012) 9:43. doi: 10.1186/1742-4690-9-43
144. Schafer F, Kewenig S, Stolte N, Stahl-Hennig C, Stallmach A, Kaup FJ, et al. Lack of simian immunodeficiency virus (SIV) specific IgA response in the intestine of SIV infected rhesus macaques. *Gut* (2002) 50:608–14. doi: 10.1136/gut.50.5.608
145. Barassi C, Lazzarin A, Lopalco L. CCR5-specific mucosal IgA in saliva and genital fluids of HIV-exposed seronegative subjects. *Blood* (2004) 104:2205–6. doi: 10.1182/blood-2004-06-2134
146. Bishop PE, McMillan A, Gilmour HM. Immunological study of the rectal mucosa of men with and without human immunodeficiency virus infection. *Gut* (1987) 28:1619–24. doi: 10.1136/gut.28.12.1619
147. Kotler DP, Scholes JV, Tierney AR. Intestinal plasma cell alterations in acquired immunodeficiency syndrome. *Dig Dis Sci* (1987) 32:129–38. doi: 10.1007/BF01297100
148. Mestecky J, Wright PF, Lopalco L, Staats HF, Kozlowski PA, Moldoveanu Z, et al. Scarcity or absence of humoral immune responses in the plasma and cervicovaginal lavage fluids of heavily HIV-1-exposed but persistently seronegative women. *AIDS Res Hum Retroviruses* (2011) 27:469–86. doi: 10.1089/aid.2010.0169
149. Nilssen DE, Oktedalen O, Brandtzaeg P. Intestinal B cell hyperactivity in AIDS is controlled by highly active antiretroviral therapy. *Gut* (2004) 53:487–93. doi: 10.1136/gut.2003.027854
150. Raux M, Finkielsztejn L, Salmon-Ceron D, Bouchez H, Excler JL, Dulioust E, et al. Comparison of the distribution of IgG and IgA antibodies in serum and various mucosal fluids of HIV type 1-infected subjects. *AIDS Res Hum Retroviruses* (1999) 15:1365–76. doi: 10.1089/088922299310070
151. Schneider T, Zippel T, Schmidt W, Pauli G, Wahnschaffe U, Chakravarti S, et al. Increased immunoglobulin G production by short term cultured duodenal biopsy samples from HIV infected patients. *Gut* (1998) 42:357–61. doi: 10.1136/gut.42.3.357
152. Scamurra RW, Nelson DB, Lin XM, Miller DJ, Silverman GJ, Kappel T, et al. Mucosal plasma cell repertoire during HIV-1 infection. *J Immunol* (2002) 169:4008–16. doi: 10.4049/jimmunol.169.7.4008
153. Xu W, Santini PA, Sullivan JS, He B, Shan M, Ball SC, et al. HIV-1 evades virus-specific IgG2 and IgA responses by targeting systemic and intestinal B cells via long-range intercellular conduits. *Nat Immunol* (2009) 10:1008–17. doi: 10.1038/ni.1753
154. Levesque MC, Moody MA, Hwang KK, Marshall DJ, Whitesides JF, Amos JD, et al. Polyclonal B cell differentiation and loss of gastrointestinal tract germinal centers in the earliest stages of HIV-1 infection. *PloS Med* (2009) 6: e1000107. doi: 10.1371/journal.pmed.1000107
155. Kok A, Hocqueloux L, Hocini H, Carriere M, Lefrou L, Guguin A, et al. Early initiation of combined antiretroviral therapy preserves immune function in the gut of HIV-infected patients. *Mucosal Immunol* (2015) 8:127–40. doi: 10.1038/mi.2014.50
156. Burgener A, McGowan I, Klatt NR. HIV and mucosal barrier interactions: consequences for transmission and pathogenesis. *Curr Opin Immunol* (2015) 36:22–30. doi: 10.1016/j.coi.2015.06.004

157. Dandekar S, George MD, Baumler AJ. Th17 cells, HIV and the gut mucosal barrier. *Curr Opin HIV AIDS* (2010) 5:173–8. doi: 10.1097/COH.0b013e328335eda3
158. Hirao LA, Grishina I, Bourry O, Hu WK, Somrit M, Sankaran-Walters S, et al. Early mucosal sensing of SIV infection by paneth cells induces IL-1beta production and initiates gut epithelial disruption. *PloS Pathog* (2014) 10: e1004311. doi: 10.1371/journal.ppat.1004311
159. Hunt PW, Sinclair E, Rodriguez B, Shive C, Clagett B, Funderburg N, et al. Gut epithelial barrier dysfunction and innate immune activation predict mortality in treated HIV infection. *J Infect Dis* (2014) 210:1228–38. doi: 10.1093/infdis/jiu238
160. Ponte R, Mehraj V, Ghali P, Couedel-Courteille A, Cheynier R, Routy JP. Reversing Gut Damage in HIV Infection: Using Non-Human Primate Models to Instruct Clinical Research. *EBioMedicine* (2016) 4:40–9. doi: 10.1016/j.ebiom.2016.01.028
161. Raehtz KD, Barrenas F, Xu C, Busman-Sahay K, Valentine A, Law L. African green monkeys avoid SIV disease progression by preventing intestinal dysfunction and maintaining mucosal barrier integrity. *PloS Pathog* (2020) 16:e1008333. doi: 10.1371/journal.ppat.1008333
162. Atarashi K, Tanoue T, Shima T, Imaoka A, Kuwahara T, Momose Y, et al. Induction of colonic regulatory T cells by indigenous Clostridium species. *Science* (2011) 331:337–41. doi: 10.1126/science.1198469
163. Furusawa Y, Obata Y, Fukuda S, Endo TA, Nakato G, Takahashi D, et al. Commensal microbe-derived butyrate induces the differentiation of colonic regulatory T cells. *Nature* (2013) 504:446–50. doi: 10.1038/nature12721
164. Hooper LV, Littman DR, Macpherson AJ. Interactions between the microbiota and the immune system. *Science* (2012) 336:1268–73. doi: 10.1126/science.1223490
165. Muranski P, Restifo NP. Essentials of Th17 cell commitment and plasticity. *Blood* (2013) 121:2402–14. doi: 10.1182/blood-2012-09-378653
166. Telesford KM, Yan W, Ochoa-Reparaz J, Pant A, Kircher C, Christy MA, et al. A commensal symbiotic factor derived from Bacteroides fragilis promotes human CD39(+)Foxp3(+) T cells and Treg function. *Gut Microbes* (2015) 6:234–42. doi: 10.1080/19490976.2015.1056973
167. Wu HJ, Wu E. The role of gut microbiota in immune homeostasis and autoimmunity. *Gut Microbes* (2012) 3:4–14. doi: 10.4161/gmic.19320
168. Hegazy AN, West NR, Stubbington MJT, Wendt E, Suijker KIM, Datsi A, et al. Circulating and Tissue-Resident CD4(+) T Cells With Reactivity to Intestinal Microbiota Are Abundant in Healthy Individuals and Function Is Altered During Inflammation. *Gastroenterology* (2017) 153:1320–37 e16. doi: 10.1053/j.gastro.2017.07.047
169. Gutzeit C, Magri G, Cerutti A. Intestinal IgA production and its role in host-microbe interaction. *Immunol Rev* (2014) 260:76–85. doi: 10.1111/imr.12189
170. Jones L, Ho WQ, Ying S, Ramakrishna L, Srinivasan KG, Yurieva M, et al. A subpopulation of high IL-21-producing CD4(+) T cells in Peyer's Patches is induced by the microbiota and regulates germinal centers. *Sci Rep* (2016) 6:30784. doi: 10.1038/srep30784
171. Maruya M, Kawamoto S, Kato LM, Fagarasan S. Impaired selection of IgA and intestinal dysbiosis associated with PD-1-deficiency. *Gut Microbes* (2013) 4:165–71. doi: 10.4161/gmic.23595
172. Kawamoto S, Tran TH, Maruya M, Suzuki K, Doi Y, Tsutsui Y, et al. The inhibitory receptor PD-1 regulates IgA selection and bacterial composition in the gut. *Science* (2012) 336:485–9. doi: 10.1126/science.1217718
173. Teng F, Klinger CN, Felix KM, Bradley CP, Wu E, Tran NL, et al. Gut Microbiota Drive Autoimmune Arthritis by Promoting Differentiation and Migration of Peyer's Patch T Follicular Helper Cells. *Immunity* (2016) 44:875–88. doi: 10.1016/j.immuni.2016.03.013
174. Ballesteros-Tato A, Leon B, Graf BA, Moquin A, Adams PS, Lund FE, et al. Interleukin-2 inhibits germinal center formation by limiting T follicular helper cell differentiation. *Immunity* (2012) 36:847–56. doi: 10.1016/j.immuni.2012.02.012
175. Johnston RJ, Choi YS, Diamond JA, Yang JA, Crotty S. STAT5 is a potent negative regulator of TFH cell differentiation. *J Exp Med* (2012) 209:243–50. doi: 10.1084/jem.20111174
176. Proietti M, Cornacchione V, Rezzonico Jost T, Romagnani A, Faliti CE, Perruzza L, et al. ATP-gated ionotropic P2X7 receptor controls follicular T helper cell numbers in Peyer's patches to promote host-microbiota mutualism. *Immunity* (2014) 41:789–801. doi: 10.1016/j.immuni.2014.10.010
177. Dillon SM, Frank DN, Wilson CC. The gut microbiome and HIV-1 pathogenesis: a two-way street. *AIDS* (2016) 30:2737–51. doi: 10.1097/QAD.0000000000001289
178. Zevin AS, McKinnon L, Burgener A, Klatt NR. Microbial translocation and microbiome dysbiosis in HIV-associated immune activation. *Curr Opin HIV AIDS* (2016) 11:182–90. doi: 10.1097/COH.0000000000000234
179. Dillon SM, Lee EJ, Kotter CV, Austin GL, Dong Z, Hecht DK, et al. An altered intestinal mucosal microbiome in HIV-1 infection is associated with mucosal and systemic immune activation and endotoxemia. *Mucosal Immunol* (2014) 7:983–94. doi: 10.1038/mi.2013.116
180. Mutlu EA, Keshavarzian A, Losurdo J, Swanson G, Siewe B, Forsyth C, et al. A compositional look at the human gastrointestinal microbiome and immune activation parameters in HIV infected subjects. *PloS Pathog* (2014) 10:e1003829. doi: 10.1371/journal.ppat.1003829
181. Vujkovic-Cvijin I, Dunham RM, Iwai S, Maher MC, Albright RG, Broadhurst MJ, et al. Dysbiosis of the gut microbiota is associated with HIV disease progression and tryptophan catabolism. *Sci Transl Med* (2013) 5:193ra91. doi: 10.1126/scitranslmed.3006438
182. Le Chatelier E, Nielsen T, Qin J, Prifti E, Hildebrand F, Falony G, et al. Richness of human gut microbiome correlates with metabolic markers. *Nature* (2013) 500:541–6. doi: 10.1038/nature12506
183. Lozupone CA, Li M, Campbell TB, Flores SC, Linderman D, Gebert MJ, et al. Alterations in the gut microbiota associated with HIV-1 infection. *Cell Host Microbe* (2013) 14:329–39. doi: 10.1016/j.chom.2013.08.006
184. Noguera-Julian M, Rocafort M, Guillen Y, Rivera J, Casadella M, Nowak P, et al. Gut Microbiota Linked to Sexual Preference and HIV Infection. *EBioMedicine* (2016) 5:135–46. doi: 10.1016/j.ebiom.2016.01.032
185. Vazquez-Castellanos JF, Serrano-Villar S, Latorre A, Artacho A, Ferrus ML, Madrid N, et al. Altered metabolism of gut microbiota contributes to chronic immune activation in HIV-infected individuals. *Mucosal Immunol* (2015) 8:760–72. doi: 10.1038/mi.2014.107
186. Yu G, Fadrosh D, Ma B, Ravel J, Goedert JJ. Anal microbiota profiles in HIV-positive and HIV-negative MSM. *AIDS* (2014) 28:753–60. doi: 10.1097/QAD.0000000000000154
187. Blum FC, Hardy BL, Bishop-Lilly KA, Frey KG, Hamilton T, Whitney JB, et al. Microbial Dysbiosis During Simian Immunodeficiency Virus Infection is Partially Reverted with Combination Anti-retroviral Therapy. *Sci Rep* (2020) 10:6387. doi: 10.1038/s41598-020-63196-0
188. Handley SA, Thackray LB, Zhao G, Presti R, Miller AD, Droit L, et al. Pathogenic simian immunodeficiency virus infection is associated with expansion of the enteric virome. *Cell* (2012) 151:253–66. doi: 10.1016/j.cell.2012.09.024
189. Monaco CL, Gootenberg DB, Zhao G, Handley SA, Ghebremichael MS, Lim ES, et al. Altered Virome and Bacterial Microbiome in Human Immunodeficiency Virus-Associated Acquired Immunodeficiency Syndrome. *Cell Host Microbe* (2016) 19:311–22. doi: 10.1016/j.chom.2016.02.011
190. Nowak P, Troseid M, Avershina E, Barqasho B, Neogi U, Holm K, et al. Gut microbiota diversity predicts immune status in HIV-1 infection. *AIDS* (2015) 29:2409–18. doi: 10.1097/QAD.0000000000000869

Conflict of Interest: The authors declare that the research was conducted in the absence of any commercial or financial relationships that could be construed as a potential conflict of interest.

frontiers in Immunology

ORIGINAL RESEARCH
published: 16 April 2021
doi: 10.3389/fimmu.2021.666388

Role of Circulating T Follicular Helper Cells and Stem-Like Memory CD4$^+$ T Cells in the Pathogenesis of HIV-2 Infection and Disease Progression

Sivasankaran Munusamy Ponnan[1,2†], Vidyavijayan KK[1†], Kannan Thiruvengadam[1], Nancy Hilda J[1], Manikannan Mathayan[3], Kailapuri Gangatharan Murugavel[4] and Luke Elizabeth Hanna[1]*

[1] Department of HIV/AIDS, National Institute for Research in Tuberculosis (Indian Council of Medical Research), Chennai, India, [2] Centre for Infectious Disease Research, Indian Institute of Science, Bangalore, India, [3] Centre for Drug Discovery and Development, Sathyabama Institute of Science and Technology, Chennai, India, [4] Division of Immunology, YRG Centre for AIDS Research and Education, Chennai, India

CD4$^+$ T cells are critical players in the host adaptive immune response. Emerging evidence suggests that certain CD4$^+$ T cell subsets contribute significantly to the production of neutralizing antibodies and help in the control of virus replication. Circulating T follicular helper cells (Tfh) constitute a key T cell subset that triggers the adaptive immune response and stimulates the production of neutralizing antibodies (NAbs). T cells having stem cell-like property, called stem-like memory T cells (Tscm), constitute another important subset of T cells that play a critical role in slowing the rate of disease progression through the differentiation and expansion of different types of memory cell subsets. However, the role of these immune cell subsets in T cell homeostasis, CD4$^+$ T cell proliferation, and progression of disease, particularly in HIV-2 infection, has not yet been elucidated. The present study involved a detailed evaluation of the different CD4$^+$ T cell subsets in HIV-2 infected persons with a view to understanding the role of these immune cell subsets in the better control of virus replication and delayed disease progression that is characteristic of HIV-2 infection. We observed elevated levels of CD4$^+$ Tfh and CD4$^+$ Tscm cells along with memory and effector T cell abundance in HIV-2 infected individuals. We also found increased frequencies of CXCR5$^+$ CD8$^+$ T cells and CD8$^+$ Tscm cells, as well as memory B cells that are responsible for NAb development in HIV-2 infected persons. Interestingly, we found that the frequency of memory CD4$^+$ T cells as well as memory B cells correlated significantly with neutralizing antibody titers in HIV-2 infected persons. These observations point to a more robust CD4$^+$ T cell response that supports B cell differentiation, antibody production, and CD8$^+$ T cell development in HIV-2 infected persons and contributes to better control of the virus and slower rate of disease progression in these individuals.

Keywords: HIV-2, ART, CTL, TSCM cells, TFH cells, CXCR5+ CD8+ cells, B cells

OPEN ACCESS

Edited by:
Sunil Kannanganat Sidharthan, Baylor College of Medicine, United States

Reviewed by:
Shetty Ravi Dyavar, University of Nebraska Medical Center, United States
Riti Sharan, Texas Biomedical Research Institute, United States

****Correspondence:***
Luke Elizabeth Hanna
hanna@nirt.res.in

[†]These authors have contributed equally to this work

Specialty section:
This article was submitted to Viral Immunology, a section of the journal Frontiers in Immunology

Received: *10 February 2021*
Accepted: *23 March 2021*
Published: *16 April 2021*

Citation:
Ponnan SM, Vidyavijayan KK, Thiruvengadam K, Hilda J N, Mathayan M, Murugavel KG and Hanna LE (2021) Role of Circulating T Follicular Helper Cells and Stem-Like Memory CD4$^+$ T Cells in the Pathogenesis of HIV Infection and Disease Progression. Front. Immunol. 12:666388. doi: 10.3389/fimmu.2021.666388

INTRODUCTION

Acquired immunodeficiency in humans is caused by two types of human immunodeficiency virus (HIV), namely HIV-1 and HIV-2 (1). HIV-2 is less pathogenic than HIV-1, the course of disease is slower, and the proportion of disease controllers is significantly greater with HIV-2 infection (2). Unlike the case in HIV-1 infection, reduction in $CD4^+$ T cells is much slower in HIV-2 infection (2). Several studies have documented the significance of antiviral $CD4^+$ as well as $CD8^+$ T cells in the control of infection in HIV-1 non-progressors and HIV-2 slow progressors (3–7). Studies have also shown differences in levels of expression of immune activation as well exhaustion markers including HLA-DR, PD1, CCR5, SAMHD1, Blimp-1 and TRIM5α on $CD4^+$ T cell subsets in HIV-1 and HIV-2 infected individuals (8). Other factors that have been implicated in slower disease progression associated with HIV-2 infection include higher frequencies of virus-specific highly differentiated polyfunctional T cells and high titers of neutralizing antibodies (7, 9). However, the role of recently identified CD4+ T cell subsets like the T follicular helper cells and stem cell like memory T cells that are known to play a critical role in the control of HIV infection have not been investigated in the context of HIV-2 infection.

B cell-helping follicular T helper cells (Tfh cells) are reported to be an important subset of T cells involved in the production of high titers of neutralizing antibodies during the course of HIV disease as well as vaccination (10, 11). Earlier studies have documented the central role of Tfh cells in the control of HIV infection in long-term non-progressors (LTNPs) (8). A recent study found that Tfh cells constitute major viral reservoirs even in HIV-2 infected individuals with undetectable viremia and preserved blood $CD4^+$ T cell counts (12). Since the last decade, T cells having stem cell-like properties (T_{SCM} cells) have gained much focus. The self-renewal capacity and longer survival period of T_{SCM} cells gives them the opportunity to differentiate into effector T cells (13). Increased frequency of T_{SCM} cells has also been reported in HIV-vaccinated individuals as well as elite controllers (EC) (14, 15). While there is evidence to suggest that T_{SCM} cells are essential for differentiation and enrichment of mature central effector (CE), effector memory (EM), and terminal effector (TE) cells in HIV-1 infected individuals (16–18), the possible role of these cells in HIV-2 infection has not been well explored.

It has been reported that the total number of B cells in peripheral blood also increases with an increase in $CD4^+$ T cell count after initiation of ART (19, 20), since the $CD4^+$ T cells connect the cellular and humoral arms of the immune system. Studies have reported that memory B cell subsets are significantly expanded in HIV-2 infected persons as compared to HIV-1 infected individuals irrespective of their treatment status (21–23). Our data also demonstrate a significant expansion in the antigen-specific $CD4^+$ T cell subset in HIV-2 infected individuals, and suggest that these cells could support the activation of plasmablasts, atypical and memory B cells, as well as polyfunctional T cell and antigen-presenting cell (APC) activity (24), thus providing the basis for a robust host immune response against the pathogen. Similarly, studies on NK cells in HIV infection have critically acclaimed their role in antiviral activity (25–27). Functional and genetic studies have demonstrated the role of NK cells in slowing down disease progression (28). However, as infection progresses, NK cell subsets undergo phenotypic and functional abnormalities resulting in failure to control viral movement (28). While a large number of studies have focused on understanding the phenotype and function of NK cells in HIV-1 infection, very little is known about the role of these cell subsets in HIV-2 disease and their contribution to viral control.

The current study was undertaken to understand the role of Tfh cells, T_{SCM} cells, follicular homing $CD8^+$ T cells, as well as B cells and NK cells in determining the course of disease progression in HIV infection. We found elevated levels of $CD4^+$ as well as $CD8^+$ T cells that are phenotypically unique and express higher levels of markers pertaining to T stem cell–likeness and follicular homing phenotype, as well as CXCR5 on their surface in HIV-2 infected persons. Furthermore, we observed a higher frequency of memory B cells and NK cells in these individuals. Our observations throw light on some of the critical $CD4^+$ and $CD8^+$ T cell subsets and immune responses associated with better protection against disease progression in HIV-infected individuals and suggest that a successful HIV vaccine should elicit some of these key immune responses in order to confer protection in vaccine recipients.

MATERIALS AND METHODS

Ethics Statement

The study protocol was approved by the Scientific Advisory Committee of the ICMR-National Institute for Research in Tuberculosis (NIRT), Chennai, India, and the study was conducted in accordance with Good Clinical Laboratory Practice (GCLP) guidelines. The study protocol was also reviewed and approved by the Institutional Ethics Committee of ICMR-NIRT (TRC IEC No: 2009009) and the Institutional Review Board of the Y. R. Gaitonde Centre for AIDS Research and Education (YRG IRB No: 279), Chennai, India.

Study Participants

The study was carried out on samples collected during the period 2016-2018. Sample collection was performed at YRG CARE, one of the largest tertiary referral HIV Care Centres in southern India, providing medical care and support for more than 22,000 patients, and the study was conducted at ICMR-NIRT. The study population comprised of 4 groups of individuals: (i) HIV-2 infected persons (HIV-2; n=37), (ii) HIV-1 infected individuals on antiretroviral therapy (HIV-1+ART+; n=10),(iii) HIV-infected individuals naïve to ART (HIV-1+ART-; n=10), and (iv) HIV–unexposed uninfected healthy women (HU; n=35). Individuals in groups 1 & 2 received ZDV (Zidovudine) + 3TC (Lamivudine) + NVP (Nevirapine) or TDF (Tenofovir) + 3TC (Lamivudine) + EFV (Efavirenz) as per the National Technical Guidelines on Antiretroviral Treatment (NACO, 2018). In addition, we also included a group of HIV exposed

seronegative (HESN) individuals who were HIV-uninfected female spouses of HIV-1 seropositive men (HIV discordant couples; n=35) from one of our earlier studies (unpublished data) for comparison. Enrolment into the study required the willingness of participants to provide written informed consent for specimen collection and storage. All HIV-2 infected persons were free of HIV-1 co-infection at the time of sampling (**Table 1**). Diagnosis and confirmation of HIV-2 infection was based on serological and molecular diagnostic tests. Serological testing was done using the Retro quick rapid test (Qualpro Diagnostics) and HIV-1/2 Tridot (J. Mitra). Samples were further tested using molecular tests to confirm the absence of HIV-1 co-infection with negative detection in HIV-1 DNA-PCR and positive detection in HIV-2 gene-specific PCR.

Isolation and Cryopreservation of PBMC

Ten milliliters of blood was collected from all study participants by venepuncture in a green top VACUTAINER® containing sodium heparin as the anticoagulant and used for the isolation of peripheral blood mononuclear cells (PBMC). PBMC were isolated by density gradient centrifugation and cryopreserved at <-190°C.

Phenotypic Analysis of Immune Cell Subsets

Cryopreserved PBMC obtained from the study participants were used for immunophenotyping by flow cytometry. Briefly, two million cells were washed with FACS buffer and stained with Live/Dead Fixable Aqua blue dye (Invitrogen). The following cocktail of monoclonal antibodies were used to enumerate the different cell types: T follicular helper and Treg panel: CD3-APC H7 (SK7), CD4-BUV 737 (SK3), CD8-APC R 700 (RPA-T8), CD45RO BUV395 (UCHL-1),CCR7-PEcy7 (G043H7), CXCR3-PERCP Cy5.5 (IC6), CXCR5-BB515 (RF8B2), PD-1-PE (EH12.1), CD25-APC (A251) and CD127-PECF594 (HIL.7R.M21); B cell panel: CD3-APC H7(SK7), CD38-APC (HIT2), CD20-PE (HIB19), CD19-BUV395 (3H7), IgD-BUV737 (IA6.2), CD27-BB515 (0323; Memory T cell and T_{SCM} panel: CD3-APCH7 (SK7), CD8-APCR700 (RPA.T8), CD4-BUV737 (RPA-T4), CD45RO-BUV395 (UCHL-1), CCR7-PEcy7 (G043H7),CD95-PECF594 (DX2), CD28-APC (28.2), CD122-PE (MIKB2). NK cell panel: CD3-APCH7 (SK7), CD56-APC (B519), CD16-BUV737 (3CG8), CD95- PECF594 (DX2), NKG2D-PERCP CY5.5 (1D11). Cells were stained with the antibodies for 20 minutes at 4°C (antibody and clone description are provided in **Table S1**). About 2×10^6 cells were stained for each panel. After staining, the cells were washed, fixed with BD Cytofix (2% paraformaldehyde), and analyzed on a FACS ARIA III SORP flow cytometer (Becton Dickinson). A minimum of 1,000,000 total events were acquired, and data were analyzed using FlowJo software, version 10.5 (Tree Star Inc., Ashland, Oregon, USA).

Statistical Analysis

Statistical analyses were performed using GraphPad Prism, version 7.05 (GraphPad Software, Inc., CA). Values are presented as median and interquartile range. Percentage frequency of the immune cell subsets like memory T cells, follicular helper-like $CD8^+$ T cells (CXCR5+ $CD8^+$ T cells), T_{SCM} cells, B cells and NK cells were compared between the HIV-2, HIV-1, HESN and HU groups using Kruskal-Wallis test, followed by subgroup analysis using Dunn's multiple comparison test. Correlation analysis was performed to determine the relationship between the frequency of different immune cell types and broadly neutralizing antibodies titer. For all analyses, differences were considered significant if the p-value was <0.05.

RESULTS

Expansion of Circulating T Follicular Helper Cells, Stem-Like Memory $CD4^+$ T Cells, and $CXCR5^+CD8^+$ T Cells in HIV-2 Infected Individuals

Recent studies suggest that follicular $CXCR5^+$ $CD8^+$ T cells and $CD8^+$ stem-like memory cells are involved in the control of HIV/SIV infection (29, 30). We therefore, evaluated the frequencies of these T cell subsets in HIV-2 infected individuals and compared it with that seen in HIV-exposed seronegative (HESN) individuals, HIV-1 infected persons on antiretroviral treatment (HIV-1+ART+) as well as those not on treatment (HIV-1+ART-), and HIV-unexposed healthy individuals (HU). Polychromatic flow cytometry was used to enumerate the different T cell subsets, including circulating Tfh cells, CXCR5 expressing $CD8^+$ T cells, stem-like memory T cells, and regulatory T cells. Tfh and CXCR5 expressing $CD8^+$ T cells were defined using CXCR5 and PD-1, T stem-like memory cells were identified using CD28 and CD95 expression on naïve T cells, and T regs were identified based on the expression of CD25 on $CD127^-$ $CD4^+$ T cells (**Figure 1A**).

TABLE 1 | Demographic characteristics of Study Populations Groups.

	HIV-2 N=37	HU N=35	HIV+ART+ N=10	HIV+ART- N=10	HE SN N=35
Age mean (range)	43 (18-57)	33(22-42)	34(32-39)	35(30-48)	36(27-42)
STDs (BV, CT, NG)	0	0	0	0	0
ART details	37(100%)	0	10(100%)	NA	NA
Viral Load, Log10 copies/mL, mean (SD)	NA	NA	2.14	4.4943(0.9036)	NA
CD4 Count at treatment initiation (cells/mL), median (IQR)	617(33-3097)	NA	392(289-492)	NA	NA

BV, Bacterial Vaginitis; CT, Chlamydia trachomatis; NG, Neisseria gonorrhoeae; HESN, HIV exposed seronegative; HIV+ART+, HIV-infected women on ART; HIV+ART-, HIV-infected women naïve to ART; HU, HIV unexposed seronegative controls.

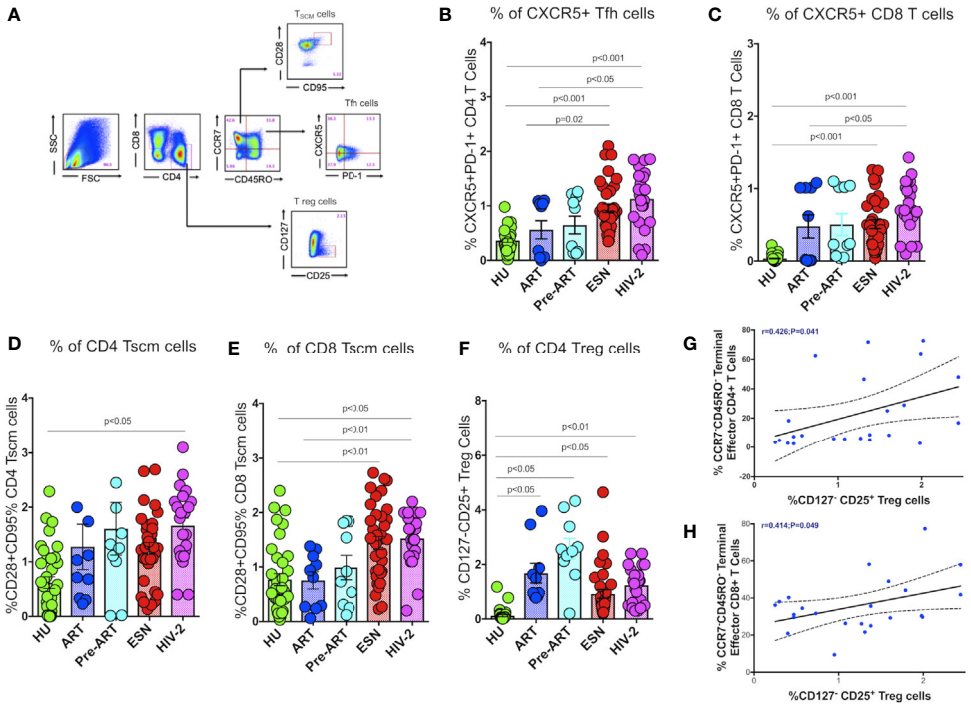

FIGURE 1 | Distribution of Tfh cells and stem-like memory T cells in the study population. **(A)** Representative flow plots for enumeration of Tfh cells, CXCR5$^+$ T cells, Tscm cells and regulatory T cells. **(B)** Frequency of CXCR5$^+$ CD4$^+$ Tfh cells in the HU, HIV-1+ART+, HIV-1+ART-, HESN and HIV-2 groups. **(C)** Frequency of CXCR5$^+$ CD8$^+$ T cells in the HU, HIV-1+ART+, HIV-1+ART-, HESN and HIV-2 groups. **(D)** Frequency of CCR7-CD28+CD95+ stem-like memory CD4$^+$ T cells in the HU, HIV-1+ART+, HIV-1+ART-, HESN and HIV-2 groups. **(E)** Cumulative frequency of CCR7-CD28+CD95+ stem-like memory CD8$^+$ T cells in the HU, HIV-1+ART+, HIV-1+ART-, HESN and HIV-2 groups. **(F)** Frequency of CD127- CD25+ regulatory T cells in the HU, HIV-1+ART+, HIV-1+ART-, HESN and HIV-2 groups. Scatter dot plots summarize the % frequency of total CXCR5+ T cells, Tscm cells and Treg cells (median, 1st and 3rd quartiles). P values were calculated using the K-Wallis test. Sub-group analysis was performed using Dunn's test. **(G)** Correlation between frequency of CCR7-CD45RO- Terminal Effector Memory CD4$^+$T cells and frequency of CD25+127- CD4$^+$ T Regulatory cells in HIV-2 infected individuals. **(H)** Correlation between frequency of CCR7-CD45RO- Terminal Effector Memory CD8$^+$ T cells and frequency of CD25+127- CD4$^+$ T regulatory cells in HIV-2 infected individuals. (Note: HU: HIV unexposed seronegative controls, n = 35; HIV-1+ART+: HIV-1-infected women on ART, n = 10; HIV-1+ART-: HIV-infected women naïve to ART, n = 10; HESN: HIV exposed seronegative individuals, n = 35; HIV-2: HIV-2 infected persons, n = 37).

We found significantly elevated numbers of CD4$^+$ Tfh cells in HIV-2 infected individuals (median: 1.21%; range: 0.70-1.56%) as compared to HIV-1 infected persons (median: 0.58%; range: 0.04-1.04%; p<0.05) as well as unexposed healthy individuals (median: 0.37%; range: 0.23-0.44%; p<0.001) (**Figure 1B**). Incidentally, we also found higher numbers of CD4$^+$ Tfh cells in the ESN group (median: 0.86%; range: 0.61-1.27%) as compared to the HIV-infected (median: 0.58%; range: 0.04-1.04%; p=0.02) and HIV-unexposed healthy control groups (median: 0.37%; range: 0.23-0.44%; p<0.001). Further, we found significantly higher frequencies of CXCR5$^+$CD8$^+$ T cells in HIV-2 infected individuals (median: 0.90%; range: 0.61-1.10%) as compared to HIV-1 infected individuals on ART (median: 0.32%; range: 0.01-1.01%; p<0.05) as well as HIV-unexposed healthy controls (median: 0.01; range: 0.01-0.04%) (p<0.001) (**Figure 1C**). Collectively, our findings reveal significant expansion of critical T cell subsets that help boost the host immune response leading to better control of the virus and slower course of disease progression in HIV-2 infected individuals.

Earlier studies have reported that the self-renewing and multipotent Tscm cells mature into memory cells or reservoirs of effector T lymphocytes, which continue to persist in the host even in the absence of antigen (31). Hence, expansion of Tscm cells appears to be a very critical component in the control of HIV infection. Very interestingly, we found significantly increased numbers of Tscm cells in both the CD4$^+$ and CD8$^+$ T cell compartments in HIV-2 infected individuals as compared to HIV-1-infected persons (**Figures 1D, E**). The median frequency of circulating CD4$^+$ Tscm cells in the HIV-2 group was 1.80% (range: 1.10-2.10%), HIV-1 infected group on ART was 0.8% (range: 0.31-1.80%), HIV infected group naïve to ART was 1.20% (range: 0.70-2.10%), and unexposed healthy groups was 0.63% (range: 0.01-1.45%) respectively. The median frequency of circulating CD8$^+$ Tscm cells in the HIV-2 group was 1.70% (range: 1.21-2.21%), HIV-1 infected group on ART was 0.877% (range: 0.26-1.23%), HIV infected group naïve to ART was 0.82% (range: 0.21-1.81%), and unexposed healthy groups was 0.56% (range: 0.23-1.17%). Another striking observation was the presence of a significantly higher

frequency of CD8$^+$ Tscm cells in the HESN population (median 1.26%; range: 0.71-1.93%) as compared to the HIV-1 infected and HU groups.

In contrast, we observed a decreased frequency of Treg cells in the HIV-2 and HESN groups as compared to the other groups. The ART-naive HIV-infected group had a significantly higher proportion of CD4$^+$ Treg cells as compared to the other study groups ($p<0.01$) (**Figure 1F**). We further analyzed the correlation between the Tregs and memory T cell subsets and found an inverse correlation between Tregs and effector memory T cells in both CD4$^+$ (r-0.4, p=0.04) and CD8$^+$ (r-0.4, p=0.05) T cell compartments in HIV-2 infected individuals (**Figures 1G, H**). These findings clearly indicate that increased frequency of Tregs help maintain immune homeostasis by controlling the exaggerated immune response and promoting the development of long-lived memory cells during HIV-2 infection.

Increased Frequency of Memory B Cells and Plasmablast B Cells in HIV-2 Infection

We analyzed the frequency of different memory B cell subsets in the study groups. Surface markers CD27 and CD38 were used to identify plasmablast B cells (CD19+CD38+CD27+). Memory B cell subsets were distinguished based on IgD and CD27 expression as unswitched memory B cells (IgD+CD27+), class switched memory B cells (IgD- CD27+), atypical memory B cells (IgD-CD27-), and naive B cells (IgD+CD27-) as described by Kaminski et al. (32) (**Figure 2A**). We found a higher frequency of short-lived antibody-secreting plasmablast cells in the HIV-2 positive (median:1.91%; range 1.50 - 2.40%) as well as HESN (median:1.44%; range: 1.05 - 2.14%) groups as compared to treated HIV-1 infected and healthy uninfected groups (median: 1.01%; range: 0.64 -1.69%; $p<0.001$). Numbers of plasmablast cells were also significantly higher in ART-naïve HIV-1-infected individuals as compared to treated individuals (median:1.95%; range: 1.30- 3.61% $p<0.05$) (**Figure 2B**). These observations suggest that HIV infection, in general, is associated with an increase in the numbers of antibody-secreting plasmablast cells that further differentiate into long-lived plasma cells and contribute to better control of infection, but their role in slowing down disease progression remains to be clarified.

The HIV-2 and HESN groups were found to possess significantly higher frequencies of class-switched memory B cells and IgM memory B cells (unswitched) as compared to the HIV-1 and HU groups ($p<0.001$). The median frequency of class-switched memory B cells was 18.2% (range: 12.5 - 23.2%) and unswitched memory B cells was 27.6% (range: 22.8 - 35.4%) in the HIV-2 group (**Figures 2C, D**). We observed a significantly higher proportion of atypical memory B cells in both HIV-1+ART+ and HIV-2 groups as compared to the other groups (**Figure 2E**).

We found a direct correlation between the frequency of atypical memory B cells and the titer of neutralizing antibodies in HIV-2 infected persons (r=0.61, p=0.002) (**Figure 2F**) (neutralizing antibody titres of HIV-2 infected persons is provided in Supplementary Table 1). Levels of atypical

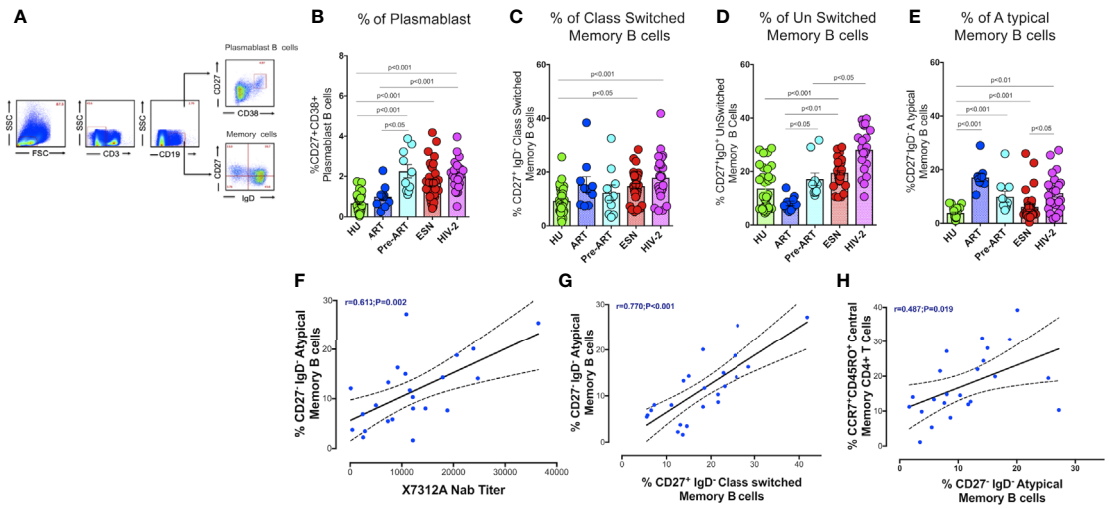

FIGURE 2 | Distribution of Memory B cells and Plasmablast B cells in the study groups. **(A)** Representative flow plots for enumeration of memory B cells and Plasmablast B cells (CD27+CD38+ expression on B cells) among the HU, HIV-1+ART+, HIV-1+ART-, HESN and HIV-2 groups. **(B)** Frequency of CD27+CD38+ Plasmablast B cells in the HU, HIV-1+ART+, HIV-1+ART-, HESN and HIV-2 groups. **(C)** Frequency of CD27+IgD- Class Switched Memory B cells in the HU, HIV-1+ ART+, HIV-1+ART-, HESN and HIV-2 groups. **(D)** Frequency of CD27-IgD- unswitched Memory B cells in HU, HIV-1+ART+, HIV-1+ART-, HESN and HIV-2 groups. **(E)** Frequency of CD27+IgD+ Atypical Memory B cells in HU, HIV-1+ART+, HIV-1+ART-, HESN and HIV-2 groups. The scatter dot plots summarize the % frequency of total memory B cells and Plasmablast cells (median, 1st and 3rd quartiles). P values were calculated using the K-Wallis test. Sub-group analysis was performed using Dunn's test. **(F)** Correlation between frequency of CD27-IgD- Atypical Memory B cells and X7312A neutralizing antibody titers in HIV-2 infected individuals. **(G)** Correlation between frequency of CD27-IgD- Atypical memory B cells and frequency of CD27+IgD- Class Switched Memory B cells in HIV-2 infected individuals. **(H)** Correlation between frequency of CCR7+ CD45RO+ Central Memory CD4$^+$ T cells and frequency of CD27-IgD- Atypical Memory B cells in HIV-2 infected individuals. (HU, HIV unexposed seronegative controls, HIV-1+ART+: HIV-1-infected women on ART; HIV-1+ART-: HIV-1-infected women naïve to ART; HESN: HIV exposed seronegative individuals; HIV-2: HIV-2 infected persons).

memory B cells also correlated positively with the frequency of class-switched memory B cells and central memory CD4$^+$ T cells (r=0.48, p<0.019 and r=0.77, p<0.001 respectively) (**Figures 2G, H**). These observations provide further evidence to suggest that early HIV-2 infection is associated with increased CD4$^+$ T cell help for B cell differentiation resulting in the development of increased numbers of memory B cell subsets as well as antibody-secreting plasma B cells, thus constituting a robust immune response to fight the infection.

Increased Frequency of Effector Memory CD4$^+$ and CD8$^+$ T Cells in HIV-2 Infected Individuals

We examined the distribution of memory CD4$^+$ and CD8$^+$ T cells in HIV-2 infected individuals, given the potential role of these cell types in slowing down disease progression. Effector memory cells are characterized by the expression of C-C chemokine receptor type-7 and CD45RO on their cell surface. Based on their function, 4 distinct populations of effector cells have been described by Gattinoni et al. (31). These include the central memory (CM) T cells defined as CD3+CD4+/CD8+CD45RO+CCR7+ cells, effector memory (EM) T cells defined as CD3+CD4+/CD8+ CD45RO+CCR7- cells, terminal effector (TE) T cells defined as CD3+CD4+/CD8+CD45RO-CCR7- cells and naïve T cells (TN) defined as CD3+CD4+/CD8+CD45RO-CCR7+ cells.

The proportion of CD4$^+$ and CD8$^+$ naïve T cells was significantly lower in the HIV-2, HESN, HIV-1+ART+ and HIV-1+ART- groups as compared to the HU group (**Figure 3A**). On the other hand, the frequency of CD4$^+$ effector memory T cells and terminal effector T cells was significantly higher in the HIV-2 and HESN groups (**Figures 3B, C**). While the median frequency of CD4$^+$ terminal effector T cells was 18.6 % (range: 12.7- 36.5%) in the HIV-2 group and 14.31% (range: 11.40 - 20.21%) in the HESN group, the median frequency of CD4$^+$ effector memory T cells was 43.6% (range: 31.5 - 52.3%) in the HIV-2 group and 44.1% (range: 39.5 - 55.1%) in the HESN group. Earlier studies have also reported a progressive expansion of terminal effector T cells during viral infections, including HIV-1 infection (33–35). We also found that the proportion of cytotoxic function exhibiting terminal effector T cells was very high in HIV-2 infected individuals as compared to HIV-1 infected persons and healthy controls. On the other hand, the proportion of CD4$^+$ central memory T cells was higher in the HIV-1 group as compared to the HIV-2 group (**Figure 3D**).

We examined the correlation between the frequency of memory T cell subsets and neutralizing antibody titers in

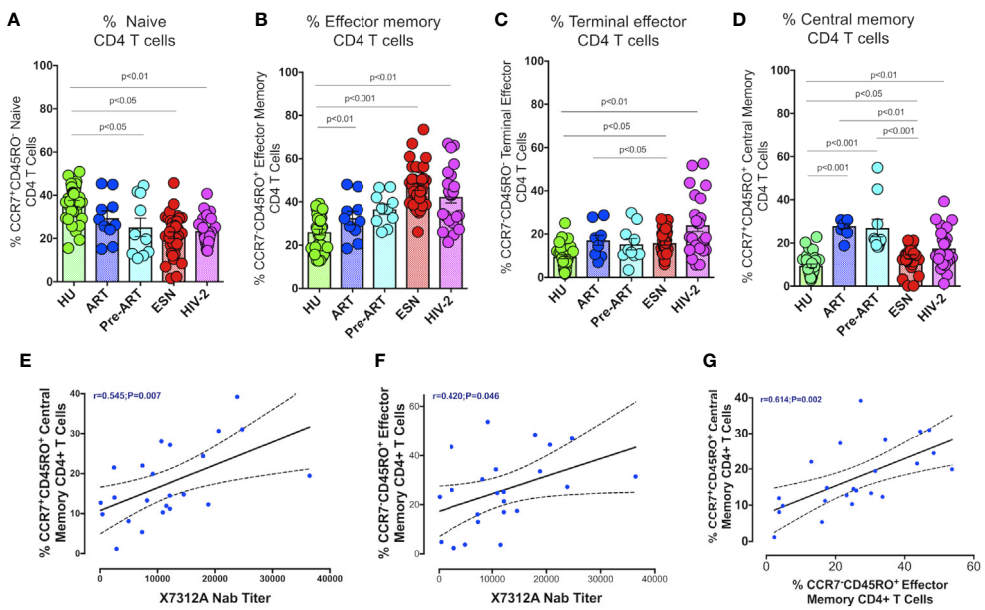

FIGURE 3 | Distribution of CD4$^+$ Memory T cell subsets in the study groups. Graphical representation showing the enumeration of CD4$^+$ Memory T cells subsets defined using CCR7 and CD45RO expression. **(A)** Frequency of CCR7+CD45RO- naïve CD4$^+$ T cells in the HU, HIV-1+ART+, HIV-1+ART-, HIV-2 and HESN groups. **(B)** Frequency of CCR7-CD45RO+ Effector Memory CD4$^+$ T cells in the HU, HIV-1+ART+, HIV-1+ART-, HIV-2 and HESN groups. **(C)** Frequency of CCR7-CD45RO- Terminal Effector Memory CD4$^+$ T cells HU, HIV-1+ART+, HIV-1+ART-, HIV-2 and HESN groups. **(D)** Frequency of CCR7+CD45RO+ Central Memory CD4$^+$ T cells in the HU, HIV-1+ART+, HIV-1+ART-, HIV-2 and HESN groups. The scatter dot plots summarize the % frequency of total memory T cells (median, 1st, and 3rd quartiles). P values were calculated using the K-Wallis test. Sub-group analysis was performed using Dunn's test. **(E)** Correlation between frequency of CCR7+ CD45RO+ Central memory CD4$^+$ T cells and X7312A neutralizing antibody titers in HIV-2 infected individuals. **(F)** Correlation between frequency of CCR7-CD45RO+ Effector Memory CD4$^+$ T cells and X7312A neutralizing antibody titers in HIV-2 infected individuals. **(G)** Correlation between frequency of CCR7+ CD45RO+ Central Memory CD4$^+$ T cells and frequency of CCR7-CD45RO+ Effector Memory CD4$^+$ T cells in HIV-2 infected individuals. (Note: HU: HIV unexposed seronegative controls, HIV-1+ART+: HIV-1-infected women on ART; HIV-1+ART-: HIV-1-infected women naïve to ART; HESN: HIV exposed seronegative individuals; HIV-2: HIV-2 infected persons).

HIV-2 infected individuals. Interestingly, we found a positive correlation between the frequency of $CD4^+$ central memory cells as well as effector memory T cells with X731A neutralizing antibodies titer (r=0.54, p=0.007, and r=0.42, p=0.046 respectively) in HIV-2 infected individuals (**Figures 3E, F**). In addition, we noticed a correlation between $CD4^+$ central memory T cells and $CD4^+$ effector memory T cells (r-0.61, p=0.002) (**Figure 3G**) in the study population.

We also examined the distribution of $CD8^+$ memory T cells in HIV-2 infected individuals. As seen with $CD4^+$ T cells, naïve $CD8^+$ T cells were present at significantly lower levels in the HIV-1 and HIV-2 infected groups as compared to the healthy controls (**Figure 4A**). On the other hand, $CD8^+$ terminal effector memory T cells were significantly higher in the HIV-2 and HESN groups as compared to the other groups ($p<0.05$). The median frequency of $CD8^+$ terminal effector T cells was 40.3% (range: 30.4 - 49.4%) in the HIV-2 group and 48.30% (range: 44.31-55.30%) in the HESN group (**Figure 4C**). In contrast, HIV-1-infected persons had a significantly higher proportion of $CD8^+$ effector and central memory T cells ($p<0.001$) (**Figure 4B**). The median frequency of CD8+ effector memory T cells was 44.6% (range: 40.6 - 49.9%) in the HIV-1+ART- group and 38.6% (range: 29.5 - 43.3%) in the HIV-1+ART+ group. The median frequency of $CD8^+$ central memory T cells was 24.4% (range: 20.7 - 34.8%) in the HIV-1+ART- group and 32.2% (range: 22.4 - 36.1%) in the HIV-1+ART+ group (**Figure 4D**).

In HIV-2 infected individuals, correlation analysis revealed a significant correlation between the frequency of $CD4^+$ effector memory T cells and $CD8^+$ central memory T cells (r=0.49, p=0.016) (**Figure 4E**). Similarly, $CD4^+$ effector memory T cells correlated significantly with levels of $CD8^+$ effector memory T cells and $CD8^+$ central memory T cells (r=0.46, p=0.016 and r=0.48, p=0.020) (**Figure 4F**). Levels of $CD8^+$ central memory T cells correlated positively with $CD8^+$ effector memory T cells (r-0.69, $p<0.001$) (**Figure 4G**).

Increased Frequency of NKG2D Expressing CD56 Negative CD16+ NK Cells in HIV-2 Infected Persons

NK cell-mediated ADCC is thought to be an essential mechanism involved in controlling HIV infection. Several studies have described NK cell activation and cytolytic function in HIV-1 infected individuals as well as in long-term non-progressors (LTNP) and elite controllers (EC) (36–39). However, the distribution of NK cells and their profile in HIV-2 disease remains mostly undefined. To address this knowledge gap, we characterized the population of NK cell subsets

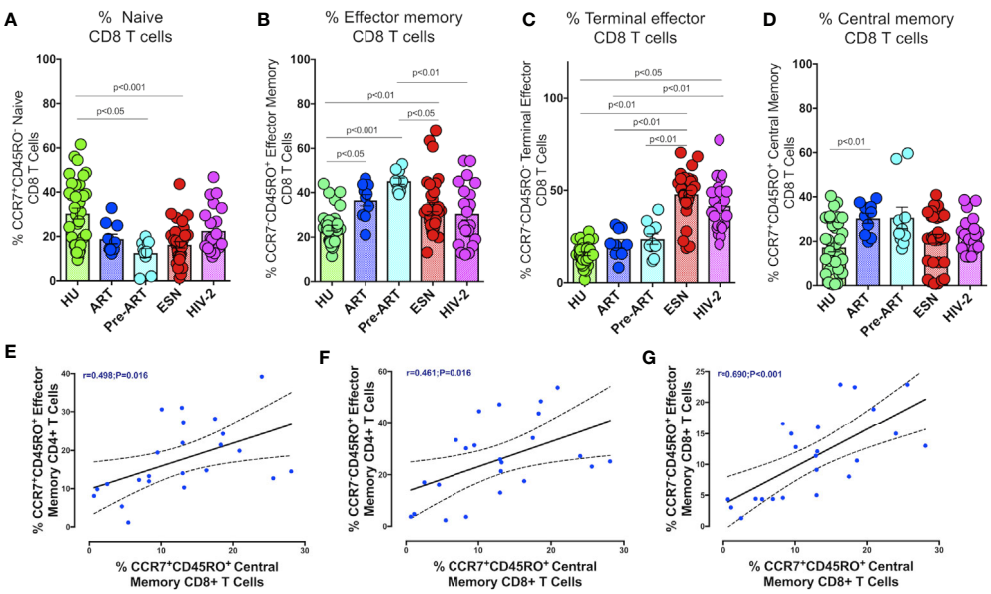

FIGURE 4 | Distribution of $CD8^+$memory T cells responses in the study groups. Graphical representation of the enumeration of $CD8^+$memory T cells subsets defined using CCR7 and CD45RO expression. **(A)** Frequency of CCR7+CD45RO- naïve $CD8^+$ T cells in the HU, HIV-1+ART+, HIV-1+ART-, HIV-2 and HESN groups. **(B)** Frequency of CCR7-CD45RO+ Effector Memory $CD8^+$ T cells in the HU, HIV-1+ART+, HIV-1+ART-, HIV-2 and HESN groups. **(C)** Frequency of CCR7-CD45RO- Terminal Effector Memory $CD8^+$ T cells HU, HIV-1+ART+, HIV-1+ART-, HIV-2 and HESN groups. **(D)** Frequency of CCR7+CD45RO+ Central Memory $CD8^+$ T cells in the HU, HIV-1+ART+, HIV-1+ART-, HIV-2 and HESN groups. The scatter dot plots summarize the % frequency of total memory T cells (median, 1st, and 3rd quartiles). P values were calculated using the K-Wallis test. Sub-group analysis was performed using Dunn's test. **(E)** Correlation between frequency of CCR7-CD45RO+ Effector Memory $CD4^+$ T cells and frequency of CCR7+CD45RO+ Central Memory $CD8^+$ T cells in HIV-2 infected individuals. **(F)** Correlation between frequency of CCR7-CD45RO+ Effector Memory $CD4^+$ T cells and frequency of CCR7-CD45RO+ Effector Memory $CD8^+$ T cells in HIV-2 infected individuals. **(G)** Correlation between frequency of CCR7-CD45RO+ Effector Memory $CD4^+$ T cells and frequency of CCR7+CD45RO+ Central Memory $CD8^+$ T cells in HIV-2 infected individuals. (Note: HU: HIV unexposed seronegative controls, HIV-1+ART+: HIV-1-infected women on ART; HIV-1+ART-: HIV-1-infected women naïve to ART; HESN: HIV exposed seronegative individuals; HIV-2: HIV-2 infected persons).

expressing the activation receptor NKG2D and the exhaustion marker CD95 receptor in the study population (**Figure 5A**).

We observed significantly higher frequencies of CD56^{negative} CD16^{+} NK cells in HIV-2 infected individuals as compared to HIV-1-infected persons and unexposed healthy individuals (p=0.036) (**Figure 5B**). The median frequency of CD56^{negative} CD16^{+} NK cells in the HIV-2 group was 25% (range:14.1 - 38.5%) and 12.9% (range: 10.4 - 17.1%) in the HIV-1 group. On the other hand, there was no difference in the proportion of CD56^{dim} CD16^{+} NK cells as well as CD56^{bright} CD16^{+} NK cells between the groups (**Figures 5C, D**). However, earlier studies have documented a significant reduction in the proportion of mature CD56^{dim} NK cells as well as immature CD56^{bright} NK cells in HIV-1 infection (40), with a concomitant increase in the numbers of CD56^{negative} NK cells (41). Our study demonstrates a greater increase in the proportion of CD56^{negative} NK cells than CD56^{bright} and CD56^{dim} NK cells in HIV-2 infected individuals.

We also found significantly higher numbers of CD56^{negative} NK cells expressing the NKG2D activating receptor in HIV-2 infected individuals than in HIV-1 and HU individuals (p<0.001 and p<0.05, respectively) (**Figure 5E**). On the other hand, HIV-1 infected individuals had significantly higher numbers of NKG2D expressing CD56^{bright} and CD56^{dim} NK cells (**Figures 5F, G**). Similarly, CD95 expressing CD56^{bright} and CD56^{dim} NK cells were also significantly more in HIV-2 infected persons as compared to HIV-1-infected individuals and healthy unexposed controls. However, there was no difference between the groups with respect to CD95 expression on CD56^{negative} NK cells (**Figures 5H-J**).

We also examined the correlation between levels of CD56^{negative} NK cells and neutralizing antibodies titer as well as other memory T cells and B cell subsets in HIV-2 infected individuals. Interestingly, we found that levels of CD56^{negative} NK cells correlated significantly with levels of CD27^{+} IgD^{-} class-switched memory B cells as well as CD27^{-} IgD^{-} atypical memory B cells (r-0.70, p=0.0001 and r-0.47, p=0.022) (**Figures 5K, L**). Overall, our results indicate that the unconventional cytotoxic CD56^{negative} NK cells in HIV-2 infected individuals possess

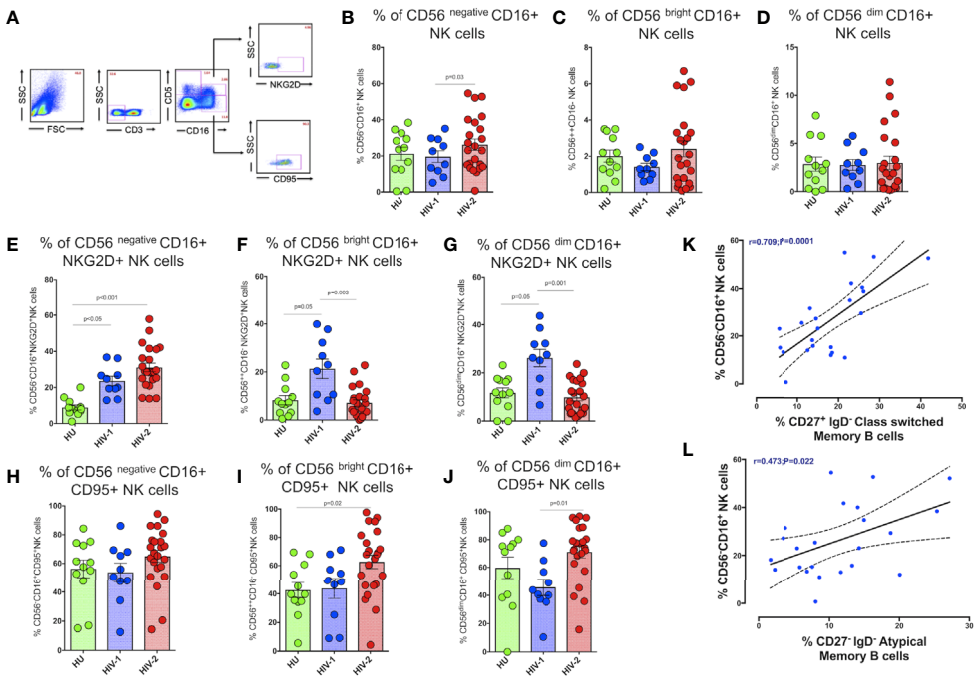

FIGURE 5 | Distribution of NK cell subsets in the study population. **(A)** Representative flow plots showing the enumeration of NK cell subsets based on CD16 and CD56 expression in the study population (HU N=35, HIV-1+ART+ N=10, and HIV-2 N=37). **(B)** Frequency of CD56 negative CD16+ NK cells in the HU, HIV-1+ART+ and HIV-2 groups. **(C)** Frequency of CD56 bright CD16+ NK cells in the HU, HIV-1+ART+ and HIV-2 groups. **(D)** Frequency of CD56 dim CD16+ NK cells in the HU, HIV-1+ART+ and HIV-2 groups. **(E)** Frequency of CD56 negative CD16+NKG2D+ NK cells in the HU, HIV-1+ART+ and HIV-2 groups. **(F)** Frequency of CD56 bright CD16+NKG2D+ NK cells in the HU, HIV-1+ART+ and HIV-2 groups. **(G)** Frequency of CD56 dim CD16+NKG2D+ NK cells in the HU, HIV-1+ART+ and HIV-2 groups. **(H)** Frequency of CD56 negative CD16+CD95+ NK cells in the HU, HIV-1+ART+ and HIV-2 groups. **(I)** Frequency of CD56 bright CD16+CD95+ NK cells in the HU, HIV-1+ART+ and HIV-2 groups. **(J)** Frequency of CD56 dim CD16+95+ NK cells in the HU, HIV-1+ART+ and HIV-2 groups. The scatter dot plots summarize the % frequency of NK cell subsets with differential expression of CD56 and CD16 (median, 1st and 3rd quartiles). P values were calculated using the K-Wallis test. Sub-group analysis was performed using Dunn's test. **(K)** Correlation between the frequency of CD56 negative CD16+ NK cells and frequency of CD27+ IgD- Class Switched Memory B cells in HIV-2 infected individuals. **(L)** Correlation between the frequency of CD56 negative CD16+ NK cells and frequency of CD27- IgD- Atypical Memory B cells in HIV-2 infected individuals. (Note: HU: HIV-unexposed seronegative controls; HIV-1+ART+: HIV-1-infected women on ART; HIV-2: HIV-2 infected individuals.

increased activation and reduced exhaustion properties and suggest a possible role for these cells in the slower course of disease progression that is characteristic of HIV-2 infection.

DISCUSSION

$CD4^+$ T cells are the central mediators of the adaptive immune response. $CD4^+$ T cell depletion is the hallmark of the pathogenesis of HIV-1 and HIV-2 infection (42). However, the host immune system continuously exchanges dying $CD4^+$ T cells with naïve $CD4^+$ T cells during the early stages of HIV infection (43). Compared to HIV-1, HIV-2 is less pathogenic and is associated with a long asymptomatic phase after infection, reduced viral load and slower decline of $CD4^+$ T cells (44, 45). It may be assumed that elevated effector and memory cell differentiation could contribute to better control of viremia and slower disease progression in controllers of HIV infection (46). Earlier studies have reported a higher proportion of HIV-1 specific T_{SCM} cells and effector memory cells in elite controllers, suggesting a role for these cells in the resistance to HIV infection/disease progression (47, 48). Vigano et al. observed an inverse correlation between the frequency of total t_{SCM} cells and levels of plasma viremia in untreated HIV-1 infected individuals (49). A more recent study showed that, relative to effector $CD4^+$ T cells, Tfh cells serve as the major viral reservoirs in HIV-2 infected persons (12). This makes it important to understand the role of different subsets of $CD4^+$ T cells in HIV-2 infection in order to identify the correlates of delayed disease progression and slower course of disease associated with HIV-2 infection.

In the current study, we analyzed the role of key $CD4^+$ T cell subsets in the control of HIV infection and disease progression in HIV-2 infected individuals by analyzing the expression of phenotypic and functional makers pertaining to memory differentiation, stem cell-likeness and follicular homing. We also investigated the correlation between neutralizing antibody titer and $CD8^+$ memory T cell subsets in HIV-2 infected persons. We found significant expansion and enrichment of effector memory and terminal effector cells in the HIV-2 group. These findings are in line with those found in literature, where an increase in effector and terminal effector cell frequency has been reported in multiple viral infections, including HIV-1 infection (34, 50). Very interestingly, we found a significant association between central and effector memory $CD4^+$ T cells and neutralizing antibody titer (neutralizing antibody data has been reported in an earlier publication from our group) (9). Just as in the case of $CD4^+$ T cells, the frequency of effector memory and Terminal effector $CD8^+$ T cells were also substantially higher in the HIV-2 infected group. These findings suggest that HIV-2 infection elicits a robust immune response capable of activating $CD4^+$ T cells to provide continuous help to $CD8^+$ T cells as well as B cells, leading to better control of viral replication and slower progression of disease.

Tscm cells are a small subset of T cells possessing self-renewal capabilities, that when stimulated via the T cell receptor, may divide into mature memory or effector T cells (49, 51). Many studies have consistently reported a close and robust association between the proliferation of effector cells and memory T cells and virus control in HIV infection (1, 2, 52). However, there is a lack of clarity in this line with regard to HIV-2 infection due to the limited number of studies in HIV-2 individuals. Interestingly, in the present study we found that HIV-2 infected persons had significantly higher levels of stem cell-like memory cells in both the $CD4^+$ and $CD8^+$ T cell compartments. Similarly, there was a significantly enriched population of Tfh cells in HIV-2-infected individuals as compared to HIV-1 infected persons. However, we found no correlation between levels of Tfh cells and B cells/ neutralizing antibody titer. This could possibly due to the small sample size in the study. HIV-2 infected individuals also had significantly elevated numbers of circulating follicular homing $CXCR5^+CD8^+$ T cells as compared to HIV-1 infected individuals.

HIV-1 natural controllers are known to possess high levels of $CXCR5^+$ $CD8^+$ Tscm cells, which correlate inversely with the viral load (14). We found higher frequencies of Tscm and $CXCR5^+$ $CD8^+$ T cells with effector memory phenotype in HIV-2 individuals as compared to HIV-1 infected persons. All this evidence suggests a plausible role for HIV-2-specific Tscm cells and Tfh cells in slowing down disease progression in HIV-2 infected persons. To the best of our knowledge, the present study constitutes the first research to record elevated frequencies of Tfh cells, Tscm cells, and follicular homing $CXCR5^+$ $CD8^+$ T cells in an HIV-2 cohort from India. However, the mechanisms by which these cells reduce the viral load in HIV-2 individuals requires further investigation.

In healthy individuals, most B cells in peripheral blood are either resting naive B cells or classical type memory B cells that express either switched or unswitched antibody isotypes (IgG, IgE, and IgA, or IgM and IgD respectively) (32). In chronic HIV infection, absolute numbers of both classical and memory B cells are decreased in the peripheral circulation (53). Moir et al. reported that ART-naïve HIV-1 individuals with chronic infection had a highly expanded population of immature/ transitional B cells, whereas in early infection, plasmablasts and atypical memory B cells were more prevalent (19). A previous study showed that plasmablasts and class-switched memory B cells were induced upon vaccination in a phase-1 MVA and ADVAX prime-boost vaccine trial carried out in India (54). As with other studies, we too documented an expansion of peripheral plasmablasts as well as atypical exhausted memory B cells in both HIV-1 and 2 infected groups (19, 55, 56). Evidence suggests that atypical memory B cells can efficiently present antigens to T cells (57). This is evident from the positive correlation found between atypical memory B cells and memory $CD4^+$ T cells in our study. The expanded plasmablasts, atypical and memory cells are likely to be responsible for the increase in B cell turn over and slower disease progression associated with HIV-2 infection.

NK cells also influence the transition between innate and adaptive immune responses via the production of cytokines and chemokines (58). NK cell specificity for target cells and the

ensuing effector functions are dependent on signalling from receptors that are expressed on the surface of NK cells (38, 59). Earlier studies have documented a dramatic increase in $CD56^{neg}$ NK cells (60, 61) with low cytolytic, proliferative, and cytokine-producing capabilities in HIV-1 infection (28, 62, 63), that lyse HLA-I-deficient target cells and participate in antibody-dependent cytotoxicity (ADCC) (64, 65). Similarly, a subpopulation of $CD56^{dim}$ NK cells called terminally matured NK cells express CD57, a marker that identifies antigen-experienced NK cells, was found to be elevated in elite controllers (66). In addition, NK cells expressing NKG2D, an activation receptor used for contacting target cells and subsequently resulting in the release of perforin and other cytotoxic molecules, were reported to be higher in these individuals (67). We found an increased frequency of $CD56^{dim}$ NK cells as well as NKG2D expressing $CD56^{neg}$ NK cells in HIV-2 infected individuals as compared to those with HIV-1 infection.

To summarize, HIV infection and the onset of AIDS is characterized by extensive interaction between the host immune system and the virus. The interaction results in profound quantitative and qualitative changes in both adaptive and innate immune cells, including T and B lymphocytes and natural killer cells in infected individuals. Both host genetic and viral factors are thought to contribute to non-progression of HIV disease (68), but the features of antiviral immunity that result in an effective immune response are only partially understood. The findings of the present study reveal that HIV-2 infection elicits a superior T cell response with high levels of critical T cell subsets including Tfh cells and stem cell-like $CD4^+$ T cells that support the development of follicular homing T cells and other immune cell subsets and contribute to the control of infection. The study also documents robust memory B cell and NK cell responses that contribute to better control of HIV-2 infection and disease. We believe that vaccination strategies designed to elicit durable cellular immunity should target the generation of these immune cell types in order to provide adequate control of HIV infection. Further studies should be undertaken to fully understand the contribution and mechanistic role of these consequential cell types in HIV control.

DATA AVAILABILITY STATEMENT

The original contributions presented in the study are included in the article/**Supplementary Material**. Further inquiries can be directed to the corresponding author.

ETHICS STATEMENT

The study protocol was also reviewed and approved by the Institutional Ethics Committee of ICMR-NIRT (TRC IEC No: 2009009) and the Institutional Review Board of the Y. R. Gaitonde Centre for AIDS Research and Education (YRG IRB No: 279), Chennai, India. The patients/participants provided their written informed consent to participate in this study.

AUTHOR CONTRIBUTIONS

SMP, VV and LH designed the conceptual framework of the study. SP, VV and NH performed the experiments. SMP analyzed the data. KT contributed to statistical analyses. KM contributed to specimen collection. MM and LH contributed to the review and editing of the manuscript. SP and VV wrote the manuscript. All authors contributed to the article and approved the submitted version.

FUNDING

The present study was supported by the Department of Health Research (Human Resource Development Young Scientist Fellowship) and The Indian Council of Medical Research, Govt. of India.

SUPPLEMENTARY MATERIAL

The Supplementary Material for this article can be found online at: https://www.frontiersin.org/articles/10.3389/fimmu.2021.666388/full#supplementary-material

REFERENCES

1. Esbjornsson J, Jansson M, Jespersen S, Mansson F, Honge BL, Lindman J, et al. HIV-2 as a model to identify a functional HIV cure. *AIDS Res Ther* (2019) 16(1):24. doi: 10.1186/s12981-019-0239-x
2. Salwe S, Padwal V, Nagar V, Patil P, Patel V. T cell functionality in HIV-1, HIV-2 and dually infected individuals: correlates of disease progression and immune restoration. *Clin Exp Immunol* (2019) 198(2):233–50. doi: 10.1111/cei.13342
3. Honge BL, Petersen MS, Jespersen S, Medina C, Te DDS, Kjerulff B, et al. T-cell and B-cell perturbations are similar in ART-naive HIV-1 and HIV-1/2 dually infected patients. *AIDS (London England)* (2019) 33(7):1143–53. doi: 10.1097/QAD.0000000000002185
4. Honge BL, Petersen MS, Jespersen S, Medina C, Te DDS, Kjerulff B, et al. T-cell and B-cell perturbations identify distinct differences in HIV-2 compared with HIV-1-induced immunodeficiency. *AIDS (London England)* (2019) 33 (7):1131–41. doi: 10.1097/QAD.0000000000002184
5. Kumar P. Long term non-progressor (LTNP) HIV infection. *Indian J Med Res* (2013) 138(3):291–3.
6. de Silva TI, Peng Y, Leligdowicz A, Zaidi I, Li L, Griffin H, et al. Correlates of T-cell-mediated viral control and phenotype of CD8(+) T cells in HIV-2, a naturally contained human retroviral infection. *Blood* (2013) 121(21):4330–9. doi: 10.1182/blood-2012-12-472787
7. Duvall MG, Precopio ML, Ambrozak DA, Jaye A, McMichael AJ, Whittle HC, et al. Polyfunctional T cell responses are a hallmark of HIV-2 infection. *Eur J Immunol* (2008) 38(2):350–63. doi: 10.1002/eji.200737768
8. Diallo MS, Samri A, Charpentier C, Bertine M, Cheynier R, Thiebaut R, et al. A Comparison of Cell Activation, Exhaustion, and Expression of HIV Coreceptors and Restriction Factors in HIV-1- and HIV-2-Infected Nonprogressors. *AIDS Res Hum Retroviruses* (2021) 37(3):214–23. doi: 10.1089/aid.2020.0084
9. Vidyavijayan KK, Cheedarala N, Babu H, Precilla LK, Sathyamurthi P, Chandrasekaran P, et al. Cross Type Neutralizing Antibodies Detected in a Unique HIV-2 Infected Individual From India. *Front Immunol* (2018) 9:2841. doi: 10.3389/fimmu.2018.02841
10. Munusamy Ponnan S, Swaminathan S, Tiruvengadam K, KV K, Cheedarla N, Nesakumar M, et al. Induction of circulating T follicular helper cells and

regulatory T cells correlating with HIV-1 gp120 variable loop antibodies by a subtype C prophylactic vaccine tested in a Phase I trial in India. *PloS One* (2018) 13(8):e0203037. doi: 10.1371/journal.pone.0203037
11. Lu J, Lv Y, Lv Z, Xu Y, Huang Y, Cui M, et al. Expansion of circulating T follicular helper cells is associated with disease progression in HIV-infected individuals. *J Infect Public Health* (2018) 11(5):685–90. doi: 10.1016/j.jiph.2018.01.005
12. Godinho-Santos A, Foxall RB, Antao AV, Tavares B, Ferreira T, Serra-Caetano A, et al. Follicular Helper T Cells Are Major Human Immunodeficiency Virus-2 Reservoirs and Support Productive Infection. *J Infect Dis* (2020) 221(1):122–6. doi: 10.1093/infdis/jiz431
13. Guan L, Li X, Wei J, Liang Z, Yang J, Weng X, et al. Antigen-specific CD8+ memory stem T cells generated from human peripheral blood effectively eradicate allogeneic targets in mice. *Stem Cell Res Ther* (2018) 9(1):337. doi: 10.1186/s13287-018-1080-1
14. Rutishauser RL, Deguit CDT, Hiatt J, Blaeschke F, Roth TL, Wang L, et al. TCF-1 regulates the stem-like memory potential of HIV-specific CD8+ T cells in elite controllers. *JCI Insight* (2021) 6(3):e136648.8. doi: 10.1172/jci.insight.136648
15. Munusamy Ponnan S, Hayes P, Fernandez N, Thiruvengadam K, Pattabiram S, Nesakumar M, et al. Evaluation of antiviral T cell responses and TSCM cells in volunteers enrolled in a phase I HIV-1 subtype C prophylactic vaccine trial in India. *PloS One* (2020) 15(2):e0229461. doi: 10.1371/journal.pone.0229461
16. Chahroudi A, Silvestri G, Lichterfeld M. T memory stem cells and HIV: a long-term relationship. *Curr HIV/AIDS Rep* (2015) 12(1):33–40. doi: 10.1007/s11904-014-0246-4
17. Ribeiro SP, Milush JM, Cunha-Neto E, Kallas EG, Kalil J, Somsouk M, et al. The CD8+ memory stem T cell (TSCM) subset is associated with improved prognosis in chronic HIV-1 infection. *J Virol* (2014) 88(23):13836–44. doi: 10.1128/JVI.01948-14
18. Gattinoni L, Lugli E, Ji Y, Pos Z, Paulos CM, Quigley MF, et al. A human memory T cell subset with stem cell–like properties. *Nat Med* (2011) 17 (10):1290. doi: 10.1038/nm.2446
19. Moir S, Buckner CM, Ho J, Wang W, Chen J, Waldner AJ, et al. B cells in early and chronic HIV infection: evidence for preservation of immune function associated with early initiation of antiretroviral therapy. *Blood* (2010) 116 (25):5571–9. doi: 10.1182/blood-2010-05-285528
20. Moir S, Malaspina A, Ho J, Wang W, Dipoto AC, O'Shea MA, et al. Normalization of B cell counts and subpopulations after antiretroviral therapy in chronic HIV disease. *J Infect Dis* (2008) 197(4):572–9. doi: 10.1086/526789
21. Bjorling E, Scarlatti G, von Gegerfelt A, Albert J, Biberfeld G, Chiodi F, et al. Autologous neutralizing antibodies prevail in HIV-2 but not in HIV-1 infection. *Virology* (1993) 193(1):528–30. doi: 10.1006/viro.1993.1160
22. Marcelino JM, Nilsson C, Barroso H, Gomes P, Borrego P, Maltez F, et al. Envelope-specific antibody response in HIV-2 infection: C2V3C3-specific IgG response is associated with disease progression. *AIDS (London England)* (2008) 22(17):2257–65. doi: 10.1097/QAD.0b013e3283155546
23. Kong R, Li H, Bibollet-Ruche F, Decker JM, Zheng NN, Gottlieb GS, et al. Broad and potent neutralizing antibody responses elicited in natural HIV-2 infection. *J Virol* (2012) 86(2):947–60. doi: 10.1128/JVI.06155-11
24. Duvall MG, Jaye A, Dong T, Brenchley JM, Alabi AS, Jeffries DJ, et al. Maintenance of HIV-specific CD4+ T cell help distinguishes HIV-2 from HIV-1 infection. *J Immunol* (2006) 176(11):6973–81. doi: 10.4049/jimmunol.176.11.6973
25. Vivier E, Raulet DH, Moretta A, Caligiuri MA, Zitvogel L, Lanier LL, et al. Innate or adaptive immunity? The example of natural killer cells. *Science* (2011) 331(6013):44–9. doi: 10.1126/science.1198687
26. Cerwenka A, Lanier LL. Natural killer cells, viruses and cancer. *Nat Rev Immunol* (2001) 1(1):41–9. doi: 10.1038/35095564
27. Nuvor SV, van der Sande M, Rowland-Jones S, Whittle H, Jaye A. Natural killer cell function is well preserved in asymptomatic human immunodeficiency virus type 2 (HIV-2) infection but similar to that of HIV-1 infection when CD4 T-cell counts fall. *J Virol* (2006) 80(5):2529–38. doi: 10.1128/JVI.80.5.2529-2538.2006
28. Alter G, Teigen N, Davis BT, Addo MM, Suscovich TJ, Waring MT, et al. Sequential deregulation of NK cell subset distribution and function starting in acute HIV-1 infection. *Blood* (2005) 106(10):3366–9. doi: 10.1182/blood-2005-03-1100
29. Mylvaganam GH, Rios D, Abdelaal HM, Iyer S, Tharp G, Mavigner M, et al. Dynamics of SIV-specific CXCR5+ CD8 T cells during chronic SIV infection. *Proc Natl Acad Sci* (2017) 114(8):1976–81. doi: 10.1073/pnas.1621418114
30. Petrovas C, Ferrando-Martinez S, Gerner MY, Casazza JP, Pegu A, Deleage C, et al. Follicular CD8 T cells accumulate in HIV infection and can kill infected cells in vitro via bispecific antibodies. *Sci Trans Med* (2017) 9(373):eaag2285. doi: 10.1126/scitranslmed.aag2285
31. Gattinoni L, Lugli E, Ji Y, Pos Z, Paulos CM, Quigley MF, et al. A human memory T cell subset with stem cell–like properties. *Nat Med* (2011) 17:1290. doi: 10.1038/nm.2446
32. Kaminski DA, Wei C, Qian Y, Rosenberg AF, Sanz I. Advances in human B cell phenotypic profiling. *Front Immunol* (2012) 3:302. doi: 10.3389/fimmu.2012.00302
33. Weiskopf D, Bangs DJ, Sidney J, Kolla RV, De Silva AD, deSilva AM, et al. Dengue virus infection elicits highlypolarized CX3CR1+ cytotoxic CD4+ T cells associated with protective immunity. *Proc Natl Acad Sci USA* (2015) 112 (31):E4256-63. doi: 10.1073/pnas.1505956112
34. Tian Y, Babor M, Lane J, Schulten V, Patil VS, Seumois G, et al. Unique phenotypes and clonal expansions of human CD4 effector memory T cells re-expressing CD45RA. *Nat Commun* (2017) 8(1):1–13. doi: 10.1038/s41467-017-01728-5
35. Condotta SA, Richer MJ. The immune battlefield: The impact ofinflammatory cytokines on CD8+ T-cell immunity. *PLoS Pathog* (2017) 13(10):e1006618. doi: 10.1371/journal.ppat.1006618
36. Marras F, Nicco E, Bozzano F, Di Biagio A, Dentone C, Pontali E, et al. Natural killer cells in HIV controller patients express an activated effector phenotype and do not up-regulate NKp44 on IL-2 stimulation. *Proc Natl Acad Sci U S A* (2013) 110(29):11970–5. doi: 10.1073/pnas.1302090110
37. Luo Z, Li Z, Martin L, Hu Z, Wu H, Wan Z, et al. Increased Natural Killer Cell Activation in HIV-Infected Immunologic Non-Responders Correlates with CD4+ T Cell Recovery after Antiretroviral Therapy and Viral Suppression. *PloS One* (2017) 12(1):e0167640. doi: 10.1371/journal.pone.0167640
38. Mikulak J, Oriolo F, Zaghi E, Di Vito C, Mavilio D. Natural killer cells in HIV-1 infection and therapy. *AIDS (London England)* (2017) 31(17):2317–30. doi: 10.1097/QAD.0000000000001645
39. Kulkarni AG, Paranjape RS, Thakar MR. Higher Expression of Activating Receptors on Cytotoxic NK Cells is Associated with Early Control on HIV-1C Multiplication. *Front Immunol* (2014) 5:222. doi: 10.3389/fimmu.2014.00222
40. Milush JM, Lopez-Verges S, York VA, Deeks SG, Martin JN, Hecht FM, et al. CD56negCD16(+) NK cells are activated mature NK cells with impaired effector function during HIV-1 infection. *Retrovirology* (2013) 10(1):158. doi: 10.1186/1742-4690-10-158
41. Hu PF, Hultin LE, Hultin P, Hausner MA, Hirji K, Jewett A, et al. Natural killer cell immunodeficiency in HIV disease is manifest by profoundly decreased numbers of CD16+CD56+ cells and expansion of a population of CD16dimCD56- cells with low lytic activity. *J Acquired Immune Deficiency Syndromes Hum Retrovirol Off Publ Int Retrovirol Assoc* (1995) 10(3):331–40. doi: 10.1097/00042560-199511000-00005
42. Cooper A, Garcia M, Petrovas C, Yamamoto T, Koup RA, Nabel GJ. HIV-1 causes CD4 cell death through DNA-dependent protein kinase during viral integration. *Nature* (2013) 498(7454):376–9. doi: 10.1038/nature12274
43. Lee HG, Cho MZ, Choi JM. Bystander CD4(+) T cells: crossroads between innate and adaptive immunity. *Exp Mol Med* (2020) 52(8):1255–63. doi: 10.1038/s12276-020-00486-7
44. Reeves JD, Doms RW. Human immunodeficiency virus type 2. *J Gen Virol* (2002) 83(Pt 6):1253–65. doi: 10.1099/0022-1317-83-6-1253
45. Nyamweya S, Hegedus A, Jaye A, Rowland-Jones S, Flanagan KL, Macallan DC. Comparing HIV-1 and HIV-2 infection: Lessons for viral immunopathogenesis. *Rev Med Virol* (2013) 23(4):221–40. doi: 10.1002/rmv.1739
46. de Silva TI, Cotten M, Rowland-Jones SL. HIV-2: the forgotten AIDS virus. *Trends Microbiol* (2008) 16(12):588–95. doi: 10.1016/j.tim.2008.09.003
47. Borrow P, Lewicki H, Hahn BH, Shaw GM, Oldstone M. Virus-specific CD8+ cytotoxic T-lymphocyte activity associated with control of viremia in primary human immunodeficiency virus type 1 infection. *J Virol* (1994) 68(9):6103–10. doi: 10.1128/JVI.68.9.6103-6110.1994

48. Wodarz D. Helper-dependent vs. helper-independent CTL responses in HIV infection: implications for drug therapy and resistance. *J Theor Biol* (2001) 213 (3):447–59. doi: 10.1006/jtbi.2001.2426
49. Vigano S, Negron J, Ouyang Z, Rosenberg ES, Walker BD, Lichterfeld M, et al. Prolonged antiretroviral therapy preserves HIV-1-specific CD8 T cells with stem cell-like properties. *J Virol* (2015) 89(15):7829–40. doi: 10.1128/JVI.00789-15
50. Porichis F, Kaufmann DE. HIV-specific CD4 T cells and immune control of viral replication. *Curr Opin HIV AIDS* (2011) 6(3):174–80. doi: 10.1097/COH.0b013e3283454058
51. Hou S, Hyland L, Ryan KW, Portner A, Doherty PC. Virus-specific CD8+ T-cell memory determined by clonal burst size. *Nature* (1994) 369(6482):652–4. doi: 10.1038/369652a0
52. Salwe S, Singh A, Padwal V, Velhal S, Nagar V, Patil P, et al. Immune signatures for HIV-1 and HIV-2 induced CD4(+)T cell dysregulation in an Indian cohort. *BMC Infect Dis* (2019) 19(1):135. doi: 10.1186/s12879-019-3743-7
53. Hart M, Steel A, Clark SA, Moyle G, Nelson M, Henderson DC, et al. Loss of discrete memory B cell subsets is associated with impaired immunization responses in HIV-1 infection and may be a risk factor for invasive pneumococcal disease. *J Immunol* (2007) 178(12):8212–20. doi: 10.4049/jimmunol.178.12.8212
54. Ponnan SM, Swaminathan S, Tiruvengadam K, Vidyavijayan KK, Cheedarla N, Nesakumar M, et al. Induction of circulating T follicular helper cells and regulatory T cells correlating with HIV-1 gp120 variable loop antibodies by a subtype C prophylactic vaccine tested in a Phase I trial in India. *PloS One* (2018) 13(8):e0203037. doi: 10.1371/journal.pone.0203037
55. Levesque MC, Moody MA, Hwang KK, Marshall DJ, Whitesides JF, Amos JD, et al. Polyclonal B cell differentiation and loss of gastrointestinal tract germinal centers in the earliest stages of HIV-1 infection. *PloS Med* (2009) 6(7): e1000107. doi: 10.1371/journal.pmed.1000107
56. Perreau M, Savoye AL, De Crignis E, Corpataux JM, Cubas R, Haddad EK, et al. Follicular helper T cells serve as the major CD4 T cell compartment for HIV-1 infection, replication, and production. *J Exp Med* (2013) 210(1):143–56. doi: 10.1084/jem.20121932
57. Fecteau JF, Cote G, Neron S. A new memory CD27-IgG+ B cell population in peripheral blood expressing VH genes with low frequency of somatic mutation. *J Immunol* (2006) 177(6):3728–36. doi: 10.4049/jimmunol.177.6.3728
58. Andoniou CE, Andrews DM, Degli-Esposti MA. Natural killer cells in viral infection: more than just killers. *Immunol Rev* (2006) 214:239–50. doi: 10.1111/j.1600-065X.2006.00465.x
59. Scully E, Alter G. NK Cells in HIV Disease. *Curr HIV/AIDS Rep* (2016) 13 (2):85–94. doi: 10.1007/s11904-016-0310-3
60. Mavilio D, Benjamin J, Daucher M, Lombardo G, Kottilil S, Planta MA, et al. Natural killer cells in HIV-1 infection: dichotomous effects of viremia on inhibitory and activating receptors and their functional correlates. *Proc Natl Acad Sci U S A* (2003) 100(25):15011–6. doi: 10.1073/pnas.2336091100
61. Eller MA, Eller LA, Ouma BJ, Thelian D, Gonzalez VD, Guwatudde D, et al. Elevated natural killer cell activity despite altered functional and phenotypic profile in Ugandans with HIV-1 clade A or clade D infection. *J Acquired Immune Deficiency Syndromes (1999)* (2009) 51(4):380–9. doi: 10.1097/QAI.0b013e3181aa256e
62. Sondergaard SR, Ullum H, Pedersen BK. Proliferative and cytotoxic capabilities of CD16+CD56- and CD16+/-CD56+ natural killer cells. *APMIS* (2000) 108(12):831–7. doi: 10.1111/j.1600-0463.2000.tb00006.x
63. Vieillard V, Fausther-Bovendo H, Samri A, Debre PFrench Asymptomatiques a Long Terme A-COSG. Specific phenotypic and functional features of natural killer cells from HIV-infected long-term nonprogressors and HIV controllers. *J acquired Immune deficiency syndromes (1999)* (2010) 53(5):564–73. doi: 10.1097/QAI.0b013e3181d0c5b4
64. Mavilio D, Lombardo G, Kinter A, Fogli M, La Sala A, Ortolano S, et al. Characterization of the defective interaction between a subset of natural killer cells and dendritic cells in HIV-1 infection. *J Exp Med* (2006) 203(10):2339–50. doi: 10.1084/jem.20060894
65. Brunetta E, Fogli M, Varchetta S, Bozzo L, Hudspeth KL, Marcenaro E, et al. The decreased expression of Siglec-7 represents an early marker of dysfunctional natural killer-cell subsets associated with high levels of HIV-1 viremia. *Blood* (2009) 114(18):3822–30. doi: 10.1182/blood-2009-06-226332
66. Pohlmeyer CW, Gonzalez VD, Irrinki A, Ramirez RN, Li L, Mulato A, et al. Identification of NK Cell Subpopulations That Differentiate HIV-Infected Subject Cohorts with Diverse Levels of Virus Control. *J Virol* (2019) 93(7): e01790–18. doi: 10.1128/JVI.01790-18
67. Bryceson YT, March ME, Ljunggren HG, Long EO. Activation, coactivation, and costimulation of resting human natural killer cells. *Immunol Rev* (2006) 214:73–91. doi: 10.1111/j.1600-065X.2006.00457.x
68. Gaardbo JC, Hartling HJ, Gerstoft J, Nielsen SD. Thirty years with HIV infection—nonprogression is still puzzling: lessons to be learned from controllers and long-term nonprogressors. *AIDS Res Treat* (2012) 2012:161584. doi: 10.1155/2012/161584

Conflict of Interest: The authors declare that the research was conducted in the absence of any commercial or financial relationships that could be construed as a potential conflict of interest.

frontiers in Immunology

ORIGINAL RESEARCH
published: 19 April 2021
doi: 10.3389/fimmu.2021.661990

The Architecture of Circulating Immune Cells Is Dysregulated in People Living With HIV on Long Term Antiretroviral Treatment and Relates With Markers of the HIV-1 Reservoir, Cytomegalovirus, and Microbial Translocation

Lisa Van de Wijer[1†], Wouter A. van der Heijden[1†], Rob ter Horst[1], Martin Jaeger[1], Wim Trypsteen[2], Sofie Rutsaert[2], Bram van Cranenbroek[3], Esther van Rijssen[3], Irma Joosten[3], Leo Joosten[1], Linos Vandekerckhove[2], Till Schoofs[4], Jan van Lunzen[4], Mihai G. Netea[1,5], Hans J.P.M. Koenen[3], André J.A.M. van der Ven[1] and Quirijn de Mast[1]*

[1] Department of Internal Medicine and Radboud Center for Infectious Diseases, Radboud University Medical Center, Nijmegen, Netherlands, [2] HIV Cure Research Center, Department of Internal Medicine and Paediatrics, Faculty of Medicine and Health Sciences, Ghent University and Ghent University Hospital, Ghent, Belgium, [3] Laboratory for Medical Immunology, Department of Laboratory Medicine, Radboud University Medical Center, Nijmegen, Netherlands, [4] ViiV Healthcare, Brentford, United Kingdom, [5] Department for Genomics & Immunoregulation, Life and Medical Sciences 12 Institute (LIMES), University of Bonn, Bonn, Germany

OPEN ACCESS

Edited by:
Constantinos Petrovas, Centre Hospitalier Universitaire Vaudois (CHUV), Switzerland

Reviewed by:
Stéphane Isnard, McGill University Health Centre, Canada
Susanne Dam Nielsen, Copenhagen University Hospital, Denmark

***Correspondence:**
Lisa Van de Wijer
L.vandewijer@radboudumc.nl

†These authors have contributed equally to this work and share first authorship

Specialty section:
This article was submitted to T Cell Biology, a section of the journal Frontiers in Immunology

Received: *31 January 2021*
Accepted: *29 March 2021*
Published: *19 April 2021*

Citation:
Van de Wijer L, van der Heijden WA, Horst Rt, Jaeger M, Trypsteen W, Rutsaert S, van Cranenbroek B, van Rijssen E, Joosten I, Joosten L, Vandekerckhove L, Schoofs T, van Lunzen J, Netea MG, Koenen HJPM, van der Ven AJAM and de Mast Q (2021) The Architecture of Circulating Immune Cells Is Dysregulated in People Living With HIV on Long Term Antiretroviral Treatment and Relates With Markers of the HIV-1 Reservoir, Cytomegalovirus, and Microbial Translocation. Front. Immunol. 12:661990. doi: 10.3389/fimmu.2021.661990

Long-term changes in the immune system of successfully treated people living with HIV (PLHIV) remain incompletely understood. In this study, we assessed 108 white blood cell (WBC) populations in a cohort of 211 PLHIV on stable antiretroviral therapy and in 56 HIV-uninfected controls using flow cytometry. We show that marked differences exist in T cell maturation and differentiation between PLHIV and HIV-uninfected controls: PLHIV had reduced percentages of CD4+ T cells and naïve T cells and increased percentages of CD8+ T cells, effector T cells, and T helper 17 (Th17) cells, together with increased Th17/regulatory T cell (Treg) ratios. PLHIV also exhibited altered B cell maturation with reduced percentages of memory B cells and increased numbers of plasmablasts. Determinants of the T and B cell composition in PLHIV included host factors (age, sex, and smoking), markers of the HIV reservoir, and CMV serostatus. Moreover, higher circulating Th17 percentages were associated with higher plasma concentrations of interleukin (IL) 6, soluble CD14, the gut homing chemokine CCL20, and intestinal fatty acid binding protein (IFABP). The changes in circulating lymphocytes translated into functional changes with

reduced interferon (IFN)- γ responses of peripheral blood mononuclear cells to stimulation with *Candida albicans* and *Mycobacterium tuberculosis*. In conclusion, this comprehensive analysis confirms the importance of persistent abnormalities in the number and function of circulating immune cells in PLHIV on stable treatment.

Keywords: HIV, Th17 & Tregs cells, CD4+/CD8+ lymphocytes, B cell, HIV reservoir, CMV, Interferon gama (IFN-γ), Natural killer cell (NK cells)

INTRODUCTION

Combination antiretroviral therapy (cART) has drastically curtailed morbidity and mortality in people living with HIV (PLHIV) (1). Still, PLHIV remain at an increased risk for pneumococcal infections, *Mycobacterium tuberculosis* (*M. tuberculosis*) reactivation and impaired vaccine responses (2–6). Moreover, HIV infection predisposes to non-infectious comorbidities, such as cardiovascular disease and non-AIDS-related cancer, which share an underlying pathophysiological pathway characterized by a persisting and inappropriate activation of innate and adaptive immune cells (7, 8). Together, these observations point towards a disbalance in the homeostasis of the immune system, characterized by immunodeficiency on the one hand, and chronic inflammation on the other hand.

HIV-1 preferentially infects and kills activated CD4+ T cells, leading to rapid and severe CD4+ T cell depletion in the gut and increased microbial translocation (9–12). A small proportion of these cells remains latently infected with replication competent virus and defective proviruses, called the HIV-1 reservoir (13). The HIV-1 reservoir and increased microbial translocation, together with lifestyle factors and co-infections such as cytomegalovirus (CMV) may all contribute to the disrupted immune function in PLHIV (10, 13–17). However, published data have shown inconsistent or even contradictory findings. Heterogeneity in study populations, limited sample sizes of study populations and differences in lifestyle factors, including use of tobacco and recreational drugs, may underlie these inconsistencies and emphasize the need for an integrative approach in evaluating the immune system in PLHIV on stable cART.

The Human Functional Genomics Project (HFGP) aims to disentangle variation in the immune system in different cohorts of healthy individuals and individuals with underlying conditions. It combines multiple levels of analyses and data integration, including demographic and lifestyle data, data from 'omics technologies', and functional immune data (18). As part of this project, we previously identified relevant environmental and host factors for circulating white blood cell (WBC) populations in healthy individuals (19). Embedded within the HFGP, we established a cohort of 211 virally suppressed PLHIV (200HIV) and showed that these individuals exhibited a sustained pro-inflammatory immune phenotype with priming of the interleukin (IL)-1β pathway (20). In the present study, we used the same cohort to comprehensively assess the peripheral WBC composition during treated HIV infection with a special focus on the adaptive immune system. We compared their WBC populations with those of healthy individuals and assessed associations with demographic and lifestyle factors, different HIV-specific factors, and *ex vivo* cytokine responses of peripheral blood mononuclear cells (PBMCs) to stimulation with different bacterial, fungal and viral antigens.

METHODS

Study Population

This study is part of the HFGP (www.humanfunctionalgenomics.org) (18). Between 14 December 2015 and 6 February 2017, individuals living with HIV were recruited from the HIV clinic of Radboud university medical center. Inclusion criteria were Caucasian ethnicity, age ≥ 18 years, receiving cART > 6 months, and latest HIV-RNA levels ≤200 copies/ml. Exclusion criteria were: signs of acute or opportunistic infections, antibiotic use <1 month prior to study visit, and active hepatitis B/C. The control population consisted of 56 healthy adult individuals (56P cohort), who did not suffer from any acute or chronic conditions and who were longitudinally sampled four times in three-month intervals. Inclusion, sampling and sample processing of both cohorts were conducted simultaneously and by the same personnel. The 56P participants were selected as a subset of a larger cohort of 534 healthy individuals (500FG) which was phenotypically assessed two years earlier according to the same methods (19, 21). Differences in cell-cell associations were compared between 200 HIV and 500FG cohort. The reason is that the larger sample size of this control cohort (n=534 vs n=56) improved statistical power, whilst batch effects between PLHIV and 500FG were deemed of less significance when comparing within-group correlations between cohorts. General information from all participants was recorded in the Castor Electronic Data Capture program (Castor EDC, CIWIT B.V., Amsterdam, The Netherlands), using questionnaires on socio-demographic information, lifestyle and life-events. Clinical data were extracted from medical files and the 'Stichting HIV Monitoring' registry (Amsterdam, The Netherlands).

Ethics

The study protocols were approved by the Medical Ethical Review Committee region Arnhem-Nijmegen (ref. 42561.091.122) and conducted in accordance with the principles of the Declaration of Helsinki. All study participants provided written informed consent.

Cell Processing

Venous blood was collected in sterile 10 ml EDTA BD Vacutainer® tubes between 8 and 11 am and processed within 1-4 hours. Cell counts were determined using a Sysmex XN-450 automated hematology analyzer (Sysmex Corporation, Kobe, Japan). Erythrocyte-lysed whole blood samples were obtained after 10 minutes incubation of 1.5 ml EDTA-anticoagulated blood with lysis buffer containing 3.0 M NH_4Cl, 0.2 M $KHCO_3$ and 2 mM Na_4EDTA. The remaining WBC were washed twice, by adding 25 ml phosphate-buffered saline 1x (PBS, Braun, Melsungen, Germany) and centrifuging at 452 x g for 5 min at room temperature. Before staining, cells were resuspended in 300 µl of PBS enriched with 0.2% bovine serum albumin (BSA, Sigma-Aldrich, Zwijndrecht, Netherlands). Isolation of PBMCs was performed by density centrifugation of EDTA-anticoagulated blood diluted 1:1 in pyrogen-free PBS over Ficoll-Paque (VWR, Amsterdam, The Netherlands) as described previously (22). Cells were adjusted to 5.0 x 10^6 cells/ml.

Flow Cytometry

Supplementary Table 1 summarizes the antibody clones and the fluorochrome conjugates used for the different panel fluorescent staining mixes. Staining was performed on 100 µl/well erythrocyte-lysed blood (panel 1-3,5) or 0.5 x 10^6 cells/well freshly isolated PBMCs (panel 4). Cells were stained according to previously described procedures (see also **Supplementary Methods**) (19).

Samples were measured on a 10-color Navios flow cytometer (Beckman Coulter, Fullerton, CA, USA), equipped with three solid-state lasers (488 nm, 638 nm, and 405 nm) (19). Gating was conducted manually and verified by two independent specialists to prevent gating errors. Samples were analyzed within 4-5 hr after blood collection, using five distinct and complementary 10-color antibody panels: 1. general; 2. T cell; 3. B cell; 4. intracellular T cell/Treg; 5. chemokine receptors (CCR). Staining and gating strategies can be found in **Supplementary Figure 1**. Flow cytometry data were analyzed using Kaluza software version 1.3. In our analyses, we focused on a set of 108 manually annotated WBC subsets based on the original 500FG study (panel 1-4) (19), with the addition of a fifth panel in which we classified monocytes, CD4+ memory and regulatory T cells, and CD8+ cells according to their expression of the CXCR3, CCR4, and CCR6 (panel 5).

PBMC Stimulation Experiments

Freshly isolated PBMCs were incubated with different stimuli (**Supplementary Table 2**) including bacterial (*Staphylococcus aureus*, *M. tuberculosis*, *Streptococcus pneumoniae [S. pneumoniae]*), fungal (*Cryptococcus gattii*, *Candida albicans [C. albicans]* hyphae and yeast) and other relevant antigens (Imiquimod, TLR7 ligand), in round-bottom 96-well plates (Greiner Bio-One, Frickenhausen, Germany) with 0.5 x 10^6 cells/well at 37°C and 5% CO_2 in the presence of 10% human pooled serum for seven days. Supernatants were stored at -20°C. Levels of the lymphocyte-derived cytokines IL-17, IL-22, and interferon (IFN)-γ were measured in the supernatants (PeliKine Compact or Duoset ELISA, R&D Systems).

Plasma Markers

Serum levels of immunoglobulin (Ig)M and IgG were measured by immunonephelometry using a Beckman Coulter Imager and Beckman Coulter reagents. Measurements were standardized using certified European reference material 470 (ERM®-DA470). CMV IgG antibodies were measured in serum using ELISA (Genway Biotech Inc., San Diego, CA, USA) according to the manufacturer's instructions. Markers of systemic inflammation, high-sensitive C-reactive protein (hsCRP) and soluble CD14 (sCD14), and microbial translocation, intestinal fatty acid binding protein (IFABP), were measured by ELISA (Quantikine, R&D Systems) according to the manufacturer's instructions. IL-6 was measured using a SimplePlex Cartridge (Protein Simple, San Jose, CA, USA). Circulating plasma CCL20, IL-17A, and IFN-γ were measured using the commercially available Olink Proteomics AB Inflammation Panel as described previously (23, 24).

Cell-Associated HIV-1 DNA and Cell-Associated HIV-1 RNA Quantification in CD4+ T Cells

The HIV reservoir was assessed by analyzing CD4+ cell-associated HIV-1 DNA (CA-DNA) and CA-RNA. In virally suppressed patients, the CA-DNA roughly equals the integrated HIV-1 DNA, being replication competent or not (25), while CA-RNA is associated with recent HIV-1 transcriptional activity and serves as a proxy for the active proviral reservoir (26). CA-DNA and CA-RNA were measured in triplicate by droplet digital PCR (ddPCR – Bio-Rad) in CD4+ T cells isolated using EasySep Human CD4+ T Cell Isolation Kit (Stemcell technologies, Vancouver, Canada) as described previously (27). CA-DNA was extracted by the DNeasy Blood & Tissue kit (Qiagen, Hilden, Germany) according to the manufacturer's protocol with the addition of 75µl elution buffer on the column heated at 56°C for 10 minutes. CA-RNA was extracted using the Innuprep RNA kit (Westburg, Leusden, The Netherlands) with 30µl elution buffer. Total RNA was reversely transcribed to cDNA by qScript cDNA SuperMix according to manufacturer's protocol (Quantabio, Beverly, MA, USA). CA-DNA was normalized by measuring the reference gene RPP30 (**Supplementary Table 3** and **Supplementary Methods**) in duplicate by ddPCR and expressed per million CD4+ T cells. CA-RNA was normalized using three reference genes per patient, (B2M, ACTB and GADPH), which were measured with LightCycler 480 SYBR Green I Master mix. HIV-1 RNA copies were divided by the geometric mean of the reference genes and expressed per million PBMCs. ddPCR data analysis was performed using the ddpcRquant tool with standard settings for thresholding and absolute quantification (28).

Statistical Analyses

A detailed description of the statistical methods can be found in the **Supplementary Methods**. Given the impact of cohort

differences in the absolute cell numbers of main WBC types (e.g. CD4+) on the numbers of their subsets (e.g. CD4+ regulatory T cells [Tregs]), results were primarily reported as WBC percentages, unless stated otherwise. WBC percentages were calculated by dividing the cell count of each subpopulation by its respective parent (one level up) or, where relevant, grandparent (two levels up; **Supplementary Table 4**). Data curation of cytokine, soluble marker, and immunoglobulin data was done according to previous methods (21). For comparisons between cohorts, we used all four longitudinally collected data points from the 56P cohort as independent measurements. Because of the known seasonality effects on WBC, this approach was considered preferable over selecting one of the data collection points or summarizing the data points. Data were normalized using an inverse rank transformation algorithm.

Comparisons in baseline characteristics between groups were made using Student's t-test (or Mann-Whitney U test) for continuous variables, and Pearson's Chi-square test (or Fisher's exact) for categorical variables. Linear regression was used to compare WBC between cohorts, and to calculate associations between WBC and clinical and virological factors. All analyses were corrected for age, sex, time since January 2015 and seasonal effects. Cytokine analyses between cohorts were also corrected for CD4+ and CD8+ T cell percentages. Spearman correlations were used as the distance metric for unsupervised hierarchical WBC count clustering. Two-sided FDR-corrected p-values < 0.05 were considered statistically significant (29). Effect sizes are reported as Spearman's Rho or standardized beta coefficients (β). Data were analyzed using the statistical programming language R (version 3.4.3, R Core Team, 2012).

RESULTS

General and HIV-Specific Characteristics

Data from 211 PLHIV and 56 controls were analyzed in this study (**Table 1**). PLHIV were older (median [IQR] 52.5 [46.2 – 59.4] vs 30.0 [25.1 – 52.2] years, $p<0.0001$) and more often male (193/211 [91.5%] vs 34/56 [60.7%], $p<0.0001$) than controls. PLHIV had received cART for a median of 6.6 (4.2–11.9) years and 205/210 (98%) had plasma HIV-1 RNA <50 copies/mL at time of study visit. Analyzing the HIV reservoir, we found detectable levels of total CA-DNA in 207/208 (99.5%) and CA-RNA in 210/210 (100%); CA-DNA and CA-RNA levels were highly correlated (**Supplementary Figure 2A**; R=0.68, $p<2.2{\cdot}10^{-16}$). In general, PLHIV with higher CA-DNA and CA-RNA levels were older, had been living with and treated

TABLE 1 | General characteristics.

Characteristic	PLHIV (n = 211)	HC (n = 56)	P-value
Age, years	52.5 (46.2 – 59.4)	30.0 (25.1 – 52.2)	<0.0001
Sex, female, n/N (%)	19/211 (9.0)	22/56 (39.3)	<0.0001
BMI, kg/m^2	24.2 (22.1 – 26.1)	23.6 (21.6 – 25.2)	0.41
Time since HIV diagnosis, years	8.5 (9.5)	–	–
Way of transmission, n/N (%)		–	–
MSM	159/211 (75.4)	–	–
Heterosexual contact	9 (4.3)	–	–
IDU	3 (1.4)	–	–
Other or unknown	40 (19.0)		
Nadir CD4$^+$ cell count, cells/μl	250 (130 - 360)	–	–
CD4$^+$ count, cells/μl	660 (480 - 810)	–	–
Zenith HIV-RNA, copies/mL	100 000 (50 000 - 391182)	–	–
HIV-RNA >50 copies/mL ≤1 yr. prior to inclusion, n/N (%)	23/210 (11.0)	–	–
CA-DNA (copies per million CD4+ cells)	1547 (584 - 2802)		
CA-RNA (copies per million CD4+ cells)	157 (74 - 299)		
cART-naive, n/N (%)	30/211 (14.2)	–	–
Time on cART, years	6.6 (4.2 – 11.9)	–	–
ARV classes, n/N (%)			
NNRTI	63/211 (29.9)	–	–
PI	32/211 (15.2)	–	–
INSTI	141/211 (66.8)	–	–
Co-medication, n/N (%)			
Cholesterol lowering drugs	58/211 (27.5)	–	–
Antihypertensive drugs	50/211 (23.7)	–	–
Metformin	9/211 (4.3)	–	–
Active smoking, n/N (%)	63/211 (29.9)	2/56 (3.6)	<0.0001
Heavy drinking, n/N (%)*	28/211 (13.3)	11/56 (19.6)	0.29
Regular substance use, n/N (%)†	61/211 (28.9)	3/56 (5.4)	<0.0001

Data depicted as median (IQR) unless stated otherwise. Data analyzed using Mann-Whitney U or χ^2 (or Fisher's exact) where applicable.

**Classified according to the CDC definition: for men, ≥15 drinks per week and for women, ≥8 drinks/week.*

†Defined as use of any psychoactive substance (with the exception of alcohol and tobacco) during periods ≥ 1 time per week including ≥ 1 time during the 30 days prior to the study visit. ARV, antiretroviral drug; BMI, body mass index; CA-DNA, CD4-cell-associated HIV-1 DNA; CA-RNA, CD4-cell-associated HIV-1 RNA; HC, healthy control; cART, combination antiretroviral therapy; INSTI, integrase inhibitor; IDU, intravenous drug use; MSM, men who have sex with men; NNRTI, non-nucleoside reverse transcriptase inhibitor; PLHIV, people living with HIV; PI, protease inhibitor.

for HIV for a longer period, and had lower nadir CD4+ T cell counts (**Supplementary Figure 2A**). We observed no significant differences in CA-RNA and CA-DNA between PLHIV with plasma HIV-1 RNA <50 copies/mL (205/210 [98%]) and those with plasma HIV-1 RNA 50-200 copies/mL (5/210 [2%]; **Supplementary Figure 2B**). PLHIV with at least once a viral load of >50 copies/mL during year prior to study visit (23/210 [11.0%]) had higher levels of CA-RNA (p=0.0077), but no differences in CA-DNA (p=0.076; **Supplementary Figure 2B**).

Alterations in WBC Composition and Cell-Cell Associations in Chronic HIV

We analyzed 108 WBC populations, including 93/107 (87%) B and T cell subsets and 14/107 (13%) innate cell subsets (neutrophils, monocytes, natural killer [NK] and natural killer T cells [NKT]). **Figure 1** and **Supplementary Figure 3** show the differences in WBC composition between PLHIV and controls. An overview of median (IQR) WBC percentages and numbers in PLHIV and controls can be found in **Supplementary Table 5**.

Principal component analysis (PCA) of all WBC populations only explained a limited amount of the total variance. Still, the PCA plot showed clear differences in clustering between PLHIV and controls (**Figure 1A**). As expected, PLHIV exhibited an expansion of CD8+ and a reduction of CD4+ T cell numbers and percentages (**Figure 1B** and **Supplementary Table 5**). Functionally, CD4+ T cells comprise a diverse population of cells. CD4+ T helper (Th) cells fulfill essential roles for viral (Th1, CCR6-CXCR3+CCR4-), parasitic (Th2, CCR6-CXCR3-CCR4+), and mucosal (Th17, $CCR6^+CXCR3$-CCR4+) immunity (30). In addition, CD4+ Tregs are essential for controlling inflammation (31). Despite reduced CD4+ T cell counts, numbers of all Th cell subsets (CD4+ CD45RA- CD25-) were markedly increased in PLHIV compared to controls (**Figure 1B** and **Supplementary Table 5**). Within the Th pool, Th2 percentages were reduced in PLHIV compared to controls, whereas Th1 percentages did not differ. Remarkably, Th17 percentages and numbers were increased in PLHIV (**Figures 1B, C** and **Supplementary Table 5**). While Treg percentages (of CD4+ cells), including highly suppressive Tregs co-expressing the transcription factors FoxP3 and Helios, were also increased in PLHIV, absolute Treg numbers were reduced (**Figures 1B, C** and **Supplementary Table 5**). This relative increase of Tregs may result from a loss of other CD4+ subsets (32). Among Tregs, we found no differences in the percentage of activated (HLA-DR+) and effector Tregs (CD45RA-). The relationship between pro-inflammatory Th17 cells and Treg must remain balanced to preserve functional immunity. Altered ratios have been described in untreated HIV (lower Th17/Treg), autoimmune disease and cancer (higher Th17/Treg) (9, 33, 34). Here, we found increased Th17/Treg ratios among virally suppressed PLHIV, irrespective of the Treg identification marker used (**Figure 1C** and **Supplementary Figure 4).** Furthermore, out of the Treg population, the percentage of Th17-like CCR6+ Tregs was increased in PLHIV, further contributing to a pro-inflammatory state. Developmentally, T cells evolve from naive T cells to antigen experienced central memory (CM), effector memory (EM), and effector cells (35, 36). HIV not only differentially affects functional subpopulations, but also disrupts these developmental stages. While naïve $CD4^+$ and $CD8^+$ T cells were reduced, memory and effector cells were expanded in PLHIV (**Figure 1B** and **Supplementary Table 5**). Likewise, we found higher percentages of proliferating (Ki67+) CD4+ and CD8+ T cells in PLHIV, indicating increased cell turnover. These results suggest a shift from naive cells towards terminally differentiated cells in HIV, even if viral replication is under control (37), which cannot be explained by age, sex, or season as we corrected our models for these factors.

Changes in the B cell compartment have also been described in PLHIV, including loss of CD27+ memory B cells (38, 39). Furthermore, viremia and low CD4+ T cell counts have been associated with the expansion of terminally differentiated B cells and immature B cells respectively (38, 39). In our study, we observed clear differences in B cell development in PLHIV illustrated by increased percentages of naïve B cells (IgD+IgM+ CD27-) and reduced percentages of memory B cells (IgD+IgM+ CD27+), transitional B cells (CD24++CD38++) and natural effector B cells (CD24+CD38+IgD+IgM+). In addition, the number of plasmablasts (IgD- IgM- CD38++) was increased in PLHIV, (**Figures 1B, C** and **Supplementary Table 5**). Adequate B cell maturation further requires optimal communication between B and T cells. We therefore sought to identify differences in WBC co-regulation between PLHIV and HIV-uninfected individuals by comparing cell-cell associations between PLHIV and participants from the 500FG cohort. Details of this 500FG cohort have been reported previously (500FG, n=534) (19). Using the same immunophenotyping techniques, we observed weaker correlations between naïve, CM and EM CD4+ T cells and several B cell subpopulations (including class-switch memory B cells) within PLHIV than in participants of the 500FG cohort, suggesting altered B/T cell interactions (**Figure 2**). These differences were not attributable to the influence of age, sex, or season as these factors were regressed out of the analysis.

Apart from changes in the adaptive cell compartment, we observed clear changes in the innate WBC compartment in PLHIV. Monocyte and NKT cell numbers and percentages were increased, whereas NK cell numbers and percentages were reduced, specifically the cytokine-producing NK bright cells (**Figure 1B** and **Supplementary Table 5**) Together, these data show a widespread functional and developmental dysregulation of the immune system in virally suppressed PLHIV. This dysregulation encompasses both the innate and the adaptive compartment and results in a pro-inflammatory immune environment with an expansion of monocytes, pro-inflammatory Th and effector T cells, and dysregulated B cell memory responses.

Lifestyle, Demographic, and Clinical Factors Influence the WBC Composition During Chronic HIV Infection

Apart from the effects of HIV, demographic and lifestyle-related factors may influence the composition of the circulating WBC populations. Indeed, we found that older age was associated with an increase of innate immune cells and differential effects on B and T cell populations, for example with lower percentages of naïve T cells (CD4+ T cells β=-0.29, p=0.00020; CD8+ T cells

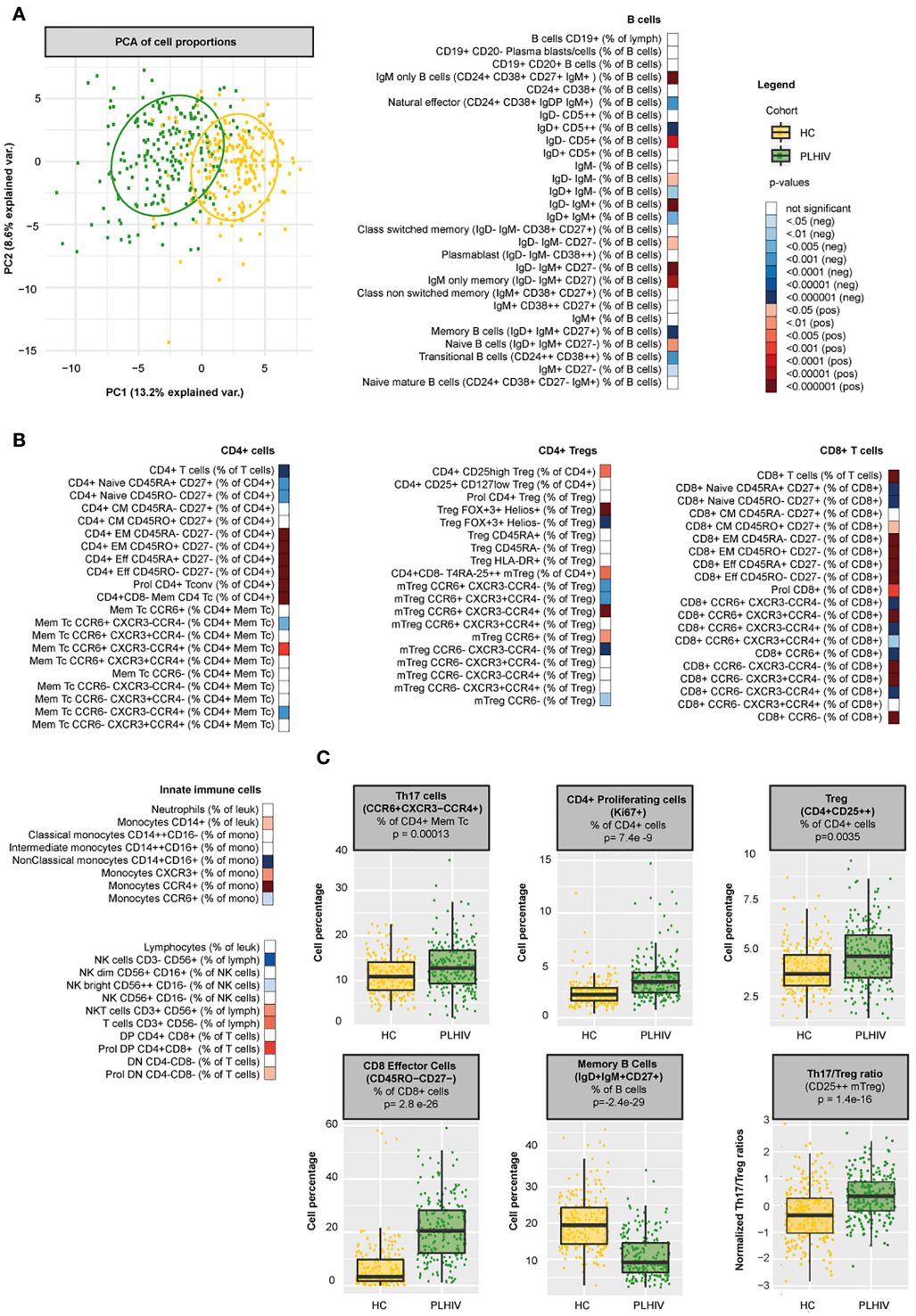

FIGURE 1 | Differences in WBC percentages between PLHIV and healthy individuals **(A)** Principal component biplot showing standardized variance for the two principal component of all WBC subsets. The ovals represent the different cohorts. **(B)** Differences in WBC percentages (n=108 WBC subsets) between PLHIV (n=211) and healthy controls (n=56) **(C)** Boxplots showing examples of cohort differences in cell percentages and Th17/Treg ratios (Treg identification marker CD25++). Inverse-rank transformed data were analyzed using multiple linear regression and adjusted for age, sex, sampling time, and season. For color coding of the FDR-adjusted p-values see legend.

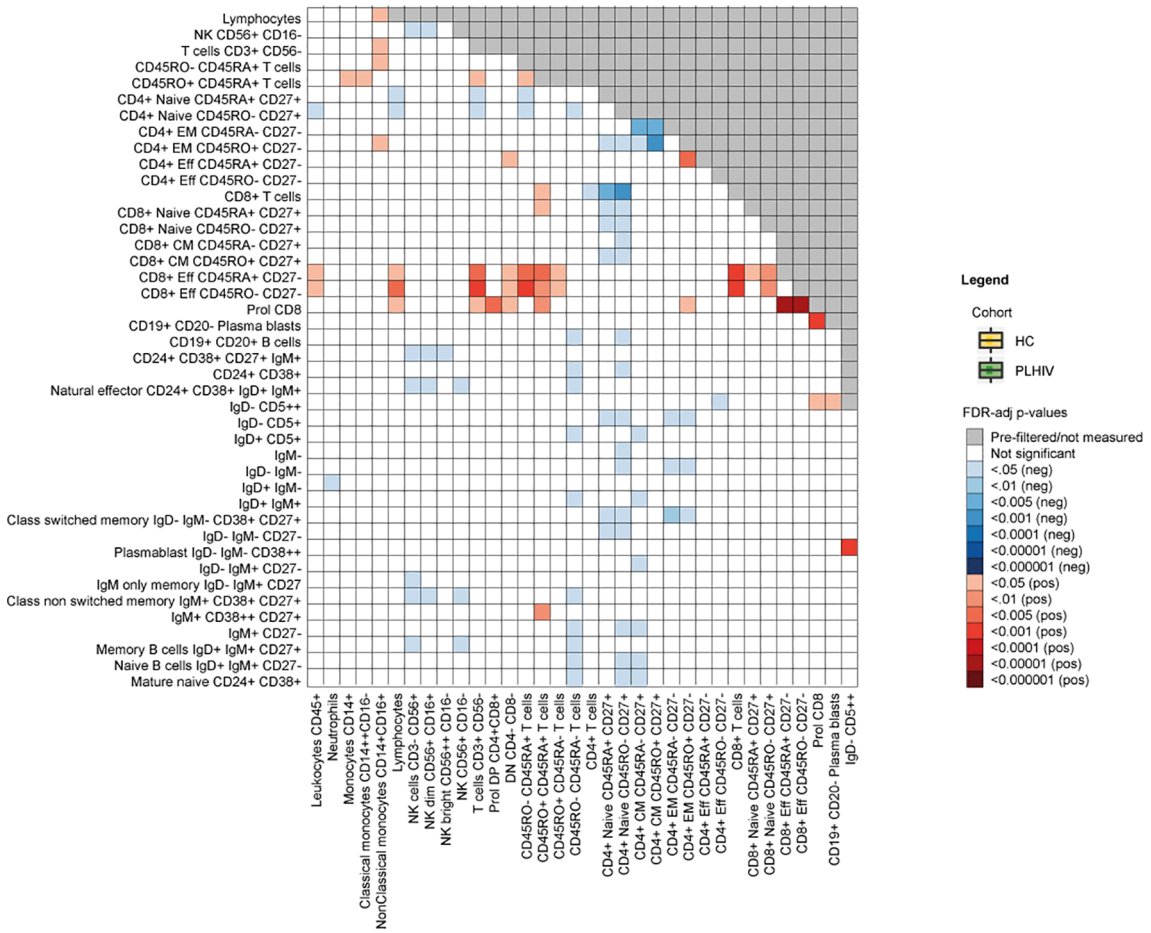

FIGURE 2 | Differences in cell-cell associations between PLHIV and healthy individuals. Exploratory analysis depicting cell-cell associations between a total of 77 available WBC subsets that were significantly stronger (red) or weaker (blue) in PLHIV compared to healthy controls (n=534). FDR-adjusted p-values are obtained after 10 000 permutations and adjusted for age, sex, sampling time and season. HC, healthy control; PLHIV, people living with HIV; WBC, white blood cells.

β=-0.29, p=0.00020) and B memory cells (β=-0.39, $p=1.5{\cdot}10^{-7}$) and higher percentages of memory T cells (e.g. CD8+ CM β=0.22, p=0.00064) and mature naïve B cells in PLHIV (β=0.25, p=0.00087, **Figure 3** and **Supplementary Table 6**). Sex-dependent influences of the WBC composition, reflected by more effector and EM cells and fewer naïve (B and T) cells in males in HIV infection, resembled those observed previously observed in healthy individuals (21, 40).

Lifestyle risk behaviors such as smoking [63/211 (29.9%)], heavy drinking [28/211 (13.3%)], and regular drug use [61/211 (28.9%)] were highly prevalent in PLHIV (**Table 1**). We found that packyears (reflecting total tobacco exposure) were associated with higher frequencies of neutrophils (β=0.22, p=0.033), Treg (β=0.22, p=0.033), CD8+ subsets (e.g. CCR6-CXCR3-CCR4+ β=0.24, p=0.025), and class switched memory B cells (β=0.20, p=0.042, **Supplementary Table 6**). Active smoking correlated with higher percentages of Th17 (β=0.21, p=0.031) and CCR6+ Tregs (β=0.26, p=0.0028, **Figure 3** and **Supplementary Table 6**). Neither heavy drinking, nor regular drug use affected the WBC composition.

We further assessed the effects of relevant clinical factors on the WBC composition in PLHIV, by exploring associations with the history of immune suppression and treatment-related factors. We found that nadir CD4+ cell counts were closely associated with both B and T cell percentages in PLHIV (**Figure 3** and **Supplementary Table 6**). For example, higher counts were associated with higher percentages of naïve CD4+ T cells (β=0.45, $p=1.2{\cdot}10^{-9}$) and memory B cells (β=0.18, p=0.034). In contrast, we observed no effects of the duration of HIV infection or cART (regimen) on the WBC composition (**Supplementary Tables 6**).

HIV-1 Reservoir and CMV Affect the WBC Composition in Chronic HIV Infection

First, we explored the relationship with markers of the HIV reservoir. CA-DNA was negatively associated with CD4+ T cell percentages (β=-0.33, $p=9.8{\cdot}10^{-5}$) and positively with CD8+ T cell percentages (β=0.34, $p=7.0{\cdot}10^{-5}$). Within the CD4+ T cell pool, CA-DNA correlated with higher percentages of CM and Th17 cells (β=0.21, p=0.026 and β=0.24, p=0.0081 respectively;

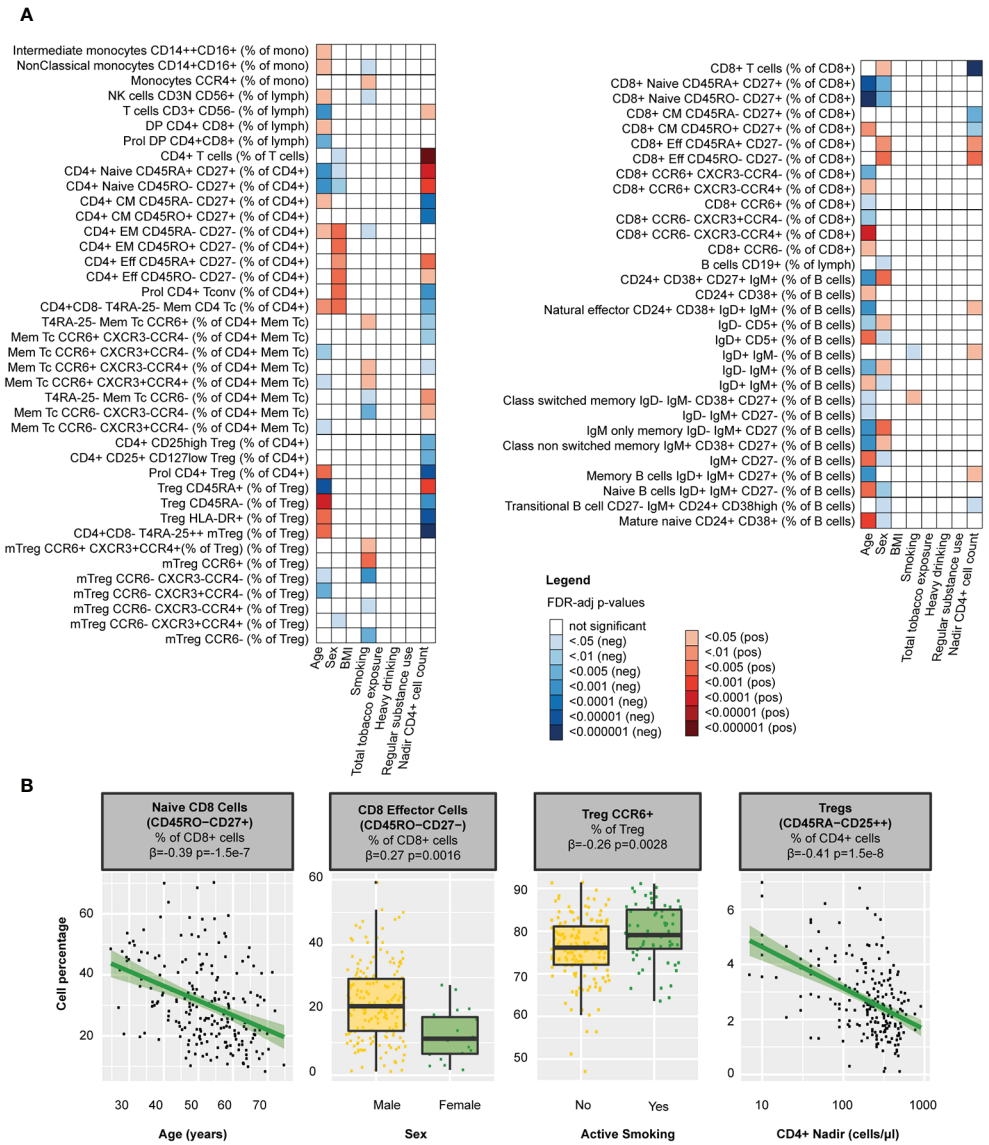

FIGURE 3 | Clinical determinants of WBC percentages in PLHIV **(A)** Heatmap of WBC percentages (n=108 WBC subsets) that were significantly associated with any of the clinical determinants tested in 211 PLHIV; WBC subsets that showed no significant correlations with any of the parameters (n=37) have been removed from the figure. **(B)** Examples of WBC subsets that were significantly associated with age, sex, smoking, or CD4 nadir. Inverse-rank transformed data were analyzed using linear regression and adjusted for age, sex, sampling time, and season. For color coding of the FDR-adjusted p-values see legend. PLHIV, people living with HIV; WBC, white blood cells.

Figure 4 and **Supplementary Table 7**) Higher CA-DNA was also associated with more CD4+ T cell proliferation (Ki67+, β=0.35, $p=3.3{\cdot}10^{-5}$) and Treg activation (HLA-DR+, β=0.23, p=0.0081). We found similar associations between T cells and CA-RNA, whereas we found no relation between T cells and the relative HIV transcription level (CA-RNA/CA-DNA ratios; **Supplementary Table 7**). Lastly, we observed several associations between CA-DNA and B cells: higher CA-DNA levels correlated with reduced percentages of IgD+ only memory B cells (β=-0.27, p=0.00068) and, albeit non-significantly, with reduced percentages of natural effector B cells (CD24+CD38+ IgD+IgM+, β=-0.18, p=0.056), and class unswitched memory B cells (IgD+IgM+CD27+, β=-0.18, p=0.053). Exclusion of PLHIV with HIV-RNA 50-200 copies/mL at time of study visit (5/210 [2%]) did not change the main conclusions of our paper (**Supplementary Tables 8, 9**).

Second, CMV co-infection may contribute to immune dysregulation in both treated and untreated PLHIV. As CMV is known to affect WBC populations in healthy controls (41), we explored the association of CMV serostatus with WBC composition. 198 of the PLHIV (93.8%) were seropositive for CMV. In line with findings in healthy individuals (41), CMV

seropositivity correlated with higher percentages of effector, EM T cells (e.g. with CD8+ effector cells β=0.43, p=1.7·10^{-9} and CD4+ EM cells β=0.30, p=0.00011; **Figure 4** and **Supplementary Table 7**) and NKT cells (β=0.29, p=0.00029), yet with lower percentages of Th17 cells (β=-0.26, p=0.00065). We observed no associations between B cell subsets and CMV.

Microbial Translocation, Inflammation and Th17 Differentiation in Chronic HIV Infection

Our main findings include a loss of naïve T cells and an expansion of Th17 in PLHIV compared to healthy controls, which related with lower nadir CD4+ T cells counts and higher levels of CA-DNA. To further assess the potential underlying mechanisms, we explored the relationship between these WBC subsets, markers of chronic inflammation, and markers of microbial translocation. As discussed above, naïve T cells are able to differentiate into different Th subsets depending on the cytokine environment (42). We previously showed that PLHIV in our cohort exhibited a pro-inflammatory profile with increased levels of hsCRP (p=0.00022) and sCD14 (a marker of monocyte activation, p=0.0025; **Figure 5A**) as well as markedly elevated monocyte-derived cytokine responses, particularly IL-1β (20). Such a pro-inflammatory cytokine environment may push the differentiation of naive CD4+ cells into Th17 cells (42). Indeed, we observed positive associations between Th17 percentages and circulating IL-6 (β=0.21, p=0.014) and sCD14 (β =0.17, p=0.035; **Figures 5B, C**). Notably, Th17 cells fulfill an essential role in mucosal defense and gut Th17 cells are known to be severely depleted during acute HIV (9). To test whether gut integrity might have been compromised in our cohort, we measured levels of the microbial translocation marker IFABP and found increased levels in PLHIV compared to healthy controls (p=7.6·10^{-5}; **Figure 5D**), suggesting ongoing microbial

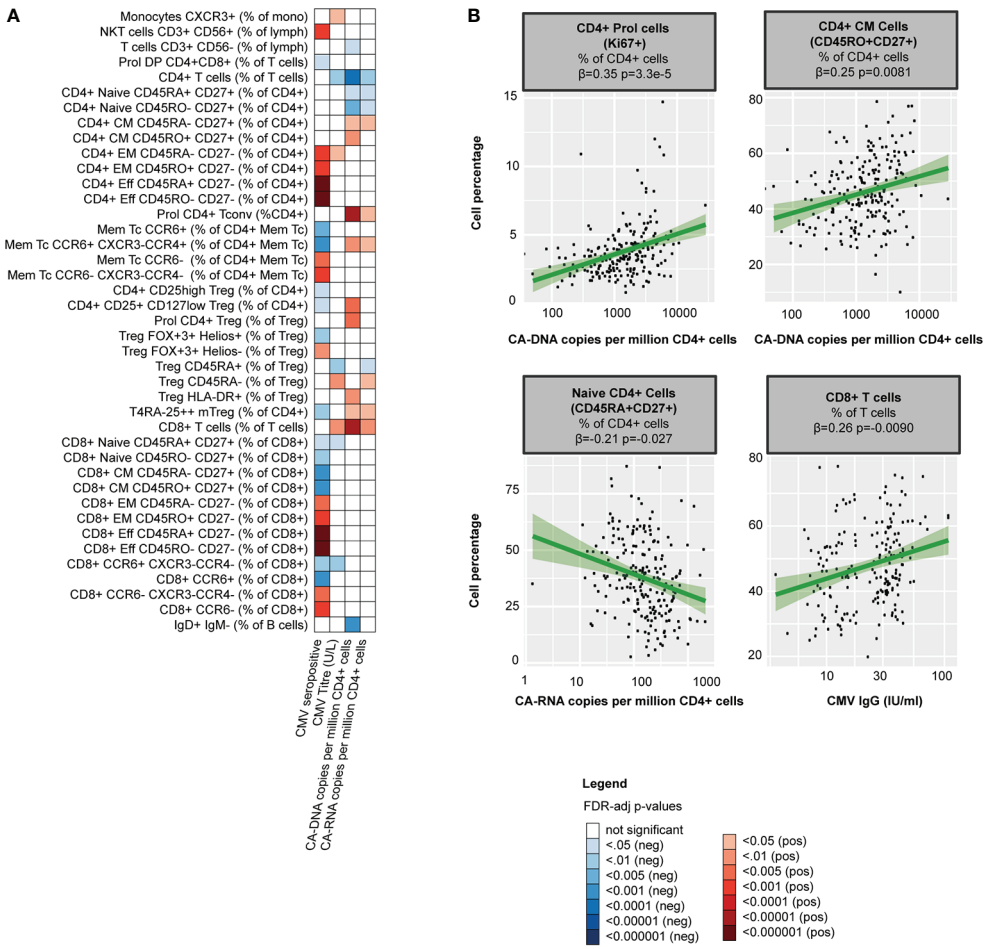

FIGURE 4 | The HIV-1 reservoir, CMV serostatus and WBC percentages in PLHIV **(A)** Heatmap of significant associations between WBC percentages (total n=108), CMV co-infection (serostatus and IgG titers in 198 seropositive PLHIV) and markers of the HIV-1 reservoir (CA -DNA and CA- RNA) in 211 PLHIV; WBC subsets that showed no significant correlations with any of the parameters (n=41) have been removed from the figure. **(B)** Examples of WBC percentages that were significantly associated with the viral reservoir or CMV IgG titers. Inverse-rank transformed data were analyzed using linear regression and adjusted for age, sex, sampling time, and season. For color coding of the FDR-adjusted p-values see legend. CA-DNA, CD4-cell-associated HIV-1 DNA; CA-RNA, CD4-cell-associated HIV-1 RNA; CMV, cytomegalovirus; PLHIV, people living with HIV; WBC, white blood cells.

translocation in chronic treated HIV, especially in those with higher CA-RNA and CA-DNA (CA-RNA β =0.18, p=0.0091 and CA-DNA β=0.21, p=0.0025, **Figure 5E**). Higher levels of IFABP were associated with an expansion of peripheral blood Th17 (β=0.17, p0.043; **Figure 5B**). Homing of Th17 to the gut (and other tissues, such as the skin) is directed by the chemokine CCL20, which is produced by tissue and immune cells (neutrophils and monocytes) and binds uniquely to the CCR6+ receptor (43). Correspondingly, we found strong associations between CCL20 and Th17 percentages (β=0.22, p=0.0037), CCL20 and Th17/Treg (β=0.26, p=0.00081 for Th17/FoxP3+ Treg, β=0.27, p=0.00081 for Th17/CD127low Treg, and β=0.19, p=0.013 for Th17/CD25++ Treg), CCL20 and circulating IL-17A levels (β=0.47, p=$1.2{\cdot}10^{-11}$) and CCL20 and IFABP (β=0.24, p=0.0011; **Figure 5F**). Together, these results suggest that the pro-inflammatory environment in chronic HIV may promote the differentiation of circulating naïve CD4+ T cells into Th17 cells and that these changes may be associated with changes in gut permeability and gut homing.

Functional Consequences of Changes in Adaptive Immune Cells in Chronic HIV

As our results indicated significant changes in circulating immune cell populations in PLHIV, we next analyzed the

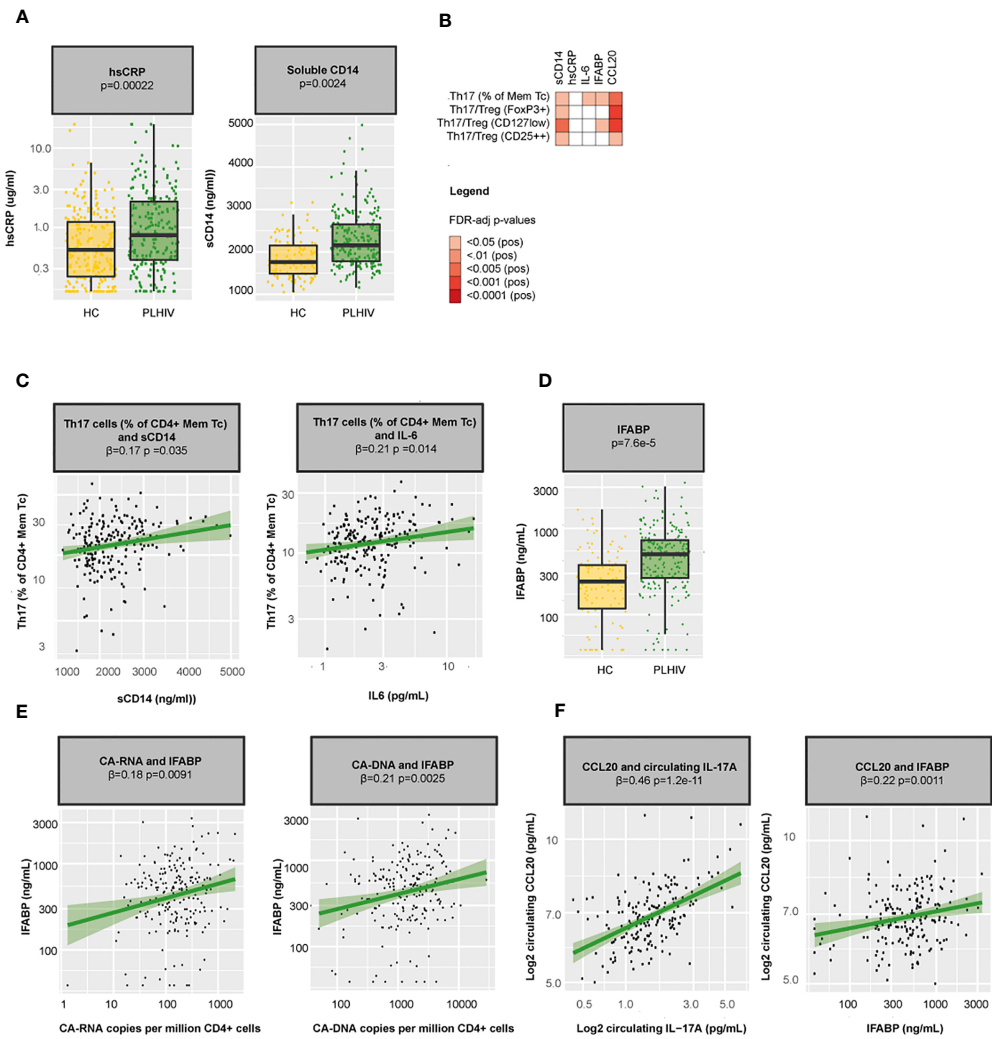

FIGURE 5 | Inflammation, microbial translocation, and Th17 cells in PLHIV **(A)** Boxplots showing differences in hsCRP and sCD14 between PLHIV (n=211) and healthy controls (n=56). **(B)** Heatmap showing associations between Th17 percentages, Th17/Treg ratios and sCD14, hsCRP, IFABP, and CCL20. **(C)** Associations between Th17 percentages and sCD14 and circulating IL-6 in PLHIV. **(D)** Levels of the microbial translocation marker IFABP in PLHIV and healthy controls. **(E)** Associations between IFABP and CA-RNA and CA-DNA in PLHIV. **(F)** Associations between CCL20 and circulating IL-17A and IFABP. Inverse-rank transformed data were analyzed using linear regression analyses and corrected for sampling time. CA-DNA, CD4-cell-associated HIV-1 DNA; CA-RNA, CD4-cell-associated HIV-1 RNA; CCL20, Chemokine (C-C motif) ligand 20; HC, healthy control; hsCRP, high-sensitivity CRP; IFABP, intestinal fatty-acid binding protein; IL-6, interleukin 6; IL-17A, interleukin 17A; Mem Tc, CD4+ memory T cell; PLHIV, people living with HIV; sCD14, soluble CD14; Th17 percentages, T-helper 17 cell percentages (Mem Tc CCR6+ CXCR3-CCR4+ as percentage of CD4+ Mem Tc); Treg, regulatory T cells; WBC, white blood cells.

possible functional consequences. First, we measured *ex vivo* cytokine responses of PBMCs after stimulation with different stimuli. We found strong correlations between NK and T-cell percentages and *ex vivo* IFN-γ, IL-17, and IL-22 responses (**Figure 6A** and **Supplementary Table 10**): IFN-γ responses correlated with percentages of NK dim, CD4+ and CD8+ EM cells, whereas IL-22 responses correlated with CCR6+ CM CD4+ cell percentages. As expected, Th17 percentages were associated with increased circulating IL-17A (β=0.16, p=0.029) and *ex vivo* IL-17 responses to *C. albicans* (β=0.19, p=0.047) and with reduced IFN-γ responses (**Figures 6A, E** and **Supplementary Table 10**). Despite the expansion of Th17 cells among PLHIV compared to controls, *ex vivo* responses of IL-17 or IL-22 did not differ, suggesting that the functional capacity of these cells may be compromised. In contrast, IFN-γ production upon stimulation with *C. albicans* hyphae (p=0.012) and *M. tuberculosis* (p=0.0025) was reduced in PLHIV (**Figure 6B**). Among PLHIV, lower *ex vivo* IFN-γ production to stimulation with Imiquimod (β =-0.21, p=0.0020) and *S. pneumoniae* (β=-0.22, p=0.0011) and lower circulating IFN-γ concentrations (β=-0.18, p=0.014) were associated with higher CA-DNA levels (**Figures 6C, D**). No associations were found between *ex vivo* cytokine production and CMV seropositivity.

Second, we measured serum immunoglobulins and found significant correlations between serum IgM and IgM+ B cell populations (**Figure 6F**), but no cohort differences in IgM levels [median (IQR) 0.76 (0.56 – 1.05) g/L in PLHIV versus 0.82 (0.65 – 1.21) g/L in controls, p= 0.22] or IgG levels [10.03 (8.34 - 11.59) g/L in PLHIV versus 9.10 (7.59 – 11.38) g/L in controls, p= 0.12]. These results indicate that while some of the alterations in adaptive immune function may be reversed by long-term cART (44, 45), others, such as impaired IFN-γ responses, remain.

DISCUSSION

In this study we show that, despite suppressive cART, the circulating innate and adaptive immune cell composition in PLHIV differs from that of HIV-uninfected individuals. We confirm that PLHIV exhibit a WBC profile characterized by proliferating memory and effector CD4+ and CD8+ T cells. While untreated HIV infection has been associated with a loss of circulating Th17 cells (9), we observed an expansion of circulating Th17 cells and increased Th17/Treg ratios during stable suppressive treatment, which was associated with plasma concentrations of IL-6, CCL20 and the microbial translocation marker IFABP. Furthermore, PLHIV showed clear changes in B cell maturation with reduced memory B cell percentages and increased plasmablast numbers. In the innate compartment, we observed an expansion of monocytes together with a loss of NK cells, specifically NK bright cells. In addition to age, sex, smoking, and CMV, we found strong associations between WBC populations and markers of the HIV-1 reservoir (CA-DNA and CA-RNA). Functionally, Th17 responses seemed to be preserved, whereas IFN-γ responses to *C. albicans* and *M. tuberculosis* were compromised, especially in those with higher CA-DNA. The compromised IFN-γ responses may affect host defense against some important bacterial pathogens (including *M. tuberculosis*) and the HIV-1 reservoir.

Prior studies have shown that untreated HIV infection results in a massive depletion of Th17 cells from the peripheral blood and the mucosa (9), a process that may partially be reversed by cART (46–48). We recently showed that PLHIV from the same cohort exhibited a pro-inflammatory profile with increased monocyte-derived cytokines, particularly IL-1β (20). IL-1β and IL-6 are among the critical cytokines driving differentiation of Th17 (42), and we postulate that these cytokines may have contributed to the higher circulating Th17 numbers. Th17 cells in the peripheral blood poorly reflect mucosal Th17 numbers (49) and it is possible that mucosal Th17 depletion with increased microbial translocation and altered Th17 recruitment occurs in the participants of our study. The gut-inflammatory marker generating islet-derived protein 3α (REG3α) would be of interest for future studies on the interplay between Th17 and epithelial gut damage in PLHIV (50).Concurrently to increased Th17 cells and pro-inflammatory Th17-like (CCR6+) mTregs, PLHIV showed increased peripheral blood Th17/Treg ratios. Increased Th17/Treg ratios have been linked to cardiovascular disease and atherosclerosis (33), cancer (34), and major depressive disorder (51), which are all highly prevalent in long-term treated PLHIV. Th17-mediated auto-immune diseases like psoriasis are also common among PLHIV, although they mostly occur during periods of severe immunosuppression and resolve upon cART initiation (52). Despite these changes in Th17, IL-17 and IL-22 cytokine responses did not differ between PLHIV and healthy controls. In contrast, we observed reduced *ex vivo* IFN-γ responses to *C. albicans* and *M. tuberculosis* in PLHIV. IFN-γ is predominantly produced by NK(T) cells, Th1, and CD8+ cells (44). Given that CD8+ cells were increased in PLHIV and Th1 cells did not differ between PLHIV and controls, we postulate that the reduced IFN-γ responses may have resulted from the loss of NK cells, which has been reported previously in both untreated and treated PLHIV (53, 54). In line with prior data, we observed an inverse relationship between IFN-γ responses and CA-DNA, suggesting that the failure to restore the NK cell compartment after cART initiation may be important for the containment of the HIV-1 reservoir (55).Moreover, IFN-γ is a key cytokine in the immune response against *M. tuberculosis* which remains an important pathogen in treated PLHIV (56). Improving IFN-γ responses, may therefore be relevant in the context of *M. tuberculosis* and HIV cure.

Different factors may contribute to the variation in T-cells repertoire in PLHIV. First, the effects of demographic factors such as age, sex, and smoking resembled those observed previously in healthy individuals (19, 41). Second, PLHIV in our study were almost universally coinfected with CMV and, in line with earlier data in HIV-infected and uninfected individuals, CMV seropositivity was associated with the expansion of effector and EM CD4+ and CD8+ T cells (14, 41, 57, 58). Of note, high CMV IgG levels may reflect frequent CMV reactivations or result from a stronger immune response (including adequate B/T cell interactions and B cell responses) and, consequently, fewer activations (59). Importantly, higher CMV IgG titers have been linked to microbial translocation and the development of non-AIDS-defining events such as cardiovascular disease (14, 60).

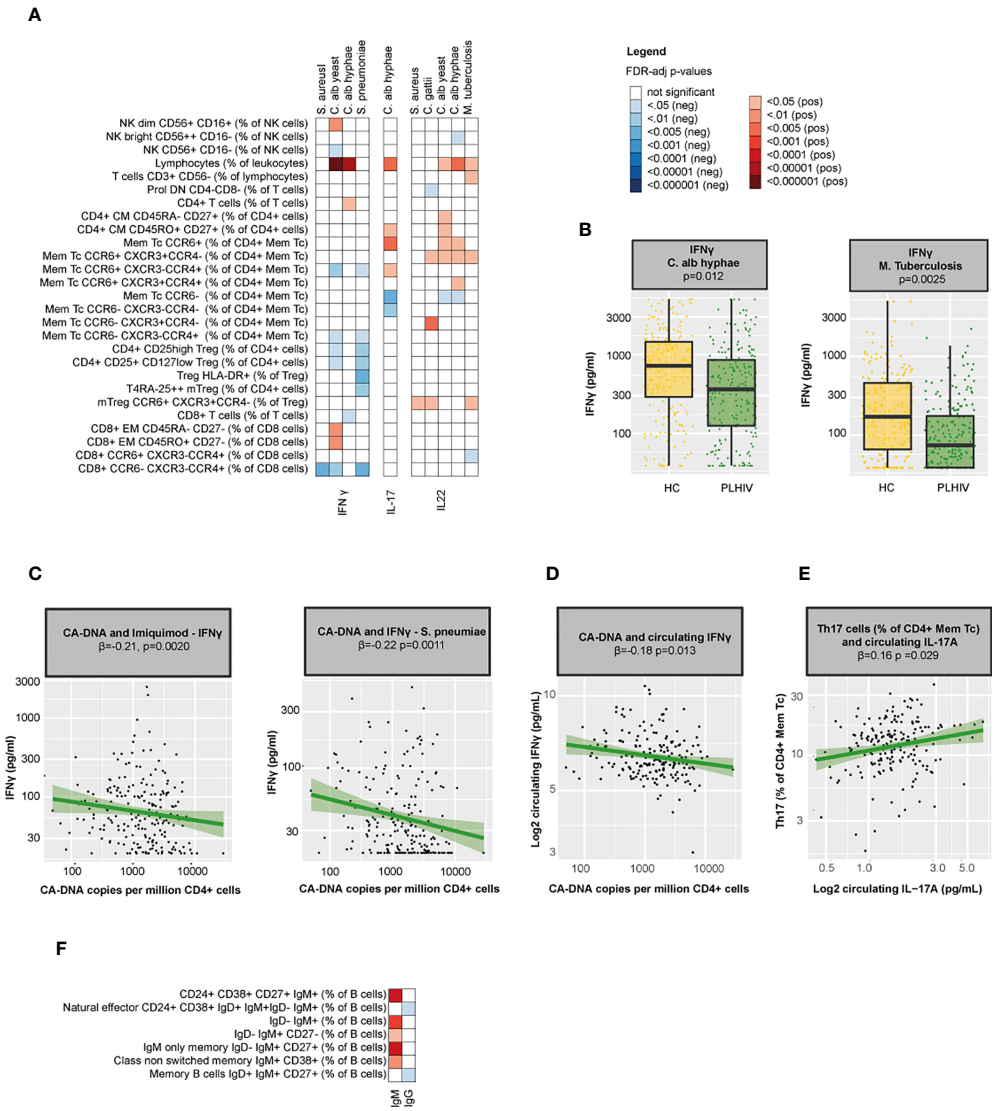

FIGURE 6 | Functional consequences of WBC alterations in PLHIV **(A)** Heatmap of NK(T) and T cell percentages (total n=71) that were significantly associated with the ex vivo production of IFN-γ, IL-17, and IL-22 upon seven days ex vivo stimulation of PBMCs with different stimuli (n=7) in 211 PLHIV; WBC subsets that showed no significant correlations with any of the parameters (n=44) have been removed from the figure. **(B)** Boxplot showing differences in ex vivo IFN-γ responses upon stimulation with *C. albicans* and *M. tuberculosis* between PLHIV (n=211) and healthy controls (n=56). **(C)** Association between CA-DNA and *ex vivo* IFN-γ responses to stimulation with Imiquimod and S. pneumoniae in PLHIV. **(D)** Association between CA-DNA and circulating IFN-γ in PLHIV. **(E)** Association between Th17 percentages and circulating IL-17A in PLHIV. **(F)** Heatmap of B cell percentages (total n=28) that were significantly correlated with IgM or IgG levels in PLHIV; WBC subsets that showed no significant correlations with any of the parameters (n=21) have been removed from the figure. Inverse-rank transformed data were analyzed using linear regression analyses and corrected for sampling time. For cohort comparisons, data were corrected for age, sex, sampling time, season and the CD4+ and CD8+ cell percentages. For color coding of the FDR-adjusted p-values see legend. CA-DNA, CD4-cell-associated HIV-1 DNA; HC, healthy control; IFN-γ, interferon gamma; Ig, immunoglobulin; IL-17(A), interleukin 17(A); IL-22, interleukin 22; Mem Tc, CD4+ memory T cell; NK(T) cells, natural killer (T) cells; PBMC, peripheral blood mononuclear cell; PLHIV, people living with HIV; sCD14, soluble CD14; Th17 percentages, T-helper 17 cell percentages (Mem Tc CCR6+ CXCR3-CCR4+ as percentage of CD4+ Mem Tc); WBC, white blood cell.

Third, we found substantial associations between WBC subsets and CD4+ nadir and markers of the HIV-1 reservoir. Overall, CA-DNA showed more and stronger correlations with WBC subsets than did CA-RNA, which may be explained by the fact that CA-RNA levels, reflecting transcriptional activity, are low during viral suppression and subtle effects may be missed (13, 61).

Next to T cell dysfunction, HIV is characterized by aberrant B cell responses and B cell dysfunction. Using a different set of B cell markers than earlier studies in PLHIV (62, 63), we confirm their observations that percentages of naïve B cells are increased and memory B cells are reduced in PLHIV. Moreover, adequate B cell maturation requires optimal communication between T and B cells, which, according to

our data, might be compromised in chronic stable PLHIV. B/T cell interactions take place in the germinal centers in lymph nodes and are orchestrated by follicular Th cells (Tfh) (64). As these cells are known to be highly permissive to HIV infection and serve as reservoirs during chronic infection, they could potentially explain these disrupted B/T cell interactions (64–66). Clinically, compromised B/T cells interactions may contribute to impaired immune responses to vaccination as well as increased risks for infections, such as invasive pneumococcal disease (5, 67). Finally, improvement of B/T cell communication is crucial for the development of broadly neutralizing antibodies and thus functional cure in PLHIV (68).

Our findings support the relevance of new immune modulating strategies in ART-treated PLHIV. Examples of interventions with potent anti-inflammatory properties in PLHIV include the IL-1β-inhibiting agent canakinumab (69) and the epigenetic modifier panobinostat (HDACi) (70, 71). Moreover, checkpoint inhibitors (e.g. those targeting PD1, PD-L1, and CTLA4) have been shown to, transiently, reverse latency of the viral reservoir, to restore cytotoxic T cell functions (72–75), and to enhance B-cell germinal responses to HIV-1 envelope vaccines (76). Further research is required to establish whether these agents are safe and effective long-term options to mitigate inflammation and to reverse immune exhaustion and HIV latency in stable HIV infection.

Several limitations should be considered when interpreting our data. First, the observational study design limits causal inferences. Second, generalizability of our findings to women, children and non-European populations requires further studying. Third, participants from the HIV cohort were older and more often male and age and sex both have known effects on the immune system (19, 21) To adjust for these differences, we used multivariable regression models which allowed us to take into account the effects of these independent predictors (age and sex) on our outcome of interest (HIV status). Fourth, we used a predefined set of markers and flow cytometry panels. While this standardized approach enhances validity and reproducibility and enabled us to compare our results with those of a large cohort of healthy controls, some interesting WBC subsets and markers for HIV have not been included (e.g. Tfh cells, CD38 HLA-DR co-expression, and PD-1/CD57 expression in the context of B/T cell interactions, T-cell activation, and immune cell exhaustion respectively). Furthermore, data on intracellular production of IL-17 and IFN-γ in maximally stimulated sorted cell populations (e.g. Th17 or NK cells) may provide a better understanding of the changes in cytokine production capacity per WBC subset. Finally, our WBC data are limited to the peripheral blood and we have no data on tissue-specific WBC composition (e.g. lymph nodes or the gut).

In summary, we show that the circulating innate and adaptive immune cell composition is altered in a large group of PLHIV receiving cART for more than six months. Furthermore, our findings suggest that some of the adaptive immune responses (Th17) are preserved while IFN-γ responses are compromised. Our comprehensive approach provides new insight into the changes in the immune cell architecture and functional immunity in treated HIV and highlights associations with the HIV-reservoir, underlining the need for early cART initiation. Our results are currently validated and extended in a multi-omics study including 2000 virally suppressed PLHIV (clinicaltrials.gov identifier: NCT03994835).

DATA AVAILABILITY STATEMENT

The raw data supporting the conclusions of this article will be made available by the authors, without undue reservation.

ETHICS STATEMENT

The studies involving human participants were reviewed and approved by Medical Ethical Review Committee region Arnhem-Nijmegen (ref. 42561.091.122). The patients/participants provided their written informed consent to participate in this study.

AUTHOR CONTRIBUTIONS

WH, QM, MN, HK, IJ, and AV designed the study. WH, LW and MJ recruited and included the participants. WH, LW, MJ, WT, SR, BC, and ER performed the laboratory experiments. RH, LW and WH analyzed the data and interpreted the data together with QM, AV, MN, LK, HK, IJ and JL. LW, WH, AV and QM wrote the manuscript. All authors contributed to the article and approved the submitted version.

FUNDING

QM, AV, and MN receive research support from ViiV Healthcare. The funders were not involved in the study design, data interpretation or the submission.

ACKNOWLEDGMENTS

We thank all volunteers from the 200HIV and 56P cohorts of the HFGP for participation in the study. We thank the clinicians and nurse practitioners of the HIV clinic of the Radboud university medical center for their help with participant recruitment and Anouk Janssen, Sanne Smeekens and Marije Oosting for their help with participant inclusion.

SUPPLEMENTARY MATERIAL

The Supplementary Material for this article can be found online at: https://www.frontiersin.org/articles/10.3389/fimmu.2021.661990/full#supplementary-material

REFERENCES

1. Smit M, Brinkman K, Geerlings S, Smit C, Thyagarajan K, Sighem A, et al. Future challenges for clinical care of an ageing population infected with HIV: a modelling study. *Lancet Infect Dis* (2015) 15(7):810–8. doi: 10.1016/S1473-3099(15)00056-0
2. Harboe ZB, Larsen MV, Ladelund S, Kronborg G, Konradsen HB, Gerstoft J, et al. Incidence and Risk Factors for Invasive Pneumococcal Disease in HIV-Infected and Non-HIV-Infected Individuals Before and After the Introduction of Combination Antiretroviral Therapy: Persistent High Risk Among HIV-Infected Injecting Drug Users. *Clin Infect Dis* (2014) 59(8):1168–76. doi: 10.1093/cid/ciu558
3. Kerneis S, Launay O, Turbelin C, Batteux F, Hanslik T, Boelle PY. Long-term Immune Responses to Vaccination in HIV-Infected Patients: A Systematic Review and Meta-Analysis. *Clin Infect Dis* (2014) 58(8):1130–9. doi: 10.1093/cid/cit937
4. O'Connor J, Vjecha MJ, Phillips AN, Angus B, Cooper D, Grinsztejn B, et al. Effect of immediate initiation of antiretroviral therapy on risk of severe bacterial infections in HIV-positive people with CD4 cell counts of more than 500 cells per muL: secondary outcome results from a randomised controlled trial. *Lancet HIV* (2017) 4(3):E105-E12. doi: 10.1016/S2352-3018(16)30216-8
5. Garcia Garrido HM, Mak AMR, Wit F, Wong GWM, Knol MJ, Vollaard A, et al. Incidence and Risk Factors for Invasive Pneumococcal Disease and Community-acquired Pneumonia in Human Immunodeficiency Virus-Infected Individuals in a High-income Setting. *Clin Infect Dis* (2020) 71 (1):41–50. doi: 10.1093/cid/ciz728
6. Ganatra SR, Bucsan AN, Alvarez X, Kumar S, Chatterjee A, Quezada M, et al. Antiretroviral therapy does not reduce tuberculosis reactivation in a tuberculosis-HIV coinfection model. *J Clin Invest* (2020) 130(10):5171–9. doi: 10.1172/JCI136502
7. Titanji B, Gavegnano C, Hsue P, Schinazi R, Marconi VC. Targeting Inflammation to Reduce Atherosclerotic Cardiovascular Risk in People With HIV Infection. *J Am Heart Assoc* (2020) 9(3):e014873. doi: 10.1161/JAHA.119.014873
8. Deeks SG. HIV infection, inflammation, immunosenescence, and aging. *Annu Rev Med* (2011) 62:141–55. doi: 10.1146/annurev-med-042909-093756
9. Chevalier MF, Petitjean G, Dunyach-Remy C, Didier C, Girard PM, Manea ME, et al. The Th17/Treg Ratio, IL-1RA and sCD14 Levels in Primary HIV Infection Predict the T-cell Activation Set Point in the Absence of Systemic Microbial Translocation. *PloS Pathog* (2013) 9(6). doi: 10.1371/journal.ppat.1003453
10. Brenchley JM. Microbial translocation is a cause of systemic immune activation in chronic HIV infection. *Retrovirology* (2006) 3. doi: 10.1186/1742-4690-3-S1-S98
11. Perkins, Wolinsky D. The Interplay Between Host Genetic Variation, Viral Replication, and Microbial Translocation in Untreated HIV-Infected Individuals (vol 212, pg 578, 2015). *J Infect Dis* (2015) 212(10):1686–6. doi: 10.1093/infdis/jiv089
12. Siedner MJ, Zanni M, Tracy RP, Kwon DS, Tsai AC, Kakuhire B, et al. Increased Systemic Inflammation and Gut Permeability Among Women With Treated HIV Infection in Rural Uganda. *J Infect Dis* (2018) 218(6):922–6. doi: 10.1093/infdis/jiy244
13. Cohn LB, Chomont N, Deeks SG. The Biology of the HIV-1 Latent Reservoir and Implications for Cure Strategies. *Cell Host Microbe* (2020) 27(4):519–30. doi: 10.1016/j.chom.2020.03.014
14. Ramendra R, Isnard S, Lin J, Fombuena B, Ouyang J, Mehraj V, et al. Cytomegalovirus Seropositivity Is Associated With Increased Microbial Translocation in People Living With Human Immunodeficiency Virus and Uninfected Controls. *Clin Infect Dis* (2020) 71(6):1438–46. doi: 10.1093/cid/ciz1001
15. Isnard S, Ramendra R, Dupuy FP, Mehraj V, Lin J, Kokinov N, et al. Relevance of Reg3 alpha and I-FABP on microbial translocation, inflammation and reservoir size in people living with HIV. *J Int AIDS Soc* (2019) 22:67–8. doi: 10.1016/S2055-6640(20)31030-X
16. Mehraj V, Ramendra R, Isnard S, Dupuy FP, Ponte R, Chen J, et al. Circulating (1–>3)-beta-D-glucan Is Associated With Immune Activation During Human Immunodeficiency Virus Infection. *Clin Infect Dis* (2020) 70(2):232–41. doi: 10.1093/cid/ciz212
17. Olson A, Coote C, Snyder-Cappione JE, Lin N, Sagar M. HIV-1 transcription but not intact provirus levels are associated with systemic inflammation. *J Infect Dis* (2020). doi: 10.1093/infdis/jiaa657
18. Netea MG, Joosten LA, Li Y, Kumar V, Oosting M, Smeekens S, et al. Understanding human immune function using the resources from the Human Functional Genomics Project. *Nat Med* (2016) 22(8):831–3. doi: 10.1038/nm.4140
19. Aguirre-Gamboa R, Joosten I, Urbano PC, van der Molen RG, van Rijssen E, van Cranenbroek B, et al. Differential Effects of Environmental and Genetic Factors on T and B Cell Immune Traits. *Cell Rep* (2016) 17(9):2474–87. doi: 10.1016/j.celrep.2016.10.053
20. van der Heijden WA, van de Wijer L, Keramati F, Trypsteen W, Rutsaert S, Ter Horst R, et al. Chronic HIV infection induces transcriptional and functional reprogramming of innate immune cells. *JCI Insight* (2021) 6(7): e145928. doi: 10.1172/jci.insight.145928
21. Ter Horst R, Jaeger M, Smeekens SP, Oosting M, Swertz MA, Li Y, et al. Host and Environmental Factors Influencing Individual Human Cytokine Responses. *Cell* (2016) 167(4):1111–24.e13. doi: 10.1016/j.cell.2016.10.018
22. Oosting M, Buffen K, Cheng SC, Verschueren IC, Koentgen F, van de Veerdonk FL, et al. Borrelia-induced cytokine production is mediated by spleen tyrosine kinase (Syk) but is Dectin-1 and Dectin-2 independent. *Cytokine* (2015) 76(2):465–72. doi: 10.1016/j.cyto.2015.08.005
23. Assarsson E, Lundberg M, Holmquist G, Bjorkesten J, Thorsen SB, Ekman D, et al. Homogenous 96-plex PEA immunoassay exhibiting high sensitivity, specificity, and excellent scalability. *PloS One* (2014) 9(4):e95192. doi: 10.1371/journal.pone.0095192
24. Koeken VACM, de Bree LCJ, Mourits VP, Moorlag SJCFM, Walk J, Cirovic B, et al. BCG vaccination in humans inhibits systemic inflammation in a sex-dependent manner. *J Clin Invest* (2020) 130(10):5591–602. doi: 10.1172/JCI133935
25. Chomont N, El-Far M, Ancuta P, Trautmann L, Procopio FA, Yassine-Diab B, et al. HIV reservoir size and persistence are driven by T cell survival and homeostatic proliferation. *Nat Med* (2009) 15(8):893–900. doi: 10.1038/nm.1972
26. Pasternak AO, Lukashov VV, Berkhout B. Cell-associated HIV RNA: a dynamic biomarker of viral persistence. *Retrovirology* (2013) 10:41. doi: 10.1186/1742-4690-10-41
27. Rutsaert S, De Spiegelaere W, De Clercq L, Vandekerckhove L. Evaluation of HIV-1 reservoir levels as possible markers for virological failure during boosted darunavir monotherapy. *J Antimicrobial Chemotherapy* (2019) 74 (10):3030–4. doi: 10.1093/jac/dkz269
28. Trypsteen W, Vynck M, De Neve J, Bonczkowski P, Kiselinova M, Malatinkova E, et al. ddpcRquant: threshold determination for single channel droplet digital PCR experiments. *Anal Bioanal Chem* (2015) 407 (19):5827–34. doi: 10.1007/s00216-015-8773-4
29. Benjamini Y, Hochberg Y. Controlling the False Discovery Rate - a Practical and Powerful Approach to Multiple Testing. *J R Stat Soc Ser B-Statistical Method* (1995) 57(1):289–300. doi: 10.1111/j.2517-6161.1995.tb02031.x
30. Becattini S, Hochberg Y. T cell immunity. Functional heterogeneity of human memory CD4(+) T cell clones primed by pathogens or vaccines. *Science* (2015) 347(6220):400–6. doi: 10.1126/science.1260668
31. Li ZY, Latorre D, Mele F, Foglierini M, De Gregorio C, Cassotta A, et al. FOXP3(+) regulatory T cells and their functional regulation. *Cell Mol Immunol* (2015) 12(5):558–65. doi: 10.1038/cmi.2015.10
32. Schulze Zur Wiesch J, Li D, Tsun A, Li B. Comprehensive analysis of frequency and phenotype of T regulatory cells in HIV infection: CD39 expression of FoxP3+ T regulatory cells correlates with progressive disease. *J Virol* (2011) 85(3):1287–97. doi: 10.1128/JVI.01758-10
33. Saigusa R, Winkels H, Ley K. T cell subsets and functions in atherosclerosis. *Nat Rev Cardiol* (2020) 17(7):387–401. doi: 10.1038/s41569-020-0352-5
34. Knochelmann HM, Dwyer CJ, Bailey SR, Amaya SM, Elston DM, Mazza-McCrann JM, et al. When worlds collide: Th17 and Treg cells in cancer and autoimmunity. *Cell Mol Immunol* (2018) 15(5):458–69. doi: 10.1038/s41423-018-0004-4
35. Sallusto F, Geginat J, Lanzavecchia A. Central memory and effector memory T cell subsets: function, generation, and maintenance. *Annu Rev Immunol* (2004) 22:745–63. doi: 10.1146/annurev.immunol.22.012703.104702
36. Mahnke YD, Brodie TM, Sallusto F, Roederer M, Lugli E. The who's who of T-cell differentiation: human memory T-cell subsets. *Eur J Immunol* (2013) 43 (11):2797–809. doi: 10.1002/eji.201343751
37. Sachsenberg N, Perelson AS, Yerly S, Schockmel GA, Leduc D, Hirschel B, et al. Turnover of CD4(+) and CD8(+) T lymphocytes in HIV-1 infection as measured by Ki-67 antigen. *J Exp Med* (1998) 187(8):1295–303. doi: 10.1084/jem.187.8.1295

38. Moir S, Fauci AS. Insights into B cells and HIV-specific B-cell responses in HIV-infected individuals. *Immunol Rev* (2013) 254(1):207–24. doi: 10.1111/imr.12067
39. Moir S, Buckner CM, Ho J, Wang W, Chen J, Waldner AJ, et al. B cells in early and chronic HIV infection: evidence for preservation of immune function associated with early initiation of antiretroviral therapy. *Blood* (2010) 116 (25):5571–9. doi: 10.1182/blood-2010-05-285528
40. Arts RJ, Novakovic B, Ter Horst R, Carvalho A, Bekkering S, Lachmandas E, et al. Glutaminolysis and Fumarate Accumulation Integrate Immunometabolic and Epigenetic Programs in Trained Immunity. *Cell Metab* (2016) 24(6):807–19. doi: 10.1016/j.cmet.2016.10.008
41. Patin E, Hasan M, Bergstedt J, Rouilly V, Libri V, Urrutia A, et al. Natural variation in the parameters of innate immune cells is preferentially driven by genetic factors. *Nat Immunol* (2018) 19(3):302–14 doi: 10.1038/s41590-018-0049-7.
42. Acosta-Rodriguez EV, Napolitani G, Lanzavecchia A, Sallusto F. Interleukins 1 beta and 6 but not transforming growth factor-beta are essential for the differentiation of interleukin 17-producing human T helper cells. *Nat Immunol* (2007) 8(9):942–9. doi: 10.1038/ni1496
43. Schutyser E, Struyf S, Van Damme J. The CC chemokine CCL20 and its receptor CCR6. *Cytokine Growth Factor Rev* (2003) 14(5):409–26. doi: 10.1016/S1359-6101(03)00049-2
44. Roff SR, Noon-Song EN, Yamamoto JK. The Significance of Interferon-gamma in HIV-1 Pathogenesis, Therapy, and Prophylaxis. *Front Immunol* (2014) 4:498. doi: 10.3389/fimmu.2013.00498
45. Kim CJ, Nazli A, Rojas OL, Chege D, Alidina Z, Huibner S, et al. A role for mucosal IL-22 production and Th22 cells in HIV-associated mucosal immunopathogenesis. *Mucosal Immunol* (2012) 5(6):670–80. doi: 10.1038/mi.2012.72
46. Gosselin A, Monteiro P, Chomont N, Diaz-Griffero F, Said EA, Fonseca S, et al. Peripheral Blood CCR4(+)CCR6(+) and CXCR3(+)CCR6(+) CD4(+) T Cells Are Highly Permissive to HIV-1 Infection. *J Immunol* (2010) 184 (3):1604–16. doi: 10.4049/jimmunol.0903058
47. He Y, Li J, Zheng YH, Luo Y, Zhou HY, Yao YH, et al. A Randomized Case-Control Study of Dynamic Changes in Peripheral Blood Th17/Treg Cell Balance and Interleukin-17 Levels in Highly Active Antiretroviral-Treated HIV Type 1/AIDS Patients. *AIDS Res Hum Retroviruses* (2012) 28(4):339–45. doi: 10.1089/aid.2011.0140
48. Kim CJ, McKinnon LR, Kovacs C, Kandel G, Huibner S, Chege D, et al. Mucosal Th17 cell function is altered during HIV infection and is an independent predictor of systemic immune activation. *J Immunol* (2013) 191(5):2164–73. doi: 10.4049/jimmunol.1300829
49. Nayrac M, Requena M, Loiseau C, Cazabat M, Suc B, Carrere N, et al. Th22 cells are efficiently recruited in the gut by CCL28 as an alternative to CCL20 but do not compensate for the loss of Th17 cells in treated HIV-1-infected individuals. *Mucosal Immunol* (2021) 14(1):219–28. doi: 10.1038/s41385-020-0286-6
50. Isnard S, Ramendra R, Dupuy FP, Lin J, Fombuena B, Kokinov N, et al. Plasma Levels of C-Type Lectin REG3alpha and Gut Damage in People With Human Immunodeficiency Virus. *J Infect Dis* (2020) 221(1):110–21. doi: 10.1093/infdis/jiz423
51. Ghosh R, Kumar PK, Mitra P, Purohit P, Nebhinani N, Sharma P. Circulating T helper 17 and IFN-gamma positive Th17 cells in Major Depressive Disorder. *Behav Brain Res* (2020) 394:112811. doi: 10.1016/j.bbr.2020.112811
52. Morar N, Willis-Owen SA, Maurer T, Bunker CB. HIV-associated psoriasis: pathogenesis, clinical features, and management. *Lancet Infect Dis* (2010) 10 (7):470–8. doi: 10.1016/S1473-3099(10)70101-8
53. Dillon SM, Lee EJ, Bramante JM, Barker E, Wilson CC. The Natural Killer Cell Interferon-Gamma Response to Bacteria Is Diminished in Untreated HIV-1 Infection and Defects Persist Despite Viral Suppression. *Jaids-Journal Acquired Immune Deficiency Syndromes* (2014) 65(3):259–67. doi: 10.1097/01.qai.0000435603.50598.2b
54. Azzoni L, Papasavvas E, Chehimi J, Kostman JR, Mounzer K, Ondercin J, et al. Sustained impairment of IFN-gamma secretion in suppressed HIV-infected patients despite mature NK cell recovery: evidence for a defective reconstitution of innate immunity. *J Immunol* (2002) 168(11):5764–70. doi: 10.4049/jimmunol.168.11.5764
55. Marras F, Casabianca A, Bozzano F, Ascierto ML, Orlandi C, Di Biagio A, et al. Control of the HIV-1 DNA Reservoir Is Associated In Vivo and In Vitro with NKp46/NKp30 (CD335 CD337) Inducibility and Interferon Gamma Production by Transcriptionally Unique NK Cells. *J Virol* (2017) 91(23). doi: 10.1128/JVI.00647-17
56. Flynn JL, Chan J. Tuberculosis: latency and reactivation. *Infect Immun* (2001) 69(7):4195–201. doi: 10.1128/IAI.69.7.4195-4201.2001
57. Tu WJ, Rao S. Mechanisms Underlying T Cell Immunosenescence: Aging and Cytomegalovirus Infection. *Front Microbiol* (2016) 7:2111. doi: 10.3389/fmicb.2016.02111
58. Freeman ML, Mudd JC, Shive CL, Younes SA, Panigrahi S, Sieg SF, et al. CD8 T-Cell Expansion and Inflammation Linked to CMV Coinfection in ART-treated HIV Infection. *Clin Infect Dis* (2016) 62(3):392–6. doi: 10.1093/cid/civ840
59. Gianella S, Morris SR, Tatro E, Vargas MV, Haubrich RH, Daar ES, et al. Virologic Correlates of Anti-CMV IgG Levels in HIV-1-Infected Men. *J Infect Dis* (2014) 209(3):452–6. doi: 10.1093/infdis/jit434
60. Lichtner M, Cicconi P, Vita S, Cozzi-Lepri A, Galli M, Lo Caputo S, et al. Cytomegalovirus Coinfection Is Associated With an Increased Risk of Severe Non-AIDS-Defining Events in a Large Cohort of HIV-Infected Patients. *J Infect Dis* (2015) 211(2):178–86. doi: 10.1093/infdis/jiu417
61. Pasternak AO, Berkhout B. What do we measure when we measure cell-associated HIV RNA. *Retrovirology* (2018) 15(1):13. doi: 10.1186/s12977-018-0397-2
62. Pensieroso S, Galli L, Nozza S, Ruffin N, Castagna A, Tambussi G, et al. B-cell subset alterations and correlated factors in HIV-1 infection. *AIDS* (2013) 27 (8):1209–17. doi: 10.1097/QAD.0b013e32835edc47
63. Buckner CM, Kardava L, Zhang X, Gittens K, Justement JS, Kovacs C, et al. Maintenance of HIV-Specific Memory B-Cell Responses in Elite Controllers Despite Low Viral Burdens. *J Infect Dis* (2016) 214(3):390–8. doi: 10.1093/infdis/jiw163
64. Vinuesa CG. HIV and T follicular helper cells: a dangerous relationship. *J Clin Invest* (2012) 122(9):3059–62. doi: 10.1172/JCI65175
65. Lindqvist M, van Lunzen J, Soghoian DZ, Kuhl BD, Ranasinghe S, Kranias G, et al. Expansion of HIV-specific T follicular helper cells in chronic HIV infection. *J Clin Invest* (2012) 122(9):3271–80. doi: 10.1172/JCI64314
66. Planchais C, Hocqueloux L, Ibanez C, Gallien S, Copie C, Surenaud M, et al. Early Antiretroviral Therapy Preserves Functional Follicular Helper T and HIV-Specific B Cells in the Gut Mucosa of HIV-1-Infected Individuals. *J Immunol* (2018) 200(10):3519–29. doi: 10.4049/jimmunol.1701615
67. Abzug MJ, Warshaw M, Rosenblatt HM, Levin MJ, Nachman SA, Pelton SI, et al. Immunogenicity and Immunologic Memory after Hepatitis B Virus Booster Vaccination in HIV-Infected Children Receiving Highly Active Antiretroviral Therapy. *J Infect Dis* (2009) 200(6):935–46. doi: 10.1086/605448
68. Moir S, Fauci AS. B-cell responses to HIV infection. *Immunological Rev* (2017) 275(1):33–48. doi: 10.1111/imr.12502
69. Hsue PY, Li D, Ma Y, Ishai A, Manion M, Nahrendorf M, et al. IL-1beta Inhibition Reduces Atherosclerotic Inflammation in HIV Infection. *J Am Col Cardiol* (2018) 72:2809–11. doi: 10.1016/j.jacc.2018.09.038
70. Brinkmann CR, Hojen JF, Rasmussen TA, Kjaer AS, Olesen R, Denton PW, et al. Treatment of HIV-Infected Individuals with the Histone Deacetylase Inhibitor Panobinostat Results in Increased Numbers of Regulatory T Cells and Limits Ex Vivo Lipopolysaccharide-Induced Inflammatory Responses. *mSphere* (2018) 3(1):e00616–17. doi: 10.1128/mSphere.00616-17
71. Hogh Kolbaek Kjaer AS, Brinkmann CR, Dinarello CA, Olesen R, Ostergaard L, Sogaard OS, et al. The histone deacetylase inhibitor panobinostat lowers biomarkers of cardiovascular risk and inflammation in HIV patients. *AIDS* (2015) 29:1195–200. doi: 10.1097/QAD.0000000000000678
72. Chen H, Moussa M, Catalfamo M. The Role of Immunomodulatory Receptors in the Pathogenesis of HIV Infection: A Therapeutic Opportunity for HIV Cure? *Front Immunol* (2020) 11(1):1223. doi: 10.3389/fimmu.2020.01223
73. Evans VA, van der Sluis RM, Solomon A, Dantanarayana A, McNeil C, Garsia R, et al. Programmed cell death-1 contributes to the establishment and maintenance of HIV-1 latency. *AIDS* (2018) 32(1):1491–7. doi: 10.1097/QAD.0000000000001849
74. Le Garff G, Samri A, Lambert-Niclot S, Even S, Lavole A, Cadranel J, et al. Transient HIV-specific T cells increase and inflammation in an HIV-infected patient treated with nivolumab. *AIDS* (2017) 31:1048–51. doi: 10.1097/QAD.0000000000001429

75. Gay CL, Bosch RJ, Ritz J, Hataye JM, Aga E, Tressler RL, et al. Clinical Trial of the Anti-PD-L1 Antibody BMS-936559 in HIV-1 Infected Participants on Suppressive Antiretroviral Therapy. *J Infect Dis* (2017) 215:1725–33. doi: 10.1093/infdis/jix191
76. Bradley T, Kuraoka M, Yeh CH, Tian M, Chen H, Cain DW, et al. Immune checkpoint modulation enhances HIV-1 antibody induction. *Nat Commun* (2020) 11:948. doi: 10.1038/s41467-020-14670-w

Conflict of Interest: This study was supported by an AIDS-fonds (#P-29001) Netherlands and an ERC Advanced Grant (#833247). LV was supported by FWO (grant 1.8.020.09.N.00) and Collen-Francqui Research Professor Mandate. SR received a strategic basic research fund of the Research Foundation – Flanders (FWO, 1S32916N). TS and JL were employed by ViiV Healthcare.

The remaining authors declare that the research was conducted in the absence of any commercial or financial relationships that could be construed as a potential conflict of interest.

frontiers in Immunology

ORIGINAL RESEARCH
published: 09 June 2021
doi: 10.3389/fimmu.2021.683396

In Situ Characterization of Human Lymphoid Tissue Immune Cells by Multispectral Confocal Imaging and Quantitative Image Analysis; Implications for HIV Reservoir Characterization

Eirini Moysi[1], *Perla M. Del Rio Estrada*[2], *Fernanda Torres-Ruiz*[2], *Gustavo Reyes-Terán*[2,3], *Richard A. Koup*[1] *and Constantinos Petrovas*[1,4]*

[1] Vaccine Research Center, National Institute of Allergy and Infectious Diseases, National Institutes of Health, Bethesda, MD, United States, [2] Centro de Investigación en Enfermedades Infecciosas, Instituto Nacional de Enfermedades Respiratorias, Mexico City, Mexico, [3] Comisión Coordinadora de Institutos Nacionales de Salud y Hospitales de Alta Especialidad, Secretaría de Salud, Mexico City, Mexico, [4] Institute of Pathology, Department of Laboratory Medicine and Pathology, Lausanne University Hospital, Lausanne, Switzerland

OPEN ACCESS

Edited by:
Xu Yu,
Massachusetts General Hospital and Harvard Medical School, United States

Reviewed by:
Zaza Mtine Ndhlovu,
Ragon Institute of MGH, MIT and Harvard, United States
Jacob D. Estes,
Oregon Health & Science University, United States

***Correspondence:**
Constantinos Petrovas
petrovasc@mail.nih.gov

Specialty section:
This article was submitted to Viral Immunology, a section of the journal Frontiers in Immunology

Received: 20 March 2021
Accepted: 13 May 2021
Published: 09 June 2021

Citation:
Moysi E, Del Rio Estrada PM, Torres-Ruiz F, Reyes-Terán G, Koup RA and Petrovas C (2021) In Situ Characterization of Human Lymphoid Tissue Immune Cells by Multispectral Confocal Imaging and Quantitative Image Analysis; Implications for HIV Reservoir Characterization. Front. Immunol. 12:683396. doi: 10.3389/fimmu.2021.683396

CD4 T cells are key mediators of adaptive immune responses during infection and vaccination. Within secondary lymphoid organs, helper CD4 T cells, particularly those residing in germinal centers known as follicular helper T cells (Tfh), provide critical help to B-cells to promote their survival, isotype switching and selection of high affinity memory B-cells. On the other hand, the important role of Tfh cells for the maintenance of HIV reservoir is well documented. Thus, interrogating and better understanding the tissue specific micro-environment and immune subsets that contribute to optimal Tfh cell differentiation and function is important for designing successful prevention and cure strategies. Here, we describe the development and optimization of eight multispectral confocal microscopy immunofluorescence panels designed for in depth characterization and immune-profiling of relevant immune cells in formalin-fixed paraffin-embedded human lymphoid tissue samples. We provide a comprehensive library of antibodies to use for the characterization of CD4+ T-cells -including Tfh and regulatory T-cells- as well as CD8 T-cells, B-cells, macrophages and dendritic cells and discuss how the resulting multispectral confocal datasets can be quantitatively dissected using the HistoCytometry pipeline to collect information about relative frequencies and immune cell spatial distributions. Cells harboring actively transcribed virus are analyzed using an in-situ hybridization assay for the characterization of HIV mRNA positive cells in combination with additional protein markers (multispectral RNAscope). The application of this methodology to lymphoid tissues offers a means to interrogate multiple relevant immune cell targets simultaneously at increased resolution in a reproducible manner to guide CD4 T-cell studies in infection and vaccination.

Keywords: lymph nodes, Tfh, confocal imaging, tissue architecture, HIV reservoir

INTRODUCTION

To understand the tissue specific mechanisms that govern successful clinical outcomes in infection and vaccination, for example pathogen clearance or the production of neutralizing antibodies, it is important to understand the context in which these outcomes arise. Lymphoid tissues and secondary lymphoid organs (SLOs) are anatomical sites with a key role in the generation of adaptive immune responses (1). They are characterized by a high density of lymphocytes compared to peripheral blood (estimated at ~60% in SLOs compared to 2.2% in blood) (2, 3) and are also populated by cell subsets such as fibroblasts and stromal cells that perform critical immune related functions (4–7) but are less amenable to isolation for *ex vivo* study. Traditionally, the study of immune cell dynamics in lymphoid tissues has been performed using single-cell methodologies such as flow cytometry and more recently mass cytometry (i.e. CyTOF) and single-cell or bulk RNAseq after dissociating the cells from the tissue. Such methodologies have greatly enriched our understanding of circulating and tissue-resident immunophenotypes, their transcriptional programs and population kinetics at different life stages or in pathology (8–11). However, methodologies employing cell suspensions do not interrogate by design the microanatomical segregation or positioning of immune subsets relative to each other despite the importance of these two parameters for mechanism and function (12).

HIV infection profoundly affects the microarchitecture of lymphoid tissues and lymph nodes (LN) (13). The virus is detected in LN shortly after infection (14) where it persists for life, even in the context of antiretroviral therapy (13, 15). Structural damage of B-cell follicles, LN fibrosis as well as acute lymphadenitis characterized by focal hemorrhages, extensive cellular destruction, accumulation of neutrophils, phagocytosis of nuclear debris, proliferation of blood vessels, presence of immunoblasts and clear cell aggregation are some of the changes that have been described in individuals affected by the virus (13). The CD4 T cell lineage, which comprises several subsets including Th1, Th2, Th9, Th17, Th22, regulatory T cells (Treg) and follicular helper T cells (Tfh) (16, 17) is a major target of HIV infection (18). CD4 T cell lineage subsets show varying distributions in peripheral blood and lymphoid tissue compartments depending on their trafficking and functional profiles as well as status of differentiation (naïve; central memory Tcm; effector memory Tem; terminal effector Temra) (8, 11). Of particular interest among these subsets are Tfh, a CD4 T cell population that was first identified in tonsillar tissues, in microanatomical regions known as germinal centers (GC) that develop after antigenic challenge (4, 19). Tfh are phenotypically characterized by the expression of the transcriptional regulator Bcl-6 and chemokine receptor CXCR5, as well as by the concurrent expression of the costimulatory receptors PD-1, CD40L and ICOS (4, 20). Their role is to provide critical help to B-cells to promote their survival, isotype switching and selection of high affinity memory B cells (21). In line with the heterogeneity observed in other CD4 T-cell subsets, Tfh also display phenotypic heterogeneity that has been shown to associate with function (21, 22). Furthermore, the exact topology of Tfh within GCs is also emerging as an important dimension for their analysis (23, 24) HIV infection has been shown to perturb Tfh numbers both in humans as well as in NHP animal models of the disease (25, 26). In addition, Tfh have been shown to represent an important reservoir of HIV during chronic infection (27, 28). Understanding thus the changes that come about in lymphoid tissues during a chronic infection is important for appreciating the mechanisms leading to pathology, disease progression as well as neutralizing – and broadly neutralizing- antibody formation.

In this study, we describe the development of eight multispectral confocal imaging panels designed for the analysis of CD4+ T-cells -including Tfh and regulatory T-cells- as well as CD8 T-cells, B-cells, macrophages and dendritic cells in tissue sections. Two additional panels designed for the characterization of key lymphoid stromal elements and HIV RNA positioning are also presented. We discuss how to prepare the confocal microscope for image acquisition, provide a comprehensive list of validated antibodies to use and suggest a framework for the quantitative analysis of the imaging results using the HistoCytometry pipeline (29). The proposed tissue analysis can be applied in studies of natural HIV infection as well as in experimental vaccination protocols to supplement existing datasets with spatial information to aid the generation of hypothesis-driven questions regarding the mechanisms underlying successful immune responses.

MATERIALS AND METHODS

Ethics Statement

Signed informed consent was obtained before all procedures in accordance with the Declaration of Helsinki and approved by the appropriate Institutional Review Board. Tonsils were obtained from anonymized discarded pathologic specimens from Children's National Medical Center (CNMC) under the auspices of the Basic Science Core of the District of Columbia Developmental Center for AIDS Research. The CNMC Institutional Review Board determined that study of anonymized discarded tissues did not constitute 'human subjects research'. The inguinal lymph nodes used for the RNAscope and for LN-specific validations were from HIV+ donors recruited at Centro de Investigación en Enfermedades Infecciosas (CIENI), Instituto Nacional de Enfermedades Respiratorias (INER) in Mexico City, Mexico. Informed consent was obtained before the procedures in line with the protocols approved by the INER-CIENI Ethics Committee.

Tissue Processing

Upon receipt of tissue, lymph nodes and tonsils were washed with ice-cold medium R-10 (RPMI 1640 supplemented with 10% fetal bovine serum, 2 mM L-glutamine, 100 U/mL penicillin and 100 µg/mL streptomycin (Invitrogen). The surrounding fatty tissue was removed, and tissues were cut into small pieces and

immediately placed in fixative for 24hrs that was either in 10% Neutral Buffered Formalin (tonsils) or 4% neutral buffered paraformaldehyde for RNAscope as preliminary experiments showed superior results using this type of fixation (lymph node samples). Specimens were then embedded in paraffin and sectioned for multiplex confocal microscopy analysis. Tonsillar mononuclear cells used in flow cytometry experiments were isolated from specimens by mechanical disruption and subsequent Ficoll-Paque density gradient centrifugation.

Antibodies

The following antibodies were used in the study (also summarized in **Table 1**).

Flow Cytometry

CD3 BB700 (clone SP34-2, Beckton Dickenson) or CD3 H7APC (clone SK7, BD Biosciences); Ki67 Brilliant Violet 421 (clone B56, BD Horizon); CD20 Brilliant Violet 570 (clone 2H7, Biolegend); CD4 Brilliant Violet 650 (clone SK3, BD

TABLE 1 | Antibodies used for confocal imaging and flow cytometry.

Confocal Imaging Biomarker	Fluorochrome	Clone	Catalog Number	Source	Dilution
Bcl-6	Unconjugated	PG-B6p	M7211	DAKO	1:100
Bcl-6	Unconjugated	LN22	MAB9607	Abnova	1:50
Ki67	Brilliant Violet 421	B56	562899	BD Horizon	1:50
Ki67	Brilliant Violet 480	B56	566109	BD Horizon	1:50
Ki67	Alexa Fluor 647	B56	558615	BD Biosciences	1:50
PD-1	Alexa Fluor 488	polyclonal	FAB7115G	R&D Systems	1:20
CD20	eFluor 615	L26	42-0202-82	eBioscience	1:50
CD57	Brilliant Violet 480	NK-1	555618	BD Horizon	1:50
FoxP3	Alexa Fluor 647	206D	320114	Biolegend	1:10
CD4	Alexa Fluor 700	polyclonal	FAB8165N	R&D Systems	1:50
CD138	Unconjugated	Ep201	BSB6530	BioSB	1:200
CD38	Unconjugated	SPC32	BioSB6201	BioSB	1:200
H2Ax	Alexa Fluor 647	N1-431	560447	BD Biosciences	1:10
Helios	Unconjugated	polyclonal	GTX115629	GeneTex	1:20
CD25	Unconjugated	4C9	BSB6320	BioSB	1:10
IL-10	Alexa Fluor 546	E-10	Sc-8438 AF546	Santa Cruz	1:10
MPO	Unconjugated	polyclonal	A0398	Agilent-DAKO	1:300
CD68	Unconjugated	KP-1	M0814	Agilent-DAKO	1:200
CD163	Alexa Fluor 647	EDHu-1	NB110-40686AF647	Novus	1:100
FasL	Unconjugated	polyclonal	Ab134401	Abcam	1:10
CD8	Unconjugated	4B11	4B11	Invitrogen	1:100
Granzyme B	Unconjugated	GrB-7	M7235	DAKO	1:100
CD11c	Unconjugated	2F1C10	60258-1-IG	ProteinTech	1:200
CD123	Unconjugated	BSB-59	BSB5327	BioSB	1:50
CLEC9A	Unconjugated	polyclonal	ab223188	Abcam	1:10
CD31	Unconjugated	polyclonal	ab28364	Abcam	1:10
CD20	Unconjugated	L26	14-0202-82	eBioscience	1:50
IgD	Alexa Fluor 488*	EPR6146	ab124795	Abcam	1:10
FDC	Unconjugated	CNA.42	F3803	Sigma	1:200
Collagen I	Unconjugated	3G3	LS-B5932	LSBio	1:500
Collagen IV	Unconjugated	LS-B16212	LS-B16212	LSBio	1:500
CD3	Unconjugated	F7.2.38	M7254	DAKO	1:300
CD4	Unconjugated	polyclonal	ab133616	Abcam	1:10

Flow Cytometry Biomarker	Fluorochrome	Clone	Catalog Number	Source
CD3	BB700	SP34-2	566518	Beckton Dickenson
Ki67	Brilliant Violet 241	B56	562899	BD Horizon
CD3	H7APC	SK7	641406	BD Biosciences
CD8	Pacific Blue	RPA-T8	558207	BD Pharmingen
CD20	Brilliant Violet 570	2H7	302332	Biolegend
CD4	Brilliant Violet 650	SK3	563875	BD Biosciences
PD-1	Brilliant Violet 711	EH12.2H7	329928	Biolegend
Bcl-6	PE	K112-91	561522	BD Pharmingen
CD57	Alexa Fluor 594	NK-1	NBP2-47789AF594	Novus Biotechne
CXCR5	Cy7PE	MU5UBEE	25-9185-42	Thermo Fisher
CD19	FITC	J3-119	IM1284U	Beckman-Coulter
CD38	Brilliant Violet 786	HIT2	303530	Biolegend
IgG	BUV395	G17-1	104385	BD Biosciences
H2Ax	Alexa Fluor 647	N1-431	560447	BD Biosciences

Biosciences); PD-1 Brilliant Violet 711 (clone EH12.2H7, Biolegend); Bcl-6 PE (clone K112-91, BD Pharmingen); CD57 Alexa Fluor 594 (clone NK-1, Novus Biotechne); CXCR5 (CD185) Cy7PE (clone MU5UBEE, Thermo Fisher); CD8 Pacific Blue (clone RPA-T8, BD Pharmingen); CD19 FITC (clone J3-119, Beckman-Coulter); CD38 Brilliant Violet 786 (clone HIT2, Biolegend); IgG1 BUV395 (clone G17-1, BD Biosciences); H2AX (pS139) Alexa Fluor 647 (clone N1-431, BD Pharmingen).

Imaging

Primary/Conjugated

Tfh panel: Bcl-6 unconjugated (clone PG-B6p, DAKO); Ki67 Brilliant Violet 421 (clone B56, BD Horizon); PD-1 Alexa Fluor 488 (goat polyclonal, R&D systems); CD20 eFluor 615 (clone L26, eBioscience); CD57 Brilliant Violet 480 (clone NK-1, BD Horizon); FoxP3 Alexa Fluor 647 (Clone 206D, Biolegend); CD4 Alexa Fluor 700 (goat polyclonal, R&D systems) *B-cell panel:* CD138 unconjugated (clone Ep201, BioSB); CD38 unconjugated (clone SPC32, BioSB); Bcl-6 unconjugated (clone LN22, Abnova); Ki67 Brilliant Violet 480 (clone B56, BD Horizon); CD20 eFluor 615 (clone L26, eBioscience); H2Ax Alexa Fluor 647 (clone N1-431, BD Pharmingen); CD4 Alexa Fluor 700 (polyclonal, R&D systems) *Regulatory T-cell panel:* Helios unconjugated (polyclonal, GeneTex); CD25 unconjugated (clone 4C9, BioSB); Ki67 Brilliant Violet 480 (clone B56, BD Horizon); CD20 eFluor 615 (clone L26, eBioscience); FoxP3 Alexa Fluor 647 (clone 206D, Biolegend); IL-10 Alexa Fluor 546 (clone E-10, Santa Cruz); CD4 Alexa Fluor 700 (polyclonal, R&D systems) *Inflammation panel:* MPO unconjugated (polyclonal, Agilent-DAKO); CD68 unconjugated (KP-1, Agilent-DAKO); PD-1 Alexa Fluor 488 (goat polyclonal, R&D systems); CD20 eFluor 615 (clone L26, eBioscience); Ki67 Brilliant Violet 480 (clone B56, BD Horizon); CD163 Alexa Fluor 647 (clone EDhu-1, Novus); CD4 Alexa Fluor 700 (polyclonal, R&D systems) *CD8 T cell panel:* FasL unconjugated (polyclonal, Abcam); CD8 unconjugated (4B11, Invitrogen); Granzyme B (GrB-7, DAKO); CD20 eFluor 615 (clone L26, eBioscience); CD57 Brilliant Violet 480 (clone NK-1, BD Horizon); CD4 Alexa Fluor 700 (polyclonal, R&D systems); Ki67 Alexa Fluor 647 (B56, BD Biosciences) or for the *alternative CD8 T cell panel:* FasL unconjugated (polyclonal, Abcam); CD8 unconjugated (4B11, Invitrogen); Granzyme B (GrB-7, DAKO); CD3 (F7.2.38, Dako); CD20 eFluor 615 (clone L26, eBioscience); Ki67 Brilliant Violet 480 (clone B56, BD Horizon); CD4 Alexa Fluor 700 (polyclonal, R&D systems); *DC panel:* CD11c unconjugated (clone 2F1C10, ProteinTech); CD123 unconjugated (clone BSB-59, BioSB); CLEC9A (polyclonal, Abcam); Ki67 Brilliant Violet 480 (clone B56, BD Horizon); CD20 eFluor 615 (clone L26, eBioscience); CD4 Alexa Fluor 700 (polyclonal, R&D systems); CD8 unconjugated (4B11, Invitrogen); CD8 unconjugated (4B11, Invitrogen) *Structure panel:* CD31 unconjugated (polyclonal, Abcam); CD20 unconjugated (L26, eBioscience); IgD Alexa Fluor 488 (polyclonal, R&D systems – custom made on AF488), FDC unconjugated (CNA.42, Sigma); Collagen I (3G3, LSBio); Collagen IV (LS-B16212; LSBio); Ki67 Brilliant Violet 480 (B56, BD Horizon).

Secondary

Tfh panel: Goat anti-Mouse IgG1 Alexa Fluor 546 (A21123, Life Technologies); *B-cell panel:* Donkey anti-rabbit Brilliant Violet 421 (poly4064,406410, Biolegend); Goat anti-mouse IgG1 Alexa Fluor 546 (A21123, Life Technologies); Goat anti-mouse IgG2b Alexa Fluor 488 (A21141, Thermo Scientific) *Regulatory T-cell panel:* Donkey anti-rabbit Brilliant Violet 421 (poly4064, 406410, Biolegend); Goat anti-mouse IgG2b Alexa Fluor 488 (A21141, Thermo Scientific) *Inflammation panel:* Donkey anti-rabbit Brilliant Violet 421 (poly4064, 406410, Biolegend); Goat anti-mouse IgG1 Alexa Fluor 546 (A21123, Life Technologies) *CD8 T cell panel:* Donkey anti-rabbit Brilliant Violet 421 (poly4064, 406410, Biolegend); Goat anti-mouse IgG2b Alexa Fluor 488 (A21141, Thermo Scientific); Goat anti-mouse IgG2a Alexa Fluor 546 (A21133, Thermo Scientific) *Alternative CD8 T cell panel:* Donkey anti-rabbit Brilliant Violet 421 (poly4064, 406410, Biolegend); Goat anti-mouse IgG2b Alexa Fluor 488 (A21141, Thermo Scientific); Goat anti-mouse IgG2a Alexa Fluor 546 (A21133, Thermo Scientific); Goat anti-mouse IgG1 Alexa Fluor 647 (A-21240, Thermo Scientific). *DC panel:* Donkey anti-rabbit Brilliant Violet 421 (poly4064, 406410, Biolegend); Goat anti-mouse IgG2a Alexa Fluor 488 (A-21131, Thermo Scientific); Goat anti-mouse IgG1 Alexa Fluor 546 (A-21123, Thermo Scientific); Goat anti-mouse IgG2b Alexa Fluor 647 (A-21242, Thermo Scientific) *Structure panel:* Donkey anti-rabbit Brilliant Violet 421 (poly4064, 406410, Biolegend); Goat anti-mouse IgG2a Alexa Fluor 546 (A-21133, Thermo Scientific); Goat anti-mouse IgM Alexa Fluor 647 (115-607-020, Jackson ImmunoResearch); Goat anti-mouse IgG3 Alexa Fluor 594 (A-21155, Thermo Scientific); Goat anti-mouse IgG1 Alexa Fluor 594 (A-21125, Thermo Scientific).

Flow Cytometry

Tonsil cells (1-2 x 10^6) were stained with the Aqua Live/Dead Viability Dye (Invitrogen) and titrated amounts of antibodies against CD3, CD20, CD4, CD8, PD-1, CD57 and CXCR5 or CD3, CD8, CD19, CD38, IgG and CD20. ICS staining for Ki67 and Bcl-6 or H2Ax was performed using the BD Cytofix/Cytoperm Kit (BD Biosciences. At the end of the protocol cells were fixed with 1% parafolmaldehyde and acquired on a BD FACSymphony Flow Cytometer (BD Biosciences) running the BD FACSDiva software.

Immunofluorescent Tissue Staining

Tonsillar tissue was used in seven out of the eight panels described (GC reactivity, T-cell regulation, B-cell immunity, CD8 T-cell positioning and function, monocyte and inflammatory markers, GC microarchitecture, tissue-specific DC subpopulations). Confocal imaging of tonsil sections (~10um in thickness) was performed using formalin fixed paraffin embedded (FFPE) tissues. Tissue sections were baked at 60°C for 1 hour and deparaffinized by serial immersions in xylene and ethanol dilutions. Antigen retrieval was performed at 110°C for 15 minutes using Borg RTU (Biocare Medical).

Tissue sections were blocked and permeabilized for 1 hour at room temperature (RT) (1M Tris, 0.3% Triton X-100, 1% Bovine Serum Albumin) and stained with titrated amounts of antibodies. Stainings were carried out consecutively with the primary antibodies being added first and incubated overnight at 4°C, followed by staining with the appropriate secondary antibody. Conjugated antibody stainings were performed for 2 hours at RT, after which sections were stained with JOPRO-1 Iodide (Invitrogen) for nucleus identification and mounted with Fluoromount G (SouthernBiotech).

Multispectral RNAscope

vRNA+ detection was based on specimens originating from HIV+ individuals (**Table 2**). For this purpose, formalin-fixed, paraffin-embedded lymph node tissue sections (~10um thick) were stained with HIV RNA probes (Cat No. 416111) using the RNAscope Multiplex Fluorescent Reagent Kit v2 (ACD) according to the manufacturer's instructions. Briefly, sections were baked for 1 hour at 60°C and deparaffinized using serial xylene and ethanol baths. This was followed by an antigen retrieval step performed at 100°C for 15 minutes and a proteinase K treatment step for 20 minutes at 40°C. Subsequently, sections were incubated with HIV-1 Clade B-specific RNA probes (ACD) at 40°C for 2 hours in a HybEz hybridization oven (ACD) before being subjected to 4 rounds of signal amplification performed using the RNAscope amplification reagents. To visualize the RNA signal a tyramide-based detection system was used (TSA Plus Cyanine 5, Akoya Biosciences) per manufacturer's instructions. To ascertain the specificity of the vRNA+ signal a modified version of the RNAscope protocol was used in which tissues were pretreated with 150ul of RNase A/T1 mix in 1x PBS (RNase cocktail Enzyme mix, 500U/ml A; 20.000 U/ml T1, Thermo Fisher) for 30mins at 40°C prior to target probe hybridization. For CD4+ T cell subset and FDC visualization sections were stained with antibodies against CD3 (F7.2.38, Dako), CD4 (rabbit polyclonal, abcam) and FDC (CNA.42, Sigma) at the end of the RNAscope protocol. The following secondary antibodies were used for CD3, CD4 and FDC visualization: Goat anti-Mouse IgG1 Alexa Fluor 546 (A21123, Life Technologies), Donkey anti-Rabbit Brilliant Violet 421 (406410, Biolegend) and Goat anti-Mouse IgM Alexa Fluor 594 (A21125, Life Technologies).

Confocal Imaging and Analysis

Images were acquired on a Leica TCS SP8 confocal platform running LAS-X at a 512 x 512 pixel density with a 1x optical zoom using a 40x objective (NA 1.3) unless otherwise stated. The microscope was equipped with 3 HyD and 2 PMT detectors and 11 laser lines (405, 457, 476, 488, 496, 514, 561, 594, 633, 685 and 730nm). Panels consisted of antibodies conjugated to the following fluorophores: BV421, BV480, AF488, JOPRO-1, AF546, eF615, AF647, AF700. Images were tiled and merged using LAS X Navigator software. To ensure accurate representation and minimize selection bias at least 50% of the tissue was imaged or 5 follicles were captured on average in line with previously published research in our lab (24, 30). Replicate markers, shared among all panels, were also included in the analysis to ensure reproducibility across tissue sections and orientations. For analysis, we focused on well-defined areas devoid of background staining and quantified the data either as relative frequencies or as cell counts normalized to total tissue area (**Main Figures** and **Supplementary Figure 1A**). The latter is an alternative way to present the data that takes into consideration potential differences in tissue size allowing for this parameter to be controlled during quantification. Cell numbers (counts) for this alternative analysis were obtained from HistoCytometry using the program FlowJo whilst the total tissue area was calculated using the Imaris software through the surface creation module (**Supplementary Figure 1B**). The Imaris software was also used to calculate the number of FDC-bound virions in RNAscope analysis. Quantitation in this case was performed using the Spots creation feature after appropriately masking the vRNA+ channel to reveal colocalization with FDC surfaces. To minimize spectral spill-over among the various channels, fluorophore emission was collected on separate detectors with fluorophores being excited sequentially (2-3 fluorophores/sequential). Furthermore, spectral areas corresponding to each fluorophore were carefully selected after testing each fluorophore separately to verify the exact emission curve. Of note, staining of tissues with single antibody-fluorophore specificities was performed under the exact same conditions as the full panels in order for any protocol-associated shifts in emission curves to be accounted for. Fluorophore spillover, where present, was corrected by imaging tissues stained with single antibody-fluorophore combinations and by creating a compensation matrix *via* the Leica LAS-AF Channel Dye Separation module (Leica Microsystems) per user's manual. Images were collected as z-stacks and are presented as maximum intensity projections (MIP) throughout the manuscript. Spillover corrected images were analyzed with the Imaris software version 9.6.0 (Bitplane Scientific) and the HistoCytometry pipeline was applied as previously described (29, 31). Briefly, 3- dimensional imaging datasets were segmented based on their nuclear staining signal and marker(s) of interest using the Surface Creation Module and

TABLE 2 | Demographic and clinical details of study participants.

Experiment	Tissue ID	Age	Gender	VL (copies/uL)	CD4 count	Classification
Bcl-pH2Ax	HIV-1 #1	28	M	91357	261	Tx Naïve, Chronic
Bcl-pH2Ax	HIV-1 #2	34	M	84687	142	Tx Naïve, Chronic
RNAscope_main	HIV-1 #3	23	M	1,205,036	315	Tx Naïve, Chronic
RNAscope_controls	HIV-1 #4	19	M	621,622	290	Tx Naïve, Chronic
CD8-FasL	HIV-1 #5	31	M	67,764	721	Tx Naïve, Chronic

average voxel intensities for all channels were calculated. Average voxel intensities for all channels of interest, within these surfaces, along with the X, Y positioning of the cell centroids (sphericity, volume), were then exported to Excel and combined into a unified spreadsheet file (comma separated values format). This spreadsheet was then imported into the FlowJo v 10 program for further analysis.

Statistical Analysis

Statistical analyses were performed with GraphPad Prism 9.0 (GraphPad Software, Inc, San Diego, CA). We compared differences among groups using one-way analysis of variance (ANOVA) and Tukey's multiple-comparison posttest. Differences between groups were considered to be significant at a P value of <0.05.

RESULTS

Evaluation of GC Reactivity in Lymphoid Tissues

To investigate GC reactivity, we designed a panel combining the GC relevant markers CD20, Ki67, Bcl-6, PD-1, CD4, CD57 and FoxP3 (**Figure 1A**) and performed quantification of immune cell frequencies in selected tonsillar topologies by HistoCytometry (29). We used CD20, Ki67 and Bcl-6 to map B cell follicles ($CD20^{hi/dim}$) or GCs ($CD20^{hi/dim}Ki67^{+}$) as well as for the delineation of the mantle zone (MZ; $CD20^{dim}Ki67^{-}$) where most naïve B-cells reside, dark zone (DZ; $CD20^{dim}Ki67^{+}$), where clonal expansion and antigen receptor diversification occurs, and light zone (LZ; $CD20^{hi/dim}Ki67^{+/-}$) where B-cells undergo selection (19). Bcl-6 is a transcriptional repressor that is required for mature B-cell GC formation. Within the B-cell lineage, Bcl-6 expression is mainly confined to GC B cells where it acts to promote the selection of B-cells by silencing the antiapoptotic molecule Bcl-2, enhancing the ability of GC B cells to tolerate DNA damage, preserve B cell identity and fine-tune BCR mediated responsiveness (19) Bcl-6 is also expressed in CD4+ T-cells and has been shown to direct Tfh lineage commitment (32). Bcl-6 further distinguishes i) follicular B-cell subsets; GC B-cells (DZ: $CD20^{dim}Ki67^{+}Bcl\text{-}6^{+}$, LZ: $CD20^{hi/dim}Ki67^{+/-}Bcl\text{-}6^{+}$) and non-GC ($CD20^{hi}$ $Ki67^{-}Bcl\text{-}6^{-}$) and ii) Tfh cell subsets ($PD\text{-}1^{hi}$ $Bcl\text{-}6^{hi/dim}$) (**Figure 1B**). Furthermore, we used the marker CD57, an epitope expressed in a subset of CD4 T cells that are positive for CD69 and CD45RO and detected in approximately 15-25% of tonsil CXCR5+ CD4 T cells (33), to track two distinct GC-Tfh populations ($CD57^{+}$ and $CD57^{-}$) that have been shown to possess divergent immunophenotypes (24). Potential regulatory CD4 T cells were also measured and localized based on the expression of the transcription factor FoxP3. Quantitative analysis revealed an overall higher frequency of $Ki67^{-}$ cells within follicular areas (**Figure 1C**). $Ki67^{+}$ cells were in their majority $Bcl\text{-}6^{hi}$ and represented 10-38% of the total $CD20^{hi/dim}$ population. $Bcl\text{-}6^{lo}$ B-cells were also present within the $Ki67^{+}$ DZ compartment but at a very low frequency (<1%) (**Figure 1C**) Our analysis thus, confirms Ki67 and Bcl-6 co-staining as a meaningful way to topologically define the LZ/DZ compartments. When CD4 T-cells were examined, a variable percentage of $PD\text{-}1^{hi}$ CD4+ T-cells (Tfh) was observed among the follicles measured. Within follicular areas, $PD\text{-}1^{hi}$ cells represented on average 20% of the total CD4 population (**Figure 1C**) or 69% of the total CD4 population when a stricter follicular definition was applied that excluded $PD\text{-}1^{lo}$ and $PD\text{-}1^{dim}$ CD4 T -cells residing outside the LZ/DZ localities (GC only) (**Figure 1D** and **Supplementary Figure 1C**). Analysis of Tfh subpopulations revealed a trend for higher frequencies of $CD57^{-}$ Tfh within tonsillar B-cell follicles compared to $CD57^{+}$ irrespective of the B-cell follicle definition used with the latter being localized closer to the DZ as we have previously reported (24) (**Figures 1A, C, D**). We also measured Bcl-6 and FoxP3 expression within follicular areas. We found 5-10% of follicular CD4 T-cells to possess the $Bcl\text{-}6^{hi}$ signature, whilst FoxP3+ expression was seen in <2% of CD4 T-cells (**Figure 1C**). In GCs, B-cells were the most abundant population (~83% of GC cells) whilst CD4 T cells, Tfh and Tfrs represented ~6%, 4% and 0,03% of the total cells respectively as measured by HistoCytometry (**Figure 1D**). Consistent with previous reports, FoxP3 expression within tonsillar follicular areas was detected primarily at the B-T cell border and only rarely in the GC (34) (**Figure 1A**). Cross-validation of the studied populations by flow cytometry revealed comparable frequencies and trends (**Figure 1E** and **Supplementary Figures 1C, D**). Our GC reactivity pipeline thus tracks B-cells, CD4+ T-cells (including Tfh) and Tregs in tonsillar tissue subanatomical localities accurately and in line with previously published reports.

Assessment of Tissue-Specific T-Cell Regulation

FoxP3+ CD4 T-cells have been shown to represent critical regulators of the GC size and activity, including that of Tfh cells, in both mice (35) and humans (36). To allow for a more detailed study of regulatory T-cells in lymphoid tissues, we designed a dedicated panel consisting of the Treg- specific markers CD4, CD25 and FoxP3 all of which are typical phenotypic markers of natural (thymus-derived) Tregs (37) (**Figure 2A**). Helios, an Ikaros transcription factor family member that has been shown to stabilize the Treg phenotype (38), was also included in the panel as it has been associated with a better capacity for immunosuppression in some studies (39) as well as with vaccine-induced Treg kinetics in tonsillar tissues (30). We also probed for IL-10, a cytokine linked to the functional capacity of Tregs, in line with reports suggesting a role for Tfr cell-derived IL-10 in the modulation of GC responses in acute viral infection (40, 41). In line with previous reports, quantitative analysis of relevant Treg populations in tonsillar tissue using the HistoCytometry pipeline revealed a higher percentage of regulatory T cells in EF areas ($CD20^{lo}$) compared with follicular areas (30, 34) (**Figures 2B, C**, upper graph). This trend was true for all populations measured irrespective of their specific phenotype ($CD25^{hi}FoxP3^{+}$ or $CD25^{hi}Helios^{+}$ or $CD25^{hi}FoxP3^{+}Helios^{+}$ or $CD25^{hi}FoxP^{+}IL10^{hi}$). Within GCs,

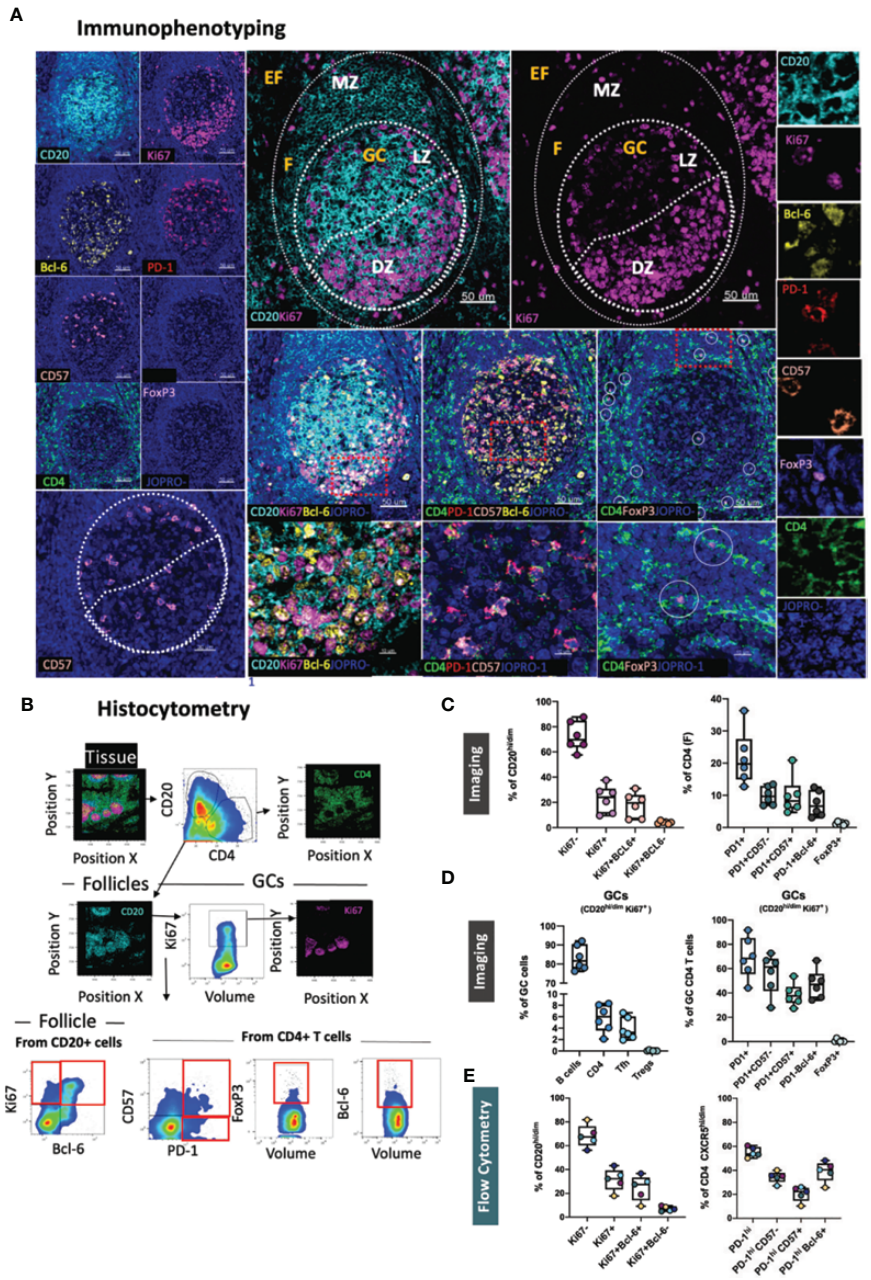

FIGURE 1 | Development of a multispectral panel for the characterization of GC reactivity. **(A)** Representative example of Ki67 (magenta), CD20 (cyan), PD-1 (red), Bcl-6 (yellow), CD57 (orange), CD4 (green) and FoxP3 (pink) staining patterns in a tonsillar tissue section (left and right panels) and concomitant B-cell follicle and GC boundary delineations (Extrafollicular CD20lo and Follicular CD20hi/dim; Mantle Zone; MZ: CD20dimKi67lo, Light Zone; LZ: CD20hiKi67lo and Dark Zone; DZ: CD20dim Ki67hi) (middle panel). Circles in lower middle panels denote single FoxP3 events. **(B)** Histocytometry immunophenotyping gating strategy used for the sequential identification of B cells (CD20+Bcl-6+/- Ki67+/-), Tfh (CD4+PD-1hiBcl-6+/- CD57+/-), and Tfr (CD4+FoxP3+) in tonsillar tissue after nuclear staining based cell segmentation on Imaris and FlowJo analysis. F and EF and GC areas were defined based on the respective staining signals for CD20, Ki67 and CD4 and manually gated on FlowJo to extract frequencies for specific tissue localities. **(C)** Box plots showing the representative frequencies of B cell and CD4+ T-cell populations (Tfh, Treg) in B-cell follicles ($CD20^{hi/dim}$ areas) as defined by the expression of Ki67/Bcl-6, PD-1/CD57/Bcl-6 and FoxP3 in tonsillar tissue after application of the GC reactivity pipeline. Each box plot circle represents an individual follicle. Colors represent different phenotypic groups. **(D)** Box plots showing the relative frequencies of B-cells, CD4 T cells, Tfh and Tregs (Tfr) as well as the frequencies of select CD4 T cell subpopulations in GCs ($CD20^{hi/dim}$ Ki67+ areas) expressed as percentages of total GC cells measured. Circles represent distinct follicles and colors denote individual subpopulations. **(E)** Box plots showing the relative frequencies of B cell and CD4+ T-cell populations in B-cell follicles as measured by flow cytometry (n=5). CD4 T cells proximal to follicular localities and within GCs were identified through the expression of the B-cell follicle-specific chemokine receptor CXCR5 ($CXCR5^{hi/dim}$). Images were acquired at 40x (NA 1.3) with 1% magnification. Scale bars are 50um, 30um (CD57 positional image) and 10um (lower panel zoomed details) respectively.

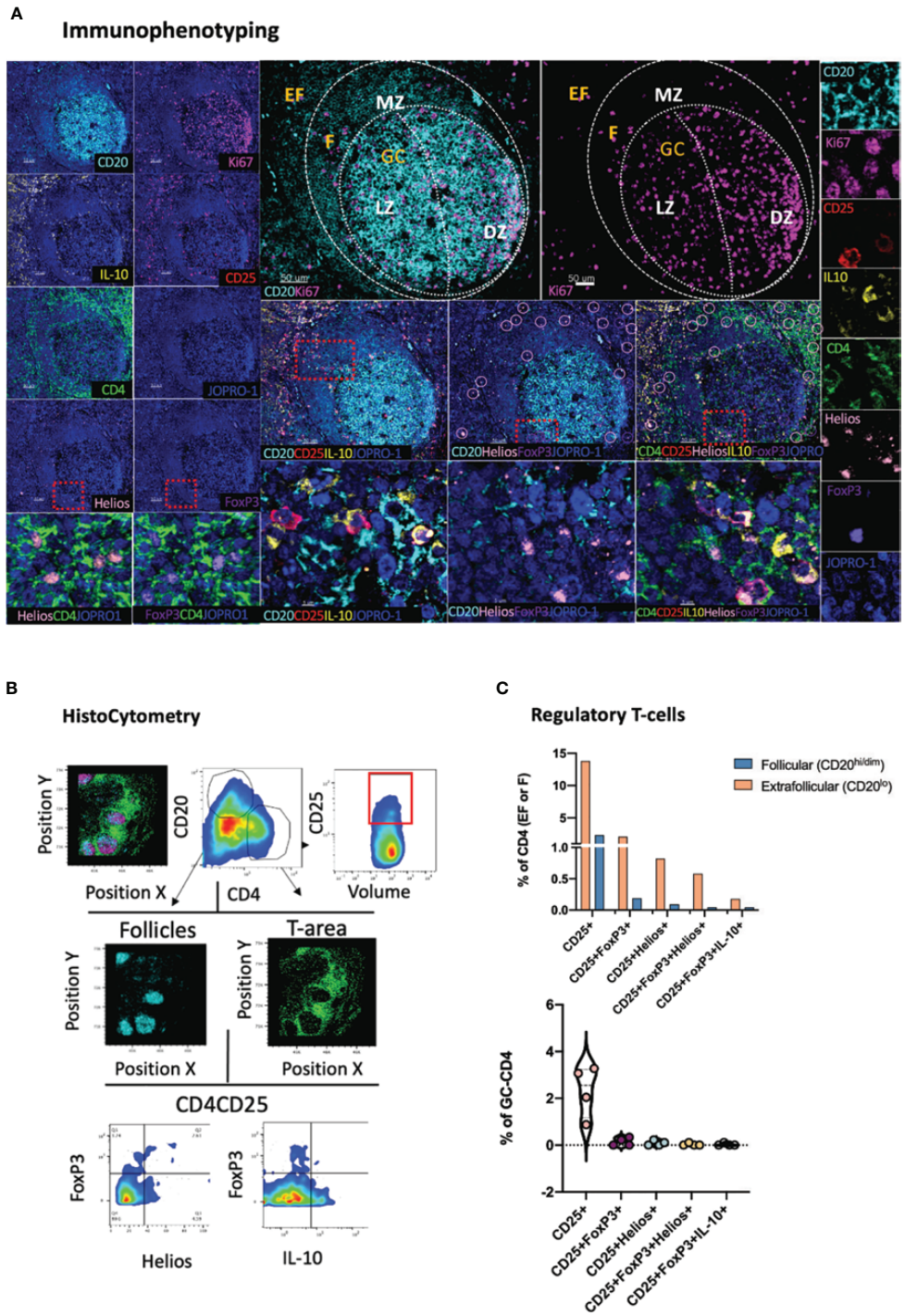

FIGURE 2 | Development of a multispectral panel for the assessment of tissue-specific T-cell regulation. **(A)** Representative example of antibody staining patterns for Helios (pink), CD20 (cyan), CD25 (red), IL-10 (yellow), Ki67 (magenta), CD4 (green) and FoxP3 (purple) in a tonsillar tissue section (left and right panels) and distribution of each marker with respect to the MZ, LZ and DZ (middle panels). Circles (pink/purple) in lower middle panels denote individual Helios (pink) and FoxP3 (purple) events. **(B)** Immunophenotyping gating strategy used for the identification of Tregs and Tfrs in lymphoid tissues of interest based on the expression and coexpression of the transcription factors FoxP3, Helios, the protein marker CD25 and IL10 in histocytometry. **(C)** Bar graphs (upper row) and violin plots (lower row) showing the frequencies of Tregs and Tfrs in follicular and extrafollicular areas and frequencies of Tfr subsets in a tonsillar tissue section. Circles in violin plots represent individual follicles whereas colors represent different phenotypic subgroups. Images were acquired at 40x (NA 1.3) with 1% magnification. Scale bars are 50um, 10um (zoomed in details) and 5um (Helios and FoxP3 staining patterns) respectively.

regulatory T-cells (Tfr) were rare. The frequency of $CD25^{hi}FoxP3^{+}$ Tfrs in all follicles combined did not exceed 0.2% whilst that of $CD25^{hi}FoxP3^{+}Helios^{+}$ and $CD25^{hi}FoxP3^{-}Helios^{+}$ was lower than 0.05% (**Figure 2C**, lower graph). CD25+FoxP3^{+} Tregs had the highest frequency in the T cell zone (up to 2% of total CD4+ T-cells). We also observed the presence of $CD25^{hi}FoxP3^{+i}IL10^{hi}$ Tregs, albeit at a low frequency (~0.3% of EF CD4 T-cells). Taken together, these data suggest that CD25, FoxP3, Helios and IL10 in combination with CD4, CD20 and Ki67 can be used to map and quantify Tregs and Tfrs effectively in microanatomical sites of interest including the GC, B cell follicle – T cell zone border where Tfr-mediated suppression may be more efficient (34) as well as in paracortical T-cell zones ($CD20^{-}CD4^{+}$ areas).

Topological Quantification of B-Cell Immunity

Whilst a topological examination of B cells in GCs can be achieved through the combinatorial examination of CD20, Ki67 and Bcl-6, a more granular view of B cell subsets is often necessary to appreciate the microenvironment that leads to the development of GC B cells and plasma cells. A deeper understanding of the role that specific B cell subsets might have in modulating the evolution of GC reactions is also desirable (42). This topological distribution becomes of particular relevance in the context of infection, such as chronic HIV infection, where B-cell responses become overtly dysregulated (43). To address the limitations of a tripartite CD20-Ki67-Bcl-6 analysis, a panel incorporating three additional markers, namely CD138, CD38 and pH2Ax was developed (**Figure 3A**). In this panel CD38, a marker of activated T and B lymphocytes (44) is used alongside the plasma cell marker CD138 (45) to inform on the tissue-specific positioning of B cells ($CD20^{hi}CD38^{lo}$; $CD20^{hi}$ $CD38^{dim}$ $CD138^{lo}$) and plasma cells ($CD20^{lo}$ $CD38^{hi}$ $CD138^{hi}$) (**Figure 3B**) in follicular and extrafollicular (CD20-$CD4^{hi}$) areas. In addition, pH2Ax, a histone that becomes rapidly phosphorylated in response to DNA double-strand breaks (DSBs) (46) serves as proxy for class switch recombination (CSR) (47). First, B-cells in tonsillar tissue were dissected by means of Ki67 and Bcl-6 expression. As expected, and consistent to our previous analysis (**Figure 1C**), we found a significantly higher frequency of $Ki67^{-}$ B cells within total follicular areas compared to the frequencies of all other measured populations (*vs* $Ki67^{+}$, p=0.004; *vs* $Ki67^{+}Bcl\text{-}6^{-}$, p <0.0001 and *vs* $Ki67^{+}Bcl\text{-}6^{+}$; p=0.0028) (**Figure 3C**, upper panel). Within B cell follicles, we also measured the frequency of pH2Ax positive CD20+ cells. Since phosphorylation of H2AX can take place in cells undergoing cell death as well, we focused our analysis on cells that displayed higher overall volumes in HistoCytometry as measured by nuclear staining ($Volume^{hi}$ for live cells). We found that pH2Ax/$Volume^{hi}$ frequencies were higher in GCs as compared to the total follicle, consistent with the role of GCs in class switch recombination and somatic hypermutation (**Figures 3B** for gating and **3C**, upper right panel). To address the low overall frequency of pH2Ax ($Volume^{hi}$) events in tonsils, a confirmatory analysis of the specificity of the detected signal by flow cytometry was undertaken. Unswitched (IgG^{lo}) B-cells within distinct tonsillar localities were defined by the combined expression of CD20 and CD38 as $CD20^{dim}CD38^{lo}$, $CD20^{hi}CD38^{dim}$ and $CD20^{lo}CD38^{hi}$. We observed pH2Ax frequencies to be the highest within the $CD20^{hi}CD38^{dim}$ compartment (**Supplementary Figure 2A**). pH2Ax expression was also examined in LN sections from HIV+ individuals. The latter analysis revealed higher frequencies of pH2Ax ($Volume^{hi}$) in the follicles and GCs of HIV+ LN specimens compared to the frequencies seen in HIV- tonsillar tissues, consistent with the higher levels of GC reactivity expected in chronic HIV+ infection (**Supplementary Figure 2A**). Taken together these data suggested that pH2Ax is meaningful biomarker for monitoring B-cell responses. We also addressed in our analyses the frequency of $CD38^{hi}CD138^{hi}$ cells in tonsillar EF, F and GC bound localities and observed a higher prevalence $CD38^{hi}CD138^{hi}$ cells in EF areas (~5% of total EF cells) and GCs as compared to $CD20^{hi/dim}$ areas, which confirmed the MZ as the area with the higher density of naïve B cells. When different follicles were examined, variable frequencies of $CD38^{hi}CD138^{hi}$ cells were found (0.65-3% of total cells in $CD20^{hi/dim}$ localities) (**Figure 3C**, lower panel). Our data therefore confirm the combination of these six B cell specific markers as a valid means to interrogate the topologies, and associated frequencies of several relevant B cell subsets in lymphoid tissues for analyses of B cell dynamics.

Evaluation of CD8 T-Cell Positioning and Function

Another tissue-resident immune subset of great importance, especially in the context of viral infection, is CD8 T-cells. Within tonsillar tissues, CD8 T cells have been shown to localize in extrafollicular ($CXCR5^{-}CD8^{+}$) and to a lesser extend within follicular ($CXCR5^{+}CD8^{+}$) spaces, with the latter (follicular CD8+ T-cells or fCD8) displaying an early effector phenotype associated with a non-cytolytic (granzyme $A^{+}perforin^{-}$) profile that sets them apart from their CXCR5- counterparts (48). Traditionally, cytotoxic T cells, such as CD8 T cells, have been defined by the expression of perforin, granzyme B as well as their expression of high levels of the transcription factor T-bet that regulates the cytotoxic effector gene program (49) In the context of lymphoid tissues however, and in particular in HIV/SIV infection, CD8 T cells have been shown to possess a low level, discordant expression of perforin and granzyme B (50). To address the topology of CD8 CTLs in lymphoid tissues we designed a panel using the lineage-specific marker CD8 ($CD8^{bright}$) in combination with Granzyme B, FasL, an alternative major mediator of CTL killing, and CD57, a marker of senescence of CD8 T cells (51), as well as the GC and T-cell zone markers CD20, Ki67 and CD4 (**Figure 4A**). These markers allow for the spatial distribution of CD8 populations to be dissected by means of marker co-expression as $CD8^{bright}GrzB^{+/-}$, $CD8^{bright}FasL^{+/-}$ or $CD8^{bright}GrzB^{+}FasL^{+}$ either in stand-alone topologies or in relation to the positioning of intrafollicular $CD4^{+}CD57^{+/-}$ as well as $CD20^{hi/dim}Ki67^{+/-}$ B-cells (**Figures 4A, B**). In absence of the lineage marker CD3, analysis in of CD8 T cells

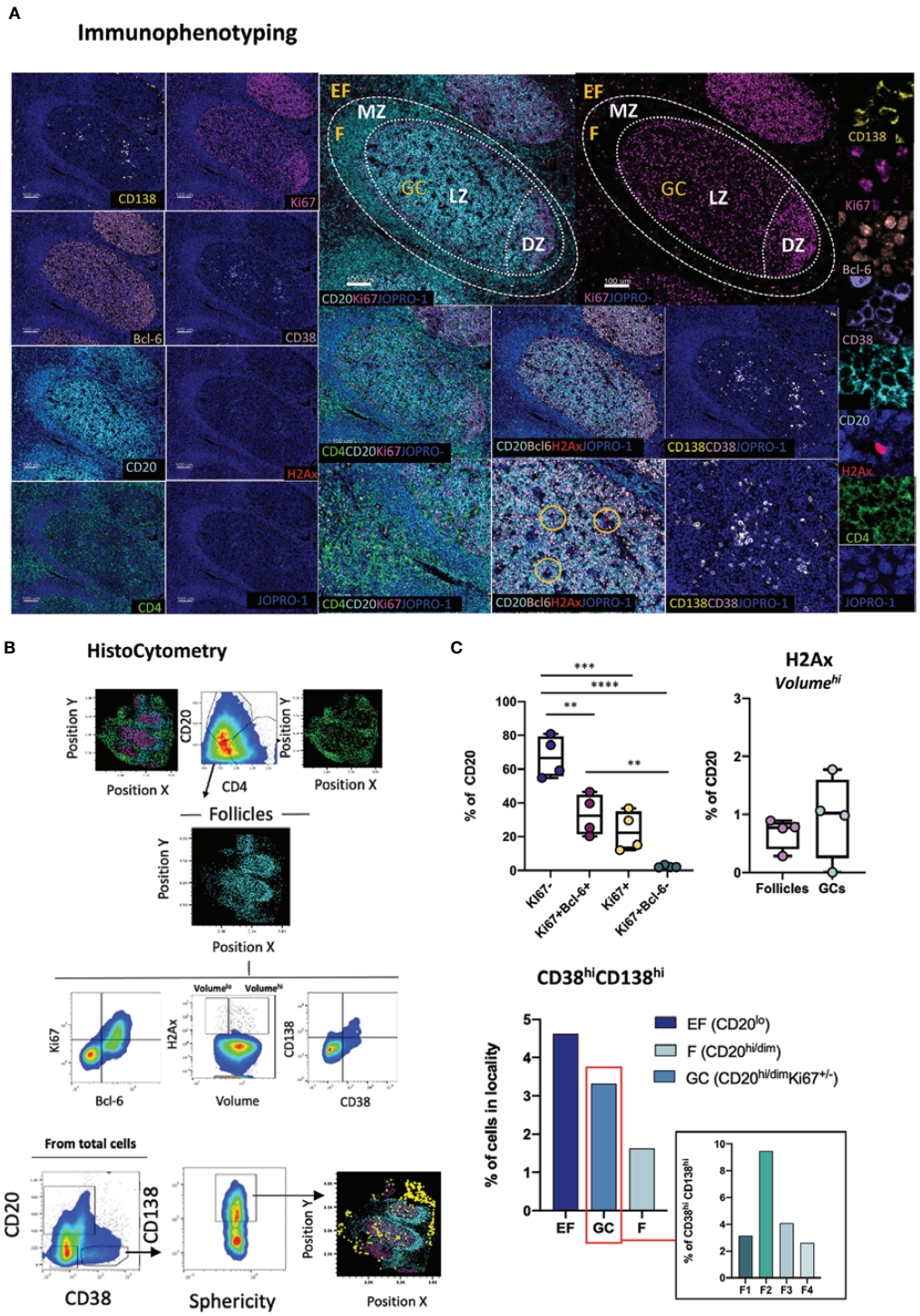

FIGURE 3 | Development of a multispectral panel for the topological examination of B cells. **(A)** Representative example of antibody staining patterns for CD138 (yellow), Ki67(magenta), Bcl-6 (orange), CD38 (violet), CD20 (cyan), H2Ax (red), CD4 (green) and nuclar staining (JOPRO-1, blue) and distribution of each marker with respect to the MZ, LZ and DZ (middle panels). Orange circles in the lower row images denote H2Ax events. **(B)** Gating strategy used for the immunophenotyping of various B cell populations and CD38hiCD138hi cells in GC ($CD20^{dim}Ki67^{hi}$), F ($CD20^{hi/dim}$) and EF ($CD20^{lo}$) areas. **(C)** Box plots showing the frequencies of various B cell populations (as defined by the expression of Ki67 and Bcl-6), H2Ax $Volume^{hi}$ CD20+ cells and $CD38^{hi}CD138^{hi}$ cells in a representative tonsil tissue section. Each circle represents a distinct follicle and each color denotes a distinct subpopulation. p values were derived from ANOVA analysis (Tukey's multiple comparisons test). Images were acquired at 40x (NA 1.3) with 1% magnification. Scale bars are 100um for all panels displaying an entire follicle), 50um for the middle panel close ups and 5um for the right panel single staining close ups. $^{**}p < 0.01$, $^{***}p < 0.001$, $^{****}p < 0.0001$.

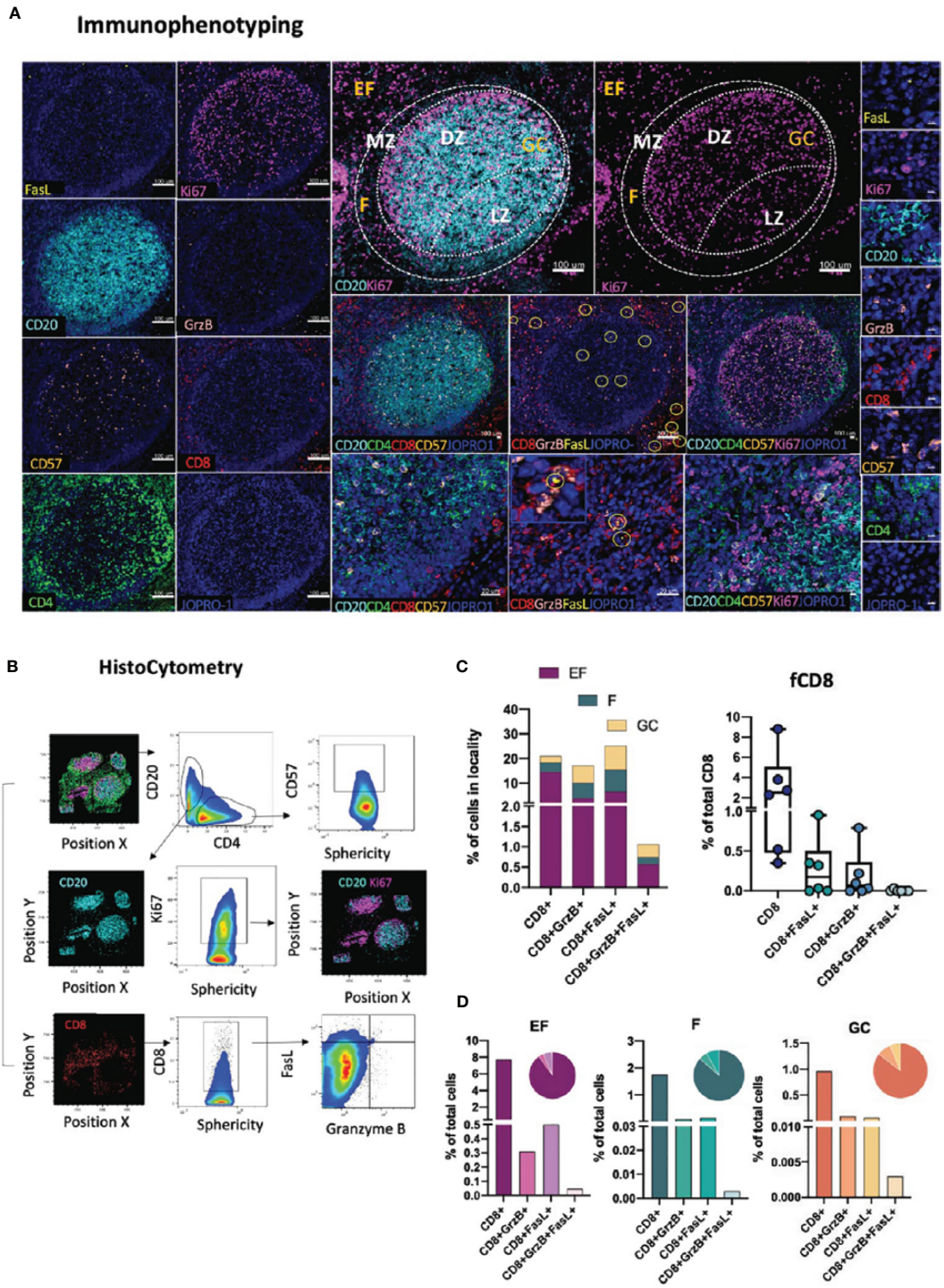

FIGURE 4 | Development of a multispectral panel for the topological examination of CD8 T cells. **(A)** Representative example of antibody staining patterns for FasL (yellow), Ki67 (magenta), CD20 (cyan), Granzyme B (pink), CD57 (orange), CD4 (green) and the nuclear marker JOPRO-1 (blue) and distribution of each protein marker with respect to the MZ, LZ and DZ (middle panels). Yellow circles in lower middle panels denote individual FasL events. **(B)** Gating strategy used for the immunophenotyping of various CD8 T cell populations ($CD8^{hi}$; $CD8^{hi}$GrzB+, $CD8^{hi}$FasL+ and $CD8^{hi}$ GrzB+ FasL+) in in GC ($CD20^{dim}Ki67^{hi}$), F ($CD20^{hi/dim}$)and EF ($CD20^{lo}$) areas. **(C)** Box plots and bar graphs showing the relative frequencies of four distinct CD8 T cell populations in EF, F and GC; the frequencies of follicular $CD8^{hi}$; $CD8^{hi}$GrzB+, $CD8^{hi}$FasL+ and $CD8^{hi}$GrzB+ FasL+ in six distinct follicles and **(D)** proportion of each CD8+ cell subset within each locality (EF, F and GC) as a percentage of total cells. Each circle represents a follicle and each color stands for a distinct subpopulation. Images were acquired at 40x (NA 1.3) with 1% magnification. Scale bars are 100um for all panels displaying an entire follicle), 20um in the middle panel close ups and 5um in the right panel single staining close ups.

in tonsillar tissues was restricted on $CD8^{bright}$ T cells which excluded the majority of $CD8^{dim}$ $CD3^-$ T cells present in the tonsils (**Supplementary Figure 2B**). However, in cases where NK cell frequencies are of interest, CD3 can be easily incorporated into the panel in the place of CD57 to facilitate the characterization of the $CD3^-CD8^{dim}$ population (**Supplementary Figure 2C**). In the absence of perforin staining, we use granzyme B and FasL – two molecules with potential for upregulation in infection, in particular HIV infection (31, 52) to denote CD8 T cells with potential for cytotoxicity. As expected, analysis of CD8 distributions in tonsillar tissue with histocytometry revealed a higher frequency of CD8 T cells in EF localities than in F or GC localities and comparable frequencies of CD8 within the latter two (**Figure 4C**, upper panel). We also found considerable variations in the frequencies of follicular CD8 T-cells amongst different follicles that ranged from 0.3 to 9% of total CD8 T-cells. In their majority fCD8 lacked expression of Granzyme B+ or FasL+ with only a small minority expressing either of these two markers (<0.6% of total GC cells). Double positive $GranzymeB^+$ $FasL^+$ $fCD8^+$ T-cells were also rare (<0.020% of total GC cells) in tonsils (**Figure 4C**, lower panel) but their expression is upregulated in HIV infected LNs (**Supplementary Figure 3A**). Despite the differences however in the CD8+ T cell subset frequencies found in tonsils, no significant differences were observed when the relative proportions of each population within EF, F and GC areas were examined (**Figure 4D**). Taken together, our data show that in line with previous reports, CD8+ T-cells in tonsillar tissues are mainly extrafollicular in nature and display a phenotype that is consistent with a reduced cytotoxic potential. HIV infection however can increase the frequencies of these rare populations, including those of CD8+ FasL+ T-cells in follicular localities (**Supplementary Figure 3A**). Application of this panel thus can provide important information on CD8 T-cell GC infiltration and fCD8 dynamics in pathological contexts. It can also be used to reveal possible functional correlations between CD8-CD4 T cells and CD8-B cells especially in HIV infection where Tfh have been shown to represent an active tissue reservoir (27).

Topological Distribution of Monocytic and Inflammatory Markers

Antigenic challenge upregulates inflammatory markers in draining lymphoid sites and encourages innate immune cell infiltration (53). Whilst in a non-pathological context inflammatory processes serve to orchestrate innate and adaptive immune responses (54), chronic inflammation, such as the one triggered by HIV infection, can profoundly dysregulate immune dynamics through the disruption of immune cell trafficking (55), induction of skewed immune cell topologies (31), and through dysregulation of immune cell ratios (56). The spatial dynamics of immune cells with pro- or anti-inflammatory potential therefore holds particular prognostic relevance in studies of infection and vaccination. Towards this end, we developed a panel consisting of the markers CD163, CD68, MPO, CD4, CD20, Ki67 and PD-1 (**Figure 5A**). In this panel, subsets of the monocyte/macrophage lineage are defined as $CD163^{hi}CD68^{lo}$, $CD163^{lo}CD68^{hi}$ and $CD163^{hi}CD68^{hi}$ based on the expression of the markers CD163 (a type B scavenger receptor) and CD68, a marker expressed by mature macrophages and resident histiocytes (57, 58). In addition, cells expressing myeloperoxidase (MPO^{hi}), a heme-containing enzyme found in the primary azurophilic granules of neutrophils (59), one of the main cell types involved in the inflammatory response- (60) are mapped relative to GC or Tfh positioning ($CD4^+PD\text{-}1^+$) (**Figure 5B**). Application of this panel to tonsillar tissue revealed that MPO^{hi}, $CD163^{hi}CD68^{lo}$ and $CD163^{hi}CD68^{hi}$ cells are preferentially localized in EF areas with only exception being $CD163^{lo}CD68^{hi}$ cells which showed comparable distributions in EF ($CD20^{lo}$) and F areas (1.85% and 1.81% of total cells in EF and F areas respectively) consistent with previously published reports (61) (**Figure 5C**). In GCs, $CD163^{lo}CD68^{hi}$ cells were the most abundant of the four populations measured (1.1% of total cells), a signal most likely originating from tingible body macrophages (TBMs) (62). No significant proportional variations were observed in the frequencies of these four subsets among individual follicles (**Figure 5C**, lower graph). Taken together, our data suggest that meaningful information on the position and relative abundance of pro-inflammatory cells in lymphoid tissues can be obtained by co-staining for MPO, CD163 and CD68.

Evaluation of GC Microarchitecture

The preservation of lymphoid tissue architecture, and by extension GC microarchitecture is of paramount importance for the evolution local immune responses. Loss of GC topology due to ageing or pathology negatively impacts responses to infection and vaccination (63, 64). Reversible lymphatic remodeling occurs with every round of antigenic challenge and is mediated by distinct stromal cell populations with differential expression of CD31 (PECAM1) including T cell zone reticular cells (TRECs), follicular dendritic cells (FDC), marginal reticular cells (MRC), lymphatic endothelial cells (LECs), blood endothelial cells (BEC) and high endothelial cells (HECs) (65, 66). HIV infection in particular profoundly perturbs the architecture of lymphoid organs through progressive collagen deposition and fibrosis, that disrupts and damages the important follicular reticular cell (FRC) network (13, 67) To map stroma and GC specific changes we developed a panel consisting of markers CD31, IgD, CD20, FDC, Ki67, Collagen I and Collagen IV (**Figure 6A**). In this panel, CD20, Ki67 and IgD are used to define the follicular mantle ($CD20^{dim}IgD^+$), GC-LZ ($IgD^-CD20^{hi}Ki67^{lo}$) and GC-DZ ($IgD^-CD20^{dim}Ki67^{hi}$) for assessment of GC reactivity as well as quantification of naïve $CD20^{dim}IgD^{hi}$ or non-GC memory ($CD20^{dim}IgD^{lo}$ $Ki67^-$) B cells (**Figure 6B**). FDCs hold a key role in the maintenance of GCs and retention of antigen (66) and their disruption has been shown to directly impact GC stability (68), especially in the context of chronic HIV infection (69, 70). FDC disruption can be measured by applying this panel as a reduction of the total area

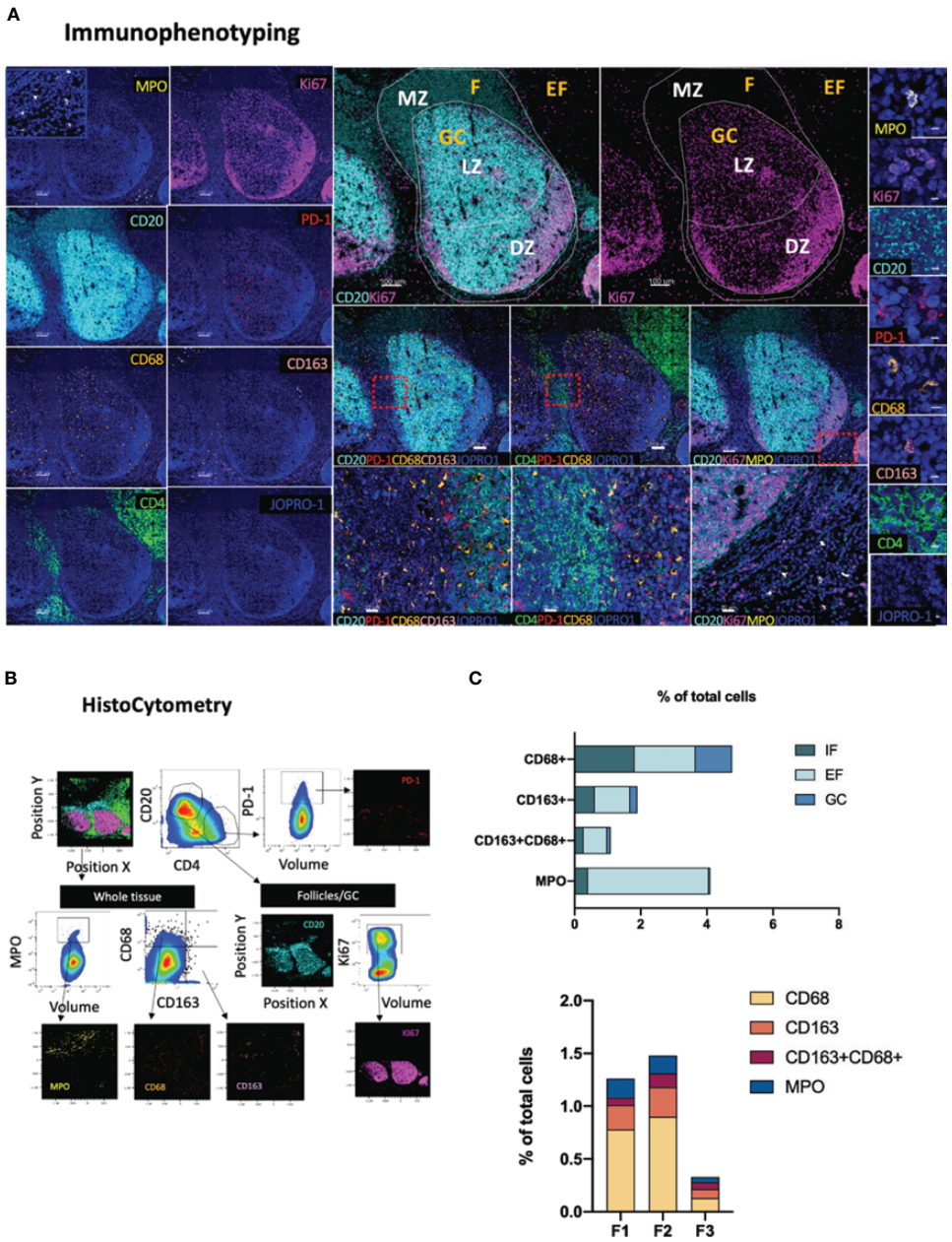

FIGURE 5 | Development of a multispectral panel for the topological examination of monocytes and inflammatory markers. **(A)** Representative example of antibody staining patterns for MPO (yellow), CD20 (cyan), Ki67 (magenta), PD-1 (red), CD68 (orange), CD163 (pink), CD4 (green) and JOPRO (nucleus, blue) and distribution of each protein marker with respect to the MZ, LZ and DZ (middle panels). Red dotted enclosures in lower middle panels denote the areas for which zoom ins are given (lower middle panels). **(B)** Gating strategy used for the immunophenotyping of neutrophils (MPOhi), monocytic populations ($CD163^{hi}CD68^{lo}$, $CD68^{hi}CD163^{lo}$, $CD68^{hi}CD163^{hi}$) and Tfh ($CD4+PD\text{-}1^{hi}$) in GC ($CD20^{dim}Ki67^{hi}$), F ($CD20^{hi/dim}$) and EF ($CD20^{lo}$) areas. **(C)** Bar graphs showing the relative frequencies of MPO^{hi} and various monocytic populations in intrafollicular (IF), EF and GCs as well as the frequencies of the same populations in three distinct follicles imaged. Images were acquired at 40x (NA 1.3) with 1% magnification. Scale bars are 100um for all panels displaying an entire follicle), 20um in the middle panel close ups and 5um in the right panel single staining close ups.

occupied by these cells compared to the total area of the follicle as previously reported (71). Topological mapping of BECs and LECs is also possible through combinatorial analysis of CD31 and Collagen I+IV staining ($CD31^{hi}Collagen^{hi}$) whilst cumulative changes in the reticulum can be traced by quantification of the total $collagen^{hi}$ signal present in select topological compartments (**Figure 6B**). We applied this panel to map intrafollicular variation in tonsillar tissues and found considerable variation amongst follicles in $CD20^{hi/dim}$, $CD20^{dim}Ki67^{hi}$, IgD^{hi} and FDC^{hi} areas, which was reflective of

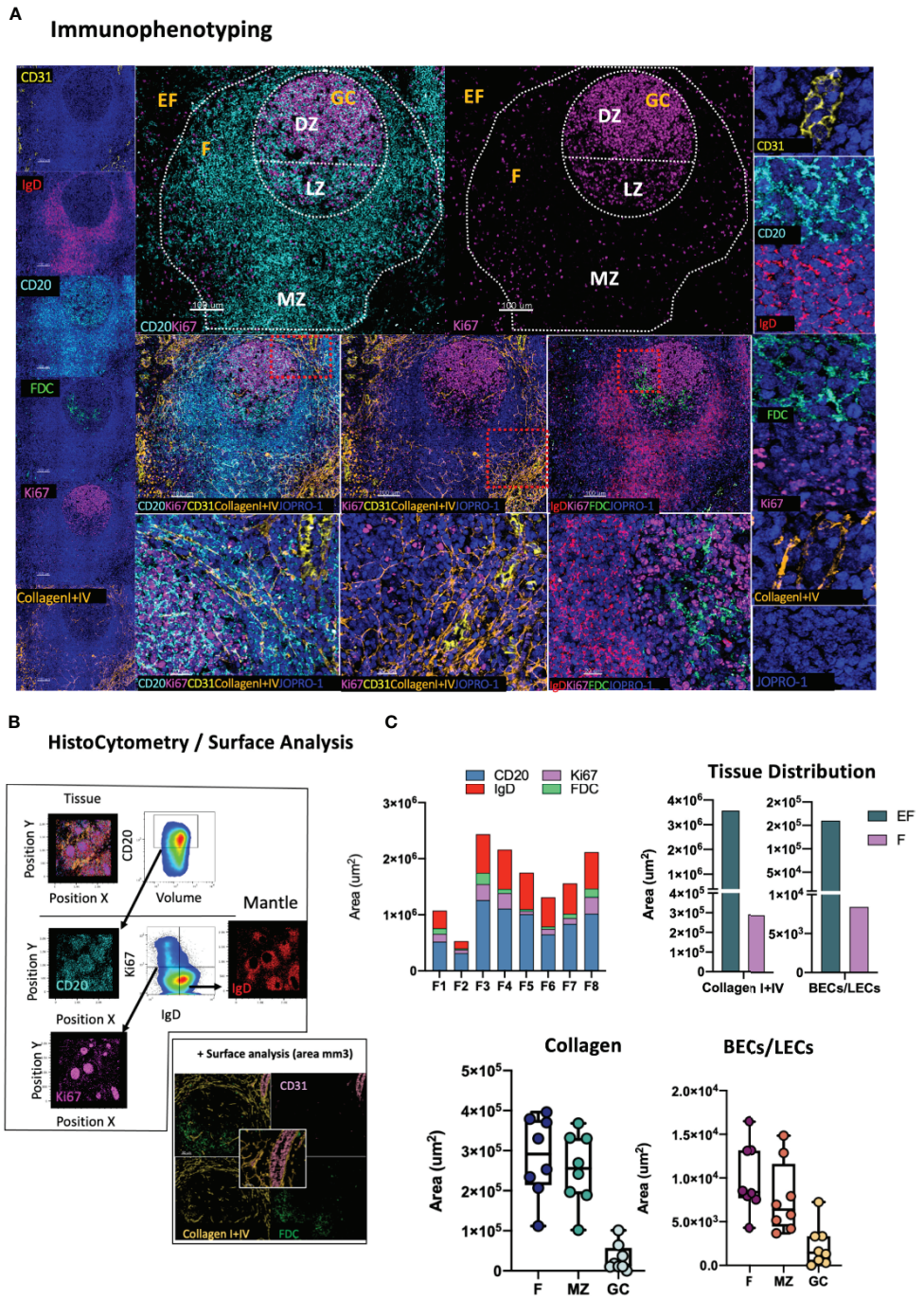

FIGURE 6 | Development of a multispectral panel for the evaluation of GC microarchitecture. **(A)** Representative images showing staining for CD31 (yellow), IgD (red), CD20 (cyan), FDC (green), KI67 (magenta) and Collagen I+IV (orange) in a tonsillar tissue section and individual protein marker distributions with respect to the MZ, LZ and DZ of a B-cell follicle (middle panels). Red dotted square enclosures in lower middle panels denote the areas that are presented magnified in the lower middle panels. **(B)** Gating strategy used for the sequential positional immunophenotyping of naïve B-cells (IgD^{hi}) in F ($CD20^{hi/dim}$) areas using histocytometry. **(C)** Box plots showing the areas (um3) occupied by each individual microarchitectural component namely B-cell follicle; $CD20^{hi/dim;}$ mantle zone: IgD^{hi}, GC ($CD20^{dim}Ki67^{hi}$) and FDC network (FDC^{hi}) in eight distinct B cell follicles as measured by surface analysis in the program Imaris as well as the relative areas occupied by Collagen (Collagen I+IVhi) and vascular and lymphatic endothelium ($CD31^{hi}$CollagenI+IV^{hi}) in EF areas, F areas and GCs. Images were acquired at 40x (NA 1.3) with 1% magnification. Scale bars are 100um for all panels displaying an entire follicle), 20um in the middle panel close ups and 5um in the right panel single staining close ups. BEC, Blood Endothelial Cell; LEC, Lymphatic Endothelial Cell.

the overall size of individual follicles (**Figure 6C**, first graph). In addition, analysis of collagen I+IV and CD31 staining distribution either as a single stain (Collagen I+IV^{hi}) or in combination (vascular and lymphatic endothelium) showed preferential segregation of BECs and LECs in extrafollicular spaces and within MZs but only minimal staining was seen in GCs (**Figure 6C**).Taken together these data suggest lymphoid tissue specific microarchitectural niches can be successfully mapped by CD20, IgD, Ki67, FDC, CD31 and collagen staining to yield important information regarding stromal changes, especially in the context of pathology when variations are likely to be tied to clinical outcomes.

Positioning of Tissue-Specific DC Subpopulations

DCs are innate immune, antigen presenting cells with a key role in the induction of adaptive immune responses. Several DC subsets exist in humans with varying migratory potentials, tissue distributions, microanatomical compartmentalization and functions. These subsets fall under three major groups: CD11c+ myeloid DCs (mDCs), monocyte-derived DCs (moDCs) and CD123+ plasmacytoid DCs (pDCs) (72). The latter is a major interferon type I producing cell type in response to viral infection (73) and key spatiotemporal CD8 T-cell priming orchestrator within lymphoid tissues (74). CD141+ CLEC9A+ DCs of the CD11c+ subset on the other hand have been shown to be particularly efficiently in promoting naïve T cell activation (72). To map DC subpopulations in lymphoid tissues in studies of infection or vaccination we developed a panel consisting of the markers CD123, CLECL9A and CD11c in combination with CD20, Ki67 as well as CD4 and CD8 (**Figure 7A**). We used CD123, the a chain of the IL-3 receptor, for topological examination of pDCs (CD11c$^-$CD123$^+$CLEC9A$^-$) (73) and CD11c, a β2-integrin (75), and CLEC9A, a C-type Lectin-like receptor (76) to interrogate the spatial distribution of CD11c$^+$CD123$^-$CLEC9A$^+$ DC in subcapsular areas and conduits surrounding B cell follicles (**Figure 7B**). Cells of myeloid lineage (CD11c^{hi}), CD8 T -cells and CD4 T -cells were also mapped using this panel to infer mechanistic insights regarding potential cell-to-cell interactions as well as for quantification of immune cell dynamics for hypothesis-driven discovery and experimental testing. Tonsillar tissue analysis revealed similar distributions of CD11c+, CD11c-CD123+ and CD11c+CLEC9A+ events between EF and perifollicular (CD20$^{hi/dim}$, non-GC) spaces albeit at markedly different frequencies (**Figure 7C**, upper row, left). CD11c-CD123+ and CD11c+ CLEC9A+ events were rare within GCs (<0.3%) whilst CD11c+ cells were the most abundant of the three populations measured (~1% of total GC cells and 2% of total B-cell follicle cells) with individual distributions ranging from 0.1 to 1.2% within follicles (**Figure 7C**, upper low, right and lower panel). Some CD123+ staining was also observed in vascular lumen. This however was excluded from analysis at the stage of segmentation as it did not represent signal bound to a nucleus. Our data thus confirm that in tonsillar tissues CD11c-CD123+ and CD11c+CLEC9A+ signal is mainly located outside GCs which is consistent with the known positioning of DC and associated role of these cells in immune cell priming (53, 77).

Detection of Cells Harboring Actively Transcribing HIV

The determination of the localization of a pathogen following infection is of great importance for the development of successful, targeted prevention and cure strategies. HIV infection is a chronic infection that persists in lymphoid tissues even in the context of antiretroviral therapy causing profound tissue-specific alterations (15, 55, 78–80). This characteristic of HIV pathogenesis has prompted several cure strategies aiming at viral reservoir elimination to be developed over the past years (81). In this context, we designed a panel that leverages the analytical strength of the RNAscope *in situ* hybridization platform (ACD) and resolving power of confocal microscopy for topological examination and quantification of HIV-specific RNA in tissues. RNAscope is a widely used methodology that employs RNA probe hybridization and a system of cascading fluorescent probes to detect viral RNA, a surrogate of actively transcribing virus, *in situ* with high specificity and signal-to-noise resolution (82, 83). In this application, viral RNA detection is extended to include relevant immune cell populations of interest by staining fluorescently for CD3, CD4 and FDC (**Figure 8A**). A nuclear stain is also used to allow for individual cell segmentation whilst the specificity of the vRNA+ signal in the assay was ascertained through RNAse -mediated signal elimination in a control experiment (**Supplementary Figure 3B**). We use this panel to map virus RNA expression based on the RNAscope signal and quantify infected cells in intra-follicular (CD4^{lo}CD3^{lo}) as well as extra-follicular (CD4^{hi}CD3^{hi}) locations using HistoCytometry as well as FDC-bound virions using Spots analysis (**Figure 8B**). Analysis of a lymph node tissue section from an HIV+ individual revealed a trend for higher numbers of FDC-bound virions in follicles with lower overall frequencies of CD4$^{hi/dim}$ T-cells (**Figure 8C**). Follicular (F) spaces harbored a higher proportion of vRNA$^+$ CD4 T cells compared to EF spaces (**Figure 8D**, pie charts) however the frequency of CD4^{dim} T cells harboring actively transcribing virus was higher in EF compared with F areas in the absence of therapy. In addition, within F areas, higher levels of vRNA+ signal were observed in CD3^{hi}CD4^{dim} T cells compared to CD3^{hi}CD4^{hi} T cells (**Figure 8D**). This approach thus offers an integrative way to study tissue-specific viral burden and kinetics in relation to T cell immune dynamics at different infection stages or after the initiation of therapy.

DISCUSSION

The integration of lymphoid tissue analysis in studies of infection and vaccination can offer important insights into the mechanisms underlying disease progression or protection. In this study, we describe the development of a pipeline of eight multispectral confocal panels that can be used to track a multitude of immune cell subsets *in situ*, both innate and adaptive, in relevant lymphoid tissue localities for mechanistic insights and hypothesis-driven experimentation (**Supplementary Figure 1B**). The adoption of laser-scanning

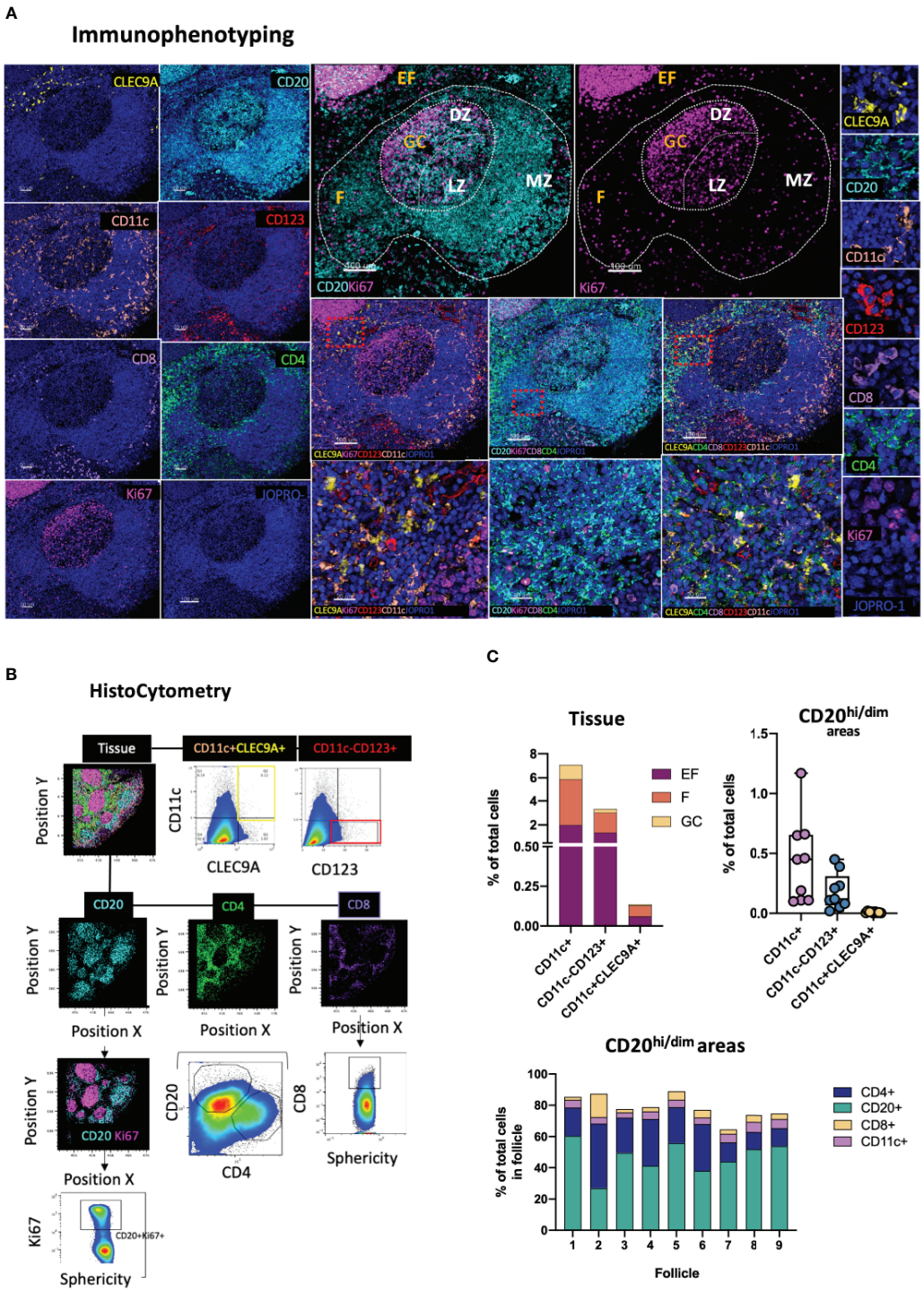

FIGURE 7 | Development of a multispectral panel for the topological examination of DCs. **(A)** Representative images showing staining for CLEC9A (yellow), CD20 (cyan), CD11c (orange), CD123 (red), CD8 (pink), CD4 (green), Ki67 (magenta) and JOPRO-1 (blue) in a tonsillar tissue section and the distribution of each protein marker with respect to the MZ, LZ and DZ (middle panels). Red dotted square enclosures in lower middle panels denote the areas that are presented magnified in the lower middle panels. **(B)** Gating strategy used for the sequential positional immunophenotyping of CD4, CD8, CD20, CD11c+, CD11c+CLEC9A+CD123- and CD11c-CD123+CLEC9A- in GC ($CD20^{dim}Ki67^{hi}$), F ($CD20^{hi/dim}$) and EF ($CD20^{lo}$) areas using histocytometry. **(C)** Box graphs and box plots showing the relative frequencies of CD11c+, CD11c+CLEC9A+CD123- and CD11c-CD123+CLEC9A- immune cells in tonsillar tissue as well as in $CD20^{hi/dim}$ areas (upper panels) and relative frequencies of CD20, CD4, CD8 and CD11c+ immune cells in nine individual follicles. Images were acquired at 40x (NA 1.3) with 1% magnification. Scale bars are 100um for all panels displaying an entire follicle), 20um in the middle panel close ups and 5um in the right panel single staining close ups.

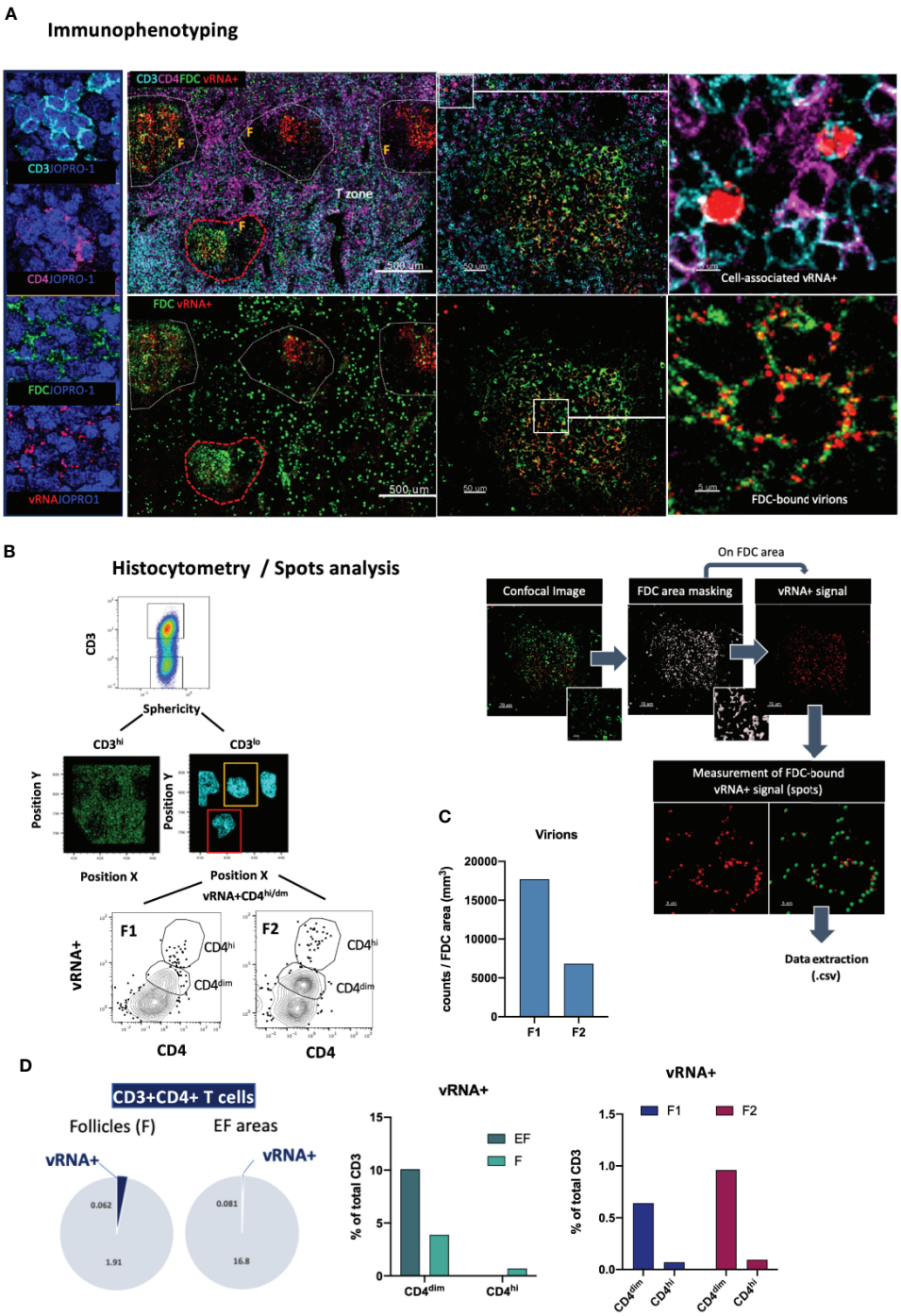

FIGURE 8 | Immunofluorescent *in situ* hybridization (IF-FISH) for the visualization of actively transcribed HIV (vRNA+) in lymph nodes. **(A)** Representative images showing staining for CD3 (cyan), CD4 (magenta), FDC (green) and HIV RNA (red) and the nuclear stain JOPRO-1 (blue) in a lymph node section from a viremic HIV+ individual. Images shown (50um,5um) are sequential close ups of the red dotted enclosures and white enclosures respectively and depict the staining seen in a B-cell follicle and distinct patterns of associated vRNA+ staining (cell-associated vs FDC-bound virions). **(B)** Gating strategy used for the quantification of vRNA+ signal in CD3+ $CD4^{hi/dim}$ T cells in two well defined B-cell follicles using HistoCytometry (left) and graphic panel summarizing the approach used to quantitate FDC-bound virions in lymphoid tissues (right). **(C)** Bar graph showing the FDC-associated virion burden in the two follicles examined as measured by histocytometry and surface spot analysis on Imaris. **(D)** Bar graphs showing the distribution of the vRNA+ signal in EF and F spaces as well as the relative distribution of the signal in $CD4^{hi}$ *vs* $CD4^{dim}$ cells and pie charts depicting the proportions of CD3+CD4+ T cells that are vRNA+/vRNA- in F and EF spaces as measured by HistoCytometry. The percentages given represent the frequency of each respective CD4 T cell population (EF vRNA+ or vRNA-/F vRNA+ or vRNA-) as a percentage of total cells d) and FDC-associated virion burden as Images were acquired at 40x (NA 1.3) with 1% magnification.

confocal microscopy (LSCM) for image acquisition offers many advantages over traditional widefield methodologies including high lateral and axial spatial resolution as well as capacity for volumetric 3D analysis and high multiplexing (84), especially when iterative staining protocols, such as CyCIF are employed (85). Even though in this study we used tissues with a thickness of ~10um, thicker tissues have successfully been imaged by us and others using immunofluorescence and confocal microscopy (24, 86). To allow for increased accuracy in downstream image segmentation we imaged tissues at 40x magnification and recorded between 40000 and 70000 individual cells. Furthermore, accurate representation and minimization of selection bias was ensured by imaging at least 50% of the tissue or by capturing 5 follicles on average in line with previously published research in our lab (24, 30) We also opted to repeat selected markers among the different panels to address sampling errors arising from the analysis of a single tissue, measured populations with and without area normalization and examined key tonsillar B cell and Tfh cell populations by flow cytometry to further confirm the validity of our tissue analysis observations (**Supplementary Figure 1A**). Wherever possible, we used previously validated antibodies in our assays. For antibodies not previously tested with FFPE tissues specificity was confirmed by i) checking the staining localization with respect to the nuclear staining, ii) studying the localization of the staining on the tissue iii) confirming the co-localization profile on lineage markers and iv) by including wherever possible an isotype control (**Supplementary Figure 3C**). Image acquisition was performed in a microscope fitted with 11 lasers. Spill-over among the various channels was minimized by: i) carefully selecting the spectral areas corresponding to each fluorophore after testing each fluorophore separately to verify the exact emission curve (**Supplementary Figures 4A, B**), ii) titrating the antibodies for optimal signal, iii) collecting fluorophore emission on separate detectors with fluorophores being excited sequentially (2-3 fluorophores/sequential, and iv) creating a spillover compensation matrix using singly stained samples and applying it to the collected dataset. In our applications autofluorescence-specific background elimination was not necessary for the most part as the validated antibodies gave excellent signal-to-noise ratios after titration. However, when this was of relevance autofluorescence was eliminated by recording the autofluorescent signal in a separate channel and subtracting it from all other channels post-acquisition or for mutually exclusive markers only, through paired subtraction. On the Imaris software this can be achieved through the channel arithmetics module. We used 8 lasers to acquire our images (**Supplementary Figure 4A**) but instruments with fewer lasers can also be used. In this case, spectrally neighboring fluorescent stains (i.e. Alexa Fluor 647 and Alexa Fluor 700) can be acquired with live spectral unmixing under a single laser. In such a scenario antibody titration is highly recommended for optimal live spectral unmixing as the intensity of the staining may vary depending on target protein expression levels and the staining protocol used. Even though our study did not make use of iterative staining protocols such as Cy-CIF (85), evaluation of such protocols in future studies is warranted as a means to increase dimensionality and maximize the use of tissue specimens with low availability. Our panels employ a total of 28 individual protein markers used to characterize ~8 distinct immune and stromal cell lineages (CD20, CD4, CD8, Neutrophils, Monocytes, FDCs, BECs/LECs, DCs) or ~ 32 distinct immune subpopulations. Staining in tandem could thus increase the dimensionality and throughput of proposed single-cell analyses to >30 distinct marker combinations. To demonstrate application in seven out of eight panels (GC reactivity; T-cell regulation; B-cell immunity; CD8 T-cell positioning and function; monocyte and inflammatory markers; GC microarchitecture; and tissue-specific DC subpopulations), we chose to focus on tonsillar tissues and defined B-cell follicles either as $CD20^{hi/dim}$ or as GCs ($CD20^{hi/dim}$ $Ki67^{+}$) (**Supplementary Figure 1C**). We found that each definition has its own merits in terms of quantification but selection of either for analysis should be carefully considered as distinct topologies may be associated with distinct functions and phenotypes. We chose tonsillar tissue because this type of tissue is easier to obtain compared to resting, HIV negative LNs. In addition, tonsillar tissue represents a chronically inflamed tissue exhibiting a highly organized stereotypical microanatomy compared to LNs and as such it is ideal for the study of tissue resident populations connected to activation and secondary B-cell follicle formation, such as monocytes and Tfh (30). In addition, previous research in our lab has shown that HIV negative tonsils and HIV negative LNs share several common topological microanatomical attributes including i) common secondary B-cell follicle microarchitecture (MZ, LZ, DZ); ii) common GC ($CD20^{hi}Ki67^{hi}$) polarization, and iii) comparable aspects of Tfh heterogeneity and polarization (24). LNs on the other hand can acquire divergent phenotypes in states of pathology, as in the case of HIV infection, that complicate the interpretation of physiological microanatomical boundaries (87). Even though discussion of LN-associated pathology extends beyond the scope of this article, the application of the panels to different tissue preparations is warranted. This is especially informative for infections that persist chronically by establishing life-long reservoirs in the tissues of infected hosts. The detection and persistence of a pathogen in tissues can be address using a number of different methodologies. These range, depending on the size of the pathogen, from direct microscopic examination to detection of pathogen-associated proteins using monoclonal antibodies (88) or associated DNA/RNA using molecular probes (89). In the case of HIV infection in particular, one of the main challenges that need to be overcome for cure is the presence of tissue-specific reservoirs that persist in infected individuals for life seeding viral replication (78, 90). Tissue analysis and *in situ* tracking of viral RNA can help address several key questions that remain in this field. For example, what is the *in vivo* phenotype of cells harboring actively transcribing virus or latent infection? Where do these cells localize and what are the micro-geographical patterns or cell-to-cell interactions that enable persistence? Does tissue-specificity modulate the function and phenotype of

latently infected cells? Are latency and persistence associated with distinct non-immune tissue-specific biomarkers (i.e. stromal cells) or soluble factor distributions *in situ* (i.e pro-inflammatory chemokines and cytokines)? Tissue analysis also offers a tangible way to measure the effect of latency reversal interventions and a means to assess the reactogenicity and immunogenicity of novel vaccine formulations. Confocal imaging in particular, with its high resolution and volumetric capacity, offers an ideal platform for the comprehensive mapping of protein markers at subcellular level.

In summary, we have described a detailed tissue analysis pipeline that can be used to characterize geographical patterns, immune-cell distributions and relationships in lymphoid tissues. Application of this type of analysis can increase the dimensionality and predictive power of flow-cytometry and single-cell RNA expression analyses and accelerate biomarker discovery in the context of infection and vaccination.

DATA AVAILABILITY STATEMENT

The original contributions presented in the study are included in the article/**Supplementary Material**. Further inquiries can be directed to the corresponding author.

ETHICS STATEMENT

The studies involving human participants were reviewed and approved by INER-CIENI Ethics Committee. The patients/participants provided their written informed consent to participate in this study.

AUTHOR CONTRIBUTIONS

EM, CP, and RK conceived and designed the study. PR, FT-R, and GR-T collected samples. EM performed the experiments, undertook the analysis and wrote the manuscript. CP and RK supervised the study. All authors contributed to the article and approved the submitted version.

FUNDING

This research was supported by the Intramural Research Program of the Vaccine Research Center, NIAID, National Institutes of Health; and a CAVD grant (#OP1032325) from the Bill and Melinda Gates Foundation.

ACKNOWLEDGMENTS

The authors would like to acknowledge Dr. Owen M Schwartz and the staff at the NIAID Bioimaging facility, in particular Dr. Juraj Kabat, Dr. Margery Smelkinson and Dr. Sundar Ganesan for assisting with microscopy related questions and for offering valuable advice on imaging analysis.

SUPPLEMENTARY MATERIAL

The Supplementary Material for this article can be found online at: https://www.frontiersin.org/articles/10.3389/fimmu.2021.683396/full#supplementary-material

Supplementary Figure 1 | Quantitation of relevant immune cell populations using HistoCytometry and Flow Cytometry, confocal imaging method overview and positional heterogeneity of CD4+ T cell subsets in tonsillar B-cell follicles. **(A)** Box plots showing the relative frequencies of CD4 T cells, CD20 and $CD20^{+}Ki67^{+}$ B cells as well as CD8 T cells in tonsillar sections as well as the cell numbers for each population normalized by the total corresponding tissue area scanned (mm3). B cells (CD20+) were the most abundant population in tonsils (median frequency 35%) followed by CD4 T cells (median frequency 27%) whilst the frequency of CD8 T cells was relatively low (7-9.5% of total cells). Higher ratios (CD20+ cells/mm^3) represent tissues with higher B-cell (CD20+) abundance. The frequencies of the corresponding tonsillar populations as determined by flow cytometry (n=6) are also shown. **(B)** Schematic illustrating the methodology used for the acquisition and analysis of the eight multispectral confocal datasets. (1) Tissues are stained with pre-titrated combinations of antibodies (2) and images are acquired on a laser scanning confocal microscope (Leica TCS SP8) using a 40x (NA 1.3) objective at 512x512 pixel density and 1% zoom. (3) Image segmentation for single cells is performed with the program Imaris based on the nuclear stain (JOPRO-1) and associated surface marker intensities and areas are then exported for graphing (4a) or combined with X-Y positional information (4b) and exported to excel to create a csv file for FlowJo import (5) and further gating and analysis (6). **(C)** (Left) Representative confocal microscopy image of a tonsillar B cell follicle as determined by immunofluorescent staining against the B cell marker CD20 (cyan) and the DZ/LZ specific marker Ki67 (magenta). White enclosures denote the boundaries of the T zone (T), follicle (F), marginal zone (MZ) and germinal center (GC) (Middle) Bar graph summarizing the frequencies of $PD\text{-}1^{hi}$ CD4+ T-cells in the area surrounding a B-cell follicle (T-zone), as well as within the F, MZ and GC. Each circle represents an individual follicle (n=6) and data were obtained from the analysis of a single tonsil tissue section (n=1) (Right) Confocal microscopy images showing the CD4 T cell populations corresponding to each individual B-cell follicle locality as determined by the distribution of the CD4 (green) and PD-1 (red). For visualization purposes MZ and GC images were masked post-acquisition on Imaris to only show the cells that belong to the area indicated. Tfh are identified by the co-expression of CD4 (green) and PD-1 (red). (D) Gating strategy used for the characterization of B-cell and Tfh populations ($CXCR5^{hi}PD\text{-}1^{hi}CD57^{+/-}$) using flow cytometry. Images were acquired at 40x (NA 1.3) with 1% zoom. Scale bars = 100um and 10um (close-ups).

Supplementary Figure 2 | Patterns of H2Ax staining, enumeration of CD3-CD8+ NK cells in tonsils and alternative CD8+ T cell imaging panel. **(A)** Representative confocal images showing the distribution of pH2Ax in GCs after staining for pH2Ax (red), CD20 (cyan) and Ki67 (magenta) (left) and representative gating strategy used for the characterization of the frequencies of $pH2Ax^{hi}$ expression in $CD20^{dim}CD38^{lo}$, $CD20^{hi}CD38^{dim}$ and $CD20^{lo}CD38^{hi}$ B cells in a flow cytometry experiment. The frequencies of $pH2Ax/Volume^{hi}$ events in F and GCs as measured by confocal imaging and HistoCytometry in two tonsils (n=2). and two HIV+ LN (n=2) are summarized in the bar graph shown. Circles represent individual follicles whilst different specimens are demarcated by individual colors. **(B)** Gating strategy used for the flow cytometrical characterization of CD8+ CD3- T cells in tonsils and histogram depicting the proportion of $CD3^{+}$ and $CD3^{-}$ cells within the $CD8^{bright}$ and $CD8^{dim}$ gates. A summary of the relative frequencies of $CD8^{bright}CD3^{-}$ cells in five tonsils is given in the bar graph shown. **(C)** Alternative CD8+ T cell confocal imaging panel combining the markers CD3 (purple), CD8 (red), FasL (yellow) and GrzB (orange) for the characterization of $CD3^{+}CD8^{+}$ and $CD3^{-}CD8^{+}$ lymphocytes in lymphoid tissues where higher NK frequencies are expected and b) relative frequencies of CD3+CD8+ and CD3-CD8+ populations as measured by histocytometry in one tonsillar tissue and one HIV+ LN

after application of the alternative CD8 T cell imaging panel. Images were acquired at 40x (NA 1.3) with 1% zoom. Scale bars are 100um, 50um and 10um.

Supplementary Figure 3 | CD8+ FasL$^{+/-}$ GrzB $^{+/-}$ T cells in tonsils and LNs, IF-FISH RNAscope staining controls and fluorescence minus one (FMO) controls. **(A)** Histocytometry plots showing the distribution of imaged follicles in one tonsillar and one HIV+ LN tissue as denoted by CD20 (cyan) and Ki67 (magenta) staining and the gating strategy used for the identification of CD8+ FasL GrzB expressing populations within these localities. Red circles denote individual follicles. The cumulative frequencies of CD8+ Fas$^{L+/-}$ GrzB $^{+/-}$ T cells for all follicles measured in the two types of samples are shown in the bar graph. Each type of sample is denoted by a different colour. **(B)** Confocal microscopy images showing two sequential LN tissue sections from an HIV+ individual stained with an HIV+ vRNA+ specific probe and antibodies specific for the protein markers CD3 (cyan) CD4 (magenta) and FDC (green) in the absence (section 1) or presence (section 2) of an RNase A/T1 pretreatment step. The localization of the vRNA+ signal (red) on the FDC network (green) is shown. **(C)** Representative example of FMO controls used to establish the specificity of the detected signals in each channel. Fluorescence in the FMO channel was detected only when the corresponding antibody was present but not when omitted or replaced by an isotype control. Images were acquired at 40x (NA 1.3) with 1% zoom. Scale bars = 500um, 50um (close-ups).

Supplementary Figure 4 | Fluorescence acquisition spectral regions and cross-talk among acquisition channels. **(A)** Schematic showing the lasers, fluorochromes used and photon detection regions used for image acquisition in the eight multispectral panels described in this study. Regions were adjusted after acquiring real-time single fluorochrome emission curves to maximize signal-to-noise ratios and minimize cross-talk between channels. **(B)** Representative example of single fluorochrome emission cross-over into neighboring channels as detected after staining for BV421, JOPRO-1, eF615, AF488, AF546, AF647, BV480 or AF700. Each horizontal line corresponds to a single fluorochrome that was acquired under the same conditions as the full panel in order to visualize and resolve potential fluorescence cross-over issues. Images were acquired at 40x (NA 1.3) with 1% zoom. Scale bars are 100um.

REFERENCES

1. Qi H, Kastenmuller W, Germain RN. Spatiotemporal Basis of Innate and Adaptive Immunity in Secondary Lymphoid Tissue. *Annu Rev Cell Dev Biol* (2014) 30:141–67. doi: 10.1146/annurev-cellbio-100913-013254
2. Kumar BV, Connors TJ, Farber DL. Human T Cell Development, Localization, and Function Throughout Life. *Immunity* (2018) 48(2):202–13. doi: 10.1016/j.immuni.2018.01.007
3. Trepel F. Number and Distribution of Lymphocytes in Man. *A Crit Anal Klin Wochenschr* (1974) 52(11):511–5. doi: 10.1007/BF01468720
4. Breitfeld D, Ohl L, Kremmer E, Ellwart J, Sallusto F, Lipp M, et al. Follicular B Helper T Cells Express CXC Chemokine Receptor 5, Localize to B Cell Follicles, and Support Immunoglobulin Production. *J Exp Med* (2000) 192 (11):1545–52. doi: 10.1084/jem.192.11.1545
5. Cremasco V, Woodruff MC, Onder L, Cupovic J, Nieves-Bonilla JM, Schildberg FA, et al. B Cell Homeostasis and Follicle Confines Are Governed by Fibroblastic Reticular Cells. *Nat Immunol* (2014) 15(10):973–81. doi: 10.1038/ni.2965
6. Fletcher AL, Acton SE, Knoblich K. Lymph Node Fibroblastic Reticular Cells in Health and Disease. *Nat Rev Immunol* (2015) 15(6):350–61. doi: 10.1038/nri3846
7. Link A, Vogt TK, Favre S, Britschgi MR, Acha-Orbea H, Hinz B, et al. Fibroblastic Reticular Cells in Lymph Nodes Regulate the Homeostasis of Naive T Cells. *Nat Immunol* (2007) 8(11):1255–65. doi: 10.1038/ni1513
8. Sathaliyawala T, Kubota M, Yudanin N, Turner D, Camp P, Thome JJ, et al. Distribution and Compartmentalization of Human Circulating and Tissue-Resident Memory T Cell Subsets. *Immunity* (2013) 38(1):187–97. doi: 10.1016/j.immuni.2012.09.020
9. Szabo PA, Levitin HM, Miron M, Snyder ME, Senda T, Yuan J, et al. Single-Cell Transcriptomics of Human T Cells Reveals Tissue and Activation Signatures in Health and Disease. *Nat Commun* (2019) 10(1):4706. doi: 10.1038/s41467-019-12464-3
10. Thome JJ, Yudanin N, Ohmura Y, Kubota M, Grinshpun B, Sathaliyawala T, et al. Spatial Map of Human T Cell Compartmentalization and Maintenance Over Decades of Life. *Cell* (2014) 159(4):814–28. doi: 10.1016/j.cell.2014.10.026
11. Wong MT, Ong DE, Lim FS, Teng KW, McGovern N, Narayanan S, et al. A High-Dimensional Atlas of Human T Cell Diversity Reveals Tissue-Specific Trafficking and Cytokine Signatures. *Immunity* (2016) 45(2):442–56. doi: 10.1016/j.immuni.2016.07.007
12. Willard-Mack CL. Normal Structure, Function, and Histology of Lymph Nodes. *Toxicol Pathol* (2006) 34(5):409–24. doi: 10.1080/01926230600867727
13. Estes JD. Pathobiology of HIV/SIV-Associated Changes in Secondary Lymphoid Tissues. *Immunol Rev* (2013) 254(1):65–77. doi: 10.1111/imr.12070
14. Leyre L, Kroon E, Vandergeeten C, Sacdalan C, Colby DJ, Buranapraditkun S, et al. Abundant HIV-Infected Cells in Blood and Tissues Are Rapidly Cleared Upon ART Initiation During Acute HIV Infection. *Sci Transl Med* (2020) 12 (533):1–13. doi: 10.1126/scitranslmed.aav3491
15. Lorenzo-Redondo R, Fryer HR, Bedford T, Kim EY, Archer J, Pond SLK, et al. Persistent HIV-1 Replication Maintains the Tissue Reservoir During Therapy. *Nature* (2016) 530(7588):51–6. doi: 10.1038/nature16933
16. Annunziato F, Romagnani S. Heterogeneity of Human Effector CD4+ T Cells. *Arthritis Res Ther* (2009) 11(6):257. doi: 10.1186/ar2843
17. Zhu J, Paul WE. Heterogeneity and Plasticity of T Helper Cells. *Cell Res* (2010) 20(1):4–12. doi: 10.1038/cr.2009.138
18. Finzi D, Blankson J, Siliciano JD, Margolick JB, Chadwick K, Pierson T, et al. Latent Infection of CD4+ T Cells Provides a Mechanism for Lifelong Persistence of HIV-1, Even in Patients on Effective Combination Therapy. *Nat Med* (1999) 5(5):512–7. doi: 10.1038/8394
19. Victora GD, Nussenzweig MC. Germinal Centers. *Annu Rev Immunol* (2012) 30:429–57. doi: 10.1146/annurev-immunol-020711-075032
20. Crotty S. Follicular Helper CD4 T Cells (TFH). *Annu Rev Immunol* (2011) 29:621–63. doi: 10.1146/annurev-immunol-031210-101400
21. Crotty S. T Follicular Helper Cell Biology: A Decade of Discovery and Diseases. *Immunity* (2019) 50(5):1132–48. doi: 10.1016/j.immuni.2019.04.011
22. Song W, Craft J. T Follicular Helper Cell Heterogeneity: Time, Space, and Function. *Immunol Rev* (2019) 288(1):85–96. doi: 10.1111/imr.12740
23. Donnadieu E, Reisinger KB, Scharf S, Michel Y, Bein J, Hansen S, et al. Landscape of T Follicular Helper Cell Dynamics in Human Germinal Centers. *J Immunol* (2020) 205(5):1248–55. doi: 10.4049/jimmunol.1901475
24. Padhan K, Moysi E, Noto A, Chassiakos A, Ghneim K, Perra MM, et al. Acquisition of Optimal TFH Cell Function Is Defined by Specific Molecular, Positional, and TCR Dynamic Signatures. *Proc Natl Acad Sci USA* (2021) 118 (18):1–11. doi: 10.1073/pnas.2016855118
25. Lindqvist M, van Lunzen J, Soghoian DZ, Kuhl BD, Ranasinghe S, Kranias G, et al. Expansion of HIV-Specific T Follicular Helper Cells in Chronic HIV Infection. *J Clin Invest* (2012) 122(9):3271–80. doi: 10.1172/JCI64314
26. Petrovas C, Yamamoto T, Gerner MY, Boswell KL, Wloka K, Smith EC, et al. Cd4 T Follicular Helper Cell Dynamics During SIV Infection. *J Clin Invest* (2012) 122(9):3281–94. doi: 10.1172/JCI63039
27. Perreau M, Savoye AL, De Crignis E, Corpataux JM, Cubas R, Haddad EK, et al. Follicular Helper T Cells Serve as the Major CD4 T Cell Compartment for HIV-1 Infection, Replication, and Production. *J Exp Med* (2013) 210 (1):143–56. doi: 10.1084/jem.20121932
28. Aid M, Dupuy FP, Moysi E, Moir S, Haddad EK, Estes JD, et al. Follicular CD4 T Helper Cells as a Major Hiv Reservoir Compartment: A Molecular Perspective. *Front Immunol* (2018) 9:895. doi: 10.3389/fimmu.2018.00895
29. Gerner MY, Kastenmuller W, Ifrim I, Kabat J, Germain RN. Histo-Cytometry: A Method for Highly Multiplex Quantitative Tissue Imaging Analysis Applied to Dendritic Cell Subset Microanatomy in Lymph Nodes. *Immunity* (2012) 37 (2):364–76. doi: 10.1016/j.immuni.2012.07.011
30. Amodio D, Cotugno N, Macchiarulo G, Rocca S, Dimopoulos Y, Castrucci MR, et al. Quantitative Multiplexed Imaging Analysis Reveals a Strong Association Between Immunogen-Specific B Cell Responses and Tonsillar Germinal Center Immune Dynamics in Children After Influenza Vaccination. *J Immunol* (2018) 200(2):538–50. doi: 10.4049/jimmunol.1701312

31. Petrovas C, Ferrando-Martinez S, Gerner MY, Casazza JP, Pegu A, Deleage C, et al. Follicular CD8 T Cells Accumulate in HIV Infection and Can Kill Infected Cells *In Vitro Via* Bispecific Antibodies. *Sci Transl Med* (2017) 9 (373):1–28. doi: 10.1126/scitranslmed.aag2285
32. Yu D, Rao S, Tsai LM, Lee SK, He Y, Sutcliffe EL, et al. The Transcriptional Repressor Bcl-6 Directs T Follicular Helper Cell Lineage Commitment. *Immunity* (2009) 31(3):457–68. doi: 10.1016/j.immuni.2009.07.002
33. Kim CH, Rott LS, Clark-Lewis I, Campbell DJ, Wu L, Butcher EC. Subspecialization of CXCR5+ T Cells: B Helper Activity Is Focused in a Germinal Center-Localized Subset of CXCR5+ T Cells. *J Exp Med* (2001) 193 (12):1373–81. doi: 10.1084/jem.193.12.1373
34. Sayin I, Radtke AJ, Vella LA, Jin W, Wherry EJ, Buggert M, et al. Spatial Distribution and Function of T Follicular Regulatory Cells in Human Lymph Nodes. *J Exp Med* (2018) 215(6):1531–42. doi: 10.1084/jem.20171940
35. Linterman MA, Pierson W, Lee SK, Kallies A, Kawamoto S, Rayner TF, et al. Foxp3+ Follicular Regulatory T Cells Control the Germinal Center Response. *Nat Med* (2011) 17(8):975–82. doi: 10.1038/nm.2425
36. Lim HW, Hillsamer P, Kim CH. Regulatory T Cells can Migrate to Follicles Upon T Cell Activation and Suppress GC-Th Cells and GC-Th Cell-Driven B Cell Responses. *J Clin Invest* (2004) 114(11):1640–9. doi: 10.1172/JCI200422325
37. Hori S, Nomura T, Sakaguchi S. Control of Regulatory T Cell Development by the Transcription Factor Foxp3. *Science* (2003) 299(5609):1057–61. doi: 10.1126/science.1079490
38. Elkord E. Helios Should Not Be Cited as a Marker of Human Thymus-Derived Tregs. Commentary: Helios(+) and Helios(-) Cells Coexist Within the Natural Foxp3(+) T Regulatory Cell Subset in Humans. *Front Immunol* (2016) 7:276. doi: 10.3389/fimmu.2016.00276
39. Elkord E, Al-Ramadi BK. Helios Expression in Foxp3(+) T Regulatory Cells. *Expert Opin Biol Ther* (2012) 12(11):1423–5. doi: 10.1517/14712598.2012.711310
40. Laidlaw BJ, Lu Y, Amezquita RA, Weinstein JS, Vander Heiden JA, Gupta NT, et al. Interleukin-10 From CD4(+) Follicular Regulatory T Cells Promotes the Germinal Center Response. *Sci Immunol* (2017) 2(16):1–10. doi: 10.1126/sciimmunol.aan4767
41. Susan Pereira Ribeiro MA, Dupuy FP, Chan CN, Hultquist J, Delage C, Moysi E, et al. IL-10 Driven Memory T Cell Survival and Tfh Differentiation Promote HIV Persistence. *bioRxiv* (2021). doi: 10.1101/2021.02.26.432955
42. Pelletier N, McHeyzer-Williams LJ, Wong KA, Urich E, Fazilleau N, McHeyzer-Williams MG. Plasma Cells Negatively Regulate the Follicular Helper T Cell Program. *Nat Immunol* (2010) 11(12):1110–8. doi: 10.1038/ni.1954
43. Moir S, Fauci AS. B Cells in HIV Infection and Disease. *Nat Rev Immunol* (2009) 9(4):235–45. doi: 10.1038/nri2524
44. Deterre P, Berthelier V, Bauvois B, Dalloul A, Schuber F, Lund F. CD38 in T- and B-Cell Functions. *Chem Immunol* (2000) 75:146–68. doi: 10.1159/000058767
45. Sanderson RD, Lalor P, Bernfield M. Lymphocytes-B Express and Lose Syndecan At Specific Stages of Differentiation. *Cell Regul* (1989) 1(1):27–35. doi: 10.1091/mbc.1.1.27
46. Rogakou EP, Pilch DR, Orr AH, Ivanova VS, Bonner WM. DNA Double-Stranded Breaks Induce Histone H2AX Phosphorylation on Serine 139. *J Biol Chem* (1998) 273(10):5858–68. doi: 10.1074/jbc.273.10.5858
47. Reina-San-Martin B, Difilippantonio S, Hanitsch L, Masilamani RF, Nussenzweig A, Nussenzweig MC. H2AX Is Required for Recombination Between Immunoglobulin Switch Regions But Not for Intra-Switch Region Recombination or Somatic Hypermutation. *J Exp Med* (2003) 197(12):1767–78. doi: 10.1084/jem.20030569
48. Quigley MF, Gonzalez VD, Granath A, Andersson J, Sandberg JK. Cxcr5+ CCR7- Cd8 T Cells Are Early Effector Memory Cells That Infiltrate Tonsil B Cell Follicles. *Eur J Immunol* (2007) 37(12):3352–62. doi: 10.1002/eji.200636746
49. Nguyen S, Sada-Japp A, Petrovas C, Betts MR. Jigsaw Falling Into Place: A Review and Perspective of Lymphoid Tissue CD8+ T Cells and Control of HIV. *Mol Immunol* (2020) 124:42–50. doi: 10.1016/j.molimm.2020.05.016
50. Reuter MA, Del Rio Estrada PM, Buggert M, Petrovas C, Ferrando-Martinez S, Nguyen S, et al. Hiv-Specific Cd8(+) T Cells Exhibit Reduced and Differentially Regulated Cytolytic Activity in Lymphoid Tissue. *Cell Rep* (2017) 21(12):3458–70. doi: 10.1016/j.celrep.2017.11.075
51. Brenchley JM, Karandikar NJ, Betts MR, Ambrozak DR, Hill BJ, Crotty LE, et al. Expression of CD57 Defines Replicative Senescence and Antigen-Induced Apoptotic Death of CD8+ T Cells. *Blood* (2003) 101(7):2711–20. doi: 10.1182/blood-2002-07-2103
52. Nguyen S, Deleage C, Darko S, Ransier A, Truong DP, Agarwal D, et al. Elite Control of HIV Is Associated With Distinct Functional and Transcriptional Signatures in Lymphoid Tissue CD8(+) T Cells. *Sci Transl Med* (2019) 11 (523):1–12. doi: 10.1126/scitranslmed.aax4077
53. Leal JM, Huang JY, Kohli K, Stoltzfus C, Lyons-Cohen MR, Olin BE, et al. Innate Cell Microenvironments in Lymph Nodes Shape the Generation of T Cell Responses During Type I Inflammation. *Sci Immunol* (2021) 6(56):1–16. doi: 10.1126/sciimmunol.abb9435
54. Chatziandreou N, Farsakoglu Y, Palomino-Segura M, D'Antuono R, Pizzagalli DU, Sallusto F, et al. Macrophage Death Following Influenza Vaccination Initiates the Inflammatory Response That Promotes Dendritic Cell Function in the Draining Lymph Node. *Cell Rep* (2017) 18(10):2427–40. doi: 10.1016/j.celrep.2017.02.026
55. Schacker TW, Brenchley JM, Beilman GJ, Reilly C, Pambuccian SE, Taylor J, et al. Lymphatic Tissue Fibrosis Is Associated With Reduced Numbers of Naive CD4+ T Cells in Human Immunodeficiency Virus Type 1 Infection. *Clin Vaccine Immunol* (2006) 13(5):556–60. doi: 10.1128/CVI.13.5.556-560.2006
56. Favre D, Mold J, Hunt PW, Kanwar B, Loke P, Seu L, et al. Tryptophan Catabolism by Indoleamine 2,3-Dioxygenase 1 Alters the Balance of TH17 to Regulatory T Cells in HIV Disease. *Sci Transl Med* (2010) 2(32):32ra6. doi: 10.1126/scitranslmed.3000632
57. Barros MH, Hauck F, Dreyer JH, Kempkes B, Niedobitek G. Macrophage Polarisation: An Immunohistochemical Approach for Identifying M1 and M2 Macrophages. *PLoS One* (2013) 8(11):e80908. doi: 10.1371/journal.pone.0080908
58. Shankwitz K, Pallikkuth S, Sirupangi T, Kirk Kvistad D, Russel KB, Pahwa R, et al. Compromised Steady-State Germinal Center Activity With Age in Nonhuman Primates. *Aging Cell* (2020) 19(2):e13087. doi: 10.1111/acel.13087
59. Aratani Y. Myeloperoxidase: Its Role for Host Defense, Inflammation, and Neutrophil Function. *Arch Biochem Biophys* (2018) 640:47–52. doi: 10.1016/j.abb.2018.01.004
60. Li Y, Wang W, Yang F, Xu Y, Feng C, Zhao Y. The Regulatory Roles of Neutrophils in Adaptive Immunity. *Cell Commun Signal* (2019) 17(1):147. doi: 10.1186/s12964-019-0471-y
61. Saylor J, Ma Z, Goodridge HS, Huang F, Cress AE, Pandol SJ, et al. Spatial Mapping of Myeloid Cells and Macrophages by Multiplexed Tissue Staining. *Front Immunol* (2018) 9:2925. doi: 10.3389/fimmu.2018.02925
62. Bellomo A, Gentek R, Bajenoff M, Baratin M. Lymph Node Macrophages: Scavengers, Immune Sentinels and Trophic Effectors. *Cell Immunol* (2018) 330:168–74. doi: 10.1016/j.cellimm.2018.01.010
63. Kityo C, Makamdop KN, Rothenberger M, Chipman JG, Hoskuldsson T, Beilman GJ, et al. Lymphoid Tissue Fibrosis Is Associated With Impaired Vaccine Responses. *J Clin Invest* (2018) 128(7):2763–73. doi: 10.1172/JCI97377
64. Linterman MA. How T Follicular Helper Cells and the Germinal Centre Response Change With Age. *Immunol Cell Biol* (2014) 92(1):72–9. doi: 10.1038/icb.2013.77
65. Thierry GR, Gentek R, Bajenoff M. Remodeling of Reactive Lymph Nodes: Dynamics of Stromal Cells and Underlying Chemokine Signaling. *Immunol Rev* (2019) 289(1):42–61. doi: 10.1111/imr.12750
66. Heesters BA, Myers RC, Carroll MC. Follicular Dendritic Cells: Dynamic Antigen Libraries. *Nat Rev Immunol* (2014) 14(7):495–504. doi: 10.1038/nri3689
67. Estes J, Baker JV, Brenchley JM, Khoruts A, Barthold JL, Bantle A, et al. Collagen Deposition Limits Immune Reconstitution in the Gut. *J Infect Dis* (2008) 198(4):456–64. doi: 10.1086/590112
68. Wang X, Cho B, Suzuki K, Xu Y, Green JA, An J, et al. Follicular Dendritic Cells Help Establish Follicle Identity and Promote B Cell Retention in Germinal Centers. *J Exp Med* (2011) 208(12):2497–510. doi: 10.1084/jem.20111449
69. Moysi E, Pallikkuth S, De Armas LR, Gonzalez LE, Ambrozak D, George V, et al. Altered Immune Cell Follicular Dynamics in HIV Infection Following Influenza Vaccination. *J Clin Invest* (2018) 128(7):3171–85. doi: 10.1172/JCI99884

70. Burton GF, Masuda A, Heath SL, Smith BA, Tew JG, Szakal AK. Follicular Dendritic Cells (FDC) in Retroviral Infection: Host/Pathogen Perspectives. *Immunol Rev* (1997) 156:185–97. doi: 10.1111/j.1600-065X.1997.tb00968.x
71. Zhang ZQ, Schuler T, Cavert W, Notermans DW, Gebhard K, Henry K, et al. Reversibility of the Pathological Changes in the Follicular Dendritic Cell Network With Treatment of HIV-1 Infection. *Proc Natl Acad Sci USA* (1999) 96(9):5169–72. doi: 10.1073/pnas.96.9.5169
72. Granot T, Senda T, Carpenter DJ, Matsuoka N, Weiner J, Gordon CL, et al. Dendritic Cells Display Subset and Tissue-Specific Maturation Dynamics Over Human Life. *Immunity* (2017) 46(3):504–15. doi: 10.1016/j.immuni.2017.02.019
73. Dave B, Kaplan J, Gautam S, Bhargava P. Plasmacytoid Dendritic Cells in Lymph Nodes of Patients With Human Immunodeficiency Virus. *Appl Immunohistochem Mol Morphol* (2012) 20(6):566–72. doi: 10.1097/PAI.0b013e318251d8a4
74. Brewitz A, Eickhoff S, Dahling S, Quast T, Bedoui S, Kroczek RA, et al. Cd8(+) T Cells Orchestrate Pdc-XCR1(+) Dendritic Cell Spatial and Functional Cooperativity to Optimize Priming. *Immunity* (2017) 46(2):205–19. doi: 10.1016/j.immuni.2017.01.003
75. Schittenhelm L, Hilkens CM, Morrison VL. Beta2 Integrins as Regulators of Dendritic Cell, Monocyte, and Macrophage Function. *Front Immunol* (2017) 8:1866. doi: 10.3389/fimmu.2017.01866
76. Huysamen C, Willment JA, Dennehy KM, Brown GD. CLEC9A is a Novel Activation C-Type Lectin-Like Receptor Expressed on BDCA3+ Dendritic Cells and a Subset of Monocytes. *J Biol Chem* (2008) 283(24):16693–701. doi: 10.1074/jbc.M709923200
77. Vermi W, Riboldi E, Wittamer V, Gentili F, Luini W, Marrelli S, et al. Role of ChemR23 in Directing the Migration of Myeloid and Plasmacytoid Dendritic Cells to Lymphoid Organs and Inflamed Skin. *J Exp Med* (2005) 201(4):509–15. doi: 10.1084/jem.20041310
78. Chaillon A, Gianella S, Dellicour S, Rawlings SA, Schlub TE, De Oliveira MF, et al. HIV Persists Throughout Deep Tissues With Repopulation From Multiple Anatomical Sources. *J Clin Invest* (2020) 130(4):1699–712. doi: 10.1172/JCI134815
79. Schacker TW, Nguyen PL, Martinez E, Reilly C, Gatell JM, Horban A, et al. Persistent Abnormalities in Lymphoid Tissues of Human Immunodeficiency Virus-Infected Patients Successfully Treated With Highly Active Antiretroviral Therapy. *J Infect Dis* (2002) 186(8):1092–7. doi: 10.1086/343802
80. Zeng M, Southern PJ, Reilly CS, Beilman GJ, Chipman JG, Schacker TW, et al. Lymphoid Tissue Damage in HIV-1 Infection Depletes Naive T Cells and Limits T Cell Reconstitution After Antiretroviral Therapy. *PLoS Pathog* (2012) 8(1):e1002437. doi: 10.1371/journal.ppat.1002437
81. Bailon L, Mothe B, Berman L, Brander C. Novel Approaches Towards a Functional Cure of HIV/AIDS. *Drugs* (2020) 80(9):859–68. doi: 10.1007/s40265-020-01322-y
82. Wang F, Flanagan J, Su N, Wang LC, Bui S, Nielson A, et al. Rnascope: A Novel in Situ RNA Analysis Platform for Formalin-Fixed, Paraffin-Embedded Tissues. *J Mol Diagn* (2012) 14(1):22–9. doi: 10.1016/j.jmoldx.2011.08.002
83. Deleage C, Wietgrefe SW, Del Prete G, Morcock DR, Hao XP, Piatak M Jr, et al. Defining HIV and SIV Reservoirs in Lymphoid Tissues. *Pathog Immun* (2016) 1(1):68–106. doi: 10.20411/pai.v1i1.100
84. Moysi E, Estes JD, Petrovas C. Novel Imaging Methods for Analysis of Tissue Resident Cells in HIV/SIV. *Curr HIV/AIDS Rep* (2016) 13(1):38–43. doi: 10.1007/s11904-016-0300-5
85. Lin JR, Fallahi-Sichani M, Sorger PK. Highly Multiplexed Imaging of Single Cells Using a High-Throughput Cyclic Immunofluorescence Method. *Nat Commun* (2015) 6:8390. doi: 10.1038/ncomms9390
86. Li W, Germain RN, Gerner MY. Multiplex, Quantitative Cellular Analysis in Large Tissue Volumes With Clearing-Enhanced 3D Microscopy (Ce3D). *Proc Natl Acad Sci USA* (2017) 114(35):E7321–E30. doi: 10.1073/pnas.1708981114
87. Paiva DD, Morais JC, Pilotto J, Veloso V, Duarte F, Lenzi HL. Spectrum of Morphologic Changes of Lymph Nodes in HIV Infection. *Mem Inst Oswaldo Cruz* (1996) 91(3):371–9. doi: 10.1590/S0074-02761996000300023
88. Eyzaguirre E HAK. Application of Immunohistochemistry to Infections. *Arch Pathol Lab Med* (2008) 132(3):424–31. doi: 10.5858/2008-132-424-AOITI
89. Frickmann H, Zautner AE, Moter A, Kikhney J, Hagen RM, Stender H, et al. Fluorescence In Situ Hybridization (FISH) in the Microbiological Diagnostic Routine Laboratory: A Review. *Crit Rev Microbiol* (2017) 43(3):263–93. doi: 10.3109/1040841X.2016.1169990
90. Wong JK, Yukl SA. Tissue Reservoirs of HIV. *Curr Opin HIV AIDS* (2016) 11(4):362–70. doi: 10.1097/COH.0000000000000293

Conflict of Interest: The authors declare that the research was conducted in the absence of any commercial or financial relationships that could be construed as a potential conflict of interest.

frontiers in Immunology

ORIGINAL RESEARCH
published: 16 June 2021
doi: 10.3389/fimmu.2021.695148

CD32$^+$CD4$^+$ T Cells Sharing B Cell Properties Increase With Simian Immunodeficiency Virus Replication in Lymphoid Tissues

*Nicolas Huot[1], Philippe Rascle[1,2], Cyril Planchais[3], Vanessa Contreras[4], Caroline Passaes[1], Roger Le Grand[4], Anne-Sophie Beignon[4], Etienne Kornobis[5,6], Rachel Legendre[5,6], Hugo Varet[5,6], Asier Saez-Cirion[1], Hugo Mouquet[3], Beatrice Jacquelin[1] and Michaela Müller-Trutwin[1]**

[1] Institut Pasteur, Unité HIV, Inflammation et Persistance, Paris, France, [2] Université Paris Diderot, Sorbonne Paris Cité, Paris, France, [3] Institut Pasteur, INSERM U1222, Laboratoire d'Immunologie Humorale, Paris, France, [4] CEA-Université Paris Sud-Inserm, U1184, IDMIT Department, IBFJ, Fontenay-aux-Roses, France, [5] Hub de Bioinformatique et Biostatistique - Département Biologie Computationnelle, Institut Pasteur, Paris, France, [6] Plate-forme Technologique Biomics – Centre de Ressources et Recherches Technologiques (C2RT), Institut Pasteur, Paris, France

OPEN ACCESS

Edited by:
Monica Vaccari,
Tulane University,
United States

Reviewed by:
Constantinos Petrovas,
Centre Hospitalier Universitaire Vaudois (CHUV),
Switzerland
Haitao Hu,
University of Texas Medical Branch at Galveston,
United States

***Correspondence:**
Michaela Müller-Trutwin
mmuller@pasteur.fr

Specialty section:
This article was submitted to T Cell Biology, a section of the journal Frontiers in Immunology

Received: 14 April 2021
Accepted: 25 May 2021
Published: 16 June 2021

Citation:
Huot N, Rascle P, Planchais C, Contreras V, Passaes C, Le Grand R, Beignon A-S, Kornobis E, Legendre R, Varet H, Saez-Cirion A, Mouquet H, Jacquelin B and Müller-Trutwin M (2021) CD32$^+$CD4$^+$ T Cells Sharing B Cell Properties Increase Concomitantly With Simian Immunodeficiency Virus Replication in Lymphoid Tissues. Front. Immunol. 12:695148. doi: 10.3389/fimmu.2021.695148

CD4 T cell responses constitute an important component of adaptive immunity and are critical regulators of anti-microbial protection. CD4$^+$ T cells expressing CD32a have been identified as a target for HIV. CD32a is an Fcγ receptor known to be expressed on myeloid cells, granulocytes, B cells and NK cells. Little is known about the biology of CD32$^+$CD4$^+$ T cells. Our goal was to understand the dynamics of CD32$^+$CD4$^+$ T cells in tissues. We analyzed these cells in the blood, lymph nodes, spleen, ileum, jejunum and liver of two nonhuman primate models frequently used in biomedical research: African green monkeys (AGM) and macaques. We studied them in healthy animals and during viral (SIV) infection. We performed phenotypic and transcriptomic analysis at different stages of infection. In addition, we compared CD32+CD4+ T cells in tissues with well-controlled (spleen) and not efficiently controlled (jejunum) SIV replication in AGM. The CD32$^+$CD4$^+$ T cells more frequently expressed markers associated with T cell activation and HIV infection (CCR5, PD-1, CXCR5, CXCR3) and had higher levels of actively transcribed SIV RNA than CD32$^-$CD4$^+$T cells. Furthermore, CD32$^+$CD4$^+$ T cells from lymphoid tissues strongly expressed B-cell-related transcriptomic signatures, and displayed B cell markers at the cell surface, including immunoglobulins CD32+CD4+ T cells were rare in healthy animals and blood but increased strongly in tissues with ongoing viral replication. CD32$^+$CD4$^+$ T cell levels in tissues correlated with viremia. Our results suggest that the tissue environment induced by SIV replication drives the accumulation of these unusual cells with enhanced susceptibility to viral infection.

Keywords: SIV, HIV, CD4, CD20, LN, intestine, natural host, CD32

INTRODUCTION

HIV-infected individuals mount immune responses resulting in a decrease of viral load by the end of the acute infection but, even in HIV controllers, the host is not able of clearing the infection. Combined antiretroviral therapy (ART) has changed HIV infection from a lethal disease into a manageable chronic infection. Indeed, ART efficiently controls HIV replication leading to undetectable virus in the blood and considerably increasing the life expectancy of people living with HIV (PLH). However, the virus persists in cellular and anatomical reservoirs, from which the virus most often rapidly rebounds in case of ART interruption (1–3). Although tremendous progress has been made in our understanding of HIV biology and pathogenesis, the composition and dynamics of the viral reservoir and the mechanisms of HIV persistence remain ill-defined.

Studies in non-human primates (NHP) infected with SIVmac have shown that viral seeding occurs in the first hours and days post-infection (4, 5). Several factors can influence the establishment and persistence of HIV/SIV reservoirs, such as the timing of initiation of ART. When ART is initiated in primary infection, the subsequent long-term decline of the reservoir is stronger than if ART is initiated in chronic infection (6, 7). Immune activation could also modify viral seeding as well as related cell trafficking (8). Moreover, HIV reservoir cells can hide from the immune system by residing in anatomical sanctuaries (1, 9–11). Follicular helper T cells (T_{FH}) in B cell follicles of secondary lymphoid tissues (SLT) as well as Treg cells (CTLA-4$^+$ CD4$^+$ T cells) in the T zone of SLT have been shown to be potential major reservoirs of HIV/SIV viruses during ART (12–16). Many efforts have been made to identify cellular markers specific to reservoir cells, in particular latently infected cells, i.e. cells harboring viral DNA in the cellular genome without expressing viral proteins. It is though not excluded that low-level viral replication contributes to the viral reservoir. It has been shown that CD4$^+$ T cells expressing high CD2 surface levels harbor higher HIV DNA copy numbers (range, 3- to 10.8-fold) compared to total CD4$^+$ T cells (17). It has also been shown that cells expressing exhaustion markers such as PD-1, TIGIT, and LAG-3 were positively associated with the frequency of CD4$^+$ T cells harboring HIV DNA (18). Memory CD4$^+$ T cells co-expressing these three markers were up to 10-fold enriched for HIV compared to total CD4$^+$ T cells (18). In the blood of HIV-infected individuals on suppressive ART for more than 3 years, CXCR3$^+$CCR6$^+$ central memory CD4$^+$ T cells were shown to contain the highest amount of integrated HIV DNA and the lowest ratio of cell-associated (ca)-unspliced HIV RNA to DNA compared to all T-cell subsets studied (19). Blood CXCR3-expressing CD4 T cells represented the major blood compartment containing inducible replication-competent virus in treated aviremic HIV-infected individuals (20). CD30$^+$CD4$^+$ T cells have been shown to be enriched for ca-HIV RNA (21). However, this enrichment was not observed in all studied individuals, and CD30$^+$CD4$^+$ T cells were not significantly enriched for HIV DNA. CD20, normally expressed on B cells, has recently been described as a marker for HIV-infected cells in patients (22, 23). The use of latent reversal agents and anti-CD20 monoclonal antibody therapy allowed the depletion of a part of HIV-reservoir cells after viral reactivation *ex vivo* (23). CD32a (Fcγ RIIa)—a low-affinity IgG receptor known to be expressed on myeloid cells, granulocytes, NK cells and B cells (24), has been proposed as a surface marker for *in vitro* HIV-infected quiescent CD4$^+$ T cells and for persistent HIV-infected CD4$^+$ T cells in the blood of ART-treated PLH (25). Analyses of CD32$^+$ CD4$^+$ T cells in tissues from ART-treated PLH were associated with a T_{FH} phenotype, consistent with a role for CD32$^+$CD4$^+$ T cells in reservoir composition (26). Optimization of the CD32$^+$CD4$^+$ T cell purification protocol revealed significant enrichment for HIV DNA in these cells (27). Of note, several reports clearly showed that CD32 is not a marker for latently-infected CD4$^+$ T cells *in vivo* (22, 28–30). It was rather demonstrated that CD32 expression on CD4$^+$ T cells is frequently associated with actively transcribed virus (31). While CD32 is unlikely to be a marker of latently infected cells, the description of CD32$^+$CD4$^+$ T cells raises the question of the origin and the role CD32a$^+$CD4$^+$ T cells.

We addressed the question if a HIV infection favors the emergence of these cells. To determine the dynamics of CD32$^+$ CD4$^+$ T cells in distinct tissues *in vivo*, we studied two nonhuman primate models frequently used in biomedical research: African green monkeys (AGM) and macaques. Asian species of NHP, such as rhesus and cynomolgus macaques (MAC), experimentally infected by SIVmac, experience a spectrum of disorders similar to those seen in HIV-1 infected humans (32). Nonhuman primates from Africa, such as AGM, sooty mangabeys, and mandrills, are natural hosts of SIV (33–35). SIV infection in these natural hosts generally does not lead to any signs of disease, even though they carry high plasma and intestinal viral load (36, 37). An important common feature of SIV infection in natural hosts is that these animals rapidly resolve inflammation and consistently exhibit lower levels of immune activation than PLH or MAC infected with SIV (36). Natural hosts of SIV also harbor extremely low levels of infected CD4$^+$ T cells in lymph nodes (LN) and spleen in contrast to PLH and MAC infected with SIVmac (Huot et al., 2016). In this context, the difference in viral reservoir in SLT between the natural host and MAC could be useful to understand the dynamics of CD32$^+$CD4$^+$ T cells during HIV/SIV infection. We analyzed CD32$^+$CD4$^+$ T cells in healthy animals and during SIV infection. We performed phenotypic and transcriptomic characterization of CD32$^+$CD4$^+$ T cells at different stages of infection in lymphoid and non-lymphoid tissues (LN, spleen, jejunum, ileum, liver, blood). Since several studies suggested that these cells could correspond to doublets (28–30), we performed several controls including imaging experiments to ensure that the analyses were made on single cells. We show here that CD32$^+$CD4$^+$ T cells were not or only slightly increased in blood and liver, while strongly increased in LNs, spleen, and intestine during SIVmac infection. CD32$^+$CD4$^+$ T cells displayed higher levels of actively transcribed SIV RNA than CD32$^-$CD4$^+$ T cells in SLT and gut during both SIVmac and

SIVagm chronic infection. $CD32^+CD4^+$ T cell levels correlated with viremia. $CD32^+CD4^+$ T cells from lymphoid tissues shared properties with B cells (CD20, IgG, IgM) and also expressed markers that were described to be often expressed on HIV infected and/or reservoir cells (CCR5, PD-1, CXCR5, CXCR3). Our results support the hypothesis that $CD32^+CD4^+$ T cells are a target for productive viral replication and suggest that general immune activation and local inflammation drives the accumulation of these peculiar cells with enhanced susceptibility to HIV infection.

MATERIAL AND METHODS

Monkeys and SIV Infections

African green monkeys (Caribbean *Chlorocebus sabaeus*, AGM) and cynomolgus macaques (*Macaca fascicularis*, MAC) were included in this study (**Supplementary Figure 1**). The AGM were infected with SIVagm.sab92018, and the MAC with SIVmac251 as previously described (38, 39). The viremia levels are shown in **Supplementary Table 1**. All SIV-infected MAC where viremic.

The AGM and MAC were housed at the IDMIT Center (Fontenay-aux-Roses, France). All experimental procedures were conducted in strict compliance with the international European guidelines 2010/63/UE for the protection of animals used for experimentation and other scientific purposes and the French law (French decree 2013-118). The IDMIT center complies with the Standards for Human Care and Use of the Office for Laboratory Animal Welfare (OLAW, USA) under OLAW Assurance number A5826-86. Monkeys were monitored under the supervision of the veterinarians in charge of the animal facilities. Animal experimental protocols were approved by the Ethical Committee of Animal Experimentation (CETEA-DSV, IDF, France) (Notification 12-098 and A17-044). The pVISCONTI study was approved and accredited under statement number A15-035 by the ethics committee "*Comité d'Ethique en Expérimentation Animale du CEA*", registered and authorized under Number 2453-2015102713323361v2 by the French Ministry of Education and Research.

Monkeys were sedated before handling with Ketamine Chlorhydrate (Rhone-Mérieux, Lyons, France. The sample size varied from 3 to 9 monkeys per group (n = 6 in most experiments). Samples were collected in random order according to the tripartite harmonized International Council for Harmonization of Technical Requirements for Pharmaceuticals for Human Use (ICH) Guideline on Methodology (previously coded Q2B). The investigators were not blinded while the animal handlers were blinded to group allocation.

Tissue Collections and Processing

Whole venous blood was collected in ethylenediaminetetraacetic acid (EDTA) tubes. Peripheral blood mononuclear cells (PBMCs) were isolated by Ficoll density-gradient centrifugation. Biopsies of peripheral LNs (pLN) were performed by excision. Other tissues were collected at autopsy. After careful removal of adhering connective and fat tissues, pLN, spleen, liver, and gut tissue were dissociated using the gentlemacS™ Dissociator technology (Miltenyi Biotec, Germany). Red blood cells were lysed in hypotonic solution and washed twice in PBS. The cell suspension was subsequently filtered through 100- and 40-µm cell strainers, and cells were washed with cold phosphate-buffered saline (PBS). Cells were either immediately stained for flow cytometry or cryopreserved in 90% foetal bovine serum (FBS) and 10% dimethyl sulfoxide (DMSO) and stored in liquid nitrogen vapour.

Quantification of Viral Load

Viral RNA copy numbers in plasma and cell-associated (ca) viral DNA and RNA from the animals were quantified as previously described (38–40). For plasma, the cut-off value corresponded to 60 viral copies or below per ml of plasma. Ultrasensitive determinations of plasma viral loads were achieved by concentrating the virus from a larger volume of material available by ultracentrifugation. For the quantification of ca-viral DNA and RNA, total nucleic acids were extracted from cells sorted as described below. The number of cells analyzed for viral load was the same for each cellular fraction of each sample. The relative fold-change of SIV transcripts was determined using the delta-delta CT method normalized to the 18s RNA levels, as described (38).

Production of Recombinant Anti-CD32 Monoclonal Antibody

IgH and IgL DNA fragments coding for human MDE8 (41) antibody were prepared by PCR-amplification from codon-optimized synthetic genes (Life Technologies, Thermo Fisher Scientific). Purified digested DNA fragments were cloned into human Igγ1-and Igλ-expressing vectors (42), and human MDE8 IgG1 antibod-ies were produced by transient co-transfection of Freestyle™ 293-F suspension cells (Thermo Fisher Scientific) using PEI-precipitation method as previously described (43). Recombinant IgG1 antibodies were purified by batch/gravity-flow affinity chromatog-raphy using protein G sepharose 4 fast flow beads (GE Healthcare, Chicago, IL) according to the manufacturer's instructions, extensively dialyzed against PBS using Slide-A-Lyzer® dial-ysis cassettes (Thermo Fisher Scientific) and quantified using NanoDrop 2000 instrument (Thermo Fisher Scientific) (43).

Polychromatic Flow Cytometry

Cryopreserved cells were thawed in foetal bovine serum. Cryopreserved or freshly isolated cells were counted, examined for viability, and then incubated with Fcγ receptor blocker from Biolegend for 10 minutes. Undiluted extracellular antibody cocktail mix was added and incubated for 20 minutes. All incubations were performed in the dark at room temperature. If no intracellular staining was done, the cells were washed, fixed with a 4% paraformaldehyde solution and stored in the dark at 4°C until acquisition. Intracellular staining was performed as follows: after staining for cell surface molecules, cells were fixed/permeabilized using the "BD Cytofix/Cytoperm Plus Fixation/Permeabilization" kit. Intracellular markers were stained with the antibody cocktail for one hour. Finally, cells were fixed with a 4% paraformaldehyde solution and stored in the dark at 4°C until

acquisition. All phenotyping data were acquired on a BD FACS LSR II (BD Biosciences) or on a LSR Fortessa (BD Immunocytometry Systems). The data were further analyzed using FlowJo 10.4.2 software (FlowJo, LLC, Ashland, OR, USA). *T*-SNE was performed using FlowJo isuali FlowJo, LLC, Ashland, OR, USA). The antibodies used are listed below: anti-CD45 (clone D058-1283, BD bioscience); anti-CD3 (clone SP34-2, BD bioscience); anti-CD4 (clone L200, BD bioscience); anti-CD32 (cloneFLI8.26)(BD bioscience); anti-CD20 (clone 2H7, (BD bioscience); anti-CD14 (clone TÜK4,M iltenyi Biotec); anti-CD28 (clone CD28.2, BD bioscience); anti-CD95 (clone DX2, BD bioscience), anti-CXCR3 (clone 1C6/CXCR3, BD bioscience); anti-CXCR5 (clone MU5UBEE, Ebioscience); anti-PD-1 (clone EH12.1, BD bioscience), anti-CXCR4 (clone 12G5,B D bioscience); anti-CCR5 (clone 3A9, BD bioscience); anti-CD86 (clone FUN-1, BD bioscience); anti-CD83 (clone HB15e, BD bioscience); anti-CD39 (clone A1, Biolegend); anti-CD25 (cloneM-A251, BD bioscience); anti-MHC-E (clone 3D12HLA-E, ebioscience), anti-TIM-3 (clone 7D3, BD bioscience); anti-CD8alpha (clone SK1, BD bioscience); anti-NKG2a/c (clone Z199, Beckman-Coulter); anti-IgG (cloneG18-145, BD bioscience); anti-IgM (clone G20-127, BD bioscience). The anti-CD32 antibody used recognizes CD32A and not the CD32B isoform.

Immunofluorescence Staining

Purified splenic CD4 T cells were isolated from five MAC and five AGM, using a MACS negative selection CD4 T Cell Isolation Kit (Miltenyi Biotec, Boston, MA). Cells were then adhered to the poly-l-lysine-coated glass slides at 37°C in RPMI 1640 containing 10% FCS. After 2 hours, CD4 T cells were prepared for fixed cell immunofluorescent confocal microscopy. Briefly, cells were blocked with 5% heat-inactivated goat serum in PBS for 20 min at room temperature. Anti CD20-APC (clone 2H7), anti CD4-alexa700 clone (clone L200), and anti CD32 antibodies described in the method section were added to the culture for 1h. Antibodies were used in the range of 0.5–2 μg/ml. The slides were rinsed in PBS containing 2% FCS and the cells were fixed and permeabilized. A secondary goat α-human IgG conjugated to Alexa Fluor 488 (Molecular Probes, Grand Island, NY) was used to detect the anti-CD32 antibody. Slides were then covered with 0.15-mm coverslips (VWR Scientific, Philadelphia, PA), using mounting media (Vectashield, Burlingame, CA) containing DAPI (Invitrogen, Carlsbad, CA) to visualize nuclear chromatin. Two-dimensional micrographs were taken using a multilaser-based spinning disk confocal microscope (Zeiss).

Cell Sorting of CD32$^+$CD4$^+$ T Cells

We performed cell sorting on frozen spleen and jejunum from chronically infected MAC or AGM. All incubations were performed in the dark at room temperature. Cells were thawed in 20% FBS-containing media supplemented with benzonase nuclease and counts and viabilities were performed (Life Technologies). Cells were incubated with Fcγ receptor blocker for 10 minutes. The antibody cocktail mix was added and incubated for 20 minutes. A viability dye for flow cytometry (LIVE/DEAD Fixable Dead Cell Stain Kit, Invitrogen) was included in all experiments to determine cell viability. The antibodies used are listed below: anti-CD45 (clone D058-1283) (BD bioscience); anti-CD3 (clone SP34-2) (BD bioscience); anti-CD4 (clone L200) (BD bioscience); anti-CD32 (cloneFLI8.26) (BD bioscience); anti-CD20 (clone 2H7, BD bioscience); anti-CD14 (clone TÜK4, Miltenyi Biotec); anti-CD8alpha (clone SK1, BD bioscience); anti-NKG2a/c (clone Z199, Beckman-Coulter). After surface staining, cells were washed and resuspended in complete medium and stored in the dark at 4°C until acquisition. Cells were sorted on a FACSAria II (BD Biosciences) in purity mode. The gating strategy is shown in **Supplemental Figure 1**. Doublet cells were excluded from the sorting using the FSC-H and FSC-A parameters. For RNA extraction, cells were directly collected in a lysis buffer containing TCEP (Qiagen). The purity of the cells was >97%.

Genome-Wide RNA Sequencing

RNA was isolated from the sorted cell populations using the Rneasy® Mini Kit (205113, Qiagen). RNA integrity was checked using the Agilent Bioanalyzer System. Dnase-treated RNA was treated for library preparation using the Truseq Stranded mRNA Sample Preparation Kit (Illumina, San Diego, CA), according to manufacturer's instructions. An initial poly(A) RNA isolation step (included in the Illumina protocol) is performed on 10 ng of total RNA to keep only the polyadenylated RNA fraction and remove the ribosomal RNA. A fragmentation step is then performed on the enriched fraction, by divalent ions at high temperature. The fragmented RNA samples were randomly primed for reverse transcription, followed by second-strand synthesis to create double-stranded cDNA fragments. No end repair step was necessary. An adenine was added to the 3'-end and specific Illumina adapters were ligated. Ligation products were submitted to PCR amplification. The obtained oriented libraries were controlled by Bioanalyzer DNA1000 Chips (Agilent, # 5067-1504) and quantified by spectrofluorimetry (Quant-iT^{TM} High-Sensitivity DNA Assay Kit, #Q33120, Invitrogen). Sequencing was performed on the Illumina Hiseq2500 platform to generate single-end 100 bp reads bearing strand specificity.

Bioinformatic Analysis of the Genome-Wide Sequence Data

Bioinformatic analyses were performed using the RNA-seq pipeline from Sequana (44). Reads were cleaned of adapter sequences, and low-quality sequences were removed using cutadapt version 1.11. Only sequences ≥ 25 nucleotides (nt) in length were considered for further analysis. STAR version 2.5.0a, with default parameters, was used for alignment on the reference genome (*Chlorocebus sabaeus*, from Ensembl release 90). Genes were counted using featureCounts version 1.4.6-p3 (45) from Subreads package (parameters: -t gene, -g ID and -s 1).

Data were analyzed using R version 3.4.3 and the Bioconductor package DESeq2 version 1.18.1. Normalization and dispersion estimation were performed with DESeq2, using the default parameters, and statistical tests for differential expression were performed by applying the independent filtering algorithm. A generalized linear model, including the

monkey identifier as a blocking factor, was used to test for the differential expression between the biological conditions. For each pairwise comparison, raw p values were adjusted for multiple testing according to the Benjamini and Hochberg (BH) procedure (46). Genes with an adjusted p value <0.05 were considered differentially expressed.

Analyses and visualization of GO terms associated with differentially expressed genes were performed using **ClueGO** (47). Both groups of genes (up- and downregulated, p value < 0.05) were used as dual input for GO and pathway annotation networks of the expressed genes and proteins pathway enrichment analysis. Each list was used to query the Kyoto Encyclopedia of Genes and Genomes (KEGG), GO-biological function database and Wiki pathways. ClueGo parameters were set as follows: Go Term Fusion selected; only display pathways with p values ≤ 0.05; GO tree interval, all levels; GO term minimum genes, 3; threshold of 4% of genes per pathway; and a kappa score of 0.42. GO terms are presented as nodes and clustered together based on the similarity of genes present in each term or pathway. The most significant term was chosen as a representative of the group (Benjamini-Hochberg correction).

Statistical Analyses

Continuous variables were compared between groups throughout using non-parametric tests. Where three groups were compared, a Kruskal–Wallis test was used; pairwise comparisons were performed on all combinations of groups only if the overall test *p*-value was <0.05. To compare differences between two independent groups, the Mann-Whitney U test was used. Correlative analyses were performed using Spearman's rank correlation. Correlation analyses were performed according to the Spearman coefficient of correlation.

Analyses were performed using GraphPad Prism (GraphPad Software, La Jolla, CA, USA) version 7.0 or R version 3.2.2.

RESULTS

Tissue-Dependent Dynamics of CD32$^+$CD4$^+$ T Cells in Response to SIV Infection

To track and characterize CD32$^+$CD4$^+$ T cells within tissue compartments, we first performed a longitudinal measurement of CD32$^+$CD4$^+$ T cells in tissues before infection and during SIV infection in a natural host (AGM, N=17 animals) and a heterologous host (MAC, N=18 animals). AGM from the sabaeus species and cynomolgus MAC were respectively infected with the wild-type SIVagm.sab92018 and the SIVmac251 isolate (**Table S1**). We analyzed blood, LNs, spleen, ileum, jejunum and liver from uninfected, acutely infected and chronically infected animals (**Table S1**).

To quantify the frequency of CD4$^+$ T cells expressing CD32, we used for comparison CD32 expression levels on myeloid cells. The latter are well known to express high levels of CD32. We specifically defined a CD32 gate for each tissue and monkey using the level of expression of CD32 on blood monocytes as an internal positive control and fluorescence minus one (FMO) as a negative control (**Figure 1A** and **Figure S1**). The median of CD32$^+$CD4$^+$ T cells in blood, peripheral LN (pLN), spleen, liver, ileum, jejunum was 0.59%, 1.23%, 1.15%, 3.02%, 2.45% and 0.65%, respectively, in MAC and 0.53%, 0.32%, 0.79%, 3.62%, 4.11% and 3%, respectively, in AGM. After SIV infection, we observed an increase in CD32$^+$CD4$^+$ T cells in all lymphoid tissues (pLN, spleen, ileum and jejunum) of SIVmac-infected MAC, the average levels varying between 4.5% and 19% (**Figure 1B**). During SIVagm infection, a significant increase in CD32$^+$CD4$^+$ T cells was seen in the jejunum but not in LN (**Figure 1B**). Of note, the frequencies of CD32$^+$CD4$^+$ T cells were not increased in blood for neither MAC nor AGM, although we cannot exclude modest increases in some MAC. Altogether, these results showed that CD32$^+$CD4$^+$ T cells increased more in lymphoid tissues than in blood during SIV infection. CD32$^+$CD4$^+$ T cells were increased in both SLT and gut during SIVmac infection, but only in gut during chronic SIVagm infection.

Increases in Viremia of SIV-Infected African Green Monkeys Are Associated With Increases in Tissue CD32$^+$ CD4$^+$ T Cell Frequencies

We wondered whether the lower increase of CD32$^+$CD4$^+$ T cells in SLT of AGM could be related to the strong control of SIV replication in SLT. To address this question, we investigated the levels of CD32$^+$CD4$^+$ T cells in NK-cell depleted AGMs infected with SIV. We and others have previously shown that anti-IL-15 treatment efficiently depletes NK cells *in vivo* in NHP (38, 48). Such NK cell depletion in chronically infected AGM increased both viremia as well as ca-viral DNA and RNA in SLT (38). We retrospectively monitored the frequency of CD32$^+$CD4$^+$ T cells from blood and LN of anti-IL15-treated and non-treated chronically infected AGM. There was an increase at day 42 post-anti-IL-15 of CD32$^+$CD4$^+$ T cells in blood and LN after NK cell depletion when compared to the frequency of these cells before anti IL-15 treatment (**Figures 1C, D**). We also compared the frequencies before and after NK cell depletion in other tissues (spleen, ileum, jejunum and in liver) (**Figures 1E, F**). There was a trend toward an increase in CD32$^+$CD4$^+$ T cells in the lymphoid tissues, such as ileum, but not in the liver (**Figure 1F**). The frequencies of CD32$^+$CD4$^+$ T cells in blood at day 42 post-anti-IL-15 correlated with viremia levels and there may be a trend toward correlation of CD32$^+$CD4$^+$ T cells with ca-viral DNA in the LN (**Figures 1G, H**). Taken together, these results show that CD32$^+$CD4$^+$ T cell frequencies increased in chronically infected AGMs in blood and LN, concomitant with an experimentally induced increase in viremia.

CD32$^+$CD4$^+$ T Cells Are Enriched for SIV RNA in Secondary Lymphoid Tissues and Intestine

We next determined the level of viral replication in CD32$^+$CD4$^+$ T cells in tissues. We quantified ca-SIV RNA in CD32$^+$CD4$^+$ T cells from SLT (spleen) and intestinal mucosa (jejunum) of chronically infected MAC and AGM. The CD32$^+$ and CD32$^-$

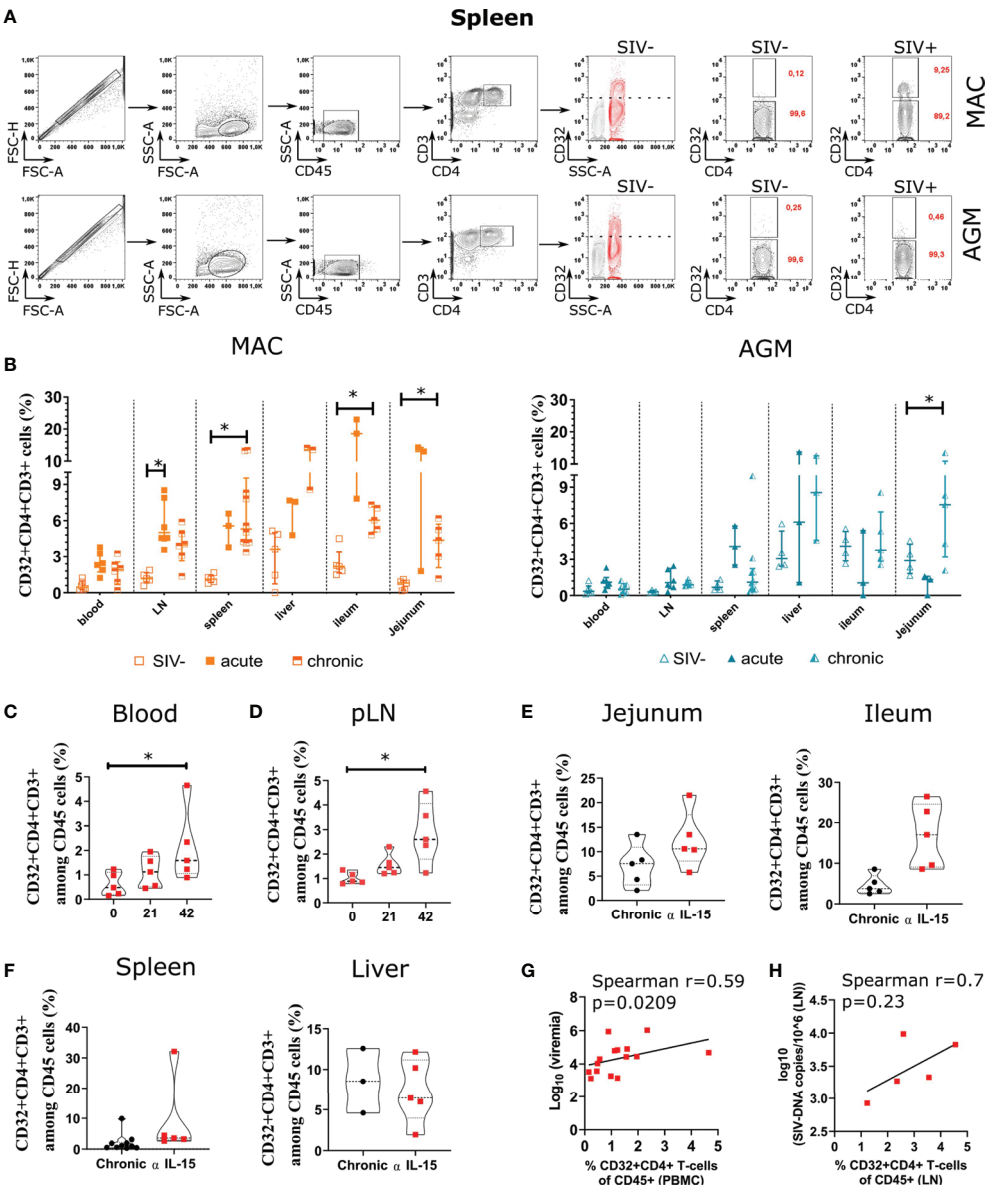

FIGURE 1 | Quantification of CD4+ T cells expressing CD32 and/or viral RNA in tissues during pathogenic and natural host SIV infections. **(A)** Representative gating strategy for CD32+CD4+ T cells. A representative example from the spleen of a chronically infected cynomolgus macaque (MAC) (upper part), and a chronically infected AGM (lower part) are shown. The position of the $CD32^+$ gate on CD4+ T cells was chosen according to the level of CD32 expression on myeloid cells (overlaid red population) in SIV-negative monkeys. In red is indicated the percentage of the gated population in both SIV- and SIV+ monkeys. **(B)** Graphs showing the frequency of CD32+CD4+ T cells in six tissues in SIV-uninfected, SIV acutely infected (day 9 p.i.) and SIV chronically infected MAC (orange) and AGM (blue). Values indicate the percentage of CD32+CD4+ T cells among total CD4+ T cells. Each individual monkey is represented by a square (MAC) or a triangle (AGM). The number of animals analyzed varied from three to six, depending on the compartment and time point studied. Time points or tissues with only three animals corresponding to liver and acute infection in gut were not included in the statistical comparisons. **(C, D)** Dynamics of CD32+CD4+CD3+ cells in blood and pLN of chronically SIV-infected AGM before, during and after anti-IL-15 administration. CD4+T cells were analyzed in blood and pLN before and at days 21 and 42 after initiation of anti-IL-15 treatment. The anti-IL-15 treatment of the chronically infected AGM (n=5 animals) has been previously reported (38). Violin plots showing the frequency of CD32+ CD4+T cells among CD45+ cells in blood **(C)** and pLN **(D)** in non-treated and anti-IL-15 treated chronically SIV-infected AGM. **(E, F)** Comparison of CD32+CD4+ T cells in tissues at necropsy, between chronically infected AGM treated or not with anti-IL-15. Violin plots show the distribution of CD32+CD4+CD3+ cells among CD45+ cells from chronically infected AGM (black) and anti-IL-15 treated chronically infected AGM (red) in the indicated tissue. **(G)** Frequencies of CD32+CD4+ T cells in PBMC of treated animals (day 42 post-anti-IL15) were plotted against viremia levels. **(H)** The frequencies of CD32+CD4+ T cells of treated animals (day 42 post-anti-IL15) were plotted against ca-viral DNA in LN. In **(B)**, statistical differences were assessed by ANOVA with Tukey adjustment for multiple comparisons. In **(C–F)**, a Kruskal-Wallis test was applied. Asterisks indicate p-values < 0.05. Each symbol represents a single animal.

$CD4^+$ T cell fractions were isolated by cell sorting. Cells were gated as Lin-$CD45^+CD3^+CD4^+CD32^+$/- (**Figure S1**). We detected viral RNA in each cellular fraction in all monkeys and all tissues analyzed. With the exception of the spleen of one chronically infected MAC, SIV RNA levels in the $CD32^+CD4^+$ T cell fraction were always higher compared to the $CD32^-CD4^+$ T cell fraction (**Figures 2A, B**). In the spleen, the fold change difference (median) of SIV ca-RNA was 12.4 and 3.9 in MAC and AGM, respectively, whereas in the jejunum it was 11.9 and 10.3 in MAC and AGM, respectively. Thus, $CD32^+CD4^+$T cells displayed higher levels of actively transcribed SIV RNA than $CD32^-CD4^+$T cells in SLT and gut in both SIVmac and SIVagm chronic infection. In SIVagm infection, the difference was less pronounced in SLT than in gut, consistent with lower viral replication levels in SLT of AGM.

$CD32^+CD4^+$ T Cells in Secondary Lymphoid Tissues Express Markers of Activation and Preferential SIV Infection

We next assessed the phenotype of $CD32^+CD4^+$ T cells in SLT and gut. In a first step, we compared differentiation, homing, and exhaustion markers by multiparameter flow cytometry on $CD32^+$ versus $CD32^-CD4^+$ T cells from blood, peripheral LN, spleen, ileum, and jejunum of chronically infected MAC and AGM. $CD32^+CD4^+$ T cells in blood and SLT were frequently $PD\text{-}1^+$ compared to the respective $CD32^-$ population in both species (**Figure 3A**). In SLT, $CD32^+CD4^+$ T cells also expressed more often CXCR5 and also more often CXCR3 in the spleen than $CD32^-CD4^+$ T cells in both MAC and AGM. In the gut, $CD32^+CD4^+$ T cells were also more often PD-1+, $CXCR5^+$ and/or $CXCR3^+$ than respective $CD32^-$ cells in AGM. Given the common markers between TFH and $CD32^+CD4^+$ T cells, we analyzed if there is a correlation between these two cell populations. The TFH cell frequency correlated positively with the frequency $CD32^+CD4^+$ T cells in the pLN (**Figure S2**). Allover, $CD32^+CD4^+$ T cells expressed more frequently markers that were described to be often expressed on HIV-infected and/or HIV-reservoir cells in lymphoid tissues (i.e. PD-1 and CXCR5 in blood and SLT; CXCR3 in blood, SLT and mucosa) (8, 12, 14, 18–21).

We next turned our attention to the main co-receptors of SIV (CXCR4, CCR5), as well as markers known as evidence of activation (CD25), IFN-stimulation (CD83, CD86, MHC-E) and regulation (CD25, CD39, CD83, and TIM-3), with a focus on SLT (spleen and pLN) (**Figures 3B, C**). Strikingly, the differences between $CD32^+$ and $CD32^-CD4^+$ T cells for all these 8 markers were generally the same for both species, indicating that the differences were not random. For instance, the frequencies of $CD32^+CD4^+$ T cells positive for CD25, CD39, CD83, CD86, and MHC-E were higher as for $CD32^-CD4^+$ T cells in both pLN and spleen of MAC and AGM. The $CCR5^+CD4^+$ T cells were also more frequent in the spleen within the $CD32^+$ than the CD32- fraction in both species. Most of the $CD32^+CD4^+$ T cells also expressed CXCR4, although not to higher levels than the $CD32^-$ cells because CXCR4 expression was already frequent among the latter. TIM-3 was most often increased in the $CD32^+$ fraction of SLT as well (**Figure 3C**). All these markers were thus either similar or more frequent within the $CD32^+CD4^+$ T cells when compared to the $CD32^-$ cells. CD25 is well known to be up-regulated upon $CD4^+$ T cell

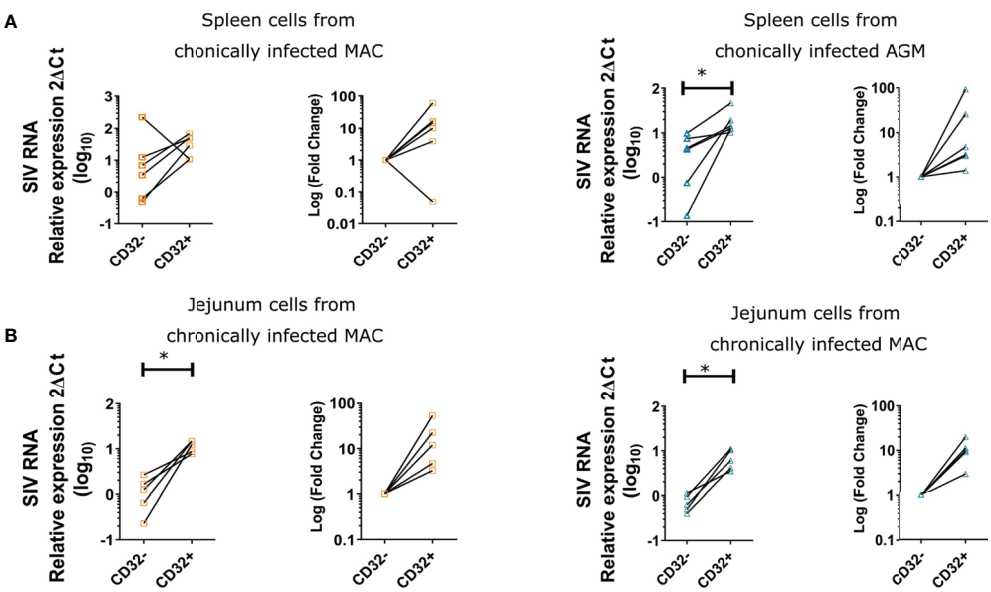

FIGURE 2 | Quantification of ca-SIV RNA in CD32+ and CD32- CD4+ T cells. Cells were isolated from **(A)** spleen and **(B)** jejunum of chronically infected MAC and AGM. Graphs show the ca-SIV RNA amount relative to 18sRNA (left graph) and the fold change in ca-SIV RNA in $CD32^+$ cells compared to $CD32^-$ $CD4^+$ T cells (right graph) for each species. The amount of RNA in $CD32^-$ cells of each respective tissue was arbitrarily set to 1. Orange symbols refer to MAC and blue symbols to AGM. Each symbol represents a single animal. Statistical difference was assessed by a Mann-Whitney U-test. Asterisks indicate p-values < 0.05.

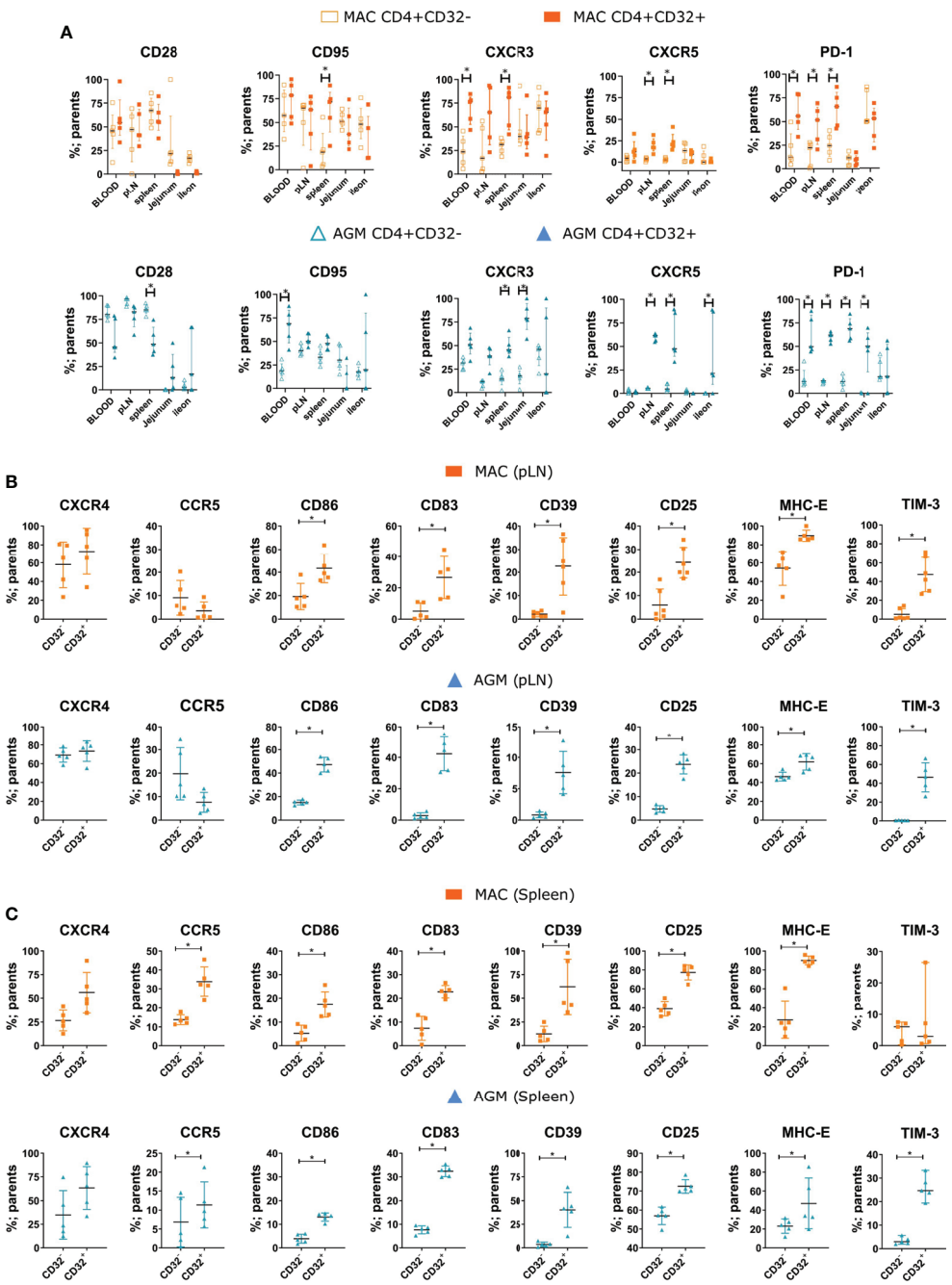

FIGURE 3 | Phenotypic characterization of CD32+CD4+ T cells in tissues during SIV infection. **(A)** Frequencies of the indicated marker on $CD32^-$ (empty symbols) and CD32+ (full symbols) for CD4+ T cells from different tissues during chronic SIV infection in MAC (orange) and AGM (blue). **(B, C)** Frequency of $CD32^-$ and CD32+CD4+ T cells expressing a given marker in **(B)** peripheral LN (pLN) and **(C)** spleen during chronic SIV infection in MAC (orange) and AGM (blue). Each symbol represents a single animal (N=5 animals for each species). In **(A)**, two-way *ANOVA* with *Sidak* test for multiple comparisons was performed. In **(B, C)**, statistical difference was assessed by a Mann-Whitney U-test. Asterisks indicate p-values < 0.05.

activation and can be expressed at high levels on Treg. TIM-3 is known to be expressed by a subset of activated or exhausted $CD4^+$ T cells and by polarized Th1 cells (49). CD39 is known to be found on activated $CD4^+$ T cells with signs of metabolic stress (50, 51). There is increasing evidence that CD83 regulates $CD4^+$ T cell development and peripheral activation (52–54). Altogether, these results suggest that $CD32^+CD4^+$ T cells are in a more activated state than $CD32^-CD4^+$T cells.

CD32+CD4+CD3+ Cells Show Up-Regulated Expression of Genes Associated With B Cell Function

To investigate on a global scale, using a non-hypothesis-driven approach, the markers that distinguish CD32+ from CD32-CD4+ T cells in lymphoid tissues during SIV infection, we determined their genome-wide transcriptomic signature. CD32+CD4+ and CD32-CD4+ T cells were isolated as described above (**Figure 1A** and **Figure S1**). Cells were isolated from the spleen of three chronically SIVmac-infected MAC and three chronically SIVagm-infected AGM. CD32+ CD4+ and CD32- CD4+ T cells clustered separately (**Figure 4A**) in both MAC and AGM. There were 881 and 1665 differentially expressed genes in CD32+ compared to CD32-CD4+ T cells for MAC and AGM, respectively (**Figure 4A** and **Table S2**). The genes that showed the highest expression in CD32+CD4+ T cells included T cell receptors (TRAV, CD3), but also many genes related to the B cell receptor rearrangement and other B cell markers, such as BANK1, a B cell transcription factor (**Figure 4B**). We also found upregulation of TBC1D9, a key regulator of TBK1. We did not found genes specifically related to the myeloid lineage, with one exception. Indeed, we observed an up-regulation of CD68 mRNA expression in CD32+ T cells of AGM (**Table S2**). However, any other classical monocyte-related gene, such as CD14, was not up-regulated. It has been shown that low levels of CD68 can be expressed in lymphoid cells such as CD19+ B lymphocytes and CD4+ T lymphocytes (55). Moreover, in vitro stimulation with T-cell mitogen or recombinant interleukin-2 (rIL-2) induced expression of CD68 antigen in activated CD4+ and CD8+ T lymphocytes (56). Thus, higher expression of CD68 in the CD32+ T cells is in agreement with CD32+ T cells harboring a higher state of activation than their CD32- counterpart.

To analyze the activation state of the cells, we assessed the level of major histocompatibility complex II (MHC II) receptor expression in CD32+CD4+ T cells. The level of HLA-DR transcripts in CD32+CD4+ T cells was higher compared with CD32-CD4+ T cells. Moreover, CD32+CD4+ T cells also expressed higher levels of MHC class II-transcripts encoding HLA-DP, -DQ, -DO, and -DM (**Figure 4C**).

We next analyzed in more detail all surface markers that were up- or down-regulated on the CD32+ cells compared to the CD32- fraction (**Figure 4D**). Ninety-four genes encoding surface markers were differentially modulated in MAC and AGM together, out of which 38 genes were common between MAC and AGM (**Figure S3**). Many of these common genes that were up-regulated in the CD32+ cells are normally attributed to the B cell lineage, such as *MS4A1* (CD20), *CD22, CD40, CD72, CD79b, CD83 and CD74*, whereas transcripts encoding the CD4+ T cell lineage (i.e., *CD4, CD3e, CD3D, CD28, ICOS, CD5, IL7r, CTLA-4, and IL2RB*) were less expressed in CD32+ cells compared to CD32-CD4+ T cells (**Figure 4D** and **Figure S2**). Down-regulation of CD3 chains and CD4 mRNA is typical for activated CD4+ T cells (57–59). Both isoforms of CD32 were expressed, the CD32a isoform being less frequent than the CD32b isoform.

Cell types are also defined by transcription factors. We focused on the transcription factors that were commonly up- or down-regulated by CD32+CD4+ T cells in both MAC and AGM when compared to the CD32- fraction (**Figure 4E**). Fifty-five genes encoding transcription factors were differentially modulated between the CD32+ and CD32- fractions in AGM and MAC (**Figure S4**). The CD32+ fraction expressed a high number of transcription factors linked to the B cell lineage, such as *PAX5*, whereas some key transcription factors for the T cell lineage were less expressed than in the CD32-CD4+ fraction (i.e. *BCL11B*, *GATA3*, *Notch1*).

We next attempted to understand the interferon-stimulated gene (ISG) expression profiles in the CD32+CD4+ T cells when compared to the CD32-CD4+ T cells. Many ISGs are known, and we included in particular those ISGs which are considered to have an antiviral function (60). The number of ISGs that were expressed to higher levels in CD32+ compared to CD32-CD4+ T cells was moderate: only 11 and 2 ISGs out of 41 ISGs analysed in, respectively, AGM and MAC (**Figure S5**). CD74 was the only ISG among those analysed that was commonly up-regulated in the CD32+ CD4+ T cells in both MAC and AGM.

To decipher the major functional pathways activated in the CD32+ and CD32- fractions, a Gene Ontology (GO) enrichment analysis was performed (**Figure S6A** and **Tables S3**, **S4**). Most of the pathways that were up-regulated both in MAC and AGM during SIV infection belonged to B cell receptor signaling pathways, while the pathways that were often down-regulated in both MAC and AGM in the CD32+CD4+ T cells as compared to the CD32- fraction belonged to pathways involved in TCR signaling, T cell activation and differentiation (**Figure S6A** and **Tables S3**, **S4**). This was particularly true for CD32+ CD4+ T cells from MAC compared to AGM (**Figure S6B** and **Table S5**). Overall, this shows that the CD32+ cell fraction expressed many genes and pathways specific for B cells.

CD32+CD4+CD3+ Cells Shared Phenotypic and Functional Aspects of B Cells

The genome wide RNAseq thus revealed the expression of many genes associated with B cell function in the CD32+CD4+ T cells. This presence of a strong B cell signature within CD4+ T cells is generally unusual. We controlled for potential cell doublets. We coated freshly sorted spleen CD4+ T cells from chronically infected MAC and AGM and stained them for expression of CD4, CD20 and CD32. Confocal microscopy revealed the existence of cells co-stained positive for the three markers (**Figures 5A, B**). Most of the cells were CD3+CD4+CD32- CD20- (>1.5 log more frequent than CD3+CD4+CD32+CD20- cells). The CD20- and CD20+ frequencies among CD32+CD4+ T cells were comparable. Cells staining positive for CD20 were also observed within the CD32- fraction but represented 1 log fewer cells than within CD32+ cells. This distribution was similar in MAC and AGM.

We then compared such CD32+ CD4+ T cells expressing CD20 to other immune cell subsets in the spleen. We performed a force-directed clustering analysis of total spleen cells isolated from chronically SIV-infected MAC and AGM based on the

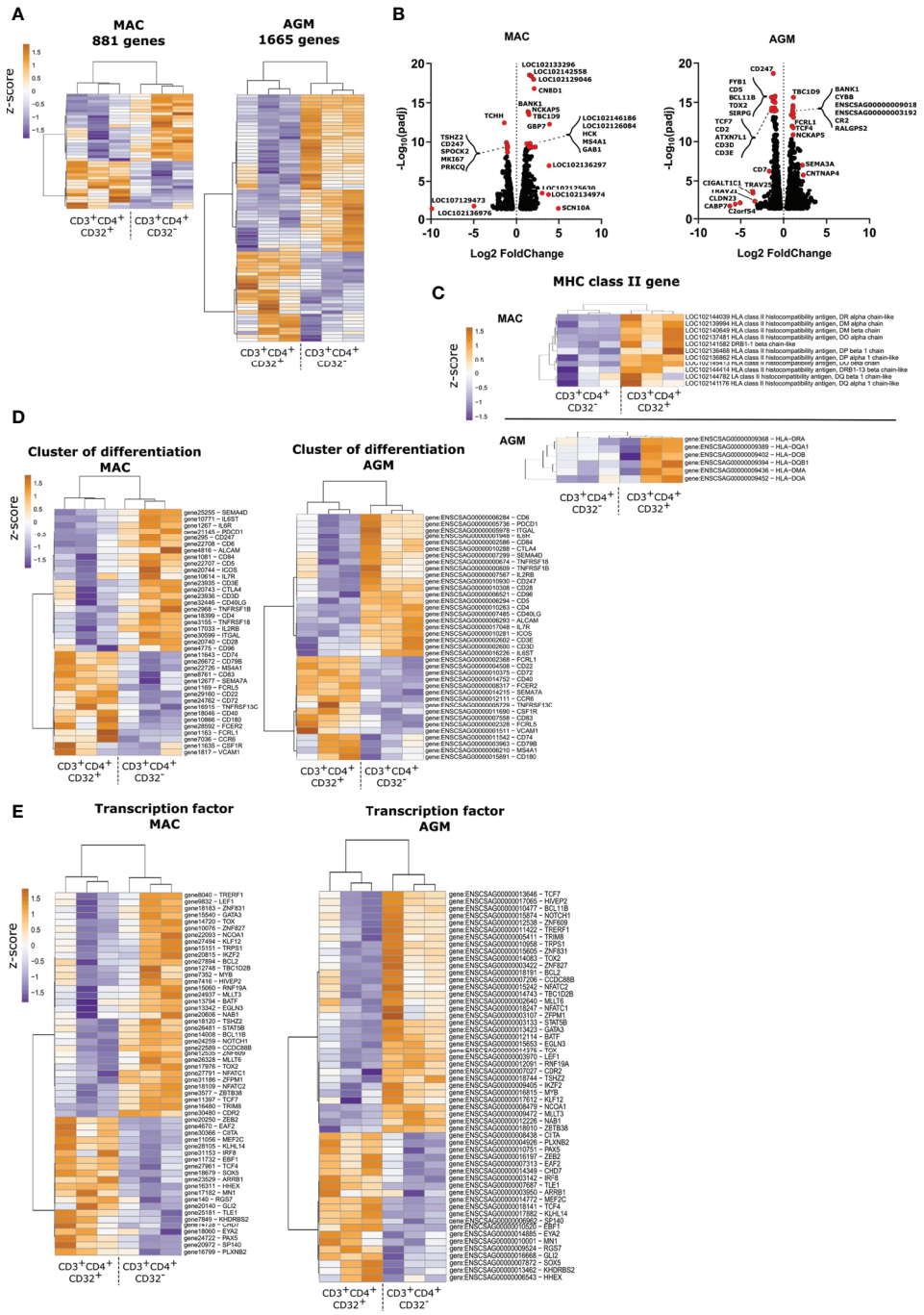

FIGURE 4 | Genome-wide transcriptome analysis of CD4+ T cell subsets according to CD32 expression from spleen during pathogenic and non-pathogenic SIV infection. **(A)** Heatmaps of transcript signatures in CD32+ and CD32$^-$CD4+ splenic T cells from chronically SIV-infected MAC and AGM. **(B)** Volcano plots of gene regulation between CD32+ and CD32$^-$ CD4+ T cells. Red dots represent highly differentially regulated genes. Many of them are associated with the B cell lineage. **(C, E)** Heatmaps showing **(C)** MHC-II molecules **(D)** cluster of differentiation transcripts and **(E)** transcription factors mRNA levels on CD4+ T cell subsets according to CD32+ expression. In each panel, subsets were organized based on the overall similarity in gene expression patterns by an unsupervised hierarchical clustering algorithm of variable genes. A dendrogram, in which the pattern of branch length reflects the comparative difference in gene expression profiles between samples is shown. A p-value adjustment was performed to account for multiple comparisons and control the false positive rate to a chosen level. Transcriptome similarity between clusters of spleen sample was evaluated by the Euclidean distance and visualized *via* heatmap. Each row represents a variable gene among clusters, and each column represents one subset per monkey. Deep sequencing results were deposited in the Gene Expression Omnibus database; the accession number is GSE169736.

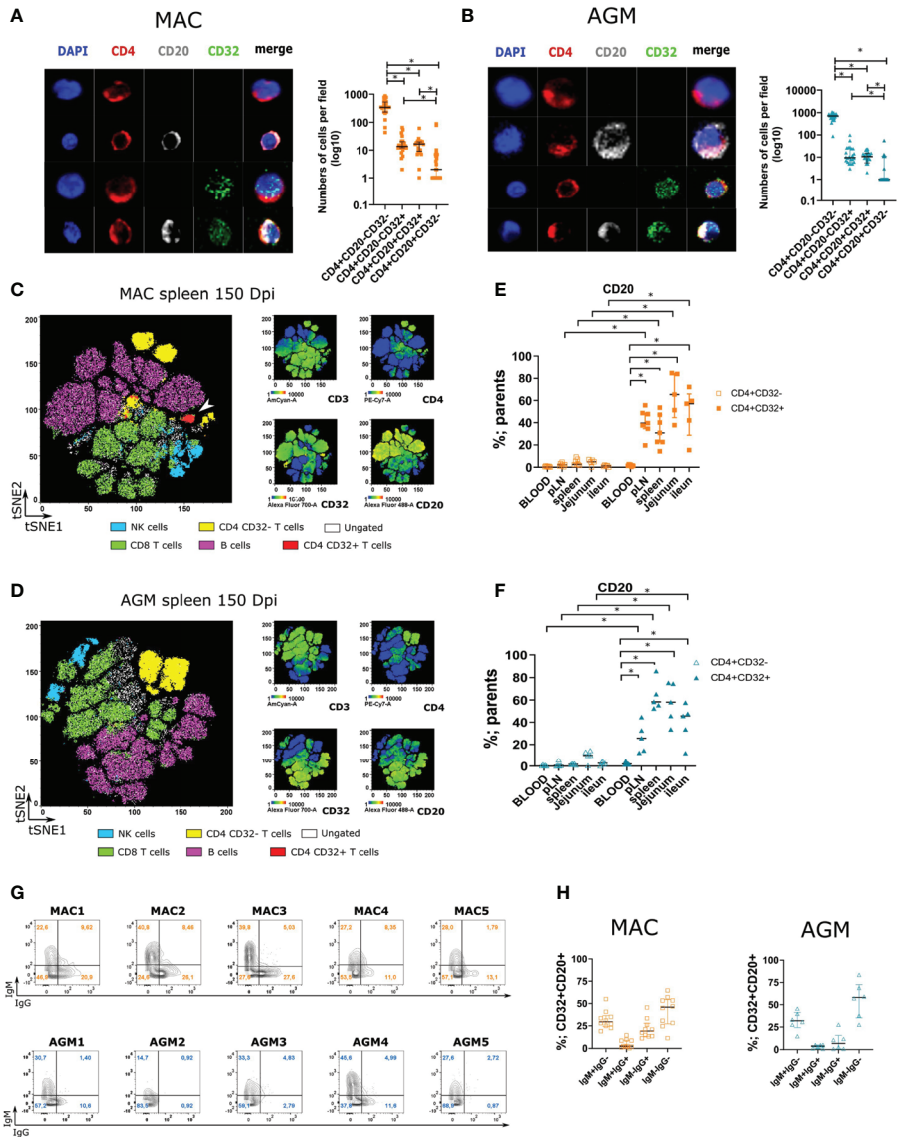

FIGURE 5 | Analyses of CD32+CD4+CD3+ cells expressing CD20 in the spleen of SIV-infected animals. **(A, B)** Confocal images of CD4+ T cells according to CD4, CD20, and CD32 staining. Staining was performed on CD4+CD3+ cells isolated from chronically SIV-infected MAC **(A)** and AGM **(B)**. Graphs with cell numbers per field are shown on the right. The experiment was performed with samples from three monkeys per species and eight fields were counted per monkey. **(C, D)** viSNE map representing concatenated spleen cells from 6 MAC **(D)** and 6 AGM **(C)**. Cells were stained with 9 markers and measured by flow cytometry. viSNE analysis was performed on 60000 live CD45$^+$ single cells per sample using all 8 surface markers. viSNE map shows concatenated flow cytometry standard files for all **(C)** MAC and **(D)** AGM samples. Overlay of 6 manually gated cell populations on viSNE plots, defined as: CD8+T cells (live, CD45+CD3+CD8+), NK cells (live, CD45+ CD3-NKG2a+), B cells (live, CD45+CD3-CD20+), CD32+CD4+ T cells (live, CD45+CD3+CD4+ CD32+), CD32-CD4+ T cells (live, CD45+CD3+CD4+CD32-). Intensity of CD3, CD32, CD4, CD20, is shown for all samples, overlaid on the viSNE map. White arrows indicate CD32+CD4+ T cells. Cells not identified by such biaxial gating within CD45$^+$ cells in the viSNE plots are shown in white. **(E, F)** Percentage of CD20+ cells within CD32+ CD4+ and CD32$^-$ CD4+ according to their expression of IgM and IgG in MAC (orange) and AGM (blue). In Figure cells from distinct tissues of chronically infected **(E)** MAC and **(F)** AGM. **(G)** Frequency of IgM and IgG on CD4+CD20+CD32+ T cells in the spleen of chronically infected MAC (upper part) and AGM (lower part). **(H)** Distribution of CD32+CD20+CD4+ T cells according to their expression of IgM and IgG in MAC (orange) and AGM (blue). In **Figures 4A, B**, a Friedman test was applied. In **Figures 4C, D**, statistical differences were assessed by ANOVA with Tukey adjustment for multiple comparisons. Asterisks indicate p-values < 0.05.

expression of eight markers. Individual flow cytometry standard files were concatenated into single flow cytometry standard files from which spatially distinct populations were obtained. To help identifying cell populations, traditional biaxial gating strategies based on surface markers were used as follows: CD4$^+$ T cells (TCRβ$^+$CD4$^+$), CD8$^+$ T cells (TCRβ$^+$CD8$^+$), B cells (CD20$^+$), NK cells (NKG2A$^+$). We overlaid immune cell populations identified by traditional gating strategies on viSNE plots and

compared them to viSNE heat maps (**Figures 5C, D**). This allowed to easily identify spatially distinct populations corresponding to B cells, $CD8^+$ T cells, $CD32^-$ $CD4^+$ T cells and NK cells in both species (**Figures 5C, D**). $CD8^+$ T cells and NK cells showed some overlapping which is expected since some but not all NK cells express CD8 in tissues (61). The $CD32^+CD4^+$ cells (red) of MAC clustered in a unique, spatially distinct population expressing CD3, CD4, CD20 and CD32 markers. In AGM, the very low numbers of this population in spleen did not allow to define such clusters.

We next used the same technique to compare the frequency of $CD32^+CD4^+$ and $CD32^-CD4^+$ T cells expressing CD20 in distinct body compartments. We analyzed four tissues (spleen, LN, jejunum, ileum) and blood from MAC and AGM during chronic infection. In all lymphoid tissues analyzed, a high frequency of $CD20^+$ cells was detected in the $CD32^+CD4^+CD3^+$ population whereas a very low amount of $CD32^-CD4^+CD3^+$ cells expressed this marker (**Figures 5E**, **F**). This differed from blood, where CD20 expression was also rare within $CD32^+CD4^+$T cells and not higher than for $CD32^-$ cells. The frequencies of the $CD20^+CD32^+CD4^+CD3^+$ cells were thus much higher in SLT and gut than in blood.

To further confirm the sharing with B cell properties of the $CD32^+CD4^+$T cells, we analyzed functional markers of B cells in these cells. We determined the single and co-expression of IgM and IgG on $CD32^+CD20^+CD4^+$ T cells from the spleen (**Figure 5G**). There was an absence of staining for both IgG and IgM antibodies on NK cells, $CD3^+CD4^-$ T cells, and $CD4^+$ CD32- T cells, whereas a high frequency of B cells as well as $CD32^+CD4^+$ T cells expressed those markers (**Figure S7**). The $CD32^+CD20^+CD4^+$ T cells generally expressed either IgM or IgG, or none of them. Thus, >25% of the $CD32^+CD4^+CD20^+$ T cells expressed IgM and not IgG, while some expressed IgG and no IgM (**Figure 5H**). About half of the $CD32^+CD4^+$ $CD20^+$ T cells expressed neither IgG nor IgM.

DISCUSSION

The knowledge and understanding of the characteristics of $CD4^+$ T cell subsets preferentially infected by HIV has considerably increased in the last years (62–64). Recent studies also provided information on major reservoir cells in tissues (12, 16, 65). Cell types are generally defined by specific markers. It is not unusual for some markers classically attributed to one type of cells to also be shared by a subfraction of other cell types For instance, mature $CD8^+$ T cells, when activated, can co-express CD4 (66). Previous studies have identified $CD4^+$ T cells expressing CD32a (25, 67–69). CD32a is an FcgR and is known to be primarily expressed on cell types such as myeloid cells, granulocytes, B cells and NK cells. Little is known about the function and biology of $CD32^+CD4^+$ T cells. Here, we analyzed $CD32^+CD4^+$ T cells in different tissues from two NHP models frequently used in biomedical research: AGM and cynomolgus MAC and investigated their dynamics in response to a viral infection. To this end, we studied these cells in healthy animals and during acute and chronic SIV infection. We performed tissue-level phenotypic and/or transcriptomic characterization at different stages of infection in lymphoid and non-lymphoid tissues. In addition, we characterized $CD32^+CD4^+$ T cells in the natural courses of SIV infection in AGM and compared these cells in tissues with well controlled (SLT) and not efficiently controlled (jejunum) SIV replication.

Our results show that $CD32^+CD4^+$ T cells were relatively rare in healthy NHP, similar to humans. The frequency of these cells strongly increased after SIV infection. The increase was compartment-specific, as the increase was very strong in lymphoid tissues (SLT, intestine) but not in blood, nor liver, during SIVmac infection. Some studies in humans also showed no significant differences in $CD32^+CD4^+$T cell frequencies in blood between HIV-1 negative, viremic and ART-treated individuals (31). Similar to MAC, an increase in $CD32^+CD4^+$T cells in the natural host was found in tissues and not in blood after SIV infection. However, the increases were pronounced only in the jejunum but not in LN. Natural hosts exhibit high viral replication in intestinal tissues, in contrast to SLT, where the viral replication is well controlled (37, 39, 70–73). Depletion of NK cells leads to loss of viral control in SLT in SIVagm infection (38). We show here that NK cell depleted SIVagm-infected AGM increase their $CD32^+CD4^+$T cells in SLT and that $CD32^+CD4^+$ T cell frequencies correlate with viremia levels. Altogether this shows that $CD32^+CD4^+$ T cells were preferentially increased in tissues with ongoing high-level viral replication.

Our genome-wide transcriptome analysis coupled with the phenotypic data indicated that $CD32^+CD4^+$ T cells were in a more activated state than $CD32^-CD4^+$T cells. In line with this, $CD32^{high}$ CD4 T cells from blood of treated PLH have been described to express higher levels of HLA-DR and CD69 than other subsets (22). Other studies also suggested that CD32 marks highly activated/exhausted memory $CD4^+$ T-cell subsets (74). The increased expression of CD32, which is an Fcγ receptor (FcγRIIa), could also make $CD4^+$ T cells more susceptible to activation by IgG immune complexes.

CD32 expression might increase on $CD4^+$ T cells as a direct consequence of the virus, either through viral infection and/or antigenic stimulation (25). Indeed, stimulation of $CD4^+$ T cells with anti-CD3/CD28 antibodies has been described to induce CD32 co-expression (75). The $CD32^+CD4^+$ T cell profiles in SLT and gut upon SIVagm infection suggest such a direct effect of the virus. However, the inflammatory environment induced by chronic viral replication might also favor the emergence of such cells. External factors, such as IL-2, IL-7 and PHA, have been shown to induce CD32 expression on $CD4^+$ T cells *in vitro* (75). The experimental NK cell depletion in AGM was induced by anti-IL-15. While most NK cell populations collapse in the absence of IL-15, effector memory $CD4^+$ T cells can be maintained in the face of IL-15 inhibition by the activity of other homeostatic regulators, such as IL-7 (48). Interestingly IL-7 is known to maintain B cell potential in common lymphoid progenitors (76). Anti-IL15 treatment was associated with an increase in $CD32^+CD4^+$ T cells. Therefore, it cannot be excluded that the anti-IL-15 treatment, by inducing IL-7 as a homeostatic

response, promoted the appearance of $CD32^+CD4^+$ T cells through a bystander effect in anti-IL-15 treated animals. IL-7 can also be increased in HIV-1 and SIVmac infection as a consequence of $CD4^+$ T cell depletion, as shown during primary infection in the blood and intestine (77–79). Thus, the increase in $CD32^+$ $CD4^+$ T cells might be a mixture of factors directly and indirectly related to HIV/SIV replication.

The higher activation state of $CD32^+CD4^+$ T cells may explain the higher frequency of HIV RNA transcription that we observed compared to the other $CD4^+$ T cells. The CD32 in splenic $CD4^+$ T cells marked highly transcriptionally active CD4 T cells. Our data are in agreement with other studies reporting transcriptionally active virus in these cells in blood (29, 31, 80), and with data on LN from HIV-infected individuals showing HIV RNA in $CD32^+$ cells inside B cell follicles (31, 81, 82). We also observed an up-regulation of CD74, an ISG known to be up-regulated in activated infected cells (83, 84) and known to be involved in the formation and transport of MHC class II peptide complexes for the generation of $CD4^+$ T cell responses. The viral DNA has not been measured here and future studies will need to address if $CD32^+$CD4 T cells from tissues contain more SIV DNA than CD32-$CD4^+$ T cells and if the frequency $CD32^+$CD4 T cells in tissues correlates with ca-SIV DNA. Altogether, $CD32^+CD4^+$ T cells displayed higher levels of actively transcribed SIV RNA than $CD32^-CD4^+$ T cells in SLT and gut during both SIVmac and SIVagm chronic infection.

We also show that $CD32^+CD4^+$ T cells from the spleen expressed more often CCR5 than the other $CD4^+$ T cells. $CD32^{high}$CD4 T cells from the blood of treated PLH have indeed been described in other studies to express higher levels of HIV co-receptor expression than other subsets (22). Our data are therefore compatible with a phenotype of these $CD32^+$ $CD4^+$ T cells being particularly susceptible to HIV/SIV infection.

The $CD32^+CD4^+$ T cells often expressed PD-1 and CXCR5. This could have several explanations. It has been suggested that they resemble T_{FH} cells (81). We show here that approximately 90% of $CD32^+CD4^+$ T cells from LN were MHC-E positive. We have previously reported that T_{FH} cells in SLT express MHC-E more frequently than any other $CD4^+$ T cell subset (85). This is an additional argument for $CD32^+$ T cells exhibiting T_{FH} cell characteristics. However, it could also be that CXCR5 and PD-1 expression is associated with the B cell phenotypical characteristics of these cells. In the lymphoid tissues, but not in the blood, about half of the $CD32^+$ $CD4^+$ T cells in the SIV-infected NHPs also expressed the B lymphocyte antigen CD20 at the cell surface. The observation that $CD20^+CD4^+CXCR4^+$ T cells can be infected with HIV-1 *in vitro* was reported many years ago (68). More recently, Serra-Peinado et al. described that $CD20^+CD4^+$ T cells from blood and LN of patients on antiretroviral therapy (ART) were significantly enriched in HIV transcripts (23). Our study supports that CD20 can be expressed on target cells of HIV *in vivo*. Here, we provide an in-depth analysis of the molecular properties of $CD32^+CD20^+CD4^+$ T cells. We combined distinct genomic, immunological and imaging methods to confirm the existence of this peculiar cellular subset. The high content of mRNA encoding transcription factors and surface markers usually attributed to the B cell lineage in the transcriptome analysis of $CD32^+$ $CD4^+$ T cells made the presence of contaminating cells unlikely. Furthermore, mRNA expression excluded the possibility of an acquisition of surface molecules attributed to the B cell lineage by trogocytosis as previously proposed (26, 29). Previous reports also have proposed that T-cell–B-cell conjugates may be the source of CD32 and CD4 co-expression (26). The imaging analyzes performed here on total CD4 T isolated from infected monkeys confirmed the existence of cells co-expressing CD32, CD4, and CD20. However, it is difficult to completely exclude the possibility of doublets contributing to this signal in some of the FACS based experiments. Of note, several reports have shown that B cells exclusively express the CD32b isoform (29, 86). Here, we found that the CD32 a isoform was present in all sorted $CD32^+$ $CD4^+$ T cell fractions of SIV-infected monkeys. This also demonstrates that CD32 co-expression on the $CD4^+$ T cells cannot be solely explained by eventual doublets. Our results are in agreement with other studies showing that many of the $CD32^{high}$ $CD4^+$ T cells from HIV-1^+ patients, and from healthy donors, co-express multiple B cell markers (22, 23, 29). Of note, we show here that CD20 expression was frequent on $CD32^+CD4^+$ T cells from gut and SLT but not for blood $CD32^+CD4^+$ T cells during SIV infection, underlining tissue-dependent distribution.

In the present study, genome-wide transcriptome analysis revealed that the $CD32^+CD4^+$ T cells detected here expressed low levels of *GATA-3*, *BCL11b* and *Notch1*, but high levels of *IRF8* compared with the $CD32^-CD4^+$ cell fraction. Previous studies showed that IRF8 could play a role in the earliest stages of B-cell development (87). Notch induces T cell factor 1 (Tcf1), which is the first T cell-specific protein in the thymus, leading to the activation of two major target genes, *Gata3* and *Bcl11b*. GATA-3 is known to critically suppress a latent B-cell potential in pro–T cells (88–90). BCL11B also supports the maintenance of T-cell fate by continuously suppressing epigenetic changes in the B-lineage-specific gene program (91). Thus, the expression pattern indicates the presence of transcription factors down-regulating T cell pathways in favor of the B cell lineage. Overall, the differential expression of checkpoint molecules of the T and B cell lineage fates suggests the presence of regulatory mechanisms of the early T and B cell differentiation pathways in this $CD32^+CD4^+$ T cell subset.

Recent data provided strong evidence that compartmentalization of T and other cells, such as B cells, is not absolute: violators of this paradigm can indeed be generated under specific conditions (92–95). CD20-expressing T cell populations have been found in healthy individuals as well as in a variety of non-malignant disease states (92, 94, 96–100). $CD20^+$ inflammatory T-cells have been described in blood and brain of multiple sclerosis patients (94, 101, 102). Murayama and colleagues reported significant increase of $CD3^+CD4^+CD20^+$ T cells in lymph nodes and not in blood during SIV infection in MAC at the stage of lymphadenopathy (103).

Thus, under conditions where the tissue microenvironment is modified, such as during chronic HIV/SIV infection in lymphoid tissues, modifications in cell differentiation could be favored.

Whether $CD32^+CD20^+$ T cells have a specific function or are only a byproduct remains to be clarified. In the case of HIV/SIV infection, the expansion of such cells might be harmful as they seem highly susceptible to infection. The fact that they increase already in acute infection, as shown here, raises the question of their contribution to the viral reservoir that is established early on after HIV/SIV infection. It is not excluded though, that these $CD32^+CD20^+CD4^+$ T cells also have a beneficial role in viral or immunological diseases. This question needs to be addressed in future studies.

Altogether, we show that $CD32^+CD4^+$ T cells had an activated profile, more frequently expressed markers associated with HIV infected and/or reservoir cells (CCR5, PD-1, CXCR5, CXCR3) and displayed higher levels of actively transcribed SIV RNA than $CD32^-CD4^+$T cells. We show that $CD4^+$ T cells expressing CD32 were rare in healthy animals but strongly increased after SIV infection in tissues exhibiting higher replication and immune activation. These $CD32^+CD4^+$ T cells in tissues also often expressed B cell markers. Genome-wide transcriptome revealed a coordinated regulation of T and B cell fate checkpoint molecules. Our results suggest that the tissue microenvironment associated with viral replication in gut and SLT drives the differentiation of a functionally not well-described subpopulation of activated $CD4^+$ T cells with enhanced susceptibility to HIV infection in lymphoid tissues.

DATA AVAILABILITY STATEMENT

Deep sequencing results have been deposited in the Gene Expression Omnibus database; the accession number is GSE169736. The authors declare that all other data supporting the findings of this study are available within the article and its Supplementary Information files or are available from the authors upon request.

ETHICS STATEMENT

The animal study was reviewed and approved by Animal experimental protocols were approved by the Ethical Committee of Animal Experimentation (CETEA-DSV, IDF, France) (Notification 12-098 and A17-044). The pVISCONTI study was approved and accredited under statement number A15-035 by the ethics committee "Comité d'Ethique en Expérimentation Animale du CEA", registered and authorized under Number 2453-2015102713323361v2 by the French Ministry of Education and Research.

AUTHOR CONTRIBUTIONS

NH and MM-T designed the study. NH designed the experiments. NH, PR, CyP, BJ, ET, RL and HV performed experiments. NH, HV, EK and RL performed statistical and bio-informatic analyses. NH, PR, Cyp, A-SB, AS-C, HM, BJ and MM-T analyzed the data. VC, Cap, RG and BJ coordinated the animal studies. NH and MM-T wrote the manuscript and all co-authors reviewed it. All authors contributed to the article and approved the submitted version.

FUNDING

For sequencing and analysis support, we thank the Biomics Platform, C2RT, Institut Pasteur, Paris, France, supported by France Génomique (ANR-10-INBS-09-09) and IBISA. NH was supported by the Fondation Jacquelin Beytout and Institut Pasteur. PR was recipient of a PhD fellowship from the University Paris Diderot, Sorbonne Paris Cité and also supported by the NIH (R01AI143457). CP was the recipient of a PhD fellowship from the ANRS. HM received core grants from the Institut Pasteur, the INSERM and the Milieu Intérieur Program (ANR-10-LABX-69-01). We would like to acknowledge funding support from ANRS, MSDAvenir and Institut Pasteur to MM-T and AS-C. We gratefully acknowledge the support to IDMIT from the French government: Investments for the Future program for infrastructures (PIA) through the ANR-11-INBS-0008 grant as well as from the PIA grant ANR-10-EQPX-02-01 to the FlowCyTech facility at IDMIT.

ACKNOWLEDGMENTS

We are grateful for the excellent help from the veterinarians and staff at the IDMIT Center (Benoit Delache, Jean-Marie Helies, Raphaël Ho Tsong Fang and Julie Morin).

SUPPLEMENTARY MATERIAL

The Supplementary Material for this article can be found online at: https://www.frontiersin.org/articles/10.3389/fimmu.2021.695148/full#supplementary-material

Supplementary Figure 1 | Gating strategy used to identify and isolate CD32+CD4+ T cells in tissues from uninfected and SIV-infected AGM and MAC. **(A)** Example of the gating strategy used to isolate CD32+CD4+ T cells from healthy MAC. The red square highlights the dot plot showing CD3+CD20+ cells **(B)** Example of dot plot showing CD3+CD20+ cells obtained during FACS sorting from chronically infected MAC and healthy or chronically infected AGM.

Supplementary Figure 2 | Gating strategy used to identify TFH cells in pLN from uninfected and SIV-infected MAC and AGM. Graph showing Spearman's correlation between TFH and CD32+CD4+ T cell frequencies. Each dot represents an individual from acutely (day 9 Pi; purple dot) or chronically infected animals (black dot). The Spearman correlation is shown, and r and p values are indicated in each graph.

Supplementary Figure 3 | Venn diagrams generated by the intersection of transcripts encoding clusters of differentiation (CD) with a p-adj <0.05 when CD32+ CD4+ are compared with CD32-CD4+ fraction in the spleen of chronically SIV-infected MAC (orange circle) and AGM (blue circle). Up-regulated clusters of differentiation (CD) are shown in the top of the figure and down-regulated clusters of differentiation (CD) are shown in the bottom part. The number of differentially regulated genes is indicated in each circle, and the list of each gene is below the circles.

Supplementary Figure 4 | Venn diagrams generated by the intersection of transcripts encoding transcription factors (TFs) with a p-adj <0.05 when CD32+CD4+ T cells are compared with CD32- CD4+ T cell fraction isolated from the spleen of chronically SIV-infected MAC (orange circle) and AGM (blue circle). Up-regulated TFs are shown in the top of the figure and down-regulated TFs are shown in the bottom parts. The number of genes is indicated in each circle, and the list of each gene is provided below.

Supplementary Figure 5 | Interferon-stimulated-genes (ISGs) differentially expressed within CD32+CD4+ T cells. The Venn diagram was generated by the intersection of all differentially expressed transcripts with a p-adj <0.05 found in CD32+CD4+ T cells from the spleen of chronically SIV-infected MAC (red circle), AGM (green circle) and ISG genes (blue circle). The ISG genes are as reported by Schoggins and Rice (60). In AGM, Eleven ISG genes were found to be differentially expressed within CD32+CD4+ T cells (i.e, OAS, GBP1, OAS2, SLC15A3, MAP3K14, ZC3HAV1, DDX60, MOV10, IFI6, IFI44L, DDX58), whereas two ISG genes were found to be differentially expressed in MAC (i.e, SSBP3, ISG20). Only CD74 is found to be differentially expressed within CD32+CD4+ T cells in both MAC and AGM.

Supplementary Figure 6 | (A) Pie chart showing the up- and down-regulated signaling pathways in CD32+CD4+ T cells isolated from the spleen of chronically SIV-infected MAC and AGM. **(B)** Pie chart showing the up- and down-regulated common signaling pathways in CD32+CD4+ T cells isolated from the spleen of chronically SIV-infected MAC and AGM. Common signaling pathways between AGM and MAC were defined by using common up- and down-regulated transcripts in the CD32+CD4+ T cell subsets when compared to the CD32-CD4+ T cells.

Supplementary Figure 7 | Gating strategy used to determine the frequency of CD32+CD4+ T cells expressing IgG and/or IgM from the spleen of chronically SIV-infected AGM **(A)** and MAC **(B)**.

Supplementary Table 1 | Table showing the characteristics of the monkeys used in this study.

Supplementary Table 2 | List of genes up- and down-regulated in CD32+CD4+ T cells when compared to CD32-CD4+T cells.

Supplementary Table 3 | Pathway up- and down-regulated in CD32+CD4+ T cells when compared to CD32-CD4+T cells in chronically infected MAC.

Supplementary Table 4 | Pathway up- and down-regulated in CD32+CD4+ T cells when compared to CD32-CD4+T cells in chronically infected AGM.

Supplementary Table 5 | Common pathways up- or down-regulated in AGM and MAC between CD32+CD4+ T cells when compared to CD32-CD4+T cells. Pathway analysis was performed using all common transcripts with a p-adj <0.05 found in CD32+CD4+ T cells from the spleen of chronically SIV-infected MAC and AGM.

REFERENCES

1. Alexaki A, Liu Y, Wigdahl B. Cellular Reservoirs of HIV-1 and Their Role in Viral Persistence. *Curr HIV Res* (2008) 6(5):388–400. doi: 10.2174/157016208785861195
2. Martinez-Picado J, Deeks SG. Persistent HIV-1 Replication During Antiretroviral Therapy. *Curr Opin HIV AIDS* (2016) 11(4):417–23. doi: 10.1097/COH.0000000000000287
3. Rothenberger MK, Keele BF, Wietgrefe SW, Fletcher CV, Beilman GJ, Chipman JG, et al. Large Number of Rebounding/Founder HIV Variants Emerge From Multifocal Infection in Lymphatic Tissues After Treatment Interruption. *Proc Natl Acad Sci U S A* (2015) 112(10):E1126–34. doi: 10.1073/pnas.1414926112
4. Okoye AA, Hansen SG, Vaidya M, Fukazawa Y, Park H, Duell DM, et al. Early Antiretroviral Therapy Limits Siv Reservoir Establishment to Delay or Prevent Post-Treatment Viral Rebound. *Nat Med* (2018) 24(9):1430–40. doi: 10.1038/s41591-018-0130-7
5. Whitney JB, Hill AL, Sanisetty S, Penaloza-MacMaster P, Liu J, Shetty M, et al. Rapid Seeding of the Viral Reservoir Prior to SIV Viremia in Rhesus Monkeys. *Nature* (2014) 512(7512):74–7. doi: 10.1038/nature13594
6. Cohn LB, Chomont N, Deeks SG. The Biology of the HIV-1 Latent Reservoir and Implications for Cure Strategies. *Cell Host Microbe* (2020) 27(4):519–30. doi: 10.1016/j.chom.2020.03.014
7. Hocqueloux L, Avettand-Fènoël V, Jacquot S, Prazuck T, Legac E, Mélard A, et al. Long-Term Antiretroviral Therapy Initiated During Primary HIV-1 Infection is Key to Achieving Both Low Hiv Reservoirs and Normal T Cell Counts. *J Antimicrob Chemother* (2013) 68(5):1169–78. doi: 10.1093/jac/dks533
8. Klatt NR, Chomont N, Douek DC, Deeks SG. Immune Activation and HIV Persistence: Implications for Curative Approaches to HIV Infection. *Immunol Rev* (2013) 254(1):326–42. doi: 10.1111/imr.12065
9. Barton K, Winckelmann A, Palmer S. HIV-1 Reservoirs During Suppressive Therapy. *Trends Microbiol* (2016) 24(5):345–55. doi: 10.1016/j.tim.2016.01.006
10. Hoetelmans RM. Sanctuary Sites in HIV-1 Infection. *Antivir Ther* (1998) 3 Suppl 4:13–7.
11. Hong JJ, Chang K-T, Villinger F. The Dynamics of T and B Cells in Lymph Node During Chronic HIV Infection: TFH and HIV, Unhappy Dance Partners? *Front Immunol* (2016) 7:522. doi: 10.3389/fimmu.2016.00522/full
12. Banga R, Procopio FA, Noto A, Pollakis G, Cavassini M, Ohmiti K, et al. Pd-1(+) and Follicular Helper T Cells are Responsible for Persistent HIV-1 Transcription in Treated Aviremic Individuals. *Nat Med* (2016) 22 (7):754–61. doi: 10.1038/nm.4113
13. Fukazawa Y, Lum R, Okoye AA, Park H, Matsuda K, Bae JY, et al. B Cell Follicle Sanctuary Permits Persistent Productive Simian Immunodeficiency Virus Infection in Elite Controllers. *Nat Med* (2015) 21(2):132–9. doi: 10.1038/nm.3781
14. Harper J, Gordon S, Chan CN, Wang H, Lindemuth E, Galardi C, et al. CTLA-4 and PD-1 Dual Blockade Induces SIV Reactivation Without Control of Rebound After Antiretroviral Therapy Interruption. *Nat Med* (2020) 26(4):519–28. doi: 10.1038/s41591-020-0782-y
15. Kaufmann DE, Walker BD. PD-1 and CTLA-4 Inhibitory Co-Signaling Pathways in HIV Infection and the Potential for Therapeutic Intervention. *J Immunol Baltim Md 1950* (2009) 182(10):5891–7.
16. McGary CS, Deleage C, Harper J, Micci L, Ribeiro SP, Paganini S, et al. CTLA-4+PD-1– Memory Cd4+ T Cells Critically Contribute to Viral Persistence in Antiretroviral Therapy-Suppressed, SIV-infected Rhesus Macaques. *Immunity 17 oct* (2017) 47(4):776–88.e5. doi: 10.1016/j.immuni.2017.09.018
17. Iglesias-Ussel M, Vandergeeten C, Marchionni L, Chomont N, Romerio F. High Levels of CD2 Expression Identify HIV-1 Latently Infected Resting Memory Cd4+ T Cells in Virally Suppressed Subjects. *J Virol* (2013) 87 (16):9148–58. doi: 10.1128/JVI.01297-13
18. Fromentin R, Bakeman W, Lawani MB, Khoury G, Hartogensis W, DaFonseca S, et al. Cd4+ T Cells Expressing Pd-1, TIGIT and LAG-3 Contribute to HIV Persistence During Art. *PloS Pathog* (2016) 12(7): e1005761. doi: 10.1371/journal.ppat.1005761
19. Khoury G, Anderson JL, Fromentin R, Hartogenesis W, Smith MZ, Bacchetti P, et al. Persistence of Integrated HIV DNA in CXCR3 + CCR6 + memory Cd4+ T Cells in HIV-infected Individuals on Antiretroviral Therapy. *AIDS Lond Engl* (2016) 30(10):1511–20. doi: 10.1097/QAD.0000000000001029
20. Banga R, Procopio FA, Ruggiero A, Noto A, Ohmiti K, Cavassini M, et al. Blood CXCR3+ Cd4 T Cells Are Enriched in Inducible Replication Competent HIV in Aviremic Antiretroviral Therapy-Treated Individuals. *Front Immunol* (2018) 9:144. doi: 10.3389/fimmu.2018.00144
21. Hogan LE, Vasquez J, Hobbs KS, Hanhauser E, Aguilar-Rodriguez B, Hussien R, et al. Increased HIV-1 Transcriptional Activity and Infectious Burden in Peripheral Blood and Gut-Associated Cd4+ T Cells Expressing Cd30. *PloS Pathog* (2018) 14(2):e1006856. doi: 10.1371/journal.ppat.1006856
22. Martin GE, Pace M, Thornhill JP, Phetsouphanh C, Meyerowitz J, Gossez M, et al. Cd32-Expressing Cd4 T Cells Are Phenotypically Diverse and Can Contain Proviral Hiv Dna. *Front Immunol* (2018) 9:928. doi: 10.3389/fimmu.2018.00928
23. Serra-Peinado C, Grau-Expósito J, Luque-Ballesteros L, Astorga-Gamaza A, Navarro J, Gallego-Rodriguez J, et al. Expression of CD20 After Viral

Reactivation Renders HIV-Reservoir Cells Susceptible to Rituximab. *Nat Commun* (2019) 10(1):3705. doi: 10.1038/s41467-019-11556-4
24. Anania JC, Chenoweth AM, Wines BD, Hogarth PM. The Human Fcγrii (Cd32) Family of Leukocyte Fcr in Health and Disease. *Front Immunol* (2019) 10:464. doi: 10.3389/fimmu.2019.00464/full
25. Descours B, Petitjean G, López-Zaragoza J-L, Bruel T, Raffel R, Psomas C, et al. CD32a Is a Marker of a CD4 T-Cell HIV Reservoir Harbouring Replication-Competent Proviruses. *Nature* (2017) 543(7646):564–7. doi: 10.1038/nature21710
26. Thornhill JP, Pace M, Martin GE, Hoare J, Peake S, Herrera C, et al. Cd32 Expressing Doublets in HIV-infected Gut-Associated Lymphoid Tissue are Associated With a T Follicular Helper Cell Phenotype. *Mucosal Immunol* (2019) 12(5):1212–9. doi: 10.1038/s41385-019-0180-2
27. Darcis G, Kootstra NA, Hooibrink B, van Montfort T, Maurer I, Groen K, et al. Cd32+Cd4+ T Cells Are Highly Enriched for HIV DNA and Can Support Transcriptional Latency. *Cell Rep* (2020) 30(7):2284–96.e3. doi: 10.1016/j.celrep.2020.01.071
28. Bertagnolli LN, White JA, Simonetti FR, Beg SA, Lai J, Tomescu C, et al. The Role of CD32 During HIV-1 Infection. *Nature* (2018) 561(7723):E17–9. doi: 10.1038/s41586-018-0494-3
29. Osuna CE, Lim S-Y, Kublin JL, Apps R, Chen E, Mota TM, et al. Evidence That Cd32a Does Not Mark the HIV-1 Latent Reservoir. *Nature* (2018) 561 (7723):E20–8. doi: 10.1038/s41586-018-0495-2
30. Pérez L, Anderson J, Chipman J, Thorkelson A, Chun T-W, Moir S, et al. Conflicting Evidence for HIV Enrichment in CD32+ Cd4 T Cells. *Nature* (2018) 561(7723):E9–16. doi: 10.1038/s41586-018-0493-4
31. Abdel-Mohsen M, Kuri-Cervantes L, Grau-Exposito J, Spivak AM, Nell RA, Tomescu C, et al. CD32 is Expressed on Cells With Transcriptionally Active HIV But Does Not Enrich for HIV DNA in Resting T Cells. *Sci Transl Med* (2018) 10(437):eaar6759. doi: 10.1126/scitranslmed.aar6759
32. Hatziioannou T, Evans DT. Animal Models for HIV/AIDS Research. *Nat Rev Microbiol* (2012) 10(12):852–67. doi: 10.1038/nrmicro2911
33. Chahroudi A, Bosinger SE, Vanderford TH, Paiardini M, Silvestri G. Natural SIV Hosts: Showing AIDS the Door. *Science* (2012) 335(6073):1188–93. doi: 10.1126/science.1217550
34. Garcia Tellez T, Huot N, Ploquin MJ-Y, Rascle P, Jacquelin B, Müller-Trutwin M. Non-Human Primates in HIV Research: Evidences, Limits and Alternatives. *Infect Genet Evol* (2016) 46:324–32. doi: 10.1016/j.meegid.2016.07.012
35. Sodora DL, Allan JS, Apetrei C, Brenchley JM, Douek DC, Else JG, et al. Toward an AIDS Vaccine: Lessons From Natural Simian Immunodeficiency Virus Infections of African Nonhuman Primate Hosts. *Nat Med* (2009) 15 (8):861–5. doi: 10.1038/nm.2013
36. Huot N, Rascle P, Garcia-Tellez T, Jacquelin B, Müller-Trutwin M. Innate Immune Cell Responses in Non Pathogenic Versus Pathogenic Siv Infections. *Curr Opin Virol* (2016) 19:37–44. doi: 10.1016/j.coviro.2016.06.011
37. Pandrea I, Sodora DL, Silvestri G, Apetrei C. Into the Wild: Simian Immunodeficiency Virus (SIV) Infection in Natural Hosts. *Trends Immunol* (2008) 29(9):419–28. doi: 10.1016/j.it.2008.05.004
38. Huot N, Jacquelin B, Garcia-Tellez T, Rascle P, Ploquin MJ, Madec Y, et al. Natural Killer Cells Migrate Into and Control Simian Immunodeficiency Virus Replication in Lymph Node Follicles in African Green Monkeys. *Nat Med* (2017) 23(11):1277–86. doi: 10.1038/nm.4421
39. Diop OM, Gueye A, Dias-Tavares M, Kornfeld C, Faye A, Ave P, et al. High Levels of Viral Replication During Primary Simian Immunodeficiency Virus Sivagm Infection Are Rapidly and Strongly Controlled in African Green Monkeys. *J Virol* (2000) 74(16):7538–47. doi: 10.1128/JVI.74.16.7538-7547.2000
40. Jacquelin B, Petitjean G, Kunkel D, Liovat A-S, Jochems SP, Rogers KA, et al. Innate Immune Responses and Rapid Control of Inflammation in African Green Monkeys Treated or Not With Interferon-Alpha During Primary Sivagm Infection. *PloS Pathog 3 juill* (2014) 10(7):e1004241. doi: 10.1371/journal.ppat.1004241
41. van Royen-Kerkhof A, Sanders EAM, Walraven V, Voorhorst-Ogink M, Saeland E, Teeling JL, et al. A Novel Human CD32 Mab Blocks Experimental Immune Haemolytic Anaemia in FcgammaRIIA Transgenic Mice. *Br J Haematol* (2005) 130(1):130–7. doi: 10.1111/j.1365-2141.2005.05571.x
42. Tiller T, Meffre E, Yurasov S, Tsuiji M, Nussenzweig MC, Wardemann H. Efficient Generation of Monoclonal Antibodies From Single Human B Cells by Single Cell RT-PCR and Expression Vector Cloning. *J Immunol Methods* (2008) 329(1–2):112–24. doi: 10.1016/j.jim.2007.09.017
43. Lorin V, Mouquet H. Efficient Generation of Human Iga Monoclonal Antibodies. *J Immunol Methods* (2015) 422:102–10. doi: 10.1016/j.jim.2015.04.010
44. Cokelaer T, Desvillechabrol D, Legendre R, Cardon M. « Sequana »: A Set of Snakemake Ngs Pipelines. *J Open Source Softw* (2017) 2(16):352. doi: 10.21105/joss.00352
45. Liao Y, Smyth GK, Shi W. Featurecounts: An Efficient General Purpose Program for Assigning Sequence Reads to Genomic Features. *Bioinformatics* (2014) 30(7):923–30. doi: 10.1093/bioinformatics/btt656
46. Benjamini Y, Hochberg Y. Controlling the False Discovery Rate: A Practical and Powerful Approach to Multiple Testing. *J R Stat Soc Ser B Methodol* (1995) 57(1):289–300. doi: 10.1111/j.2517-6161.1995.tb02031.x
47. Bindea G, Mlecnik B, Hackl H, Charoentong P, Tosolini M, Kirilovsky A, et al. Cluego: A Cytoscape Plug-in to Decipher Functionally Grouped Gene Ontology and Pathway Annotation Networks. *Bioinformatics* (2009) 25 (8):1091–3. doi: 10.1093/bioinformatics/btp101
48. DeGottardi MQ, Okoye AA, Vaidya M, Talla A, Konfe AL, Reyes MD, et al. Effect of Anti-IL-15 Administration on T Cell and NK Cell Homeostasis in Rhesus Macaques. *J Immunol Baltim Md 1950* (2016) 197(4):1183–98. doi: 10.4049/jimmunol.1600065
49. Hastings WD, Anderson DE, Kassam N, Koguchi K, Greenfield EA, Kent SC, et al. TIM-3 is Expressed on Activated Human Cd4+ T Cells and Regulates Th1 and Th17 Cytokines. *Eur J Immunol* (2009) 39(9):2492–501. doi: 10.1002/eji.200939274
50. Fang F, Yu M, Cavanagh MM, Saunders JH, Qi Q, Ye Z, et al. Expression of CD39 on Activated T Cells Impairs Their Survival in Older Individuals. *Cell Rep* (2016) 14(5):1218–31. doi: 10.1016/j.celrep.2016.01.002
51. Lee GR, Shaefi S, Otterbein LE. HO-1 and CD39: it Takes Two to Protect the Realm. *Front Immunol* (2019) 10:1765. doi: 10.3389/fimmu.2019.01765/full
52. Fujimoto Y, Tu L, Miller AS, Bock C, Fujimoto M, Doyle C, et al. Cd83 Expression Influences Cd4+ T Cell Development in the Thymus. *Cell* (2002) 108(6):755–67. doi: 10.1016/S0092-8674(02)00673-6
53. Liedtke K, Alter C, Günther A, Hövelmeyer N, Klopfleisch R, Naumann R, et al. Endogenous CD83 Expression in CD4+ Conventional T Cells Controls Inflammatory Immune Responses. *J Immunol* (2020) 204(12):3217–26. doi: 10.4049/jimmunol.2000042
54. Reinwald S, Wiethe C, Westendorf AM, Breloer M, Probst-Kepper M, Fleischer B, et al. Cd83 Expression in CD4+ T Cells Modulates Inflammation and Autoimmunity. *J Immunol* (2008) 180(9):5890–7. doi: 10.4049/jimmunol.180.9.5890
55. Chistiakov DA, Killingsworth MC, Myasoedova VA, Orekhov AN, Bobryshev YV. Cd68/Macrosialin: Not Just a Histochemical Marker. *Lab Investig J Tech Methods Pathol* (2017) 97(1):4–13. doi: 10.1038/labinvest.2016.116
56. Hameed A, Hruban RH, Gage W, Pettis G, Fox WM. Immunohistochemical Expression of CD68 Antigen in Human Peripheral Blood T Cells. *Hum Pathol* (1994) 25(9):872–6. doi: 10.1016/0046-8177(94)90005-1
57. José ES, Borroto A, Niedergang F, Alcover A, Alarcón B. Triggering the TCR Complex Causes the Downregulation of Nonengaged Receptors by a Signal Transduction-Dependent Mechanism. *Immunity* (2000) 12(2):161–70. doi: 10.1016/S1074-7613(00)80169-7
58. Krishnan S, Warke VG, Nambiar MP, Wong HK, Tsokos GC, Farber DL. Generation and Biochemical Analysis of Human Effector Cd4 T Cells: Alterations in Tyrosine Phosphorylation and Loss of CD3ζ Expression. *Blood* (2001) 97(12):3851–9. doi: 10.1182/blood.V97.12.3851
59. Paillard F, Sterkers G, Vaquero C. Transcriptional and Post-Transcriptional Regulation of TcR, CD4 and CD8 Gene Expression During Activation of Normal Human T Lymphocytes. *EMBO J* (1990) 9(6):1867–72. doi: 10.1002/j.1460-2075.1990.tb08312.x
60. Schoggins JW, Rice CM. Interferon-Stimulated Genes and Their Antiviral Effector Functions. *Curr Opin Virol* (2011) 1(6):519–25. doi: 10.1016/j.coviro.2011.10.008
61. Huot N, Rascle P, Petitdemange C, Contreras V, Palgen J-L, Stahl-Hennig C, et al. Non-Human Primate Determinants of Natural Killer Cells in Tissues at

Steady-State and During Simian Immunodeficiency Virus Infection. *Front Immunol* (2020) 11:2134. doi: 10.3389/fimmu.2020.02134
62. Chomont N, El-Far M, Ancuta P, Trautmann L, Procopio FA, Yassine-Diab B, et al. Hiv Reservoir Size and Persistence are Driven by T Cell Survival and Homeostatic Proliferation. *Nat Med* (2009) 15(8):893–900. doi: 10.1038/nm.1972
63. Clerc I, Moussa DA, Vahlas Z, Tardito S, Oburoglu L, Hope TJ, et al. Entry of Glucose- and Glutamine-Derived Carbons Into the Citric Acid Cycle Supports Early Steps of HIV-1 Infection in CD4 T Cells. *Nat Metab* (2019) 1(7):717–30. doi: 10.1038/s42255-019-0084-1
64. Valle-Casuso JC, Angin M, Volant S, Passaes C, Monceaux V, Mikhailova A, et al. Cellular Metabolism is a Major Determinant of HIV-1 Reservoir Seeding in CD4+ T Cells and Offers an Opportunity to Tackle Infection. *Cell Metab* (2019) 29(3):611–26.e5. doi: 10.1016/j.cmet.2018.11.015
65. Damouche A, Lazure T, Avettand-Fènoël V, Huot N, Dejucq-Rainsford N, Satie A-P, et al. Adipose Tissue is a Neglected Viral Reservoir and an Inflammatory Site During Chronic HIV and SIV Infection. *PloS Pathog* (2015) 11(9):e1005153. doi: 10.1371/journal.ppat.1005153
66. Sullivan YB, Landay AL, Zack JA, Kitchen SG, Al-Harthi L. Upregulation of CD4 on CD8+ T Cells: Cd4dimcd8bright T Cells Constitute an Activated Phenotype of CD8+ T Cells. *Immunology* (2001) 103(3):270–80. doi: 10.1046/j.1365-2567.2001.01243.x
67. Hua J, Davis SP, Hill JA, Yamagata T. Diverse Gene Expression in Human Regulatory T Cell Subsets Uncovers Connection Between Regulatory T Cell Genes and Suppressive Function. *J Immunol* (2015) 195(8):3642–53. doi: 10.4049/jimmunol.1500349
68. Moir S, Lapointe R, Malaspina A, Ostrowski M, Cole CE, Chun T-W, et al. Cd40-Mediated Induction of CD4 and CXCR4 on B Lymphocytes Correlates With Restricted Susceptibility to Human Immunodeficiency Virus Type 1 Infection: Potential Role of B Lymphocytes as a Viral Reservoir. *J Virol* (1999) 73(10):7972–80. doi: 10.1128/JVI.73.10.7972-7980.1999
69. Truong K-L, Schlickeiser S, Vogt K, Boës D, Stanko K, Appelt C, et al. Killer-Like Receptors and GPR56 Progressive Expression Defines Cytokine Production of Human Cd4 + Memory T Cells. *Nat Commun* (2019) 10 (1):2263. doi: 10.1038/s41467-019-10018-1
70. Gueye A, Diop OM, Ploquin MJY, Kornfeld C, Faye A, Cumont M-C, et al. Viral Load in Tissues During the Early and Chronic Phase of non-Pathogenic SIVagm Infection. *J Med Primatol* (2004) 33(2):83–97. doi: 10.1111/j.1600-0684.2004.00057.x
71. Huot N, Bosinger SE, Paiardini M, Reeves RK, Müller-Trutwin M. Lymph Node Cellular and Viral Dynamics in Natural Hosts and Impact for HIV Cure Strategies. *Front Immunol* (2018) 9:780. doi: 10.3389/fimmu.2018.00780
72. Silvestri G. Immunity in Natural Siv Infections. *J Intern Med* (2009) 265 (1):97–109. doi: 10.1111/j.1365-2796.2008.02049.x
73. Silvestri G, Paiardini M, Pandrea I, Lederman MM, Sodora DL. Understanding the Benign Nature of SIV Infection in Natural Hosts. *J Clin Invest* (2007) 117(11):3148–54. doi: 10.1172/JCI33034
74. Adams P, Fievez V, Schober R, Amand M, Iserentant G, Rutsaert S, et al. Cd32+Cd4+ Memory T Cells are Enriched for Total Hiv-1 DNA in Tissues From Humanized Mice. *iScience* (2021) 24(1):101881. doi: 10.1016/j.isci.2020.101881
75. Badia R, Ballana E, Castellví M, García-Vidal E, Pujantell M, Clotet B, et al. Cd32 Expression is Associated to T-cell Activation and is Not a Marker of the HIV-1 Reservoir. *Nat Commun* (2018) 9(1):2739. doi: 10.1038/s41467-018-05157-w
76. Dias S, Silva H, Cumano A, Vieira P. Interleukin-7 is Necessary to Maintain the B Cell Potential in Common Lymphoid Progenitors. *J Exp Med* (2005) 201(6):971–9. doi: 10.1084/jem.20042393
77. Hodge JN, Srinivasula S, Hu Z, Read SW, Porter BO, Kim I, et al. Decreases in IL-7 Levels During Antiretroviral Treatment of HIV Infection Suggest a Primary Mechanism of Receptor-Mediated Clearance. *Blood* (2011) 118 (12):3244–53. doi: 10.1182/blood-2010-12-323600
78. Muthukumar A, Zhou D, Paiardini M, Barry AP, Cole KS, McClure HM, et al. Timely Triggering of Homeostatic Mechanisms Involved in the Regulation of T-cell Levels in SIVsm-infected Sooty Mangabeys. *Blood* (2005) 106(12):3839–45. doi: 10.1182/blood-2005-01-0394
79. Ponte R, Rancez M, Figueiredo-Morgado S, Dutrieux J, Fabre-Mersseman V, Charmeteau-de-Muylder B, et al. Acute Simian Immunodeficiency Virus Infection Triggers Early and Transient Interleukin-7 Production in the Gut, Leading to Enhanced Local Chemokine Expression and Intestinal Immune Cell Homing. *Front Immunol* (2017) 8:588. doi: 10.3389/fimmu.2017.00588/full
80. Holgado MP, Sananez I, Raiden S, Geffner JR, Arruvito L. Cd32 Ligation Promotes the Activation of CD4+ T Cells. *Front Immunol* (2018) 9:2814. doi: 10.3389/fimmu.2018.02814
81. Noto A, Procopio FA, Banga R, Suffiotti M, Corpataux J-M, Cavassini M, et al. CD32+ and PD-1+ Lymph Node Cd4 T Cells Support Persistent HIV-1 Transcription in Treated Aviremic Individuals. *J Virol* (2018) 92(20): e00901-18. doi: 10.1128/JVI.00901-18
82. Vásquez JJ, Aguilar-Rodriguez BL, Rodriguez L, Hogan LE, Somsouk M, McCune JM, et al. Cd32-RNA Co-localizes With HIV-RNA in CD3+ Cells Found Within Gut Tissues From Viremic and ART-Suppressed Individuals. *Pathog Immun* (2019) 4(1):147–60. doi: 10.20411/pai.v4i1.271
83. Ghiglione Y, Rodriguez AM, De Candia C, Carobene M, Benaroch P, Schindler M, et al. Hiv-Mediated Up-Regulation of Invariant Chain (Cd74) Correlates With Generalized Immune Activation in HIV+ Subjects. *Virus Res* (2012) 163(1):380–4. doi: 10.1016/j.virusres.2011.09.011
84. Le Noury DA, Mosebi S, Papathanasopoulos MA, Hewer R. Functional Roles of HIV-1 Vpu and CD74: Details and Implications of the Vpu-CD74 Interaction. *Cell Immunol* (2015) 298(1–2):25–32. doi: 10.1016/j.cellimm.2015.08.005
85. Huot N, Rascle P, Petitdemange C, Contreras V, Stürzel CM, Baquero E, et al. Siv-Induced Terminally Differentiated Adaptive Nk Cells in Lymph Nodes Associated With Enhanced Mhc-E Restricted Activity. *Nat Commun* (2021) 12(1):1282. doi: 10.1038/s41467-021-21402-1
86. Veri M-C, Gorlatov S, Li H, Burke S, Johnson S, Stavenhagen J, et al. Monoclonal Antibodies Capable of Discriminating the Human Inhibitory Fcγ-Receptor IIB (Cd32b) From the Activating Fcγ-Receptor IIA (Cd32a): Biochemical, Biological and Functional Characterization. *Immunology* (2007) 121(3):392–404. doi: 10.1111/j.1365-2567.2007.02588.x
87. Wang H, Lee CH, Qi C, Tailor P, Feng J, Abbasi S, et al. Irf8 Regulates B-Cell Lineage Specification, Commitment, and Differentiation. *Blood* (2008) 112 (10):4028–38. doi: 10.1182/blood-2008-01-129049
88. García-Ojeda ME, Klein Wolterink RGJ, Lemaître F, Richard-Le Goff O, Hasan M, Hendriks RW, et al. Gata-3 Promotes T-Cell Specification by Repressing B-Cell Potential in Pro–T Cells in Mice. *Blood* (2013) 121 (10):1749–59. doi: 10.1182/blood-2012-06-440065
89. Rothenberg EV. Transcriptional Control of Early T and B Cell Developmental Choices. *Annu Rev Immunol* (2014) 32(1):283–321. doi: 10.1146/annurev-immunol-032712-100024
90. Scripture-Adams DD, Damle SS, Li L, Elihu KJ, Qin S, Arias AM, et al. Gata-3 Dose-Dependent Checkpoints in Early T Cell Commitment. *J Immunol* (2014) 193(7):3470–91. doi: 10.4049/jimmunol.1301663
91. Ikawa T, Masuda K, Endo TA, Endo M, Isono K, Koseki Y, et al. Conversion of T Cells to B Cells by Inactivation of Polycomb-Mediated Epigenetic Suppression of the B-lineage Program. *Genes Dev* (2016) 30(22):2475–85. doi: 10.1101/gad.290593.116
92. Ahmed R, Omidian Z, Giwa A, Cornwell B, Majety N, Bell DR, et al. A Public Bcr Present in a Unique Dual-Receptor-Expressing Lymphocyte From Type 1 Diabetes Patients Encodes a Potent T Cell Autoantigen. *Cell 30* (2019) 177(6):1583–99.e16. doi: 10.1016/j.cell.2019.05.007
93. de ruyn M, Wiersma VR, Wouters MCA, Samplonius DF, Klip HG, Helfrich W, et al. Cd20+ T Cells Have a Predominantly Tc1 Effector Memory Phenotype and Are Expanded in the Ascites of Patients With Ovarian Cancer. *Oncoimmunology* (2015) 4(4):e999536. doi: 10.1080/2162402X.2014.999536
94. Schuh E, Berer K, Mulazzani M, Feil K, Meinl I, Lahm H, et al. Features of Human Cd3+Cd20+ T Cells. *J Immunol* (2016) 197(4):1111–7. doi: 10.4049/jimmunol.1600089
95. Förster F, Singla A, Arora SK, Schmidt RE, Jacobs R. Cd20+ T Cell Numbers are Decreased in Untreated Hiv-1 Patients and Recover After Haart. *Immunol Lett* (2012) 146(1):74–8. doi: 10.1016/j.imlet.2012.05.004
96. Eggleton P, Bremer E, Tarr JM, de Bruyn M, Helfrich W, Kendall A, et al. Frequency of Th17 Cd20+ Cells in the Peripheral Blood of Rheumatoid Arthritis Patients is Higher Compared to Healthy Subjects. *Arthritis Res Ther* (2011) 13(6):R208. doi: 10.1186/ar3541

97. Katopodis O, Liossis S-N, Viglis V, Pouli A, Dimopoulos M-A, Sfikakis PP. Expansion of CD8+ T Cells That Express Low Levels of the B Cell-Specific Molecule CD20 in Patients With Multiple Myeloma. *Br J Haematol* (2003) 120(3):478–81. doi: 10.1046/j.1365-2141.2003.04087.x
98. Niu J, Zhai Z, Hao F, Zhang Y, Song Z, Zhong H. Dissection of a Circulating Cd3+Cd20+ T Cell Subpopulation in Patients With Psoriasis. *Clin Exp Immunol* (2018) 192(2):206–12. doi: 10.1111/cei.13106
99. Palanichamy A, Jahn S, Nickles D, Derstine M, Abounasr A, Hauser SL, et al. Rituximab Efficiently Depletes Increased Cd20 Expressing T Cells in Multiple Sclerosis Patients. *J Immunol Baltim Md 1950* (2014) 193(2):580–6. doi: 10.4049/jimmunol.1400118
100. Wilk E, Witte T, Marquardt N, Horvath T, Kalippke K, Scholz K, et al. Depletion of Functionally Active Cd20+ T Cells by Rituximab Treatment. *Arthritis Rheum* (2009) 60(12):3563–71. doi: 10.1002/art.24998
101. Chen Q, Yuan S, Sun H, Peng L. Cd3+Cd20+ T Cells and Their Roles in Human Diseases. *Hum Immunol* (2019) 80(3):191–4. doi: 10.1016/j.humimm.2019.01.001
102. Holley JE, Bremer E, Kendall AC, de Bruyn M, Helfrich W, Tarr JM, et al. Cd20+Inflammatory T-Cells Are Present in Blood and Brain of Multiple Sclerosis Patients and Can Be Selectively Targeted for Apoptotic Elimination. *Mult Scler Relat Disord* (2014) 3(5):650–8. doi: 10.1016/j.msard.2014.06.001
103. Murayama Y, Mukai R, Sata T, Matsunaga S, Noguchi A, Yoshikawa Y. Transient Expression of CD20 Antigen (Pan B Cell Marker) in Activated Lymph Node T Cells. *Microbiol Immunol* (1996) 40(6):467–71. doi: 10.1111/j.1348-0421.1996.tb01096.x

Conflict of Interest: The authors declare that the research was conducted in the absence of any commercial or financial relationships that could be construed as a potential conflict of interest.

frontiers in Immunology

SYSTEMATIC REVIEW
published: 21 July 2021
doi: 10.3389/fimmu.2021.695674

The Hitchhiker Guide to CD4$^+$ T-Cell Depletion in Lentiviral Infection. A Critical Review of the Dynamics of the CD4$^+$ T Cells in SIV and HIV Infection

*Quentin Le Hingrat[1], Irini Sereti[2], Alan L. Landay[3], Ivona Pandrea[4,5] and Cristian Apetrei[1,5]**

[1] Division of Infectious Diseases, DOM, School of Medicine, University of Pittsburgh, Pittsburgh, PA, United States, [2] HIV Pathogenesis Section, Laboratory of Immunoregulation, National Institute of Allergy and Infectious Diseases, National Institutes of Health, Bethesda, MD, United States, [3] Department of Internal Medicine, Rush University Medical Center, Chicago, IL, United States, [4] Department of Pathology, School of Medicine, University of Pittsburgh, Pittsburgh, PA, United States, [5] Department of Infectious Diseases and Immunology, Graduate School of Public Health, University of Pittsburgh, Pittsburgh, PA, United States

OPEN ACCESS

Edited by:
Vijayakumar Velu,
Emory University, United States

Reviewed by:
Jerome Estaquier,
Laval University, Canada
Matthew Wood,
Seattle Children's Research Institute, United States

***Correspondence:**
Cristian Apetrei
apetreic@pitt.edu

Specialty section:
This article was submitted to Viral Immunology, a section of the journal Frontiers in Immunology

Received: 15 April 2021
Accepted: 09 June 2021
Published: 21 July 2021

Citation:
Le Hingrat Q, Sereti I, Landay AL, Pandrea I and Apetrei C (2021) The Hitchhiker Guide to CD4$^+$ T-Cell Depletion in Lentiviral Infection. A Critical Review of the Dynamics of the CD4$^+$ T Cells in SIV and HIV Infection. Front. Immunol. 12:695674. doi: 10.3389/fimmu.2021.695674

CD4$^+$ T-cell depletion is pathognomonic for AIDS in both HIV and simian immunodeficiency virus (SIV) infections. It occurs early, is massive at mucosal sites, and is not entirely reverted by antiretroviral therapy (ART), particularly if initiated when T-cell functions are compromised. HIV/SIV infect and kill activated CCR5-expressing memory and effector CD4$^+$ T-cells from the intestinal lamina propria. Acute CD4$^+$ T-cell depletion is substantial in progressive, nonprogressive and controlled infections. Clinical outcome is predicted by the mucosal CD4$^+$ T-cell recovery during chronic infection, with no recovery occurring in rapid progressors, and partial, transient recovery, the degree of which depends on the virus control, in normal and long-term progressors. The nonprogressive infection of African nonhuman primate SIV hosts is characterized by partial mucosal CD4$^+$ T-cell restoration, despite high viral replication. Complete, albeit very slow, recovery of mucosal CD4+ T-cells occurs in controllers. Early ART does not prevent acute mucosal CD4$^+$ T-cell depletion, yet it greatly improves their restoration, sometimes to preinfection levels. Comparative studies of the different models of SIV infection support a critical role of immune activation/inflammation (IA/INFL), in addition to viral replication, in CD4$^+$ T-cell depletion, with immune restoration occurring only when these parameters are kept at bay. CD4$^+$ T-cell depletion is persistent, and the recovery is very slow, even when both the virus and IA/INFL are completely controlled. Nevertheless, partial mucosal CD4$^+$ T-cell recovery is sufficient for a healthy life in natural hosts. Cell death and loss of CD4$^+$ T-cell subsets critical for gut health contribute to mucosal inflammation and enteropathy, which weaken the mucosal barrier, leading to microbial translocation, a major driver of IA/INFL. In turn, IA/INFL trigger CD4$^+$ T-cells to become either viral targets or apoptotic, fueling their loss. CD4$^+$ T-cell depletion also drives opportunistic infections, cancers, and

comorbidities. It is thus critical to preserve CD4+ T cells (through early ART) during HIV/SIV infection. Even in early-treated subjects, residual IA/INFL can persist, preventing/delaying CD4+ T-cell restoration. New therapeutic strategies limiting mucosal pathology, microbial translocation and IA/INFL, to improve CD4+ T-cell recovery and the overall HIV prognosis are needed, and SIV models are extensively used to this goal.

Keywords: human immunodeficiency virus, simian immunodeficiency virus (SIV), AIDS, microbial translocation, immune activation (IA), inflammation, CD4+ T cells

INTRODUCTION

Even before HIV was formally established as the cause of AIDS, CD4+ T-cell depletion was identified as a key feature of HIV infection. Indeed, lymphocytopenia was among the first biological findings described in the early days of the AIDS pandemic (1). Lymphocytopenia was notably due to a depletion of CD4+ T cells and, in addition to their decrease in absolute number and percentage of total T cells, residual CD4+ T cells were dysfunctional in AIDS patients (1). Later, CD4 was identified as HIV/SIV receptor (2, 3), and CD4+ T cell counts in peripheral blood were reported to predict the risk of progression to AIDS (4).

However, the notions of CD4+ T-cell depletion and restoration encompass processes that are vastly different for different CD4+ T-cell subsets and according to their tissue location (5–8). As longitudinal studies cannot access and sample all body compartments, reasonable knowledge on CD4+ T-cell dynamics during HIV infection was obtained from descriptive studies of cohorts of HIV-1 infected patients and experimental studies of simian immunodeficiency virus (SIV) infection in nonhuman primates (NHP). Depending on whether or not an NHP is a natural host of SIV (9), the infection will be nonpathogenic or pathogenic, respectively, and CD4+ T-cell dynamics will also vary accordingly.

Here, we will review the general features of the depletion of the different CD4+ T-cell subsets and their restoration during pathogenic and nonpathogenic HIV/SIV infections, as well as the consequences of CD4+ T-cell depletion, and the potential approaches that could help reverse CD4+ T-cell depletion and prevent its deleterious consequences.

CD4+ T-CELL SUBSETS

Different CD4+ T-cell subsets are defined, according to their differentiation status or phenotype. CD4+ T cells from humans and NHP are classified as naïve (CD45RA+ CCR7+ CD28+ CD95neg) or memory T cells (CD45RO+ CD95+) (10, 11). Memory T cells are subdivided into stem cell memory (Tscm; CD45RA+ CCR7+ CD28+ CD95+) (12, 13), central memory (Tcm; CD45RAneg CCR7+ CD62L+) (11), transitional memory (Ttm; CD45RAneg CCR7neg CD95+ CD62L+), effector memory (Tem; CD45RAneg CCR7neg CD95+ CD28neg CD62Lneg) (14), terminal effector (Tte; CD45RA+ CCR7neg CD95+ CD28neg CD62Lneg) (14) and resident memory (Trm; CD45RAneg CCR7neg CD69+ ± CD103+) (15) T cells. Meanwhile, based on their functional status, CD4+ T cells can be classified as Th1 (IFN-γ producing; transcription factor: T-bet), Th2 (IL-4 producing; GATA3), Th17 (IL-17 producing; RORγt), regulatory T cells (Tregs) (suppressive function; FoxP3) and follicular helper T cells (Tfh) (IL-21 producing; Bcl6).

Additional phenotypic markers can be used to differentiate CD4+ T cells, notably CCR5, the main coreceptor of HIV/SIV (16–18), and markers of cell proliferation (Ki-67, BrdU), activation (HLA-DR, CD38, CD69), exhaustion (PD-1, CTLA-4, Tim-3) or senescence (CD57, KLRG-1) (19).

Finally, CD4+ T cells can also be subdivided according to their metabolic status, with memory cells tending to have higher metabolic activities, notably glycolysis and oxidative phosphorylation (20).

The multiple CD4+ T cell populations defined using any of these features are differentially infected, depleted, and restored. Note that during the course of the HIV/SIV infection other immune cells (CD4+CD8+ T cells, γδTCR T cells, innate lymphoid cells type 2 and 3, circulating dendritic cells) (21–26) can be depleted and restored, but their dynamics will not be detailed in this review.

CD4+ T-CELL DEPLETION IN PATHOGENIC HIV/SIV INFECTIONS

Circulation and Lymph Nodes

When CD4+ T-cell depletion was first investigated in people with HIV (PWH), research focused on CD4+ T cells dynamics in blood and superficial LNs, notably tonsils, as they were more accessible. Circulating CD4+ T cells are moderately depleted during acute HIV or SIV infection (21, 27, 28). A slight increase in the CD4+ T cell counts occurs as a consequence of the postacute partial control of viral replication and establishment of the steady-state set-points (27, 29). During chronic HIV/SIV infection, a slow and continuous decline of circulating CD4+ T cells is observed, eventually leading to severe lymphopenia, rendering persons living with HIV susceptible to opportunistic infections and eventually leading to AIDS (30). Annual rate of CD4+ T cell decline in circulation in untreated patients is correlated to plasma viral loads, and was found to be higher in persons living with HIV-1 than with HIV-2 (-15.9% *vs*. -4.1% per year, respectively), due to major differences in the levels of viral

replication between these two infections (31). Meanwhile, in the superficial and mesenteric lymph nodes, $CD4^+$ T-cell depletion is minimal during acute HIV or SIV infection (32–35). However, during the very advanced stages of HIV/SIV infection, $CD4^+$ T-cell depletion may occur even in lymph nodes and is associated with lymphadenopathy and fibrosis (34, 36, 37).

With the discovery that HIV-1, HIV-2, and most of the SIV use the chemokine receptor CCR5 as a coreceptor (16–18), and therefore preferentially infect memory T cells (38, 39), numerous studies then aimed at describing the dynamics of the different $CD4^+$ T-cell subsets in PWH and SIV-infected NHPs. In young, uninfected humans, most $CD4^+$ T cells in peripheral circulation and the lymph nodes are naïve, while the fraction of naïve $CD4^+$ T cells declines in older individuals (40). Naïve T cells also represent the majority of $CD4^+$ T cells in blood and lymph nodes of young (less than 4 years) rhesus macaques (RMs), the animal model of reference for HIV infection (11, 30). In Indian RMs, it has been estimated that, on average, less than 15% of $CD4^+$ T cells from circulation and the lymph nodes express CCR5 (30, 32, 41), while over 75% of them express CXCR4. In both humans and macaques, the vast majority of $CCR5^+$ $CD4^+$ T cells are memory T cells (30, 42, 43). As a result, the majority of circulating $CD4^+$ T cells are not direct targets for HIV and SIV, as emphasized by the low fraction of circulating $CD4^+$ T cells that are HIV-infected (44). This could explain why the loss of peripheral $CD4^+$ T cells is limited to 50-60% in most patients during acute HIV infection, with a median nadir of $CD4^+$ T cells ranging between 340 and 510/mm^3 (27, 45, 46). Similar decline in circulating $CD4^+$ T cells is also observed in SIV-infected NHP during acute pathogenic (21), non-pathogenic (47) and controlled SIV infections (48). In addition to this total $CD4^+$ T-cell depletion, a preferential depletion of the memory $CD4^+$ T cells, especially those expressing CCR5, can be seen as early as 7-14 days postinfection (dpi) in the lymph nodes and periphery, whereas naïve T cells are preserved (6, 28, 32, 49).

Once the strategies for the detailed characterization of the different memory $CD4^+$ T-cell subsets, notably Tcm, Ttm, Tem, became available, studies were performed on sorted $CD4^+$ T-cell subsets to assess the frequency of infection, in addition to monitoring the evolution of each of those subsets throughout HIV/SIV infection. These studies established that, in blood, Tcms represent the major cellular reservoir in HIV-1 infected individuals (50), while Ttms and/or Tems form the bulk of the reservoir in HIV-1 long term nonprogressors, SIVsmm-infected sooty mangabeys (a prototypic nonpathogenic infection) and HIV-2-infected individuals (51–53). In pathogenic hosts of SIV, the frequency of HIV/SIV infected cells is also high in the recently described Tscm subset, which expresses high levels of CCR5 (5, 54). In patients with progressive infection, as a result of a prolonged and continuous depletion of the target Tcm and Tem cells, due to cell death and reduced proliferation of Tcm, the majority of the remaining $CD4^+$ T cells are naïve (5, 6).

Dynamics of the $CD4^+$ T cells with specific functions have also been probed. Both HIV and SIV preferentially infect Th1 and Th17 cells (55). As a result, HIV and SIV infections are characterized by a switch from Th1 to Th2 phenotype (56), and a significant depletion of Th17 cells is observed among circulating lymphocytes throughout the infection (7). HIV-1 can also infect Tregs (57), and, although reduced (7, 58–60), stable, and increased (61, 62) absolute circulating Treg counts have all been reported during chronic infections, a decreased Th17/Treg ratio is commonly observed in pathogenic infections and was linked to immune activation and disease progression (7, 62). Furthermore, a selective depletion of circulating $CD4^+$ T cells with gut homing potential (i.e., expressing the $\alpha4\beta7$ integrin) preferentially occurs in untreated PWH (63) and in SIV-infected RMs in which those cells are selectively infected in the first days of infection (8). Most $CD4^+$ T cells expressing $\alpha4\beta7$ integrin are Tcm with a Th17 phenotype, and their dynamics in blood reflects the evolution of intestinal $CD4^+$ T cells in jejunum (8, 64).

A subset of $CD4^+$ T cells T follicular helper (Tfh), identified based on the expression of the surface markers $CXCR5^+$ PD-1^{high}, and preferentially found in B follicles in lymph nodes and spleen, can also be infected by HIV/SIV and is slightly depleted during acute infection, before accumulating during chronic infection (65–68). This chronic accumulation of Tfh might be due to a lack of regulation by the local Tregs, the follicular regulatory T cells (Tfr), as suggested by the decreased Tfr/Tfh ratio (69). Tfh cells are depleted during the AIDS stage (65). Signals provided by Tfh cells are crucial for the development of memory B cells, and the expansion of Tfh cells has been associated with B cell dysregulation, notably a reduced number of antigen-specific memory B cells, increased germinal center B cells, hypergammaglobulinemia, and lower Env-specific antibody titers (67, 70).

Finally, *in vivo*, $CD4^+$ T cells can be also selectively infected according to their metabolic status (71). HIV-1 tends to infect $CD4^+$ T cells with high oxidative phosphorylation and glycolysis, two metabolic activities more frequently enhanced in memory $CD4^+$ T cells (71). The dynamics of $CD4^+$ T cells during HIV/SIV infection according to their metabolic activities remain to be determined.

Gastrointestinal (GI) Tract

While the circulating lymphocytes only account for 2 to 5% of the total lymphocytes, intestinal lymphocytes represent a tremendous fraction of total lymphocytes (over 60%) in both humans and NHPs. In the GI tract, lymphocytes exist in three major forms: (i) intraepithelial lymphocytes (IEL), (ii) lamina propria lymphocytes (LPL), and iii) lymphocytes organized in lymphoid formations (i.e., the Peyer's patches and the solitary lymphoid follicles). There are strong similarities between human and NHPs' gut-associated lymphoid tissue (GALT) regarding the distribution of the immune cells, with the CD4/CD8 ratios being about 1:2 and 1:1 in IEL and LPL, respectively (72).

In the years following the identification of AIDS, prompted partly by the high frequency of enteropathies in PWH (73), histological studies identified a loss of $CD4^+$ T cells in gastrointestinal biopsies of PWH (74–79). Lim and colleagues also proved that, similar to circulation, memory $CD4^+$ T cells were the preferentially depleted cell subset in the gut during HIV infection (80). However, results were sometimes contradictory,

some studies reported that CD4+ T-cell depletion only affected the LPLs, while others described CD4+ T-cell depletion as impacting both LPLs and IELs (77, 81). Furthermore, almost all intestinal biopsies were obtained from clinically indicated procedures in patients presenting with AIDS or late-stage disease, limiting the insights on the dynamics of CD4+ T-cell depletion at this site (75).

It was only a decade later that, due to research performed in SIV-infected RMs, the early dynamics of CD4+ T-cell depletion in GI tissues were described (21, 33, 82). These studies reported that a massive CD4+ T-cell depletion occurs as early as 7 dpi in SIVmac-infected RMs, leading to more than 90% of intestinal CD4+ T cells being lost at 14-21 dpi (21, 33, 83) (**Figure 1**). SIV-infected cells can be detected within 7 dpi in the gut (21, 33, 93). The peak of viral replication in the gut occurs approximately 10 dpi and the vast majority of the SIV-infected cells during the acute infection are found within the lamina propria, the remaining infected cells being mainly detected in organized lymphoid tissues and macrophages (33, 77, 94). CD4+ T-cell depletion occurs earlier in the jejunum than in the ileum and colon, and affects mostly LPL (33), probably because most of the lymphocytes in jejunum are found within the lamina propria, while organized lymphoid tissues are more common to the ileum and colon. The first studies reporting this massive and rapid CD4+ T-cell depletion in the gut were performed on animals intravenously inoculated, but later the same pathogenic features were confirmed in studies in which animals were infected either intrarectally or intravaginally (83, 94).

Phenotypic analyses of the intestinal CD4+ T cells enabled further characterization of the CD4+ T-cell subsets that were preferentially depleted in the gut. Contrary to circulating lymphocytes, most of the CD4+ T LPL have an activated (HLA-DR+ CD25+) and memory (CD45RA^{neg} CD95+) phenotype (49, 95). Activated, CCR5-expressing memory CD4+ T cells, which are the preferential targets of HIV and SIV, are frequent in the gut (30, 49, 96). The predominance of this activated, memory CD4+ T cell phenotype at the mucosal sites is common to both humans and macaques, being observed even in the newborns (95), and likely occurs as a consequence of exposure to antigens *in utero*. Interestingly, mucosal CD4+ T cells of humans and NHPs that are not natural hosts of SIV express higher levels of CCR5 compared to African natural host species (30, 41, 47, 84). At 14 dpi, virtually all memory CCR5+ CD4+ T cells are lost in the lamina propria and effector sites of the gut of SIV-infected RMs, with the spared intestinal CCR5+CD4+ T cells being naïve T cells (30). This swift depletion of CD4+ T cells has been confirmed to occur as well during acute HIV-1 infections (35, 97–99), and intestinal CD4+

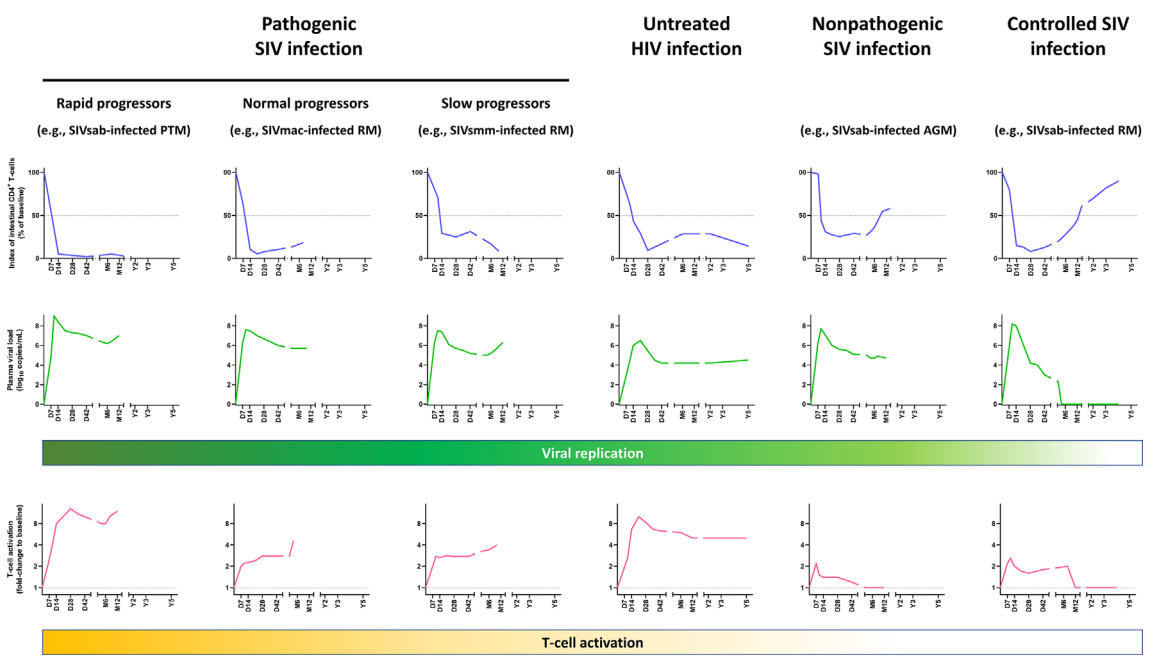

FIGURE 1 | Comparative dynamics of intestinal CD4+ T-cell depletion, plasma viral loads and immune activation/inflammation in untreated HIV and SIV infections. Schematic representation of intestinal CD4+ T-cell depletion, viral replication and immune activation is inferred from data reported in references (21, 33, 48, 84–91). Longitudinal data are presented, with the X axis representing days (D), months (M) and years (Y) postinfection. The Y axis illustrates the magnitude of lamina propria CD4+ T-cell depletion (upper panels, blue), viral replication (middle panels, green), and the levels of T-cell activation (lower panels, yellow). Intestinal CD4+ T-cell depletion is illustrated as the index of lamina propria CD4+ T cells (i.e., percentage of CD4+ T cell fraction within the CD3+ T cell population, divided by this percentage at baseline). Viral replication is represented as plasma viral loads. From the plethora of biomarkers of immune activation/inflammation, we selected the fold-change of HLA-DR+ CD8+ T cells in SIV-infected NHPs, compared to the baseline preinfection levels, except for persons living with HIV, for which the fold-changes of HLA-DR+ CD38+ CD8+ T cells were used. Note that in other primate models of rapid progressors, T-cell activation might be more blunted (92). AGM, African green monkeys; PTM, Pigtailed macaques; RM, Rhesus macaques.

T-cell depletion persists through the course of the disease in untreated PWH (35) (**Figure 1**).

As described for the circulating $CD4^+$ T cells, several experiments have shown that the initial $CD4^+$ T-cell depletion in the gut is driven by the coreceptor usage of the virus. NHP infection with X4-tropic viruses resulted in a rapid, profound depletion of the naïve $CXCR4^+$ $CD4^+$ T cells from the circulation and the lymph nodes, instead of the canonical depletion of memory $CD4^+$ T cells in the GALT, typical of the R5-tropic viruses (100–102).

Furthermore, mucosal $CD4^+$ T-cell depletion in the gut directly affects cell subsets that are involved in the maintenance of the mucosal barrier. As such, HIV/SIV infection can disrupt the production of IL-17 and IL-22, two cytokines that are essential for maintaining the tight epithelial barrier of the GI tract and gut integrity, by selectively depleting the lymphocytes producing those cytokines. Indeed, while Th1 and Th17 cell subsets are equally depleted in peripheral blood and they did not differ in frequency of infected cells, Th17 memory $CD4^+$ T cells are selectively depleted from the lamina propria and effector sites of the GI tract of PWH and SIV-infected RMs, as early as 2 weeks postinfection (55, 62, 85, 103). lL-22 producing lymphocytes are also depleted during SIV (104, 105) and HIV infections (85). Other IL-17 and/or IL-22 producing cells exist in the GI tract, but for most of them a preferential depletion and/or a reduced IL-17 production has been reported during SIV infection (25, 105–107). Moreover, IL-21-producing $CD4^+$ T lymphocytes are also depleted during SIV infection, thus limiting Th17 differentiation pathways, which are controlled by IL-21 *in vivo* (108).

Despite being susceptible to HIV and SIV infections, intestinal Tregs are increased during chronic infections, leading to a decreased Th17/Treg ratio (60, 62, 109). This could be due to limited productive infection and reduced cell death in the Tregs, as well as to an increased differentiation of naïve $CD4^+$ T cells into Tregs in the GI tract (109–112).

Note that, in addition to $CD4^+$ T-cell loss, RMs infected with SIVmac were reported to suffer a massive loss of the "double positive" ($CD4^+$ $CD8^+$) T cells, which express high levels of CCR5 and are highly activated (113), within days following SIV infection (30, 62).

Other Organs

$CD4^+$ T-cell depletion is not limited to the GI tract, lymph nodes, or circulation. It also occurs in the spleen and in the liver of NHP, within 21 dpi in the spleen and during the AIDS stage in the liver (67, 114, 115). In the bone marrow, the reduction of the pool of $CD4^+$ T cells reflects decreases in circulating $CD4^+$ T cells, with the loss affecting mainly memory cells (116). Meanwhile, $CD4^+$ T cell counts in the bronchoalveolar lavages (BAL) have been used as a proxy for the $CD4^+$ T cell counts in the lung parenchyma. Most $CD4^+$ T cells in the lung are of memory phenotype and express CCR5. A nearly complete loss of the $CD4^+$ T cells was observed in the BAL by 3 weeks postinfection (114), while other teams reported that both memory $CCR5^+$ $CD4^+$ T cells and Th17 cell subsets were maintained in the lungs (55, 117). Recently, a study in humanized mice demonstrated that SIV and HIV infections lead to a rapid loss of resident-memory $CD4^+$ T cells from the lung interstitium in the first weeks postinfection, which could participate in the increased susceptibility to pulmonary infections (118).

Finally, $CD4^+$ T-cell depletion can also be detected in the genital tract. As for $CD4^+$ T cells in the GI tract, most of the $CD4^+$ T cells found in the vaginal mucosa display an activated, memory phenotype (119). Differently from the intestinal $CD4^+$ T cells, almost all $CD4^+$ T cells from the vaginal mucosa express CXCR4, while CCR5 is expressed by only half of them. Within 14 dpi, depletion of $CD4^+$ T cells, particularly those with $CCR5^+$ expression, occurs in the vaginal mucosa of SIV-infected RMs, and lasts throughout the follow-up, until progression to AIDS (119). In HIV-infected women, vaginal $CD4^+$ T-cell depletion is strongly correlated to the depletion of circulating $CD4^+$ T cells (120). Regarding the male genital tract, $CD4^+$ T cells are depleted in the semen of PWH (121) and of SIV-infected cynomolgus macaques during acute and chronic infections (122).

$CD4^+$ T-CELL DYNAMICS DURING THE NONPATHOGENIC AND CONTROLLED SIV INFECTIONS

$CD4^+$ T-cell dynamics during nonpathogenic and controlled SIV infections have been extensively studied. Acute SIV infection induces a slight decline in the $CD4^+$ T cell counts from the lymph nodes and circulation in natural hosts (e.g., sooty mangabeys, African green monkeys, mandrills etc.), which is followed by a return to virtually preinfection levels at both sites within the first year (47, 123). As a result, the levels of circulating $CD4^+$ T cells are virtually normal in chronically SIV-infected African NHPs (124–127). Meanwhile, acute SIV infection induces a massive $CD4^+$ T-cell depletion at the mucosal sites, which largely exceeds the number of CCR5-expressing $CD4^+$ T cells that is particularly low at the mucosal sites in the natural hosts of SIVs (47, 84). This excess of $CD4^+$ T-cell depletion is not due to a different coreceptor usage by SIVs compared to HIV-1, as most SIV use CCR5 (128). The exceptions are strains of SIVsab that naturally infect sabaeus AGMs in West Africa and SIVmnd-1 that infects mandrills, which were reported to also use CXCR4 and/or CXCR6 (129–131), and SIVrcm that naturally infects red-capped mangabeys in West-Central African that was reported to exclusively use CCR2 (132–134). However, *in vivo*, SIVsab was shown to use CCR5 and preferentially deplete CCR5-expressing $CD4^+$ T cells (84).

Thus, severe acute $CD4^+$ T-cell depletion in GALT is not specific to pathogenic infection, nor is it predictive of the virulence of a retroviral infection, as shown by Pandrea et al., who proposed that the magnitude of the $CD4^+$ T-cell restoration was a better predictor of disease progression (84). This conclusion was also supported by studies in rhesus macaques (6). Interestingly, when cross-species infections of rhesus macaques with SIVsmm (47) and SIVagm (48) were performed, they resulted in pathogenic and controlled

infections, respectively. Yet, despite these completely opposite outcomes, in both instances, a severe mucosal $CD4^+$ T-cell depletion occurred during acute and early chronic infection (47, 48) (**Figure 1**). However, later on in the follow-up, a nearly complete restoration to baseline levels was observed in SIVagm-infected rhesus macaques (48), similarly to long-term nonprogressors (135), while SIVsmm-infected rhesus macaques experienced a progressive loss of intestinal $CD4^+$ T cells (47) (**Figure 1**). The SIVsmm-infected rhesus macaques eventually progressed to AIDS (47), and were classified as slow progressors, in comparison to rapid progressors (86, 136) and normal progressors (21, 33). In **Figure 1**, the rapidly progressive and normal progressive SIV infections are illustrated by the dynamics observed in SIVagm-infected pigtailed macaques and SIVmac-infected rhesus macaques, respectively. Note that such different patterns of disease progression can be observed in multiple species.

The presentation of SIV infection in natural hosts is intermediate between the two extreme patterns described above (i.e., pathogenic and controlled infections), consisting of a massive intestinal $CD4^+$ T-cell depletion during acute infection followed by a partial $CD4^+$ T-cell restoration during chronic SIV infection (**Figure 1**). This pattern is characteristic to SIVsmm infection of sooty mangabeys, SIVagm infection of African green monkeys and patas monkeys, and SIVmnd infection of mandrills (47, 84, 126, 137, 138). A relatively limited impact of the SIV infection on the mucosal $CD4^+$ T cells can also be observed in a subset of animals with pathogenic infections, the long-term nonprogressors which restore intestinal $CD4^+$ T lymphocytes and $CCR5^+$ memory T cells to higher values than normal progressors (97, 139), as long as viral replication is limited (**Figure 1**).

The relatively robust mucosal $CD4^+$ T-cell restoration occurs in natural hosts of SIV in the context of the control of chronic T-cell activation and inflammation. Thus, while T-cell activation and inflammation transiently increase during acute SIV infection, immune activation and inflammation are resolved during the transition between acute and chronic SIV infection, in spite of a relatively sustained, robust viral replication (47, 84, 123, 126, 140). This supports a paradigm in which acute $CD4^+$ T-cell depletion is driven in natural hosts of SIV by both viral replication and increased inflammation and immune activation, while partial recovery of intestinal $CD4^+$ T cells during chronic infection is enabled by the control of immune activation and inflammation, with the remaining mucosal CD4+ T-cell loss being due to the persistent viral replication.

Two important lessons can be drawn from nonpathogenic and controlled SIV infections. First, nonpathogenic SIV infections highlight that a moderate mucosal $CD4^+$ T-cell depletion has no discernible pathogenic consequences if immune activation and inflammation are kept at bay. Second, when immune activation, inflammation and viral replication are entirely contained, such as in the controlled SIV infections, total recovery of intestinal $CD4^+$ T cells is achievable, although it might take years to reach the preinfection levels (48) (**Figure 1**).

In the natural hosts, the control of the deleterious consequences of SIV infection (which include a moderate chronic $CD4^+$ T-cell depletion) resulted from multiple host adaptations that occurred over millions of years of host coevolution with their species-specific viruses (141). One of the keys to this exquisite control of the deleterious consequences of SIV infection in natural hosts of SIVs is the maintenance of the epithelial gut integrity *via* enhanced repair mechanisms (142, 143) and the absence of consequent microbial translocation, which is the main trigger of chronic T-cell activation in pathogenic infections (144). Some of the other host adaptations to elude SIV pathogenicity involve protection from $CD4^+$ T-cell depletion, either by preserving the pool of precursors, or by limiting the number of target cells. Interestingly, species which are natural SIV hosts usually present a reduced expression of CCR5 on circulating and mucosal $CD4^+$ T cells (41). It has also been reported that Tcm from sooty mangabeys were less frequently infected, potentially due to their lower CCR5 expression (52). By sparing Tcm precursors, as well as Tscm, sooty mangabeys might preserve their capacity to restore the pool of intestinal $CD4^+$ T cells (5, 52). Furthermore, lower levels of immune activation and apoptosis of the $CD4^+$ T cells from the LNs and circulation may help protect the immune system of the natural SIV hosts from the immune exhaustion described in the late-stage diseases of pathogenic HIV/SIV infections (92, 140, 145). This might be partly due to difference in the dynamics of type 1 interferons. Type 1 interferons are beneficial in the control of SIV infection during acute infection (146, 147), but persistent, dysregulated production is known to contribute to immune activation (147, 148), to induce the expression of proapoptotic markers in uninfected cells (149), and to be associated with disease progression (146). Interestingly, during chronic SIV infection, type 1 interferon response returns to preinfection levels in natural SIV hosts, while it remains elevated during pathogenic infections (62, 150, 151). Thus, the early control of type 1 interferon production in natural SV hosts might also play a role in preventing disease progression, by limiting immune activation and apoptosis of nearby uninfected $CD4^+$ T cells.

Additionally, limited $CD4^+$ T cell proliferation was described in AGMs, sooty mangabeys, and mandrills, notably among Tcm, with limited to no increase in proliferating $CD4^+$ T cells after acute infection (137, 152–156). Additionally, during SIV infection, CCR5 expression is not upregulated on memory $CD4^+$ T cells in sooty mangabeys, limiting new rounds of infection (52). By limiting bystander apoptosis, controlling cell proliferation after acute infection, and by limiting upregulation of CCR5 expression on the surface of the $CD4^+$ T cells, natural hosts of SIVs limit the production of new susceptible cells which might slow down the pace of $CD4^+$ T cell destruction.

Another consequence of the limited expression of CCR5 on the surface of target cells at the mucosal sites is the reduction in the virus ability to initiate mucosal infection (157). Limited expression of CCR5 by the $CD4^+$ T cells in the GI mucosa may also significantly impact the rates of maternal-to-infant transmission. CCR5 expression on the $CD4^+$ T cells is extremely low at birth and increases with age in both pathogenic and nonpathogenic hosts (156). However, this increase is delayed in

natural hosts of SIVs, and memory CD4+ T cells from the newborns express lower percentages of CCR5+ compared to non-natural SIV hosts, which creates the premise for a reduced rate of maternal-to-infant transmission rates of SIV in natural hosts (about 5%, compared to 20-25% in HIV-1, prior to antiretroviral therapy) (9, 158).

Another significant particularity of several African NHP species is their ability to downregulate CD4 receptor expression at the surface of their CD4+ T cells when they enter in the memory pool, rendering them resistant to SIV infection (137, 159, 160).

Through these mechanisms, natural hosts of SIVs spare specific CD4+ T-cell subsets, which could contribute to the control of inflammation and maintenance of gut integrity, despite high viral replication during chronic nonpathogenic infections. Multiple immune cell populations are involved in these processes. As an anti-inflammatory milieu, notably containing TGFβ, is rapidly established, this enhances Treg production, thus preventing the chronic immune activation (87). Furthermore, Th17 cells are spared in both gut and blood of SIVsmm-infected SMs and SIVagm-infected AGMs (55, 62, 104). The Th17/Treg ratio remains stable during SIV infection in natural SIV hosts, while it correlates with disease progression in pathogenic infections (62). Similarly, Th17 cells, as well as $\beta7^{hi}$ CD4+ T cells, are maintained in the blood and in the colon of HIV-1 long-term nonprogressors (135). Moreover, the $CD4^{neg}$ $CD8\alpha^{dim}$ T cells and the $CD4^{neg}$ $CD8^{neg}$ (DN) T cells are able to retain some of the helper T cells functions in the African NHPs that are natural hosts of SIV (34, 160, 161).

MECHANISMS OF CD4+ T-CELL DEPLETION

The loss of CD4+ T cells is caused by different intertwined mechanisms (162). Viral replication significantly contributes at least to the initial CD4+ T cell loss, which occurs rapidly in infected individuals and animal models during the acute stage of infection and mirror that of the dynamics of viral replication. Several mechanisms of cell death are directly induced by the infection of those cells by the virus: (i) cytolysis due to increased permeability of cell membrane after viral budding and/or syncytium formation (163), (ii) targeting by HIV/SIV-specific cytotoxic T lymphocytes (164, 165), and (iii) programmed cell death of cells undergoing productive infection, due to caspase-3 and/or Bax activation (166–168) (**Figure 2**). Antibody-dependent or complement-mediated mechanisms are also involved in the destruction of HIV/SIV-infected cells [antibody-dependent cellular cytotoxicity (ADCC) (169), antibody-dependent phagocytosis (170), complement-mediated phagocytosis and lysis (171)], although escape mechanisms have been described for HIV and SIV (172–174).

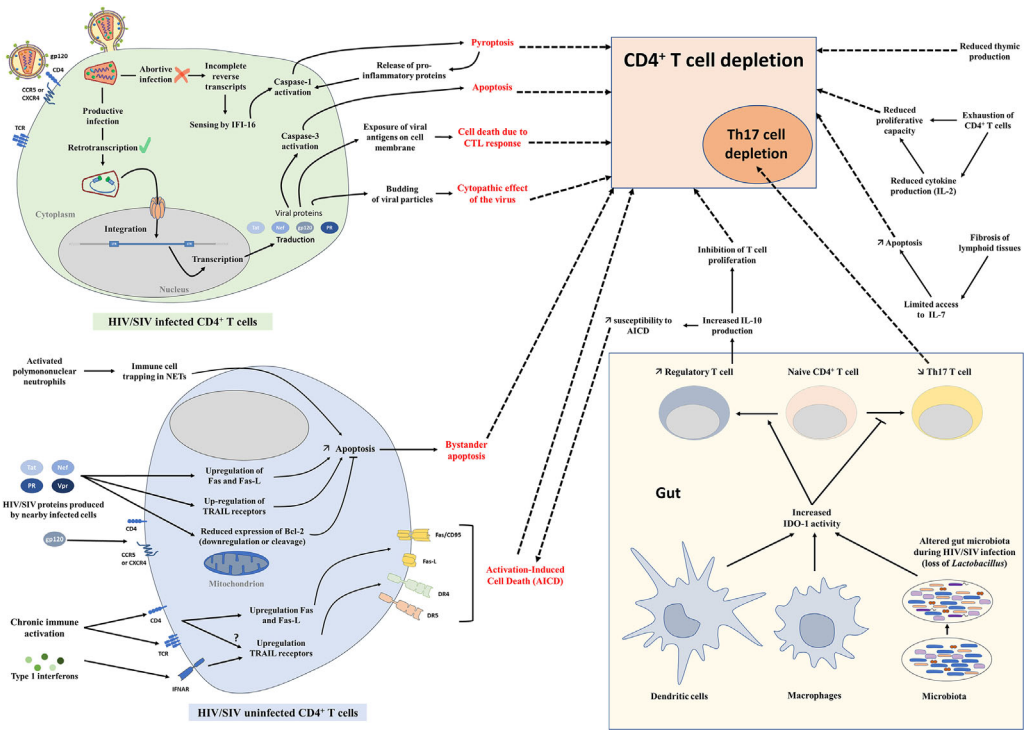

FIGURE 2 | Mechanisms of CD4+ T-cell depletion. Schematic representation of different mechanisms involved in CD4+ T-cell depletion during HIV and SIV infections. AICD, Activation-induced cell death; CTL, Cytotoxic T lymphocytes; IDO-1, Indoleamine 2,3-dioxygenase 1; NETs, Neutrophil extracellular traps.

There are several lines of evidence to support this direct impact of viral replication on $CD4^+$ T-cell depletion. First, there is a clear temporal association between viral loads and $CD4^+$ T-cell depletion, with the most prominent depletion in the gut closely following the peak of viral replication, which occurs circa one to two weeks postinfection (33, 83, 175) (**Figure 1**). Moreover, there is a clear correlation between the levels of viral replication during acute infection and the magnitude of the $CD4^+$ T-cell depletion, particularly in the gut (94). Studies have shown that mucosal depletion is minimal if peak viral loads are below 10^6 vRNA copies/ml of plasma (48, 137). Furthermore, despite their exquisite ability to finely tune inflammation and T-cell immune activation, NHP species that are natural hosts of SIVs also experience a residual $CD4^+$ T-cell depletion during chronic infection when inflammation and immune activation are controlled (47, 84), highlighting the role of viral replication in the persistence of intestinal $CD4^+$ T-cell depletion.

Despite this proven impact of viral replication on $CD4^+$ T cells at every stage of HIV/SIV infection, the extent of $CD4^+$ T-cell loss during the acute infection far exceeds the number of infected lymphocytes (32, 94). Multiple mechanisms have been proposed to explain this excess of $CD4^+$ T-cell depletion in HIV infection and pathogenic SIV infections (**Figure 2**): (i) Bystander apoptosis (140, 176), due to viral proteins promoting apoptosis of nearby cells, notably HIV-1 gp120 after its interactions with CD4 and CCR5 or CXCR4 coreceptor (177, 178),; note that in natural hosts of SIVs the levels of bystander apoptosis are kept at bay (84, 140, 145); (ii) Activation-Induced Cell Death (AICD) due to immune activation which induces FasL production and Fas (CD95) expression in nearby, uninfected $CD4^+$ T cells, shortening their lifespan and increasing their sensibility to AICD (179–182); interestingly, plasma FasL expression does not significantly increase in animals with nonpathogenic SIV infections (148, 183, 184) (iii) Abortive infection leading to pyroptosis through the caspase-1 pathway, due to an accumulation of incomplete reverse transcripts and induction of antiviral and inflammatory responses (185); (iv) Trapping of immune cells in neutrophil extracellular traps (NETs) induced by SIV infection, followed by an induction of apoptosis or lysis of those trapped $CD4^+$ T cells, as recently described (186) (**Figure 2**).

In addition to these general mechanisms involved in total $CD4^+$ T-cell depletion, preferential depletion of Th17 cells could be partly due to the induction of indoleamine 2,3-dioxygenase (IDO-1), caused by sustained microbial translocation and immune activation in pathogenic infections (110, 187) (**Figure 2**). Catabolites produced by the degradation of tryptophan by IDO-1 enhance Treg and deplete Th17 cells (110). As adaptive Tregs can produce IL-10 that inhibits T cell proliferation (188) and increases susceptibility to AICD (180, 189), accumulation of Tregs during chronic HIV/SIV infection could also exacerbate $CD4^+$ T-cell depletion.

Furthermore, in late stages of HIV/SIV infection, immune exhaustion plays a role in total $CD4^+$ T-cell depletion. During chronic infection, increased expression of PD-1 and other immune check-point inhibitors is observed on $CD8^+$ T cells, but also on $CD4^+$ T cells. Exhausted HIV/SIV-specific $CD4^+$ T cells, which are associated with high plasma viremia, have a decreased proliferative capacity and reduced polyfunctional cytokine response, including decreased production of IL-2 (190–192). This fuels gradual $CD4^+$ T-cell depletion, in combination with the reduced production of naïve T cells by the thymus (193) and TGF-β-driven fibrosis of lymphoid tissues (194, 195) that are observed during HIV and SIV infections (**Figure 2**).

CONSEQUENCES OF THE $CD4^+$ T-CELL DEPLETION

The consequences of $CD4^+$ T-cell depletion have been widely scrutinized, highlighting the critical roles of this cell subset for disease progression and development of comorbidities during pathogenic infections (4, 196–198). The first observation made in patients and NHPs with low peripheral $CD4^+$ T-cell counts ($<200/mm^3$) was their extreme susceptibility to opportunistic infections (notably fungal infections including *Pneumocystis jirovecii* pneumonia, mycobacterial infections, and cytomegalovirus disease) (199, 200). In addition, PWH with a lower nadir of $CD4^+$ T-cell count are also at higher risk of developing AIDS-defining cancers (non-Hodgkin lymphoma, cervical cancer, and Kaposi sarcoma) (201, 202).

However, it was reported that the profound, but transient, $CD4^+$ T-cell depletion observed during acute nonpathogenic SIV infections and the residual mucosal CD4+ T-cell depletion persisting during chronic nonpathogenic SIV infections were not sufficient to trigger disease progression (203). As such, a new paradigm emerged in which the combination of $CD4^+$ T-cell depletion (notably Th17 cells), inflammation and immune activation in the GI tract drive the deleterious consequences of HIV infection. During HIV/SIV infection, $CD4^+$ T cells but also myeloid cells are killed, releasing inflammatory cytokines (204, 205), including IL-1β, thus creating an inflammatory environment (185, 206). Combined with the loss of IL-17 and IL-22-producing cells that are involved in epithelial integrity maintenance and homeostasis, as well as in antimicrobial defense (25, 104, 207), this leads to damage of the gut epithelial integrity, enteropathy and microbial translocation (83, 93, 144). The role of impaired epithelial integrity in driving microbial translocation was confirmed by the demonstration of the leakage of microbial products occurring near breaks in the epithelial lining (144). Microbial translocation can be detected in mucosal tissues (lamina propria, gut-associated lymphoid tissue, mesenteric lymph nodes), but also in distant lymph nodes and circulation (144, 208, 209). These microbial products fuel local and systemic inflammation, and macrophage activation (144, 210). Sustained inflammation and immune activation trigger a vicious cycle by attracting new $CD4^+$ T cells, increasing the number of susceptible cells, and by reactivating proviruses in latently-infected cells (206). Newly produced viral proteins and viruses can in turn boost inflammation, tissue damage, and microbial translocation.

The importance of the maintenance of the integrity of the intestinal epithelium was demonstrated recently (209). DSS-induced colitis in SIV-infected AGMs disrupted the intestinal epithelium integrity, recapitulating the characteristics of a pathogenic SIV infection, i.e. increased local inflammation and immune activation, detection of microbial products in lymphoid tissues and increased viral replication (209). Meanwhile, in the inflammatory bowel diseases (IBD), mucosal inflammation is associated with loss of intestinal epithelial integrity and massive infiltration of immune cells, including T cells, in the lamina propria. In response to their exposure to microbial antigens, these T cells produce inflammatory cytokines (IFNγ, TNFα) which disrupt tight-junctions function and worsen intestinal epithelial integrity. However, unlike during HIV/SIV infection, local inflammation does not lead to $CD4^+$ T-cell depletion in patients with IBD; on the contrary, most IBD patients present with increased numbers of intestinal $CD4^+$ T cells, including Th17 cells (211). As such, comparison with IBD demonstrates that inflammation *per se*, in the absence of the viral trigger, can damage the gut integrity, but it is not sufficient to deplete intestinal $CD4^+$ T cells. However, in the context of HIV/SIV infection, inflammation drives T-cell activation (209) and eventually leads to T cell loss through increased viral replication and/or activation-induced cell death (AICD). It is possible that the persistent expression of high levels of type 1 interferons during chronic, pathogenic HIV/SIV infections play a role in this T cell loss, as type 1 interferons are known to induce AICD. Conversely, treatment with type 1 interferons had been evaluated in IBD (212), due to their ability to inhibit Th17 cell differentiation (213).

Chronic inflammation has been linked to numerous non-AIDS comorbidities, notably cardiovascular diseases, liver fibrosis and thromboembolism (214–216). Inflammation and immune activation also promote a procoagulant state in infected animals (217), and they are positively correlated with disease progression (217).

RESTORATION OF $CD4^+$ T CELLS DURING ART

Assessment of the extent of $CD4^+$ T-cell restoration in the GI tract that can be expected in patients initiating ART during acute or chronic HIV infection is complex, as most studies focused on the total $CD4^+$ T cell counts and only few investigated specific $CD4^+$ T-cell subsets, such as memory or Th17 cells. Furthermore, the replenishment of mucosal $CD4^+$ T cells can take time, requiring long follow-up of PWH or NHP.

However, there is a general consensus in the field that the efficacy of the $CD4^+$ T-cell restoration on ART vastly depends on the stage of the infection and the degree of immunosuppression at the time of treatment initiation. Guadalupe et al., reported that when ART was initiated at 6 weeks post-HIV infection and was maintained for 14 months, the levels of mucosal $CD4^+$ T cells were close to values observed in uninfected individuals (97). Further studies have found that, when ART was initiated in the first weeks postinfection, and viral replication was suppressed in plasma and decreased by 1,000-fold in the GALT, a significant, albeit incomplete, restoration of mucosal $CD4^+$ T cells was observed in all humans and macaques (88, 99, 218) (**Figure 3**). In rhesus macaques in which ART was initiated prior to the acute mucosal $CD4^+$ T-cell depletion (i.e., 7 days post-SIVmac251 infection), ART failed to prevent $CD4^+$ T-cell depletion in the GALT, but enabled a virtually complete $CD4^+$ T-cell restoration by 6 months postinfection, particularly through a significant increase in the Tcm levels (88). Meanwhile, while early ART initiation at 3 to 4 days postinfection did not prevent the establishment of the SIV reservoir in lymph nodes (222), it prevented Th17 depletion in the lymphoid tissues (61). Similarly, early treatment of acutely HIV-infected individuals (Fiebig stage I or II) could not halt mucosal $CD4^+$ T-cell depletion in the first weeks post-treatment but generated a strong restoration of $CD4^+$ T cells in the lamina propria at 96 weeks post-treatment (99) (**Figure 3**).

Meanwhile, most data on patients which initiated ART during chronic HIV/SIV infection suggest a modest $CD4^+$ T-cell restoration in the GI tract (97, 98, 219), at least when considering the relative $CD4^+$ T cell counts (223). Finally, in patients in which ART was initiated during the AIDS stage, the immune restoration was minimal and occurred very slowly (224) (**Figure 3**).

In patients on ART, a more robust restoration of mucosal $CD4^+$ T cells was observed in patients with higher frequency of Tcm in the lamina propria of the jejunum, suggesting that the maintenance and/or the restoration of this subset is critical for an important restoration of intestinal $CD4^+$ T cells (219). Furthermore, Th17 cells were also restored in patients receiving ART, especially in those in which therapy was initiated very early in infection (85). However, Th17/Treg ratio remained reduced, as Treg cell counts in lymph nodes and in GALT did not return to baseline levels in PWH receiving ART (60, 61), which might be due to the residual viral replication and immune activation in the GALT of those patients (219).

Overall, as a near-total restoration of mucosal CD4+ T cells is observed only in early ART-treated patients, this is a strong incentive for a generalization of early antiretroviral treatment in all PWH.

OTHER TYPES OF $CD4^+$ T-CELL DEPLETION

Important insight on the impact of $CD4^+$ T-cell depletion on HIV pathogenesis has been gained by directly depleting the $CD4^+$ T cells with monoclonal antibodies, or by using knock-out models in different animal species, as well as through the study of genetic diseases in humans.

Experimental $CD4^+$ T-Cell Depletions

Total CD4+ T-Cell Depletion

The first studies on $CD4^+$ cell depletion in SIV-infected and SIV-uninfected NHP, performed with anti-CD4 monoclonal

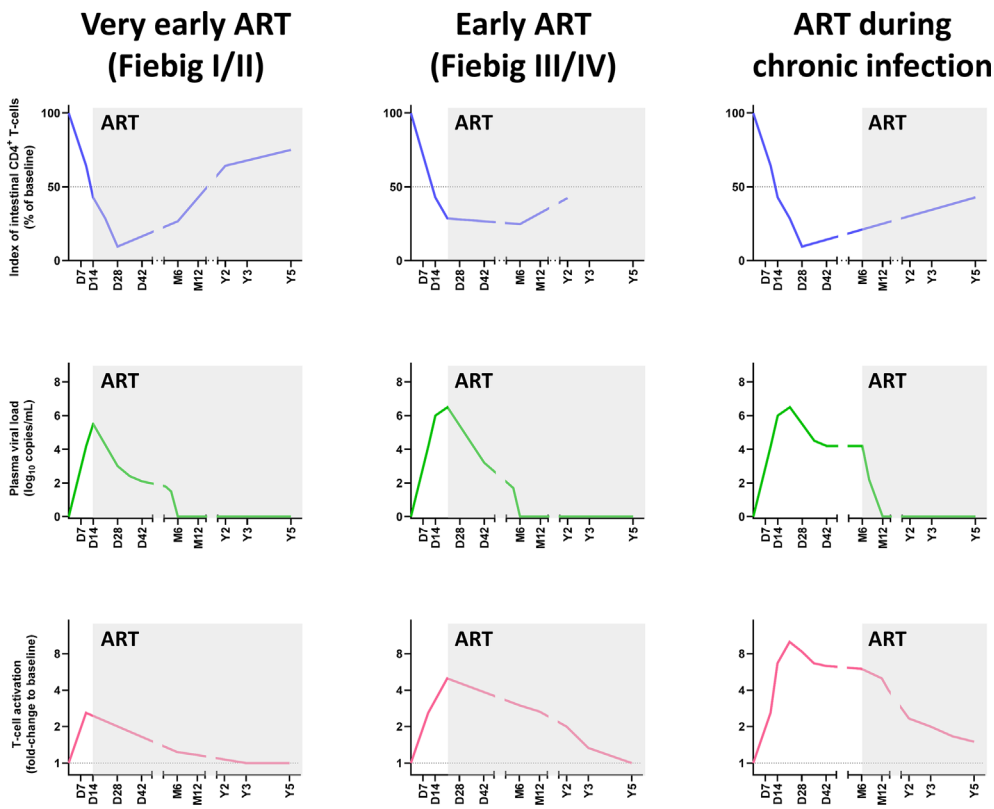

FIGURE 3 | Comparative dynamics of intestinal CD4+ T-cell depletion, plasma viral load and immune activation/inflammation in treated HIV infections, according to the timing of initiation of antiretroviral therapy ART. Schematic representation of intestinal CD4+ T-cell depletion, viral replication and immune activation is inferred from data reported in references (85, 90, 91, 99, 219–221). Longitudinal data are presented, with the X axis representing days (D), months (M) and years (Y) postinfection. The Y axis illustrates the magnitude of mucosal CD4+ T-cell depletion (upper panels), viral replication (middle panels), and the levels of immune activation/inflammation (lower panels). Intestinal CD4+ T-cell depletion is illustrated as the index of CD4+ T cells (i.e., percentage of CD4+ T cell fraction within the CD3+ T cell population, divided by this percentage at baseline). Viral replication is represented as plasma viral loads. From the plethora of biomarkers of immune activation/inflammation, we selected the fold-change of HLA-DR+ CD38+ CD8+ T cells in persons living with HIV, compared to uninfected individuals. ART, Antiretroviral therapy.

antibodies, were published over a decade ago (225–228), and reported that, despite an increased percentage of proliferating (Ki-67+) CD4+ T cells, reconstitution of CD4+ T cell population was slower than what was reported for CD8+ T cells in CD8-depleted animals, regardless of SIV infection status (226, 227). Interestingly, CD4+ T-cell restoration postexperimental depletion did not differ between natural and non-natural SIV hosts (227), reinforcing the previous finding that the higher restoration of intestinal CD4+ T cells in natural hosts of SIV was not due to a higher cell proliferation.

In CD4-depleted, SIV-infected NHPs, plasma viral loads decreased, in relation with the low number of CD4+ T cells (225). However, when CD4+ T-cell depletion was induced prior to SIV inoculation, this led to persisting high plasma viral loads in CD4+ T-cell-depleted monkeys, with no postpeak decline of viremia, and accelerated disease progression (229, 230).

Interestingly, microbial translocation was not increased in SIV-uninfected CD4-depleted animals (227), and CD4+ T-cell depletion was not sufficient to reactivate viral replication in CD4-depleted, ART-treated NHPs (228). This limited clinical impact of experimentally-induced CD4+ T-cell depletion might be explained by the limited CD4+ T-cell depletion at the mucosal effector sites, notably in the GI tract (<50%), in those studies during which anti-CD4 monoclonal antibodies were administered over a short period of time.

Selective Treg Depletion

Since Treg are usually accumulating throughout chronic HIV/SIV infection, are frequently infected and suppress HIV/SIV-specific cytotoxic T cell responses (231), different Treg-specific depletion strategies, targeting either CD25 (IL-2 receptor subunit) (232–234) or CCR4 (234, 235), have been investigated. Despite achieving only partial Treg depletion with maximal effect in blood and lymph nodes, and minimal depletion in GI tract, this usually led to increased SIV-specific T cell responses (232, 234), and increased immune activation (232–234). Another strategy aimed at blocking CTLA-4 also resulted in increased SIV-specific T cell responses (236). Viral reactivation occurred in most NHPs in which Treg functions were blocked by anti-CTLA-4 monoclonal antibodies, or in

which Treg were depleted (232–234, 237, 238). Higher viral loads in mucosal tissues and greater loss of CCR5$^+$ CD4$^+$ T cells in the rectal mucosa have been reported to occur in the NHPs receiving an anti-CTLA-4 blocking monoclonal antibody (237).

Knock-Out Models

Numerous CD4 knock-out mice models have been developed (239–241). In these mice, the TCR$\alpha\beta^+$ $\gamma\delta^-$ CD4^{neg} CD8^{neg} (double negative, or DN) T-cell subset is expanded (239). The TCR repertoire of those DN T cells is more polyclonal than in wild-type mice, and these cells are able to maintain part of the helper T cell functions, similarly to natural hosts of SIV (240, 241). However, it was reported that memory cytotoxic CD8$^+$ T lymphocytes could be reduced in CD4-deficient mice (242).

Idiopathic CD4 Lymphopenia

In the late 1980s, a severe lymphopenia, preferentially impacting CD4$^+$ T cells, was identified in HIV-uninfected patients with no other condition or treatment known to induce lymphocytopenia (243). This condition was termed idiopathic CD4 lymphopenia (ICL) (244). This disease is rare, with less than 0.5% of blood donors in the United States meeting the definition criteria (245, 246). Due to their low levels of circulating CD4$^+$ T cells, ICL patients develop opportunistic infections, some similar to AIDS patients, notably fungal, nontuberculosis mycobacterial and HPV-associated infections (247, 248). A recent work suggests that ICL could have an autoimmune component linked to the production of auto-antibodies directed against CD4$^+$ T lymphocytes (249). In some cases, genetic mutations have also been linked to ICL (250).

In addition to CD4$^+$ T-cell lymphopenia, an increase in circulating Treg was observed and, in some patients, decreases in CD8$^+$ T cells and/or CD19$^+$ B cells and/or NK cell counts were also reported (247, 248). Furthermore, CD4$^+$ T cells are more activated and proliferating in ICL patients than in controls (247, 251). No specific depletion of CD4$^+$ T- cell subsets (Th1, Th2, Th17) was observed in peripheral blood, but a reduction of the percentage of naïve CD4$^+$ T cells was seen, compared to controls and PWH (251). Monitoring the CD4$^+$ T-cell counts in the mucosal tissues of ICL patients also identified a profound CD4$^+$ T-cell loss, although less severe than in PWH, as only a 3-fold reduction in the number of intestinal CD4$^+$ T cells was observed (252). This CD4$^+$ T-cell loss did not affect the functionality of mucosal Th1 and Th17 cells (252). While an initial study on 10 ICL patients reported a slight increase in microbial translocation (251), a more recent study of 46 ICL patients found normal levels of LPS, and only slight increases of sCD14 (252). We can hypothesize that, similarly to natural hosts of SIV, despite CD4$^+$ T cell loss, the maintained functionality of remaining Th17 cells and/or other IL-17 producing cells such as mucosa-associated immune T cells (MAIT) might be sufficient to preserve gut epithelial integrity and limit microbial translocation in ICL patients (253).

Genetic Mutations

Absolute CD4+ T-Cell Depletion

Genetic mutations leading to absolute CD4$^+$ T-cell depletion have been reported in two patients, one 22-year-old female with a mutation in the translation initiation codon of the CD4 gene (254) and a 45-year-old female with a mutation in a splice acceptor site leading to the expression of a CD4 protein lacking its anchoring domain to the cellular membrane (255). In the first case, neither CD4 expression on cell membrane, nor soluble CD4 were detected, whereas for the second patient, only CD4 expression on cell membrane was abrogated, while soluble CD4 could still be detected in plasma (254, 255). The first patient was hospitalized for severe viral respiratory infection which led to the discovery of her primary immunodeficiency. Both patients presented numerous HPV-associated warts. However, in both cases, immunodeficiencies were only detected when patients were adults, later than most other primary cellular immunodeficiencies. Interestingly, in both cases, it was shown that helper T cell functions could be performed by DN T cells and/or CD8$^+$ T cells (254, 255), similarly to what has been described in in natural hosts of SIV (160, 161) and in CD4 knock-out models in mice (240, 241). The DN T-cell subset was also expanded, similarly to CD4 KO mice. These two reports illustrate that this rescue mechanism can also be found in humans. This absence of CD4$^+$ T cells has also been reported in one patas monkey with near-complete loss of peripheral and mucosal CD4$^+$ T cells, which protected it from productive SIV infection when intravenously-inoculated with SIVsab (137).

Depletion of the Th17 Subset of CD4$^+$ T Cells

Patients with hyper-IgE syndromes present with elevated IgE serum levels, decreased Th17 cells, and higher susceptibility to *Staphylococcus aureus* pulmonary, skin infections and *Candida* infections (256, 257). Multiple genetic mutations have been associated with this syndrome, and patients with DOCK8 mutation also present with HPV-associated warts, cutaneous manifestations of *Molluscum contagiosum* and/or Herpes simplex virus infections (258, 259). These studies highlight the importance of Th17 cells in the protection of the organism from bacterial and fungal infections, notably through the maintenance of the integrity of the intestinal barrier, as also emphasized by the increased microbial translocation observed during HIV and SIV pathogenic infections in which Th17 cells are depleted and the intestinal barrier is damaged, with visible breaches in the intestinal epithelium.

PERSPECTIVES FOR THERAPEUTIC APPROACHES AIMED AT PREVENTING OR LIMITING CD4$^+$ T-CELL DEPLETION AND ITS CONSEQUENCES

The most effective treatment currently available for preventing or limiting CD4$^+$ T-cell depletion is the early initiation of ART, ideally during Fiebig stages I or II. This is the only treatment which has proved a high efficacy in restoring intestinal CD4$^+$ T cell in PWH and can have additional positive impact on limiting size of viral reservoirs (**Figure 3**). However, as there is persistent immune activation in PWH on ART, which could cause a limited CD4$^+$ T cell loss, early ART might not be sufficient to entirely

restore mucosal CD4+ T cells in all patients. It should also be acknowledged that, even when viral replication is suppressed, restoration can take time, as evidenced in elite controllers SIVagm-infected RMs, in which complete recovery of intestinal CD4+ T cells was only observed after 4 years of absence of viral replication in plasma and tissues (48) (**Figure 1**). Thus, complete recovery of intestinal CD4+ T cells in PWH could take even longer, especially if the treatment could not be initiated early in the infection.

As the crucial role of IL-17 and IL-22 producing T cells in preserving the mucosal integrity emerged recently, it has been hypothesized that treatments aiming at maintaining or restoring those cell subsets could limit the deleterious impact of CD4+ T-cell depletion in HIV/SIV-infected NHPs, i.e., microbial translocation, inflammation, and immune activation. As pointed out, a long follow-up of PWH receiving those treatments will probably be necessary before being able to definitively rule on their efficacy.

IL-21

IL-21 has been described to enhance several immune functions, including long-term maintenance of CD8+ T cells, differentiation of memory B cells and differentiation of naïve CD4+ T cells into Th17 cells (108, 260–262). Several studies have explored its potential to limit Th17 depletion in SIV-infected NHPs. In a preliminary study, Micci et al., observed that, after 5 weekly doses of recombinant IL-21, the frequency of circulating Th17 cells increased in chronically SIVmac-infected macaques (108). Paiardini et al., confirmed these findings in a subsequent study in rhesus macaques treated with IL-21 between weeks 2 and 6 postinfection (263). They observed no difference with respect to the total CD4+ T cell counts in circulation, lymph nodes and the GI tract, but intestinal Th17 cells were maintained at week 6 postinfection in IL-21-treated macaques, while a severe depletion was observed in controls (263). This preservation of the Th17 cell subset was associated with lower intestinal inflammation and microbial translocation, as expected (263). Unfortunately, this protective effect on Th17 depletion faded away and intestinal Th17 cell loss was similar in both groups 23 weeks postinfection (263). Similarly, in ART-treated SIV-infected macaques, treatment with IL-21 did not enhance total CD4+ T-cell restoration in the circulation, lymph nodes and GI tract, but both intestinal Th17 and IL-22- producing CD4+ T cells were restored to near-baseline levels (264). Th17 cells were more frequently polyfunctional in IL-21-treated macaques, and this effect was more robust in jejunum than in rectal biopsies (265). This was sufficient to limit neutrophil infiltration in intestinal tissues, as well as T cell activation and proliferation. However, these positive effects were also blunted over time (264, 265). Conversely, one recent study reported a reduction in immune activation and T-cell exhaustion in IL-21 treated rhesus macaques, but did not see any impact on Th17 CD4+ T cells (266).

IL-7

IL-7 was among the first cytokines investigated, as it was shown to boost CD4+ T-cell regeneration (267–269). In SIV-infected rhesus macaques on ART, rsIL-7 induced a transient increase in CD4+ and CD8+ T-cell counts (270). Similarly, in virologically-suppressed PWH on ART, rhIL-7 increased CD4+ T-cell counts in circulation and in the gut (268, 271, 272). Although transient viral reactivations were detected, mainly in patients receiving high rhIL-7 doses (268, 271), and a slight increase in viral reservoir was reported (273), those preliminary results were promising for restoring T cells but clinical trials investigating IL-7 were interrupted due to the appearance of neutralizing antibodies in IL-7-treated patients and production issues.

IDO-1 Inhibitors

Metabolites generated by the catabolism of tryptophan by IDO-1 (kynurenine pathway) can lead to an increase in the number of Treg while depleting Th17 CD4+ T cells (110), Specific IDO-1 inhibitors have been used in oncology, but none has been tested in PWH and only one in SIV-infected RMs (274, 275). Until now, in the HIV/SIV field, in order to reduce IDO-1 expression, most studies focused on altering gut microbiota. A recent study by Vujkovic-Cvijn and colleagues showed that dysbiosis caused by acute SIV infection, notably loss of *Lactobacillus* spp, increased IDO-1 activity and was correlated with Th17 depletion in peripheral blood (187). Interestingly, enhanced IDO-1 activity due to SIV infection could be thwarted by supplementing SIV-infected macaques with *Lactobacillus* (187). The addition of IL-21 did not further lower IDO-1 activity (187, 265). However, the beneficial effect of those probiotic treatments on Th17 cell restoration still has to be demonstrated.

Alterations of intestinal microbiota in PWH and in SIV-infected NHPs have been extensively described (276). In pigtailed macaques (PTM), prebiotics/probiotics improved intestinal CD4+ T cell counts, enhanced functionality of colonic Th17 and Th1 CD4+ T cells, but did not prevent systemic microbial translocation as shown by the presence of microbial products in peripheral lymph nodes (277). Clinical trials have suggested a potential beneficial effect of probiotics on circulating CD4+ T-cell counts or intestinal Th17 cells (278–280). However, the varying compositions of probiotic supplements hindered comparisons between studies, and most of these studies were underpowered due to a low number of included patients. Moreover, other confounding factors complicated the evaluation of those strategies: both HIV-1 and LPS induce IDO-1 expression (112, 281), and thus ART itself could reduce IDO-1 activity in PWH (282).

Another inhibitor of the kynurenine pathway has been recently evaluated in NHPs, a kynurenine 3-monooxygenase inhibitor which increased circulating CD4+ T cells but failed to increase intestinal Th17 cell restoration and to prevent microbial translocation (283). Recently, one work reported increased Th17 and Th22 populations among circulating CD4+ T cells in ART-treated, SIV-infected rhesus macaques that received a fecal microbial transplantation (284). This restoration of Th17 and Th22 subsets in the blood needs to be confirmed in intestinal tissues in further studies.

Others

Other strategies have been suggested. One of them consists of targeting CD4+ T cells expressing α4β7 integrin, which is a gut-

homing signal (285), using an anti-α4β7 monoclonal antibody, to reduce the number of susceptible cells in mucosal tissues and preserve $CD4^+$ T cells in the GALT (286). In preliminary works, SIV-infected NHPs receiving anti-α4β7 monoclonal antibody had higher $CD4^+$ T cell counts than controls in both peripheral blood and in intestinal tissues (286, 287). However, in PWH, despite a slight increase in the circulating $CD4^+$ T cell counts at 10 weeks postinfusion, this increase was not sustained (288). Furthermore, even though gut homing was limited, treatment with anti-α4β7 monoclonal antibody did not prevent HIV or SIV infection, viral reservoir seeding, nor it delayed viral rebound post-treatment interruption (288, 289). Recently, an anti-caspase inhibitor administered to RMs in the first days following SIVmac infection has been shown to reduce T cell death and maintenance of CD4/CD8 T cell ratios (290). Furthermore, memory CD4+ T cells were preserved after the early administration of this inhibitor (290).

CONCLUSION

In his literary masterpiece "*The Restaurant at the End of the Universe*", Douglas Adams states that "It is a curious fact, and one to which no-one knows quite how much importance to attach, that something like 85 percent of all known worlds in the Galaxy, be they primitive or highly advanced, have invented a drink called jynnan tonyx, or gee-N'N-T'N-ix, or jinond-o-nicks, […] 'chinanto/mnigs,' […] 'tzjin-anthony-ks'". Similarly, acute mucosal $CD4^+$ T-cell depletion is a common feature of all HIV and SIV infections, be they pathogenic, nonpathogenic, or controlled. However, as clearly demonstrated by the data presented here, acute $CD4^+$ T-cell depletion is only the spark that can ignite the wildfire in the woods, while chronic inflammation and immune activation that lead to comorbidities and disease progression, and the ability of the host to manage these features associated with HIV/SIV infection, are driving the prognosis.

The natural hosts of SIV seem to be also a good example of convergent evolution to develop strategies to thwart retroviral infections. These NHP species are able to constrain this fire to a limited timing by: (i) spacing the trees, i.e. limiting the number of target cells by having a reduced number of $CD4^+$ T cells expressing CCR5 and/or down-regulating CCR5 expression when entering the memory pool, (ii) limiting the propagation of fire to unburnt trees, i.e. hampering by-stander apoptosis that is the main driver of cell death in HIV/SIV infections, (iii) preserving specific trees that protects the soil, i.e., Th17 cells that are crucial in the maintenance of gut integrity and protecting from bacterial and fungal infections, or trees that will help the regrowth of the forest, i.e. sparing Tcm cells, that have a higher expansion potential, and (iv) growing fire-resistant trees that are able to maintain wild-life in the absence of the other trees, i.e. $CD3^+$ $CD4^{neg}$ $CD8^{neg}$ T cells that exhibit some of the helper T cell functions and that are frequent in most natural hosts of SIV.

DATA AVAILABILITY STATEMENT

The original contributions presented in the study are included in the article/supplementary material. Further inquiries can be directed to the corresponding author.

AUTHOR CONTRIBUTIONS

QLH, IP, and CA designed the manuscript and contributed to drafting. QLH, IS, AL, IP, and CA drafted and revised the manuscript. QLH, IP, and CA prepared the figures. QLH, IS, AL, IP, and CA edited the manuscript. All authors contributed to the article and approved the submitted version.

FUNDING

QLH, IP, and CA are supported by grants from the National Institutes of Health/National Institute of Diabetes and Digestive and Kidney Diseases/National Heart, Lung and Blood Institute/National Institute of Allergy and Infectious Diseases: R01DK113919 (IP/CA), R01DK119936 (CA), R01 AI119346 (CA), RO1 HL117715 (IP), R01 HL123096 (IP). The work of IS was supported by the intramural research program of NIAID/NIH. ALL is supported by UM1-AI106701 AIDS Clinical Trials Group Immunology Support Laboratory. The content of this publication does not necessarily reflect the views or policies of the Department of Health and Human Services, nor does mention of trade names, commercial products, or organizations imply endorsement by the U.S. Government. The funders had no role in study design, data collection and analysis, decision to publish, or preparation of the manuscript.

ACKNOWLEDGMENTS

We would like to thank Adam Kleinman for helpful discussion and critical reading of the manuscript.

REFERENCES

1. Gottlieb MS, Schroff R, Schanker HM, Weisman JD, Fan PT, Wolf RA, et al. Pneumocystis Carinii Pneumonia and Mucosal Candidiasis in Previously Healthy Homosexual Men: Evidence of a New Acquired Cellular Immunodeficiency. *N Engl J Med* (1981) 305:1425–31. doi: 10.1056/NEJM198112103052401
2. Dalgleish AG, Beverley PC, Clapham PR, Crawford DH, Greaves MF, Weiss RA. The CD4 (T4) Antigen Is an Essential Component of the Receptor for the AIDS Retrovirus. *Nature* (1984) 312:763–7. doi: 10.1038/312763a0
3. Klatzmann D, Champagne E, Chamaret S, Gruest J, Guetard D, Hercend T, et al. T-Lymphocyte T4 Molecule Behaves as the Receptor for Human Retrovirus LAV. *Nature* (1984) 312:767–8. doi: 10.1038/312767a0

4. Fahey JL, Taylor JM, Detels R, Hofmann B, Melmed R, Nishanian P, et al. The Prognostic Value of Cellular and Serologic Markers in Infection With Human Immunodeficiency Virus Type 1. *N Engl J Med* (1990) 322:166–72. doi: 10.1056/NEJM199001183220305
5. Cartwright EK, McGary CS, Cervasi B, Micci L, Lawson B, Elliott ST, et al. Divergent CD4+ T Memory Stem Cell Dynamics in Pathogenic and Nonpathogenic Simian Immunodeficiency Virus Infections. *J Immunol* (2014) 192:4666–73. doi: 10.4049/jimmunol.1303193
6. Okoye A, Meier-Schellersheim M, Brenchley JM, Hagen SI, Walker JM, Rohankhedkar M, et al. Progressive CD4+ Central Memory T Cell Decline Results in CD4+ Effector Memory Insufficiency and Overt Disease in Chronic SIV Infection. *J Exp Med* (2007) 204:2171–85. doi: 10.1084/jem.20070567
7. Prendergast A, Prado JG, Kang YH, Chen F, Riddell LA, Luzzi G, et al. HIV-1 Infection is Characterized by Profound Depletion of CD161+ Th17 Cells and Gradual Decline in Regulatory T Cells. *AIDS* (2010) 24:491–502. doi: 10.1097/QAD.0b013e3283344895
8. Kader M, Wang X, Piatak M, Lifson J, Roederer M, Veazey R, et al. Alpha4 (+)beta7(hi)CD4(+) Memory T Cells Harbor Most Th-17 Cells and are Preferentially Infected During Acute SIV Infection. *Mucosal Immunol* (2009) 2:439–49. doi: 10.1038/mi.2009.90
9. Pandrea I, Sodora DL, Silvestri G, Apetrei C. Into the Wild: Simian Immunodeficiency Virus (SIV) Infection in Natural Hosts. *Trends Immunol* (2008) 29:419–28. doi: 10.1016/j.it.2008.05.004
10. Picker LJ, Treer JR, Ferguson-Darnell B, Collins PA, Buck D, Terstappen LW. Control of Lymphocyte Recirculation in Man. I. Differential Regulation of the Peripheral Lymph Node Homing Receptor L-Selectin on T Cells During the Virgin to Memory Cell Transition. *J Immunol* (1993) 150:1105–21.
11. Pitcher CJ, Hagen SI, Walker JM, Lum R, Mitchell BL, Maino VC, et al. Development and Homeostasis of T Cell Memory in Rhesus Macaque. *J Immunol* (2002) 168:29–43. doi: 10.4049/jimmunol.168.1.29
12. Gattinoni L, Lugli E, Ji Y, Pos Z, Paulos CM, Quigley MF, et al. A Human Memory T Cell Subset With Stem Cell-Like Properties. *Nat Med* (2011) 17:1290–7. doi: 10.1038/nm.2446
13. Lugli E, Dominguez MH, Gattinoni L, Chattopadhyay PK, Bolton DL, Song K, et al. Superior T Memory Stem Cell Persistence Supports Long-Lived T Cell Memory. *J Clin Invest* (2013) 123:594–9. doi: 10.1172/JCI66327
14. Viollet L, Monceaux V, Petit F, Ho Tsong Fang R, Cumont MC, Hurtrel B, et al. Death of CD4+ T Cells From Lymph Nodes During Primary SIVmac251 Infection Predicts the Rate of AIDS Progression. *J Immunol* (2006) 177:6685–94. doi: 10.4049/jimmunol.177.10.6685
15. Pichyangkul S, Yongvanitchit K, Limsalakpetch A, Kum-Arb U, Im-Erbsin R, Boonnak K, et al. Tissue Distribution of Memory T and B Cells in Rhesus Monkeys Following Influenza A Infection. *J Immunol* (2015) 195:4378–86. doi: 10.4049/jimmunol.1501702
16. Dragic T, Litwin V, Allaway GP, Martin SR, Huang Y, Nagashima KA, et al. HIV-1 Entry Into CD4+ Cells is Mediated by the Chemokine Receptor CC-CKR-5. *Nature* (1996) 381:667–73. doi: 10.1038/381667a0
17. Deng H, Liu R, Ellmeier W, Choe S, Unutmaz D, Burkhart M, et al. Identification of a Major Co-Receptor for Primary Isolates of HIV-1. *Nature* (1996) 381:661–6. doi: 10.1038/381661a0
18. Rucker J, Edinger AL, Sharron M, Samson M, Lee B, Berson JF, et al. Utilization of Chemokine Receptors, Orphan Receptors, and Herpesvirus-Encoded Receptors by Diverse Human and Simian Immunodeficiency Viruses. *J Virol* (1997) 71:8999–9007. doi: 10.1128/jvi.71.12.8999-9007.1997
19. Nixon DE, Landay AL. Biomarkers of Immune Dysfunction in HIV. *Curr Opin HIV AIDS* (2010) 5:498–503. doi: 10.1097/COH.0b013e32833ed6f4
20. Saez-Cirion A, Sereti I. Immunometabolism and HIV-1 Pathogenesis: Food for Thought. *Nat Rev Immunol* (2021) 21:5–19. doi: 10.1038/s41577-020-0381-7
21. Smit-McBride Z, Mattapallil JJ, McChesney M, Ferrick D, Dandekar S. Gastrointestinal T Lymphocytes Retain High Potential for Cytokine Responses But Have Severe CD4(+) T-Cell Depletion at All Stages of Simian Immunodeficiency Virus Infection Compared to Peripheral Lymphocytes. *J Virol* (1998) 72:6646–56. doi: 10.1128/JVI.72.8.6646-6656.1998
22. Hermier F, Comby E, Delaunay A, Petitjean J, Favennec L, Bazin C, et al. Decreased Blood TcR Gamma Delta+ Lymphocytes in AIDS and P24-Antigenemic HIV-1-infected Patients. *Clin Immunol Immunopathol* (1993) 69:248–50. doi: 10.1006/clin.1993.1176
23. Kloverpris HN, Kazer SW, Mjosberg J, Mabuka JM, Wellmann A, Ndhlovu Z, et al. Innate Lymphoid Cells Are Depleted Irreversibly During Acute HIV-1 Infection in the Absence of Viral Suppression. *Immunity* (2016) 44:391–405. doi: 10.1016/j.immuni.2016.01.006
24. Mudd JC, Busman-Sahay K, DiNapoli SR, Lai S, Sheik V, Lisco A, et al. Hallmarks of Primate Lentiviral Immunodeficiency Infection Recapitulate Loss of Innate Lymphoid Cells. *Nat Commun* (2018) 9:3967. doi: 10.1038/s41467-018-05528-3
25. Xu H, Wang X, Liu DX, Moroney-Rasmussen T, Lackner AA, Veazey RS. IL-17-producing Innate Lymphoid Cells are Restricted to Mucosal Tissues and are Depleted in SIV-Infected Macaques. *Mucosal Immunol* (2012) 5:658–69. doi: 10.1038/mi.2012.39
26. Donaghy H, Pozniak A, Gazzard B, Qazi N, Gilmour J, Gotch F, et al. Loss of Blood CD11c(+) Myeloid and CD11c(-) Plasmacytoid Dendritic Cells in Patients With HIV-1 Infection Correlates With HIV-1 RNA Virus Load. *Blood* (2001) 98:2574–6. doi: 10.1182/blood.V98.8.2574
27. Robb ML, Eller LA, Kibuuka H, Rono K, Maganga L, Nitayaphan S, et al. Prospective Study of Acute HIV-1 Infection in Adults in East Africa and Thailand. *N Engl J Med* (2016) 374:2120–30. doi: 10.1056/NEJMoa1508952
28. Mattapallil JJ, Letvin NL, Roederer M. T-Cell Dynamics During Acute SIV Infection. *AIDS* (2004) 18:13–23. doi: 10.1097/00002030-200401020-00002
29. Letvin NL, Daniel MD, Sehgal PK, Desrosiers RC, Hunt RD, Waldron LM, et al. Induction of AIDS-like Disease in Macaque Monkeys With T-Cell Tropic Retrovirus STLV-III. *Science* (1985) 230:71–3. doi: 10.1126/science.2412295
30. Veazey RS, Mansfield KG, Tham IC, Carville AC, Shvetz DE, Forand AE, et al. Dynamics of CCR5 Expression by CD4(+) T Cells in Lymphoid Tissues During Simian Immunodeficiency Virus Infection. *J Virol* (2000) 74:11001–7. doi: 10.1128/JVI.74.23.11001-11007.2000
31. Gottlieb GS, Sow PS, Hawes SE, Ndoye I, Redman M, Coll-Seck AM, et al. Equal Plasma Viral Loads Predict a Similar Rate of CD4+ T Cell Decline in Human Immunodeficiency Virus (HIV) Type 1- and HIV-2-infected Individuals From Senegal, West Africa. *J Infect Dis* (2002) 185:905–14. doi: 10.1086/339295
32. Mattapallil JJ, Douek DC, Hill B, Nishimura Y, Martin M, Roederer M. Massive Infection and Loss of Memory CD4+ T Cells in Multiple Tissues During Acute SIV Infection. *Nature* (2005) 434:1093–7. doi: 10.1038/nature03501
33. Veazey RS, DeMaria M, Chalifoux LV, Shvetz DE, Pauley DR, Knight HL, et al. Gastrointestinal Tract as a Major Site of CD4+ T Cell Depletion and Viral Replication in SIV Infection. *Science* (1998) 280:427–31. doi: 10.1126/science.280.5362.427
34. Milush JM, Mir KD, Sundaravaradan V, Gordon SN, Engram J, Cano CA, et al. Lack of Clinical AIDS in SIV-Infected Sooty Mangabeys With Significant CD4+ T Cell Loss is Associated With Double-Negative T Cells. *J Clin Invest* (2011) 121:1102–10. doi: 10.1172/JCI44876
35. Brenchley JM, Schacker TW, Ruff LE, Price DA, Taylor JH, Beilman GJ, et al. CD4+ T Cell Depletion During All Stages of HIV Disease Occurs Predominantly in the Gastrointestinal Tract. *J Exp Med* (2004) 200:749–59. doi: 10.1084/jem.20040874
36. Mangkornkanok-Mark M, Mark AS, Dong J. Immunoperoxidase Evaluation of Lymph Nodes From Acquired Immune Deficiency Patients. *Clin Exp Immunol* (1984) 55:581–6.
37. Janossy G, Pinching AJ, Bofill M, Weber J, McLaughlin JE, Ornstein M, et al. An Immunohistological Approach to Persistent Lymphadenopathy and its Relevance to AIDS. *Clin Exp Immunol* (1985) 59:257–66.
38. Willerford DM, Gale MJJr., Benveniste RE, Clark EA, Gallatin WM. Simian Immunodeficiency Virus is Restricted to a Subset of Blood CD4+ Lymphocytes That Includes Memory Cells. *J Immunol* (1990) 144:3779–83.
39. Schnittman SM, Lane HC, Greenhouse J, Justement JS, Baseler M, Fauci AS. Preferential Infection of CD4+ Memory T Cells by Human Immunodeficiency Virus Type 1: Evidence for a Role in the Selective T-cell Functional Defects Observed in Infected Individuals. *Proc Natl Acad Sci USA* (1990) 87:6058–62. doi: 10.1073/pnas.87.16.6058
40. Hulstaert F, Hannet I, Deneys V, Munhyeshuli V, Reichert T, De Bruyere M, et al. Age-Related Changes in Human Blood Lymphocyte Subpopulations. II.

Varying Kinetics of Percentage and Absolute Count Measurements. *Clin Immunol Immunopathol* (1994) 70:152–8. doi: 10.1006/clin.1994.1023
41. Pandrea I, Apetrei C, Gordon S, Barbercheck J, Dufour J, Bohm R, et al. Paucity of CD4+CCR5+ T Cells Is a Typical Feature of Natural SIV Hosts. *Blood* (2007) 109:1069–76. doi: 10.1182/blood-2006-05-024364
42. Sallusto F, Lenig D, Mackay CR, Lanzavecchia A. Flexible Programs of Chemokine Receptor Expression on Human Polarized T Helper 1 and 2 Lymphocytes. *J Exp Med* (1998) 187:875–83. doi: 10.1084/jem.187.6.875
43. Bleul CC, Wu L, Hoxie JA, Springer TA, Mackay CR. The HIV Coreceptors CXCR4 and CCR5 are Differentially Expressed and Regulated on Human T Lymphocytes. *Proc Natl Acad Sci USA* (1997) 94:1925–30. doi: 10.1073/pnas.94.5.1925
44. Chun TW, Stuyver L, Mizell SB, Ehler LA, Mican JA, Baseler M, et al. Presence of an Inducible HIV-1 Latent Reservoir During Highly Active Antiretroviral Therapy. *Proc Natl Acad Sci USA* (1997) 94:13193–7. doi: 10.1073/pnas.94.24.13193
45. Ghosn J, Deveau C, Chaix ML, Goujard C, Galimand J, Zitoun Y, et al. Despite Being Highly Diverse, Immunovirological Status Strongly Correlates With Clinical Symptoms During Primary HIV-1 Infection: A Cross-Sectional Study Based on 674 Patients Enrolled in the ANRS Co 06 PRIMO Cohort. *J Antimicrob Chemother* (2010) 65:741–8. doi: 10.1093/jac/dkq035
46. Ananworanich J, Sacdalan CP, Pinyakorn S, Chomont N, de Souza M, Luekasemsuk T, et al. Virological and Immunological Characteristics of HIV-Infected Individuals at the Earliest Stage of Infection. *J Virus Erad* (2016) 2:43–8. doi: 10.1016/S2055-6640(20)30688-9
47. Gordon SN, Klatt NR, Bosinger SE, Brenchley JM, Milush JM, Engram JC, et al. Severe Depletion of Mucosal CD4+ T Cells in AIDS-free Simian Immunodeficiency Virus-Infected Sooty Mangabeys. *J Immunol* (2007) 179:3026–34. doi: 10.4049/jimmunol.179.5.3026
48. Pandrea I, Gaufin T, Gautam R, Kristoff J, Mandell D, Montefiori D, et al. Functional Cure of SIVagm Infection in Rhesus Macaques Results in Complete Recovery of CD4+ T Cells and is Reverted by CD8+ Cell Depletion. *PloS Pathog* (2011) 7:e1002170. doi: 10.1371/journal.ppat.1002170
49. Veazey RS, Tham IC, Mansfield KG, DeMaria M, Forand AE, Shvetz DE, et al. Identifying the Target Cell in Primary Simian Immunodeficiency Virus (SIV) Infection: Highly Activated Memory CD4(+) T Cells are Rapidly Eliminated in Early SIV Infection In Vivo. *J Virol* (2000) 74:57–64. doi: 10.1128/JVI.74.1.57-64.2000
50. Chomont N, El-Far M, Ancuta P, Trautmann L, Procopio FA, Yassine-Diab B, et al. HIV Reservoir Size and Persistence are Driven by T Cell Survival and Homeostatic Proliferation. *Nat Med* (2009) 15:893–900. doi: 10.1038/nm.1972
51. Descours B, Avettand-Fenoel V, Blanc C, Samri A, Melard A, Supervie V, et al. Immune Responses Driven by Protective Human Leukocyte Antigen Alleles From Long-Term Nonprogressors are Associated With Low HIV Reservoir in Central Memory CD4 T Cells. *Clin Infect Dis* (2012) 54:1495–503. doi: 10.1093/cid/cis188
52. Paiardini M, Cervasi B, Reyes-Aviles E, Micci L, Ortiz AM, Chahroudi A, et al. Low Levels of SIV Infection in Sooty Mangabey Central Memory CD(4)(+) T Cells are Associated With Limited CCR5 Expression. *Nat Med* (2011) 17:830–6. doi: 10.1038/nm.2395
53. Samri A, Charpentier C, Diallo MS, Bertine M, Even S, Morin V, et al. Limited HIV-2 Reservoirs in Central-Memory CD4 T-Cells Associated to CXCR6 Co-Receptor Expression in Attenuated HIV-2 Infection. *PloS Pathog* (2019) 15:e1007758. doi: 10.1371/journal.ppat.1007758
54. Buzon MJ, Sun H, Li C, Shaw A, Seiss K, Ouyang Z, et al. HIV-1 Persistence in CD4+ T Cells With Stem Cell-Like Properties. *Nat Med* (2014) 20:139–42. doi: 10.1038/nm.3445
55. Brenchley JM, Paiardini M, Knox KS, Asher AI, Cervasi B, Asher TE, et al. Differential Th17 CD4 T-cell Depletion in Pathogenic and Nonpathogenic Lentiviral Infections. *Blood* (2008) 112:2826–35. doi: 10.1182/blood-2008-05-159301
56. Clerici M, Hakim FT, Venzon DJ, Blatt S, Hendrix CW, Wynn TA, et al. Changes in Interleukin-2 and Interleukin-4 Production in Asymptomatic, Human Immunodeficiency Virus-Seropositive Individuals. *J Clin Invest* (1993) 91:759–65. doi: 10.1172/JCI116294
57. Oswald-Richter K, Grill SM, Shariat N, Leelawong M, Sundrud MS, Haas DW, et al. HIV Infection of Naturally Occurring and Genetically Reprogrammed Human Regulatory T-Cells. *PloS Biol* (2004) 2:E198. doi: 10.1371/journal.pbio.0020198
58. Eggena MP, Barugahare B, Jones N, Okello M, Mutalya S, Kityo C, et al. Depletion of Regulatory T Cells in HIV Infection Is Associated With Immune Activation. *J Immunol* (2005) 174:4407–14. doi: 10.4049/jimmunol.174.7.4407
59. Andersson J, Boasso A, Nilsson J, Zhang R, Shire NJ, Lindback S, et al. The Prevalence of Regulatory T Cells in Lymphoid Tissue is Correlated With Viral Load in HIV-infected Patients. *J Immunol* (2005) 174:3143–7. doi: 10.4049/jimmunol.174.6.3143
60. Epple HJ, Loddenkemper C, Kunkel D, Troger H, Maul J, Moos V, et al. Mucosal But Not Peripheral FOXP3+ Regulatory T Cells are Highly Increased in Untreated HIV Infection and Normalize After Suppressive HAART. *Blood* (2006) 108:3072–8. doi: 10.1182/blood-2006-04-016923
61. Yero A, Farnos O, Rabezanahary H, Racine G, Estaquier J, Jenabian MA. Differential Dynamics of Regulatory T-Cell and Th17 Cell Balance in Mesenteric Lymph Nodes and Blood Following Early Antiretroviral Initiation During Acute Simian Immunodeficiency Virus Infection. *J Virol* (2019) 93(19):e00371-19. doi: 10.1128/JVI.00371-19
62. Favre D, Lederer S, Kanwar B, Ma ZM, Proll S, Kasakow Z, et al. Critical Loss of the Balance Between Th17 and T Regulatory Cell Populations in Pathogenic SIV Infection. *PloS Pathog* (2009) 5:e1000295. doi: 10.1371/journal.ppat.1000295
63. Krzysiek R, Rudent A, Bouchet-Delbos L, Foussat A, Boutillon C, Portier A, et al. Preferential and Persistent Depletion of CCR5+ T-Helper Lymphocytes With Nonlymphoid Homing Potential Despite Early Treatment of Primary HIV Infection. *Blood* (2001) 98:3169–71. doi: 10.1182/blood.V98.10.3169
64. Wang X, Xu H, Gill AF, Pahar B, Kempf D, Rasmussen T, et al. Monitoring alpha4beta7 Integrin Expression on Circulating CD4+ T Cells as a Surrogate Marker for Tracking Intestinal CD4+ T-Cell Loss in SIV Infection. *Mucosal Immunol* (2009) 2:518–26. doi: 10.1038/mi.2009.104
65. Xu H, Wang X, Malam N, Lackner AA, Veazey RS. Persistent Simian Immunodeficiency Virus Infection Causes Ultimate Depletion of Follicular Th Cells in AIDS. *J Immunol* (2015) 195:4351–7. doi: 10.4049/jimmunol.1501273
66. Petrovas C, Yamamoto T, Gerner MY, Boswell KL, Wloka K, Smith EC, et al. CD4 T Follicular Helper Cell Dynamics During SIV Infection. *J Clin Invest* (2012) 122:3281–94. doi: 10.1172/JCI63039
67. Moukambi F, Rabezanahary H, Rodrigues V, Racine G, Robitaille L, Krust B, et al. Early Loss of Splenic Tfh Cells in SIV-Infected Rhesus Macaques. *PloS Pathog* (2015) 11:e1005287. doi: 10.1371/journal.ppat.1005287
68. Moukambi F, Rabezanahary H, Fortier Y, Rodrigues V, Clain J, Benmadid-Laktout G, et al. Mucosal T Follicular Helper Cells in SIV-Infected Rhesus Macaques: Contributing Role of IL-27. *Mucosal Immunol* (2019) 12:1038–54. doi: 10.1038/s41385-019-0174-0
69. Chowdhury A, Del Rio Estrada PM, Tharp GK, Trible RP, Amara RR, Chahroudi A, et al. Decreased T Follicular Regulatory Cell/T Follicular Helper Cell (TFH) in Simian Immunodeficiency Virus-Infected Rhesus Macaques may Contribute to Accumulation of TFH in Chronic Infection. *J Immunol* (2015) 195:3237–47. doi: 10.4049/jimmunol.1402701
70. Lindqvist M, van Lunzen J, Soghoian DZ, Kuhl BD, Ranasinghe S, Kranias G, et al. Expansion of HIV-Specific T Follicular Helper Cells in Chronic HIV Infection. *J Clin Invest* (2012) 122:3271–80. doi: 10.1172/JCI64314
71. Valle-Casuso JC, Angin M, Volant S, Passaes C, Monceaux V, Mikhailova A, et al. Cellular Metabolism Is a Major Determinant of HIV-1 Reservoir Seeding in CD4(+) T Cells and Offers an Opportunity to Tackle Infection. *Cell Metab* (2019) 29:611–626 e5. doi: 10.1016/j.cmet.2018.11.015
72. Veazey RS, Rosenzweig M, Shvetz DE, Pauley DR, DeMaria M, Chalifoux LV, et al. Characterization of Gut-Associated Lymphoid Tissue (GALT) of Normal Rhesus Macaques. *Clin Immunol Immunopathol* (1997) 82:230–42. doi: 10.1006/clin.1996.4318
73. Kotler DP, Gaetz HP, Lange M, Klein EB, Holt PR. Enteropathy Associated With the Acquired Immunodeficiency Syndrome. *Ann Intern Med* (1984) 101:421–8. doi: 10.7326/0003-4819-101-4-421
74. Rodgers VD, Fassett R, Kagnoff MF. Abnormalities in Intestinal Mucosal T Cells in Homosexual Populations Including Those With the

Lymphadenopathy Syndrome and Acquired Immunodeficiency Syndrome. *Gastroenterology* (1986) 90:552–8. doi: 10.1016/0016-5085(86)91108-X
75. Ellakany S, Whiteside TL, Schade RR, van Thiel DH. Analysis of Intestinal Lymphocyte Subpopulations in Patients With Acquired Immunodeficiency Syndrome (AIDS) and AIDS-related Complex. *Am J Clin Pathol* (1987) 87:356–64. doi: 10.1093/ajcp/87.3.356
76. Budhraja M, Levendoglu H, Kocka F, Mangkornkanok M, Sherer R. Duodenal Mucosal T Cell Subpopulation and Bacterial Cultures in Acquired Immune Deficiency Syndrome. *Am J Gastroenterol* (1987) 82:427–31.
77. Jarry A, Cortez A, Rene E, Muzeau F, Brousse N. Infected Cells and Immune Cells in the Gastrointestinal Tract of AIDS Patients. An Immunohistochemical Study of 127 Cases. *Histopathology* (1990) 16:133–40. doi: 10.1111/j.1365-2559.1990.tb01081.x
78. Schneider T, Jahn HU, Schmidt W, Riecken EO, Zeitz M, Ullrich R. Loss of CD4 T Lymphocytes in Patients Infected With Human Immunodeficiency Virus Type 1 Is More Pronounced in the Duodenal Mucosa Than in the Peripheral Blood. Berlin Diarrhea/Wasting Syndrome Study Group. *Gut* (1995) 37:524–9. doi: 10.1136/gut.37.4.524
79. Bishop PE, McMillan A, Gilmour HM. A Histological and Immunocytochemical Study of Lymphoid Tissue in Rectal Biopsies From Homosexual Men. *Histopathology* (1987) 11:1133–47. doi: 10.1111/j.1365-2559.1987.tb01854.x
80. Lim SG, Condez A, Lee CA, Johnson MA, Elia C, Poulter LW. Loss of Mucosal CD4 Lymphocytes Is an Early Feature of HIV Infection. *Clin Exp Immunol* (1993) 92:448–54. doi: 10.1111/j.1365-2249.1993.tb03419.x
81. Ullrich R, Zeitz M, Heise W, L'Age M, Ziegler K, Bergs C, et al. Mucosal Atrophy Is Associated With Loss of Activated T Cells in the Duodenal Mucosa of Human Immunodeficiency Virus (HIV)-Infected Patients. *Digestion* (1990) 46(Suppl 2):302–7. doi: 10.1159/000200401
82. Mattapallil JJ, Smit-McBride Z, McChesney M, Dandekar S. Intestinal Intraepithelial Lymphocytes Are Primed for Gamma Interferon and MIP-1beta Expression and Display Antiviral Cytotoxic Activity Despite Severe CD4(+) T-Cell Depletion in Primary Simian Immunodeficiency Virus Infection. *J Virol* (1998) 72:6421–9. doi: 10.1128/JVI.72.8.6421-6429.1998
83. Kewenig S, Schneider T, Hohloch K, Lampe-Dreyer K, Ullrich R, Stolte N, et al. Rapid Mucosal CD4(+) T-Cell Depletion and Enteropathy in Simian Immunodeficiency Virus-Infected Rhesus Macaques. *Gastroenterology* (1999) 116:1115–23. doi: 10.1016/S0016-5085(99)70014-4
84. Pandrea IV, Gautam R, Ribeiro RM, Brenchley JM, Butler IF, Pattison M, et al. Acute Loss of Intestinal CD4+ T Cells Is Not Predictive of Simian Immunodeficiency Virus Virulence. *J Immunol* (2007) 179:3035–46. doi: 10.4049/jimmunol.179.5.3035
85. Schuetz A, Deleage C, Sereti I, Rerknimitr R, Phanuphak N, Phuang-Ngern Y, et al. Initiation of ART During Early Acute HIV Infection Preserves Mucosal Th17 Function and Reverses HIV-Related Immune Activation. *PloS Pathog* (2014) 10:e1004543. doi: 10.1371/journal.ppat.1004543
86. Mandell DT, Kristoff J, Gaufin T, Gautam R, Ma D, Sandler N, et al. Pathogenic Features Associated With Increased Virulence Upon Simian Immunodeficiency Virus Cross-Species Transmission From Natural Hosts. *J Virol* (2014) 88:6778–92. doi: 10.1128/JVI.03785-13
87. Kornfeld C, Ploquin MJ, Pandrea I, Faye A, Onanga R, Apetrei C, et al. Antiinflammatory Profiles During Primary SIV Infection in African Green Monkeys are Associated With Protection Against AIDS. *J Clin Invest* (2005) 115:1082–91. doi: 10.1172/JCI23006
88. Verhoeven D, Sankaran S, Silvey M, Dandekar S. Antiviral Therapy During Primary Simian Immunodeficiency Virus Infection Fails to Prevent Acute Loss of CD4+ T Cells in Gut Mucosa But Enhances Their Rapid Restoration Through Central Memory T Cells. *J Virol* (2008) 82:4016–27. doi: 10.1128/JVI.02164-07
89. Staprans SI, Dailey PJ, Rosenthal A, Horton C, Grant RM, Lerche N, et al. Simian Immunodeficiency Virus Disease Course is Predicted by the Extent of Virus Replication During Primary Infection. *J Virol* (1999) 73:4829–39. doi: 10.1128/JVI.73.6.4829-4839.1999
90. Ananworanich J, Eller LA, Pinyakorn S, Kroon E, Sriplenchan S, Fletcher JL, et al. Viral Kinetics in Untreated Versus Treated Acute HIV Infection in Prospective Cohort Studies in Thailand. *J Int AIDS Soc* (2017) 20:21652. doi: 10.7448/IAS.20.1.21652
91. Ndhlovu ZM, Kamya P, Mewalal N, Kloverpris HN, Nkosi T, Pretorius K, et al. Magnitude and Kinetics of CD8+ T Cell Activation During Hyperacute HIV Infection Impact Viral Set Point. *Immunity* (2015) 43:591–604. doi: 10.1016/j.immuni.2015.08.012
92. Cumont MC, Diop O, Vaslin B, Elbim C, Viollet L, Monceaux V, et al. Early Divergence in Lymphoid Tissue Apoptosis Between Pathogenic and Nonpathogenic Simian Immunodeficiency Virus Infections of Nonhuman Primates. *J Virol* (2008) 82:1175–84. doi: 10.1128/JVI.00450-07
93. Heise C, Miller CJ, Lackner A, Dandekar S. Primary Acute Simian Immunodeficiency Virus Infection of Intestinal Lymphoid Tissue Is Associated With Gastrointestinal Dysfunction. *J Infect Dis* (1994) 169:1116–20. doi: 10.1093/infdis/169.5.1116
94. Li Q, Duan L, Estes JD, Ma ZM, Rourke T, Wang Y, et al. Peak SIV Replication in Resting Memory CD4+ T Cells Depletes Gut Lamina Propria CD4+ T Cells. *Nature* (2005) 434:1148–52. doi: 10.1038/nature03513
95. Wang X, Rasmussen T, Pahar B, Poonia B, Alvarez X, Lackner AA, et al. Massive Infection and Loss of CD4+ T Cells Occurs in the Intestinal Tract of Neonatal Rhesus Macaques in Acute SIV Infection. *Blood* (2007) 109:1174–81. doi: 10.1182/blood-2006-04-015172
96. Lapenta C, Boirivant M, Marini M, Santini SM, Logozzi M, Viora M, et al. Human Intestinal Lamina Propria Lymphocytes are Naturally Permissive to HIV-1 Infection. *Eur J Immunol* (1999) 29:1202–8. doi: 10.1002/(SICI)1521-4141(199904)29:04<1202::AID-IMMU1202>3.0.CO;2-O
97. Guadalupe M, Reay E, Sankaran S, Prindiville T, Flamm J, McNeil A, et al. Severe CD4+ T-Cell Depletion in Gut Lymphoid Tissue During Primary Human Immunodeficiency Virus Type 1 Infection and Substantial Delay in Restoration Following Highly Active Antiretroviral Therapy. *J Virol* (2003) 77:11708–17. doi: 10.1128/JVI.77.21.11708-11717.2003
98. Mehandru S, Poles MA, Tenner-Racz K, Horowitz A, Hurley A, Hogan C, et al. Primary HIV-1 Infection Is Associated With Preferential Depletion of CD4+ T Lymphocytes From Effector Sites in the Gastrointestinal Tract. *J Exp Med* (2004) 200:761–70. doi: 10.1084/jem.20041196
99. Deleage C, Schuetz A, Alvord WG, Johnston L, Hao XP, Morcock DR, et al. Impact of Early cART in the Gut During Acute HIV Infection. *JCI Insight* (2016) 1(10):e87065. doi: 10.1172/jci.insight.87065
100. Harouse JM, Gettie A, Tan RC, Blanchard J, Cheng-Mayer C. Distinct Pathogenic Sequela in Rhesus Macaques Infected With CCR5 or CXCR4 Utilizing SHIVs. *Science* (1999) 284:816–9. doi: 10.1126/science.284.5415.816
101. Picker LJ, Hagen SI, Lum R, Reed-Inderbitzin EF, Daly LM, Sylwester AW, et al. Insufficient Production and Tissue Delivery of CD4+ Memory T Cells in Rapidly Progressive Simian Immunodeficiency Virus Infection. *J Exp Med* (2004) 200:1299–314. doi: 10.1084/jem.20041049
102. Ho SH, Shek L, Gettie A, Blanchard J, Cheng-Mayer C. V3 Loop-Determined Coreceptor Preference Dictates the Dynamics of CD4+-T-cell Loss in Simian-Human Immunodeficiency Virus-Infected Macaques. *J Virol* (2005) 79:12296–303. doi: 10.1128/JVI.79.19.12296-12303.2005
103. Cecchinato V, Trindade CJ, Laurence A, Heraud JM, Brenchley JM, Ferrari MG, et al. Altered Balance Between Th17 and Th1 Cells at Mucosal Sites Predicts AIDS Progression in Simian Immunodeficiency Virus-Infected Macaques. *Mucosal Immunol* (2008) 1:279–88. doi: 10.1038/mi.2008.14
104. Klatt NR, Estes JD, Sun X, Ortiz AM, Barber JS, Harris LD, et al. Loss of Mucosal CD103+ DCs and IL-17+ and IL-22+ Lymphocytes is Associated With Mucosal Damage in SIV Infection. *Mucosal Immunol* (2012) 5:646–57. doi: 10.1038/mi.2012.38
105. Kim CJ, Nazli A, Rojas OL, Chege D, Alidina Z, Huibner S, et al. A Role for Mucosal IL-22 Production and Th22 Cells in HIV-associated Mucosal Immunopathogenesis. *Mucosal Immunol* (2012) 5:670–80. doi: 10.1038/mi.2012.72
106. Reeves RK, Rajakumar PA, Evans TI, Connole M, Gillis J, Wong FE, et al. Gut Inflammation and Indoleamine Deoxygenase Inhibit IL-17 Production and Promote Cytotoxic Potential in NKp44+ Mucosal NK Cells During SIV Infection. *Blood* (2011) 118:3321–30. doi: 10.1182/blood-2011-04-347260
107. Campillo-Gimenez L, Cumont MC, Fay M, Kared H, Monceaux V, Diop O, et al. AIDS Progression is Associated With the Emergence of IL-17-producing Cells Early After Simian Immunodeficiency Virus Infection. *J Immunol* (2010) 184:984–92. doi: 10.4049/jimmunol.0902316
108. Micci L, Cervasi B, Ende ZS, Iriele RI, Reyes-Aviles E, Vinton C, et al. Paucity of IL-21-producing CD4(+) T Cells is Associated With Th17 Cell Depletion

in SIV Infection of Rhesus Macaques. *Blood* (2012) 120:3925–35. doi: 10.1182/blood-2012-04-420240
109. Allers K, Loddenkemper C, Hofmann J, Unbehaun A, Kunkel D, Moos V, et al. Gut Mucosal FOXP3+ Regulatory CD4+ T Cells and Nonregulatory CD4+ T Cells Are Differentially Affected by Simian Immunodeficiency Virus Infection in Rhesus Macaques. *J Virol* (2010) 84:3259–69. doi: 10.1128/JVI.01715-09
110. Favre D, Mold J, Hunt PW, Kanwar B, Loke P, Seu L, et al. Tryptophan Catabolism by Indoleamine 2,3-Dioxygenase 1 Alters the Balance of TH17 to Regulatory T Cells in HIV Disease. *Sci Transl Med* (2010) 2:32ra36. doi: 10.1126/scitranslmed.3000632
111. Jenabian MA, Patel M, Kema I, Kanagaratham C, Radzioch D, Thebault P, et al. Distinct Tryptophan Catabolism and Th17/Treg Balance in HIV Progressors and Elite Controllers. *PloS One* (2013) 8:e78146. doi: 10.1371/journal.pone.0078146
112. Manches O, Munn D, Fallahi A, Lifson J, Chaperot L, Plumas J, et al. HIV-Activated Human Plasmacytoid DCs Induce Tregs Through an Indoleamine 2,3-Dioxygenase-Dependent Mechanism. *J Clin Invest* (2008) 118:3431–9. doi: 10.1172/JCI34823
113. Pahar B, Lackner AA, Veazey RS. Intestinal Double-Positive CD4+CD8+ T Cells are Highly Activated Memory Cells With an Increased Capacity to Produce Cytokines. *Eur J Immunol* (2006) 36:583–92. doi: 10.1002/eji.200535520
114. Vajdy M, Veazey R, Tham I, deBakker C, Westmoreland S, Neutra M, et al. Early Immunologic Events in Mucosal and Systemic Lymphoid Tissues After Intrarectal Inoculation With Simian Immunodeficiency Virus. *J Infect Dis* (2001) 184:1007–14. doi: 10.1086/323615
115. Ahsan MH, Gill AF, Lackner AA, Veazey RS. Acute and Chronic T Cell Dynamics in the Livers of Simian Immunodeficiency Virus-Infected Macaques. *J Virol* (2012) 86:5244–52. doi: 10.1128/JVI.07080-11
116. Hoang TN, Harper JL, Pino M, Wang H, Micci L, King CT, et al. Bone Marrow-Derived CD4(+) T Cells Are Depleted in Simian Immunodeficiency Virus-Infected Macaques and Contribute to the Size of the Replication-Competent Reservoir. *J Virol* (2019) 93(1):e01344-18. doi: 10.1128/JVI.01344-18
117. Brenchley JM, Knox KS, Asher AI, Price DA, Kohli LM, Gostick E, et al. High Frequencies of Polyfunctional HIV-Specific T Cells Are Associated With Preservation of Mucosal CD4 T Cells in Bronchoalveolar Lavage. *Mucosal Immunol* (2008) 1:49–58. doi: 10.1038/mi.2007.5
118. Corleis B, Bucsan AN, Deruaz M, Vrbanac VD, Lisanti-Park AC, Gates SJ, et al. HIV-1 and SIV Infection Are Associated With Early Loss of Lung Interstitial CD4+ T Cells and Dissemination of Pulmonary Tuberculosis. *Cell Rep* (2019) 26:1409–1418 e5. doi: 10.1016/j.celrep.2019.01.021
119. Veazey RS, Marx PA, Lackner AA. Vaginal CD4+ T Cells Express High Levels of CCR5 and are Rapidly Depleted in Simian Immunodeficiency Virus Infection. *J Infect Dis* (2003) 187:769–76. doi: 10.1086/368386
120. Gumbi PP, Jaumdally SZ, Salkinder AL, Burgers WA, Mkhize NN, Hanekom W, et al. CD4 T Cell Depletion at the Cervix During HIV Infection is Associated With Accumulation of Terminally Differentiated T Cells. *J Virol* (2011) 85:13333–41. doi: 10.1128/JVI.05671-11
121. Politch JA, Mayer KH, Anderson DJ. Depletion of CD4+ T Cells in Semen During HIV Infection and Their Restoration Following Antiretroviral Therapy. *J Acquir Immune Defic Syndr* (2009) 50:283–9. doi: 10.1097/QAI.0b013e3181989870
122. Bernard-Stoecklin S, Gommet C, Corneau AB, Guenounou S, Torres C, Dejucq-Rainsford N, et al. Semen CD4+ T Cells and Macrophages are Productively Infected at All Stages of SIV Infection in Macaques. *PloS Pathog* (2013) 9:e1003810. doi: 10.1371/journal.ppat.1003810
123. Pandrea I, Apetrei C, Dufour J, Dillon N, Barbercheck J, Metzger M, et al. Simian Immunodeficiency Virus SIVagm.sab Infection of Caribbean African Green Monkeys: A New Model for the Study of SIV Pathogenesis in Natural Hosts. *J Virol* (2006) 80:4858–67. doi: 10.1128/JVI.80.10.4858-4867.2006
124. Pandrea I, Onanga R, Kornfeld C, Rouquet P, Bourry O, Clifford S, et al. High Levels of SIVmnd-1 Replication in Chronically Infected Mandrillus Sphinx. *Virology* (2003) 317:119–27. doi: 10.1016/j.virol.2003.08.015
125. Sumpter B, Dunham R, Gordon S, Engram J, Hennessy M, Kinter A, et al. Correlates of Preserved CD4(+) T Cell Homeostasis During Natural, Nonpathogenic Simian Immunodeficiency Virus Infection of Sooty Mangabeys: Implications for AIDS Pathogenesis. *J Immunol* (2007) 178:1680–91. doi: 10.4049/jimmunol.178.3.1680
126. Apetrei C, Sumpter B, Souquiere S, Chahroudi A, Makuwa M, Reed P, et al. Immunovirological Analyses of Chronically Simian Immunodeficiency Virus SIVmnd-1- and SIVmnd-2-infected Mandrills (Mandrillus Sphinx). *J Virol* (2011) 85:13077–87. doi: 10.1128/JVI.05693-11
127. Apetrei C, Gautam R, Sumpter B, Carter AC, Gaufin T, Staprans SI, et al. Virus Subtype-Specific Features of Natural Simian Immunodeficiency Virus SIVsmm Infection in Sooty Mangabeys. *J Virol* (2007) 81:7913–23. doi: 10.1128/JVI.00281-07
128. Apetrei C, Robertson DL, Marx PA. The History of SIVS and AIDS: Epidemiology, Phylogeny and Biology of Isolates From Naturally SIV Infected non-Human Primates (NHP) in Africa. *Front Biosci* (2004) 9:225–54. doi: 10.2741/1154
129. Pandrea I, Kornfeld C, Ploquin MJ, Apetrei C, Faye A, Rouquet P, et al. Impact of Viral Factors on Very Early In Vivo Replication Profiles in Simian Immunodeficiency Virus SIVagm-infected African Green Monkeys. *J Virol* (2005) 79:6249–59. doi: 10.1128/JVI.79.10.6249-6259.2005
130. Riddick NE, Wu F, Matsuda K, Whitted S, Ourmanov I, Goldstein S, et al. Simian Immunodeficiency Virus SIVagm Efficiently Utilizes Non-CCR5 Entry Pathways in African Green Monkey Lymphocytes: Potential Role for GPR15 and CXCR6 as Viral Coreceptors. *J Virol* (2015) 90:2316–31. doi: 10.1128/JVI.02529-15
131. Schols D, De Clercq E. The Simian Immunodeficiency Virus Mnd(GB-1) Strain Uses CXCR4, Not CCR5, as Coreceptor for Entry in Human Cells. *J Gen Virol* (1998) 79(Pt 9):2203–5. doi: 10.1099/0022-1317-79-9-2203
132. Chen Z, Kwon D, Jin Z, Monard S, Telfer P, Jones MS, et al. Natural Infection of a Homozygous Delta24 CCR5 Red-Capped Mangabey With an R2b-tropic Simian Immunodeficiency Virus. *J Exp Med* (1998) 188:2057–65. doi: 10.1084/jem.188.11.2057
133. Beer BE, Foley BT, Kuiken CL, Tooze Z, Goeken RM, Brown CR, et al. Characterization of Novel Simian Immunodeficiency Viruses From Red-Capped Mangabeys From Nigeria (SIVrcmNG409 and -NG411). *J Virol* (2001) 75:12014–27. doi: 10.1128/JVI.75.24.12014-12027.2001
134. Georges-Courbot MC, Lu CY, Makuwa M, Telfer P, Onanga R, Dubreuil G, et al. Natural Infection of a Household Pet Red-Capped Mangabey (Cercocebus Torquatus Torquatus) With a New Simian Immunodeficiency Virus. *J Virol* (1998) 72:600–8. doi: 10.1128/JVI.72.1.600-608.1998
135. Ciccone EJ, Greenwald JH, Lee PI, Biancotto A, Read SW, Yao MA, et al. CD4+ T Cells, Including Th17 and Cycling Subsets, are Intact in the Gut Mucosa of HIV-1-infected Long-Term Nonprogressors. *J Virol* (2011) 85:5880–8. doi: 10.1128/JVI.02643-10
136. Hirsch VM, Dapolito G, Johnson PR, Elkins WR, London WT, Montali RJ, et al. Induction of AIDS by Simian Immunodeficiency Virus From an African Green Monkey: Species-Specific Variation in Pathogenicity Correlates With the Extent of In Vivo Replication. *J Virol* (1995) 69:955–67. doi: 10.1128/jvi.69.2.955-967.1995
137. Apetrei C, Gaufin T, Gautam R, Vinton C, Hirsch V, Lewis M, et al. Pattern of SIVagm Infection in Patas Monkeys Suggests That Host Adaptation to Simian Immunodeficiency Virus Infection may Result in Resistance to Infection and Virus Extinction. *J Infect Dis* (2010) 202(Suppl 3):S371–6. doi: 10.1086/655970
138. Onanga R, Kornfeld C, Pandrea I, Estaquier J, Souquiere S, Rouquet P, et al. High Levels of Viral Replication Contrast With Only Transient Changes in CD4(+) and CD8(+) Cell Numbers During the Early Phase of Experimental Infection With Simian Immunodeficiency Virus SIVmnd-1 in Mandrillus Sphinx. *J Virol* (2002) 76:10256–63. doi: 10.1128/JVI.76.20.10256-10263.2002
139. Ling B, Veazey RS, Hart M, Lackner AA, Kuroda M, Pahar B, et al. Early Restoration of Mucosal CD4 Memory CCR5 T Cells in the Gut of SIV-infected Rhesus Predicts Long Term Non-Progression. *AIDS* (2007) 21:2377–85. doi: 10.1097/QAD.0b013e3282f08b32
140. Estaquier J, Idziorek T, de Bels F, Barre-Sinoussi F, Hurtrel B, Aubertin AM, et al. Programmed Cell Death and AIDS: Significance of T-Cell Apoptosis in Pathogenic and Nonpathogenic Primate Lentiviral Infections. *Proc Natl Acad Sci USA* (1994) 91:9431–5. doi: 10.1073/pnas.91.20.9431
141. Ma D, Jasinska A, Kristoff J, Grobler JP, Turner T, Jung Y, et al. SIVagm Infection in Wild African Green Monkeys From South Africa: Epidemiology,

Natural History, and Evolutionary Considerations. *PloS Pathog* (2013) 9: e1003011. doi: 10.1371/journal.ppat.1003011
142. Raehtz KD, Barrenas F, Xu C, Busman-Sahay K, Valentine A, Law L, et al. African Green Monkeys Avoid SIV Disease Progression by Preventing Intestinal Dysfunction and Maintaining Mucosal Barrier Integrity. *PloS Pathog* (2020) 16:e1008333. doi: 10.1371/journal.ppat.1008333
143. Barrenas F, Raehtz K, Xu C, Law L, Green RR, Silvestri G, et al. Macrophage-Associated Wound Healing Contributes to African Green Monkey SIV Pathogenesis Control. *Nat Commun* (2019) 10:5101. doi: 10.1038/s41467-019-13816-9
144. Estes JD, Harris LD, Klatt NR, Tabb B, Pittaluga S, Paiardini M, et al. Damaged Intestinal Epithelial Integrity Linked to Microbial Translocation in Pathogenic Simian Immunodeficiency Virus Infections. *PloS Pathog* (2010) 6:e1001052. doi: 10.1371/journal.ppat.1001052
145. Silvestri G, Sodora DL, Koup RA, Paiardini M, O'Neil SP, McClure HM, et al. Nonpathogenic SIV Infection of Sooty Mangabeys Is Characterized by Limited Bystander Immunopathology Despite Chronic High-Level Viremia. *Immunity* (2003) 18:441–52. doi: 10.1016/S1074-7613(03)00060-8
146. Sandler NG, Bosinger SE, Estes JD, Zhu RT, Tharp GK, Boritz E, et al. Type I Interferon Responses in Rhesus Macaques Prevent SIV Infection and Slow Disease Progression. *Nature* (2014) 511:601–5. doi: 10.1038/nature13554
147. Carnathan D, Lawson B, Yu J, Patel K, Billingsley JM, Tharp GK, et al. Reduced Chronic Lymphocyte Activation Following Interferon Alpha Blockade During the Acute Phase of Simian Immunodeficiency Virus Infection in Rhesus Macaques. *J Virol* (2018) 92(9):e01760-17. doi: 10.1128/JVI.01760-17
148. Meythaler M, Martinot A, Wang Z, Pryputniewicz S, Kasheta M, Ling B, et al. Differential CD4+ T-Lymphocyte Apoptosis and Bystander T-Cell Activation in Rhesus Macaques and Sooty Mangabeys During Acute Simian Immunodeficiency Virus Infection. *J Virol* (2009) 83:572–83. doi: 10.1128/JVI.01715-08
149. Herbeuval JP, Grivel JC, Boasso A, Hardy AW, Chougnet C, Dolan MJ, et al. CD4+ T-cell Death Induced by Infectious and Noninfectious HIV-1: Role of Type 1 Interferon-Dependent, TRAIL/DR5-mediated Apoptosis. *Blood* (2005) 106:3524–31. doi: 10.1182/blood-2005-03-1243
150. Jacquelin B, Mayau V, Targat B, Liovat AS, Kunkel D, Petitjean G, et al. Nonpathogenic SIV Infection of African Green Monkeys Induces a Strong But Rapidly Controlled Type I IFN Response. *J Clin Invest* (2009) 119:3544–55. doi: 10.1172/JCI40093
151. Harris LD, Tabb B, Sodora DL, Paiardini M, Klatt NR, Douek DC, et al. Downregulation of Robust Acute Type I Interferon Responses Distinguishes Nonpathogenic Simian Immunodeficiency Virus (SIV) Infection of Natural Hosts From Pathogenic SIV Infection of Rhesus Macaques. *J Virol* (2010) 84:7886–91. doi: 10.1128/JVI.02612-09
152. Chan ML, Petravic J, Ortiz AM, Engram J, Paiardini M, Cromer D, et al. Limited CD4+ T Cell Proliferation Leads to Preservation of CD4+ T Cell Counts in SIV-Infected Sooty Mangabeys. *Proc Biol Sci* (2010) 277:3773–81. doi: 10.1098/rspb.2010.0972
153. McGary CS, Cervasi B, Chahroudi A, Micci L, Taaffe J, Meeker T, et al. Increased Stability and Limited Proliferation of CD4+ Central Memory T Cells Differentiate Nonprogressive Simian Immunodeficiency Virus (SIV) Infection of Sooty Mangabeys From Progressive SIV Infection of Rhesus Macaques. *J Virol* (2014) 88:4533–42. doi: 10.1128/JVI.03515-13
154. Ortiz AM, Carnathan DG, Yu J, Sheehan KM, Kim P, Reynaldi A, et al. Analysis of the In Vivo Turnover of CD4+ T-Cell Subsets in Chronically SIV-Infected Sooty Mangabeys. *PloS One* (2016) 11:e0156352. doi: 10.1371/journal.pone.0156352
155. Chakrabarti LA, Lewin SR, Zhang L, Gettie A, Luckay A, Martin LN, et al. Normal T-Cell Turnover in Sooty Mangabeys Harboring Active Simian Immunodeficiency Virus Infection. *J Virol* (2000) 74:1209–23. doi: 10.1128/JVI.74.3.1209-1223.2000
156. Ma D, Jasinska AJ, Feyertag F, Wijewardana V, Kristoff J, He T, et al. Factors Associated With Siman Immunodeficiency Virus Transmission in a Natural African Nonhuman Primate Host in the Wild. *J Virol* (2014) 88:5687–705. doi: 10.1128/JVI.03606-13
157. Pandrea I, Parrish NF, Raehtz K, Gaufin T, Barbian HJ, Ma D, et al. Mucosal Simian Immunodeficiency Virus Transmission in African Green Monkeys: Susceptibility to Infection is Proportional to Target Cell Availability at Mucosal Sites. *J Virol* (2012) 86:4158–68. doi: 10.1128/JVI.07141-11
158. Pandrea I, Onanga R, Souquiere S, Mouinga-Ondeme A, Bourry O, Makuwa M, et al. Paucity of CD4+ CCR5+ T Cells may Prevent Transmission of Simian Immunodeficiency Virus in Natural Nonhuman Primate Hosts by Breast-Feeding. *J Virol* (2008) 82:5501–9. doi: 10.1128/JVI.02555-07
159. Beaumier CM, Harris LD, Goldstein S, Klatt NR, Whitted S, McGinty J, et al. CD4 Downregulation by Memory CD4+ T Cells In Vivo Renders African Green Monkeys Resistant to Progressive SIVagm Infection. *Nat Med* (2009) 15:879–85. doi: 10.1038/nm.1970
160. Vinton C, Klatt NR, Harris LD, Briant JA, Sanders-Beer BE, Herbert R, et al. CD4-Like Immunological Function by CD4- T Cells in Multiple Natural Hosts of Simian Immunodeficiency Virus. *J Virol* (2011) 85:8702–8. doi: 10.1128/JVI.00332-11
161. Sundaravaradan V, Saleem R, Micci L, Gasper MA, Ortiz AM, Else J, et al. Multifunctional Double-Negative T Cells in Sooty Mangabeys Mediate T-Helper Functions Irrespective of SIV Infection. *PloS Pathog* (2013) 9: e1003441. doi: 10.1371/journal.ppat.1003441
162. Doitsh G, Greene WC. Dissecting How CD4 T Cells Are Lost During HIV Infection. *Cell Host Microbe* (2016) 19:280–91. doi: 10.1016/j.chom.2016.02.012
163. Leonard R, Zagury D, Desportes I, Bernard J, Zagury JF, Gallo RC. Cytopathic Effect of Human Immunodeficiency Virus in T4 Cells Is Linked to the Last Stage of Virus Infection. *Proc Natl Acad Sci USA* (1988) 85:3570–4. doi: 10.1073/pnas.85.10.3570
164. Borrow P, Lewicki H, Hahn BH, Shaw GM, Oldstone MB. Virus-Specific CD8+ Cytotoxic T-lymphocyte Activity Associated With Control of Viremia in Primary Human Immunodeficiency Virus Type 1 Infection. *J Virol* (1994) 68:6103–10. doi: 10.1128/jvi.68.9.6103-6110.1994
165. Jones RB, Walker BD. HIV-Specific CD8(+) T Cells and HIV Eradication. *J Clin Invest* (2016) 126:455–63. doi: 10.1172/JCI80566
166. Gandhi RT, Chen BK, Straus SE, Dale JK, Lenardo MJ, Baltimore D. HIV-1 Directly Kills CD4+ T Cells by a Fas-independent Mechanism. *J Exp Med* (1998) 187:1113–22. doi: 10.1084/jem.187.7.1113
167. Petit F, Arnoult D, Lelievre JD, Moutouh-de Parseval L, Hance AJ, Schneider P, et al. Productive HIV-1 Infection of Primary CD4+ T Cells Induces Mitochondrial Membrane Permeabilization Leading to a Caspase-Independent Cell Death. *J Biol Chem* (2002) 277:1477–87. doi: 10.1074/jbc.M102671200
168. Laforge M, Petit F, Estaquier J, Senik A. Commitment to Apoptosis in CD4 (+) T Lymphocytes Productively Infected With Human Immunodeficiency Virus Type 1 Is Initiated by Lysosomal Membrane Permeabilization, Itself Induced by the Isolated Expression of the Viral Protein Nef. *J Virol* (2007) 81:11426–40. doi: 10.1128/JVI.00597-07
169. Hessell AJ, Hangartner L, Hunter M, Havenith CE, Beurskens FJ, Bakker JM, et al. Fc Receptor But Not Complement Binding Is Important in Antibody Protection Against HIV. *Nature* (2007) 449:101–4. doi: 10.1038/nature06106
170. Musich T, Li L, Liu L, Zolla-Pazner S, Robert-Guroff M, Gorny MK. Monoclonal Antibodies Specific for the V2, V3, CD4-Binding Site, and gp41 of HIV-1 Mediate Phagocytosis in a Dose-Dependent Manner. *J Virol* (2017) 91(8):e02325-16. doi: 10.1128/JVI.02325-16
171. Solder BM, Schulz TF, Hengster P, Lower J, Larcher C, Bitterlich G, et al. HIV and HIV-infected Cells Differentially Activate the Human Complement System Independent of Antibody. *Immunol Lett* (1989) 22:135–45. doi: 10.1016/0165-2478(89)90180-6
172. Chung AW, Isitman G, Navis M, Kramski M, Center RJ, Kent SJ, et al. Immune Escape From HIV-specific Antibody-Dependent Cellular Cytotoxicity (ADCC) Pressure. *Proc Natl Acad Sci USA* (2011) 108:7505–10. doi: 10.1073/pnas.1016048108
173. Schmitz J, Zimmer JP, Kluxen B, Aries S, Bogel M, Gigli I, et al. Antibody-Dependent Complement-Mediated Cytotoxicity in Sera From Patients With HIV-1 Infection Is Controlled by CD55 and CD59. *J Clin Invest* (1995) 96:1520–6. doi: 10.1172/JCI118190
174. Dufloo J, Guivel-Benhassine F, Buchrieser J, Lorin V, Grzelak L, Dupouy E, et al. Anti-HIV-1 Antibodies Trigger Non-Lytic Complement Deposition on Infected Cells. *EMBO Rep* (2020) 21:e49351. doi: 10.15252/embr.201949351
175. Mehandru S, Poles MA, Tenner-Racz K, Manuelli V, Jean-Pierre P, Lopez P, et al. Mechanisms of Gastrointestinal CD4+ T-Cell Depletion During Acute and Early Human Immunodeficiency Virus Type 1 Infection. *J Virol* (2007) 81:599–612. doi: 10.1128/JVI.01739-06

176. Finkel TH, Tudor-Williams G, Banda NK, Cotton MF, Curiel T, Monks C, et al. Apoptosis Occurs Predominantly in Bystander Cells and Not in Productively Infected Cells of HIV- and SIV-Infected Lymph Nodes. *Nat Med* (1995) 1:129–34. doi: 10.1038/nm0295-129
177. Boirivant M, Viora M, Giordani L, Luzzati AL, Pronio AM, Montesani C, et al. HIV-1 gp120 Accelerates Fas-mediated Activation-Induced Human Lamina Propria T Cell Apoptosis. *J Clin Immunol* (1998) 18:39–47. doi: 10.1016/S0165-2478(97)85516-2
178. Cicala C, Arthos J, Rubbert A, Selig S, Wildt K, Cohen OJ, et al. HIV-1 Envelope Induces Activation of Caspase-3 and Cleavage of Focal Adhesion Kinase in Primary Human CD4(+) T Cells. *Proc Natl Acad Sci USA* (2000) 97:1178–83. doi: 10.1073/pnas.97.3.1178
179. Katsikis PD, Wunderlich ES, Smith CA, Herzenberg LA, Herzenberg LA. Fas Antigen Stimulation Induces Marked Apoptosis of T Lymphocytes in Human Immunodeficiency Virus-Infected Individuals. *J Exp Med* (1995) 181:2029–36. doi: 10.1084/jem.181.6.2029
180. Estaquier J, Idziorek T, Zou W, Emilie D, Farber CM, Bourez JM, et al. T Helper Type 1/T Helper Type 2 Cytokines and T Cell Death: Preventive Effect of Interleukin 12 on Activation-Induced and CD95 (FAS/APO-1)-Mediated Apoptosis of CD4+ T Cells From Human Immunodeficiency Virus-Infected Persons. *J Exp Med* (1995) 182:1759–67. doi: 10.1084/jem.182.6.1759
181. Estaquier J, Tanaka M, Suda T, Nagata S, Golstein P, Ameisen JC. Fas-Mediated Apoptosis of CD4+ and CD8+ T Cells From Human Immunodeficiency Virus-Infected Persons: Differential In Vitro Preventive Effect of Cytokines and Protease Antagonists. *Blood* (1996) 87:4959–66. doi: 10.1182/blood.V87.12.4959.bloodjournal87124959
182. Sloand EM, Young NS, Kumar P, Weichold FF, Sato T, Maciejewski JP. Role of Fas Ligand and Receptor in the Mechanism of T-cell Depletion in Acquired Immunodeficiency Syndrome: Effect on CD4+ Lymphocyte Depletion and Human Immunodeficiency Virus Replication. *Blood* (1997) 89:1357–63. doi: 10.1182/blood.V89.4.1357
183. Kim N, Dabrowska A, Jenner RG, Aldovini A. Human and Simian Immunodeficiency Virus-Mediated Upregulation of the Apoptotic Factor TRAIL Occurs in Antigen-Presenting Cells From AIDS-Susceptible But Not From AIDS-Resistant Species. *J Virol* (2007) 81:7584–97. doi: 10.1128/JVI.02616-06
184. Diop OM, Ploquin MJ, Mortara L, Faye A, Jacquelin B, Kunkel D, et al. Plasmacytoid Dendritic Cell Dynamics and Alpha Interferon Production During Simian Immunodeficiency Virus Infection With a Nonpathogenic Outcome. *J Virol* (2008) 82:5145–52. doi: 10.1128/JVI.02433-07
185. Doitsh G, Cavrois M, Lassen KG, Zepeda O, Yang Z, Santiago ML, et al. Abortive HIV Infection Mediates CD4 T Cell Depletion and Inflammation in Human Lymphoid Tissue. *Cell* (2010) 143:789–801. doi: 10.1016/j.cell.2010.11.001
186. Sivanandham R, Brocca-Cofano E, Krampe N, Falwell E, Venkatraman SMK, Ribeiro RM, et al. Neutrophil Extracellular Trap Production Contributes to Pathogenesis in SIV-Infected Nonhuman Primates. *J Clin Invest* (2018) 128:5178–83. doi: 10.1172/JCI99420
187. Vujkovic-Cvijin I, Swainson LA, Chu SN, Ortiz AM, Santee CA, Petriello A, et al. Gut-Resident Lactobacillus Abundance Associates With IDO1 Inhibition and Th17 Dynamics in SIV-Infected Macaques. *Cell Rep* (2015) 13:1589–97. doi: 10.1016/j.celrep.2015.10.026
188. Brockman MA, Kwon DS, Tighe DP, Pavlik DF, Rosato PC, Sela J, et al. IL-10 Is Up-Regulated in Multiple Cell Types During Viremic HIV Infection and Reversibly Inhibits Virus-Specific T Cells. *Blood* (2009) 114:346–56. doi: 10.1182/blood-2008-12-191296
189. Clerici M, Sarin A, Berzofsky JA, Landay AL, Kessler HA, Hashemi F, et al. Antigen-Stimulated Apoptotic T-Cell Death in HIV Infection Is Selective for CD4+ T Cells, Modulated by Cytokines and Effected by Lymphotoxin. *AIDS* (1996) 10:603–11. doi: 10.1097/00002030-199606000-00005
190. Palmer BE, Boritz E, Wilson CC. Effects of Sustained HIV-1 Plasma Viremia on HIV-1 Gag-Specific CD4+ T Cell Maturation and Function. *J Immunol* (2004) 172:3337–47. doi: 10.4049/jimmunol.172.5.3337
191. Younes SA, Yassine-Diab B, Dumont AR, Boulassel MR, Grossman Z, Routy JP, et al. HIV-1 Viremia Prevents the Establishment of Interleukin 2-Producing HIV-Specific Memory CD4+ T Cells Endowed With Proliferative Capacity. *J Exp Med* (2003) 198:1909–22. doi: 10.1084/jem.20031598
192. Fenwick C, Joo V, Jacquier P, Noto A, Banga R, Perreau M, et al. T-Cell Exhaustion in HIV Infection. *Immunol Rev* (2019) 292:149–63. doi: 10.1111/imr.12823
193. Douek DC, McFarland RD, Keiser PH, Gage EA, Massey JM, Haynes BF, et al. Changes in Thymic Function With Age and During the Treatment of HIV Infection. *Nature* (1998) 396:690–5. doi: 10.1038/25374
194. Zeng M, Smith AJ, Wietgrefe SW, Southern PJ, Schacker TW, Reilly CS, et al. Cumulative Mechanisms of Lymphoid Tissue Fibrosis and T Cell Depletion in HIV-1 and SIV Infections. *J Clin Invest* (2011) 121:998–1008. doi: 10.1172/JCI45157
195. Estes JD, Wietgrefe S, Schacker T, Southern P, Beilman G, Reilly C, et al. Simian Immunodeficiency Virus-Induced Lymphatic Tissue Fibrosis Is Mediated by Transforming Growth Factor Beta 1-Positive Regulatory T Cells and Begins in Early Infection. *J Infect Dis* (2007) 195:551–61. doi: 10.1086/510852
196. Kaplan JE, Spira TJ, Fishbein DB, Bozeman LH, Pinsky PF, Schonberger LB. A Six-Year Follow-Up of HIV-Infected Homosexual Men With Lymphadenopathy. Evidence for an Increased Risk for Developing AIDS After the Third Year of Lymphadenopathy. *JAMA* (1988) 260:2694–7. doi: 10.1001/jama.260.18.2694
197. Mellors JW, Munoz A, Giorgi JV, Margolick JB, Tassoni CJ, Gupta P, et al. Plasma Viral Load and CD4+ Lymphocytes as Prognostic Markers of HIV-1 Infection. *Ann Intern Med* (1997) 126:946–54. doi: 10.7326/0003-4819-126-12-199706150-00003
198. Goulet JL, Fultz SL, Rimland D, Butt A, Gibert C, Rodriguez-Barradas M, et al. Aging and Infectious Diseases: do Patterns of Comorbidity Vary by HIV Status, Age, and HIV Severity? *Clin Infect Dis* (2007) 45:1593–601. doi: 10.1086/523577
199. Phair J, Munoz A, Detels R, Kaslow R, Rinaldo C, Saah A. The Risk of Pneumocystis Carinii Pneumonia Among Men Infected With Human Immunodeficiency Virus Type 1. Multicenter Aids Cohort Study Group. *N Engl J Med* (1990) 322:161–5. doi: 10.1056/NEJM199001183220304
200. Masur H, Ognibene FP, Yarchoan R, Shelhamer JH, Baird BF, Travis W, et al. CD4 Counts as Predictors of Opportunistic Pneumonias in Human Immunodeficiency Virus (HIV) Infection. *Ann Intern Med* (1989) 111:223–31. doi: 10.7326/0003-4819-111-3-223
201. Clifford GM, Polesel J, Rickenbach M, Dal Maso L, Keiser O, Kofler A, et al. Cancer Risk in the Swiss HIV Cohort Study: Associations With Immunodeficiency, Smoking, and Highly Active Antiretroviral Therapy. *J Natl Cancer Inst* (2005) 97:425–32. doi: 10.1093/jnci/dji072
202. Patel P, Hanson DL, Sullivan PS, Novak RM, Moorman AC, Tong TC, et al. Adolescent Spectrum of Disease and H.I.V.O.S. Investigators, Incidence of Types of Cancer Among HIV-Infected Persons Compared With the General Population in the United States, 1992-2003. *Ann Intern Med* (2008) 148:728–36. doi: 10.7326/0003-4819-148-10-200805200-00005
203. Milush JM, Reeves JD, Gordon SN, Zhou D, Muthukumar A, Kosub DA, et al. Virally Induced CD4+ T Cell Depletion is Not Sufficient to Induce AIDS in a Natural Host. *J Immunol* (2007) 179:3047–56. doi: 10.4049/jimmunol.179.5.3047
204. Hasegawa A, Liu H, Ling B, Borda JT, Alvarez X, Sugimoto C, et al. The Level of Monocyte Turnover Predicts Disease Progression in the Macaque Model of AIDS. *Blood* (2009) 114:2917–25. doi: 10.1182/blood-2009-02-204263
205. Laforge M, Campillo-Gimenez L, Monceaux V, Cumont MC, Hurtrel B, Corbeil J, et al. HIV/SIV Infection Primes Monocytes and Dendritic Cells for Apoptosis. *PloS Pathog* (2011) 7:e1002087. doi: 10.1371/journal.ppat.1002087
206. Doitsh G, Galloway NL, Geng X, Yang Z, Monroe KM, Zepeda O, et al. Cell Death by Pyroptosis Drives CD4 T-Cell Depletion in HIV-1 Infection. *Nature* (2014) 505:509–14. doi: 10.1038/nature12940
207. Raffatellu M, Santos RL, Verhoeven DE, George MD, Wilson RP, Winter SE, et al. Simian Immunodeficiency Virus-Induced Mucosal Interleukin-17 Deficiency Promotes Salmonella Dissemination From the Gut. *Nat Med* (2008) 14:421–8. doi: 10.1038/nm1743
208. Brenchley JM, Price DA, Schacker TW, Asher TE, Silvestri G, Rao S, et al. Microbial Translocation Is a Cause of Systemic Immune Activation in Chronic HIV Infection. *Nat Med* (2006) 12:1365–71. doi: 10.1038/nm1511
209. Hao XP, Lucero CM, Turkbey B, Bernardo ML, Morcock DR, Deleage C, et al. Experimental Colitis in SIV-uninfected Rhesus Macaques Recapitulates

Important Features of Pathogenic SIV Infection. *Nat Commun* (2015) 6:8020. doi: 10.1038/ncomms9020
210. Kristoff J, Haret-Richter G, Ma D, Ribeiro RM, Xu C, Cornell E, et al. Early Microbial Translocation Blockade Reduces SIV-mediated Inflammation and Viral Replication. *J Clin Invest* (2014) 124:2802–6. doi: 10.1172/JCI75090
211. Fujino S, Andoh A, Bamba S, Ogawa A, Hata K, Araki Y, et al. Increased Expression of Interleukin 17 in Inflammatory Bowel Disease. *Gut* (2003) 52:65–70. doi: 10.1136/gut.52.1.65
212. Wang Y, MacDonald JK, Benchimol EI, Griffiths AM, Steinhart AH, Panaccione R, et al. Type I Interferons for Induction of Remission in Ulcerative Colitis. *Cochrane Database Syst Rev* (2015) (9):CD006790. doi: 10.1002/14651858.CD006790.pub3
213. Ramgolam VS, Sha Y, Jin J, Zhang X, Markovic-Plese S. IFN-Beta Inhibits Human Th17 Cell Differentiation. *J Immunol* (2009) 183:5418–27. doi: 10.4049/jimmunol.0803227
214. Deeks SG, Tracy R, Douek DC. Systemic Effects of Inflammation on Health During Chronic HIV Infection. *Immunity* (2013) 39:633–45. doi: 10.1016/j.immuni.2013.10.001
215. Kuller LH, Tracy R, Belloso W, De Wit S, Drummond F, Lane HC, et al. Inflammatory and Coagulation Biomarkers and Mortality in Patients With HIV Infection. *PloS Med* (2008) 5:e203. doi: 10.1371/journal.pmed.0050203
216. Calmy A, Gayet-Ageron A, Montecucco F, Nguyen A, Mach F, Burger F, et al. HIV Increases Markers of Cardiovascular Risk: Results From a Randomized, Treatment Interruption Trial. *AIDS* (2009) 23:929–39. doi: 10.1097/QAD.0b013e32832995fa
217. Pandrea I, Cornell E, Wilson C, Ribeiro RM, Ma D, Kristoff J, et al. Coagulation Biomarkers Predict Disease Progression in SIV-Infected Nonhuman Primates. *Blood* (2012) 120:1357–66. doi: 10.1182/blood-2012-03-414706
218. George MD, Reay E, Sankaran S, Dandekar S. Early Antiretroviral Therapy for Simian Immunodeficiency Virus Infection Leads to Mucosal CD4+ T-Cell Restoration and Enhanced Gene Expression Regulating Mucosal Repair and Regeneration. *J Virol* (2005) 79:2709–19. doi: 10.1128/JVI.79.5.2709-2719.2005
219. Macal M, Sankaran S, Chun TW, Reay E, Flamm J, Prindiville TJ, et al. Effective CD4+ T-Cell Restoration in Gut-Associated Lymphoid Tissue of HIV-Infected Patients Is Associated With Enhanced Th17 Cells and Polyfunctional HIV-Specific T-Cell Responses. *Mucosal Immunol* (2008) 1:475–88. doi: 10.1038/mi.2008.35
220. van den Dries L, Claassen MAA, Groothuismink ZMA, van Gorp E, Boonstra A. Immune Activation in Prolonged Cart-Suppressed HIV Patients Is Comparable to That of Healthy Controls. *Virology* (2017) 509:133–9. doi: 10.1016/j.virol.2017.06.014
221. Funderburg NT, Andrade A, Chan ES, Rosenkranz SL, Lu D, Clagett B, et al. Dynamics of Immune Reconstitution and Activation Markers in HIV+ Treatment-Naive Patients Treated With Raltegravir, Tenofovir Disoproxil Fumarate and Emtricitabine. *PloS One* (2013) 8:e83514. doi: 10.1371/journal.pone.0083514
222. Whitney JB, Hill AL, Sanisetty S, Penaloza-MacMaster P, Liu J, Shetty M, et al. Rapid Seeding of the Viral Reservoir Prior to SIV Viraemia in Rhesus Monkeys. *Nature* (2014) 512:74–7. doi: 10.1038/nature13594
223. Ciccone EJ, Read SW, Mannon PJ, Yao MD, Hodge JN, Dewar R, et al. Cycling of Gut Mucosal CD4+ T Cells Decreases After Prolonged Anti-Retroviral Therapy and Is Associated With Plasma LPS Levels. *Mucosal Immunol* (2010) 3:172–81. doi: 10.1038/mi.2009.129
224. Autran B, Carcelain G, Li TS, Blanc C, Mathez D, Tubiana R, et al. Positive Effects of Combined Antiretroviral Therapy on CD4+ T Cell Homeostasis and Function in Advanced HIV Disease. *Science* (1997) 277:112–6. doi: 10.1126/science.277.5322.112
225. Klatt NR, Villinger F, Bostik P, Gordon SN, Pereira L, Engram JC, et al. Availability of Activated CD4+ T Cells Dictates the Level of Viremia in Naturally SIV-Infected Sooty Mangabeys. *J Clin Invest* (2008) 118:2039–49. doi: 10.1172/JCI33814
226. Grakoui A, Shoukry NH, Woollard DJ, Han JH, Hanson HL, Ghrayeb J, et al. HCV Persistence and Immune Evasion in the Absence of Memory T Cell Help. *Science* (2003) 302:659–62. doi: 10.1126/science.1088774
227. Engram JC, Cervasi B, Borghans JA, Klatt NR, Gordon SN, Chahroudi A, et al. Lineage-Specific T-Cell Reconstitution Following In Vivo CD4+ and CD8+ Lymphocyte Depletion in Nonhuman Primates. *Blood* (2010) 116:748–58. doi: 10.1182/blood-2010-01-263814
228. Kumar NA, McBrien JB, Carnathan DG, Mavigner M, Mattingly C, White ER, et al. Antibody-Mediated CD4 Depletion Induces Homeostatic CD4(+) T Cell Proliferation Without Detectable Virus Reactivation in Antiretroviral Therapy-Treated Simian Immunodeficiency Virus-Infected Macaques. *J Virol* (2018) 92(22):e01235-18. doi: 10.1128/JVI.01235-18
229. Ortiz AM, Klatt NR, Li B, Yi Y, Tabb B, Hao XP, et al. Depletion of CD4(+) T Cells Abrogates Post-Peak Decline of Viremia in SIV-Infected Rhesus Macaques. *J Clin Invest* (2011) 121:4433–45. doi: 10.1172/JCI46023
230. Micci L, Alvarez X, Iriele RI, Ortiz AM, Ryan ES, McGary CS, et al. CD4 Depletion in SIV-Infected Macaques Results in Macrophage and Microglia Infection With Rapid Turnover of Infected Cells. *PloS Pathog* (2014) 10:e1004467. doi: 10.1371/journal.ppat.1004467
231. Kleinman AJ, Sivanandham R, Pandrea I, Chougnet CA, Apetrei C. Regulatory T Cells As Potential Targets for HIV Cure Research. *Front Immunol* (2018) 9:734. doi: 10.3389/fimmu.2018.00734
232. He T, Brocca-Cofano E, Policicchio BB, Sivanandham R, Gautam R, Raehtz KD, et al. Cutting Edge: T Regulatory Cell Depletion Reactivates Latent Simian Immunodeficiency Virus (SIV) in Controller Macaques While Boosting SIV-Specific T Lymphocytes. *J Immunol* (2016) 197:4535–9. doi: 10.4049/jimmunol.1601539
233. Pandrea I, Gaufin T, Brenchley JM, Gautam R, Monjure C, Gautam A, et al. Cutting Edge: Experimentally Induced Immune Activation in Natural Hosts of Simian Immunodeficiency Virus Induces Significant Increases in Viral Replication and CD4+ T Cell Depletion. *J Immunol* (2008) 181:6687–91. doi: 10.4049/jimmunol.181.10.6687
234. Sivanandham R, Kleinman AJ, Sette P, Brocca-Cofano E, Kilapandal Venkatraman SM, Policicchio BB, et al. Nonhuman Primate Testing of the Impact of Different Regulatory T Cell Depletion Strategies on Reactivation and Clearance of Latent Simian Immunodeficiency Virus. *J Virol* (2020) 94(19):e00533-20. doi: 10.1128/JVI.00533-20
235. Wang Z, Pratts SG, Zhang H, Spencer PJ, Yu R, Tonsho M, et al. Treg Depletion in Non-Human Primates Using a Novel Diphtheria Toxin-Based Anti-Human CCR4 Immunotoxin. *Mol Oncol* (2016) 10:553–65. doi: 10.1016/j.molonc.2015.11.008
236. Hryniewicz A, Boasso A, Edghill-Smith Y, Vaccari M, Fuchs D, Venzon D, et al. CTLA-4 Blockade Decreases TGF-beta, IDO, and Viral RNA Expression in Tissues of SIVmac251-Infected Macaques. *Blood* (2006) 108:3834–42. doi: 10.1182/blood-2006-04-010637
237. Cecchinato V, Tryniszewska E, Ma ZM, Vaccari M, Boasso A, Tsai WP, et al. Immune Activation Driven by CTLA-4 Blockade Augments Viral Replication at Mucosal Sites in Simian Immunodeficiency Virus Infection. *J Immunol* (2008) 180:5439–47. doi: 10.4049/jimmunol.180.8.5439
238. Harper J, Gordon S, Chan CN, Wang H, Lindemuth E, Galardi C, et al. CTLA-4 and PD-1 Dual Blockade Induces SIV Reactivation Without Control of Rebound After Antiretroviral Therapy Interruption. *Nat Med* (2020) 26:519–28. doi: 10.1038/s41591-020-0782-y
239. Rahemtulla A, Fung-Leung WP, Schilham MW, Kundig TM, Sambhara SR, Narendran A, et al. Normal Development and Function of CD8+ Cells But Markedly Decreased Helper Cell Activity in Mice Lacking CD4. *Nature* (1991) 353:180–4. doi: 10.1038/353180a0
240. Rahemtulla A, Kundig TM, Narendran A, Bachmann MF, Julius M, Paige CJ, et al. Class II Major Histocompatibility Complex-Restricted T Cell Function in CD4-Deficient Mice. *Eur J Immunol* (1994) 24:2213–8. doi: 10.1002/eji.1830240942
241. Locksley RM, Reiner SL, Hatam F, Littman DR, Killeen N. Helper T Cells Without CD4: Control of Leishmaniasis in CD4-Deficient Mice. *Science* (1993) 261:1448–51. doi: 10.1126/science.8367726
242. von Herrath MG, Yokoyama M, Dockter J, Oldstone MB, Whitton JL. CD4-Deficient Mice Have Reduced Levels of Memory Cytotoxic T Lymphocytes After Immunization and Show Diminished Resistance to Subsequent Virus Challenge. *J Virol* (1996) 70:1072–9. doi: 10.1128/jvi.70.2.1072-1079.1996
243. Smith DK, Neal JJ, Holmberg SD. Unexplained Opportunistic Infections and CD4+ T-Lymphocytopenia Without HIV Infection. An Investigation of Cases in the United States. The Centers for Disease Control Idiopathic CD4+ T-lymphocytopenia Task Force. *N Engl J Med* (1993) 328:373–9. doi: 10.1056/NEJM199302113280601

244. C. Centers for Disease. Unexplained CD4+ T-Lymphocyte Depletion in Persons Without Evident HIV Infection–United States. *MMWR Morb Mortal Wkly Rep* (1992) 41:541–5. doi: 10.1001/jama.1992.03490100048012
245. Aledort LM, Operskalski EA, Dietrich SL, Koerper MA, Gjerset GF, Lusher JM, et al. Low CD4+ Counts in a Study of Transfusion Safety. The Transfusion Safety Study Group. *N Engl J Med* (1993) 328:441–2. doi: 10.1056/NEJM199302113280614
246. Busch MP, Valinsky JE, Paglieroni T, Prince HE, Crutcher GJ, Gjerset GF, et al. Screening of Blood Donors for Idiopathic CD4+ T-Lymphocytopenia. *Transfusion* (1994) 34:192–7. doi: 10.1046/j.1537-2995.1994.34394196614.x
247. Zonios DI, Falloon J, Bennett JE, Shaw PA, Chaitt D, Baseler MW, et al. Idiopathic CD4+ Lymphocytopenia: Natural History and Prognostic Factors. *Blood* (2008) 112:287–94. doi: 10.1182/blood-2007-12-127878
248. Regent A, Autran B, Carcelain G, Cheynier R, Terrier B, Charmeteau-De Muylder B, et al. Idiopathic CD4 Lymphocytopenia: Clinical and Immunologic Characteristics and Follow-Up of 40 Patients. *Medicine (Baltimore)* (2014) 93:61–72. doi: 10.1097/MD.0000000000000017
249. Perez-Diez A, Wong CS, Liu X, Mystakelis H, Song J, Lu Y, et al. Prevalence and Pathogenicity of Autoantibodies in Patients With Idiopathic CD4 Lymphopenia. *J Clin Invest* (2020) 130:5326–37. doi: 10.1172/JCI136254
250. Gorska MM, Alam R. A Mutation in the Human Uncoordinated 119 Gene Impairs TCR Signaling and Is Associated With CD4 Lymphopenia. *Blood* (2012) 119:1399–406. doi: 10.1182/blood-2011-04-350686
251. Lee PI, Ciccone EJ, Read SW, Asher A, Pitts R, Douek DC, et al. Evidence for Translocation of Microbial Products in Patients With Idiopathic CD4 Lymphocytopenia. *J Infect Dis* (2009) 199:1664–70. doi: 10.1086/598953
252. Kovacs SB, Sheikh V, Thompson WL, Morcock DR, Perez-Diez A, Yao MD, et al. T-Cell Depletion in the Colonic Mucosa of Patients With Idiopathic CD4+ Lymphopenia. *J Infect Dis* (2015) 212:1579–87. doi: 10.1093/infdis/jiv282
253. Sortino O, Dias J, Anderson M, Laidlaw E, Leeansyah E, Lisco A, et al. Preserved MAIT Cell Numbers and Function in Idiopathic CD4 Lymphocytopenia. *J Infect Dis* (2020). doi: 10.1093/infdis/jiaa782
254. Lisco A, Ye P, Wong CS, Pei L, Hsu AP, Mace EM, et al. Lost in Translation: Lack of CD4 Expression Due to a Novel Genetic Defect. *J Infect Dis* (2021) 223(4):645–54. doi: 10.1093/infdis/jiab025
255. Fernandes RA, Perez-Andres M, Blanco E, Jara-Acevedo M, Criado I, Almeida J, et al. Complete Multilineage Cd4 Expression Defect Associated With Warts Due to an Inherited Homozygous CD4 Gene Mutation. *Front Immunol* (2019) 10:2502. doi: 10.3389/fimmu.2019.02502
256. Grimbacher B, Holland SM, Gallin JI, Greenberg F, Hill SC, Malech HL, et al. Hyper-IgE Syndrome With Recurrent Infections–An Autosomal Dominant Multisystem Disorder. *N Engl J Med* (1999) 340:692–702. doi: 10.1056/NEJM199903043400904
257. Ma CS, Chew GY, Simpson N, Priyadarshi A, Wong M, Grimbacher B, et al. Deficiency of Th17 Cells in Hyper IgE Syndrome Due to Mutations in STAT3. *J Exp Med* (2008) 205:1551–7. doi: 10.1084/jem.20080218
258. Zhang Q, Davis JC, Lamborn IT, Freeman AF, Jing H, Favreau AJ, et al. Combined Immunodeficiency Associated With DOCK8 Mutations. *N Engl J Med* (2009) 361:2046–55. doi: 10.1056/NEJMoa0905506
259. Engelhardt KR, McGhee S, Winkler S, Sassi A, Woellner C, Lopez-Herrera G, et al. Large Deletions and Point Mutations Involving the Dedicator of Cytokinesis 8 (DOCK8) in the Autosomal-Recessive Form of hyper-IgE Syndrome. *J Allergy Clin Immunol* (2009) 124:1289–302 e4. doi: 10.1016/j.jaci.2009.10.038
260. Spolski R, Leonard WJ. Interleukin-21: A Double-Edged Sword With Therapeutic Potential. *Nat Rev Drug Discov* (2014) 13:379–95. doi: 10.1038/nrd4296
261. Nurieva R, Yang XO, Martinez G, Zhang Y, Panopoulos AD, Ma L, et al. Essential Autocrine Regulation by IL-21 in the Generation of Inflammatory T Cells. *Nature* (2007) 448:480–3. doi: 10.1038/nature05969
262. Korn T, Bettelli E, Gao W, Awasthi A, Jager A, Strom TB, et al. IL-21 Initiates an Alternative Pathway to Induce Proinflammatory T(H)17 Cells. *Nature* (2007) 448:484–7. doi: 10.1038/nature05970
263. Pallikkuth S, Micci L, Ende ZS, Iriele RI, Cervasi B, Lawson B, et al. Maintenance of Intestinal Th17 Cells and Reduced Microbial Translocation in SIV-Infected Rhesus Macaques Treated With Interleukin (IL)-21. *PloS Pathog* (2013) 9:e1003471. doi: 10.1371/journal.ppat.1003471
264. Micci L, Ryan ES, Fromentin R, Bosinger SE, Harper JL, He T, et al. Interleukin-21 Combined With ART Reduces Inflammation and Viral Reservoir in SIV-Infected Macaques. *J Clin Invest* (2015) 125:4497–513. doi: 10.1172/JCI81400
265. Ortiz AM, Klase ZA, DiNapoli SR, Vujkovic-Cvijin I, Carmack K, Perkins MR, et al. IL-21 and Probiotic Therapy Improve Th17 Frequencies, Microbial Translocation, and Microbiome in ARV-Treated, SIV-Infected Macaques. *Mucosal Immunol* (2016) 9:458–67. doi: 10.1038/mi.2015.75
266. Mendez-Lagares G, Lu D, Merriam D, Baker CA, Villinger F, Van Rompay KKA, et al. IL-21 Therapy Controls Immune Activation and Maintains Antiviral CD8(+) T Cell Responses in Acute Simian Immunodeficiency Virus Infection. *AIDS Res Hum Retroviruses* (2017) 33:S81–92. doi: 10.1089/aid.2017.0160
267. Fry TJ, Connick E, Falloon J, Lederman MM, Liewehr DJ, Spritzler J, et al. A Potential Role for Interleukin-7 in T-Cell Homeostasis. *Blood* (2001) 97:2983–90. doi: 10.1182/blood.V97.10.2983
268. Sereti I, Dunham RM, Spritzler J, Aga E, Proschan MA, Medvik K, et al. IL-7 Administration Drives T Cell-Cycle Entry and Expansion in HIV-1 Infection. *Blood* (2009) 113:6304–14. doi: 10.1182/blood-2008-10-186601
269. Nugeyre MT, Monceaux V, Beq S, Cumont MC, Ho Tsong Fang R, Chene L, et al. IL-7 Stimulates T Cell Renewal Without Increasing Viral Replication in Simian Immunodeficiency Virus-Infected Macaques. *J Immunol* (2003) 171:4447–53. doi: 10.4049/jimmunol.171.8.4447
270. Beq S, Nugeyre MT, Ho Tsong Fang R, Gautier D, Legrand R, Schmitt N, et al. IL-7 Induces Immunological Improvement in SIV-infected Rhesus Macaques Under Antiviral Therapy. *J Immunol* (2006) 176:914–22. doi: 10.4049/jimmunol.176.2.914
271. Levy Y, Lacabaratz C, Weiss L, Viard JP, Goujard C, Lelievre JD, et al. Enhanced T Cell Recovery in HIV-1-infected Adults Through IL-7 Treatment. *J Clin Invest* (2009) 119:997–1007. doi: 10.1172/JCI38052
272. Sortino O, Richards E, Dias J, Leeansyah E, Sandberg JK, Sereti I. IL-7 Treatment Supports CD8+ Mucosa-Associated Invariant T-cell Restoration in HIV-1-Infected Patients on Antiretroviral Therapy. *AIDS* (2018) 32:825–8. doi: 10.1097/QAD.0000000000001760
273. Vandergeeten C, Fromentin R, DaFonseca S, Lawani MB, Sereti I, Lederman MM, et al. Interleukin-7 Promotes HIV Persistence During Antiretroviral Therapy. *Blood* (2013) 121:4321–9. doi: 10.1182/blood-2012-11-465625
274. Prendergast GC, Malachowski WP, DuHadaway JB, Muller AJ. Discovery of IDO1 Inhibitors: From Bench to Bedside. *Cancer Res* (2017) 77:6795–811. doi: 10.1158/0008-5472.CAN-17-2285
275. Boasso A, Vaccari M, Fuchs D, Hardy AW, Tsai WP, Tryniszewska E, et al. Combined Effect of Antiretroviral Therapy and Blockade of IDO in SIV-Infected Rhesus Macaques. *J Immunol* (2009) 182:4313–20. doi: 10.4049/jimmunol.0803314
276. Williams B, Landay A, Presti RM. Microbiome Alterations in HIV Infection a Review. *Cell Microbiol* (2016) 18:645–51. doi: 10.1111/cmi.12588
277. Klatt NR, Canary LA, Sun X, Vinton CL, Funderburg NT, Morcock DR, et al. Probiotic/Prebiotic Supplementation of Antiretrovirals Improves Gastrointestinal Immunity in SIV-Infected Macaques. *J Clin Invest* (2013) 123:903–7. doi: 10.1172/JCI66227
278. Trois L, Cardoso EM, Miura E. Use of Probiotics in HIV-Infected Children: A Randomized Double-Blind Controlled Study. *J Trop Pediatr* (2008) 54:19–24. doi: 10.1093/tropej/fmm066
279. Anukam KC, Osazuwa EO, Osadolor HB, Bruce AW, Reid G. Yogurt Containing Probiotic Lactobacillus Rhamnosus GR-1 and L. Reuteri RC-14 Helps Resolve Moderate Diarrhea and Increases CD4 Count in HIV/AIDS Patients. *J Clin Gastroenterol* (2008) 42:239–43. doi: 10.1097/MCG.0b013e31802c7465
280. d'Ettorre G, Rossi G, Scagnolari C, Andreotti M, Giustini N, Serafino S, et al. Probiotic Supplementation Promotes a Reduction in T-Cell Activation, an Increase in Th17 Frequencies, and a Recovery of Intestinal Epithelium Integrity and Mitochondrial Morphology in ART-treated HIV-1-Positive Patients. *Immun Inflamm Dis* (2017) 5:244–60. doi: 10.1002/iid3.160
281. Fujigaki S, Saito K, Sekikawa K, Tone S, Takikawa O, Fujii H, et al. Lipopolysaccharide Induction of Indoleamine 2,3-Dioxygenase is Mediated Dominantly by an IFN-gamma-independent Mechanism. *Eur J Immunol* (2001) 31:2313–8. doi: 10.1002/1521-4141(200108)31:8<2313::AID-IMMU2313>3.0.CO;2-S
282. Byakwaga H, Boum Y2nd, Huang Y, Muzoora C, Kembabazi A, Weiser SD, et al. The Kynurenine Pathway of Tryptophan Catabolism, CD4+ T-Cell

Recovery, and Mortality Among HIV-Infected Ugandans Initiating Antiretroviral Therapy. *J Infect Dis* (2014) 210:383–91. doi: 10.1093/infdis/jiu115
283. Swainson LA, Ahn H, Pajanirassa P, Khetarpal V, Deleage C, Estes JD, et al. Kynurenine 3-Monooxygenase Inhibition During Acute Simian Immunodeficiency Virus Infection Lowers PD-1 Expression and Improves Post-Combination Antiretroviral Therapy Cd4(+) T Cell Counts and Body Weight. *J Immunol* (2019) 203:899–910. doi: 10.4049/jimmunol.1801649
284. Hensley-McBain T, Zevin AS, Manuzak J, Smith E, Gile J, Miller C, et al. Effects of Fecal Microbial Transplantation on Microbiome and Immunity in Simian Immunodeficiency Virus-Infected Macaques. *J Virol* (2016) 90:4981–9. doi: 10.1128/JVI.00099-16
285. Berlin C, Berg EL, Briskin MJ, Andrew DP, Kilshaw PJ, Holzmann B, et al. Alpha 4 Beta 7 Integrin Mediates Lymphocyte Binding to the Mucosal Vascular Addressin Madcam-1. *Cell* (1993) 74:185–95. doi: 10.1016/0092-8674(93)90305-A
286. Byrareddy SN, Kallam B, Arthos J, Cicala C, Nawaz F, Hiatt J, et al. Targeting alpha4beta7 Integrin Reduces Mucosal Transmission of Simian Immunodeficiency Virus and Protects Gut-Associated Lymphoid Tissue From Infection. *Nat Med* (2014) 20:1397–400. doi: 10.1038/nm.3715
287. Ansari AA, Reimann KA, Mayne AE, Takahashi Y, Stephenson ST, Wang R, et al. Blocking of alpha4beta7 Gut-Homing Integrin During Acute Infection Leads to Decreased Plasma and Gastrointestinal Tissue Viral Loads in Simian Immunodeficiency Virus-Infected Rhesus Macaques. *J Immunol* (2011) 186:1044–59. doi: 10.4049/jimmunol.1003052
288. Sneller MC, Clarridge KE, Seamon C, Shi V, Zorawski MD, Justement JS, et al. An Open-Label Phase 1 Clinical Trial of the anti-alpha4beta7 Monoclonal Antibody Vedolizumab in HIV-Infected Individuals. *Sci Transl Med* (2019) 11(509):eaax3447. doi: 10.1126/scitranslmed.aax3447
289. Ziani W, Shao J, Fang A, Connolly PJ, Wang X, Veazey RS, et al. Mucosal Integrin alpha4beta7 Blockade Fails to Reduce the Seeding and Size of Viral Reservoirs in SIV-Infected Rhesus Macaques. *FASEB J* (2021) 35:e21282. doi: 10.1096/fj.202002235R
290. Laforge M, Silvestre R, Rodrigues V, Garibal J, Campillo-Gimenez L, Mouhamad S, et al. The Anti-Caspase Inhibitor Q-VD-OPH Prevents AIDS Disease Progression in SIV-Infected Rhesus Macaques. *J Clin Invest* (2018) 128:1627–40. doi: 10.1172/JCI95127

Conflict of Interest: The authors declare that the research was conducted in the absence of any commercial or financial relationships that could be construed as a potential conflict of interest.

frontiers in Immunology

REVIEW
published: 12 August 2021
doi: 10.3389/fimmu.2021.726419

A Tale of Two Viruses: Immunological Insights Into HCV/HIV Coinfection

Samaa T. Gobran[1,2,3], *Petronela Ancuta*[1,2] *and Naglaa H. Shoukry*[1,4]*

[1] Centre de Recherche du Centre hospitalier de l'Université de Montréal (CRCHUM), Montréal, QC, Canada, [2] Département de microbiologie, infectiologie et immunologie, Faculté de Médecine, Université de Montréal, Montréal, QC, Canada, [3] Department of Medical Microbiology and Immunology, Faculty of Medicine, Zagazig University, Zagazig, Egypt, [4] Département de médecine, Faculté de médecine, Université de Montréal, Montréal, QC, Canada

Nearly 2.3 million individuals worldwide are coinfected with human immunodeficiency virus (HIV) and hepatitis C virus (HCV). Odds of HCV infection are six times higher in people living with HIV (PLWH) compared to their HIV-negative counterparts, with the highest prevalence among people who inject drugs (PWID) and men who have sex with men (MSM). HIV coinfection has a detrimental impact on the natural history of HCV, including higher rates of HCV persistence following acute infection, higher viral loads, and accelerated progression of liver fibrosis and development of end-stage liver disease compared to HCV monoinfection. Similarly, it has been reported that HCV coinfection impacts HIV disease progression in PLWH receiving anti-retroviral therapies (ART) where HCV coinfection negatively affects the homeostasis of $CD4^+$ T cell counts and facilitates HIV replication and viral reservoir persistence. While ART does not cure HIV, direct acting antivirals (DAA) can now achieve HCV cure in nearly 95% of coinfected individuals. However, little is known about how HCV cure and the subsequent resolution of liver inflammation influence systemic immune activation, immune reconstitution and the latent HIV reservoir. In this review, we will summarize the current knowledge regarding the pathogenesis of HIV/HCV coinfection, the effects of HCV coinfection on HIV disease progression in the context of ART, the impact of HIV on HCV-associated liver morbidity, and the consequences of DAA-mediated HCV cure on immune reconstitution and HIV reservoir persistence in coinfected patients.

Keywords: human immunodeficiency virus, hepatitis C, coinfection (HIV infection), direct acting antiviral, anti retro viral therapy, liver fibrosis, CD4 T cell

OPEN ACCESS

Edited by:
Vijayakumar Velu,
Emory University, United States

Reviewed by:
Bertram Bengsch,
University of Freiburg Medical Center, Germany
Carey Shive,
Louis Stokes Cleveland VA Medical Center, United States

***Correspondence:**
Naglaa H. Shoukry
naglaa.shoukry@umontreal.ca

Specialty section:
This article was submitted to Viral Immunology, a section of the journal Frontiers in Immunology

Received: *16 June 2021*
Accepted: *26 July 2021*
Published: *12 August 2021*

Citation:
Gobran ST, Ancuta P and Shoukry NH (2021) A Tale of Two Viruses: Immunological Insights Into HCV/HIV Coinfection. Front. Immunol. 12:726419. doi: 10.3389/fimmu.2021.726419

INTRODUCTION

Hepatitis C virus (HCV) and human immunodeficiency virus type 1 (HIV-1) are two chronic viral infections that affect millions worldwide. They share similar routes of transmission through percutaneous exposure to infected blood, sexual activity and vertical transmission from infected mother-to-child. HCV is transmitted 10-times more efficiently than HIV through percutaneous exposure resulting in a high rate of HCV/HIV coinfection among people who inject drugs (PWID) (1).

HIV infection on the other hand increases the risk of HCV acquisition through sexual contact, as demonstrated by recent outbreaks of HCV among men who have sex with men (MSM) (2, 3). Similarly, HIV infection increases the risk of vertical transmission of HCV from a mother to her infant (4, 5). Finally, people living in resource-limited countries with reduced access to diagnosis and medical care are at higher risk of being infected with both viruses (6). In absence of an effective vaccine against neither HCV nor HIV, coinfection is a seriously growing public health problem, with 2.3 million individuals affected, of whom 1.3 million are PWID (7).

The immunopathology of HCV/HIV coinfection is more deleterious than each infection separately. HIV accelerates the development of HCV-related liver disease including advanced liver fibrosis, cirrhosis, hepatocellular carcinoma (HCC) and death (8). Similarly, HCV coinfection is a major cause of non-AIDS-related morbidity and mortality in people living with HIV (PLWH) as it is associated with reduced or slower $CD4^+$ T cell reconstitution after antiretroviral therapy (ART) (9). In addition, recent studies have reported that direct acting antiviral (DAA)-mediated HCV cure leads to an increase in cell-associated HIV-DNA in the blood of ART-treated PLWH who had low viral reservoirs at baseline, likely as a consequence of viral reservoir mobilization from tissues (10, 11). Whether DAA-mediated cure of HCV represents an obstacle to HIV reservoir elimination in coinfected subjects remains an important question to address.

In this review, we will discuss the interplay between HIV and HCV during coinfection. Specifically, how HIV influences HCV infectious outcome and liver disease progression and how HCV coinfection modulates the HIV latent reservoir and immune reconstitution following DAA-mediated cure and relevance to clinical management of coinfected patients.

HCV MONOINFECTION

Epidemiology

HCV is transmitted primarily through exposure to contaminated blood. Sexual transmission and vertical transmission from an infected mother to her infant are low, but both transmissions increase in the context of HIV coinfection (3–5). It is estimated that 71 million individuals are chronically infected with HCV globally (12). Injection drug use is the main source of HCV infection in high income countries, while unsafe medical injections/procedures are the main source in the developing world (13). The opioid crisis in the USA, has led to doubling the national incidence of HCV infection between 2010 and 2014 and the numbers continue to rise (14). Globally, drug use accounts for ~23% of new HCV infections (15).

Viral Replication Cycle

The HCV genome consists of an uncapped positive single stranded RNA of approximately 9.6 kb-pairs [reviewed in (16)]. The genome represents an uninterrupted open reading frame (17), encoding a polyprotein precursor of approximately 3,000 amino acids including three structural proteins (Core, envelope glycoproteins E1, and E2) and seven non-structural (NS) proteins (P7, NS2, NS3, NS4A, NS4B, NS5A, and NS5B) (16). HCV replicates primarily in human hepatocytes. Although HCV uses multiple receptors for entry into host cells, it is dependent on four main receptors on the surface of hepatocytes: CD81, a cell membrane tetraspanin protein, the scavenger receptor class B type I (SR-BI), and the tight junction proteins claudin-1 (CLDN1) and occludin (OCLN) (16, 18). The viral envelope glycoproteins fuse with the cellular membrane by clathrin-mediated endocytosis then the viral genome is released into the cytosol (16). This is followed by translation of the open reading frame of the HCV genome generating a large polyprotein that is later processed into mature structural and non-structural proteins (16). Junctions between structural proteins are processed by host signal peptidases while the non-structural proteins are processed by the NS2/3 autoprotease and the NS3/4A serine protease. Replication of the HCV RNA takes place within endoplasmic reticulum derived structures known as the membranous web through a negative strand intermediate in a replication complex (16). This is mediated by the viral NS5B protein that acts as an RNA-dependent RNA polymerase and regulated by the NS5A protein that plays many pleiotropic functions during HCV replication and assembly (19). The progeny virion is assembled into a nucleocapsid built from the structural core proteins around the viral RNA. This is followed by virion release with a surrounding membrane derived from the human cell with embedded heterodimers of the envelope glycoproteins E1 and E2 (16).

Natural History, Pathogenesis, and Immune Responses

The acute phase of HCV is empirically defined as the first 6 months post infection. Acute HCV is asymptomatic in the majority of infected subjects. Approximately 20–30% of infected subjects are able to clear the virus spontaneously during the acute phase while 70–80% develop persistent infection (20). As the virus continues to replicate in hepatocytes, it elicits persistent inflammation with increased expression of pro-inflammatory cytokines and chemokines from hepatocytes, the liver resident macrophages known as Kupffer cells, and other immune cells such as monocyte derived macrophages, natural killer (NK) cells and dendritic cells (DCs) that are recruited to the liver. Virus replication in hepatocytes also triggers hepatocyte damage with production of reactive oxygen species (ROS), damage associated molecular patterns (DAMPs) and some apoptosis. Altogether these mediators trigger the fibrogenic process (21). Hepatic stellate cells (HSCs), the main mediators of fibrosis, are activated by these different inflammatory signals and the cytokine TGF-β and start to express alpha-smooth muscle actin (αSMA) and collagen type I. Persistent inflammation leads to continued deposition of matrix proteins and imbalance in their degradation through increased expression of tissue inhibitors of metalloproteases (TIMPs) leading to liver stiffness and gradual loss of function (22). This chronic liver damage can progress to different stages of fibrosis, cirrhosis and HCC over 5-30 years (20). Multiple host

factors including age, male sex, alcohol consumption and/or coinfection with HIV can accelerate progression to end-stage liver disease (23, 24).

HCV infection of hepatocytes triggers innate immune responses that are reviewed extensively elsewhere (25). Briefly, the cytosolic RIG-I-like receptor (RLR), retinoic acid-inducible gene-I (RIG-I), recognizes 5′-triphosphate double-stranded RNA (dsRNA) replicative intermediate and/or polyuridine (poly(U)) motifs within the HCV RNA. RIG-I then translocates to the mitochondria where it interacts with the mitochondrial antiviral-signaling protein (MAVS) to activate the downstream transcription factors IRF-3 and NF-κB, resulting in the induction of type I and type III interferons (IFNs) (25). HCV dsRNA is also sensed by the toll-like receptor 3 (TLR3) resulting in innate immune signaling through the adaptor molecule TRIF. HCV is able to evade innate immune responses by virtue of its NS3/4A protease that cleaves MAVS and inactivates its downstream signaling effect(s) (25) and by blocking the TLR3-mediated interferon signaling *via* NS4B-induced TRIF degradation (26). Finally, infected hepatocytes also shed exosomes carrying HCV RNA that are taken up by liver infiltrating plasmacytoid DCs (pDCs) that are then activated to produce type I and type III IFNs in the liver microenvironment (27). This IFN response is reflected as increased levels of interferon-induced genes (ISG), chemokines and inflammatory mediators in the liver thus activating liver resident inflammatory cells (28, 29). This response is also detectable in the peripheral blood. One notable ISG is CXCL-10 or interferon-gamma-inducible protein-10 (IP-10) that is elevated in plasma during acute HCV where high levels can predict failure to spontaneously resolve HCV (30). Levels of ISG induction correlate with single nucleotide polymorphisms in the IFN-lambda 3 (IFNλ3)/IFNλ4 region that are also associated with acute infection outcome [reviewed in (31)]. Following spontaneous resolution, ISG and inflammatory mediators return to normal levels but remain elevated in those who develop chronic infection (32). Natural killer (NK) cells are also activated during acute infection irrespective of infectious outcome and exhibit reduced production of cytokines and enhanced cytotoxic functions in chronic infection [reviewed in (33)].

A broad, polyfunctional and sustained virus-specific $CD4^+$ and $CD8^+$ T cell response is essential for spontaneous viral clearance [reviewed in (34)] where $CD127^+$ virus-specific memory T cells develop (35–38). The abrupt disappearance of HCV-specific $CD4^+$ helper T cell responses compromises $CD8^+$ T cell function(s) and facilitates emergence of viral escape mutants (39–42) resulting in chronic infection. In chronic HCV, $CD8^+$ T cells become exhausted and express different levels of exhaustion markers like programmed death-1 (PD-1), T cell immunoglobulin and mucin domain-containing protein 3 (Tim-3), and others [reviewed in (34, 43)], and lose effector functions (34). This is associated with downregulation of the transcription factor T-bet and different levels of expression of the nuclear factors T cell factor 1 (TCF1), Eomesodermin (Eomes), and thymocyte selection-associated high mobility group box protein (TOX) that distinguish different subsets of exhausted $CD8^+$ T cells (44–46). $TCF1^+CD127^+PD1^+$T-bet^{lo} HCV-specific $CD8^+$ T cells expressing both exhaustion and memory markers and of limited functionality were described in HCV chronically infected subjects and termed "memory-like" or "stem-like" T cells (47, 48). While PD-$1^{hi}Eomes^{hi}TOX^{hi}CD127^-$ were reported to be a terminally exhausted subset (49). Recent single cell RNA sequencing (scRNA-seq) analysis revealed that $TCF1^+CD127^+PD1^+$ memory-like cells are likely the progenitors of the PD-$1^{hi}Eomes^{hi}TOX^{hi}CD127^-$ terminally exhausted cells (49). Finally, escape mutations that occur in epitopes targeted by $CD8^+$ T cells influence their phenotype as they can no longer see their cognate antigen despite persistent viremia. $CD8^+$ T cells targeting epitopes that have escaped, express fewer exhaustion markers and revert to a memory phenotype where they express the memory marker CD127 and acquire transcriptomic and functional signatures that partly resemble memory $CD8^+$ T cells generated following spontaneous HCV clearance (50–52).

Increasing evidence suggest an important role for antibodies (Abs) against the HCV glycoproteins E1 and E2 in spontaneous clearance (53, 54). Development of neutralizing Abs (NAbs) is generally delayed during acute infection (55–57). Although Ab responses are short lived in resolvers (58), they appeared early during acute resolving infection(s) in some subjects following expansion of activated circulating T follicular helper cells (cTfh) expressing IL-21 that help expansion of HCV-specific B cells (59). Generation of NAbs correlated with spontaneous resolution in other studies (17, 60). Preincubation of virus inoculum with anti-HCV Abs or passive immunization resulted in reduced viral loads and/or sterilizing immunity in animal models (61–65). Broadly neutralizing Abs (bNAbs) neutralizing multiple HCV genotypes, blocked infection in humanized mice (66–68) and were isolated from spontaneous HCV resolvers (69) underscoring their protective role.

Spontaneous HCV clearance generates long-lived memory T cells with enhanced protective immunity upon reinfection (58, 70). Subsequent HCV reinfections are typically of lower viral loads, shorter viremia and higher clearance rate (80-50% *vs* 25%) (71–74). In contrast, correlates of long-term protective immunity upon repeated HCV exposures are not well understood. Depletion studies in chimpanzees underscored the essential and complementary protective roles of $CD4^+$ and $CD8^+$ memory T cells in preventing HCV persistence (42, 70). Protection in PWID was associated with increased magnitude, breadth and, polyfunctionality of HCV-specific memory T cells (71, 72) and NAbs (71). Altogether, these results suggest that long-term protective immunity against HCV is possible and effective and provide strong rationale for vaccine development.

Treatments for HCV

For nearly 30 years, interferon-based therapeutic regimens were the only option for treatment of chronic hepatitis C. These regimens were long (lasting nearly a year), had numerous side-effects, and were successful in only 50% of the treated individuals. Direct acting antivirals (DAA), targeting several key steps in the HCV replication cycle, have become increasingly available in

recent years (75). Currently approved DAA primarily target the NS3/4A protease, the NS5B polymerase and NS5A and are usually given in different combinations (76). DAA has substantially changed the management of chronic HCV, as HCV cure is achieved in >95% of cases (76). Nevertheless, DAA regimens are costly and access to diagnosis and treatment remains limited especially among the highest risk groups like PWID and MSM. Furthermore, DAA-mediated cure does not protect against HCV reinfection (77). Hence, the development of an effective prophylactic anti-HCV vaccine remains a priority to achieve HCV elimination.

HIV MONOINFECTION

Epidemiology

HIV-1 is transmitted by sexual contact across mucosal surfaces, by vertical transmission through maternal-infant exposure, and by percutaneous exposure (78). It is estimated that 37.9 million people are infected with HIV worldwide (79). HIV incidence continues to rise among PWID through sharing HIV-contaminated materials. In addition, unprotected sex is another important HIV risk factor among PWID, female sex workers, and MSM (80). HIV-infected PWID transmit HIV sexually to non-injectors, and through vertical transmission (81). Whereas overall, 10% of HIV-infected persons are coinfected with HCV, among PWID, HCV coinfection rates range from 50% to >90% (81). Other factors are associated with higher rates of HIV-1 acquisition such as high number of recent sexual partners, anal sex, concurrent sexually transmitted diseases, as well as the viral load and the clinical stage of the transmitting partner (82, 83). Access of PLWH to ART increased from 2.98 million in 2006 to 21.8 million in 2017 and was accompanied by a 51% reduction in HIV-associated mortality from 1.95 million in 2006 to 0.95 million in 2017. However, the annual incidence of new HIV infections decreased only by 17%. The combination of decreased mortality associated with ART implementation and only a small decrease in the incidence of new HIV infection has led to an overall important increase in the number of PLWH world-wide from 8.74 million in 1990 to 36.82 million in 2017 (84).

Viral Replication Cycle

HIV belongs to the genus Lentivirus within the Retroviridae family, with a virion containing two copies of positive single stranded RNA. The HIV genome of 9.2 Kb contains 9 genes encoding for multiple structural (*gag*, *pol*, *env*), regulatory (*tat*, *rev*), and accessory (*nef*, *vpr*, *vif*, *vpu*) proteins. The *env* gene encodes for the envelope glycoprotein gp160, that is further processed into gp120 and gp41. gp120 mediates HIV entry into target cells (*e.g.* $CD4^+$ T cells and macrophages) through interaction with the CD4 molecule, which is the main receptor for the virus (85), as well as the chemokine receptors CCR5 and/or CXCR4, which are the main HIV coreceptors (86, 87). The molecular tropism of HIV, dictated by the capacity of specific viral strains to use CCR5 and/or CXCR4 for entry led to classification of HIV into CCR5-tropic (R5), CXCR4-tropic (X4) or dual-tropic (R5/X4) strains (87). Once gp120 binds to CD4, the envelope undergoes conformational changes, exposing the chemokine receptor binding domains of gp120 and allowing its interaction with the coreceptors (88). This leads to further conformational changes allowing gp41 to expose its fusion peptide, which penetrates the cell membrane to deliver the viral capsid inside the target cells (89). The HIV reverse transcriptase (RT) encoded by the *pol* gene initiates the process of reverse transcription by copying the positive-sense single-stranded RNA genome into a complementary DNA (cDNA) (90). The cDNA and its complement form a double-stranded viral DNA, which is then integrated into the host cell's genome by the viral integrase (IN) encoded by the *pol* gene as well (91, 92). HIV integration is followed either by active viral transcription and production of new virion progeny or viral latency, with integrated proviral DNA persisting in many cells and tissues as latent HIV reservoirs (90, 93). The persistence of latent reservoirs despite viral-suppressive ART represents a major barrier to HIV cure (94, 95).

Natural History, Pathogenesis, and Immune Responses

The course of HIV infection includes three phases: acute, chronic, and Acquired Immunodeficiency Syndrome (AIDS) (96, 97). The acute HIV infection phase, between the time of HIV acquisition to seroconversion, can be further subdivided in four Fiebig stages (I-IV), based on the sequential detection of HIV RNA, proteins, and antibodies (98). The acute phase is associated with high levels of viremia and wide HIV dissemination into lymphoid organs (99), where the virus encounters its main targets: $CD4^+$ T cells, macrophages and dendritic cells (100–102). The concurrent HIV-specific immunity initiated during the acute phase is associated with a dramatic decline in viremia (96, 97). However, this immunity is inadequate to suppress viral replication completely, with HIV replication persisting in lymph nodes even when plasma viremia is undetectable (96, 99). After the acute phase, most patients have a period of viral latency, in which the viral genome is stably integrated in the host cell genome (96, 99). While CD4 counts normalize in the peripheral blood at the end of the acute phase, alterations in $CD4^+$ T cell homeostasis were documented in the gut-associated lymphoid tissue very early upon infection and persist during the chronic phase (96, 99, 103). These alterations are at the core of HIV pathogenesis, with a "leaky gut" being the source of microbial translocation, chronic immune activation, systemic inflammation and disease progression (104, 105). During the chronic phase, the state of viral latency is reversed upon activation of latently infected $CD4^+$ T cells upon interaction with their cognate pathogens leading to productive infection (93) and massive depletion of central memory $CD4^+$ T cells, which are the "self-renewing" source for tissue effector memory $CD4^+$ T cells (97). The HIV-dependent depletion of $CD4^+$ T cells is mediated through pyroptosis (106), apoptosis of uninfected bystander cells (107), and $CD8^+$ cytotoxic T cell killing (108). When $CD4^+$ T cell counts decline below the limit

of 200 cells/μl of blood (109), cell-mediated immunity is severely compromised, resulting in AIDS, a fatal complication characterized by life-threatening opportunistic infections and cancers (97).

In the absence of ART, the duration of the chronic phase is highly variable and can last for several years. While the majority of PLWH progress rapidly to AIDS, a minority remain immune competent (long-term non-progressors, LTNP) and a subset of those efficiently control HIV replication (elite controllers, EC) (110). LTNP are often asymptomatic for 10–20 years with $CD4^+$ T cell counts maintained within the normal range (>500 cells/μl) and plasma viral loads between 5,000 and 15,000 RNA copies/ml (111, 112). On the other hand, EC represent a small subset of the HIV-positive population (< 1%) who are able to control HIV viremia below the limit of detection in the absence of ART (113). Nevertheless, disease progression occurs as well in LTNP and EC, thus justifying the current recommendations of early ART initiation (114, 115). The natural control of HIV infection is achieved *via* multiple mechanisms including the expression of intrinsic restriction factors that limit HIV replication, the development of efficient cellular immune responses (116) in association with specific protective HLA class I alleles (117) and humoral immune responses. Furthermore, natural resistance to HIV acquisition was described in sex workers in Africa and represents a reference for studying correlates of HIV mucosal immunity (118). Finally, early treatment initiation renders a fraction of PLWH able to control HIV infection following treatment interruption (119), thus supporting the concept of "functional HIV cure" (120). However, about 10 to 40% of ART-treated individuals are immunological non-responders (INRs) (121, 122); these PLWH fail to reconstitute their $CD4^+$ T cell frequencies and functions despite controlled viremia under ART (123). This is due to the incapacity of ART to clear HIV reservoirs and diminish inflammation (124). This sub-group is at higher risk for developing AIDS and non-AIDs related morbidity and mortality (124–127).

HIV-specific $CD8^+$ T cells are also key determinants of the course of natural HIV infection. Almost all HIV infected individuals mount a strong virus-specific $CD8^+$ T cell response during the acute phase and the polyfunctionality of these $CD8^+$ T cells is key to long-term control of viremia and limiting disease progression [reviewed in (128)]. Many of the evasion mechanisms employed by HCV are also used by HIV including escape mutations in targeted epitopes and $CD8^+$ T cell exhaustion and are detailed elsewhere (128). High-dimensional functional and phenotypic analysis revealed phenotypic heterogeneity among HIV-specific $CD8^+$ T cells as well as common exhaustion signatures and pathways that are shared not only among chronic viral infections like HCV, HIV and LCMV but also in cancer (49, 129). These include increased expression of Eomes and TOX as key features of exhausted T cells associated with disease severity in HIV infection while $CD8^+$ T cells expressing lower levels of inhibitory receptors like PD-1 and higher levels of CD127, TCF1 and/or CXCR5 were associated with higher functionality, proliferation and better control of viral replication (129–131). Moreover, $CXCR5^+CD8^+$ T cells express less inhibitory receptors levels with higher cytotoxicity (132), which could contribute to improved control of viral reservoirs in lymph nodes particularly since lymphoid tissue resident memory $CD8^+$ T cells were shown to express higher levels of in CXCR5, compared with blood memory $CD8^+$ T cells (133) and that higher frequencies of follicular $CXCR5^+$ $CD8^+$ T cells correlated with lower rates of peripheral viremia (134).

HIV Treatment

ART transformed HIV infection into a manageable chronic disease (78). Multiple antiviral drugs are now available that target different steps of the HIV replication cycle including, in order of discovery, reverse transcription, protease-mediated virion maturation, entry, fusion, and integration (78). However, ART does not eradicate HIV and viral rebound occurs rapidly upon treatment interruption due to the persistence of latent HIV reservoirs in long-lived memory $CD4^+$ T cells (94). To date, HIV cure was achieved in only two people who received bone marrow transplantation to treat cancer using donor cells carrying the delta 32 mutation in the *ccr5* gene (CCR5δ32/δ32) (135), a mutation known to confer resistance to CCR5-tropic HIV infection (86).

ART is also important as a preventative measure. Early initiation of ART reduces sexual transmission of HIV-1 (136), particularly in genetically linked HIV-1 infections among serodiscordant couples (137). Pre-exposure prophylaxis (PrEP) using daily oral doses of the combined nucleoside reverse transcriptase inhibitors, tenofovir and emtricitabine, conferred higher protection against HIV than placebo in controlled trials (138–140). Furthermore, an injectable, long-acting integrase inhibitor, cabotegravir, is safe and well-tolerated and two large efficacy trials are underway in uninfected high-risk individuals (140, 141). In the past ten years, broadly neutralizing antibodies (bNAbs) targeting different HIV-1 envelope epitopes isolated from PLWH with slow disease progression were engineered (142, 143) and are currently being tested for both efficacy and safety as a potential alternative or adjuvant for ART (144).

HCV/HIV CO-INFECTION

Epidemiology

Approximately 6.2% of PLWH are also co-infected with HCV. The odds of HCV infection are six times higher in PLWH than in the HIV-negative population, with the highest prevalence among PWID and MSM, consistent with shared routes of transmission (7). Although parenteral transmission remains the principal route of HCV transmission in PWID (7), sexual transmission of HCV occurs among HIV-positive MSM (3, 145, 146).

Natural History, Pathogenesis, and Immune Responses

Multiple factors shape the natural history of coinfection including genotype/subgroup of both viruses, host factors and socioeconomic factors including access to screening and treatment services (147). As reviewed above, virus-specific

$CD8^+$ T cell responses are essential for spontaneous resolution of acute HCV infection. The magnitude, breadth and polyfunctionality of the HCV-specific $CD8^+$ T cells are key determinants of infectious outcome. These functions are dependent on $CD4^+$ T cell help (34), and virus persistence during acute HCV is temporally associated with abrupt loss and/or dysfunction of virus-specific $CD4^+$ helper T cells (148). As demonstrated in $CD4^+$ T cell depletion studies in the chimpanzee model of HCV, loss of $CD4^+$ T cells function was associated with decline in frequency of virus-specific $CD8^+$ T cells and their cytokine production resulting in accumulation of escape mutations in the targeted CD8 epitopes with impairment of HCV-specific immune responses (42). $CD4^+$ helper T cells are also essential for optimal B cell function and production of neutralizing antibodies. Specifically, antigen-specific B cell affinity maturation, isotype class switching and differentiation into antibody-secreting plasma cells in germinal centers are regulated by direct contact with $CD4^+$ Tfh cells (59, 149).

Given the central role of $CD4^+$ T cells in coordinating antiviral immune responses, it is not surprising that the immune response to HCV in the context of an HCV/HIV coinfection is compromised. HIV infection impairs the immune response to HCV, including in people who have cleared HCV infection (150). HIV-1-infected individuals with spontaneous control of HCV remain at significant risk for a second episode of HCV viremia (150). The breadth and magnitude of HCV-specific $CD8^+$ T cells correlated with $CD4^+$ T cell count (151). Similarly, coinfection and $CD4^+$ T-cell counts $<350/mm^3$ was associated with a global decline in the anti-HCV envelope antibody response, including binding antibody titers, NAb titers, and NAb breadth (152). These immunological factors are the likely cause of the observed lower rate of spontaneous clearance of acute HCV in HIV coinfected subjects (5-10%), as compared to HCV monoinfection (20-30%) (153), especially in patients with low $CD4^+$ T cell counts (154, 155). Furthermore, the overall reduction in $CD4^+$ T cells, microbial translocation, and systemic immune activation have deleterious effects on the liver with accelerated progression of liver fibrosis, early onset of cirrhosis and HCC, as compared to monoinfection (8)(discussed in the next section).

LIVER DISEASE IN HCV/HIV COINFECTED INDIVIDUALS

HCV/HIV co-infected individuals are at a higher risk of progressive liver disease, with accelerated progression to liver cirrhosis and higher rates of HCC, even when HIV is controlled by ART (24, 155, 156). HIV coinfection accelerates HCV-mediated fibrosis through both direct and indirect mechanisms that will be discussed in this section and are summarized in **Figure 1**.

Direct Effect of HIV on Liver Disease Progression

HIV gp120 interacts with CXCR4 and CCR5 on the surface of hepatocytes and HSCs, respectively (157, 175). This interaction activates HSCs and promotes ROS accumulation through an NF-κB-dependent mechanism, resulting in enhancement of the fibrogenic process (158, 159). Co-culture experiments in the presence of HCV, HIV or both HIV and HCV demonstrated an additive effect of HIV on the profibrogenic program in hepatocyte and HSC lines through ROS, NF-κB, and TGF-β1 up-regulation; resulting in increased expression of the extracellular matrix protein collagen I, and TIMP1 (176).

It was also reported that HIV can infect HSCs in a CD4/chemokine coreceptor-independent manner. HIV infection promoted HSC collagen I expression and secretion of the proinflammatory chemokine monocyte chemoattractant protein-1 (MCP-1) (162). HIV was also shown to infect Kupffer cells, the liver resident macrophages that orchestrates the intrahepatic inflammatory response. Kupffer cells express the HIV receptor CD4 and both coreceptors CCR5 and CXCR4 [reviewed in (163)]. In vitro infection of Kupffer cells by HIV led to their sensitization to lipopolysaccharide (LPS) treatment by increasing cell surface expression of CD14 and TLR4, resulting in increased secretion of TNF-α and IL-6. This effect was maintained even after suppression of HIV replication using antiretroviral drugs (164). Activation of macrophages/Kupffer cells is mirrored by increased levels of the soluble macrophage activation marker CD163 in serum of HIV/HCV coinfected subjects accompanied by periportal $CD163^+$ macrophage accumulation during fibrosis progression but not in established cirrhosis suggesting that soluble CD163 is probably a marker of active fibrogenesis rather than accumulated fibrosis (165).

HIV also enhances apoptosis of hepatocytes, another accelerator of the fibrogenic process. This effect is mediated by TNF–related apoptosis-inducing ligand (TRAIL) signaling and upregulation of TRAIL receptor 1 (DR4), and 2 (DR5) (160). The TRAIL-dependent hepatocyte apoptosis in HCV infected individuals is aggravated by HIV coinfection (161). In addition, HIV gp120 and HCV-E2 protein, can collaboratively elicit hepatocyte apoptosis *in vitro* through upregulation of Fas ligand expression and dephosphorylation of the anti-apoptotic molecule AKT (161, 177).

Indirect Effect of HIV on Liver Disease Progression

The principal mechanism through which HIV indirectly accelerates liver disease progression is increased microbial translocation. HIV infection induces severe depletion of the gastrointestinal lymphoid tissue, impairing the gastrointenstinal tract epithelial integrity and allowing bacterial LPS to translocate from the gut to the systemic circulation and through the liver (105). LPS binds to TLR4 on the surface of quiescent HSCs, leading to upregulated chemokine secretion and chemotaxis of Kupffer cells. Concurrently, this interaction induces downregulation of the TGF-β pseudoreceptor Bambi to sensitize HSCs to TGF-β-induced signals from Kupffer cells (166). Activation of HSCs is further aggravated by HIV-mediated depletion of Kupffer cells that are responsible for LPS phagocytosis (163, 178).

Elevated levels of microbial translocation markers (e.g. LPS, LPS binding protein, soluble CD14) were reported in HCV-

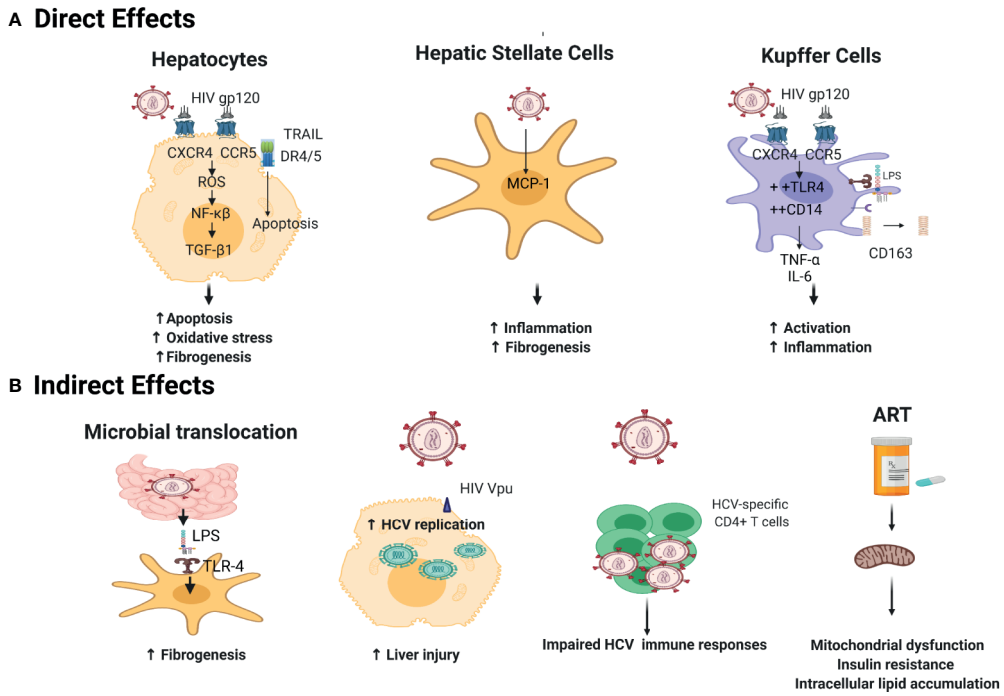

FIGURE 1 | Mechanisms underlying acceleration of liver disease progression by HIV in HCV/HIV coinfection. **(A)** Direct Mechanisms: gp120 binds to HIV coreceptors (CXCR4 and CCR5) on hepatocytes surface (157) leading to accumulation of ROS which triggers an NF-κβ mediated oxidative stress (158, 159). HIV also activates TNF–related apoptosis-inducing ligand (TRAIL)-mediated apoptosis *via* upregulation of TRAIL receptor 1 (DR4), and 2 (DR5) (160), aggravating HCV fibrotic complications (161). HIV promotes hepatic stellate cells (HSC) collagen I expression and secretion of the proinflammatory cytokine monocyte chemoattractant protein-1 (MCP-1) inducing inflammation and fibrogenesis (162). HIV sensitizes Kupffer cells to lipopolysaccharide (LPS) *via* gp120 binding to CXCR4 and CCR5 (163) increasing cell surface expression of CD14 and TLR4, resulting in increased secretion of TNF-α and IL-6 (164). This is accompanied by shedding of CD163 in serum (165). **(B)** Indirect Mechanisms: HIV indirectly augments fibrosis mainly by microbial translocation: LPS translocate through impaired gut epithelium (105) and binds to Toll-like receptor 4 TLR4 on HSCs, leading to upregulated chemokine secretion and Kupffer cells chemotaxis (166). HIV accessory proteins Vpr (167) and Nef (168) enhance HCV RNA replication creating a state of inflammation and tissue damage. HIV causes functional alterations of HCV-specific immune responses with more HCV replication and hepatic inflammation (150, 169). ART elicits insulin resistance by altering mitochondrial function (170, 171) and increased intracellular lipid accumulation (172, 173) leading to enhanced development of liver fibrosis (174). Created with Biorender.com.

infected subjects upon HIV acquisition and compared to HIV uninfected subjects (179). In addition, decreased levels of endotoxin-core antibodies (EndoCAb IgM) and increased levels of IgG, specific for a heterophilic (alpha-galactose) epitope, which has previously been associated with stage of liver disease (180), were observed in HIV-infected compared to uninfected subjects (179). All these measures were strongly associated with HCV-related liver disease progression to cirrhosis (179).

Other indirect mechanisms include the enhancement of HCV RNA replication *via* the HIV accessory proteins Vpr (167) and Nef (168); the accumulation in the liver of HIV-specific $CD8^+$ T cells creating a state of inflammation and tissue damage in co-infected patients (181, 182); and functional alterations of HCV-specific immune responses in the presence of HIV coinfection (150, 169). Also, the CD4/CD8 functional imbalance seen during HIV infection modifies the hepatic cytokine milieu, in favor of a profibrotic state in the liver (155, 183). Finally, HIV induces upregulation of the Triggering Receptor Expressed on Myeloid cells 1 (TREM1) on Kupffer cells and induces extracellular signal-regulated protein kinases 1 and 2 (ERK1/2) cascade leading to increased macrophage inflammatory response (184).

The effect of ART on liver injury in co-infected patients is controversial. Early studies suggested that nucleoside reverse transcriptase inhibitors (NRTIs) and protease inhibitors may affect mitochondrial function leading to increased insulin resistance (170, 171), and development of liver fibrosis (174). This effect is mainly mediated by polymerase-gamma suppression, a DNA polymerase necessary for mitochondrial DNA replication (185). Another proposed mechanism for ART-induced mitochondrial insufficiency is the inhibition of mitochondrial adenylate kinase and adenosine nucleotide translocator (186, 187). Studies using hepatocyte cell lines have demonstrated that non-nucleoside reverse transcriptase inhibitors (NNRTIs) can interfere with mitochondrial function leading to increase intracellular lipid accumulation which can further enhance liver damage (172, 173). In contrast, other reports suggested that ART enhances HCV-specific T cell responses with a significant decline in HCV-RNA levels (188) and reduction in the rate of hepatic decompensation events and

liver fibrosis (189, 190). Additional studies are needed to evaluate the effect new regimens of ART on liver functions.

EFFECT OF HCV INFECTION ON HIV DISEASE PROGRESSION

HCV infection impacts the natural history of HIV with increased risk of developing AIDS defining illness like HIV-related bacterial and mycotic infections in coinfected subjects (191). HCV likely contributes to increased immune activation in chronic HCV/HIV coinfection resulting in impaired immune responses and rapid progression to AIDS (192). The different effects of HCV on HIV disease progression are presented in this section and summarized in **Table 1**.

Impact of HCV on CD4$^+$ and CD8$^+$ T Cells

HCV seroconversion of HIV-infected subjects is associated with reduced CD4$^+$ T cell counts during the first few years and their reduced recovery after ART (204, 205). This deficit could be attributed to the nature of the liver as a lymphoid organ essential for maintaining T cell homeostasis, where hepatic inflammation induced by HCV infection leads to altered T cell homeostasis (193). Similarly, persistent liver inflammation may contribute to enhanced immune activation and generalized exhaustion of CD8$^+$ T cells with the upregulation of various exhaustion molecule like PD-1, Tim-3 and CD39 on total and virus-specific CD8$^+$ T cells (195–197).

Modulation of HIV Replication by HCV

HCV proteins may modulate HIV replication through multiple mechanisms [reviewed in (206)]. The HCV non-structural protein NS3/4A can activate HIV transcription through its LTR by enhancing DNA binding of the transcription factor AP-1 (199). The NS3/4A effect on HIV transcription was facilitated by the HIV protein Vpu, which mediates ubiquitination and subsequent degradation of NS4A allowing the destabilization of the NS3/4A complex and the nuclear translocation of NS3 (200). Other studies demonstrated that both, HCV core protein and HIV Nef can bind directly to the tumor necrosis factor receptor-associated factor (TRAF) 2, TRAF5, and TRAF6 and initiate the NF-κB signaling cascade thus enhancing HIV replication in monocyte-derived macrophages (201). Another *in vitro* study demonstrated that HCV core potentiates HIV-1 replication in macrophages *via* upregulation of TNF-α and IL-6 *via* TLR2, JNK, and MEK1/2-dependent pathways. Furthermore, TNF-α and IL-6 secreted from HCV core-treated macrophages reactivated pro-viral HIV-1 DNA in the latently infected monocytic U1 cell lines (207). In contrast, another study, using the HepG2 hepatocyte cell line, demonstrated that Tat-induced LTR activation was suppressed by HCV core protein restricting HIV-1 transcription and replication. This core mediated LTR inhibition was unchanged when NS3/4A protein was added to the culture. However, LTR activation and gene transcription were enhanced by infectious HCV virions suggesting the involvement of other viral or cellular proteins in this process (208).

HIV Reservoirs in HCV Coinfected Subjects

Few studies to date explored the effect of HCV coinfection on the HIV reservoir size (7). A recent study has demonstrated a larger HIV reservoir size in resting CD4$^+$ T cells in ART-treated HCV/HIV coinfected individuals with chronic HCV or who have spontaneously resolved HCV as compared to HIV mono-infected subjects (209). This increased HIV reservoir size represents a major obstacle to HIV elimination in those co-infected subjects and can be explained by several theories. First, increased immune activation during HCV coinfection, where persistently activated HCV-specific and non-specific CD4$^+$ T-

TABLE 1 | Impact of HCV on HIV disease progression.

HCV-mediated immunological and virological alterations in PLWH	Proposed Mechanism	Effect/Reversal upon DAA treatment
Compromised restoration of CD4$^+$ T cell frequency during ART	HCV induced hepatic inflammation and immune activation lead to altered T cell homeostasis (193)	Partial restoration of T cell compartment and memory profile (194)
Deterioration of CD8$^+$ T cell function	Persistent liver inflammation contributes to generalized exhaustion of CD8$^+$ T cells with upregulation of exhaustion molecules like PD-1, Tim-3 and CD39 on total and virus-specific CD8$^+$ T cells (195–197)	Partial reversal of CD8$^+$ T cell exhaustion (49, 198)
Augmentation of HIV replication.	NS3/4A: activates binding of AP-1 to LTR, facilitated by Vpu leading to increased HIV RNA reverse transcription into cDNA to be integrated in the host genome (199, 200).	Unknown
	Core protein: binds to TRAF2, TRAF5 and TRAF6, aided by Nef, initiating NFKB cascade ending in LTR stimulation (201).	Unknown
Higher HIV reservoirs size during ART	Immune activation: immune activated CD4$^+$ T cells provide targets for seeding of HIV reservoir (202)	Partial reversal of hepatic inflammation (11)
	Impaired HIV-specific cell mediated immunity responsible for clearance of HIV infected cells with high frequency of T-regs and IL-10 (203)	Unknown
	Permissiveness of HCV specific CD4$^+$ T cells to HIV infection (unproven)	Unknown
Increased risk of developing AIDS defining conditions	Increased immune activation in chronic HCV/HIV co-infection resulting in impaired immune responses (191, 192)	Unknown

cells provide new targets for HIV infection and latency, as previously observed with herpesviruses (202). This T cell activation may facilitate *de novo* infection, especially since the concentrations of antiretroviral drugs reaching lymphoid tissues are low (210). Another theory is the possibility that impaired HIV-specific cell-mediated immunity, responsible for clearance of HIV-infected cells, contributes to HIV reservoir persistence. This immune suppression may be a consequence of chronic HCV coinfection where higher frequencies of peripheral regulatory T cells (Tregs) and IL-10 producing cells were detected as compared to HIV monoinfected subjects (203). Finally, whether HCV-specific $CD4^+$ T cells represent HIV infection targets and sites of HIV reservoir persistence remains to be investigated. Previous studies reveled that in addition to HIV-specific $CD4^+$ T cells (211), increased HIV infection occurs in mycobacterium tuberculosis (MTb)-specific $CD4^+$ T cells, while cytomegalovirus (CMV)-specific $CD4^+$ T cells showed impaired permissiveness to HIV (212). Recently, several groups characterized the antigenic specificity of $CD4^+$ T cells carrying HIV reservoirs, in an effort to therapeutically prevent HIV reservoir seeding in pathogen-specific cells or to target their specific elimination in HIV cure strategies (213, 214). We have recently demonstrated that integrative HIV infection in *Staphylococcus aureus*-reactive $CD4^+$ T cells can be promoted by DCs in a retinoic acid-dependent manner (215) and the liver is an organ rich in retinoic acid (216). The liver is also an organ rich in Th7 cells (217), a subset of $CD4^+$ T cells transcriptionally programmed to be HIV infection targets (218), with a considerable fraction of HCV-specific $CD4^+$ T cells bearing the phenotypic and functional characteristics of Th17 cells (219). Therefore, it is tempting to speculate that HIV infection and viral reservoir persistence in HCV-specific $CD4^+$ T cells may explain differences observed between HIV monoinfected and HIV/HCV coinfected individuals in terms of HIV reservoir size. The clonal expansion of HIV infected memory $CD4^+$ T cells is a well-known mechanism, by which HIV latent reservoir is maintained and expanded (214, 220). A similar mechanism may be at play during concomitant HCV infection, potentially conferring preferential susceptibility of HCV-specific $CD4^+$ T cells to HIV infection and reservoir expansion.

EFFECT OF DAA-MEDIATED CURE OF HCV IN COINFECTED SUBJECTS

Before the DAA era, HCV treatment and cure in HCV/HIV coinfected subjects was a complex problem since long IFN-based therapeutic regimens had multiple side effects and the rate of sustained viral response (SVR) was much lower than in monoinfected subjects. IFN-free DAA regimens that are widely available now have been a major game changer given their relative short treatment duration, reduced side effects and a response rate of >95%. In the context of HIV/HCV coinfection however, early studies suggested a lower SVR rate to DAA (86.3%) as compared to monoinfection (94.9%) (221). Nevertheless, most recent studies reported response rates to DAA in HIV/HCV coinfection as comparable to those in HCV-monoinfected individuals (222). Predictors of failure to achieve SVR under DAA in coinfected individuals are not different from those observed in monoinfected people and include sex, immune status, HCV RNA load, severity of liver disease, and the use of suboptimal DAA-based regimens (129). Given these promising results, HCV/HIV coinfected subjects are no longer considered difficult to reach an HCV cure. Nevertheless, specific consideration should be given to negative predictors of SVR and barriers to treatment that may be more common in the coinfected population (223). Data from several cohorts have identified a clear benefit of HCV cure in limiting liver disease progression and reducing the risk of developing HCC in PLWH, especially if they are treated at an early fibrosis stage (224, 225). In this section, we will discuss the impact of DAA-mediated cure of HCV on liver disease progression, immune reconstitution and the HIV reservoir in coinfected subjects. These points are also summarized in **Table 1**.

Immune Reconstitution in HCV/HIV Coinfected Subjects Following DAA

DAA-mediated cure of HCV induces rapid decrease in serum levels of sCD163, a marker of inflammatory macrophage activity, and is associated with reduced histological inflammation in the liver (226). DAA therapy was also accompanied by a rapid decline in ISG expression in the liver and peripheral blood (227). Multianalyte profiling of 50 plasma proteins pre- and post DAA-mediated clearance in a cohort of 28 subjects with chronic HCV infection, including two HIV coinfected subjects, demonstrated that the elevated plasma cytokines and chemokines improve but do not completely normalize up to 8 months post cure (228). Interestingly, CXCL10/IP-10, an IFN induced chemokine, is usually elevated during chronic HCV infection and it rapidly decreased upon starting DAA therapy in line with reduced IFN-α signaling in the liver (228, 229). This was also associated with the normalization of NK cell phenotype and function (cytotoxicity and cytokine expression) (229)

The analysis of peripheral blood lymphocytes early during DAA therapy reported an increase in total $CD4^+$ and $CD8^+$ T cells but not NK cells or monocytes (230). At the same time, a reduction in activated ($HLA\text{-}DR^+$ and $CD38^+$) $CD4^+$ and $CD8^+$ T cells was observed in both monoinfected and coinfected subjects (230), with this effect being sustained up to one year post-SVR (231). Furthermore, there was an increase in the frequency of T cells expressing CXCR3, the CXCL10/IP-10 receptor (230), indicative of T cell redistribution in the periphery upon DAA treatment. Indeed, a reduction in liver inflammation may theoretically cause an efflux of lymphocytes from the liver and draining lymph nodes in the peripheral blood.

In HCV monoinfection, DAA treatment was associated with restoration of the proliferative capacity of HCV-specific $CD8^+$ T cells (198). However, selective maintenance of $TCF1^+CD127^+PD1^+$ memory like HCV-specific $CD8^+$ T cells was observed following cessation of therapy (47), as well as a limited impact of DAA on the functional and mitochondrial impairment of HCV-specific $CD8^+$ T cell responses (232).

In contrast, Barili et al. reported partial improvement of the mitochondrial metabolic functions of HCV-specific $CD8^+$ T cells following DAA treatment (233). However, they used *in vitro* stimulated PBMCs which may have affected mitochondrial function (233). Bulk RNA-seq and scRNA-seq analysis of HCV-specific $CD8^+$ T cells identified an antigen-dependent core exhaustion signature, with memory-like $CD8^+$ T cells targeting variant epitopes exhibiting a less pronounced exhaustion signature (49, 52). HCV-specific memory-like T cells harbored the same transcriptomic signatures before and after DAA treatment suggesting a permanent "exhaustion scar" that could not be reversed by DAA-mediated HCV cure (49). Only one study examined HCV-specific $CD4^+$ T cells in subjects undergoing DAA treatment. In this study, the frequency of HCV-specific $CD4^+$ T cells increased 2 weeks after starting DAA, with downregulation of the exhaustion and activation markers (CD38, CD39, ICOS, OX40 and PD-1) and upregulation of the memory-T cell markers (CD127 and CCR7) without complete normalization (234). As with total $CD4^+$ T cells, this transient increase in HCV-specific $CD4^+$ T cells early after starting DAA therapy is likely due to decreased liver inflammation and emigration of HCV-specific $CD4^+$ T cells from the liver. It is noteworthy that HCV-specific $CD4^+$ T cells with a Tfh phenotype and transcriptional signature were preferentially maintained following DAA-mediated HCV cure (234).

Conflicting results were reported in the setting of DAA therapy in HCV/HIV coinfection. One study reported a reduction in total activated ($HLA\text{-}DR^+$ and $CD38^+$) $CD4^+$ and $CD8^+$ T cells up to one year post-SVR (231). Another study did not observe any change in T cell activation at 12 weeks after DAA compared to baseline (235) but observed an increase in the frequency of total $CD4^+$ and $CD8^+$ T cells producing IFN-γ, IL-17, and IL-22 (235).

The frequency of $Foxp3^+CD25^+CD4^+$ Tregs is usually elevated in chronic HCV infection and contribute to the immune suppressive and anti-inflammatory immune response in the liver. However, DAA-mediated clearance of HCV does not completely normalize frequency of Tregs in neither monoinfected (236) nor coinfected subjects (237). Similarly, the frequency of $HLA\text{-}DR^-CD33^+$ $CD11b^+$ myeloid-derived suppressor cells (MDSC) are expanded in HCV monoinfected (238) and coinfected subjects (237). MDSC play a crucial role in immune suppression *via* production of arginase-1, inducible NOS, TGF-β and IL-10 that inhibit T cell functions (239). The frequency of MDSC remains elevated post-DAA therapy in HCV/HIV co-infected subjects and may contribute to generalized immune suppression (237).

In summary, studies examining DAA-mediated cure of HCV, mostly in monoinfected subjects, suggest only partial reconstitution of immune functions and persistence of immune suppressive cells like Tregs and MDSC. This immune suppressive environment may contribute to reduced immune response to vaccinations, limited immune surveillance against cancer, and increased reactivation of latent or occult infections of herpesviruses and hepatitis B virus, respectively (240, 241). Finally, this incomplete reconstitution of HCV-specific $CD4^+$ and $CD8^+$ T cells may increase the risk of HCV persistence upon re-exposure and reinfection in high-risk populations like PWID and MSM. Additional studies examining immune reconstitution post DAA-mediated cure in HCV/HIV coinfected subjects are warranted.

Liver Disease in HCV/HIV Coinfected Subjects Post DAA-Mediated Cure

As discussed above, DAA-mediated cure of HCV causes an improvement in liver fibrosis markers in both HCV monoinfected and HCV/HIV coinfected subjects (225, 242, 243). Furthermore, recent cohort studies suggest that HCV/HIV coinfected subjects with cirrhosis are no longer at higher risk for developing HCC or end-stage liver disease as compared to HCV monoinfection (225). However, the risk of developing HCC is not completely eliminated upon HCV cure and remains high in subjects with advanced fibrosis or cirrhosis pointing to an irreversible liver damage. Molecular studies using HCV-infected hepatocytes, as well as studies using liver biopsy samples from infected patients, have revealed that chronic HCV infection induces epigenetic and gene expression alterations associated with risk for HCC, alterations that persist after HCV cure (244, 245).

Other factors may contribute to continued risk of developing end-stage liver disease and HCC in HCV/HIV coinfected subjects. First, metabolic abnormalities including insulin resistance are quite common in HIV-infected individuals and result in hepatic steatosis with accumulation of triglycerides in hepatocytes, and can accelerate liver damage and increase risk of developing HCC irrespective of HCV status [reviewed in (246)]. Second, gut dysbiosis and intestinal damage are hallmarks of HIV infection that are not restored by ART [reviewed in (247)]. Considering the fact that DAA-mediated HCV clearance does not impact gut dysbiosis in cirrhotic HCV-monoinfected subjects (248), dysbiosis is highly likely to remain a prominent risk of liver damage in the context of HCV/HIV coinfection after DAA-mediated cure. Thus, new therapeutic interventions may be needed to normalize the metabolic status and restore intestinal health in DAA-treated HCV/HIV coinfected subjects.

Impact of DAA Treatment on HIV Reservoir

The HIV reservoir levels have been intensively studied in ART-treated HIV infected subjects (249, 250), but little is known about HIV persistence in the context of HIV/HCV coinfection, especially following DAA treatment. A study performed on PBMCs revealed that DAA-mediated HCV clearance did not induce a decrease in HIV reservoirs but rather an increase in integrated HIV-DNA levels, mainly in patients with low versus undetectable levels of HIV viremia before DAA (251). Similarly, Rozera et al. observed a significant rise in HIV-DNA levels in the peripheral blood of some successfully ART-treated HIV/HCV co-infected patients at the end of DAA treatment, which correlated with lower cellular HIV reservoir at baseline (10). Most recently, a study of 97 ART-treated subjects reported that

HCV/HIV coinfected subjects with chronic HCV infection, as well as HCV/HIV coinfected subjects who have spontaneously cleared HCV, showed higher levels of HIV-DNA in resting $CD4^+$ T cells ($CD25^-CD69^-HLADR^-$) compared to HIV monoinfected individuals (209). This increase in HIV reservoir size following DAA therapy may be explained by the mobilization of cells carrying HIV reservoirs from lymph nodes, liver and other tissues into the peripheral blood in response to DAA-mediated reduction of HCV-elicited immune activation and hepatic inflammation (10, 252). This is mirrored by the rapid decline of CXCL10 levels in response to DAA therapy, similar to plasma HCV RNA levels (253). In contrast, a new study demonstrated that although all three forms of HIV DNA (total, integrated, and episomal) remained stable during DAA treatment, cell-associated unspliced HIV-RNA levels (giving rise to the progeny virions) were significantly increased 12 months after the end of DAA therapy, suggesting an increased HIV transcriptional activity in reservoir cells (11). This may be explained by a decrease in IFN-mediated antiviral immunity as reflected by the observed reduction in ISG signals (227) and normalization of the expression levels of IFN-β, IFI44, and CXCL10 in the peripheral blood following DAA therapy (254). In addition, as reported by Meissner et al, liver biopsies from patients who achieved SVR showed that HCV cure was accompanied by decreased expression of type II and III IFNs, but higher expression of type I IFNs compared to pre-treatment baseline (227). Recently, diverse and opposing effects of the type I IFNα on HIV latency were described. IFNα inhibits the establishment of latency. However, once latency is established, IFNα is able to reverse it through binding to its receptor on $CD4^+$ T cells and triggering phosphorylation of STAT1, 3, and 5 proteins (255). It is well-established that STAT5 can activate HIV transcription *via* its binding to the HIV long terminal repeat (256).

Altogether, the limited data available so far suggest that the HIV reservoirs are higher in HCV/HIV coinfected compared to HIV monoinfected subjects and that DAA-mediated HCV cure does not reduce HIV persistence. However, several limitations prevent the generalization of these findings because some studies used purified memory $CD4^+$ T cells while others used total PBMCs to quantify HIV DNA (10, 11). Another issue is the extensive use of PCR-based techniques to assess the integrated HIV-DNA. These techniques tend to overestimate the size of the reservoir due to the high prevalence of defective proviruses (257). Other confounding factors include the pre-ART HIV viral load, host genetic factors and liver condition. Additional studies with well-defined cohorts and extended follow-up after DAA-mediated cure of HCV are essential to accurately evaluate the long-term effects of DAA therapy on the HIV reservoir.

CONCLUSION

Since the discovery of HIV and HCV, tremendous advances were made in understanding the molecular steps of the viral replication cycle, natural infection, pathogenesis and immune responses. Studies also documented mechanisms by which HCV and HIV reciprocally influence their pathogenesis, thus leading to exacerbated alterations of immune competence as a consequence of impaired liver functions and altered intestinal barrier integrity. Despite the absence of efficient vaccines, DAA currently cures HCV infection, while ART controls viral replication at undetectable levels, thus improving the life quality of co-infected individuals. However, DAA treatment does not completely normalize immune and liver functions. Also, ART does not eradicate HIV reservoirs, which persist in long lived memory $CD4^+$ T cells with various antigenic specificities, potentially including HCV-specific $CD4^+$ T cells.

FUTURE DIRECTIONS

New longitudinal studies should address the effect of DAA on HIV reservoir persistence in ART-treated HCV/HIV coinfected individuals in relation to age, sex, metabolic status, liver damage, drug and alcohol use, and other comorbidities. Given the fact that the pool of HCV-specific $CD4^+$ T cells contracts but still persists upon DAA, studies are also needed to evaluate whether these cells contribute to the pool of latent HIV reservoirs in ART-treated individuals and whether HCV re-exposure and/or reinfection in high-risk groups may promote HIV reservoir expansion. Finally, additional therapeutic interventions may be needed to restore immune competence and control residual HIV transcription in ART-treated individuals after DAA-mediated HCV cure.

AUTHOR CONTRIBUTIONS

SG reviewed the literature and wrote the first draft. PA and NS reviewed the literature, revised the first draft, and modified the manuscript. All authors contributed to the article and approved the submitted version.

FUNDING

Our research is funded through grants from the Canadian Institutes of Health Research CIHR (PJT-173467 (to NS), HOP-120239 and PJT-153052 (to PA)), the National Institutes of Health (NIH) (U01AI131313, R01AI136533 and U19AI159819 to NS), the Canadian HIV Cure Enterprise Team Grant (CanCURE 1.0) funded by CIHR in partnership with the Canadian Foundation for AIDS Research (CANFAR) and the International AIDS Society (IAS) (CanCURE 1.0; HIG-133050), and the CanCURE 2.0 Team Grant funded by CIHR (HB2-164064) to PA. SG is supported by a doctoral fellowship from the Canadian Network on Hepatitis C (CanHepC). CanHepC is funded by a joint initiative of the CIHR (NHC142832) and the Public Health Agency of Canada.

REFERENCES

1. Coutinho RA. HIV and Hepatitis C Among Injecting Drug Users. *BMJ (Clin Res Ed)* (1998) 317:424–5. doi: 10.1136/bmj.317.7156.424
2. Hagan H, Jordan AE, Neurer J, Cleland CM. Incidence of Sexually Transmitted Hepatitis C Virus Infection in HIV-Positive Men Who Have Sex With Men. *Aids* (2015) 29:2335–45. doi: 10.1097/QAD.0000000000000834
3. Nijmeijer BM, Koopsen J, Schinkel J, Prins M, Geijtenbeek TB. Sexually Transmitted Hepatitis C Virus Infections: Current Trends, and Recent Advances in Understanding the Spread in Men Who Have Sex With Men. *J Int AIDS Soc* (2019) 22:e25348–8. doi: 10.1002/jia2.25348
4. Thomas DL, Villano SA, Riester KA, Hershow R, Mofenson LM, Landesman SH, et al. Perinatal Transmission of Hepatitis C Virus From Human Immunodeficiency Virus Type 1-Infected Mothers. *Women Infants Transm Study J Infect Dis* (1998) 177:1480–8. doi: 10.1086/515315
5. Ferrero S, Lungaro P, Bruzzone BM, Gotta C, Bentivoglio G, Ragni N. Prospective Study of Mother-to-Infant Transmission of Hepatitis C Virus: A 10-Year Survey (1990-2000). *Acta Obstet Gynecol Scand* (2003) 82:229–34. doi: 10.1034/j.1600-0412.2003.00107.x
6. Lemoine M, Nayagam S, Thursz M. Viral Hepatitis in Resource-Limited Countries and Access to Antiviral Therapies: Current and Future Challenges. *Future Virol* (2013) 8:371–80. doi: 10.2217/fvl.13.11
7. Platt L, Easterbrook P, Gower E, McDonald B, Sabin K, McGowan C, et al. Prevalence and Burden of HCV Co-Infection in People Living With HIV: A Global Systematic Review and Meta-Analysis. *Lancet Infect Dis* (2016) 16:797–808. doi: 10.1016/S1473-3099(15)00485-5
8. Chen JY, Feeney ER, Chung RT. HCV and HIV Co-Infection: Mechanisms and Management. *Nat Rev Gastroenterol Hepatol* (2014) 11:362–71. doi: 10.1038/nrgastro.2014.17
9. Chew KW, Bhattacharya D. Virologic and Immunologic Aspects of HIV-Hepatitis C Virus Coinfection. *AIDS (Lond Engl)* (2016) 30:2395–404. doi: 10.1097/QAD.0000000000001203
10. Rozera G, Fabbri G, Lorenzini P, Mastrorosa I, Timelli L, Zaccarelli M, et al. Peripheral Blood HIV-1 DNA Dynamics in Antiretroviral-Treated HIV/HCV Co-Infected Patients Receiving Directly-Acting Antivirals. *PloS One* (2017) 12:e0187095. doi: 10.1371/journal.pone.0187095
11. Ghiglione Y, Polo ML, Urioste A, Rhodes A, Czernikier A, Trifone C, et al. Hepatitis C Virus (HCV) Clearance After Treatment With Direct-Acting Antivirals in Human Immunodeficiency Virus (HIV)-HCV Coinfection Modulates Systemic Immune Activation and HIV Transcription on Antiretroviral Therapy. *Open Forum Infect Dis* (2020) 7:ofaa115. doi: 10.1093/ofid/ofaa115
12. World Health Organization (WHO). *Hepatitis C - Fact Sheet*. (2020). Available at: https://www.who.int/news-room/fact-sheets/detail/hepatitis-c (Accessed September 2020).
13. Trickey A, Fraser H, Lim AG, Peacock A, Colledge S, Walker JG, et al. The Contribution of Injection Drug Use to Hepatitis C Virus Transmission Globally, Regionally, and at Country Level: A Modelling Study. *Lancet Gastroenterol Hepatol* (2019) 4:435–44. doi: 10.1016/S2468-1253(19)30085-8
14. Suryaprasad AG, White JZ, Xu F, Eichler BA, Hamilton J, Patel A, et al. Emerging Epidemic of Hepatitis C Virus Infections Among Young Nonurban Persons Who Inject Drugs in the United States, 2006-2012. *Clin Infect Dis* (2014) 59:1411–9. doi: 10.1093/cid/ciu643
15. World Health Organization (WHO). WHO, Access to Hepatitis C Testing and Treatment for People Who Inject Drugs and People in Prisons - a Global Perspective. In: W.H.O. (WHO), editor. Geneva: World Health Organization (WHO (2019). p. Policy brief. Available at: https://apps.who.int/iris/bitstream/handle/10665/312116/WHO-CDS-HIV-19.6-eng.pdf?ua=1 (Accessed March 2020).
16. Scheel TK, Rice CM. Understanding the Hepatitis C Virus Life Cycle Paves the Way for Highly Effective Therapies. *Nat Med* (2013) 19:837–49. doi: 10.1038/nm.3248
17. Pestka JM, Zeisel MB, Blaser E, Schurmann P, Bartosch B, Cosset FL, et al. Rapid Induction of Virus-Neutralizing Antibodies and Viral Clearance in a Single-Source Outbreak of Hepatitis C. *Proc Natl Acad Sci USA* (2007) 104:6025–30. doi: 10.1073/pnas.0607026104
18. Gerold G, Moeller R, Pietschmann T. Hepatitis C Virus Entry: Protein Interactions and Fusion Determinants Governing Productive Hepatocyte Invasion. *Cold Spring Harb Perspect Med* (2020) 10(2):a036830. doi: 10.1101/cshperspect.a036830
19. Pawlotsky JM. NS5A Inhibitors in the Treatment of Hepatitis C. *J Hepatol* (2013) 59:375–82. doi: 10.1016/j.jhep.2013.03.030
20. Hoofnagle JH. Course and Outcome of Hepatitis C. *Hepatology* (2002) 36:S21–9. doi: 10.1053/jhep.2002.36227
21. Khatun M, Ray RB. Mechanisms Underlying Hepatitis C Virus-Associated Hepatic Fibrosis. *Cells* (2019) 8(10):1249. doi: 10.3390/cells8101249
22. Zhang DY, Friedman SL. Fibrosis-Dependent Mechanisms of Hepatocarcinogenesis. *Hepatology* (2012) 56:769–75. doi: 10.1002/hep.25670
23. Poynard T, Bedossa P, Opolon P. Natural History of Liver Fibrosis Progression in Patients With Chronic Hepatitis C. The OBSVIRC, METAVIR, CLINIVIR, and DOSVIRC Groups. *Lancet* (1997) 349:825–32. doi: 10.1016/S0140-6736(96)07642-8
24. Zeremski M, Dimova RB, Pillardy J, de Jong YP, Jacobson IM, Talal AH. Fibrosis Progression in Patients With Chronic Hepatitis C Virus Infection. *J Infect Dis* (2016) 214:1164–70. doi: 10.1093/infdis/jiw332
25. Schwerk J, Negash A, Savan R, Gale MJr. Innate Immunity in Hepatitis C Virus Infection. *Cold Spring Harb Perspect Med* (2021) 11(2):a036988. doi: 10.1101/cshperspect.a036988
26. Liang Y, Cao X, Ding Q, Zhao Y, He Z, Zhong J. Hepatitis C Virus NS4B Induces the Degradation of TRIF to Inhibit TLR3-Mediated Interferon Signaling Pathway. *PloS Pathog* (2018) 14:e1007075. doi: 10.1371/journal.ppat.1007075
27. Takahashi K, Asabe S, Wieland S, Garaigorta U, Gastaminza P, Isogawa M, et al. Plasmacytoid Dendritic Cells Sense Hepatitis C Virus-Infected Cells, Produce Interferon, and Inhibit Infection. *Proc Natl Acad Sci USA* (2010) 107:7431–6. doi: 10.1073/pnas.1002301107
28. Wieland S, Makowska Z, Campana B, Calabrese D, Dill MT, Chung J, et al. Simultaneous Detection of Hepatitis C Virus and Interferon Stimulated Gene Expression in Infected Human Liver. *Hepatology* (2014) 59:2121–30. doi: 10.1002/hep.26770
29. Su AI, Pezacki JP, Wodicka L, Brideau AD, Supekova L, Thimme R, et al. Genomic Analysis of the Host Response to Hepatitis C Virus Infection. *Proc Natl Acad Sci USA* (2002) 99:15669–74. doi: 10.1073/pnas.202608199
30. Grebely J, Feld JJ, Applegate T, Matthews GV, Hellard M, Sherker A, et al. Plasma Interferon-Gamma-Inducible Protein-10 (IP-10) Levels During Acute Hepatitis C Virus Infection. *Hepatology* (2013) 57:2124–34. doi: 10.1002/hep.26263
31. Boisvert M, Shoukry NH. Type III Interferons in Hepatitis C Virus Infection. *Front Immunol* (2016) 7:628. doi: 10.3389/fimmu.2016.00628
32. Rosenberg BR, Depla M, Freije CA, Gaucher D, Mazouz S, Boisvert M, et al. Longitudinal Transcriptomic Characterization of the Immune Response to Acute Hepatitis C Virus Infection in Patients With Spontaneous Viral Clearance. *PloS Pathog* (2018) 14:e1007290. doi: 10.1371/journal.ppat.1007290
33. Rehermann B. Natural Killer Cells in Viral Hepatitis. *Cell Mol Gastroenterol Hepatol* (2015) 1:578–88. doi: 10.1016/j.jcmgh.2015.09.004
34. Abdel-Hakeem MS, Shoukry NH. Protective Immunity Against Hepatitis C: Many Shades of Gray. *Front Immunol* (2014) 5:274. doi: 10.3389/fimmu.2014.00274
35. Golden-Mason L, Burton JRJr., Castelblanco N, Klarquist J, Benlloch S, Wang C, et al. Loss of IL-7 Receptor Alpha-Chain (CD127) Expression in Acute HCV Infection Associated With Viral Persistence. *Hepatology* (2006) 44:1098–109. doi: 10.1002/hep.21365
36. Bengsch B, Spangenberg HC, Kersting N, Neumann-Haefelin C, Panther E, von Weizsacker F, et al. Analysis of CD127 and KLRG1 Expression on Hepatitis C Virus-Specific CD8+ T Cells Reveals the Existence of Different Memory T-Cell Subsets in the Peripheral Blood and Liver. *J Virol* (2007) 81:945–53. doi: 10.1128/JVI.01354-06
37. Badr G, Bedard N, Abdel-Hakeem MS, Trautmann L, Willems B, Villeneuve JP, et al. Early Interferon Therapy for Hepatitis C Virus Infection Rescues Polyfunctional, Long-Lived CD8+ Memory T Cells. *J Virol* (2008) 82:10017–31. doi: 10.1128/JVI.01083-08

38. Shin EC, Park SH, Nascimbeni M, Major M, Caggiari L, de Re V, et al. The Frequency of CD127+ HCV-Specific T Cells But Not the Expression of Exhaustion Markers Predict the Outcome of Acute Hepatitis C Virus Infection. *J Virol* (2013) 87(8):4772–4777. doi: 10.1128/JVI.03122-12
39. Bowen DG, Walker CM. Mutational Escape From CD8+ T Cell Immunity: HCV Evolution, From Chimpanzees to Man. *J Exp Med* (2005) 201:1709–14. doi: 10.1084/jem.20050808
40. Semmo N, Klenerman P. CD4+ T Cell Responses in Hepatitis C Virus Infection. *World J Gastroenterol* (2007) 13:4831–8. doi: 10.3748/wjg.v13.i36.4831
41. Schulze Zur Wiesch J, Ciuffreda D, Lewis-Ximenez L, Kasprowicz V, Nolan BE, Streeck H, et al. Broadly Directed Virus-Specific CD4+ T Cell Responses are Primed During Acute Hepatitis C Infection, But Rapidly Disappear From Human Blood With Viral Persistence. *J Exp Med* (2012) 209:61–75. doi: 10.1084/jem.20100388
42. Grakoui A, Shoukry NH, Woollard DJ, Han JH, Hanson HL, Ghrayeb J, et al. HCV Persistence and Immune Evasion in the Absence of Memory T Cell Help. *Science* (2003) 302:659–62. doi: 10.1126/science.1088774
43. Shin EC, Sung PS, Park SH. Immune Responses and Immunopathology in Acute and Chronic Viral Hepatitis. *Nat Rev Immunol* (2016) 16:509–23. doi: 10.1038/nri.2016.69
44. Alfei F, Kanev K, Hofmann M, Wu M, Ghoneim HE, Roelli P, et al. TOX Reinforces the Phenotype and Longevity of Exhausted T Cells in Chronic Viral Infection. *Nature* (2019) 571:265–9. doi: 10.1038/s41586-019-1326-9
45. Paley MA, Kroy DC, Odorizzi PM, Johnnidis JB, Dolfi DV, Barnett BE, et al. Progenitor and Terminal Subsets of CD8+ T Cells Cooperate to Contain Chronic Viral Infection. *Science* (2012) 338:1220–5. doi: 10.1126/science.1229620
46. Utzschneider DT, Charmoy M, Chennupati V, Pousse L, Ferreira DP, Calderon-Copete S, et al. T Cell Factor 1-Expressing Memory-Like CD8 (+) T Cells Sustain the Immune Response to Chronic Viral Infections. *Immunity* (2016) 45:415–27. doi: 10.1016/j.immuni.2016.07.021
47. Wieland D, Kemming J, Schuch A, Emmerich F, Knolle P, Neumann-Haefelin C, et al. TCF1(+) Hepatitis C Virus-Specific CD8(+) T Cells are Maintained After Cessation of Chronic Antigen Stimulation. *Nat Commun* (2017) 8:15050. doi: 10.1038/ncomms15050
48. Lugli E, Galletti G, Boi SK, Youngblood BA. Stem, Effector, and Hybrid States of Memory CD8(+) T Cells. *Trends Immunol* (2020) 41:17–28. doi: 10.1016/j.it.2019.11.004
49. Hensel N, Gu Z, Sagar, Wieland D, Jechow K, Kemming J, et al. Memory-Like HCV-Specific CD8(+) T Cells Retain a Molecular Scar After Cure of Chronic HCV Infection. *Nat Immunol* (2021) 22:229–39. doi: 10.1038/s41590-020-00817-w
50. Bengsch B, Seigel B, Ruhl M, Timm J, Kuntz M, Blum HE, et al. Coexpression of PD-1, 2b4, CD160 and KLRG1 on Exhausted HCV-Specific CD8+ T Cells is Linked to Antigen Recognition and T Cell Differentiation. *PloS Pathog* (2010) 6:e1000947. doi: 10.1371/journal.ppat.1000947
51. Kasprowicz V, Kang YH, Lucas M, Schulze zur Wiesch J, Kuntzen T, Fleming V, et al. Hepatitis C Virus (HCV) Sequence Variation Induces an HCV-Specific T-Cell Phenotype Analogous to Spontaneous Resolution. *J Virol* (2010) 84:1656–63. doi: 10.1128/JVI.01499-09
52. Wolski D, Foote PK, Chen DY, Lewis-Ximenez LL, Fauvelle C, Aneja J, et al. Early Transcriptional Divergence Marks Virus-Specific Primary Human CD8(+) T Cells in Chronic Versus Acute Infection. *Immunity* (2017) 47:648–663.e8. doi: 10.1016/j.immuni.2017.09.006
53. Kinchen VJ, Cox AL, Bailey JR. Can Broadly Neutralizing Monoclonal Antibodies Lead to a Hepatitis C Virus Vaccine? *Trends Microbiol* (2018) 26:854–64. doi: 10.1016/j.tim.2018.04.002
54. Shoukry NH, Vaccines HC. Antibodies, and T Cells. *Front Immunol* (2018) 9:1480. doi: 10.3389/fimmu.2018.01480
55. Farci P, London WT, Wong DC, Dawson GJ, Vallari DS, Engle R, et al. The Natural History of Infection With Hepatitis C Virus (HCV) in Chimpanzees: Comparison of Serologic Responses Measured With First- and Second-Generation Assays and Relationship to HCV Viremia. *J Infect Dis* (1992) 165:1006–11. doi: 10.1093/infdis/165.6.1006
56. Logvinoff C, Major ME, Oldach D, Heyward S, Talal A, Balfe P, et al. Neutralizing Antibody Response During Acute and Chronic Hepatitis C Virus Infection. *Proc Natl Acad Sci USA* (2004) 101:10149–54. doi: 10.1073/pnas.0403519101
57. Netski DM, Mosbruger T, Depla E, Maertens G, Ray SC, Hamilton RG, et al. Humoral Immune Response in Acute Hepatitis C Virus Infection. *Clin Infect Dis* (2005) 41:667–75. doi: 10.1086/432478
58. Takaki A, Wiese M, Maertens G, Depla E, Seifert U, Liebetrau A, et al. Cellular Immune Responses Persist and Humoral Responses Decrease Two Decades After Recovery From a Single-Source Outbreak of Hepatitis C. *Nat Med* (2000) 6:578–82. doi: 10.1038/75063
59. Salinas E, Boisvert M, Upadhyay AA, Bédard N, Nelson SA, Bruneau J, et al. Early T Follicular Helper Cell Activity Accelerates Hepatitis C Virus-Specific B Cell Expansion. *J Clin Invest* (2021) 131(2):e140590. doi: 10.1172/JCI140590
60. Osburn WO, Snider AE, Wells BL, Latanich R, Bailey JR, Thomas DL, et al. Clearance of Hepatitis C Infection Is Associated With Early Appearance of Broad Neutralizing Antibody Responses. *Hepatology* (2014) 59(6):2140–51. doi: 10.1002/hep.27013
61. Vanwolleghem T, Bukh J, Meuleman P, Desombere I, Meunier JC, Alter H, et al. Polyclonal Immunoglobulins From a Chronic Hepatitis C Virus Patient Protect Human Liver-Chimeric Mice From Infection With a Homologous Hepatitis C Virus Strain. *Hepatology* (2008) 47:1846–55. doi: 10.1002/hep.22244
62. Farci P, Alter HJ, Wong DC, Miller RH, Govindarajan S, Engle R, et al. Prevention of Hepatitis C Virus Infection in Chimpanzees After Antibody-Mediated In Vitro Neutralization. *Proc Natl Acad Sci USA* (1994) 91:7792–6. doi: 10.1073/pnas.91.16.7792
63. Farci P, Shimoda A, Wong D, Cabezon T, De Gioannis D, Strazzera A, et al. Prevention of Hepatitis C Virus Infection in Chimpanzees by Hyperimmune Serum Against the Hypervariable Region 1 of the Envelope 2 Protein. *Proc Natl Acad Sci USA* (1996) 93:15394–9. doi: 10.1073/pnas.93.26.15394
64. Krawczynski K, Alter MJ, Tankersley DL, Beach M, Robertson BH, Lambert S, et al. Effect of Immune Globulin on the Prevention of Experimental Hepatitis C Virus Infection. *J Infect Dis* (1996) 173:822–8. doi: 10.1093/infdis/173.4.822
65. Dorner M, Horwitz JA, Robbins JB, Barry WT, Feng Q, Mu K, et al. A Genetically Humanized Mouse Model for Hepatitis C Virus Infection. *Nature* (2011) 474:208–11. doi: 10.1038/nature10168
66. Law M, Maruyama T, Lewis J, Giang E, Tarr AW, Stamataki Z, et al. Broadly Neutralizing Antibodies Protect Against Hepatitis C Virus Quasispecies Challenge. *Nat Med* (2008) 14:25–7. doi: 10.1038/nm1698
67. Bailey JR, Flyak AI, Cohen VJ, Li H, Wasilewski LN, Snider AE, et al. Broadly Neutralizing Antibodies With Few Somatic Mutations and Hepatitis C Virus Clearance. *JCI Insight* (2017) 2(9):e9287. doi: 10.1172/jci.insight.92872
68. Giang E, Dorner M, Prentoe JC, Dreux M, Evans MJ, Bukh J, et al. Human Broadly Neutralizing Antibodies to the Envelope Glycoprotein Complex of Hepatitis C Virus. *Proc Natl Acad Sci USA* (2012) 109:6205–10. doi: 10.1073/pnas.1114927109
69. Kinchen VJ, Zahid MN, Flyak AI, Soliman MG, Learn GH, Wang S, et al. Broadly Neutralizing Antibody Mediated Clearance of Human Hepatitis C Virus Infection. *Cell Host Microbe* (2018) 24:717–730.e5. doi: 10.1016/j.chom.2018.10.012
70. Shoukry NH, Grakoui A, Houghton M, Chien DY, Ghrayeb J, Reimann KA, et al. Memory CD8+ T Cells Are Required for Protection From Persistent Hepatitis C Virus Infection. *J Exp Med* (2003) 197:1645–55. doi: 10.1084/jem.20030239
71. Osburn WO, Fisher BE, Dowd KA, Urban G, Liu L, Ray SC, et al. Spontaneous Control of Primary Hepatitis C Virus Infection and Immunity Against Persistent Reinfection. *Gastroenterology* (2010) 138:315–24. doi: 10.1053/j.gastro.2009.09.017
72. Abdel-Hakeem MS, Bedard N, Murphy D, Bruneau J, Shoukry NH. Signatures of Protective Memory Immune Responses During Hepatitis C Virus Reinfection. *Gastroenterology* (2014) 147:870–81.e8. doi: 10.1053/j.gastro.2014.07.005
73. Grebely J, Prins M, Hellard M, Cox AL, Osburn WO, Lauer G, et al. Hepatitis C Virus Clearance, Reinfection, and Persistence, With Insights From Studies of Injecting Drug Users: Towards a Vaccine. *Lancet Infect Dis* (2012) 12:408–14. doi: 10.1016/S1473-3099(12)70010-5

74. Sacks-Davis R, Grebely J, Dore GJ, Osburn W, Cox AL, Rice TM, et al. Hepatitis C Virus Reinfection and Spontaneous Clearance of Reinfection—the InC3 Study. *J Infect Dis* (2015) 212:1407–19. doi: 10.1093/infdis/jiv220
75. Zoulim F, Liang TJ, Gerbes AL, Aghemo A, Deuffic-Burban S, Dusheiko G, et al. Hepatitis C Virus Treatment in the Real World: Optimising Treatment and Access to Therapies. *Gut* (2015) 64:1824–33. doi: 10.1136/gutjnl-2015-310421
76. Pawlotsky JM, Feld JJ, Zeuzem S, Hoofnagle JH. From Non-A, Non-B Hepatitis to Hepatitis C Virus Cure. *J Hepatol* (2015) 62:S87–99. doi: 10.1016/j.jhep.2015.02.006
77. Cunningham EB, Hajarizadeh B, Amin J, Hellard M, Bruneau J, Feld JJ, et al. Reinfection Following Successful Direct-Acting Antiviral Therapy for Hepatitis C Infection Among People Who Inject Drugs. *Clin Infect Dis* (2020) 72(8):1392–400. doi: 10.1093/cid/ciaa253
78. Barre-Sinoussi F, Ross AL, Delfraissy JF. Past, Present and Future: 30 Years of HIV Research. *Nat Rev Microbiol* (2013) 11:877–83. doi: 10.1038/nrmicro3132
79. WHO. *WHO, HIV/AIDS Fact Sheet*. (2019). Available at: https://www.who.int/news-room/fact-sheets/detail/hiv-aids (Accessed March 2020).
80. Ochonye B, Folayan MO, Fatusi AO, Bello BM, Ajidagba B, Emmanuel G, et al. Sexual Practices, Sexual Behavior and HIV Risk Profile of Key Populations in Nigeria. *BMC Public Health* (2019) 19:1210. doi: 10.1186/s12889-019-7553-z
81. Taylor LE, Swan T, Matthews GV. Management of Hepatitis C Virus/HIV Coinfection Among People Who Use Drugs in the Era of Direct-Acting Antiviral-Based Therapy. *Clin Infect Dis* (2013) 57:S118–24. doi: 10.1093/cid/cit326
82. Dosekun O, Fox J. An Overview of the Relative Risks of Different Sexual Behaviours on HIV Transmission. *Curr Opin HIV AIDS* (2010) 5:291–7. doi: 10.1097/COH.0b013e32833a88a3
83. Shaw GM, Hunter E. HIV Transmission. *Cold Spring Harb Perspect Med* (2012) 2(11):a006965. doi: 10.1101/cshperspect.a006965
84. Pandey A, Galvani AP. The Global Burden of HIV and Prospects for Control. *Lancet HIV* (2019) 6:e809–11. doi: 10.1016/S2352-3018(19)30230-9
85. Klatzmann DR, McDougal JS, Maddon PJ. The CD4 Molecule and HIV Infection. *Immunodefic Rev* (1990) 2:43–66.
86. Deng H, Liu R, Ellmeier W, Choe S, Unutmaz D, Burkhart M, et al. Identification of a Major Co-Receptor for Primary Isolates of HIV-1. *Nature* (1996) 381:661–6. doi: 10.1038/381661a0
87. Berger EA, Doms RW, Fenyö EM, Korber BT, Littman DR, Moore JP, et al. A New Classification for HIV-1. *Nature* (1998) 391:240. doi: 10.1038/34571
88. Wyatt R, Sodroski J. The HIV-1 Envelope Glycoproteins: Fusogens, Antigens, and Immunogens. *Science* (1998) 280:1884–8. doi: 10.1126/science.280.5371.1884
89. Chan DC, Kim PS. HIV Entry and its Inhibition. *Cell* (1998) 93:681–4. doi: 10.1016/S0092-8674(00)81430-0
90. Zheng YH, Lovsin N, Peterlin BM. Newly Identified Host Factors Modulate HIV Replication. *Immunol Lett* (2005) 97:225–34. doi: 10.1016/j.imlet.2004.11.026
91. Chavez L, Calvanese V, Verdin E. HIV Latency Is Established Directly and Early in Both Resting and Activated Primary CD4 T Cells. *PloS Pathog* (2015) 11:e1004955. doi: 10.1371/journal.ppat.1004955
92. Gomez C, Hope TJ. The Ins and Outs of HIV Replication. *Cell Microbiol* (2005) 7:621–6. doi: 10.1111/j.1462-5822.2005.00516.x
93. Siliciano RF, Greene WC. HIV Latency. *Cold Spring Harb Perspect Med* (2011) 1:a007096. doi: 10.1101/cshperspect.a007096
94. Sengupta S, Siliciano RF. Targeting the Latent Reservoir for HIV-1. *Immunity* (2018) 48:872–95. doi: 10.1016/j.immuni.2018.04.030
95. Cohn LB, Chomont N, Deeks SG. The Biology of the HIV-1 Latent Reservoir and Implications for Cure Strategies. *Cell Host Microbe* (2020) 27:519–30. doi: 10.1016/j.chom.2020.03.014
96. Grossman Z, Meier-Schellersheim M, Paul WE, Picker LJ. Pathogenesis of HIV Infection: What the Virus Spares is as Important as What it Destroys. *Nat Med* (2006) 12:289–95. doi: 10.1038/nm1380
97. Douek DC, Roederer M, Koup RA. Emerging Concepts in the Immunopathogenesis of AIDS. *Annu Rev Med* (2009) 60:471–84. doi: 10.1146/annurev.med.60.041807.123549
98. Cohen MS, Gay CL, Busch MP, Hecht FM. The Detection of Acute HIV Infection. *J Infect Dis* (2010) 202:S270–7. doi: 10.1086/655651
99. Pantaleo G, Graziosi C, Fauci AS. The Immunopathogenesis of Human Immunodeficiency Virus Infection. *N Engl J Med* (1993) 328:327–35. doi: 10.1056/NEJM199302043280508
100. Feinberg MB, McCune JM, Miedema F, Moore JP, Schuitemaker H. HIV Tropism and CD4+ T-Cell Depletion. *Nat Med* (2002) 8:537. doi: 10.1038/nm0602-537a
101. Haase AT. Perils at Mucosal Front Lines for HIV and SIV and Their Hosts. *Nat Rev Immunol* (2005) 5:783–92. doi: 10.1038/nri1706
102. Orenstein JM, Fox C, Wahl SM. Macrophages as a Source of HIV During Opportunistic Infections. *Science* (1997) 276:1857–61. doi: 10.1126/science.276.5320.1857
103. Veazey RS, Lackner AA. Getting to the Guts of HIV Pathogenesis. *J Exp Med* (2004) 200:697–700. doi: 10.1084/jem.20041464
104. Brenchley JM, Price DA, Douek DC. HIV Disease: Fallout From a Mucosal Catastrophe? *Nat Immunol* (2006) 7:235–9. doi: 10.1038/ni1316
105. Brenchley JM, Price DA, Schacker TW, Asher TE, Silvestri G, Rao S, et al. Microbial Translocation Is a Cause of Systemic Immune Activation in Chronic HIV Infection. *Nat Med* (2006) 12:1365–71. doi: 10.1038/nm1511
106. Doitsh G, Galloway NL, Geng X, Yang Z, Monroe KM, Zepeda O, et al. Cell Death by Pyroptosis Drives CD4 T-Cell Depletion in HIV-1 Infection. *Nature* (2014) 505:509–14. doi: 10.1038/nature12940
107. Garg H, Mohl J, Joshi A. HIV-1 Induced Bystander Apoptosis. *Viruses* (2012) 4:3020–43. doi: 10.3390/v4113020
108. Kumar V. Robbins Basic Pathology. *Basic Pathology*. Philadelphia, PA: Elsevier/Saunders (2012).
109. Loveday C, Hill A. Prediction of Progression to AIDS With Serum HIV-1 RNA and CD4 Count. *Lancet* (1995) 345:790–1. doi: 10.1016/S0140-6736(95)90668-1
110. Migueles SA, Connors M. Success and Failure of the Cellular Immune Response Against HIV-1. *Nat Immunol* (2015) 16:563–70. doi: 10.1038/ni.3161
111. Poropatich K, Sullivan DJJr. Human Immunodeficiency Virus Type 1 Long-Term non-Progressors: The Viral, Genetic and Immunological Basis for Disease non-Progression. *J Gen Virol* (2011) 92:247–68. doi: 10.1099/vir.0.027102-0
112. Mikhail M, Wang B, Saksena NK. Mechanisms Involved in non-Progressive HIV Disease. *AIDS Rev* (2003) 5:230–44.
113. Morley D, Lambert JS, Hogan LE, De Gascun C, Redmond N, Rutishauser RL, et al. Rapid Development of HIV Elite Control in a Patient With Acute Infection. *BMC Infect Dis* (2019) 19:815. doi: 10.1186/s12879-019-4485-2
114. Gebara NY, El Kamari V, Rizk N. HIV-1 Elite Controllers: An Immunovirological Review and Clinical Perspectives. *J Virus Eradication* (2019) 5:163–6. doi: 10.1016/S2055-6640(20)30046-7
115. Goulder P, Deeks SG. HIV Control: Is Getting There the Same as Staying There? *PloS Pathog* (2018) 14:e1007222. doi: 10.1371/journal.ppat.1007222
116. Walker BD, Yu XG. Unravelling the Mechanisms of Durable Control of HIV-1. *Nat Rev Immunol* (2013) 13:487–98. doi: 10.1038/nri3478
117. Carrington M, Walker BD. Immunogenetics of Spontaneous Control of HIV. *Annu Rev Med* (2012) 63:131–45. doi: 10.1146/annurev-med-062909-130018
118. Yao XD, Omange RW, Henrick BM, Lester RT, Kimani J, Ball TB, et al. Acting Locally: Innate Mucosal Immunity in Resistance to HIV-1 Infection in Kenyan Commercial Sex Workers. *Mucosal Immunol* (2014) 7:268–79. doi: 10.1038/mi.2013.44
119. Sáez-Cirión A, Bacchus C, Hocqueloux L, Avettand-Fenoel V, Girault I, Lecuroux C, et al. Post-Treatment HIV-1 Controllers With a Long-Term Virological Remission After the Interruption of Early Initiated Antiretroviral Therapy ANRS VISCONTI Study. *PloS Pathog* (2013) 9:e1003211. doi: 10.1371/journal.ppat.1003211
120. Hamimi C, Pancino G, Barré-Sinoussi F, Sáez-Cirión A. Will it be Possible to Live Without Antiretroviral Therapy? *Curr Opin HIV AIDS* (2013) 8:196–203. doi: 10.1097/COH.0b013e32835f94d5
121. Opportunistic Infections Project Team of the Collaboration of Observational, HIVERiEiE, Young J, Psichogiou M, Meyer L, Ayayi S, Grabar S, et al. CD4 Cell Count and the Risk of AIDS or Death in HIV-Infected Adults on Combination Antiretroviral Therapy With a Suppressed

Viral Load: A Longitudinal Cohort Study From COHERE. *PloS Med* (2012) 9:e1001194–e1001194. doi: 10.1371/journal.pmed.1001194
122. Nakanjako D, Kiragga AN, Musick BS, Yiannoutsos CT, Wools-Kaloustian K, Diero L, et al. Frequency and Impact of Suboptimal Immune Recovery on First-Line Antiretroviral Therapy Within the International Epidemiologic Databases to Evaluate AIDS in East Africa. *Aids* (2016) 30:1913–22. doi: 10.1097/QAD.0000000000001085
123. Yang X, Su B, Zhang X, Liu Y, Wu H, Zhang T. Incomplete Immune Reconstitution in HIV/AIDS Patients on Antiretroviral Therapy: Challenges of Immunological non-Responders. *J Leukoc Biol* (2020) 107:597–612. doi: 10.1002/JLB.4MR1019-189R
124. Bruzzesi E, Sereti I. Residual Immune Activation and Latency. *Curr Top Microbiol Immunol* (2018) 417:157–80. doi: 10.1007/82_2018_118
125. Pacheco YM, Jarrin I, Rosado I, Campins AA, Berenguer J, Iribarren JA, et al. Increased Risk of Non-AIDS-Related Events in HIV Subjects With Persistent Low CD4 Counts Despite cART in the CoRIS Cohort. *Antiviral Res* (2015) 117:69–74. doi: 10.1016/j.antiviral.2015.03.002
126. Engsig FN, Zangerle R, Katsarou O, Dabis F, Reiss P, Gill J, et al. Long-Term Mortality in HIV-Positive Individuals Virally Suppressed for >3 Years With Incomplete CD4 Recovery. *Clin Infect Dis* (2014) 58:1312–21. doi:10.1093/cid/ciu038
127. Takuva S, Maskew M, Brennan AT, Long L, Sanne I, Fox MP. Poor CD4 Recovery and Risk of Subsequent Progression to AIDS or Death Despite Viral Suppression in a South African Cohort. *J Int AIDS Soc* (2014) 17:18651. doi: 10.7448/IAS.17.1.18651
128. Collins DR, Gaiha GD, Walker BD. CD8(+) T Cells in HIV Control, Cure and Prevention. *Nat Rev Immunol* (2020) 20:471–82. doi: 10.1038/s41577-020-0274-9
129. Bengsch B, Ohtani T, Khan O, Setty M, Manne S, O'Brien S, et al. Epigenomic-Guided Mass Cytometry Profiling Reveals Disease-Specific Features of Exhausted CD8 T Cells. *Immunity* (2018) 48:1029–1045.e5. doi: 10.1016/j.immuni.2018.04.026
130. Sekine T, Perez-Potti A, Nguyen S, Gorin JB, Wu VH, Gostick E, et al. TOX is Expressed by Exhausted and Polyfunctional Human Effector Memory CD8 (+) T Cells. *Sci Immunol* (2020) 5(49):eaba7918. doi: 10.1126/sciimmunol.aba7918
131. Rutishauser RL, Deguit CDT, Hiatt J, Blaeschke F, Roth TL, Wang L, et al. TCF-1 Regulates HIV-Specific CD8+ T Cell Expansion Capacity. *JCI Insight* (2021) 6(3):e136648. doi: 10.1172/jci.insight.136648
132. He R, Hou S, Liu C, Zhang A, Bai Q, Han M, et al. Follicular CXCR5-Expressing CD8(+) T Cells Curtail Chronic Viral Infection. *Nature* (2016) 537:412–28. doi: 10.1038/nature19317
133. Buggert M, Nguyen S, Salgado-Montes de Oca G, Bengsch B, Darko S, Ransier A, et al. Identification and Characterization of HIV-Specific Resident Memory CD8(+) T Cells in Human Lymphoid Tissue. *Sci Immunol* (2018) 3 (24):eaar4526. doi: 10.1126/sciimmunol.aar4526
134. Reuter MA, Del Rio Estrada PM, Buggert M, Petrovas C, Ferrando-Martinez S, Nguyen S, et al. HIV-Specific CD8(+) T Cells Exhibit Reduced and Differentially Regulated Cytolytic Activity in Lymphoid Tissue. *Cell Rep* (2017) 21:3458–70. doi: 10.1016/j.celrep.2017.11.075
135. Hütter G, Nowak D, Mossner M, Ganepola S, Müssig A, Allers K, et al. Long-Term Control of HIV by CCR5 Delta32/Delta32 Stem-Cell Transplantation. *N Engl J Med* (2009) 360:692–8. doi: 10.1056/NEJMoa0802905
136. Cohen MS, Chen YQ, McCauley M, Gamble T, Hosseinipour MC, Kumarasamy N, et al. Prevention of HIV-1 Infection With Early Antiretroviral Therapy. *N Engl J Med* (2011) 365:493–505. doi: 10.1056/NEJMc1110588
137. Cohen MS, Chen YQ, McCauley M, Gamble T, Hosseinipour MC, Kumarasamy N, et al. Antiretroviral Therapy for the Prevention of HIV-1 Transmission. *N Engl J Med* (2016) 375:830–9. doi: 10.1056/NEJMoa1600693
138. Anderson PL, Glidden DV, Liu A, Buchbinder S, Lama JR, Guanira JV, et al. Emtricitabine-Tenofovir Concentrations and Pre-Exposure Prophylaxis Efficacy in Men Who Have Sex With Men. *Sci Transl Med* (2012) 4:151ra125. doi: 10.1126/scitranslmed.3004006
139. McCormack S, Dunn DT, Desai M, Dolling DI, Gafos M, Gilson R, et al. Pre-Exposure Prophylaxis to Prevent the Acquisition of HIV-1 Infection (PROUD): Effectiveness Results From the Pilot Phase of a Pragmatic Open-Label Randomised Trial. *Lancet* (2016) 387:53–60. doi: 10.1016/S0140-6736(15)00056-2
140. Riddell JT, Amico KR, Mayer KH. HIV Preexposure Prophylaxis: A Review. *Jama* (2018) 319:1261–8. doi: 10.1001/jama.2018.1917
141. Markowitz M, Frank I, Grant RM, Mayer KH, Elion R, Goldstein D, et al. Safety and Tolerability of Long-Acting Cabotegravir Injections in HIV-Uninfected Men (ECLAIR): A Multicentre, Double-Blind, Randomised, Placebo-Controlled, Phase 2a Trial. *Lancet HIV* (2017) 4:e331–40. doi: 10.1016/S2352-3018(17)30068-1
142. Grobben M, Stuart RA, van Gils MJ. The Potential of Engineered Antibodies for HIV-1 Therapy and Cure. *Curr Opin Virol* (2019) 38:70–80. doi: 10.1016/j.coviro.2019.07.007
143. Caskey M, Klein F, Nussenzweig MC. Broadly Neutralizing Anti-HIV-1 Monoclonal Antibodies in the Clinic. *Nat Med* (2019) 25:547–53. doi: 10.1038/s41591-019-0412-8
144. Caskey M. Broadly Neutralizing Antibodies for the Treatment and Prevention of HIV Infection. *Curr Opin HIV AIDS* (2020) 15:49–55. doi: 10.1097/COH.0000000000000600
145. Jin F, Matthews GV, Grulich AE. Sexual Transmission of Hepatitis C Virus Among Gay and Bisexual Men: A Systematic Review. *Sex Health* (2017) 14:28–41. doi: 10.1071/SH16141
146. Nijmeijer BM, Sarrami-Forooshani R, Steba GS, Schreurs RR, Koekkoek SM, Molenkamp R, et al. HIV-1 Exposure and Immune Activation Enhance Sexual Transmission of Hepatitis C Virus by Primary Langerhans Cells. *J Int AIDS Soc* (2019) 22:e25268. doi: 10.1002/jia2.25268
147. Gupta P. Hepatitis C Virus and HIV Type 1 Co-Infection. *Infect Dis Rep* (2013) 5:e7. doi: 10.4081/idr.2013.s1.e7
148. Binder B, Thimme R. CD4+ T Cell Responses in Human Viral Infection: Lessons From Hepatitis C. *J Clin Invest* (2020) 130:595–7. doi: 10.1172/JCI133222
149. Crotty S. T Follicular Helper Cell Biology: A Decade of Discovery and Diseases. *Immunity* (2019) 50:1132–48. doi: 10.1016/j.immuni.2019.04.011
150. Kim AY, Schulze zur Wiesch J, Kuntzen T, Timm J, Kaufmann DE, Duncan JE, et al. Impaired Hepatitis C Virus-Specific T Cell Responses and Recurrent Hepatitis C Virus in HIV Coinfection. *PloS Med* (2006) 3:e492. doi: 10.1371/journal.pmed.0030492
151. Kim AY, Lauer GM, Ouchi K, Addo MM, Lucas M, Wiesch JS, et al. The Magnitude and Breadth of Hepatitis C Virus-Specific CD8+ T Cells Depend on Absolute CD4+ T-Cell Count in Individuals Coinfected With HIV-1. *Blood* (2005) 105:1170–8. doi: 10.1182/blood-2004-06-2336
152. Bailey JR, Dowd KA, Snider AE, Osburn WO, Mehta SH, Kirk GD, et al. CD4+ T-Cell-Dependent Reduction in Hepatitis C Virus-Specific Neutralizing Antibody Responses After Coinfection With Human Immunodeficiency Virus. *J Infect Dis* (2015) 212:914–23. doi: 10.1093/infdis/jiv139
153. Ganesan M, Poluektova LY, Kharbanda KK, Osna NA. Human Immunodeficiency Virus and Hepatotropic Viruses Co-Morbidities as the Inducers of Liver Injury Progression. *World J Gastroenterol* (2019) 25:398–410. doi: 10.3748/wjg.v25.i4.398
154. Sato H, Adachi E, Lim LA, Koga M, Koibuchi T, Tsutsumi T, et al. CD4/CD8 Ratio Predicts the Cellular Immune Response to Acute Hepatitis C in HIV-Coinfected Adults. *J Infect Chemother* (2019) 25:646–8. doi: 10.1016/j.jiac.2019.04.001
155. Hernandez MD, Sherman KE. HIV/hepatitis C Coinfection Natural History and Disease Progression. *Curr Opin HIV AIDS* (2011) 6:478–82. doi: 10.1097/COH.0b013e32834bd365
156. Thein HH, Yi Q, Dore GJ, Krahn MD. Natural History of Hepatitis C Virus Infection in HIV-Infected Individuals and the Impact of HIV in the Era of Highly Active Antiretroviral Therapy: A Meta-Analysis. *Aids* (2008) 22:1979–91. doi: 10.1097/QAD.0b013e32830e6d51
157. Xiao P, Usami O, Suzuki Y, Ling H, Shimizu N, Hoshino H, et al. Characterization of a CD4-Independent Clinical HIV-1 That can Efficiently Infect Human Hepatocytes Through Chemokine (C-X-C Motif) Receptor 4. *Aids* (2008) 22:1749–57. doi: 10.1097/QAD.0b013e328308937c
158. Lin W, Wu G, Li S, Weinberg EM, Kumthip K, Peng LF, et al. HIV and HCV Cooperatively Promote Hepatic Fibrogenesis *via* Induction of Reactive Oxygen Species and NFkappaB. *J Biol Chem* (2011) 286:2665–74. doi: 10.1074/jbc.M110.168286

159. Lin W, Weinberg EM, Chung RT. Pathogenesis of Accelerated Fibrosis in HIV/HCV Co-Infection. *J Infect Dis* (2013) 207:S13–8. doi: 10.1093/infdis/jis926
160. Jang JY, Shao RX, Lin W, Weinberg E, Chung WJ, Tsai WL, et al. HIV Infection Increases HCV-Induced Hepatocyte Apoptosis. *J Hepatol* (2011) 54:612–20. doi: 10.1016/j.jhep.2010.07.042
161. Zhou X, Jiang W, Liu Z, Liu S, Liang X. Virus Infection and Death Receptor-Mediated Apoptosis. *Viruses* (2017) 9(11):316. doi: 10.3390/v9110316
162. Tuyama AC, Hong F, Saiman Y, Wang C, Ozkok D, Mosoian A, et al. Human Immunodeficiency Virus (HIV)-1 Infects Human Hepatic Stellate Cells and Promotes Collagen I and Monocyte Chemoattractant Protein-1 Expression: Implications for the Pathogenesis of HIV/hepatitis C Virus-Induced Liver Fibrosis. *Hepatology* (2010) 52:612–22. doi: 10.1002/hep.23679
163. Zhang L, Bansal MB. Role of Kupffer Cells in Driving Hepatic Inflammation and Fibrosis in HIV Infection. *Front Immunol* (2020) 11:1086. doi: 10.3389/fimmu.2020.01086
164. Mosoian A, Zhang L, Hong F, Cunyat F, Rahman A, Bhalla R, et al. Frontline Science: HIV Infection of Kupffer Cells Results in an Amplified Proinflammatory Response to LPS. *J Leukoc Biol* (2017) 101:1083–90. doi: 10.1189/jlb.3HI0516-242R
165. Lidofsky A, Holmes JA, Feeney ER, Kruger AJ, Salloum S, Zheng H, et al. Macrophage Activation Marker Soluble CD163 Is a Dynamic Marker of Liver Fibrogenesis in Human Immunodeficiency Virus/Hepatitis C Virus Coinfection. *J Infect Dis* (2018) 218:1394–403. doi: 10.1093/infdis/jiy331
166. Seki E, De Minicis S, Osterreicher CH, Kluwe J, Osawa Y, Brenner DA, et al. TLR4 Enhances TGF-Beta Signaling and Hepatic Fibrosis. *Nat Med* (2007) 13:1324–32. doi: 10.1038/nm1663
167. Deng A, Chen C, Ishizaka Y, Chen X, Sun B, Yang R. Human Immunodeficiency Virus Type 1 Vpr Increases Hepatitis C Virus RNA Replication in Cell Culture. *Virus Res* (2014) 184:93–102. doi: 10.1016/j.virusres.2014.02.017
168. Park IW, Fan Y, Luo X, Ryou MG, Liu J, Green L, et al. HIV-1 Nef is Transferred From Expressing T Cells to Hepatocytic Cells Through Conduits and Enhances HCV Replication. *PloS One* (2014) 9:e99545. doi: 10.1371/journal.pone.0099545
169. Feuth T, Arends JE, Fransen JH, Nanlohy NM, van Erpecum KJ, Siersema PD, et al. Complementary Role of HCV and HIV in T-Cell Activation and Exhaustion in HIV/HCV Coinfection. *PloS One* (2013) 8:e59302. doi: 10.1371/journal.pone.0059302
170. van Vonderen MG, Blumer RM, Hassink EA, Sutinen J, Ackermans MT, van Agtmael MA, et al. Insulin Sensitivity in Multiple Pathways is Differently Affected During Zidovudine/Lamivudine-Containing Compared With NRTI-Sparing Combination Antiretroviral Therapy. *J Acquir Immune Defic Syndr* (2010) 53:186–93. doi: 10.1097/QAI.0b013e3181c190f4
171. Fleischman A, Johnsen S, Systrom DM, Hrovat M, Farrar CT, Frontera W, et al. Effects of a Nucleoside Reverse Transcriptase Inhibitor, Stavudine, on Glucose Disposal and Mitochondrial Function in Muscle of Healthy Adults. *Am J Physiol Endocrinol Metab* (2007) 292:E1666–73. doi: 10.1152/ajpendo.00550.2006
172. Blas-García A, Apostolova N, Ballesteros D, Monleón D, Morales JM, Rocha M, et al. Inhibition of Mitochondrial Function by Efavirenz Increases Lipid Content in Hepatic Cells. *Hepatology* (2010) 52:115–25. doi: 10.1002/hep.23647
173. Paemanee A, Sornjai W, Kittisenachai S, Sirinonthanawech N, Roytrakul S, Wongtrakul J, et al. Nevirapine Induced Mitochondrial Dysfunction in HepG2 Cells. *Sci Rep* (2017) 7:9194. doi: 10.1038/s41598-017-09321-y
174. Hull MW, Rollet K, Moodie EE, Walmsley S, Cox J, Potter M, et al. Insulin Resistance is Associated With Progression to Hepatic Fibrosis in a Cohort of HIV/hepatitis C Virus-Coinfected Patients. *Aids* (2012) 26:1789–94. doi: 10.1097/QAD.0b013e32835612ce
175. Bruno R, Galastri S, Sacchi P, Cima S, Caligiuri A, DeFranco R, et al. Gp120 Modulates the Biology of Human Hepatic Stellate Cells: A Link Between HIV Infection and Liver Fibrogenesis. *Gut* (2010) 59:513–20. doi: 10.1136/gut.2008.163287
176. Salloum S, Holmes JA, Jindal R, Bale SS, Brisac C, Alatrakchi N, et al. Exposure to Human Immunodeficiency Virus/Hepatitis C Virus in Hepatic and Stellate Cell Lines Reveals Cooperative Profibrotic Transcriptional Activation Between Viruses and Cell Types. *Hepatology* (2016) 64:1951–68. doi: 10.1002/hep.28766
177. Munshi N, Balasubramanian A, Koziel M, Ganju RK, Groopman JE, Hepatitis C. And Human Immunodeficiency Virus Envelope Proteins Cooperatively Induce Hepatocytic Apoptosis *via* an Innocent Bystander Mechanism. *J Infect Dis* (2003) 188:1192–204. doi: 10.1086/378643
178. Balagopal A, Ray SC, De Oca RM, Sutcliffe CG, Vivekanandan P, Higgins Y, et al. Kupffer Cells are Depleted With HIV Immunodeficiency and Partially Recovered With Antiretroviral Immune Reconstitution. *Aids* (2009) 23:2397–404. doi: 10.1097/QAD.0b013e3283324344
179. Balagopal A, Philp FH, Astemborski J, Block TM, Mehta A, Long R, et al. Human Immunodeficiency Virus-Related Microbial Translocation and Progression of Hepatitis C. *Gastroenterology* (2008) 135:226–33. doi: 10.1053/j.gastro.2008.03.022
180. Mehta AS, Long RE, Comunale MA, Wang M, Rodemich L, Krakover J, et al. Increased Levels of Galactose-Deficient Anti-Gal Immunoglobulin G in the Sera of Hepatitis C Virus-Infected Individuals With Fibrosis and Cirrhosis. *J Virol* (2008) 82:1259–70. doi: 10.1128/JVI.01600-07
181. Operskalski EA, Kovacs A. HIV/HCV Co-Infection: Pathogenesis, Clinical Complications, Treatment, and New Therapeutic Technologies. *Curr HIV/AIDS Rep* (2011) 8:12–22. doi: 10.1007/s11904-010-0071-3
182. Vali B, Yue FY, Jones RB, Sheth PM, Kaul R, Betts MR, et al. HIV-Specific T-Cells Accumulate in the Liver in HCV/HIV Co-Infection. *PloS One* (2008) 3:e3454. doi: 10.1371/journal.pone.0003454
183. Mastroianni CM, Lichtner M, Mascia C, Zuccala P, Vullo V. Molecular Mechanisms of Liver Fibrosis in HIV/HCV Coinfection. *Int J Mol Sci* (2014) 15:9184–208. doi: 10.3390/ijms15069184
184. Hyun J, McMahon RS, Lang AL, Edwards JS, Badilla AD, Greene ME, et al. HIV and HCV Augments Inflammatory Responses Through Increased TREM-1 Expression and Signaling in Kupffer and Myeloid Cells. *PloS Pathog* (2019) 15:e1007883. doi: 10.1371/journal.ppat.1007883
185. Pérez-Matute P, Pérez-Martínez L, Blanco JR, Oteo JA. Role of Mitochondria in HIV Infection and Associated Metabolic Disorders: Focus on Nonalcoholic Fatty Liver Disease and Lipodystrophy Syndrome. *Oxid Med Cell Longevity* (2013) 2013:493413. doi: 10.1155/2013/493413
186. Feeney ER, Mallon PW. Impact of Mitochondrial Toxicity of HIV-1 Antiretroviral Drugs on Lipodystrophy and Metabolic Dysregulation. *Curr Pharm Des* (2010) 16:3339–51. doi: 10.2174/138161210793563482
187. Apostolova N, Blas-García A, Esplugues JV. Mitochondrial Interference by Anti-HIV Drugs: Mechanisms Beyond Pol-γ Inhibition. *Trends Pharmacol Sci* (2011) 32:715–25. doi: 10.1016/j.tips.2011.07.007
188. Rohrbach J, Robinson N, Harcourt G, Hammond E, Gaudieri S, Gorgievski M, et al. Cellular Immune Responses to HCV Core Increase and HCV RNA Levels Decrease During Successful Antiretroviral Therapy. *Gut* (2010) 59:1252–8. doi: 10.1136/gut.2009.205971
189. Anderson JP, Tchetgen Tchetgen EJ, Lo Re V3rd, Tate JP, Williams PL, Seage GR3rd, et al. Antiretroviral Therapy Reduces the Rate of Hepatic Decompensation Among HIV- and Hepatitis C Virus-Coinfected Veterans. *Clin Infect Dis* (2014) 58:719–27. doi: 10.1093/cid/cit779
190. Price JC, Seaberg EC, Phair JP, Witt MD, Koletar SL, Thio CL. Brief Report: Highly Active Antiretroviral Therapy Mitigates Liver Disease in HIV Infection. *J Acquir Immune Defic Syndr* (2016) 72:319–23. doi: 10.1097/QAI.0000000000000981
191. d'Arminio Monforte A, Cozzi-Lepri A, Castagna A, Antinori A, De Luca A, Mussini C, et al. Risk of Developing Specific AIDS-Defining Illnesses in Patients Coinfected With HIV and Hepatitis C Virus With or Without Liver Cirrhosis. *Clin Infect Dis* (2009) 49:612–22. doi: 10.1086/603557
192. Boulougoura A, Sereti I. HIV Infection and Immune Activation: The Role of Coinfections. *Curr Opin HIV AIDS* (2016) 11:191–200. doi: 10.1097/COH.0000000000000241
193. Robinson MW, Harmon C, O'Farrelly C. Liver Immunology and its Role in Inflammation and Homeostasis. *Cell Mol Immunol* (2016) 13:267–76. doi: 10.1038/cmi.2016.3
194. Burchill MA, Golden-Mason L, Wind-Rotolo M, Rosen HR. Memory Re-Differentiation and Reduced Lymphocyte Activation in Chronic HCV-Infected Patients Receiving Direct-Acting Antivirals. *J Viral Hepat* (2015) 22:983–91. doi: 10.1111/jvh.12465
195. Rallon N, Garcia M, Garcia-Samaniego J, Rodriguez N, Cabello A, Restrepo C, et al. HCV Coinfection Contributes to HIV Pathogenesis by Increasing

Immune Exhaustion in CD8 T-Cells. *PloS One* (2017) 12:e0173943. doi: 10.1371/journal.pone.0173943
196. Gupta PK, Godec J, Wolski D, Adland E, Yates K, Pauken KE, et al. CD39 Expression Identifies Terminally Exhausted CD8+ T Cells. *PloS Pathog* (2015) 11:e1005177. doi: 10.1371/journal.ppat.1005177
197. Barrett L, Trehanpati N, Poonia S, Daigh L, Sarin SK, Masur H, et al. Hepatic Compartmentalization of Exhausted and Regulatory Cells in HIV/HCV-Coinfected Patients. *J Viral Hepat* (2015) 22:281–8. doi: 10.1111/jvh.12291
198. Martin B, Hennecke N, Lohmann V, Kayser A, Neumann-Haefelin C, Kukolj G, et al. Restoration of HCV-Specific CD8+ T Cell Function by Interferon-Free Therapy. *J Hepatol* (2014) 61:538–43. doi: 10.1016/j.jhep.2014.05.043
199. Wu X, Ishaq M, Hu J, Guo D. HCV NS3/4A Protein Activates HIV-1 Transcription From its Long Terminal Repeat. *Virus Res* (2008) 135:155–60. doi: 10.1016/j.virusres.2008.03.006
200. Kang L, Luo Z, Li Y, Zhang W, Sun W, Li W, et al. Association of Vpu With Hepatitis C Virus NS3/4A Stimulates Transcription of Type 1 Human Immunodeficiency Virus. *Virus Res* (2012) 163:74–81. doi: 10.1016/j.virusres.2011.08.011
201. Khan KA, Abbas W, Varin A, Kumar A, Di Martino V, Dichamp I, et al. HIV-1 Nef Interacts With HCV Core, Recruits TRAF2, TRAF5 and TRAF6, and Stimulates HIV-1 Replication in Macrophages. *J Innate Immun* (2013) 5:639–56. doi: 10.1159/000350517
202. Gianella S, Anderson CM, Var SR, Oliveira MF, Lada SM, Vargas MV, et al. Replication of Human Herpesviruses Is Associated With Higher HIV DNA Levels During Antiretroviral Therapy Started at Early Phases of HIV Infection. *J Virol* (2016) 90:3944–52. doi: 10.1128/JVI.02638-15
203. Garcia-Broncano P, Medrano LM, Berenguer J, González-García J, Jiménez-Sousa M, Carrero A, et al. Dysregulation of the Immune System in HIV/HCV-Coinfected Patients According to Liver Stiffness Status. *Cells* (2018) 7 (11): 196. doi: 10.3390/cells7110196
204. van Santen DK, van der Helm JJ, Touloumi G, Pantazis N, Muga R, Gunsenheimer-Bartmeyer B, et al. Effect of Incident Hepatitis C Infection on CD4+ Cell Count and HIV RNA Trajectories Based on a Multinational HIV Seroconversion Cohort. *Aids* (2019) 33:327–37. doi: 10.1097/QAD.0000000000002040
205. Potter M, Odueyungbo A, Yang H, Saeed S, Klein MB. Impact of Hepatitis C Viral Replication on CD4+ T-Lymphocyte Progression in HIV-HCV Coinfection Before and After Antiretroviral Therapy. *Aids* (2010) 24:1857–65. doi: 10.1097/QAD.0b013e32833adbb5
206. Liberto MC, Zicca E, Pavia G, Quirino A, Marascio N, Torti C, et al. Virological Mechanisms in the Coinfection Between HIV and HCV. *Mediators Inflamm* (2015) 2015:320532. doi: 10.1155/2015/320532
207. Swaminathan G, Pascual D, Rival G, Perales-Linares R, Martin-Garcia J, Navas-Martin S. Hepatitis C Virus Core Protein Enhances HIV-1 Replication in Human Macrophages Through TLR2, JNK, and MEK1/2-Dependent Upregulation of TNF-Alpha and IL-6. *FEBS Lett* (2014) 588:3501–10. doi: 10.1016/j.febslet.2014.08.009
208. Sengupta S, Powell E, Kong L, Blackard JT. Effects of HCV on Basal and Tat-Induced HIV LTR Activation. *PloS One* (2013) 8:e64956. doi: 10.1371/journal.pone.0064956
209. Lopez-Huertas MR, Palladino C, Garrido-Arquero M, Esteban-Cartelle B, Sanchez-Carrillo M, Martinez-Roman P, et al. HCV-Coinfection is Related to an Increased HIV-1 Reservoir Size in cART-Treated HIV Patients: A Cross-Sectional Study. *Sci Rep* (2019) 9:5606. doi: 10.1038/s41598-019-41788-9
210. Lorenzo-Redondo R, Fryer HR, Bedford T, Kim EY, Archer J, Pond SLK, et al. Persistent HIV-1 Replication Maintains the Tissue Reservoir During Therapy. *Nature* (2016) 530:51–6. doi: 10.1038/nature16933
211. Douek DC, Brenchley JM, Betts MR, Ambrozak DR, Hill BJ, Okamoto Y, et al. HIV Preferentially Infects HIV-Specific CD4+ T Cells. *Nature* (2002) 417:95–8. doi: 10.1038/417095a
212. Saharia KK, Koup RA. T Cell Susceptibility to HIV Influences Outcome of Opportunistic Infections. *Cell* (2013) 155:505–14. doi: 10.1016/j.cell.2013.09.045
213. Gantner P, Pagliuzza A, Pardons M, Ramgopal M, Routy JP, Fromentin R, et al. Single-Cell TCR Sequencing Reveals Phenotypically Diverse Clonally Expanded Cells Harboring Inducible HIV Proviruses During ART. *Nat Commun* (2020) 11:4089. doi: 10.1038/s41467-020-17898-8
214. Mendoza P, Jackson JR, Oliveira TY, Gaebler C, Ramos V, Caskey M, et al. Antigen-Responsive CD4+ T Cell Clones Contribute to the HIV-1 Latent Reservoir. *J Exp Med* (2020) 217(7):e20200051. doi: 10.1101/2020.01.10.902155
215. Cattin A, Wacleche VS, Fonseca Do Rosario N, Marchand LR, Dias J, Gosselin A, et al. RALDH Activity Induced by Bacterial/Fungal Pathogens in CD16(+) Monocyte-Derived Dendritic Cells Boosts HIV Infection and Outgrowth in CD4(+) T Cells. *J Immunol* (2021) 206:2638–51. doi: 10.4049/jimmunol.2001436
216. Zhong G, Kirkwood J, Won KJ, Tjota N, Jeong H, Isoherranen N. Characterization of Vitamin A Metabolome in Human Livers With and Without Nonalcoholic Fatty Liver Disease. *J Pharmacol Exp Ther* (2019) 370:92–103. doi: 10.1124/jpet.119.258517
217. Molina MF, Abdelnabi MN, Fabre T, Shoukry NH. Type 3 Cytokines in Liver Fibrosis and Liver Cancer. *Cytokine* (2019) 124:154497. doi: 10.1016/j.cyto.2018.07.028
218. Planas D, Routy JP, Ancuta P. New Th17-Specific Therapeutic Strategies for HIV Remission. *Curr Opin HIV AIDS* (2019) 14:85–92. doi: 10.1097/COH.0000000000000522
219. Kared H, Fabre T, Bédard N, Bruneau J, Shoukry NH. Galectin-9 and IL-21 Mediate Cross-Regulation Between Th17 and Treg Cells During Acute Hepatitis C. *PloS Pathog* (2013) 9:e1003422. doi: 10.1371/journal.ppat.1003422
220. Liu R, Simonetti FR, Ho YC. The Forces Driving Clonal Expansion of the HIV-1 Latent Reservoir. *Virol J* (2020) 17:4. doi: 10.1186/s12985-019-1276-8
221. Neukam K, Morano-Amado LE, Rivero-Juarez A, Mancebo M, Granados R, Tellez F, et al. HIV-Coinfected Patients Respond Worse to Direct-Acting Antiviral-Based Therapy Against Chronic Hepatitis C in Real Life Than HCV-Monoinfected Individuals: A Prospective Cohort Study. *HIV Clin Trials* (2017) 18:126–34. doi: 10.1080/15284336.2017.1330801
222. Sikavi C, Najarian L, Saab S. Similar Sustained Virologic Response in Real-World and Clinical Trial Studies of Hepatitis C/Human Immunodeficiency Virus Coinfection. *Dig Dis Sci* (2018) 63:2829–39. doi: 10.1007/s10620-018-5215-0
223. Sikavi C, Chen PH, Lee AD, Saab EG, Choi G, Saab S, et al. And Human Immunodeficiency Virus Coinfection in the Era of Direct-Acting Antiviral Agents: No Longer a Difficult-to-Treat Population. *Hepatology* (2018) 67:847–57. doi: 10.1002/hep.29642
224. Zahnd C, Salazar-Vizcaya L, Dufour JF, Müllhaupt B, Wandeler G, Kouyos R, et al. Modelling the Impact of Deferring HCV Treatment on Liver-Related Complications in HIV Coinfected Men Who Have Sex With Men. *J Hepatol* (2016) 65:26–32. doi: 10.1016/j.jhep.2016.02.030
225. Salmon-Ceron D, Nahon P, Layese R, Bourcier V, Sogni P, Bani-Sadr F, et al. Human Immunodeficiency Virus/Hepatitis C Virus (HCV) Co-Infected Patients With Cirrhosis Are No Longer at Higher Risk for Hepatocellular Carcinoma or End-Stage Liver Disease as Compared to HCV Mono-Infected Patients. *Hepatology* (2019) 70:939–54. doi: 10.1002/hep.30400
226. Lund Laursen T, Brøckner Siggard C, Kazankov K, Damgaard Sandahl T, Møller HJ, Ong A, et al. Rapid and Persistent Decline in Soluble CD163 With Successful Direct-Acting Antiviral Therapy and Associations With Chronic Hepatitis C Histology. *Scand J Gastroenterol* (2018) 53:986–93. doi: 10.1080/00365521.2018.1481996
227. Meissner EG, Wu D, Osinusi A, Bon D, Virtaneva K, Sturdevant D, et al. Endogenous Intrahepatic IFNs and Association With IFN-Free HCV Treatment Outcome. *J Clin Invest* (2014) 124:3352–63. doi: 10.1172/JCI75938
228. Hengst J, Falk CS, Schlaphoff V, Deterding K, Manns MP, Cornberg M, et al. Direct-Acting Antiviral-Induced Hepatitis C Virus Clearance Does Not Completely Restore the Altered Cytokine and Chemokine Milieu in Patients With Chronic Hepatitis C. *J Infect Dis* (2016) 214:1965–74. doi: 10.1093/infdis/jiw457
229. Serti E, Chepa-Lotrea X, Kim YJ, Keane M, Fryzek N, Liang TJ, et al. Successful Interferon-Free Therapy of Chronic Hepatitis C Virus Infection Normalizes Natural Killer Cell Function. *Gastroenterology* (2015) 149:190–200.e2. doi: 10.1053/j.gastro.2015.03.004
230. Meissner EG, Kohli A, Higgins J, Lee YJ, Prokunina O, Wu D, et al. Rapid Changes in Peripheral Lymphocyte Concentrations During Interferon-Free

Treatment of Chronic Hepatitis C Virus Infection. *Hepatol Commun* (2017) 1:586–94. doi: 10.1002/hep4.1074
231. Emmanuel B, El-Kamary SS, Magder LS, Stafford KA, Charurat ME, Poonia B, et al. Immunological Recovery in T-Cell Activation After Sustained Virologic Response Among HIV Positive and HIV Negative Chronic Hepatitis C Patients. *Hepatol Int* (2019) 13:270–6. doi: 10.1007/s12072-019-09941-8
232. Aregay A, Owusu Sekyere S, Deterding K, Port K, Dietz J, Berkowski C, et al. Elimination of Hepatitis C Virus has Limited Impact on the Functional and Mitochondrial Impairment of HCV-Specific CD8+ T Cell Responses. *J Hepatol* (2019) 71:889–99. doi: 10.1016/j.jhep.2019.06.025
233. Barili V, Fisicaro P, Montanini B, Acerbi G, Filippi A, Forleo G, et al. Targeting P53 and Histone Methyltransferases Restores Exhausted CD8+ T Cells in HCV Infection. *Nat Commun* (2020) 11:604. doi: 10.1038/s41467-019-14137-7
234. Smits M, Zoldan K, Ishaque N, Gu Z, Jechow K, Wieland D, et al. Follicular T Helper Cells Shape the HCV-Specific CD4+ T Cell Repertoire After Virus Elimination. *J Clin Invest* (2020) 130:998–1009. doi: 10.1172/JCI129642
235. Najafi Fard S, Schietroma I, Corano Scheri G, Giustini N, Serafino S, Cavallari EN, et al. Direct-Acting Antiviral Therapy Enhances Total CD4+ and CD8+ T-Cells Responses, But Does Not Alter T-Cells Activation Among HCV Mono-Infected, and HCV/HIV-1 Co-Infected Patients. *Clin Res Hepatol Gastroenterol* (2018) 42:319–29. doi: 10.1016/j.clinre.2017.11.006
236. Langhans B, Nischalke HD, Kramer B, Hausen A, Dold L, van Heteren P, et al. Increased Peripheral CD4(+) Regulatory T Cells Persist After Successful Direct-Acting Antiviral Treatment of Chronic Hepatitis C. *J Hepatol* (2017) 66:888–96. doi: 10.1016/j.jhep.2016.12.019
237. Tumino N, Casetti R, Fabbri G, Cimini E, Romanelli A, Turchi F, et al. In HIV/HCV Co-Infected Patients T Regulatory and Myeloid-Derived Suppressor Cells Persist After Successful Treatment With Directly Acting Antivirals. *J Hepatol* (2017) 67:422–4. doi: 10.1016/j.jhep.2017.03.036
238. Cai W, Qin A, Guo P, Yan D, Hu F, Yang Q, et al. Clinical Significance and Functional Studies of Myeloid-Derived Suppressor Cells in Chronic Hepatitis C Patients. *J Clin Immunol* (2013) 33:798–808. doi: 10.1007/s10875-012-9861-2
239. Marvel D, Gabrilovich DI. Myeloid-Derived Suppressor Cells in the Tumor Microenvironment: Expect the Unexpected. *J Clin Invest* (2015) 125:3356–64. doi: 10.1172/JCI80005
240. Macias J, Tellez F, Rivero-Juarez A, Palacios R, Morano LE, Merino D, et al. Early Emergence of Opportunistic Infections After Starting Direct-Acting Antiviral Drugs in HIV/HCV-Coinfected Patients. *J Viral Hepat* (2019) 26:48–54. doi: 10.1111/jvh.13003
241. Fabbri G, Mastrorosa I, Vergori A, Mazzotta V, Pinnetti C, Grisetti S, et al. Reactivation of Occult HBV Infection in an HIV/HCV Co-Infected Patient Successfully Treated With Sofosbuvir/Ledipasvir: A Case Report and Review of the Literature. *BMC Infect Dis* (2017) 17:182. doi: 10.1186/s12879-017-2287-y
242. Bachofner JA, Valli PV, Kröger A, Bergamin I, Künzler P, Baserga A, et al. Direct Antiviral Agent Treatment of Chronic Hepatitis C Results in Rapid Regression of Transient Elastography and Fibrosis Markers Fibrosis-4 Score and Aspartate Aminotransferase-Platelet Ratio Index. *Liver Int* (2017) 37:369–76. doi: 10.1111/liv.13256
243. Rial-Crestelo D, Sepúlveda MA, González-Gasca FJ, Geijo-Martínez P, Martínez-Alfaro E, Barberá JR, et al. Does Fibrosis Really Regress in HIV/hepatitis C Virus Co-Infected Patients After Treatment With Direct Antiviral Agents? *Aids* (2020) 34:427–32. doi: 10.1097/QAD.0000000000002433
244. Hamdane N, Jühling F, Crouchet E, El Saghire H, Thumann C, Oudot MA, et al. HCV-Induced Epigenetic Changes Associated With Liver Cancer Risk Persist After Sustained Virologic Response. *Gastroenterology* (2019) 156:2313–2329.e7. doi: 10.1053/j.gastro.2019.02.038
245. Perez S, Kaspi A, Domovitz T, Davidovich A, Lavi-Itzkovitz A, Meirson T, et al. Hepatitis C Virus Leaves an Epigenetic Signature Post Cure of Infection by Direct-Acting Antivirals. *PloS Genet* (2019) 15:e1008181. doi: 10.1371/journal.pgen.1008181
246. Jeyarajan AJ, Chung RT. Insights Into the Pathophysiology of Liver Disease in HCV/HIV: Does it End With HCV Cure? *J Infect Dis* (2020) 222:S802–s813. doi: 10.1093/infdis/jiaa279
247. Mudd JC, Brenchley JM. Gut Mucosal Barrier Dysfunction, Microbial Dysbiosis, and Their Role in HIV-1 Disease Progression. *J Infect Dis* (2016) 214:S58–66. doi: 10.1093/infdis/jiw258
248. Bajaj JS, Sterling RK, Betrapally NS, Nixon DE, Fuchs M, Daita K, et al. HCV Eradication Does Not Impact Gut Dysbiosis or Systemic Inflammation in Cirrhotic Patients. *Aliment Pharmacol Ther* (2016) 44:638–43. doi: 10.1111/apt.13732
249. Hong FF, Mellors JW. Changes in HIV Reservoirs During Long-Term Antiretroviral Therapy. *Curr Opin HIV AIDS* (2015) 10:43–8. doi: 10.1097/COH.0000000000000119
250. Pardons M, Baxter AE, Massanella M, Pagliuzza A, Fromentin R, Dufour C, et al. Single-Cell Characterization and Quantification of Translation-Competent Viral Reservoirs in Treated and Untreated HIV Infection. *PloS Pathog* (2019) 15:e1007619. doi: 10.1371/journal.ppat.1007619
251. Parisi SG, Andreis S, Basso M, Cavinato S, Scaggiante R, Franzetti M, et al. Time Course of Cellular HIV-DNA and Low-Level HIV Viremia in HIV-HCV Co-Infected Patients Whose HCV Infection had Been Successfully Treated With Directly Acting Antivirals. *Med Microbiol Immunol* (2017) 206:419–28. doi: 10.1007/s00430-017-0518-x
252. Schaefer CJ, Kossen K, Lim SR, Lin JH, Pan L, Bradford W, et al. Danoprevir Monotherapy Decreases Inflammatory Markers in Patients With Chronic Hepatitis C Virus Infection. *Antimicrob Agents Chemother* (2011) 55:3125–32. doi: 10.1128/AAC.00131-11
253. Balagopal A, Smeaton LM, Quinn J, Venuto CS, Morse GD, Vu V, et al. Intrahepatic Viral Kinetics During Direct-Acting Antivirals for Hepatitis C in HIV Co-Infection:The ACTG A5335S Substudy. *J Infect Dis* (2020) 222(4):601–10. doi: 10.1093/infdis/jiaa126
254. Sung PS, Lee EB, Park DJ, Lozada A, Jang JW, Bae SH, et al. Interferon-Free Treatment for Hepatitis C Virus Infection Induces Normalization of Extrahepatic Type I Interferon Signaling. *Clin Mol Hepatol* (2018) 24:302–10. doi: 10.3350/cmh.2017.0074
255. Van der Sluis RM, Zerbato JM, Rhodes JW, Pascoe RD, Solomon A, Kumar NA, et al. Diverse Effects of Interferon Alpha on the Establishment and Reversal of HIV Latency. *PloS Pathog* (2020) 16:e1008151. doi: 10.1371/journal.ppat.1008151
256. Selliah N, Zhang M, DeSimone D, Kim H, Brunner M, Ittenbach RF, et al. The Gammac-Cytokine Regulated Transcription Factor, STAT5, Increases HIV-1 Production in Primary CD4 T Cells. *Virology* (2006) 344:283–91. doi: 10.1016/j.virol.2005.09.063
257. Bruner KM, Murray AJ, Pollack RA, Soliman MG, Laskey SB, Capoferri AA, et al. Defective Proviruses Rapidly Accumulate During Acute HIV-1 Infection. *Nat Med* (2016) 22:1043–9. doi: 10.1038/nm.4156

Conflict of Interest: The authors declare that the research was conducted in the absence of any commercial or financial relationships that could be construed as a potential conflict of interest.

Publisher's Note: All claims expressed in this article are solely those of the authors and do not necessarily represent those of their affiliated organizations, or those of the publisher, the editors and the reviewers. Any product that may be evaluated in this article, or claim that may be made by its manufacturer, is not guaranteed or endorsed by the publisher.

frontiers in Immunology

ORIGINAL RESEARCH
published: 31 August 2021
doi: 10.3389/fimmu.2021.720697

The Effect of JAK1/2 Inhibitors on HIV Reservoir Using Primary Lymphoid Cell Model of HIV Latency

*Lesley R. de Armas[1], Christina Gavegnano[2,3,4], Suresh Pallikkuth[1], Stefano Rinaldi[1], Li Pan[1], Emilie Battivelli[5,6,7], Eric Verdin[5,6,7], Ramzi T. Younis[8], Rajendra Pahwa[1], Siôn L. Williams[9], Raymond F. Schinazi[4] and Savita Pahwa[1]**

[1] Department of Microbiology and Immunology, University of Miami Miller School of Medicine, Miami, FL, United States, [2] Department of Pathology and Experimental Medicine, Emory University and Children's Healthcare of Atlanta, Atlanta, GA, United States, [3] Department of Pharmacology and Chemical Biology, Emory University and Children's Healthcare of Atlanta, Atlanta, GA, United States, [4] Center for AIDS Research, Department of Pediatrics, Emory University and Children's Healthcare of Atlanta, Atlanta, GA, United States, [5] Gladstone Institute of Virology and Immunology, Gladstone Institutes, San Francisco, CA, United States, [6] Department of Medicine, University of California San Francisco, San Francisco, CA, United States, [7] Buck Institute for Research on Aging, Novato, CA, United States, [8] Department of Otolaryngology, University of Miami Miller School of Medicine, Miami, FL, United States, [9] Department of Neurology, University of Miami Miller School of Medicine, Miami, FL, United States

OPEN ACCESS

Edited by:
Sunil Kannanganat Sidharthan, Baylor College of Medicine, United States

Reviewed by:
Shetty Ravi Dyavar, University of Nebraska Medical Center, United States
Sivasankaran M. Ponnan, Indian Institute of Science (IISc), India

***Correspondence:**
Savita Pahwa
spahwa@med.miami.edu

Specialty section:
This article was submitted to Viral Immunology, a section of the journal Frontiers in Immunology

Received: *04 June 2021*
Accepted: *13 August 2021*
Published: *31 August 2021*

Citation:
de Armas LR, Gavegnano C, Pallikkuth S, Rinaldi S, Pan L, Battivelli E, Verdin E, Younis RT, Pahwa R, Williams SL, Schinazi RF and Pahwa S (2021) The Effect of JAK1/2 Inhibitors on HIV Reservoir Using Primary Lymphoid Cell Model of HIV Latency. Front. Immunol. 12:720697. doi: 10.3389/fimmu.2021.720697

HIV eradication is hindered by the existence of latent HIV reservoirs in $CD4^+$ T cells. Therapeutic strategies targeting latent cells are required to achieve a functional cure, however the study of latently infected cells from HIV infected persons is extremely challenging due to the lack of biomarkers that uniquely characterize them. In this study, the dual reporter virus HIV_{GKO} was used to investigate latency establishment and maintenance in lymphoid-derived $CD4^+$ T cells. Single cell technologies to evaluate protein expression, host gene expression, and HIV transcript expression were integrated to identify and analyze latently infected cells. FDA-approved, JAK1/2 inhibitors were tested in this system as a potential therapeutic strategy to target the latent reservoir. Latent and productively infected tonsillar $CD4^+$ T cells displayed similar activation profiles as measured by expression of CD69, CD25, and HLADR, however latent cells showed higher CXCR5 expression 3 days post-infection. Single cell analysis revealed a small set of genes, including *HIST1*-related genes and the inflammatory cytokine, *IL32*, that were upregulated in latent compared to uninfected and productively infected cells suggesting a role for these molecular pathways in persistent HIV infection. *In vitro* treatment of HIV-infected $CD4^+$ T cells with physiological concentrations of JAK1/2 inhibitors, ruxolitinib and baricitinib, used in clinical settings to target inflammation, reduced latent and productive infection events when added 24 hr after infection and blocked HIV reactivation from latent cells. Our methods using an established model of HIV latency and lymphoid-derived cells shed light on the biology of latency in a crucial anatomical site for HIV persistence and provides key insights about repurposing baricitinib or ruxolitinib to target the HIV reservoir.

Keywords: HIV, latency, tonsil, scRNAseq, JAK-STAT signaling pathway, LRA (latency reversing agent)

INTRODUCTION

The latent HIV reservoir is defined as cells carrying integrated, replication-competent provirus that do not express viral transcripts or proteins (1). $CD4^+$ T cells are recognized as the predominant cellular refuge for the latent HIV reservoir; specifically resting memory cells have been shown to be enriched in HIV provirus compared to other $CD4^+$ T cell subsets, however cells from the myeloid lineage can also be infected by HIV and contribute to persistence of latency (2–4). Studies of antiretroviral therapy (ART) initiation during acute infection in humans and non-human primates (NHP) have shown that the latent reservoir is established very early following HIV infection (5, 6). This is likely due to the ability of latently infected cells to distribute throughout the tissues with a higher viral burden detected in the gut, lymph nodes, and CNS relative to peripheral blood (7–9).

The persistence of latent HIV reservoirs despite effective ART remains the largest barrier to the cure of HIV/AIDS (10–12). Many technical challenges contribute to the difficulties in studying latent HIV infection. First, in patients under ART suppression latently infected cells are present at very low frequencies in the blood with estimates at 1-1,000 per million $CD4^+$ T cells (13, 14). Second, despite this being an area of intense research that has generated several candidate markers including CD32a, CD30, PD-1, Lag-3, Tigit, and CD127 (15–21), there are no validated phenotypic biomarkers to distinguish latently infected from uninfected cells. Third, the majority of latent HIV genomes detected in ART-treated subjects are defective and will not produce infectious virions upon viral reactivation (i.e., transcription) (22). Finally, the two methods generally accepted for quantifying the replication-competent HIV reservoir, quantitative viral outgrowth assay (QVOA) (22) and intact proviral DNA assay (IPDA) (13), do not allow for direct interrogation of latently-infected cells and thereby hinder the discovery of biomarkers and the study of mechanisms governing latency. These stringencies limit our ability to apply mechanistic pharmacological intervention studies, with a goal of understanding the direct impact of an agent on the replication competent reservoir, which is sentinel towards informed translational research that can be applied towards human studies in the cure space.

To overcome the hurdle of trying to study extremely rare latently infected $CD4^+$ T cells *in vivo*, *in vitro* models have been generated (23–25). Primary $CD4^+$ T cell models are especially useful and easily established using cells from HIV negative donors. A widely used model for HIV latency involves selection of resting $CD4^+$ T cells (negative for expression of T cell activation markers CD69, HLADR, CD25) that have been stimulated with CCR7 ligands to support viral integration with limited viral replication (24, 26–28). Primary cell models use *in vitro* infection with HIV viruses of varying subtypes (e.g. B or C) and envelope tropism (29) and assess infection efficiency through the use of Gag p24 detection or fluorescent reporter expression indicating productive infection. Unfortunately, latently infected cells are still undetectable using these techniques and the approach given this limitation is to allow confirmed infected cells (e.g., GFP^+) ample time in culture (2-8 weeks) to silence HIV transcription and convert from productive to latent (25, 30).

On the other hand, dual reporter viral constructs allow for direct and simultaneous detection of HIV infected cells at different stages (i.e., latent and productive). HIV_{GKO} is a second-generation dual reporter virus and features eGFP marker under the control of the HIV LTR promoter and a Kusabira Orange 2 (mKO2) fluorescent marker under the control of the host elongation factor 1a (EF1α) promoter (31–35). Given the propensity for HIV infected cells to be recovered from lymphoid tissues (7, 36–38), we used HIV_{GKO} to investigate latency establishment and maintenance in lymphoid-derived, tonsillar $CD4^+$ T cells. Using this system, we were able to integrate datasets from single cell technologies to evaluate protein expression, host gene expression, and HIV transcript expression to characterize latently infected cells.

Finally, we used this tool to test reactivation of latency and FDA-approved JAK1/2 inhibitors as a therapeutic intervention for silencing HIV transcription. The FDA-approved JAK1/2 inhibitor ruxolitinib was recently evaluated in an AIDS Clinical Trial Group multi-site Phase 2a study (A5336), and demonstrated safety and efficacy in virally suppressed people living with HIV, including a significant decrease in key markers associated with HIV persistence including HLA-DR/CD38, CD25, and sCD14, as well as cellular/reservoir lifespan marker Bcl-2 (39). Baricitinib is a second-generation orally bioavailable JAK1/2 inhibitor that has an improved safety profile *versus* ruxolitinib, is approved for chronic long-term use in adults and children as young as two years of age (Olumiant.com). *In vitro*, ruxolitinib treatment of HIV-infected $CD4^+$ T cells inhibits virus production, STAT5 phosphorylation, homeostatic proliferation, and Bcl-2 downregulation (40). These findings prompted us to explore the ability of the second-generation JAK1/2 inhibitor baricitinib to target the latent reservoir directly.

METHODS

Specimen Collection

Tonsil samples were obtained from HIV-negative children and adolescents during elective tonsillectomy for sleep apnea at University of Miami Hospitals with informed consent. Single cell suspensions of mononuclear cells were isolated from tonsil tissue by mechanical separation and then filtered through a 70-micron filter in RPMI 1640 (Gibco) as described previously (41). Mononuclear cells were cryopreserved in FBS containing 20% DMSO and stored in liquid nitrogen freezers.

Virus Production

Plasmid DNA for the dual reporter viral construct, HIV_{GKO}, was obtained from Eric Verdin and Emilie Battivelli (Gladstone Institute, UCSF) and the dual tropic envelope construct was obtained through the NIH HIV Reagent Program, Division of AIDS, NIAID, NIH: Plasmid pSVIII Expressing HIV-1 92HT593.1 gp160, ARP-3077, contributed by Dr. Beatrice Hahn. Plasmids were transformed in chemically competent

E. coli and plasmid DNA was expanded and isolated using Maxi-Prep (Qiagen) reagent according to manufacturer's instructions. 293FT cell lines (Invitrogen) were used to produce virus particles and were cultured in DMEM (containing 4,500 mg/L D-glucose no L-glutamine or sodium pyruvate) supplemented with 10% (v/v) FBS, 4 mM of L-glutamine, 110 mg/L (1mM) sodium pyruvate and 1% penicillin/streptomycin. Cells were transfected with both plasmids when culture flasks showed 90-95% confluency. 24 hours before transfection the culture media was changed for antibiotic-free media. Briefly, plasmid DNA was diluted in Opti-Mem media (Invitrogen) at a ratio of 1.8:1 (HIV_{GKO}: pSVIII) before mixing with Lipofectamine 2000 Transfection Reagent (Invitrogen) according to the manufacturer's instructions. The day after transfection (32-36 hr post-transfection) the supernatant was removed and replaced with fresh antibiotic-free media. The following morning, viral supernatants were harvested into 50ml tubes and centrifuged at 1000*g* for 4 min to remove cellular debris. The supernatants were filtered through a 0.45μM low protein binding filter and loaded into ultracentrifuge tubes. Virus was concentrated by ultracentrifugation (27,000*g* at 4C for 2.3 hr), resuspended by trituration in antibiotic-free DMEM medium, aliquoted, and stored at -80°C. Viral titers were quantified using p24 ELISA kits (Perkin Elmer).

In Vitro Infection With HIV_{GKO}

Cryopreserved tonsil mononuclear cells were thawed and cultured in complete medium RPMI (Invitrogen) supplemented with 10% FBS, L-glutamine, and Penicillin/Streptomycin overnight. $CD4^+$ T cells were purified using EasySep™ Human $CD4^+$ T cell enrichment kit (StemCell Technologies) by negative selection. Purified $CD4^+$ T cells were cultured at a concentration of 2-5 million/mL of complete medium and activated using soluble anti-CD3 (1 μg/mL) and anti-CD28 (1ug/ml) antibodies for 3 days in a 37°C, 5%CO_2 incubator. Activated $CD4^+$ T cells were infected with HIV_{GKO} (100 ng p24/million cells) by spinoculation at 1,200*g* for 2.2 hr. Cell pellets were resuspended in complete medium containing IL-2 (30 U/mL, Peprotech) and cultured until further analysis.

Flow Cytometry Acquisition and Sorting

For phenotypic analysis of HIV_{GKO} infected cells by flow cytometry, cells were labeled using fluorochrome-conjugated monoclonal antibodies against CD4, CD45RO, CD69, HLADR, CD25, PD-1, and CXCR5 as previously described (42) (see **Supplemental Table 1** for Ab details). Cells were also labeled with violet live/dead stain (VIVID, Molecular Probes) for dead cell exclusion and acquired on LSRII (Becton Dickinson) or SH800 Sorter (Sony). Flow cytometry data was analyzed using FlowJo (Version 10.7.1, TreeStar). Gating for productive and latent cell populations were based off of mock-infected sample (as shown in **Figure 1C**). Gating for cell surface markers were determined using unstained control samples to define negative gates. At the time of panel validation, FMO (fluorescence minus one) controls were used to define compensation parameters and compatibility of the different markers. Additionally, all antibodies were titrated for optimal concentration for labeling.

Single Cell 3' Whole Transcriptome Amplification by BD Precise Assay

Single cell sorting was performed using the Sony SH800 instrument and 'single cell' sorting mode and 100uM chip. Individual cells were sorted into each well of BD Precise Assay 96 well plates based on gating for productive, latent,

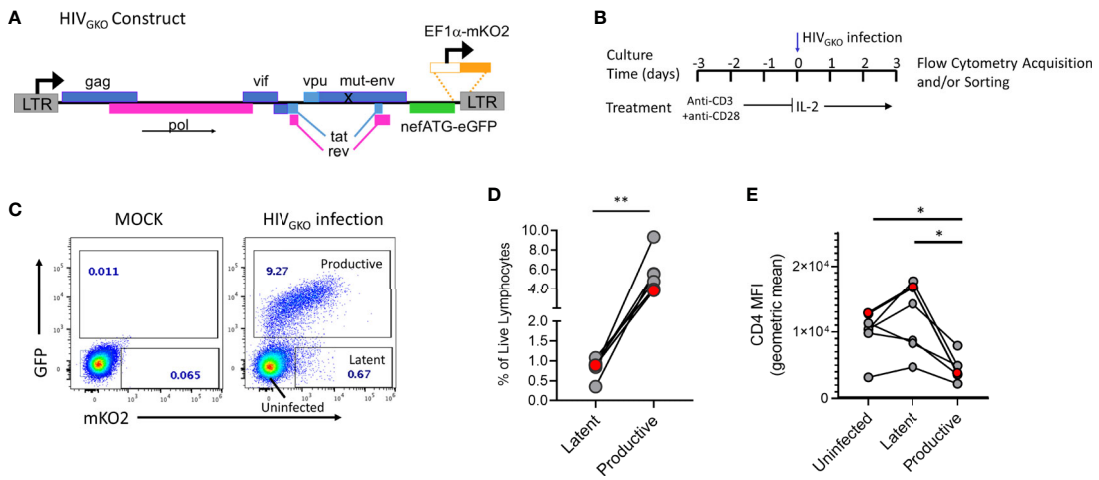

FIGURE 1 | HIV_{GKO} infection in tonsil derived $CD4^+$ T cells. **(A)** HIV_{GKO} viral construct showing mutated *env* gene, *nef* gene replaced by an eGFP reporter, and insertion of EF1a promoter directly upstream of mKO2 reporter. **(B)** Schematic showing experimental design for activation and infection with HIV_{GKO} of purified tonsillar $CD4^+$ T cells. **(C)** Representative flow plot showing expression of dual fluorescent reporters from HIV_{GKO} on day 3 post-infection. **(D)** Summary data from 6 tonsil donors with frequency of productive and latent infected cells based on gating shown in panel **(C)**. **(E)** Mean fluorescent intensity of cell surface protein expression for CD4 on cells infected with HIV_{GKO} on day 3 post-infection. Red data points in panels D and E indicate the individual donor used for single cell analyses in single cell RNA Seq experiments. Paired t test was performed to compare Uninfected, Latent, and Productive cell populations, *p < 0.05, **p < 0.01.

or uninfected cells as shown in **Figure 1A**. Immediately after sorting the plate was centrifuged at 1,000*g* for 5 min and stored at -80°C until library preparation was performed. Next-generation sequencing (NGS) library preparation was performed according to manufacturer's instructions for BD Precise Assays for patented BD™ Molecular Indexing (MI) technology with Sample Index (SI) to label individual mRNA transcripts. Briefly, during reverse transcription, the BD Precise assay applies a non-depleting pool of 65,536 barcodes termed molecular indexes (MI) for stochastic and unique labeling of mRNA transcripts. In addition to MI, a second set of barcodes (sample index, SI) are employed to identify the sample origin of each transcript according to the well position in the 96-well plate. Barcoded primers are then used to label polyadenylated RNA transcripts in each of the 96 wells, followed by a pooling step into a single tube. The resulting library was then input onto Illumina MiSeq sequencer using the appropriate sequencing kits. Each of the sequencing reads were processed to identify the MI, SI and target gene using BD primary analysis pipeline. To mitigate the effect of over-estimation of molecules from PCR and sequencing errors, the BD analysis pipeline contains Molecular Identifier (MI) adjustment algorithms recursive substitution error correction (RSEC) and distribution-based error correction (DBEC). A gene is subjected to DBEC if it meets a certain threshold for sequencing depth. If a gene passes the threshold for DBEC, the status is pass. If a gene does not pass, the status is low depth. If a gene has zero counts across all cells, the status is not detected. The MI counts detected in each plate showed comparable and similar distribution of Pass and Low Depth (see *Methods*) transcripts (**Supplemental Figure 1**). scRNA Seq data was also analyzed based on fluorescent classifications of infection status and showed comparable MI counts. Blank wells generated at the time of sorting had low MI counts compared to cell-containing wells recognizing a couple hundred genes (compared to ~17,000 for cell-containing wells) across 15 blank wells but with very low read counts per gene ≤ 3.

RT-PCR for IL32 Expression

Bulk sorting of productive, latent, and uninfected cells were sorted according to gating shown in **Figure 1C**. Cells (500) were sorted directly into CellsDirect one-step qRT-PCR reagents (Invitrogen) including primers for IL32 and GAPDH (Taqman Assay 1:100, ABI), 2x CellsDirect reaction mix, water, and SuperScript® III Reverse Transcriptase and Platinum® Taq DNA Polymerase. Eighteen cycles of pre-amplification were performed as previously described (43). The resulting cDNA was analyzed in standard Taqman qRT-PCR to assess gene transcript levels for IL32 and GAPDH. Relative quantification was performed by calculating ddCT values.

Cell Sorting and HIV Reactivation Assay

Purified $CD4^+$ T cells were infected with HIV_{GKO} as described above. On day 5 post-infection, cells were labeled with live/dead (VIVID) stain and GFP negative, latent cell-enriched gated population was sorted in purity mode using Sony SH800 sorter. The sorting gate contained ~10% of latent cells by fluorescent reporter expression (mKO2+GFP-) and the rest were uninfected (GFP-). Cells were collected in complete medium (R10), centrifuged, and resuspended in fresh medium and divided equally into 4 wells of a 96 well plate with approximately 10^4 cells/well in 150ul of R10. The cells rested overnight in presence or absence of physiologically relevant concentrations of (0.1, 1, and 10 μM) baricitinib (Selleck chemicals) before addition of LRA (1 μg/mL each of anti-CD3 and anti-CD28). Two days after LRA treatment, cells were stained for live/dead (VIVID) and acquired on Sony SH800 sorter to assess GFP and mKO2 expression for at least 25,000 cells (events). Flow cytometric data were analyzed using FlowJo version 10.7.1.

Statistical Analysis

Single cell gene expression analysis was performed using R fluidigmSC package from SINGuLAR™ Analysis Toolset which is designed specifically for single-cell studies of gene expression profiles. Pathway analysis was performed using QIAGEN Ingenuity Pathway Analysis, foldchange cutoff is 1.5, p value cutoff 0.05.

Study Approval

This study was approved by the Institutional Review Boards of University of Miami and was conducted in accordance with approved guidelines (IRB# 20140200/CR00004416). Voluntary signed informed consent was obtained from every participant prior to participating in the study.

RESULTS

Latency Is Established Early Following HIV_{GKO} Infection of Tonsil-Derived $CD4^+$ T Cells

To identify and study latently infected lymphoid-derived cells, we performed *in vitro* infection of tonsillar $CD4^+$ T cells from HIV negative donors using the lentiviral vector HIV_{GKO} (**Figure 1A**), pseudo-typed with an X4/R5 dual tropic HIV-1 envelope subtype B. In this model, purified $CD4^+$ T cells are TCR-activated prior to infection with HIV_{GKO} and evaluated 3 days after infection by flow cytometry to assess frequencies of productive and latent infected cells (**Figure 1B**). GFP and mKO2 expression were used to distinguish between the different populations compared to a mock-infected control (**Figure 1C**). mKO2 expression driven by the host-derived EF1α promoter activity in the cell nucleus signals the presence of an integrated viral genome in the cell, thus mKO2 expression in the absence of GFP expression defines the latently infected cell population in this system. GFP-expressing cells were considered productively infected though expression of mKO2 was variable, due to fluctuating expression of the EF1α promoter (44). HIV_{GKO} infection consistently established latent infection (GFP-mKO2+) in purified $CD4^+$ T cells from different tonsil donors (**Figure 1D**). However, latent infection was always established at lower frequencies compared to productive infection (GFP+) (mean 0.83% *vs* 5.5%, respectively). Productive cells infected with HIV_{GKO} also exhibited reduced CD4 expression

compared to latent and uninfected cells (**Figure 1E**) (mean CD4 MFI: productive 4,533 *vs* 11,747 and 9,633 for latent and uninfected, respectively).

CD4$^+$ T Cells With Latent Infection Can Exhibit Similar Activation Profiles as Productive Infected Cells

To characterize the cells harboring latent virus in lymphoid CD4$^+$ T cells generated in the HIV$_{GKO}$ model, surface expression of memory and activation markers 3 days after infection were assessed by flow cytometry. Productive, Latent, and uninfected cells were assessed for expression of CD45RO, CD69, HLADR, and CD25. Infected cells were enriched in the CD45RO$^+$ fraction compared to total cells, though a small fraction of infected cells were CD45RO negative (**Figure 2A** and **Supplemental Table 2**). To test the hypothesis that latent infection was the result of a transition from activated to resting state (23, 33, 45) we reasoned that productive-infected cells should have higher expression of activation markers compared to latent. However, expression of activation markers was variable on infected cells with no apparent enrichment or preference for expression of a particular marker on productive *vs.* latent cells (**Figure 2B**). T follicular helper cells (Tfh) have been shown to harbor replication competent virus in lymph nodes (8, 46), thus we assessed markers for Tfh phenotype, CXCR5 and PD-1 to determine if there was any preference for latency establishment within this subset. There was donor variation in the infection efficiency within the Tfh population (CXCR5^{hi}PD-1^{hi}), however evaluation of MFI of each marker individually showed that latent infected cells had higher CXCR5 MFI compared to productive and uninfected ($p < 0.05$) (**Figure 2C**). This association was not observed for PD-1.

Using Single-Cell RNASeq to Discover Potential Biomarkers of Latency

An important advantage of the HIV$_{GKO}$ is that using FACS sorting, mKO2$^+$ cells can be isolated without the need for virus reactivation providing a rich source of unperturbed latent cells to study gene expression and identify potential biomarkers of latency. For single cell gene expression studies, we selected one tonsil donor for downstream single cell RNA Seq analysis (donor highlighted in red datapoints in **Figures 1D, E**) in an effort to eliminate donor variation in the subsequent gene expression data. To generate RNA Seq data, we employed a plate-based platform for scRNA Seq (BD^{TM} Precise assay) to the HIV$_{GKO}$ latency model and performed whole transcriptome amplification (WTA) from a total of 462 cells from five 96-well plates across three independent experiments using a single tonsil donor. Each plate contained equal numbers of productive, latent, and uninfected cells as determined by gating using expression of the fluorescent reporters, GFP and mKO2 (index sorting data shown in **Supplemental Figure 2**). GFP$^+$ cells had varying expression of mKO2, suggesting differential activity of the EF1α promoter in this model, therefore, to exclude effects related to EF1α activity only productive cells with mKO2 expression matching that of latent cells were sorted.

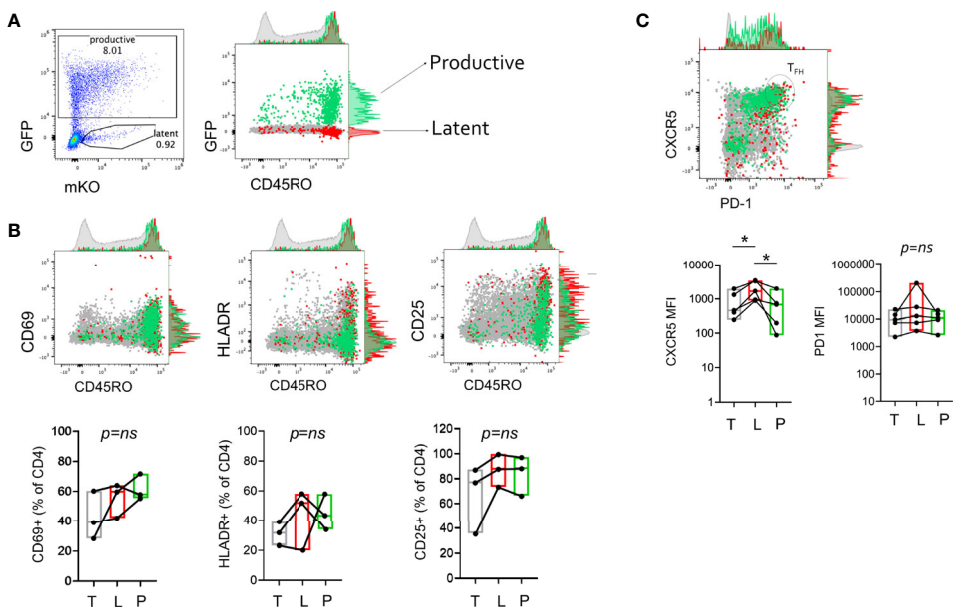

FIGURE 2 | Cellular activation and differentiation marker expression on productive and latent infected CD4$^+$ T cells. **(A)** Measurement of memory marker CD45RO expression on productive (P, GFP+, green), Latent (L, GFP-mKO+, red), and total (T, light gray) CD4$^+$ T cells 3 days post-infection with HIV$_{GKO}$. **(B)** Representative plots showing expression of activation markers (CD69, HLADR, CD25) and CD45RO expression on productive, latent, and total cells. **(C)** Representative plot showing expression of TFH markers, CXCR5 and PD-1 on productive, latent, and total cells. CXCR5^{hi}PD-1^{hi} cells define TFH population. Box and whisker plots show data from 3-5 independent experiments (individual tonsil donors). Paired t-test analysis was performed to determine differences between the groups, *$p < 0.05$, ns, not significant.

We first evaluated specific genes related to T cell activation and T helper subset differentiation within each of the sorted populations (**Supplemental Figure 3**). Transcripts for CD69 and HLADR proteins had higher expression in productive cells and expression decreased with the level of HIV transcript expression (i.e. productive>latent>uninfected). Genes related to cytokine and transcription factor expression for Th1 (*TBX21, IFNG*) and Th2 (*GATA3, IL13*) type cells did not show enrichment for either sorted population, however the Th17 transcription factor *RORC* was increased in productive compared to uninfected cells with a trend toward increased expression with greater HIV transcript expression.

To confirm the presence (or absence) of HIV transcription in the HIV_{GKO} infected cells, we aligned scRNA Seq data against the HIV_{GKO} sequence to assess expression of open reading frames (ORF) for gag, pol, tat, rev, vpr, and env genes in sorted single cells (**Figure 3A**). Productive cells expressed highest HIV transcripts per cell (median 38.5) as expected by high levels of LTR-driven GFP reporter expression (**Figure 3A**). Latent infected cells had a median of 1.5 HIV transcripts per cell, however, we observed a fraction of cells with HIV transcript levels matching GFP^+ population (22.7% with >6 MI/cell). Overall, the majority of uninfected and latent cells exhibited HIV transcript levels below the cutoff established by analysis of blank wells (no sorted cell). Desiring to have pure populations of uninfected, latent, and productive cells for gene expression analysis, we re-classified and grouped single cells on the basis of fluorescent reporter expression and HIV transcript levels (**Figure 3B**).

We performed differential gene expression analysis between 1) Uninfected HIV transcript negative (U-neg) and Latent HIV transcript negative (L-neg), 2) L-neg and Latent HIV transcript low+ (L+), 3) L-neg and Productive HIV transcript++ (P++), and 4) L+ and P++ (**Figure 3C**). The number of DEGs was highest in the comparisons of latent populations (L-neg and L+) *vs* productive with 164 and 203 DEGs respectively, while 110 DEGS from each comparison were overlapping (**Supplemental Data 1**). However, pathway analysis demonstrated that despite having several unique DEGs, the pathways involved were similar when comparing latent *vs* productive (**Figure 3D** and **Supplemental Data 2**). Enriched pathways included Sirtuin Signaling, Oxidative Phosphorylation, Mitochondrial Dysfunction, and EIF2 Signaling. In line with this observation, the contrast of gene expression between L-neg and L+ resulted in only 15 DEGs, exhibiting the high degree of similarity between the two populations (**Figure 3C**).

Gene Profiles in Latent Infected Lymphoid $CD4^+$ T Cells

We were specifically interested in the latent-infected cells and identifying a gene signature that could discriminate them from uninfected cells. To this end, we identified 24 genes with differential expression in latent *vs* uninfected cells, all of which

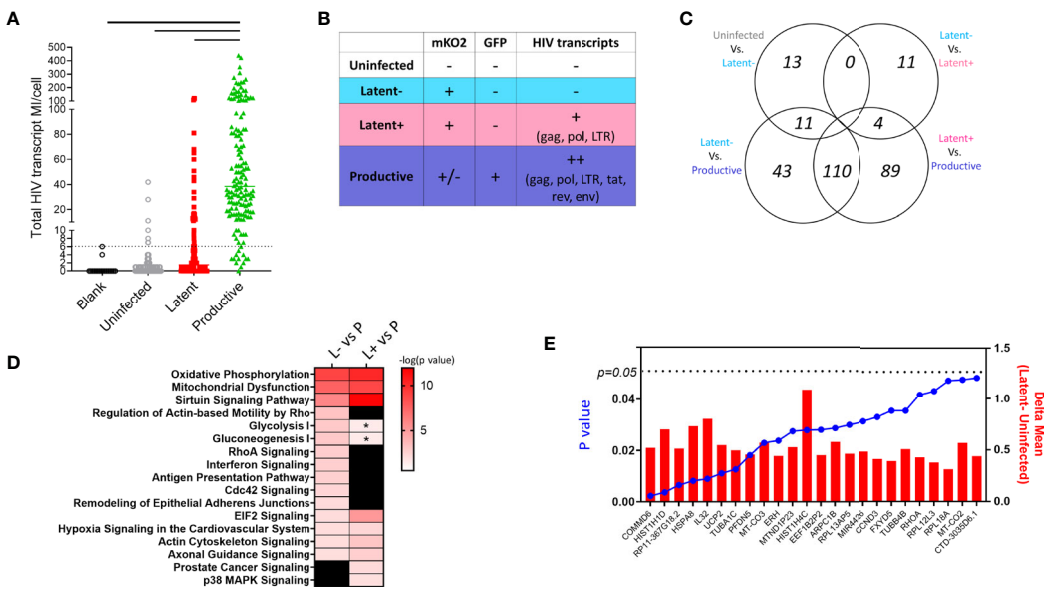

FIGURE 3 | Single cell RNA Seq in HIV_{GKO} model of latency. **(A)** HIV transcript MI counts per cell in each sorted cell type. Dotted line is cutoff for background levels of transcript expression based on blank control wells in which no cells were sorted. Solid lines indicate significant difference between productive cells and all other groups using ANOVA one-way test with multiple comparisons ($p < 0.05$). **(B)** Schematic showing cell characterization based on fluorescent reporter and HIV transcript expression. **(C)** Venn diagram showing number of differentially expressed genes between the cell populations defined in **(B)**. **(D)** Heatmap showing shared enriched pathways between Latent cell populations and productive cells. Colored boxes indicate significant pathways $p < 0.01$, * indicates pathways with $p < 0.05$ and > 0.01. **(E)** Bar graph showing the difference in average expression of each DEG between Latent and Uninfected cells with p values from ANOVA analysis shown as a super-imposed line graph (blue).

were upregulated in L-neg (**Figure 3E**). The genes were involved in protein folding (HSPA8, TUBA1C, TUBB4B, PFDN5), protein targeting/viral gene expression (RPS19, RPL18A, RPL31, RPL39), and respiratory electron transport chain (UCP2, UCP3, MT-CO2, MT-CO3) (**Supplemental Figure 4**, Genemania network analysis). We interrogated this short list of DEGs to identify 11/24 genes that exhibited enriched expression in latent cells relative to both uninfected and productive populations, indicating a potential biomarker of latency (**Figure 4A**). As a control we evaluated gene expression for EF1α (EEF1A) in each of the populations and confirmed there were no significant differences in the groups. Co-expression analysis showed strong correlation coefficients between most of the genes indicating a common pathway involving histone modification and electron transport, however *HSP8* and especially *IL32* showed low co-expression with the other genes suggesting these two genes were not related to the common pathway (**Figure 4B**, **Supplemental Figure 5**). We confirmed by RT-PCR in sorted populations (uninfected, latent, productive) that *IL32* was upregulated in latent compared to uninfected cells (**Figure 4C**).

Reactivation of Latency in HIV_{GKO} Infected Cells and Therapeutic Intervention With JAK1/2 Inhibitors

In addition to biomarker discovery, the major utility of a primary HIV latency model is to test therapeutic strategies targeting the latent reservoir, such as JAK1/2 inhibitors. Exogenous addition of ruxolitinib or baricitinib, to HIV_{GKO} infected cells reduced frequencies of productive (GFP^+) and latent ($GFP\text{-}mKO2^+$) infected cells in a dose-dependent manner with the strongest effects observed at the 10 μM concentration (**Figures 5A, B**). Molecular JAK1/2 inhibition also resulted in dose-dependent downregulation of activation markers on $CD4^+$ T cells (**Figure 5C**). CD25 expression was reduced by >80% at the highest concentration of ruxolitinib and baricitinib, while HLADR and CD69 exhibited a reduction of 60% and 50%, respectively, with both drugs (**Figure 5D**).

The approved dose for chronic long-term use of baricitinib is 2 mg (USA), or 2 and 4 mg (Japan, other non USA jurisdictions), and 4 mg is approved for hospitalized COVID-19 patients (OLUMIANT.COM, covid19treatmentguidelines.nih.gov). The plasma concentrations for both doses of baricitinib fall within

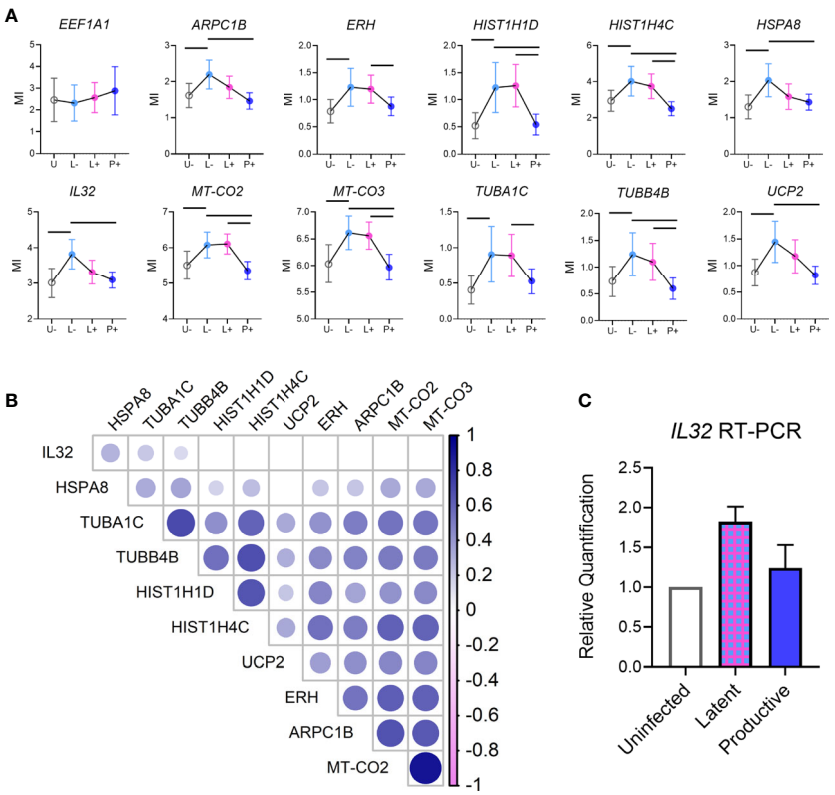

FIGURE 4 | Unique gene signature in latent cells. **(A)** Individual graphs showing mean (error bars indicate 95% Confidence Interval) expression of each of the genes identified in Differentially Expressed Gene analysis between Latent cells and other infected populations (from **Figures 3B, C**). EEF1A1 expression (gray box, top left) was used as a control for EF1α promoter activity in cells. **(B)** Correlation matrix showing the co-expression of each of the genes from **(A)** on a single cell level. Color intensity is associated with the spearman correlation coefficient and the size of circle is related to the p value (larger circle, smaller p value). **(C)** Validation of IL32 expression in bulk sort-purified cells from 2 donors by RT-PCR.

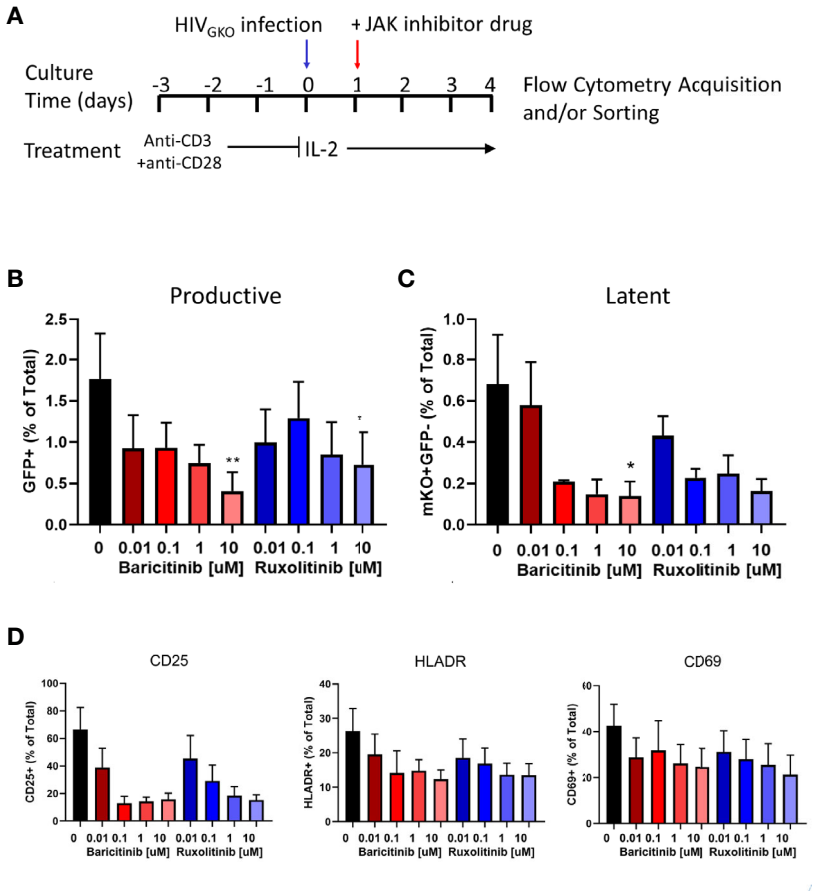

FIGURE 5 | Effect of JAK1/2 inhibitors on productive and latent infection. **(A)** Schematic showing experimental design for activation and infection with HIV$_{GKO}$ of purified tonsillar CD4$^+$ T cells. Bar graphs showing average frequency of **(B)** GFP$^+$ (productive) cells and **(C)** mKO+GFP- (latent) cells on day 4 post-infection in presence of JAK1/2 inhibitors at different concentrations. Error bars represent standard error of the mean (SEM), students t test was used to compare all conditions against the no drug control (black bar), *p < 0.05, **p < 0.01. **(D)** Bar graphs showing average frequency of cells expressing activation markers on day 4 post-infection in presence of JAK1/2 inhibitors at different concentrations. Results shown represent 3 independent experiments.

the range to effectively block both productive and latent infection in our single round replication HIV$_{GKO}$ model (**Figure 6A**). Ruxolitinib is not approved for chronic long-term use, but approved doses range within 10-25 mg (**Figure 6B**). Only the higher dose of ruxolitinib fell within plasma concentration ranges to block both productive and latent infection. Baricitinib demonstrates ~ half a log greater potency for both assays *versus* ruxolitinib (summarized in **Figure 6C**).

Finally, we designed an experiment to evaluate reactivation from latency using HIV$_{GKO}$ infected cells as shown in **Figure 7A**. At day 3 post infection, GFP negative cells were sorted (**Figure 7B**) and cultured with or without baricitinib at different concentrations for 24 hours prior to TCR stimulation as a latency reversing agent (LRA). In the absence of drug and TCR stimulus *via* anti-CD3/anti-CD28, spontaneous reactivation was observed indicated by the presence of GFP$^+$ cells. HIV reactivation above the level of spontaneous reactivation was observed in the presence of LRA, however pretreatment of cells with baricitinib abrogated the response with the greatest effect occurring at the highest concentration of drug (**Figures 7C, D**).

DISCUSSION

Primary models of HIV latency are important to enable research into mechanisms of HIV establishment and maintenance. The use of the dual reporter virus HIV$_{GKO}$ in our study and others (31, 34, 35, 47) have validated that this model recapitulates multiple aspects of latent HIV infection. The decision to infect primary CD4$^+$ T cells from tonsils rather than blood was made in order to shed light on latency establishment and maintenance in lymphoid derived cells which are critical for HIV reservoir establishment and persistence (9, 46, 48, 49). T follicular helper (Tfh) cells within lymph nodes and their counterpart in the blood peripheral Tfh (pTfh) represent a preferred cellular site of HIV reservoir (8, 50). Tfh harboring latent HIV may achieve protection from CTL recognition by hiding in follicles where

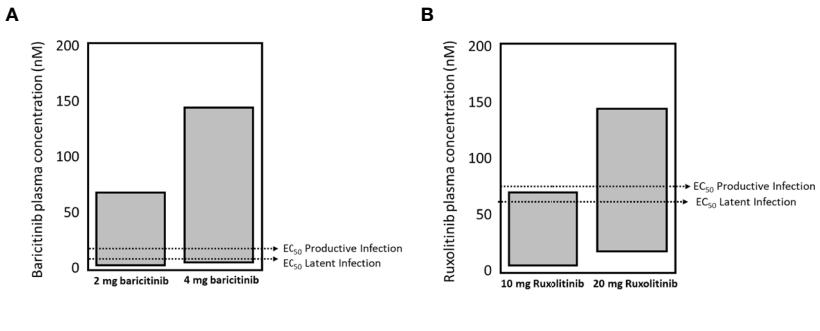

C

Drug	EC_{50} (nM) Productively Infected	EC_{50} (nM) Latently Infected
Baricitinib	10.1 ± 14.1	5.5 ± 0.7
Ruxolitinib	76.2 ± 86.1	57.0 ± 60.8

FIGURE 6 | The EC_{50} for blocking seeding of productive and latent infection with baricitinib and ruxolitinib. The approved dose for chronic long-term use of baricitinib is 2 mg (USA), or 2 and 4 mg (Japan, other non-USA jurisdictions), and 4 mg is approved for hospitalized COVID-19 patients. The plasma concentrations for both doses of baricitinib fall within the range to effectively block both productive and latent infection in our single cycle model **(A)**. Ruxolitinib is not approved for chronic long-term use, but approved doses range within 10-25 mg **(B)**. Only the higher dose of ruxolitinib fell within plasma concentration ranges to block both productive and latent infection in our single cycle model **(B)**. Baricitinib demonstrates ~ half a log greater potency for both assays *versus* ruxolitinib (summarized in **C**).

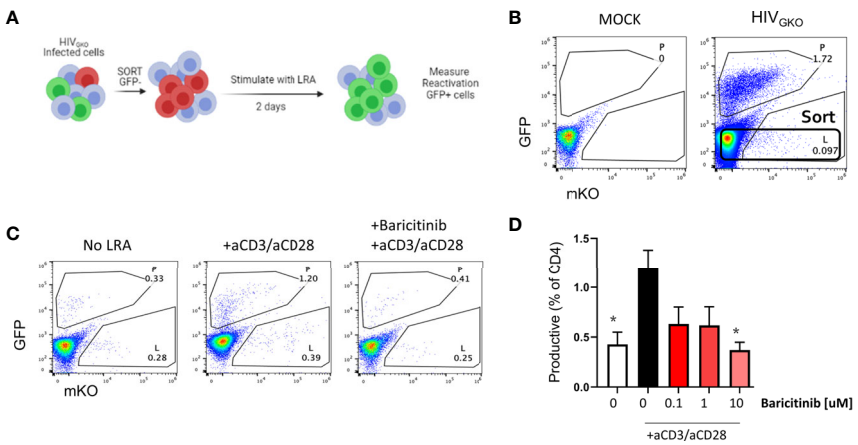

FIGURE 7 | Baricitinib inhibits viral reactivation in latent HIV_{GKO} infected $CD4^+$ T cells. **(A)** Schematic showing experimental design for sorting and re-activation of HIV_{GKO} in purified tonsillar $CD4^+$ T cells. **(B)** Representative flow plot showing expression of dual fluorescent reporters from HIV_{GKO} on day 3 post-infection and the sorting gate for reactivation experiments. **(C)** Dot plots showing expression of dual fluorescent reporters from HIV_{GKO} on day 2 following *in vitro* reactivation. **(D)** Summary bar graph showing average frequency of GFP^+ (productive) cells on day 2 post-LRA treatment in presence of Baricitinib at different concentrations. Error bars represent standard error of the mean (SEM), students t test was used to compare all conditions against the no drug control (white bar), *p < 0.05. Results shown represent 3 independent experiments.

CD8+ T cells either cannot enter due to low levels of the chemokine receptor, CXCR5 expression or are not effective at killing virus-infected cells (51, 52). Our results showed that early in the establishment of latency, tonsil $CD4^+$ T cells upregulated surface expression of CXCR5 which would allow them to enter the GC follicle. These results support a mechanism of lymph node homing as a means for HIV reservoir persistence.

An advantage of the HIV_{GKO} dual reporter system is the ability to assess uninfected and infected cells from the same treatment conditions, thereby reducing 'noise' in the data. Primary cell HIV latency models tend to be long-term experiments taking 2-12 weeks to obtain a pool of latently infected cells for analysis. On the other hand, we were able to isolate and analyze latent cells in a relatively short period of time (7 days). Multiple studies have shown that latently infected cells isolated from HIV-infected patients and NHP on long-term ART are enriched for expression of immune checkpoint molecules such as PD-1, CTLA-4, LAG-3 and TIGIT (17, 20, 21, 53).

We did not find such enrichment in latently infected cells in our model. One possible explanation for this is that in our system cells are not reactivated in order to identify latently infected cells. Most of the studies that have identified PD-1 expression as a marker of latency are stimulating *in vitro* with a strong stimulus (e.g. PMA and Ionomycin) for up to 40 hours to induce HIV gene and protein expression which will have drastic effects on cell phenotype and function. An alternative explanation is that the short-term nature of our study is not capturing these observed effects of latent HIV infection.

Our model consists of tonsil $CD4^+$ T cells which are more efficiently infected *ex vivo* by HIV strains than those from primary human peripheral blood lymphocytes (54) and we reasoned that they would allow for a larger pool of infected cells for down-stream analysis. Latent cells are often defined as 'quiescent' suggesting that the absence of cellular activity is a requirement. However, cellular activation markers are expressed at higher levels on T cells residing in tissues compared to circulating cells (55, 56) and multiple studies have shown a de-coupling between activation marker expression and productive HIV infection (57, 58), which was confirmed by our results as well. This suggests that surveillance of classical activation markers may not be sufficient to comprehend the cellular activation status as it relates to HIV transcriptional activity in the context of reactivation.

Given the difficulty of studying extremely rare and latent HIV-infected cell populations, especially in the context of viral suppression on ART, single cell analyses have allowed for enhanced resolution of *in vitro* and *ex vivo* studies (25, 30, 59). While frequencies of infected cells were low using the HIV_{GKO} system for this study, it was more robust than using patient-derived cells (1/100 *vs.* 1/million). We applied a plate-based approach to combine single cell sorting, flow cytometric phenotyping, and host and HIV gene transcript analyses to strictly define latently infected cells. Differential gene expression analysis revealed that latent cells expressed higher levels of the histone genes (*HIST1H1D, HIST1H4C*) confirming that chromatin modification is playing a role in latency establishment as was shown previously using this model (34). Histone modification controls transcription for host genes and integrated HIV (45, 60). The histone-related genes were significantly co-expressed on a single cell level with tubulin genes, mitochondrial-encoded cytochrome oxidase genes, and actin genes suggesting a connection between latency establishment and chemotaxis as reported previously in an alternative primary cell model of latency (28). Overall, these findings support the use of single cell analysis in studying HIV latency especially using technologies with advanced throughput such as 10X and Drop-seq. Identification of gene pathways in the HIV_{GKO} model that have been reported in the literature such as Sirtuin signaling (61) and upregulation of survival genes (25, 35) in latent infection reinforces the utility of this model to study the biology of and potential disruption of latent HIV infection.

We found *IL32* gene expression to be enriched in latent cells, but this transcript did not show co-expression with the histone-related genes suggesting it may be an additional molecular pathway involved in latency establishment. *IL32* is a cytokine expressed by T cells and to a lower extent in B cells and monocytes (62). The multiple isoforms of IL-32 have divergent properties and expression profiles whereby IL-32β is the most predominant and exhibits anti-inflammatory properties (along with IL-32α) and IL-32$\gamma$is pro-inflammatory (62). Compared to HIV-negative controls, all IL-32 isoforms are increased in plasma from HIV-infected individuals (62, 63). *Ex vivo* addition of IL-32 to $CD4^+$ T cells from virally suppressed HIV^+ individuals has shown conflicting results with regards to induction or suppression of HIV replication which may depend in part on the isoform used (62, 64, 65). Our results demonstrated an increase of *IL32* transcript in latent cells compared to uninfected or productively infected cells support a mechanism of transcriptional suppression of HIV as a way to establish and maintain latent infection and thus point to IL-32 as a potential target for latency reactivation.

The proposed mechanism of JAK1/2 inhibition on HIV replication is due to its effects on lowering cellular activation and increasing the pro-apoptotic protein Bcl-2, thereby reducing the lifespan of the reservoir-harboring cell while simultaneously blocking HIV-induced activation, which promotes HIV persistence and reservoir reseeding (40, 66–68). Collectively due to these tandem mechanisms, it is not surprising that baricitinib and ruxolitinib confer blockade of key events driving reservoir establishment and maintenance in this system. HIV_{GKO} is a single-round, replication deficient HIV, therefore, we cannot evaluate virus spreading in this model though it has been shown previously that ruxolitinib inhibits viral spreading *in vitro* with wild-type HIV infected cells (40), and has demonstrated efficacy towards blocking of HIV persistence markers and reservoir lifespan marker Bcl-2 in the A5336 study (39). Baricitinib (Olumiant.com) is cleared through the kidneys, significantly reducing potential for drug-drug interactions with co-administered agents that are cleared in the liver, which is a property of ruxolitinib (Jakafi.com). Further, baricitinib demonstrates a more favorable pharmacokinetic profile and efficacy in humans, at 2-4 mg once per day dosing for baricitinib *versus* 10-25 mg twice a day dosing for ruxolitinib. Recent reports have also shown that baricitinib can block key events associated with reservoir seeding and persistence in a murine model of HIV and across primary *in vitro* systems, further validating that baricitinib confers anti-HIV effects across systems within physiologically relevant concentrations found in humans (69).

Baricitinib has been shown able to block type 1 IFN-induced signaling (PMID: 30002661) in a concentration dependent manner. We also know from human studies in the COVID setting that baricitinib blocks virus induced IFN signaling in hepatocytes which correlates well with favorable clinical outcomes (PMID: 33187978). While there is nothing in the literature yet about baricitinib in the HIV space, these findings suggest that JAK1/2 inhibition by baricitinib may also block HIV-induced IFN and lead to reduction in reservoir. As baricitinib represents a next-in class JAK1/2 inhibitor with an improved safety and efficacy profile *versus* ruxolitinib, it is also

promising that our data demonstrate an increased efficacy profile compared to ruxolitnib. Together, the data reported provide a key foundation towards establishing that JAK1/2 inhibition, and in particular baricitinib, represent a potential modality towards reservoir reduction in key cells. Further, our findings demonstrate for the first time that physiologically relevant concentrations of baricitinib can reduce the HIV reservoir in lymphoid tissue derived cells. These data coupled with the body of work with this class of agents including humans (A5336), will provide an informed, robust, and mechanistic framework from which to build additional human studies with baricitinib for the indication of HIV cure.

DATA AVAILABILITY STATEMENT

The raw data supporting the conclusions of this article will be made available by the authors, without undue reservation.

ETHICS STATEMENT

The studies involving human participants were reviewed and approved by Institutional Review Boards of University of Miami (IRB# 20140200/CR00004416). Written informed consent to participate in this study was provided by the participants' legal guardian/next of kin.

AUTHOR CONTRIBUTIONS

LA, CG, SuP, SR, RP, SW, RS, and SaP provided intellectual input and contributed to the experimental design. LA and SR performed data collection. CG, RS, EB, EV, and RY provided critical reagents and/or tissue. LA, CG, and LP performed data analysis and interpretation. LA and CG wrote the manuscript. All authors provided critical feedback to produce the final manuscript. All authors contributed to the article and approved the submitted version.

FUNDING

This work was supported by grants awarded to LA and SW from the Institute of AIDS and Emerging Infectious Diseases and the Miami Center for AIDS Research (CFAR) at the University of Miami Miller School of Medicine funded by a grant (P30AI073961) from the National Institutes of Health (NIH), which is supported by the following NIH Co-Funding and Participating Institutes and Centers: NIAID, NCI, NICHD, NHLBI, NIDA, NIMH, NIA, NIDDK, NIGMS, FIC AND OAR. RS and CG were supported by NIH grant RO1-MH-116695 and in part by Emory University's CFAR NIH grant P30-AI-050409.

ACKNOWLEDGMENTS

The authors would like to thank all tonsil donors their time and cooperation and Louis Gonzalez for collecting tonsil tissue. We thank Cassandra Bazile, Omayra Mendez, Kyle Russel, Dan Kvistad, and Robert Suter for technical assistance in this study.

SUPPLEMENTARY MATERIAL

The Supplementary Material for this article can be found online at: https://www.frontiersin.org/articles/10.3389/fimmu.2021.720697/full#supplementary-material

REFERENCES

1. Abdel-Mohsen M, Richman D, Siliciano RF, Nussenzweig MC, Howell BJ, Martinez-Picado J, et al. Recommendations for Measuring HIV Reservoir Size in Cure-Directed Clinical Trials. *Nat Med* (2020) 26:1339–50. doi: 10.1038/s41591-020-1022-1
2. Honeycutt JB, Thayer WO, Baker CE, Ribeiro RM, Lada SM, Cao Y, et al. HIV Persistence in Tissue Macrophages of Humanized Myeloid-Only Mice During Antiretroviral Therapy. *Nat Med* (2017) 23:638–43. doi: 10.1038/nm.4319
3. Clayton KL, Garcia JV, Clements JE, Walker BD. HIV Infection of Macrophages: Implications for Pathogenesis and Cure. *Pathog Immun* (2017) 2:179–92. doi: 10.20411/pai.v2i2.204
4. Rodrigues V, Ruffin N, San-Roman M, Benaroch P. Myeloid Cell Interaction With HIV: A Complex Relationship. *Front Immunol* (2017) 8:1698. doi: 10.3389/fimmu.2017.01698
5. Whitney JB, Lim SY, Osuna CE, Kublin JL, Chen E, Yoon G, et al. Prevention of SIVmac251 Reservoir Seeding in Rhesus Monkeys by Early Antiretroviral Therapy. *Nat Commun* (2018) 9:5429. doi: 10.1038/s41467-018-07881-9
6. Leyre L, Kroon E, Vandergeeten C, Sacdalan C, Colby DJ, Buranapraditkun S, et al. Abundant HIV-Infected Cells in Blood and Tissues Are Rapidly Cleared Upon ART Initiation During Acute HIV Infection. *Sci Transl Med* (2020) 12:eaav3491. doi: 10.1126/scitranslmed.aav3491
7. Estes JD, Kityo C, Ssali F, Swainson L, Makamdop KN, Del Prete GQ, et al. Defining Total-Body AIDS-Virus Burden With Implications for Curative Strategies. *Nat Med* (2017) 23:1271–6. doi: 10.1038/nm.4411
8. Fukazawa Y, Lum R, Okoye AA, Park H, Matsuda K, Bae JY, et al. B Cell Follicle Sanctuary Permits Persistent Productive Simian Immunodeficiency Virus Infection in Elite Controllers. *Nat Med* (2015) 21:132–9. doi: 10.1038/nm.3781
9. Deleage C, Wietgrefe SW, Del Prete G, Morcock DR, Hao XP, Piatak M Jr, et al. Defining HIV and SIV Reservoirs in Lymphoid Tissues. *Pathog Immun* (2016) 1:68–106. doi: 10.20411/pai.v1i1.100
10. Finzi D, Hermankova M, Pierson T, Carruth LM, Buck C, Chaisson RE, et al. Identification of a Reservoir for HIV-1 in Patients on Highly Active Antiretroviral Therapy. *Science* (1997) 278:1295–300. doi: 10.1126/science.278.5341.1295
11. Palmer S, Maldarelli F, Wiegand A, Bernstein B, Hanna GJ, Brun SC, et al. Low-Level Viremia Persists for at Least 7 Years in Patients on Suppressive Antiretroviral Therapy. *Proc Natl Acad Sci USA* (2008) 105:3879–84. doi: 10.1073/pnas.0800050105
12. Andrade A, Rosenkranz SL, Cillo AR, Lu D, Daar ES, Jacobson JM, et al. Three Distinct Phases of HIV-1 RNA Decay in Treatment-Naive Patients Receiving Raltegravir-Based Antiretroviral Therapy: ACTG A5248. *J Infect Dis* (2013) 208:884–91. doi: 10.1093/infdis/jit272
13. Bruner KM, Wang Z, Simonetti FR, Bender AM, Kwon KJ, Sengupta S, et al. A Quantitative Approach for Measuring the Reservoir of Latent HIV-1 Proviruses. *Nature* (2019) 566:120–5. doi: 10.1038/s41586-019-0898-8

14. Eriksson S, Graf EH, Dahl V, Strain MC, Yukl SA, Lysenko ES, et al. Comparative Analysis of Measures of Viral Reservoirs in HIV-1 Eradication Studies. *PloS Pathog* (2013) 9:e1003174. doi: 10.1371/journal.ppat.1003174
15. Descours B, Petitjean G, Lopez-Zaragoza JL, Bruel T, Raffel R, Psomas C, et al. CD32a Is a Marker of a CD4 T-Cell HIV Reservoir Harbouring Replication-Competent Proviruses. *Nature* (2017) 543:564–7. doi: 10.1038/nature21710
16. Hogan LE, Vasquez LE, Hobbs LE, Hanhauser LE, Aguilar-Rodriguez LE, Hussien LE, et al. Increased HIV-1 Transcriptional Activity and Infectious Burden in Peripheral Blood and Gut-Associated CD4+ T Cells Expressing CD30. *PloS Pathog* (2018) 14:e1006856. doi: 10.1371/journal.ppat.1006856
17. Fromentin R, Bakeman W, Lawani MB, Khoury G, Hartogensis W, DaFonseca S, et al. CD4+ T Cells Expressing PD-1, TIGIT and LAG-3 Contribute to HIV Persistence During ART. *PloS Pathog* (2016) 12: e1005761. doi: 10.1371/journal.ppat.1005761
18. Darcis G, Berkhout B, Pasternak AO. The Quest for Cellular Markers of HIV Reservoirs: Any Color You Like. *Front Immunol* (2019) 10:2251. doi: 10.3389/fimmu.2019.02251
19. Hsiao F, Frouard J, Gramatica A, Xie G, Telwatte S, Lee GQ, et al. Tissue Memory CD4+ T Cells Expressing IL-7 Receptor-Alpha (CD127) Preferentially Support Latent HIV-1 Infection. *PloS Pathog* (2020) 16: e1008450. doi: 10.1371/journal.ppat.1008450
20. Banga R, Procopio FA, Noto A, Pollakis G, Cavassini M, Ohmiti K, et al. PD-1 (+) and Follicular Helper T Cells are Responsible for Persistent HIV-1 Transcription in Treated Aviremic Individuals. *Nat Med* (2016) 22:754–61. doi: 10.1038/nm.4113
21. Neidleman J, Luo X, Frouard J, Xie G, Hsiao F, Ma T, et al. Phenotypic Analysis of the Unstimulated *In Vivo* HIV CD4 T Cell Reservoir. *Elife* (2020) 9:e60933. doi: 10.7554/eLife.60933
22. Ho YC, Shan L, Hosmane NN, Wang J, Laskey SB, Rosenbloom DI, et al. Replication-Competent Noninduced Proviruses in the Latent Reservoir Increase Barrier to HIV-1 Cure. *Cell* (2013) 155:540–51. doi: 10.1016/j.cell.2013.09.020
23. Bosque A, Planelles V. Induction of HIV-1 Latency and Reactivation in Primary Memory CD4+ T Cells. *Blood* (2009) 113:58–65. doi: 10.1182/blood-2008-07-168393
24. Saleh S, Solomon A, Wightman F, Xhilaga M, Cameron PU, Lewin SR. CCR7 Ligands CCL19 and CCL21 Increase Permissiveness of Resting Memory CD4+ T Cells to HIV-1 Infection: A Novel Model of HIV-1 Latency. *Blood* (2007) 110:4161–4. doi: 10.1182/blood-2007-06-097907
25. Bradley T, Ferrari G, Haynes BF, Margolis DM, Browne EP. Single-Cell Analysis of Quiescent HIV Infection Reveals Host Transcriptional Profiles That Regulate Proviral Latency. *Cell Rep* (2018) 25:107–17.e103. doi: 10.1016/j.celrep.2018.09.020
26. Pace MJ, Graf EH, Agosto LM, Mexas AM, Male F, Brady T, et al. Directly Infected Resting CD4+T Cells can Produce HIV Gag Without Spreading Infection in a Model of HIV Latency. *PloS Pathog* (2012) 8:e1002818. doi: 10.1371/journal.ppat.1002818
27. Moso MA, Anderson JL, Adikari S, Gray LR, Khoury G, Chang JJ, et al. HIV Latency can be Established in Proliferating and Nonproliferating Resting CD4+ T Cells *In Vitro*: Implications for Latency Reversal. *AIDS* (2019) 33:199–209. doi: 10.1097/QAD.0000000000002075
28. Cameron PU, Saleh S, Sallmann G, Solomon A, Wightman F, Evans VA, et al. Establishment of HIV-1 Latency in Resting CD4+ T Cells Depends on Chemokine-Induced Changes in the Actin Cytoskeleton. *Proc Natl Acad Sci USA* (2010) 107:16934–9. doi: 10.1073/pnas.1002894107
29. Sarabia I, Huang SH, Ward AR, Jones RB, Bosque A. The Intact Non-Inducible Latent HIV-1 Reservoir Is Established In an *In Vitro* Primary TCM Cell Model of Latency. *J Virol* (2021) 95(7):e01297–20. doi: 10.1128/JVI.01297-20
30. Golumbeanu M, Cristinelli S, Rato S, Munoz M, Cavassini M, Beerenwinkel N, et al. Single-Cell RNA-Seq Reveals Transcriptional Heterogeneity in Latent and Reactivated HIV-Infected Cells. *Cell Rep* (2018) 23:942–50. doi: 10.1016/j.celrep.2018.03.102
31. Besnard E, Hakre S, Kampmann M, Lim HW, Hosmane NN, Martin A, et al. The mTOR Complex Controls HIV Latency. *Cell Host Microbe* (2016) 20:785–97. doi: 10.1016/j.chom.2016.11.001
32. Calvanese V, Chavez L, Laurent T, Ding S, Verdin E. Dual-Color HIV Reporters Trace a Population of Latently Infected Cells and Enable Their Purification. *Virology* (2013) 446:283–92. doi: 10.1016/j.virol.2013.07.037
33. Chavez L, Calvanese V, Verdin E. HIV Latency Is Established Directly and Early in Both Resting and Activated Primary CD4 T Cells. *PloS Pathog* (2015) 11:e1004955. doi: 10.1371/journal.ppat.1004955
34. Battivelli E, Dahabieh MS, Abdel-Mohsen M, Svensson JP, Tojal Da Silva I, Cohn LB, et al. Distinct Chromatin Functional States Correlate With HIV Latency Reactivation in Infected Primary CD4(+) T Cells. *Elife* (2018) 7: e34655. doi: 10.7554/eLife.34655
35. Kuo HH, Ahmad R, Lee GQ, Gao C, Chen HR, Ouyang Z, et al. Anti-Apoptotic Protein BIRC5 Maintains Survival of HIV-1-Infected CD4(+) T Cells. *Immunity* (2018) 48:1183–94.e1185. doi: 10.1016/j.immuni.2018.04.004
36. Chaillon A, Gianella S, Dellicour S, Rawlings SA, Schlub TE, De Oliveira MF, et al. HIV Persists Throughout Deep Tissues With Repopulation From Multiple Anatomical Sources. *J Clin Invest* (2020) 130:1699–712. doi: 10.1172/JCI134815
37. Cadena AM, Ventura JD, Abbink P, Borducchi EN, Tuyishime H, Mercado NB, et al. Persistence of Viral RNA in Lymph Nodes in ART-Suppressed SIV/SHIV-Infected Rhesus Macaques. *Nat Commun* (2021) 12:1474. doi: 10.1038/s41467-021-21724-0
38. Schacker T. The Role of Secondary Lymphatic Tissue in Immune Deficiency of HIV Infection. *AIDS* (2008) 22(Suppl 3):S13–18. doi: 10.1097/01.aids.0000327511.76126.b5
39. Marconi VC, Moser C, Gavegnano C, Deeks SG, Lederman MM, Overton ET, et al. Randomized Trial of Ruxolitinib in Antiretroviral-Treated Adults With HIV. *Clin Infect Dis* (2021) 6:ciab212. doi: 10.1093/cid/ciab212
40. Gavegnano C, Brehm JH, Dupuy FP, Talla A, Ribeiro SP, Kulpa DA, et al. Novel Mechanisms to Inhibit HIV Reservoir Seeding Using Jak Inhibitors. *PloS Pathog* (2017) 13:e1006740. doi: 10.1371/journal.ppat.1006740
41. Moysi E, Pallikkuth S, de Armas LR, Gonzalez LE, Ambrozak D, George V, et al. Altered Immune Cell Follicular Dynamics in HIV Infection Following Influenza Vaccination. *J Clin Invest* (2018) 128:3171–85. doi: 10.1172/JCI99884
42. de Armas LR, Pallikkuth S, Rinaldi S, Pahwa R, Pahwa S. Implications of Immune Checkpoint Expression During Aging in HIV-Infected People on Antiretroviral Therapy. *AIDS Res Hum Retroviruses* (2019) 35:1112–22. doi: 10.1089/AID.2019.0135
43. de Armas LR, Cotugno N, Pallikkuth S, Pan L, Rinaldi S, Sanchez MC, et al. Induction of IL21 in Peripheral T Follicular Helper Cells Is an Indicator of Influenza Vaccine Response in a Previously Vaccinated HIV-Infected Pediatric Cohort. *J Immunol* (2017) 198:1995–2005. doi: 10.4049/jimmunol.1601425
44. Kim Y, Cameron PU, Lewin SR, Anderson JL. Limitations of Dual-Fluorescent HIV Reporter Viruses in a Model of Pre-Activation Latency. *J Int AIDS Soc* (2019) 22:e25425. doi: 10.1002/jia2.25425
45. Tyagi M, Pearson RJ, Karn J. Establishment of HIV Latency in Primary CD4+ Cells Is Due to Epigenetic Transcriptional Silencing and P-TEFb Restriction. *J Virol* (2010) 84:6425–37. doi: 10.1128/JVI.01519-09
46. Perreau M, Savoye A-L, De Crignis E, Corpataux J-M, Cubas R, Haddad EK, et al. Follicular Helper T Cells Serve as the Major CD4 T Cell Compartment for HIV-1 Infection, Replication, and Production. *J Exp Med* (2013) 210:143–56. doi: 10.1084/jem.20121932
47. Vranckx LS, Demeulemeester J, Saleh S, Boll A, Vansant G, Schrijvers R, et al. LEDGIN-Mediated Inhibition of Integrase-LEDGF/p75 Interaction Reduces Reactivation of Residual Latent HIV. *EBioMedicine* (2016) 8:248–64. doi: 10.1016/j.ebiom.2016.04.039
48. Pantaleo G, Graziosi C, Butini L, Pizzo PA, Schnittman SM, Kotler DP, et al. Lymphoid Organs Function as Major Reservoirs for Human Immunodeficiency Virus. *Proc Natl Acad Sci USA* (1991) 88:9838–42. doi: 10.1073/pnas.88.21.9838
49. Okoye AA, Hansen SG, Vaidya M, Fukazawa Y, Park H, Duell DM, et al. Early Antiretroviral Therapy Limits SIV Reservoir Establishment to Delay or Prevent Post-Treatment Viral Rebound. *Nat Med* (2018) 24:1430–40. doi: 10.1038/s41591-018-0130-7
50. Pallikkuth S, Sharkey M, Babic DZ, Gupta S, Stone GW, Fischl MA, et al. Peripheral T Follicular Helper Cells Are the Major HIV Reservoir Within Central Memory CD4 T Cells in Peripheral Blood From Chronically HIV-Infected Individuals on Combination Antiretroviral Therapy. *J Virol* (2015) 90:2718–28. doi: 10.1128/JVI.02883-15

51. Petrovas C, Ferrando-Martinez S, Gerner MY, Casazza JP, Pegu A, Deleage C, et al. Follicular CD8 T Cells Accumulate in HIV Infection and Can Kill Infected Cells *In Vitro via* Bispecific Antibodies. *Sci Transl Med* (2017) 9: eaag2285. doi: 10.1126/scitranslmed.aag2285
52. Li S, Folkvord JM, Kovacs KJ, Wagstaff RK, Mwakalundwa G, Rendahl AK, et al. Low Levels of SIV-Specific CD8+ T Cells in Germinal Centers Characterizes Acute SIV Infection. *PloS Pathog* (2019) 15:e1007311. doi: 10.1371/journal.ppat.1007311
53. Harper J, Gordon S, Chan CN, Wang H, Lindemuth E, Galardi C, et al. CTLA-4 and PD-1 Dual Blockade Induces SIV Reactivation Without Control of Rebound After Antiretroviral Therapy Interruption. *Nat Med* (2020) 26:519–28. doi: 10.1038/s41591-020-0782-y
54. Moutsopoulos NM, Vazquez N, Greenwell-Wild T, Ecevit I, Horn J, Orenstein J, et al. Regulation of the Tonsil Cytokine Milieu Favors HIV Susceptibility. *J Leukoc Biol* (2006) 80:1145–55. doi: 10.1189/jlb.0306142
55. Buggert M, Nguyen S, Salgado-Montes de Oca G, Bengsch B, Darko S, Ransier A, et al. Identification and Characterization of HIV-Specific Resident Memory CD8(+) T Cells in Human Lymphoid Tissue. *Sci Immunol* (2018) 3:eaar4526. doi: 10.1126/sciimmunol.aar4526
56. Cantero-Perez J, Grau-Expósito J, Serra-Peinado C, Rosero DA, Luque-Ballesteros L, Astorga-Gamaza A, et al. Resident Memory T Cells Are a Cellular Reservoir for HIV in the Cervical Mucosa. *Nat Commun* (2019) 10:4739. doi: 10.1038/s41467-019-12732-2
57. Munoz-Arias I, Grau-Exposito J, Serra-Peinado C, Rosero DA, LuqueBallesteros L, Astorga-Gamaza A, et al. Blood-Derived CD4 T Cells Naturally Resist Pyroptosis During Abortive HIV-1 Infection. *Cell Host Microbe* (2015) 18:463–70. doi: 10.1016/j.chom.2015.09.010
58. Cavrois M, Banerjee T, Mukherjee G, Raman N, Hussien R, Rodriguez BA, et al. Mass Cytometric Analysis of HIV Entry, Replication, and Remodeling in Tissue CD4+ T Cells. *Cell Rep* (2017) 20:984–98. doi: 10.1016/j.celrep.2017.06.087
59. Sannier G, Dube M, Kaufmann DE. Single-Cell Technologies Applied to HIV-1 Research: Reaching Maturity. *Front Microbiol* (2020) 11:297. doi: 10.3389/fmicb.2020.00297
60. Krishnan V, Zeichner SL. Host Cell Gene Expression During Human Immunodeficiency Virus Type 1 Latency and Reactivation and Effects of Targeting Genes That Are Differentially Expressed in Viral Latency. *J Virol* (2004) 78:9458–73. doi: 10.1128/JVI.78.17.9458-9473.2004
61. Pagans S, Pedal A, North BJ, Kaehlcke K, Marshall BL, Dorr A, et al. SIRT1 Regulates HIV Transcription *Via* Tat Deacetylation. *PloS Biol* (2005) 3:e41. doi: 10.1371/journal.pbio.0030041
62. Zaidan SM, Leyre L, Bunet R, Larouche-Anctil E, Turcotte I, Sylla M, et al. Upregulation of IL-32 Isoforms in Virologically Suppressed HIV-Infected Individuals: Potential Role in Persistent Inflammation and Transcription From Stable HIV-1 Reservoirs. *J Acquir Immune Defic Syndr* (2019) 82:503–13. doi: 10.1097/QAI.0000000000002185
63. Santinelli L, Statzu M, Pierangeli A, Frasca F, Bressan A, Pinacchio C, et al. Increased Expression of IL-32 Correlates With IFN-Gamma, Th1 and Tc1 in Virologically Suppressed HIV-1-Infected Patients. *Cytokine* (2019) 120:273–81. doi: 10.1016/j.cyto.2019.01.012
64. Mesquita PMM, Preston-Hurlburt P, Keller MJ, Vudattu N, Espinoza L, Altrich M, et al. Role of Interleukin 32 in Human Immunodeficiency Virus Reactivation and Its Link to Human Immunodeficiency Virus-Herpes Simplex Virus Coinfection. *J Infect Dis* (2017) 215:614–22. doi: 10.1093/infdis/jiw612
65. Nold MF, Nold-Petry CA, Pott GB, Zepp JA, Saavedra MT, Kim SH, et al. Endogenous IL-32 Controls Cytokine and HIV-1 Production. *J Immunol* (2008) 181:557–65. doi: 10.4049/jimmunol.181.1.557
66. Chomont N, El-Far M, Ancuta P, Trautmann L, Procopio FA, YassineDiab B, et al. HIV Reservoir Size and Persistence Are Driven by T Cell Survival and Homeostatic Proliferation. *Nat Med* (2009) 15:893–900. doi: 10.1038/nm.1972
67. Ribeiro SP, Aid M, Dupuy FP, Chan CN, Hultquist J, Delage C, et al. IL-10 Driven Memory T Cell Survival and Tfh Differentiation Promote HIV Persistence. *BioRxIV Preprint* (2021). doi: 10.1101/2021.02.26.432955
68. Younes SA, Freeman ML, Mudd JC, Shive CL, Reynaldi A, Panigrahi S, et al. IL-15 Promotes Activation and Expansion of CD8+ T Cells in HIV-1 Infection. *J Clin Invest* (2016) 126:2745–56. doi: 10.1172/JCI85996
69. Gavegnano C HW, Koneru R, Hurwitz S, Tao S, Tyor WR, Schinazi RF, et al. Baricitinib Reverses HIV-Associated Neurocognitive Disorders in a SCID Mouse Model and Reservoir Seeding *In Vitro*. *J Neuroinflamm* (2019) 16 (1):182. doi: 10.1186/s12974-019-1565-6

Conflict of Interest: The authors declare that the research was conducted in the absence of any commercial or financial relationships that could be construed as a potential conflict of interest.

Publisher's Note: All claims expressed in this article are solely those of the authors and do not necessarily represent those of their affiliated organizations, or those of the publisher, the editors and the reviewers. Any product that may be evaluated in this article, or claim that may be made by its manufacturer, is not guaranteed or endorsed by the publisher.

frontiers in Immunology

ORIGINAL RESEARCH
published: 13 October 2021
doi: 10.3389/fimmu.2021.734871

Diminished Peripheral CD29hi Cytotoxic CD4+ T Cells Are Associated With Deleterious Effects During SIV Infection

*Omalla A. Olwenyi[1,2], Samuel D. Johnson[1,2], Kabita Pandey[1,2], Michellie Thurman[1], Arpan Acharya[1], Shilpa J. Buch[1], Howard S. Fox[3], Anthony T. Podany[4], Courtney V. Fletcher[4] and Siddappa N. Byrareddy[1,5,6,7]**

[1] Department of Pharmacology and Experimental Neuroscience, University of Nebraska Medical Center, Omaha, NE, United States, [2] Department of Pathology and Microbiology, University of Nebraska Medical Center, Omaha, NE, United States, [3] Department of Neurological Sciences, University of Nebraska Medical Center, Omaha, NE, United States, [4] Antiviral Pharmacology Laboratory, Center for Drug Discovery, University of Nebraska Medical Center (UNMC), Omaha, NE, United States, [5] Department of Genetics, Cell Biology, and Anatomy, University of Nebraska Medical Center, Omaha, NE, United States, [6] Department of Biochemistry and Molecular Biology, University of Nebraska Medical Center, Omaha, NE, United States, [7] Division of Clinical Microbiology, Department of Laboratory Medicine, Karolinska Institute, Stockholm, Sweden

OPEN ACCESS

Edited by:
Vijayakumar Velu,
Emory University, United States

Reviewed by:
Saikat Boliar,
Cornell University, United States
Nicolas HUOT,
Institut Pasteur, France
Maud Mavigner,
Emory University, United States

***Correspondence:**
Siddappa N. Byrareddy
sid.byrareddy@unmc.edu

Specialty section:
This article was submitted to Viral Immunology, a section of the journal Frontiers in Immunology

Received: *01 July 2021*
Accepted: *22 September 2021*
Published: *13 October 2021*

Citation:
Olwenyi OA, Johnson SD, Pandey K, Thurman M, Acharya A, Buch SJ, Fox HS, Podany AT, Fletcher CV and Byrareddy SN (2021) Diminished Peripheral CD29 hi Cytotoxic CD4+ T Cells Are Associated With Deleterious Effects During SIV Infection. Front. Immunol. 12:734871. doi: 10.3389/fimmu.2021.734871

Cytotoxic CD4+ T cells (CD4+ CTLs) limit HIV pathogenesis, as evidenced in elite controllers (a subset of individuals who suppress the virus without the need for therapy). CD4+ CTLs have also been shown to kill HIV-infected macrophages. However, little is known about their contribution towards HIV persistence, how they are affected following exposure to immune modulators like morphine, and what factors maintain their frequencies and function. Further, the lack of robust markers to identify CD4+ CTLs in various animal models limits understanding of their role in HIV pathogenesis. We utilized various PBMC samples obtained from SIV infected and cART treated rhesus macaques exposed to morphine or saline and subjected to flow cytometry evaluations. Thereafter, we compared and correlated the expression of CD4+ CTL-specific markers to viral load and viral reservoir estimations in total CD4+ T cells. We found that CD29 could be reliably used as a marker to identify CD4+ CTLs in rhesus macaques since CD29hi CD4+ T cells secrete higher cytotoxic and proinflammatory cytokines following PMA/ionomycin or gag stimulation. In addition, this immune cell subset was depleted during untreated SIV infection. Strikingly, we also observed that early initiation of cART reconstitutes depleted CD29hi CD4+ T cells and restores their function. Furthermore, we noted that morphine exposure reduced the secretion of proinflammatory cytokines/cytotoxic molecules in CD29hi CD4+ T cells. Lastly, increased functionality of CD29hi CD4+ T cells as depicted by elevated levels of either IL-21 or granzyme B hi T Bet+ gag specific responses were linked to limiting the size of the replication-competent reservoir during cART treatment. Collectively, our data suggest that CD4+ CTLs are crucial in limiting SIV pathogenesis and persistence.

Keywords: CD4+ CTLs, SIV, morphine, reservoirs, CD29+ CD4+ T cells, biomarker

INTRODUCTION

The proposed excision of latently infected HIV cells in a second person with HIV infection offers renewed optimism towards a cure that would usher an end to the AIDS crisis (1, 2). Although great strides have been undertaken, the cellular responses associated with sustaining persistence *versus* viral eradication remain poorly understood (3–5). HIV-infected individuals worldwide live different lifestyles stemming from varied cultural and sexual practices, co-exposures to other pathogens, and comorbid substance abuse not limited to the illicit use of drugs like morphine, cocaine, and heroin (6–11). Collectively, these behaviors differentially impact the body's immune response, alter disease pathogenesis and need to be considered during the development of a universal HIV cure (6, 12).

The body's immune system is built around the activities of CD4+ T cells (13). CD4+ T cells are a significant immune cell subset, which coordinates the immune system and also aid diverse immune (B, $CD8^+$ T, and NK) cell function (14–16). In addition, they are crucial in generating prompt and protective memory responses against recalled pathogens (17, 18). CD4+ T cells are highly plastic and exist as numerous phenotypes like T helper (Th) 1, Th 2, and Th 17, cytotoxic (CD4+ CTL), T follicular helper (Tfh), and T regulatory (T regs) (19). These diverse CD4+ T cell phenotypes express different transcriptional profiles during health and disease, have distinct fates, and carry various functions, including immune regulation (CD+ T regs) (20). Beyond the simplistic provision of help, CD4+ T cells have also been shown to play other roles like regulation of immune responses (CD4+ T regs). They could also directly target infected cells through CD4+ CTLs (13). In supercentenarians, it was suggested that CD4+ CTLs were crucial in healthy aging, where they were found to be expanded while offering long-lasting protection (21).

The hallmark of HIV infection is the progressive loss of total CD4+ T cells and dysregulation of homeostasis, later culminating in acquired immune deficiency syndrome (AIDS) (22, 23). Early during infection, HIV causes massive gut damage accompanied by leakage of microbial biproducts into the periphery (24, 25). Synchronously, gut dysbiosis occurs as the landscape of the gut microbiome shifts towards more pro-inflammatory and pathogenic bacterial communities such as *Prevotella* and *Enterobacteriaceae* (26–28). As a result of microbial translocation and gut dysbiosis, chronic immune activation and systemic inflammation later ensue (29, 30).

Progressively, enhanced CD4+ T cell activation leads to immense CD4+ T cell loss by apoptosis and exaggerated viral cytolysis (31, 32). Following combined antiretroviral therapy (cART) initiation, the recovery of absolute CD4+ T-cell counts is often viewed as the benchmark for the immune system reconstitution (33, 34). However, ongoing dysregulation of cellular function limits the implementation of robust antiviral responses (35). Furthermore, specific CD4+ T-cell lineages like Tfh have been extensively reported to harbor viral reservoirs within the periphery and lymphoid tissues (36, 37). Although CD4+ T cells are targeted during virus replication and persistence, considerable evidence supports a crucial role of cytotoxic CD4+ T-cell phenotypes in HIV control and slowing disease progression (38, 39). During acute HIV infection, a robust HIV-specific CD4+ CTL response comprised of elevated granzyme A, interferon-gamma (IFN γ+), and CD40 ligand (CD40L) has been documented to lower viral load set points (40). Johnson et al. also made similar observations and noticed that CD4+ CTLs predominantly expressed perforin, granzyme B, and Eomes during acute HIV infection (38). Subsequently, HIV Nef-specific CD4+ CTLS has been documented to suppress viral replication in macrophages *ex-vivo* (41).

The lack of a specific CD4+ CTL surface biomarker with consensus across different animal models limits the proper follow-up and interrogation of these cells. Recently, studies by Johnson et al., and Phetsouphanh et al., together used CD57 to identify and track this cell phenotype in different HIV-1 infection conditions (38, 44). Despite this, the lack of cross-reactive antibodies raised against the CD57 carbohydrate epitope in non-human primate (NHP) models limits its use (45, 46). However, recently, in a pre-print article, Nicolet et al. suggested that CD29 enriches human CD4+ CTLs (47). Nonetheless, the utility of this biomarker as a surface marker for CD4+ CTLs remains to be evaluated in NHP models. Although various efforts have been undertaken to explore the effects of CD4+ CTL with HIV disease progression (39, 48), the impact of virus-specific functionality of this cell phenotype on the size of replication-competent reservoirs remains to be studied. Moreover, the modulation of this cell lineage following exposure to substance abuse such as morphine remains unevaluated.

To address some of above-mentioned questions, we utilized samples obtained from SIV-infected rhesus macaques that were exposed to either morphine or saline. Of these animals, a subset was also treated with cART to suppress viral replication. We found that enhanced CD29+ expression on the surface of CD4+ T cells could be used to identify CD4+ CTLs. Thus, CD29hi CD4+ T cells express higher cytotoxic molecules like CD107a and granzyme B plus proinflammatory cytokines like IFN-γ and TNF-α compared to their CD29lo counterparts. In addition, increased gag-specific secretion of cytokines like IL-21 and granzyme B was accompanied by smaller sizes of replication-competent viral reservoirs suggesting that CD4+ CTLs contribute towards limiting SIV persistence in cART-treated rhesus macaques.

MATERIALS AND METHODS

Ethics Statement

This study was approved by the University of Nebraska Medical Center (UNMC) Institutional Animal Care and Use Committee (IACUC) as designated by assigned protocol numbers. For this study, we used: (1) 16-073-07-FC named "The Effect of cART and Drugs of Abuse and the Establishment of CNS Viral Reservoirs". (2) 15-113-01-FC referred to as "The Combinatorial effects of Opiates and Promoter Variant Strains of HIV-1 subtype C on Neuropathogenesis and Latency".

Rhesus Macaques Used for This Study

For protocol 16-073-07-FC, 6 animals were escalated to 6mg/kg twice daily injections of morphine alongside five rhesus macaques

exposed to saline (controls). Following this, all the animals were infected with 200 $TCID_{50}$ of SIVmac251 and later treated with a cART regimen comprising of 40 mg/ml emtricitabine (FTC), 20 mg/ml tenofovir (TFV), and 2.5 mg/ml dolutegravir (DTG). Alternatively, protocol 15-113-01-FC involved 8 rhesus macaques separately exposed to equivalent doses of either morphine (n = 4) or saline (n = 4). Similarly, this was followed with SIVmac251infection at an equivalent dose. However, no subsequent cART was administered. All animal characteristics and treatment regimen details were previously described (10). The experimental schema utilized for the study included a total of 19 rhesus macaques. Briefly, in the untreated group of eight animals, 6-mg/kg intramuscular (i.m.) injections of morphine were administered twice daily for 2 weeks to four rhesus macaques. Then, continued morphine dosing was maintained for 7 weeks while the remaining four animals received normal saline (control group). After 9 weeks, 200 $TCID_{50}$ of SIVmac251 was intravenously administered to the rhesus macaques and continued with morphine/saline treatments until the end of the study. (B) In the separate group of 11 animals exposed to cART, six were given intramuscular morphine for a total of 9 weeks while five received equal doses of saline (control group). After 9 weeks, 200 $TCID_{50}$ of SIVmac251 was intravenously administered to all animals. Five weeks later, cART was initiated and given daily at 1 ml/kg body weight up to the termination end of the study. Saline was given to the controls at a similar dose. Lastly, to evaluate the effects of cART on CD29hi CD4+ T cells, we utilized eight rhesus macaques exposed to either four drugs (FTC, tenofovir alafenamide (TAF), DTG and maraviroc (MVC); n = 4) or two drugs (DTG and FTC; n = 4) that were treated four weeks post SIV inoculation (protocol #16-001-02-FC, Assessment of Antiretroviral Pharmacology in Lymphoid Tissues using the SIV Macaque Model).

Isolation and Cryopreservation of PBMCs

Femoral blood, collected in K2-EDTA vacutainer tubes (BD, 367841), was layered above Lymphoprep™ Density Gradient Medium from STEMCELL Technologies following plasma separation. PBMCs were then later isolated using the density gradient centrifugal separation method described previously (49).

Phenotype Analysis of Immune Cells (Flow Cytometry)

Cryopreserved PBMCs processed from the blood of rhesus macaques included in this study were utilized for flow cytometry. Post-thaw viabilities of greater than 80% were considered for further experimentation. Briefly, this involved a brief 12-18h rest, and surface staining protocols proceeded at this step. First, Zombie Aqua fixable viability dye was added to discriminate dead cells. After that, all surface markers included in the lineage and integrin/chemokine receptor panels (**Supplementary Table 1**) were added at previously titrated volumes. Fixation was then performed using 2% PFA and samples acquired using the Becton Dickson Fortessa X450 flow cytometer. Intracellular staining protocols involved stimulation of SIV mac239 gag peptide mix spanning 15-mers with 11-aa overlap (ARP-6204) obtained through the NIH HIV Reagent Program, Division of AIDS, NIAID, NIH: Peptide Array, Simian Immunodeficiency Virus (SIV)mac239 Gag Protein, ARP-6204, contributed by DAIDS/NIAID) and PMA (Phorbol myristate acetate)/ionomycin (20 ng/ml and 0.5 µg/ml) respectively dissolved in 10% complete media. Simultaneously, Golgi plug containing Brefeldin A and the Golgi transport inhibitor monensin was added to inhibit the release of cytokines and cytotoxic granules into the supernatant. After 6 hours of stimulation, 20 mM EDTA solution was added. After that, live/dead exclusion was performed, and surface staining for CD29 PercpCy5.5 was carried out. For the cytotoxicity panel (**Supplementary Table 1**) involving Eomes and T-bet transcription factors, the fix/perm solution (Tonbo Biosciences) was used for fixation and permeabilization. The remaining antibody cocktail was dissolved in FoxP3 transcription factor buffer (Tonbo biosciences) and added following permeabilization. Alternatively, in the cytokine secretion panel (**Supplementary Table 1**), 2% PFA was added for fixation, followed by permeabilization using BD perm wash buffer. Then, cells were incubated with a previously prepared cocktail of antibodies. Following incubation and later washes, the acquisition was performed on the Becton Dickson Fortessa X450 flow cytometer, and analysis was carried out using Flowjo version 10.6 (Trees Star Inc., Ashland, Oregon, USA). For ICS quantification, all values were reported following background subtraction.

Quantification of Plasma Viral Load in Peripheral Blood

Quantitative real-time PCR (qRT-PCR) was utilized to estimate levels of SIV RNA in EDTA plasma (50). Briefly, RNA was extracted from EDTA plasma using a QIA amp viral RNA mini kit (Qiagen, Germantown, MD, USA; Cat no: 52906). Additional information on primers and probes with details of PCR conditions were described previously (10).

Quantitative Viral Outgrowth Assay (QVOA)

CD4+ T cells were enriched from PBMCs using the non-human primate microbead CD4+ T cell isolation kit, (STEMCELL Technologies Inc, Seattle, WA, USA) and later resuspended in complete media (RPMI1640, 10% FBS, 2 mM glutamine, Penstrep (100 U/mL penicillin and 100 µg/mL streptomycin)), 10 U/mL IL-2 and 300 nM efavirenz (EFV; NIH AIDS Reagent Program). The resultant purified CD4+ T cells were then co-stimulated with CD3/CD28 beads (Dynabeads, Life Technologies, Waltham, MA, USA) and 10-fold limiting dilutions ranging from 10^2 to 10^5 cells/mL were generated. Following 72 h of incubation, 10^5 CEMx174 cells were added to aid in viral expansion. This time point was noted as day 0 of incubation and was later prospectively followed for 21 days. SIV RNA measures were then performed using qRT-PCR. Levels of replication-competent viruses were denoted as infectious units per million (IUPM) and were estimated using the IUPMStats v1.0 infection frequency calculator (10, 51).

Statistical Analysis

Prism V9.0 (GraphPad Software) was used for Spearman's rank correlation and paired non-parametric tests with the aid of the Wilcoxon test. In addition, comparisons between morphine and

saline groups were also performed using the Mann Whitney U test. Using R version 3.4.3, a correlation matrix was generated following multiple correlations. Resultant P values were then corrected for type 1 error with the aid of Holm's correction. Lastly, following Boolean gating in FlowJo, combinatorial expression of multiple cytokines was evaluated and graphed using SPICE ("Simplified Presentation of Incredibly Complex Evaluations") (52).

RESULTS

Loss of CD29hi CD4+ T Cells Is Positively Interrelated to Declining Immune Status and Increasing Viral Loads During SIV Infection

To gain insight into cellular and virological interactions of the peripheral immune system, changes in CD29hi CD4+ T cells alongside viral load and various immune cell subsets during baseline, acute (Day 14), and chronic (Day 245) phases of SIV disease progression (**Supplementary Figure 1**). Following SIV infection, viral load levels peaked during the acute phase and were maintained through the chronic time point (**Figure 1A**). Compared to baseline, there was a progressive loss in %CD4+ T cell frequencies across the acute phase of infection (P = 0.0078) and the latter chronic phase of infection (P = 0.0003) (**Figure 1B**). Subsequently, this was accompanied by an expansion of CD8+ T cells during both the acute (P = 0.0078) and chronic (P = 0.0002) phases of untreated SIV infection (**Figure 1C**). Unsurprisingly, there was a progressive loss in the CD4/CD8 ratio across the acute (P = 0.0156) and chronic (P = 0.0156) phases of infection (**Figure 1D**). The frequencies of %CD29hi CD4+ T cells were reduced during the acute (P = 0.0469) and chronic (P = 0.0078) phases of untreated infection (**Figure 1E**). Similar trends were observed with absolute CD29hi CD4+ T cells (**Supplementary Figure 2A**) and absolute CD4+ T cells (**Supplementary Figure 2B**), while absolute CD8+ T cells were elevated during SIV progression (**Supplementary Figure 2C**). Remarkably, % CD8+/CD29+ T cells remained stabilized during the acute and chronic phases of untreated SIV infection despite the concurrent expansion of CD8+ T cells (**Figure 1F**). The percent of both CD29hi CD4+ T cells and CD29+/CD8+ T cells exhibited an increase in activation shown by increased expression of HLA-DR (P < 0.05) (**Figures 1G, H).** No changes were observed in innate-like CD8+ T cells that express CD16 (**Figure 1I**). A progressive non-significant reduction of NK cells occurs through the acute to chronic phases of untreated SIV infection (**Figure 1J**). However, NK cell subset analysis revealed that there was a reduction in % CD16+CD56- NK cells, (P = 0.024) (**Figure 1K)** together with concurrent expansions of %CD16-CD56+ NK cells, (P = 0.039) (**Figure 1L)** and %CD16-CD56- NK cells (P = 0.039) that are later maintained during chronic infection (**Figure 1M**). Multiple Spearman rank correlation analysis revealed that reduced % CD29hi CD4+ T cells were positively associated with expanding %CD8+ T cells (rho = -0.532, P = 0.0044), CD16-CD56+ NK cells (rho = -0.647, P = 0.0006) while a positive correlation was seen with improved immune status (CD4/CD8 ratio) (rho = 0.42, P = 0.044). Additionally, negative associations were noticed with CD16-CD56- NK cells (rho = -0.7278374) and CD16-CD56+ NK cells (rho = -0.3928776), (all P < 0.05) (**Figure 1N**). Furthermore, CD16+CD56- NK cells were positively correlated with absolute CD29hi CD4+ T cells (rho = 0.7510 and P = 0.00001) and absolute CD4+ T cells (rho = 0.7206 and P = 0.0002) respectively (**Supplementary Figures 2D, G**). In turn, CD16-CD56+ NK cells were associated with loss of CD29 hi CD4+ T cells (**Supplementary Figure 2E)** and declining absolute CD4+ T cells (**Supplementary Figure 2H)** during SIV disease progression. Similarly, CD16-CD56- NK cells were also associated with loss of CD29hi CD4+ T cells (**Supplementary Figure 2F)** and reduced absolute CD4+ T cells (**Supplementary Figure 2I)** during infection. Lastly, percent and absolute CD29hi CD4+ T cells were seen to negatively associate with viral loads [(rho = -0.57 and P = 0.0037) and (rho = -0.7136 and P = 0.0001)] (**Figures 1O, P**).

Early Initiation of cART (4 Weeks Post-Infection) Supports Percent CD29hi CD4+ T Cells Restoration and Rescued Polyfunctionality Within the Periphery

In a separate set of rhesus macaques (n = 8), early cART was initiated to test whether depleted peripheral CD29hi CD4+ T cells could be reconstituted. In addition, retrospective time course evaluations were carried out to evaluate how different stages of SIV disease progression and therapy affect the functionality of this cell subset. Representative gating of CD29hi CD4+ T cell subset reveals CD95+, IFN-γ+ and TNF α+ cytokine secretion following PMA/ionomycin stimulation (**Figures 2A** and **Supplementary Figure 3)**. Changes in %CD29hi CD4+ T cells, %CD95 CD29hi CD4+ T cells, IFN-γ+ CD29hi CD4+ T cells and TNF-α + CD29hi CD4+ T cells showed that six weeks post untreated SIV infection, a progressive loss CD29hi CD4+ T cells in conjunction with inflammatory cytokines occurred. CD95+ cell expression was elevated during acute SIV infection and remained steadily maintained post-therapy. In contrast, IFN-γ+ and TNF-α + cytokine levels diminished before ART but recovered after therapy (**Figures 2B, E**). Finally, early initiation of cART restored lost polyfunctionality of CD29hi CD4+ T cells (% (CD95+, IFN-γ+ and TNF α+) and [% CD95+, IFN-γ- and TNF α+)], (**Figures 2F)**.

CD29hi CD4+ T Cells Express Elevated Levels of Pro-Inflammatory and Cytolytic Mediators in Rhesus Macaques Exposed to cART and Morphine During Chronic Infection

Upon noticing that CD29hi CTLs were depleted during progressive untreated SIV infection, we next turned our efforts to characterizing these cells. Utilizing PBMCs collected from cART treated rhesus macaques, we assessed the extent to which CD4+ CD29hi T cells express diverse integrins (CD11a and CD11b) and the chemokine receptor CX3CR1 (**Supplementary Figure 4**). In addition, after PMA/ionomycin stimulation, we assessed transcription factors T bet and Eomes, the cytotoxic

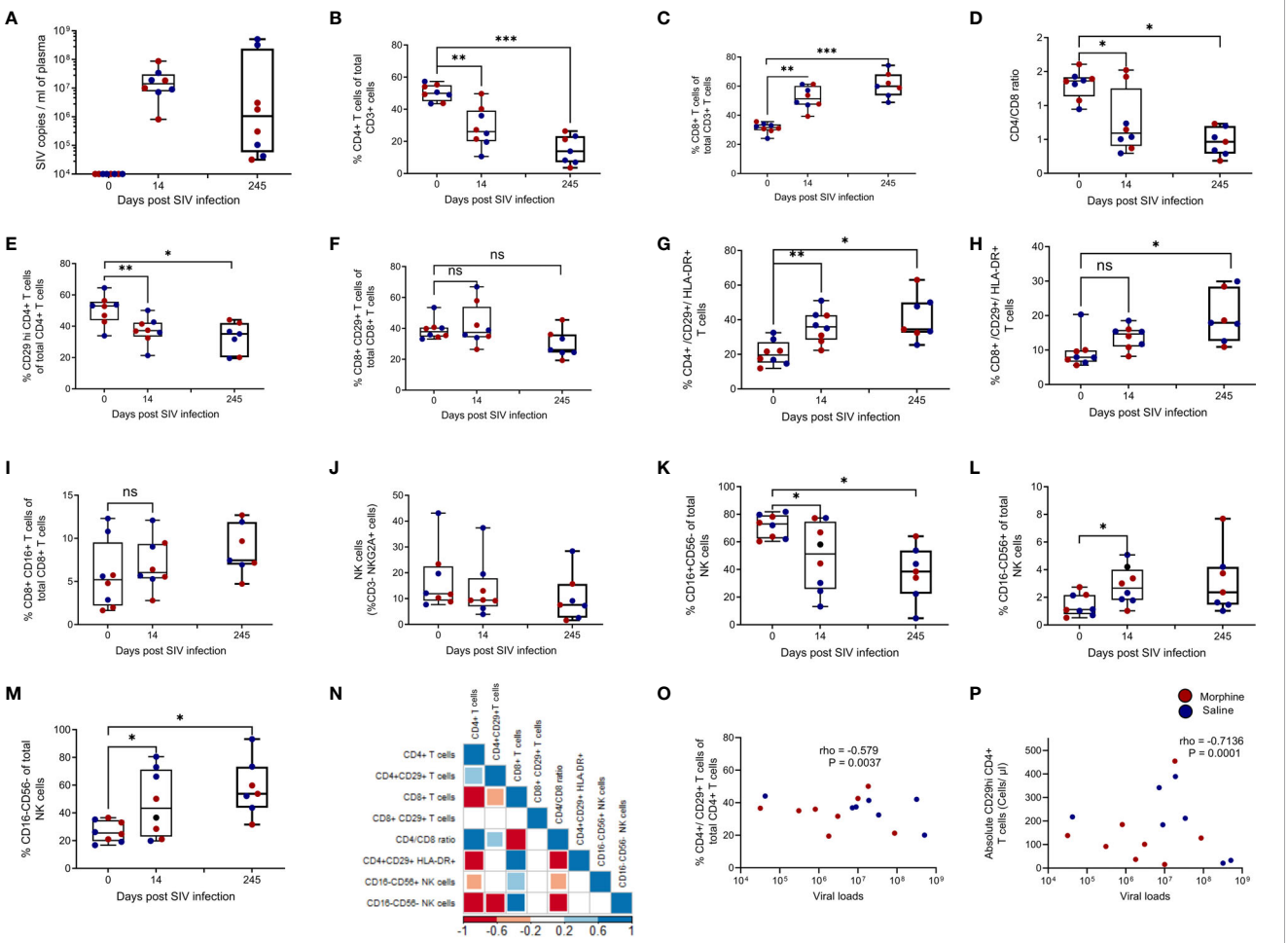

FIGURE 1 | Loss of CD29 hi CD4+ T cells are associated with increased viral loads, declining immune status, and dysregulated NK cell subsets in SIV infected rhesus macaques exposed to either morphine or saline. Viral loads at baseline (day 0), acute (day 14), and chronic (day 245) during untreated SIV infection **(A)**. Changes in percent CD4+ T cells **(B)**, percent CD8+ T cells **(C)**, CD4/CD8 ratio **(D)**, percent CD29+ CD4+ T cells **(E)**, percent CD29+ CD8+ T cells **(F)**, percent CD29+/CD4+/ HLA-DR+ **(G)**, percent CD29+/CD8+/HLA-DR+ **(H)** and CD8+/CD16+ T cells **(I)** at the three studied time points (day 0, day 14 and day 245) post infection. Evaluating NK cells and comprising subsets that include changes in total NK cells **(J)**, CD16+CD56- NK cells **(K)**, CD16-CD56+ NK cells **(L)**, and CD16-CD56- NK cells **(M)** at day 0, day 14, and day 245 post infection. **(N)** Correlogram showing correlations between various immune cell subsets and percent CD29+ CD4+ T cells.. Relationship between either **(O)** percent CD29+ CD4+ T cells or **(P)** absolute CD29+ CD4+ T cells and viral load. * shows $p < 0.05$, ** indicates $p < 0.01$ while *** denotes $p < 0.001$ resulting from Wilcoxon matched pairs signed rank tests between paired groups of the different comparisons. ns represents non significant. Per visit comparisons between morphine and saline were also performed using the Mann Whitney U test (non- significant).

mediators granzyme B and CD107a, IL-21, T helper (Th) 1 cytokines TNF-α and IFN-γ plus the Th2 cytokine IL-4 (**Supplementary Figure 5**). Surprisingly, there were no significant differences between CD11a expression in CD29hi vs. CD29lo CD4+ T cell subsets (**Figure 3A**). However, we noticed a three-fold increment of surface CD11b expression on CD29hi *versus* CD29lo CD4+ T cells (P = 0.0020) (**Figure 3B**). Similarly, we observed a close to two-fold elevation in the expression of CX3CR1 in CD29hi CD4+ T cells (P = 0.0010) **(Figure 3C).** Unexpectedly, the CD29hi CD4+ T cell subset had lower levels of Eomes (P = 0.0020) **(Figure 3D)** while expressing over two-fold levels of T bet in comparison to the CD29lo CD4+ T cell subset (P = 0.0020) **(Figure 3E)**. Moreover, elevated granzyme B expression was observed in the CD29hi CD4+ T cell subset *versus* the CD29lo CD4+ T cell subset (**Figure 3F**). Similarly, the level of granzyme B+ hi expression was elevated in the CD29hi CD4+ T cell subset (P = 0.0010) **(Figure 3G),** which remained augmented even after testing for co-expression of granzyme B hi and Tbet+ (P = 0.0010) **(Figure 3H)**. The level of IL-4 was similar between CD29hi vs CD29lo CD4+ T cells **(Figure 3I)** whilst elevated expression of diverse cytokines such as: CD107a (P = 0.0010) **(Figure 3J)**, IL-21 (P = 0.0010) **(Figure 3K),** IFN-γ (P = 0.0010) **(Figure 3L)** and TNF-α (P = 0.0010) **(Figure 3M)** were observed. Similarly, there were higher frequencies of % IFN-γ+ and TNF-α + co-expressing CD29hi CD4+ T cells in comparison to CD29lo CD4+ T cells (P = 0.0087)

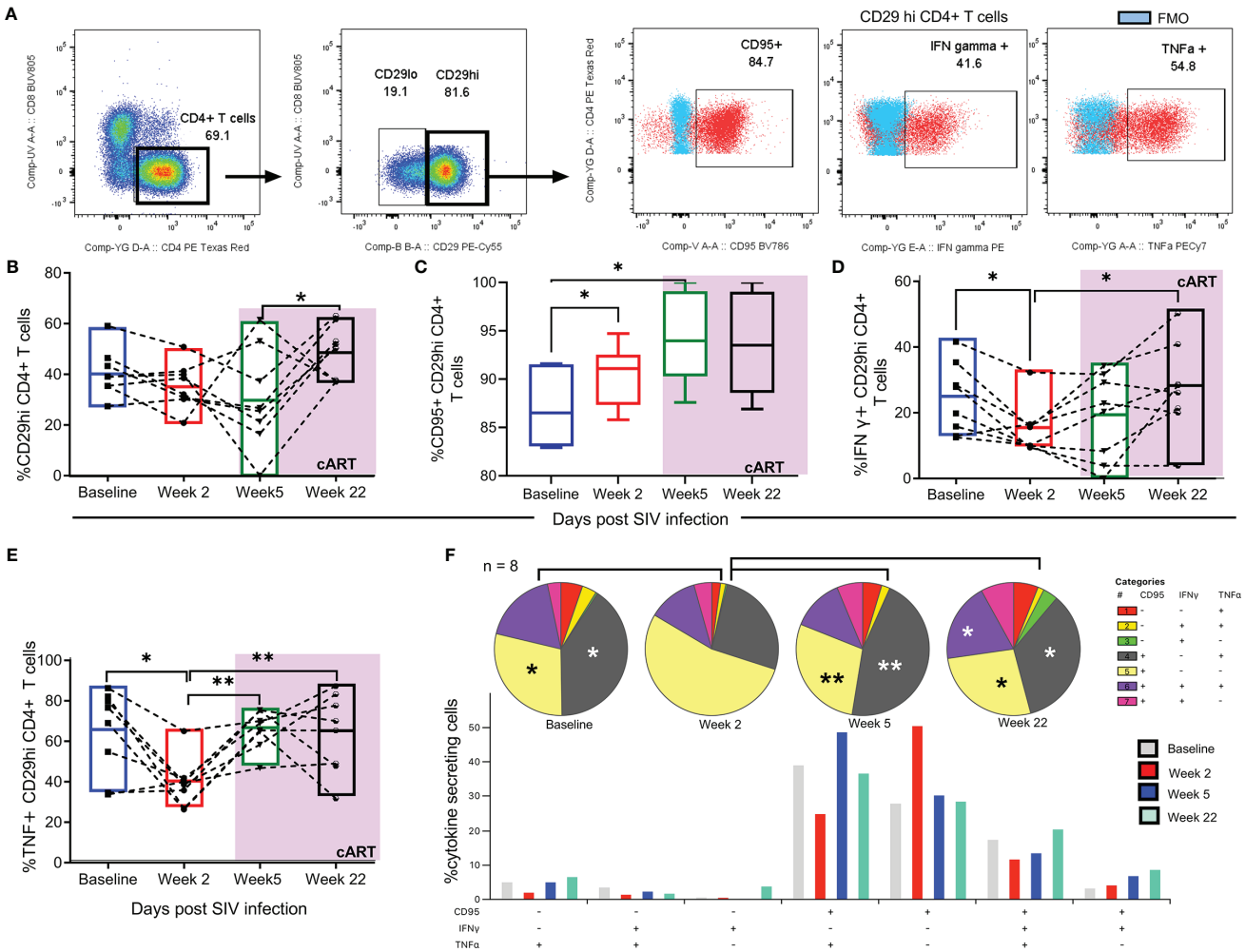

FIGURE 2 | Early cART initiation (4 weeks) restores the loss of CD29hi CD4+ T cells and restores polyfunctionality. **(A)** Representative gating used to obtain CD4+ CD29 hi T cells used for changes in cytokine secretion at different stages of SIV progression. Briefly, CD4+ T cells were obtained from gated CD3+ T cells/ lymphocytes/live cells/singlets/Time vs FSC-A populations. Thereafter, CD29 hi populations were then gated out from CD4+ T cells and the extent of CD95 expression and IFN-γ/TNF-α secretion. Following this, the changes of **(B)** %CD29hi CD4+ T cells **(C)** %CD95+ CD29hi CD4+ T cells **(D)** IFN-γ+ CD29 hi CD4+ T cells **(E)** TNF-α+ CD29hi CD4+ T cells evaluated at baseline, week 2, week 7 and week 22 post SIV infection. **(F)** Polyfunctionality profiles of CD29hi CD4+ T cells stimulated with PMA/ionomycin. Included pie charts/bar graphs represent time course changes in CD29hi poly functionality based on IFN-γ, TNF-α and CD95 expression (n = 8). Bar graphs show the median percent cytokine expressing cells. All paired comparisons across the different timepoints were performed using the non-parametric Wilcoxon test. * shows $p < 0.05$ while ** indicates $p < 0.01$.

(**Figure 3N**). Likewise, IL-21+ and IFN γ+ co-expressing cells are elevated in CD29hi CD4+ T cells in comparison to CD29lo CD4+ T cells (P = 0.0010) (**Figure 3O**). Next, we observed that morphine causes downregulation of cytokine secretion ranging from IL-21, TNF-α, IFN-γ, IFN-γ, and TNF-α dual positive plus IL-21 and IFN-γ co-expressing CD29hi CD4+ T cells (all P < 0.01) (**Figures 3P–U**). Morphine treatment was also observed to similarly downmodulate the expression of inflammatory cytokines and cytotoxic molecules in the CD29lo CD4+ T cell subset (**Supplementary Figure 6**). By evaluating polyfunctionality of CD29hi CD4+ T cells revealed that the majority of cytokine-producing cells were mainly TNF-α + cells and demonstrated greater frequencies of multiple cytokines secreting cells such as combinations with TNF-α + and CD107a cells, TNF-α + and IL-21 and TNF-α + and IFN-γ+ co-expressing cells, (all P <0.05) (**Figure 3V**).

CD29hi Gag Specific CD4+ T Cells Also Express Elevated Levels of Pro-Inflammatory and Cytolytic Mediators in Rhesus Macaques Exposed to cART and Morphine

In synchrony with earlier observations seen in **Figure 2**, CD29 hi CD4+ T cells expressed higher levels of IFN-γ (**Figure 4A**), CD107a (**Figure 4B**), IL-21 (**Figure 4C**), TNF-α (**Figure 4D**) (all P<0.05) (**Supplementary Figure 6**). The same trend was seen

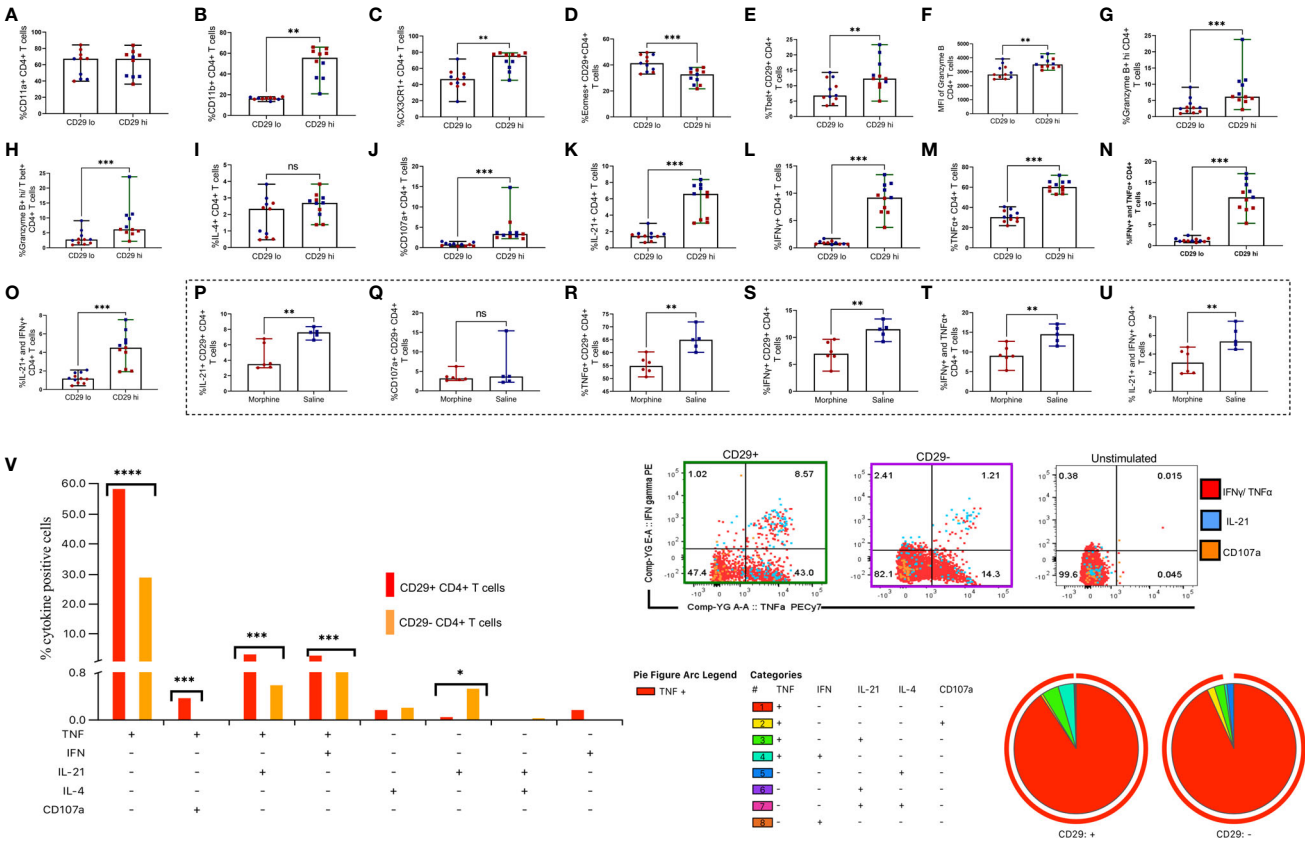

FIGURE 3 | CD29hi CD4+ T cells identify cytotoxic CD4+ T cells (CD4+ CTLs) with superior cytotoxicity, expression of inflammatory surface molecules and cytokines following stimulation with PMA/ionomycin in cART treated rhesus macaques exposed to saline or morphine during chronic infection. The expression percent CD11a **(A)**, percent CD11b **(B)**, the chemokine receptor CX3CR1 **(C)**, percent Eomes **(D)** and percent T bet **(E)** was evaluated and compared between CD29lo vs. CD29hi T cells. Similarly, cytotoxicity was evaluated based on percent granzyme B **(F)**, percent Granzyme B hi **(G)**, and Granzyme B hi and T bet co-expression **(H)**. In addition, the expression of percent IL-4 **(I)**, percent CD107a **(J)**, percent IL-21 *(K)*, percent IFN-γ **(L)**, percent TNF-α **(M)**, dual co-expression of IFN-γ and TNF-α **(N)** and IL-21 and IFN-γ co-expression **(O)** was evaluated. The changes in the secretion of cytokines and cytotoxic molecules IL-21 **(P)**, CD107a **(Q)**, TNF-α **(R)**, IFN-γ **(S)**, IFN-γ and TNF-α **(T)** and IL-21 and IFN-γ **(U)** within CD29 hi CD4+ T cells following morphine exposure were evaluated using ICS. Representative gating of CD29 hi *versus* CD29 lo cells expressing multiple cytokines such as IL-21, CD107a, TNF-α and IFN-γ **(V)**. Polyfunctional profile of CD29hi vs CD29lo CD4+ T cells responding to PMA/ionomycin. (I) Representative manual gating of CD29hi vs CD29lo CD4+ T cells used to analyze polyfunctionality. (II) and (III) Pie charts and the bar plots show the frequency of CD29+ or CD29- CD4+ T cells expressing different combinations of cytokines (TNF-α, IFN-γ, IL-21, IL-4 and CD107a) in n=11 rhesus macaques. Paired comparisons between CD29lo and CD29hi CD4+ T cells were performed using the non-parametric Wilcoxon test. Comparisons between morphine and saline were also performed in CD29+ CD4+ T cells using the Mann Whitney U test. For SPICE analyses, pie charts showing cytokine secretion patterns together with arc plots show the predominant cytokine being secreted. Bar graphs denote median cytokine expressing cells. Simultaneously, the extent of cytokine polyfunctionality was compared within CD29lo vs CD29 hi CD4+ T cell subsets with aid of the Wilcoxon test. For all comparisons, * shows $p < 0.05$, ** indicates $p < 0.01$ while *** denotes $p < 0.001$. ns represents non significant. Red dots denote morphine treated while blue dots represent rhesus macaques exposed to saline.

with TNF-α+ and CD107a- co-expressing cells (**Figure 4F**), IFN-γ-, TNF-α+ and CD107a+ co-expressing cells (**Figure 4G**), percent and MFI granzyme B hi cytolytic molecules (**Figures 4H, I**) and granzyme B hi and T Bet+ co-expressing cells (**Figure 4J**) in comparison to CD29lo CD4+ T cells, (all $P<0.05$). Notably, no significant differences were observed with levels of IL-4 (**Figure 4E**), ($P > 0.05$). In congruence with earlier observations noticed, morphine similarly led to downregulation of various gag-specific cytokines such as IL-21, TNF-α, and granzyme B hi T Bet+ in CD29hi CD4+ T cells (all $P < 0.05$) (**Figures 4K–O**). Next, we investigated whether there was a relationship between either IL-21 or granzyme B hi T Bet+ gag specific release on CD29hi CD4+ T cells with the size of the replication-competent viral reservoir as measured by quantitative viral outgrowth assay (QVOA) (**Figure 4P**). Negative correlations were observed between QVOA and either IL-21 gag specific CD4+/CD29+T cells or granzyme B hi T bet+ gag specific CD29 hi CD4+ T cells. The association between granzyme B hi T Bet+ CD29hi CD4+ (**Figures 4Q, R**).

DISCUSSION

CD4+ CTLs are crucial in limiting the pathogenesis and mediating protection against HIV/SIV infection. It was previously documented that elite controllers, a unique group of

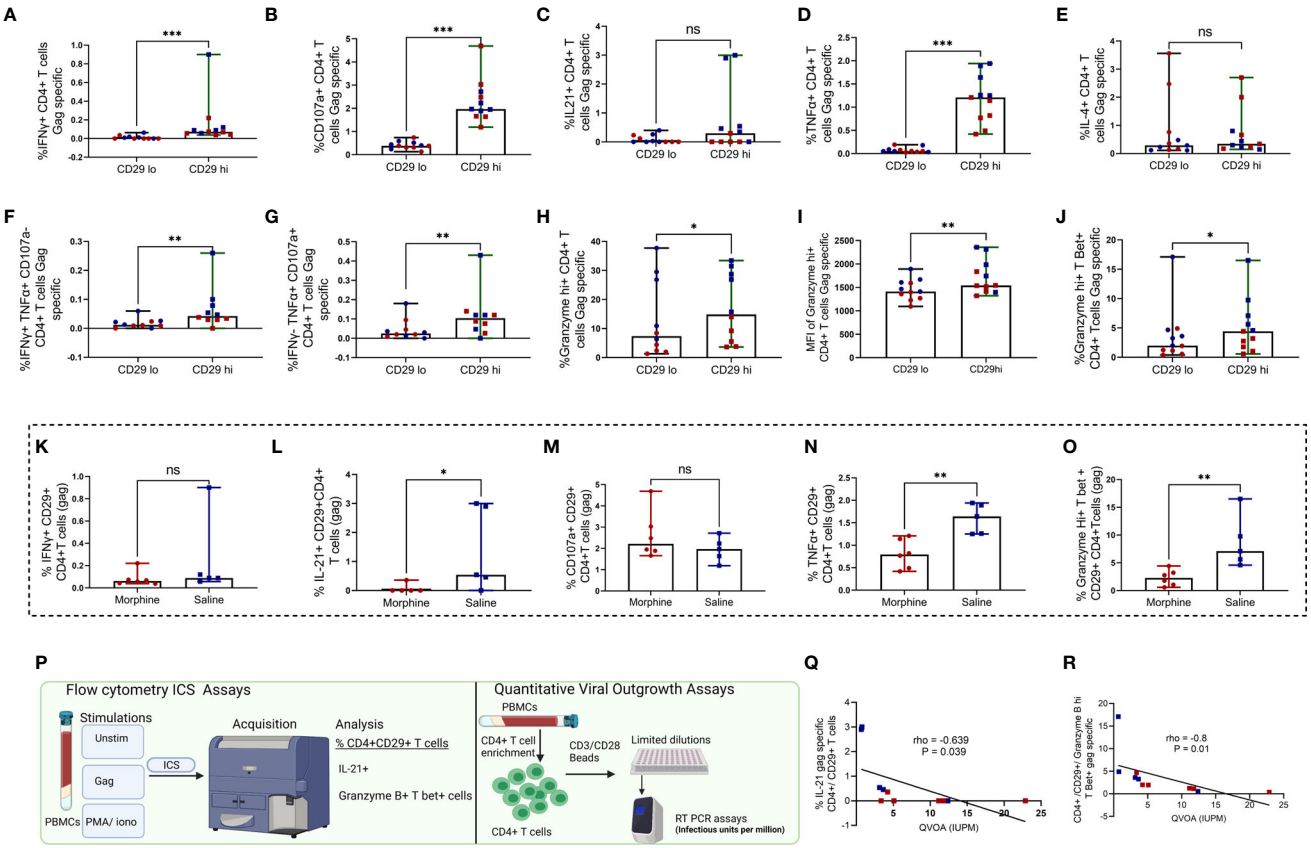

FIGURE 4 | CD29 hi CD4+ T cells express elevated inflammatory cytokines and cytotoxic molecules following stimulation with gag peptides in cART treated rhesus macaques exposed to saline or morphine during chronic infection. Comparative expression of inflammatory cytokines and cytotoxic molecules between CD29 hi vs CD29 lo CD4+ T cells was performed as depicted by percent IFN-γ **(A)**, percent CD107a **(B)**, percent IL21 **(C)**, percent TNF-α **(D)**, percent IL-4 **(E)**, percent IFN-γ+ TNF-α + and CD107a- **(F)**, percent IFN-γ- TNF-α + and CD107a+ **(G)**, Granzyme B hi **(H)**, MFI of Granzyme B+ hi **(I)**, Granzyme B+ hi T bet+ **(J)** gag specific CD4+ T cells. Immune modulation by morphine on CD29 hi CD4+ CTLS was analyzed for the expression of various cytokines such as percent IFN-γ **(K)** percent IL21 **(L)** percent CD107a **(M)**, percent TNF-α **(N)**, percent Granzyme B+ hi T bet+ cells **(O)**. Scheme for correlation analysis between gag specific IL-21 or Granzyme B hi T bet+ CD29 hi CD4+ T cells and QVOA measures of replication competent reservoirs in total CD4+ T cells **(P)**. Correlation between gag-specific IL-21+ CD29hi CD4+ T cell frequencies and QVOA **(Q)**. Correlation between gag specific Granzyme B+ hi T bet+ CD29hi CD4+ T cell frequencies and QVOA **(R)**. Paired comparisons between CD29 lo and CD29 hi CD4+ T cells were performed using the non-parametric Wilcoxon test. Comparisons between morphine and saline were also performed in CD29+ CD4+ T cells using the Mann Whitney U test. For all comparisons, * shows $p < 0.05$, ** indicates $p < 0.01$ while *** denotes $p < 0.001$. ns signifies non significant. Red dots denote morphine treated while blue dots represent rhesus macaques exposed to saline.

individuals capable of suppressing HIV without therapy, possess greater frequencies of circulating virus-specific CD4+ CTLs (44). Remarkedly, the development of CD4+ CTL escape SIV mutants is accompanied by loss of elite control in rhesus macaques (53). Thus, there is no surprise that declining immune status occurred simultaneously with the loss of proposed CD4+ CTLs and increased viral loads suggesting this cell subset is crucial in limiting HIV pathogenesis.

Similarly, the loss of HIV-specific CD4+ CTL function has been reported in chronic progressors (44). Predictably, during progressive infection, CD29hi CD4+ T cells exhibited increased HLA-DR activation levels, hinting that this cell phenotype could be targeted and depleted by the virus (54). Furthermore, the expansion of cytokine secreting (CD16-CD56+) and double negative CD16-CD56- NK cells are crucial for limiting viremia post-peak viral loads (55, 56). However, the loss of CD16 expression on prevailing NK cell subsets followed by the decrease of both CD29hi CD4+ T cells and absolute CD4+ T cells further highlights SIV-induced NK cell and CD4+ CTL dysfunction during disease progression (57).

During our time course studies, our observation that timely initiation of therapy reconstitutes peripheral CD29hi CD4+ T cells and restores IFN-γ, TNF-α, and CD95 polyfunctionality, in turn, supports findings from other groups who have reported that early ART preserves T cell function (58, 59). Following gag and PMA/ ionomycin stimulation, CD29hi CD4+ T cells display cytotoxic properties through elevated secretion of proinflammatory cytokines such as IFN-γ, TNF-α, and IL-21 or cytolytic molecules such as granzyme and CD107a (60). In turn, increased expression of T bet dually favors IFN-γ and TNF-α

secretion while supporting cytotoxicity by binding to downstream promoters of granzyme B and perforin genes (61).

Similarly, augmented expression of CX3CR1 also tends to favor CD4+ CTL transmigration into inflamed tissue, as exemplified in Dengue, where virus-specific CX3CR1 CD4+CTLs mediate protective cytotoxicity (62). Similarly, Chen et al. showed that a cytomegalovirus-driven CD57hi CD4+ CTL phenotype uses CX3CR1 to facilitate vascular trafficking by attaching to the fractalkine receptor on the endothelium during HIV infection (63).

Since CD29hi CD4+ T cells exhibit greater polyfunctionality as demonstrated by a distinct functional profile typified by elevated secretion of multiple inflammatory cytokines and cytotoxic molecules, they could serve as robust antiviral mediators that directly target virus-infected cells (59). In agreement with this, we noted that increased *ex-vivo* secretion of IL-21 in response to gag was negatively associated with the size of the replication-competent viral reservoir within the periphery. In a separate study, IL-21 secretion by CD4+ T cells was noted to support CD8+ cytotoxic T cell responses in chronic progressors, even during the late-stage infection, leading to diminished virus replication (64). Furthermore, therapeutic administration of IL-21 has been documented to reduce the size of viral reservoirs in rhesus macaques (64, 65).

The association between granzyme B hi T Bet+ CD29hi CD4+ T cells and diminished replication-competent viral reservoirs mirrors earlier findings by a separate study group found that HIV specific granzyme B and not IFN-g CD8 CTLs were linked to reduced HIV reservoirs during acute HIV infection (42). In addition, increased inflammation, as noted by elevated levels of pro inflammatory cytokines such as IL-18 (data not shown), has been linked to development of AIDS (43, 66). The observation that elevated CD29hi CD4+ CTLs were negatively associated with proinflammatory plasma IL-18 during untreated SIV infection, data not shown, corroborates the importance of these cells in fostering better disease outcomes.

The observation that morphine downmodulated the secretion of virus-specific proinflammatory cytokines and the release of granzyme B by CD4+ CD29hi CTLs coincides with several reports that suggest that this drug inhibits CD4+ T cell release of Th1 cytokines (IFN γ, TNF-α) while causing a shift towards Th2 phenotypes (67, 68). However, future studies are needed to evaluate the mechanisms by which morphine causes immune modulation of this cell subset. Further, larger sample sizes and studies using sorted CD29hi CD4+ CTLs are necessary for further validation of the contribution of this cell phenotype towards targeting persistence.

Additional future strategies aimed at improving the CD4+ CTL functionality, such as utilizing chimeric engineering strategies could reinvigorate CD4+ CTLs fostering improved disease outcomes (69, 70). Further, the unexpected transcription profile of lower Eomes expression in CD29hi CD4+ T cells while harnessing augmented levels of Tbet warrants further research in understanding how regulation of transcription factors affects CD4+ CTL functionality and differentiation. In their CD8+ T cell counterparts, Smith et al., revealed that cells expressing Tbet hi and Eomes lo profiles are more efficient in recognizing major histocompatibility complex (MHC) peptides (71). Finally, there is a need to track changes in this cell lineage in body compartments such as lymph nodes, central nervous system, and the gut that provide safe niches for low-level virus replication, evolution, and persistence following effective cART (72).

In conclusion, we demonstrate that CD29 could be reliably used to identify CD4+ CTLs in rhesus macaques. Furthermore, CD29hi CD4+ CTLs are beneficial towards limiting SIV pathogenesis by limiting virus replication and secreting crucial cytokines associated with reducing the size of the viral reservoir within the periphery.

DATA AVAILABILITY STATEMENT

The original contributions presented in the study are included in the article/**Supplementary Material**. Further inquiries can be directed to the corresponding author.

ETHICS STATEMENT

The animal study was reviewed and approved by University of Nebraska Medical Center (UNMC) Institutional Animal Care and Use Committee (IACUC).

AUTHOR CONTRIBUTIONS

OO and SNB designed the conceptual framework of the study and analyzed the data. OO performed all the flow cytometry experiments, wrote the initial draft of the manuscript. SJ, KP, MT, and AA carried out virological assays. SJB, HF, AP, CF, and SNB supported fundraising for the animal studies and edited the manuscript. All authors contributed to the article and approved the submitted version.

FUNDING

This study was supported by NIH grants R01DA043164, P30MH062261 to SNB, SJB, and HF, R01DA041751 to SNB and SJB, and R01AI124965 to CF. The funders had no role in designing the study or in the interpretation of the results.

ACKNOWLEDGMENTS

We appreciate the staff and veterinarians of the University of Nebraska Medical Center (UNMC) Comparative Medicine department for housing and animal procedures. We also appreciate other team members like Brenda M. Morsey, Benjamin Lamberty, Shannon Callen, and personnel from Dr. Byrareddy's laboratory who routinely took care of the rhesus macaques included in this study. We are also grateful to members of the flow core section at UNMC. Finally, we thank

NIH HIV Reagent Program, Division of AIDS, NIAID, NIH for the provision of Peptide Array, Simian Immunodeficiency Virus (SIV) mac239 Gag Protein, ARP-6204.

SUPPLEMENTARY MATERIAL

The Supplementary Material for this article can be found online at: https://www.frontiersin.org/articles/10.3389/fimmu.2021.734871/full#supplementary-material

Supplementary Figure 1 | Longitudinal Changes In Diverse Lymphocyte Subsets During Progressive Untreated Siv Infection. Gating strategy based on a representative sample used for delineation of lymphocyte subpopulations within PBMCs obtained from untreated SIV rhesus macaques. Lymphocytes were gated out based on size and complexity (FSC-a vs. SSC-a). NKG2A vs. CD3+ was used to exclude CD3+ T cells, NKT cells, and NK cells. CD3+ T cells were later differentiated based on CD4+ and CD8+ markers and expression of CD29 was used to mark cytotoxicity in either subset. HLA-DR levels were then used to identify activation levels in either CD4+ or CD8+ T cells. MAIT cells were also studied based on CD161 and Vα7.2Jα co-expression. CD16+ CD8+ T cells (innate like CD8+ T cells) were also evaluated. NK cell subsets based on CD16 and CD56 expression were also studied for maturity based on CD27 and activation based on HLA-DR expression.

Supplementary Figure 2 | Relationship between absolute t cell subsets and percent frequnencies of nk cell subsets during untreated siv disease progression. Changes in absolute: **(A)** CD29hi CD4+ T cells **(B)** CD4+ T cells **(C)** CD8+ T cells during baseline (day 0), day 14 and day 245 past SIV infection. Correlation between absolute CD29hi CD4+ T cells and: **(D)** %CD16+CD56- NK cells **(E)** %CD16-CD56+ NK cells **(F)** %CD16-CD56- NK cells. Additional correlations were also performed that included the association between absolute CD4+ T cells and: **(G)** %CD16+CD56- NK cells **(H)** %CD16-CD56+ NK cells **(I)** %CD16-CD56- NK cells. For **(A-C)**, ** indicates $p < 0.001$ while *** denotes $p < 0.0001$ resulting from Wilcoxon matched pairs signed rank tests between paired groups of the different comparisons. Per visit comparisons between morphine and saline were also performed using the Mann Whitney U test (non- significant).

Supplementary Figure 3 | Representative Gating Of Time Course Changes In Cd29hi Cd4+ T Cells Across The Various Studied Time Points (Baseline, Week 2, Week 7 And Week 22). Representative gating for rhesus macaque CF42 indicating changes in CD95 expression, IFN-γ and TNF-α secretion across CD29hi CD4+ T cells within the studied time points. FMO controls also included for the accurate placement of gates.

Supplementary Figure 4 | Determination Of Integrin (Cd11a And Cd11b) And Chemokine Receptor Expression (Cx3cr1) On Cd29hi Vs Cd29lo Cd4 T Cells During Art Treated Chronic Siv Infection. To achieve this, a time vs FSC-A gate was used to obtain a steady stream of cells during cell acquisition that is devoid of interruptions caused by micro bubbles, clogs or air. The FSC-A vs FSC-H gate and SSC-A vs SSC-H was used to obtain single cells. Dead cells were excluded using positive zombie aqua live dead staining. Lymphocytes were then segregated based on FSC-A vs SSC-A gate based on size and complexity and T cells later gated off using the CD3+ marker. CD4+ T cells were then further gated followed by the extent of their expression of CD29. Comparisons of CD29hi vs CD29lo CD4+ T cells were then carried out to evaluate the expression of CD11a and CD11B integrins together with the chemokine receptor CX3CR1. Fluorescent minus one (FMO) controls were included to set a background for gate placement.

Supplementary Figure 5 | Evaluation Of Cytokine Expression In Cart Treated Siv Infected Macaues Exposed To Morphine Or Saline. Cells were excluded based on the FSC-a vs. time to obtain cells in a single stream. Doublets were excluded using FSC-A vs. FSC-H/SSC-A vs. SSC-H. Live cells were then excluded based on Live Dead Zombie expression. CD3+ T cells were then identified and CD4+ or CD8+ T cells further profiled. CD29 expression in CD4+ T cells was then profiled and various cytokines such as IFN-γ, CD107a, IL21, TNF-α and IL-4 in CD29 lo vs CD29 hi CD4+ T cells unstimulated, gag and PMA/ionomycin conditions.

Supplementary Figure 6 | evaluation of cytokine secretion and cytotoxic molecule expression in cd29lo cd4+ t cells of cart treated siv infected macaques exposed to morphine or saline. Levels of **(A)** ifn-γ **(B)** il-4 **(C)** tnf-α **(D)** cd107a **(E)** mfi of granzyme b **(F)** granzyme b hi **(G)** ifn-γ and tnf-α **(H)** il-21 and ifn-γ expression in cd29lo cd4+ t cells.

Supplementary Figure 7 | evaluation of cytotoxic molecules, transcription factors in cart treated siv infected macaues exposed to morphine or saline. Cd3+ t cells were identified from live cells. Cd4+ t cells were then gated out followed by testing for cd29 expression. In unstimulated, gag or pma/ionomycin conditions, percent expression of: the cytotoxic molecule granzyme together with transcription factors like t bet or eomes were evaluated in cd29 hi vs cd29 lo subsets.

Supplementary Table 1 | various antibody panels used for the study. Exhaustive list of monoclonal antibodies with insights into specificity, fluorochrome tagged, ab clone, vendor/source together with volumes/test used.

REFERENCES

1. Kuehn BM. Study Suggests a Second Patient Has Been Cured of HIV. *JAMA* (2020) 323:1886. doi: 10.1001/jama.2020.7626
2. Woldemeskel BA, Kwaa AK, Blankson JN. Viral Reservoirs in Elite Controllers of HIV-1 Infection: Implications for HIV Cure Strategies. *EBioMedicine* (2020) 62:103118. doi: 10.1016/j.ebiom.2020.103118
3. Macedo AB, Novis CL, Bosque A. Targeting Cellular and Tissue HIV Reservoirs With Toll-Like Receptor Agonists. *Front Immunol* (2019) 10:2450. doi: 10.3389/fimmu.2019.02450
4. Chaillon A, Gianella S, Dellicour S, Rawlings SA, Schlub TE, De Oliveira MF, et al. HIV Persists Throughout Deep Tissues With Repopulation From Multiple Anatomical Sources. *J Clin Invest* (2020) 130:1699–712. doi: 10.1172/JCI134815
5. Busman-Sahay K, Starke CE, Nekorchuk MD, Estes JD. Eliminating HIV Reservoirs for a Cure: The Issue Is in the Tissue. *Curr Opin HIV AIDS* (2021) 16:200–8. doi: 10.1097/COH.0000000000000688
6. Hrdy DB. Cultural Practices Contributing to the Transmission of Human Immunodeficiency Virus in Africa. *Rev Infect Dis* (1987) 9:1109–19. doi: 10.1093/clinids/9.6.1109
7. Chang CC, Crane M, Zhou J, Mina M, Post JJ, Cameron BA, et al. HIV and Co-Infections. *Immunol Rev* (2013) 254:114–42. doi: 10.1111/imr.12063
8. Degenhardt L, Peacock A, Colledge S, Leung J, Grebely J, Vickerman P, et al. Global Prevalence of Injecting Drug Use and Sociodemographic Characteristics and Prevalence of HIV, HBV, and HCV in People Who Inject Drugs: A Multistage Systematic Review. *Lancet Global Health* (2017) 5:e1192–207. doi: 10.1016/S2214-109X(17)30375-3
9. Power J, Westle A, Dowsett GW, Lucke J, Tucker JD, Sugarman J, et al. Perceptions of HIV Cure Research Among People Living With HIV in Australia. *PloS One* (2018) 13:e0202647. doi: 10.1371/journal.pone.0202647
10. Acharya A, Olwenyi OA, Thurman M, Pandey K, Morsey BM, Lamberty B, et al. Chronic Morphine Administration Differentially Modulates Viral Reservoirs in a Simian Immunodeficiency Virus SIVmac251-Infected Rhesus Macaque Model. *J Virol* (2021) 95:e01657–01620. doi: 10.1128/JVI.01657-20
11. Olwenyi OA, Asingura B, Naluyima P, Anywar GU, Nalunga J, Nakabuye M, et al. In-Vitro Immunomodulatory Activity of Azadirachta Indica A.Juss. Ethanol: Water Mixture Against HIV Associated Chronic CD4(+) T-Cell Activation/ Exhaustion. *BMC Complement Med Ther* (2021) 21:114. doi: 10.1186/s12906-021-03288-0
12. Dybul M, Attoye T, Baptiste S, Cherutich P, Dabis F, Deeks SG, et al. The Case for an HIV Cure and How to Get There. *Lancet HIV* (2020) 8:e51–8. doi: 10.1016/S2352-3018(20)30232-0
13. Swain SL, Mckinstry KK, Strutt TM. Expanding Roles for CD4 + T Cells in Immunity to Viruses. *Nat Rev Immunol* (2012) 12:136–48. doi: 10.1038/nri3152
14. Jost S, Tomezsko PJ, Rands K, Toth I, Lichterfeld M, Gandhi RT, et al. CD4+ T-Cell Help Enhances NK Cell Function Following Therapeutic HIV-1 Vaccination. *J Virol* (2014) 88:8349–54. doi: 10.1128/JVI.00924-14

15. Ayasoufi K, Fan R, Fairchild RL, Valujskikh A. CD4 T Cell Help via B Cells Is Required for Lymphopenia-Induced CD8 T Cell Proliferation. *J Immunol* (2016) 196:3180. doi: 10.4049/jimmunol.1501435
16. Laidlaw BJ, Craft JE, Kaech SM. The Multifaceted Role of CD4(+) T Cells in CD8(+) T Cell Memory. *Nat Rev Immunol* (2016) 16:102–11. doi: 10.1038/nri.2015.10
17. Gray JI, Westerhof LM, Macleod MK. The Roles of Resident, Central and Effector Memory CD 4 T-Cells in Protective Immunity Following Infection or Vaccination. *Immunology* (2018) 154:574–81. doi: 10.1111/imm.12929
18. Beura LK, Fares-Frederickson NJ, Steinert EM, Scott MC, Thompson EA, Fraser KA, et al. CD4+ Resident Memory T Cells Dominate Immunosurveillance and Orchestrate Local Recall Responses. *J Exp Med* (2019) 216:1214–29. doi: 10.1084/jem.20181365
19. Hoefig KP, Heissmeyer V. Posttranscriptional Regulation of T Helper Cell Fate Decisions. *J Cell Biol* (2018) 217:2615–31. doi: 10.1083/jcb.201708075
20. Caza T, Landas S. Functional and Phenotypic Plasticity of CD4+ T Cell Subsets. *BioMed Res Int* (2015) 2015:521957. doi: 10.1155/2015/521957
21. Hashimoto K, Kouno T, Ikawa T, Hayatsu N, Miyajima Y, Yabukami H, et al. Single-Cell Transcriptomics Reveals Expansion of Cytotoxic CD4 T Cells in Supercentenarians. *Proc Natl Acad Sci USA* (2019) 116:24242–51. doi: 10.1073/pnas.1907883116
22. Olwenyi OA, Naluyima P, Cham F, Quinn TC, Serwadda D, Sewankambo NK, et al. Brief Report: Differential Associations of Interleukin 6 and Intestinal Fatty Acid-Binding Protein With Progressive Untreated HIV-1 Infection in Rakai, Uganda. *J acquired Immune deficiency syndromes (1999)* (2016) 72:15–20. doi: 10.1097/QAI.0000000000000915
23. Vidya Vijayan KK, Karthigeyan KP, Tripathi SP, Hanna LE. Pathophysiology of CD4+ T-Cell Depletion in HIV-1 and HIV-2 Infections. *Front Immunol* (2017) 8:580. doi: 10.3389/fimmu.2017.00580
24. Estes JD, Harris LD, Klatt NR, Tabb B, Pittaluga S, Paiardini M, et al. Damaged Intestinal Epithelial Integrity Linked to Microbial Translocation in Pathogenic Simian Immunodeficiency Virus Infections. *PloS Pathog* (2010) 6:e1001052. doi: 10.1371/journal.ppat.1001052
25. Sandler NG, Douek DC. Microbial Translocation in HIV Infection: Causes, Consequences and Treatment Opportunities. *Nat Rev Microbiol* (2012) 10:655–66. doi: 10.1038/nrmicro2848
26. Dillon SM, Frank DN, Wilson CC. The Gut Microbiome and HIV-1 Pathogenesis: A Two-Way Street. *Aids* (2016) 30:2737–51. doi: 10.1097/QAD.0000000000001289
27. Dillon SM, Lee EJ, Kotter CV, Austin GL, Gianella S, Siewe B, et al. Gut Dendritic Cell Activation Links an Altered Colonic Microbiome to Mucosal and Systemic T-Cell Activation in Untreated HIV-1 Infection. *Mucosal Immunol* (2016) 9:24–37. doi: 10.1038/mi.2015.33
28. Dubourg G, Lagier J-C, Hüe S, Surenaud M, Bachar D, Robert C, et al. Gut Microbiota Associated With HIV Infection Is Significantly Enriched in Bacteria Tolerant to Oxygen. *BMJ Open Gastroenterol* (2016) 3:e000080. doi: 10.1136/bmjgast-2016-000080
29. Klatt NR, Funderburg NT, Brenchley JM. Microbial Translocation, Immune Activation, and HIV Disease. *Trends Microbiol* (2013) 21:6–13. doi: 10.1016/j.tim.2012.09.001
30. Dillon SM, Kibbie J, Lee EJ, Guo K, Santiago ML, Austin GL, et al. Low Abundance of Colonic Butyrate-Producing Bacteria in HIV Infection Is Associated With Microbial Translocation and Immune Activation. *AIDS (London England)* (2017) 31:511–21. doi: 10.1097/QAD.0000000000001366
31. Groux H, Torpier G, Monté D, Mouton Y, Capron A, Ameisen JC. Activation-Induced Death by Apoptosis in CD4+ T Cells From Human Immunodeficiency Virus-Infected Asymptomatic Individuals. *J Exp Med* (1992) 175:331–40. doi: 10.1084/jem.175.2.331
32. Doitsh G, Cavrois M, Lassen KG, Zepeda O, Yang Z, Santiago ML, et al. Abortive HIV Infection Mediates CD4 T Cell Depletion and Inflammation in Human Lymphoid Tissue. *Cell* (2010) 143:789–801. doi: 10.1016/j.cell.2010.11.001
33. Handoko R, Colby DJ, Kroon E, Sacdalan C, De Souza M, Pinyakorn S, et al. Determinants of Suboptimal CD4(+) T Cell Recovery After Antiretroviral Therapy Initiation in a Prospective Cohort of Acute HIV-1 Infection. *J Int AIDS Soc* (2020) 23:e25585–5.
34. Hernández-Walias F, Ruiz-De-León MJ, Rosado-Sánchez I, Vázquez E, Leal M, Moreno S, et al. New Signatures of Poor CD4 Cell Recovery After Suppressive Antiretroviral Therapy in HIV-1-Infected Individuals: Involvement of miR-192, IL-6, Scd14 and miR-144. *Sci Rep* (2020) 10:2937. doi: 10.1038/s41598-020-60073-8
35. Wilson EMP, Sereti I. Immune Restoration After Antiretroviral Therapy: The Pitfalls of Hasty or Incomplete Repairs. *Immunol Rev* (2013) 254:343–54. doi: 10.1111/imr.12064
36. Aid M, Dupuy FP, Moysi E, Moir S, Haddad EK, Estes JD, et al. Follicular CD4 T Helper Cells As a Major HIV Reservoir Compartment: A Molecular Perspective. *Front Immunol* (2018) 9:895. doi: 10.3389/fimmu.2018.00895
37. Godinho-Santos A, Foxall RB, Antão AV, Tavares B, Ferreira T, Serra-Caetano A, et al. Follicular Helper T Cells Are Major Human Immunodeficiency Virus-2 Reservoirs and Support Productive Infection. *J Infect Dis* (2019) 221:122–6. doi: 10.1093/infdis/jiz431
38. Johnson S, Eller M, Teigler JE, Maloveste SM, Schultz BT, Soghoian DZ, et al. Cooperativity of HIV-Specific Cytolytic CD4 T Cells and CD8 T Cells in Control of HIV Viremia. *J Virol* (2015) 89:7494–505. doi: 10.1128/JVI.00438-15
39. Sanchez-Martinez A, Perdomo-Celis F, Acevedo-Saenz L, Rugeles MT, Velilla PA. Cytotoxic CD4(+) T-Cells During HIV Infection: Targets or Weapons? *J Clin Virol* (2019) 119:17–23. doi: 10.1016/j.jcv.2019.08.004
40. Soghoian DZ, Jessen H, Flanders M, Sierra-Davidson K, Cutler S, Pertel T, et al. HIV-Specific Cytolytic CD4 T Cell Responses During Acute HIV Infection Predict Disease Outcome. *Sci Trans Med* (2012) 4:123ra125–123ra125. doi: 10.1126/scitranslmed.3003165
41. Zheng N, Fujiwara M, Ueno T, Oka S, Takiguchi M. Strong Ability of Nef-Specific CD4+ Cytotoxic T Cells To Suppress Human Immunodeficiency Virus Type 1 (HIV-1) Replication in HIV-1-Infected CD4+ T Cells and Macrophages. *J Virol* (2009) 83:7668–77. doi: 10.1128/JVI.00513-09
42. Yue FY, Cohen JC, Ho M, Rahman A, Liu J, Mujib S, et al. HIV-Specific Granzyme B-Secreting But Not Gamma Interferon-Secreting T Cells Are Associated With Reduced Viral Reservoirs in Early HIV Infection. *J Virol* (2017) 91:e02233-02216. doi: 10.1128/JVI.02233-16
43. Iannello A, Samarani S, Debbeche O, Boulassel MR, Tremblay C, Toma E, et al. Potential Role of IL-18 in the Immunopathogenesis of AIDS, HIV-Associated Lipodystrophy and Related Clinical Conditions. *Curr HIV Res* (2010) 8:147–64. doi: 10.2174/157016210790442713
44. Phetsouphanh C, Aldridge D, Marchi E, Munier CML, Meyerowitz J, Murray L, et al. Maintenance of Functional CD57+ Cytolytic CD4+ T Cells in HIV+ Elite Controllers. *Front Immunol* (2019) 10:1844. doi: 10.3389/fimmu.2019.01844
45. Ram DR, Manickam C, Hueber B, Itell HL, Permar SR, Varner V, et al. Tracking KLRC2 (NKG2C)+ Memory-Like NK Cells in SIV+ and rhCMV+ Rhesus Macaques. *PloS Pathog* (2018) 14:e1007104. doi: 10.1371/journal.ppat.1007104
46. Resource, N.H.P.R. (2021). Available at: https://www.nhpreagents.org/ReactivityDatabase.
47. Nicolet BP, Guislain A, Wolkers MC. CD29 Enriches for Cytotoxic Human CD4+ T Cells. *BioRxiv* (2021) 2021.2002.2010.430576. doi: 10.1101/2021.02.10.430576
48. Porichis F, Kaufmann DE. HIV-Specific CD4 T Cells and Immune Control of Viral Replication. *Curr Opin HIV AIDS* (2011) 6:174–80. doi: 10.1097/COH.0b013e3283454058
49. Woollard SM, Olwenyi OA, Dutta D, Dave RS, Mathews S, Gorantla S, et al. Preliminary Studies on Immune Response and Viral Pathogenesis of Zika Virus in Rhesus Macaques. *Pathogens* (2018) 7:70. doi: 10.3390/pathogens7030070
50. Byrareddy SN, Kallam B, Arthos J, Cicala C, Nawaz F, Hiatt J, et al. Targeting α4β7 Integrin Reduces Mucosal Transmission of Simian Immunodeficiency Virus and Protects Gut-Associated Lymphoid Tissue From Infection. *Nat Med* (2014) 20:1397–400. doi: 10.1038/nm.3715
51. Olwenyi OA, Acharya A, Routhu NK, Pierzchalski K, Jones JW, Kane MA, et al. Retinoic Acid Improves the Recovery of Replication-Competent Virus From Latent SIV Infected Cells. *Cells* (2020) 9:2076. doi: 10.3390/cells9092076
52. Roederer M, Nozzi JL, Nason MC. SPICE: Exploration and Analysis of Post-Cytometric Complex Multivariate Datasets. *Cytometry Part A* (2011) 79A:167–74. doi: 10.1002/cyto.a.21015
53. Burwitz BJ, Giraldo-Vela JP, Reed J, Newman LP, Bean AT, Nimityongskul FA, et al. CD8+ and CD4+ Cytotoxic T Cell Escape Mutations Precede

Breakthrough SIVmac239 Viremia in an Elite Controller. *Retrovirology* (2012) 9:91–1. doi: 10.1186/1742-4690-9-91
54. Veazey RS, Tham IC, Mansfield KG, Demaria M, Forand AE, Shvetz DE, et al. Identifying the Target Cell in Primary Simian Immunodeficiency Virus (SIV) Infection: Highly Activated Memory CD4(+) T Cells Are Rapidly Eliminated in Early SIV Infection In Vivo. *J Virol* (2000) 74:57–64. doi: 10.1128/JVI.74.1.57-64.2000
55. Carville A, Evans TI, Reeves RK. Characterization of Circulating Natural Killer Cells in Neotropical Primates. *PloS One* (2013) 8:e78793. doi: 10.1371/journal.pone.0078793
56. Hong H, Rajakumar P, Billingsley J, Reeves RK, Johnson R. No Monkey Business: Why Studying NK Cells in Non-Human Primates Pays Off. *Front Immunol* (2013) 4:32. doi: 10.3389/fimmu.2013.00032
57. Vargas-Inchaustegui DA, Ying O, Demberg T, Robert-Guroff M. Evaluation of Functional NK Cell Responses in Vaccinated and SIV-Infected Rhesus Macaques. *Front Immunol* (2016) 7:340. doi: 10.3389/fimmu.2016.00340
58. Schuetz A, Deleage C, Sereti I, Rerknimitr R, Phanuphak N, Phuang-Ngern Y, et al. Initiation of ART During Early Acute HIV Infection Preserves Mucosal Th17 Function and Reverses HIV-Related Immune Activation. *PloS Pathog* (2014) 10:e1004543. doi: 10.1371/journal.ppat.1004543
59. Salido J, Ruiz MJ, Trifone C, Figueroa MI, Caruso MP, Gherardi MM, et al. Phenotype, Polyfunctionality, and Antiviral Activity of In Vitro Stimulated CD8+ T-Cells From HIV+ Subjects Who Initiated cART at Different Time-Points After Acute Infection. *Front Immunol* (2018) 9:2443. doi: 10.3389/fimmu.2018.02443
60. Takeuchi A, Saito T. CD4 CTL, a Cytotoxic Subset of CD4+ T Cells, Their Differentiation and Function. *Front Immunol* (2017) 8:194. doi: 10.3389/fimmu.2017.00194
61. Glimcher LH, Townsend MJ, Sullivan BM, Lord GM. Recent Developments in the Transcriptional Regulation of Cytolytic Effector Cells. *Nat Rev Immunol* (2004) 4:900–11. doi: 10.1038/nri1490
62. Weiskopf D, Bangs DJ, Sidney J, Kolla RV, De Silva AD, De Silva AM, et al. Dengue Virus Infection Elicits Highly Polarized CX3CR1+ Cytotoxic CD4+ T Cells Associated With Protective Immunity. *Proc Natl Acad Sci* (2015) 112:E4256. doi: 10.1073/pnas.1505956112
63. Chen B, Morris SR, Panigrahi S, Michaelson GM, Wyrick JM, Komissarov AA, et al. Cytomegalovirus Coinfection Is Associated With Increased Vascular-Homing CD57(+) CD4 T Cells in HIV Infection. *J Immunol* (2020) 204:2722–33. doi: 10.4049/jimmunol.1900734
64. Chevalier Mathieu F, Jülg B, Pyo A, Flanders M, Ranasinghe S, Soghoian Damien Z, et al. HIV-1-Specific Interleukin-21+ CD4+ T Cell Responses Contribute to Durable Viral Control Through the Modulation of HIV-Specific CD8+ T Cell Function. *J Virol* (2011) 85:733–41. doi: 10.1128/JVI.02030-10
65. Harper J, Huot N, Micci L, Tharp G, King C, Rascle P, et al. IL-21 and Ifnα Therapy Rescues Terminally Differentiated NK Cells and Limits SIV Reservoir in ART-Treated Macaques. *Nat Commun* (2021) 12:2866. doi: 10.1038/s41467-021-23189-7
66. Ahmad R, Sindhu Sardar TA, Toma E, Morisset R, Ahmad A. Elevated Levels of Circulating Interleukin-18 in Human Immunodeficiency Virus-Infected Individuals: Role of Peripheral Blood Mononuclear Cells and Implications for AIDS Pathogenesis. *J Virol* (2002) 76:12448–56. doi: 10.1128/JVI.76.24.12448-12456.2002
67. Roy S, Balasubramanian S, Sumandeep S, Charboneau R, Wang J, Melnyk D, et al. Morphine Directs T Cells Toward T(H2) Differentiation. *Surgery* (2001) 130:304–9. doi: 10.1067/msy.2001.116033
68. Greeneltch KM, Kelly-Welch AE, Shi Y, Keegan AD. Chronic Morphine Treatment Promotes Specific Th2 Cytokine Production by Murine T Cells In Vitro via a Fas/Fas Ligand-Dependent Mechanism. *J Immunol* (2005) 175:4999. doi: 10.4049/jimmunol.175.8.4999
69. Hensley-Mcbain T, Zevin AS, Manuzak J, Smith E, Gile J, Miller C, et al. Effects of Fecal Microbial Transplantation on Microbiome and Immunity in Simian Immunodeficiency Virus-Infected Macaques. *J Virol* (2016) 90:4981–9. doi: 10.1128/JVI.00099-16
70. Benmebarek M-R, Karches CH, Cadilha BL, Lesch S, Endres S, Kobold S. Killing Mechanisms of Chimeric Antigen Receptor (CAR) T Cells. *Int J Mol Sci* (2019) 20:1283. doi: 10.3390/ijms20061283
71. Smith C, Elhassen D, Gras S, Wynn KK, Dasari V, Tellam J, et al. Endogenous Antigen Presentation Impacts on T-Box Transcription Factor Expression and Functional Maturation of CD8+ T Cells. *Blood* (2012) 120:3237–45. doi: 10.1182/blood-2012-03-420182
72. Banga R, Munoz O, Perreau M. HIV Persistence in Lymph Nodes. *Curr Opin HIV AIDS* (2021) 16:209–14. doi: 10.1097/COH.0000000000000686

Conflict of Interest: The authors declare that the research was conducted in the absence of any commercial or financial relationships that could be construed as a potential conflict of interest.

Publisher's Note: All claims expressed in this article are solely those of the authors and do not necessarily represent those of their affiliated organizations, or those of the publisher, the editors and the reviewers. Any product that may be evaluated in this article, or claim that may be made by its manufacturer, is not guaranteed or endorsed by the publisher.

frontiers in Immunology

ORIGINAL RESEARCH
published: 18 November 2021
doi: 10.3389/fimmu.2021.778455

Low-Dose Acetylsalicylic Acid Reduces T Cell Immune Activation: Potential Implications for HIV Prevention

Julie Lajoie[1,2†], Monika M. Kowatsch[1†], Lucy W. Mwangi[2], Geneviève Boily-Larouche[1], Julius Oyugi[1,2,3], Yufei Chen[4], Makobu Kimani[5], Emmanuel A. Ho[4,6], Joshua Kimani[1,3,5] and Keith R. Fowke[1,2,5,7]*

[1] Laboratory of Viral Immunology, Department of Medical Microbiology and Infectious Diseases, University of Manitoba, Winnipeg, MB, Canada, [2] Department of Medical Microbiology, University of Nairobi, Nairobi, Kenya, [3] University of Nairobi Institute for Tropical and Infectious Diseases, University of Nairobi, Nairobi, Kenya, [4] College of Pharmacy, University of Manitoba, Winnipeg, MB, Canada, [5] Partners for Health and Development in Africa, Nairobi, Kenya, [6] Laboratory for Drug Delivery and Biomaterials, School of Pharmacy, University of Waterloo, Waterloo, ON, Canada, [7] Department of Community Health Science, University of Manitoba, Winnipeg, MB, Canada

OPEN ACCESS

Edited by:
Constantinos Petrovas, Centre Hospitalier Universitaire Vaudois (CHUV), Switzerland

Reviewed by:
Graziela Gorete Romagnoli, Oeste Paulista University - UNOESTE, Brazil
Derseree Archary, Centre for the AIDS Programme of Research in South Africa, South Africa

***Correspondence:**
Keith R. Fowke
keith.fowke@umanitoba.ca

[†]These authors have contributed equally to this work and share first authorship

Specialty section:
This article was submitted to Viral Immunology, a section of the journal Frontiers in Immunology

Received: 16 September 2021
Accepted: 22 October 2021
Published: 18 November 2021

Citation:
Lajoie J, Kowatsch MM, Mwangi LW, Boily-Larouche G, Oyugi J, Chen Y, Kimani M, Ho EA, Kimani J and Fowke KR (2021) Low-Dose Acetylsalicylic Acid Reduces T Cell Immune Activation: Potential Implications for HIV Prevention. Front. Immunol. 12:778455. doi: 10.3389/fimmu.2021.778455

Introduction: Acetylsalicylic acid (ASA) is a well-known and safe anti-inflammatory. At low-dose, it is prescribed to prevent secondary cardiovascular events in those with pre-existing conditions and to prevent preeclampsia. Little is known about how low-dose ASA affects the immune response. In this study, we followed women to assess how ASA use modifies T cells immune phenotypes in the blood and at the genital tract.

Methods: HIV uninfected women from Kenya were enrolled in this study and followed for one month to assess baseline responses including systemic/mucosal baseline immune activation. Participants then received 81mg of ASA daily for 6 weeks to assess changes to T cell immune activation (systemic and mucosal) relative to baseline levels.

Results: The concentration of ASA measured in the blood was 58% higher than the level measured at the female genital tract. In the blood, the level of ASA was inversely correlated with the following: the proportion of Th17 expressing HLA-DR (p=0.04), the proportion of effector $CD4^+$ T cells expressing CCR5 (p=0.03) and the proportion of $CD8^+$Tc17 expressing CCR5 (p=0.04). At the genital tract, ASA use correlated with a decreased of activated $CD4^+$T cells [$CD4^+CCR5^+CD161^+$ (p=0.02) and $CD4^+CCR5^+CD95^+$ (p=0.001)].

Conclusion: This study shows that ASA use impacts the immune response in both the systemic and genital tract compartments. This could have major implications for the prevention of infectious diseases such as HIV, in which the virus targets activated T cells to establish an infection. This could inform guidelines on ASA use in women.

Clinical Trial Registration: ClinicalTrials.gov, identifier NCT02079077.

Keywords: HIV, immune activation (IA), HIV risk, aspirin, Acetylsalicylic acid, inflammation, immune quiescence, HIV prevention

INTRODUCTION

Acetylsalicylic acid (ASA) belongs to the non-steroidal anti-inflammatory drug (NSAID) category. Since its discovery, it has been used for the treatment of pain and fever (1). Currently, daily low dose ASA is prescribed for prevention of secondary cardiovascular events and stroke in patients with pre-existing conditions (2). Furthermore, USA guidelines were recently modified to include the use of low-dose ASA to reduce the risk of preeclampsia (3).

At low doses, ASA acts as an anticoagulation drug, which blocks the normal function of the cyclooxygenase (COX)-1 and -2 enzymes (4). By blocking the function of the COX enzymes, ASA prevents the synthesis of the pro-inflammatory lipids thromboxane (5) and some prostaglandins (6) while inducing the synthesis of the anti-inflammatory 15-epi-lipoxin (7). Furthermore, ASA inhibits the activation of NF-κB thereby blocking transcription of pro-inflammatory mediators (8) resulting in decreased infiltration of immune cells into tissues (9).

Immune activation and inflammation are risk factors for HIV infection. Recently, the CAPRISA 004 study, which compared a placebo control group to a 1% Tenofovir vaginal gel, showed the gel had significant protection from HIV infection (adjusted odds ratio 7.15 p=0.48) (10). However, it was also shown that regardless of the study arm they were in, participants with higher baseline of immune activation were more likely to acquire HIV (adjusted odds ratio 11.27 p=.009) where as an "innate immune quiescence" phenotype was protective (adjusted odds ratio 0.06 p=0.001) (10). Importantly, the presence of genital inflammation completely abrogated the protective effect of the Tenofovir gel demonstrating that inflammation can negate the protective effects of anti-viral agents (11). On the other hand, natural protection to HIV infection has been associated with an immune phenotype of reduced inflammation which our group has called "immune quiescence". This phenotype is characterized by a lower baseline level in T cell activation and lower expression of pro-inflammatory chemokines (CXCL9 and CXCL10) (12). Together these studies show that genital inflammation impacts susceptibility to HIV infection and reducing inflammation is associated with protection from infection.

As inflammation is a major driver of disease progression among those infected with HIV, two clinical trials were conducted to determine if ASA could decrease inflammation in HIV-positive individuals. While one study showed ASA decreased the proportion of activated T cells (13), the second study showed no reduction in systemic inflammation or monocyte activation (14) suggesting that the tremendous immune activation caused by active HIV infection was not reversible with ASA. The impact of ASA use in the context of HIV infection remains debatable.

Until now, to our knowledge, no study looked at ASA to prevent HIV infection. Recently, we reported preliminary findings demonstrating that low-dose ASA treatment (81mg/day) decreased the proportion of HIV target cells at the female genital tract in HIV uninfected women and induced an immune quiescence phenotype similar to that observed in HIV-exposed seronegative (HESN) (15). Herein, we are reporting a detailed follow-up analysis to assess the immunological effects of how low-dose ASA altered the T cell compartment toward a less activated immune response which would have implications for a novel HIV prevention tool.

METHODS

Study Design and Participants

As described previously, the Inducing Immune Quiescence (IIQ) study was a randomized pilot, open-label study conducted at the Pumwani maternity and Baba Dogo community clinics located in Nairobi, Kenya (15). Thirty-eight HIV uninfected non-sex worker women were randomized into the ASA arm and were given 81mg of ASA (Bayer Canada, Mississauga, ON) per day for six weeks. The second arm consisted of 39 women treated with 200 mg of hydroxychloroquine (HCQ). As the focus of this analysis is on the mechanism of the ASA effect, the HCQ arm will not be discussed in this paper (15). Briefly, enrolment criteria were age greater than 18 and less than 55 years, not self-declaring as sex workers, presence of the uterus and cervix, willing to take the study drugs for 6 weeks, in general good health, no recent pregnancy, not breastfeeding, not currently taking anti-inflammatory or immune-suppressors, being HIV uninfected and having no history of cardiovascular diseases. Exclusion criteria included being pregnant in the last 12 months, the presence of a sexual transmissible disease (STI) at enrolment or at any time during the course of the study, menopause, taking medication that counteracts with ASA, being allergic to the study drug, having history of heartburn, stomach pain, stomach ulcers, anomia, haemophilia, kidney or liver diseases, cardiovascular diseases, or being currently involved in another clinical trial. Both the University of Nairobi/Kenyatta National Hospital and the University of Manitoba research ethic boards approved this study. The study was registered on ClinicalTrials.gov (NCT02079077).

Enrolment Procedures

Community consultative meetings were held prior to starting the study and served to introduce and discuss the study with community members, as well as assess their acceptance of the drugs, well before enrolment started. Eligible participants were screened and within two weeks were enrolled and randomized. All participants discussed the study with the study nurse and signed a consent form. Enrolled participants were followed for a 3-month period. As the immune system is known to vary during the menstrual cycle, vaginal sampling among women with a regular menstrual cycle was scheduled 5-8 days after the end of their menses. This study was designed without a placebo arm and each participant's pre-drug baseline served as her own control. At visit 1 (pre-drug baseline) and visit 3 (final day of ASA, 6 weeks post initiation of drug) blood and cervical samples were taken for the assessment of systemic and mucosal immune activation. ASA was stopped at 6 weeks and an 8-week follow-up sample was collected to assess liver/kidney function and thromboxane levels.

Sample Collection and Processing

Vaginal and blood samples were collected at each visit. A vulvovaginal swab was collected to assess for the presence of candida pseudohyphae and bacterial vaginosis by microscopy as well as *Trichomonas vaginalis*, which was diagnosed by In-Pouch kit (Biomed Diagnostics, USA). Urine samples were collected for detection of *Neisseria gonorrhea* and *Chlamydia trachomatis* (Roche Amplicor kits, USA). HIV serology using a rapid test (Determine, Inverness Medical, Japan) was performed at the first and last visit (there were no HIV seroconversions during or 6 months following the study). A questionnaire was completed at each visit. At the end of the study, to confirm adherence to the study protocol, plasma and cervico-vaginal lavage (CVL) were shipped to Winnipeg, Canada for ASA-level and cytokine and chemokine measurements (16).

Cervical cytobrushes and CVL were collected and processed according to the procedure detailed in Juno et al. (17). Blood was collected with venipuncture using heparin, and peripheral blood mononuclear cells (PBMC) were isolated by Ficoll density gradient.

PBMC and CMC Flow Cytometry

Peripheral blood mononuclear cells (PBMC) (10^6) and cervical mononuclear cells (CMC) were washed with 2% FBS-1x PBS and stained with PE.Cy5-CD3, FITC-CD4, V500-CD8, PE-CD95, APC.H7-HLA-DR, APC-CD161, Alexa700-CD45RA, V450-CCR5, PE.Cy7-CD69, PE-CF594-CCR7 (BD Biosciences, USA), or Far Red-Live Dead discriminant (Invitrogen, USA). Staining was done on fresh cells. Data were acquired on an LSRII flow cytometer (BD System, USA) and analysed using FlowJo v10.0.8r1 (TreeStar, USA). Gating strategy was to gate first on singlet, followed by lymphocytes gating and then gate on live dead and $CD3^+$. Viable $CD3^+$ cells were separated according to the $CD4^+$ and $CD8^+$ staining. For CMC, if fewer than 100 live cells were captured, the samples were excluded from the analyses. PBMCs not stained with the above panel were frozen and shipped to Winnipeg, Canada where two additional T cell phenotyping panels were used. For both assays, cells were thawed and rested overnight, 10^6 PBMCs were washed with 2% FBS-1x PBS and for the first panel, targeted at T cell trafficking, stained with APC-fire-CD3, BV605-CD4, BV650-CD8, BV421-CD161, Alexa700-CD29, Pe-Dazzle-CXCR3, PerCP-Cy5.5-Vα7.2 (BD Biosciences, USA), PE-CD103, Pe-Cy7-CD25, BB515-CCR5, APC-CCR6 (Biolegend, USA), and Aqua Vivid Dead discriminant (ThermoFisher, USA). Cells were gated first on singlets, followed by lymphocytes and then on live dead. Live cells were gated on $CD3^+$ and then separated into $CD4^+$ and $CD8^+$ subsets. Off the $CD4^+$ group Th17 cells were gated as $CD161^+CCR6^+$. From the $CD8^+$ group Tc17 cells were gated as $CD161^+V\alpha7.2$-. MAIT cells were gated off the CD3 population then CD4- followed by $CD161^{++}V\alpha7.2^+$. All trafficking markers were then gated off each subset. For the second panel, for T regulatory (Treg) identification, cells were and stained following a modified intracellular (nuclear antigen) protocol from ThermoFisher Scientific (3). Antibodies used were as follows, PeCy7-CD3, BV605-CD4, BV650-CD8, Alexa488-CD25, Alexa700-CD127, Pe-Dazzle-TIGIT, APC-Fire-CD69, BV711-HLA-DR, PerCp-Cy5.5-CTLA-4 (Biolegend, USA), PE-FoxP3, eFlour450-Helios (eBiosciences, USA), and Aqua Vivid Dead discriminant (ThermoFisher, USA). Gating strategy consisted of gating on singlets followed by lymphocytes and then live cells. From there $CD3^+$ cells were selected and then $CD4^+$ cells. Tregs were defined off the $CD4^+$ population as $CD25^+FoxP3^+$ and markers of activation and function were gated of the Treg population. To account for potential cytometer variability overtime 8 peak rainbow calibration particles (BD Biosciences, USA) were ran monthly and Fluorescent minus one controls were ran weekly using sample PBMCs. Median Fluorescence Intensity (MFI) of markers expressed on a per cell bases is described is utilized to describe "expression" of markers on a given cell.

ASA Detection

ASA levels were compared between Visit 1 (baseline) and Visit 3 (6 weeks of ASA). ASA in plasma and CVL samples were quantitated using reversed phase high-performance liquid chromatography (RP-HPLC) following previously described methods (18) with slight modifications. Briefly, HPLC analysis was performed using a Symmetry® C18 column (300Å, 3.5 µm 4.6 mm x 75 mm; Waters) with a Symmetry® C18 guard column (300Å, 5 µm, 3.9 mm x 20 mm; Waters), fitted to a Waters® Alliance® HPLC system equipped with Waters® 2690 Separations module and Waters® 996 Photodiode Array detector. The mobile phase is comprised of water, acetonitrile and orthophosphoric acid at a ratio of 74:18:0.9 (v/v, pH 2.5). Each injection (100µL) was run for 10 min at 1 mL/min with a detection wavelength set at 234 nm. The retention time for the internal standard simvastatin (SIM) and ASA were 0.97 min and 5.09 min, respectively. Plasma samples (200µL) were combined with an equivalent volume of internal standard solution. The pH of the entire solution was adjusted to 2.7 by the addition of orthophosphoric acid and the analyte was extracted using 400 µL of acetonitrile. The supernatant was then transferred into a microcentrifuge tube containing 100-120 mg of sodium chloride, vortexed and centrifuged. The upper organic phase (100 µL) was injected for HPLC analysis. CVL samples were extracted similarly except the resulting supernatant was collected and evaporated under nitrogen gas. Following the addition of 100 µL of 0.01 M hydrochloric acid into the vial for reconstitution, the entire solution was injected into the HPLC machine. For ASA, the lower limits of quantitation (LLOQ) for CVL was 39 ng/mL and for plasma was 78 ng/mL with an extraction efficiency of 92.16 ± 0.64% for CVL and 86.45 ± 1.31% (mean ± SD) for plasma. A value of half the LLOQ was assigned to participants below the LLOQ, 19.5 ng/mL for CVL and 39 ng/mL for plasma.

TXB2 Level

Thromboxane B_2 (TXB2) levels were detected in the plasma using an enzyme-linked immunosorbent assay or ELISA at a 1:5 dilution as per the protocol provided by manufacturer (Abcam, Toronto, Canada) and ran on the Spectra Max Plus plate reader

at 405nm with correction at 590 nm. Data was analysed using Wilcoxon matched-pairs signed rank on pg/mL raw data and visualized on a logarithmic scale for clearer visualization of the data.

Cytokine and Chemokine Detection

Cytokines and chemokines were assessed using Milliplex MAP multiplex kits microbead assays (Millipore, Burlington, USA) and run using the Bio-Plex 200 (BioRad, Hercules, USA). Plasmas were incubated for 2 hours and room temperature and CVLs were incubated overnight at 4°C as per manufacturers protocol. Cytokine and chemokines and their lower limit of detection ran were as follows: 0.8 pg/mL for IFN-γ, 1.1pg/mL for IL-10, 0.6 pg/mL for IL-12(p70), 5.1 pg/mL for sCD40L, 0.7 pg/mL for IL-17A, 9.4 pg/mL for IL-1α, 0.8 pg/mL for IL-1β, 1 pg/mL for IL-2, 0.4 pg/mL for IL-8, 8.6 pg/mL for IP-10, 1.9 pg/mL for MCP-1, 2.9 pg/mL for MIP-1α, 3 pg/mL for MIP-1β, 0.7 pg/mL for TNF-α, 8.3 pg/mL for IL-1RA, 10.3 pg/mL for MIG, 1.6 pg/mL for MIP-3α and 6 pg/mL for IL-2RA. It should be noted that for samples below the limit of detection an assigned value of half the manufacturers specified limit of detection was used. For CVL sample 12 cytokines and chemokines were detected in enough abundance to be used in downstream analysis.

Statistical Analysis

This was a pilot study to assess the impact of ASA on T cell immune activation. An intention to treat analysis was performed. Chi Squared (X^2) was used to assess the significance of the associations between categorical variable using Prism 6.0f (GraphPad Software, La Jolla, CA, USA) and Gaussian distribution was tested by Shapiro-Wilk normality test and normality plot using SPSS (NY, USA). To compare baseline to visit 3 two-tailed paired T test (for normally distributed data) or Wilcoxon matched-pair signed-rank test (for data not following normality distribution) were performed using Prism 6.0f (GraphPad Software, La Jolla, CA, USA) or STATA v15.0 (StataCorp LLC, USA). Using SSPS, multivariate regressions were performed to assess the impact of DMPA usage and age on the change score (Visit 3-baseline). To understand the dynamics of the immune system between systemic and musical compartments we performed correlations between plasma and CVL ASA levels were run against data from both the PBMCs and CMCs. Pearson correlation or Spearman's rank test were used for correlations between continuous variables (GraphPad Software, La Jolla, CA, USA). A p-value of <0.05 was considered as significant correction for multiple comparisons was not performed. Participants who were discontinued from the study were excluded from the analysis.

RESULTS

Sociodemographics Information

Table 1 describes the sociodemographic and clinical information about the participants. The majority of participants in this study practised vaginal douching, used depot medoxyprogesterone acetate (DMPA) as a family planning method and were in a relationship. Because age and use of DMPA are two factors known to modify the immune responses (19, 20), they were considered as confounders and entered in the multivariate regression model.

TABLE 1 | Sociodemographics information about the participants in this study.

	ASA group n = 38
Age (mean (SD))	Range (20-45) 32 (8)
Practicing vaginal douching	21
Hormonal contraception	
No HC	12
Progesterone based	21
Oral pill	2
Other or not disclosed	3
BV status at visit 1	
Normal	20
Intermediate	14
Positive	4
Regular partner	
Yes	30
No	4
Not disclosed	4
TXB2 level (pg/ml) (mean (SD))	Range (32.4 – 27673)
Visit 1 (Baseline)	3279 (4314)
Visit 3	2287 (4740)
ASA level (ng/ml) at visit 3 (mean (SD))	Range (19.5 – 616)
Plasma	111.3 (134.7)
Cervico-vaginal lavage	46.14 (29.79)

n, number; SD, standard deviation; Range, minimum to maximum concentration detected in participant samples.

TXB_2 and Immune Response

To ensure adherence to the study protocol, ASA concentration was measured at baseline and visit 3 (V3, six weeks after beginning of 81 mg ASA treatment). As suspected at baseline, we could not detect ASA in the blood or CVL of any of the participants (data not shown). At V3, ASA was detected in 94% of the participant blood and in 80% of the CVL. The concentration of ASA measured in the blood was 58% higher than the level measured at the female genital tract (**Figure 1**).

The use of low-dose ASA correlated with a reduction in the formation of thromboxane B2 (TXB_2). TXB_2 is the metabolite of TXA_2 a vasoconstrictor and a platelet coagulant (21) and therefore a direct measure of the pharmacological effect of ASA. TXB_2 measurements allow determination of an individual responsiveness to ASA (22). In our study, the level of TXB_2 dropped by 40% after six weeks on ASA, when compared to baseline level (p=0.004) and increased by 20% two weeks after the end of the treatment (**Figure 2**). The systemic level of TXB_2 did not correlate with the concentration of ASA measured at the systemic and mucosal compartment (data not shown). At visit 3, the level of TXB_2 did not correlate with cytokine/chemokine expression in the plasma but positively correlated with the level of IL-1β (p=0.0001) and IP-10 (p<0.0001) in the CVL (**Figure 3A**). TXB_2 level also positively correlated with the mucosal proportion of $CD4^+HLA\text{-}DR^+$

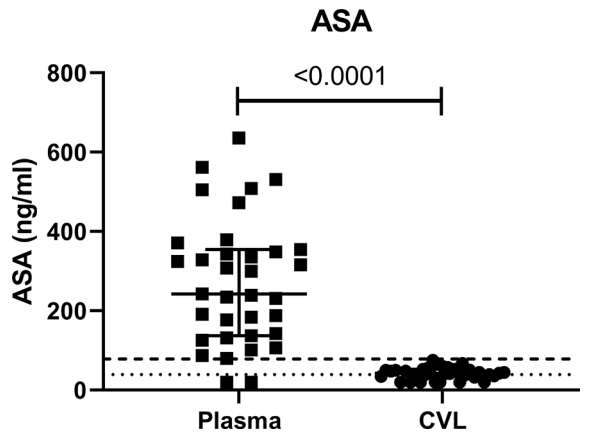

FIGURE 1 | Concentration of ASA in ng/ml measured in the systemic (plasma) and female genital tract (CVL) compartment measured at visit 3 (six weeks after starting daily ASA 81mg regimen). CVL cervico-vaginal lavage. p values < 0.05 were considered significant. The lower limits of quantitation (LLOQ) for CVL was 39 ng/mL indicated by the dotted line and for plasma was 78 ng/mL indicated by the dashed line.

T cells (p=0.0004). In the blood the proportion of central memory (p=0.04), effector memory $CD4^+$ T cells ($CD4^+CD45RA^-CCR7^-$) expressing $CD69^+$ (p=0.0007) (**Figure 3B**) and the proportion of MAIT cells ($CD4^-CD161^{+}{}^{+}V\alpha7.2^+$) expressing CCR6 (p=0.0344) (**Figure 3D**) positively correlated with the level of TXB_2. In addition, the density of HIV entry co-receptor CCR5 on systemic effector memory $CD4^+$T cells (p=0.007) (**Figure 3B**) and the proportion of MAIT cells expressing CXCR3 (p=0.0203) was inversely correlated with the TXB_2 level (**Figure 3D**). Furthermore, the proportion of $CD8^+$T cells expressing CXCR3 (p=0.0099) and proportion of effector memory $CD8^+$ expressing CCR5 was inversely correlated with TXB_2 (p=0.02) (**Figure 3C**). Finally, the expression of CD161 on Tc17 ($CD8^+CD161^+$) and the proportion of Tc17 cells expressing CXCR3 (p=0.0058) was inversely correlated with the level of plasma TXB_2 (**Figure 3D**).

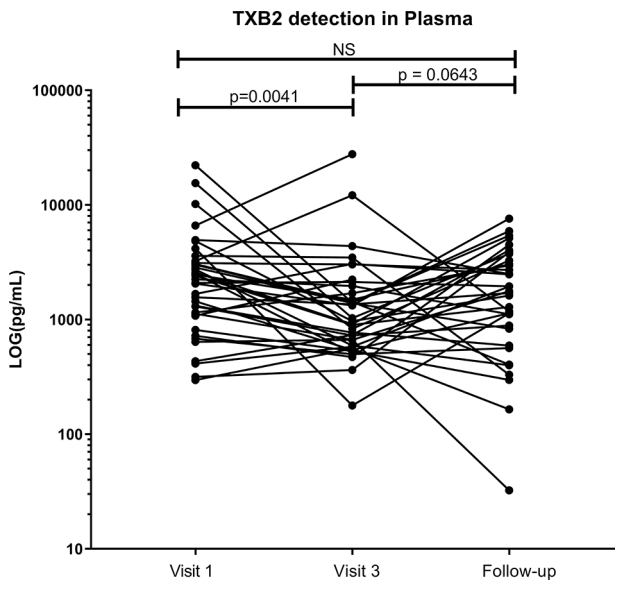

FIGURE 2 | Effect of ASA uptake on TXB2 level between baseline (Visit 1), Visit 3 (after 6 weeks on 81mg ASA drug regimen) and at follow-up (two weeks after ending ASA regimen) in the systemic compartment (plasma). Data was analyzed using Wilcoxon matched-pairs signed rank test. p values < 0.05 were considered significant, NS, non-significant. Median [IQR] values for visit 1 and visit 3 can be found in **Supplementary Table S1**.

Effect of ASA on Systemic Immune Activation in the Blood

Using flow cytometry on frozen PBMCs, we assessed how low-dose ASA modifies T cell activation. The data presented herein are new and build on those data presented in our previous paper characterizing $CD4^+CCR5^+$ HIV target cells (15). After multivariate analysis, on bulk CD4 T cells from PBMCs, we observed a decrease in the proportion of $CXCR3^+CD4^+$T cells and $CCR6^+CD4^+$ (p<0.001 and p=0.009, respectively) (**Figure 4A**).

The proportion of central memory $CD4^+$T cells ($CD4^+CCR7^+CD45RA^-$) expressing CD69 (p=0.02) was also lower at V3 and the density of CCR5 expression was decreased on bulk central memory $CD4^+$T cells (p=0.03). The proportion of naïve T cells ($CD4^+CD45RA^+CCR7^+$) expressing the activation markers CD69 or HLA-DR was lower after six weeks of ASA regimen (p=0.049 and p=0.002 respectively). However, expression of these two markers increased on naïve $CD4^+$T cells at V3 (p=0.01 and p=0.001 respectively), indicating that while there is less activation of $CD4^+$ naïve T cells in the blood at V3 compared to the baseline each cell expressed higher quantity of CD69 or HLA-DR. Furthermore, we measured a lower proportion of activated effector $CD4^+$ T cells ($CD4^+CD45RA^+CCR7^-$) expressing the activation markers CD69, CD95 or HLA-DR after six weeks on ASA (p=0.02, p=0.005, p=0.01 respectively) as well as a decrease in the expression of CCR5 on bulk effector $CD4^+$T cells (p=0.017). Finally, the proportion of effector memory T cells ($CD4^+CD45RA^-CCR7^-$) expressing HLA-DR^+ was decreased after ASA regimen (p=0.01) (**Figure 4A**). In our multivariate regression model, none of those associations were affected by the age or use of hormonal contraception (data not shown).

In addition, we also observed a decreased proportion of Th17 (defined as $CD4^+$ $CD161^+$) (p=0.009) and the proportion of Th17 expressing HLA-DR ($CD4^+CD161^+$HLA-DR^+) (p=0.01) after use of ASA. The per cell intensity of expression of CCR6 on Th17 cells was also decreased (p=0.008) following 6 weeks on ASA (**Figure 4A**). The percent of Th17 cells positive for CD103 increased following 6 weeks ASA and the expression of inhibitory molecule TIGIT on T regs decreased following 6 weeks ASA in the univariate analysis (data not shown) although the changes of both populations did not remain significant in our multivariate model adjusting for age and method of contraception.

ASA use correlated with alterations in the $CD8^+$ population in the blood. The proportion of $CD8^+$T cells (p=0.0001) and Tc17

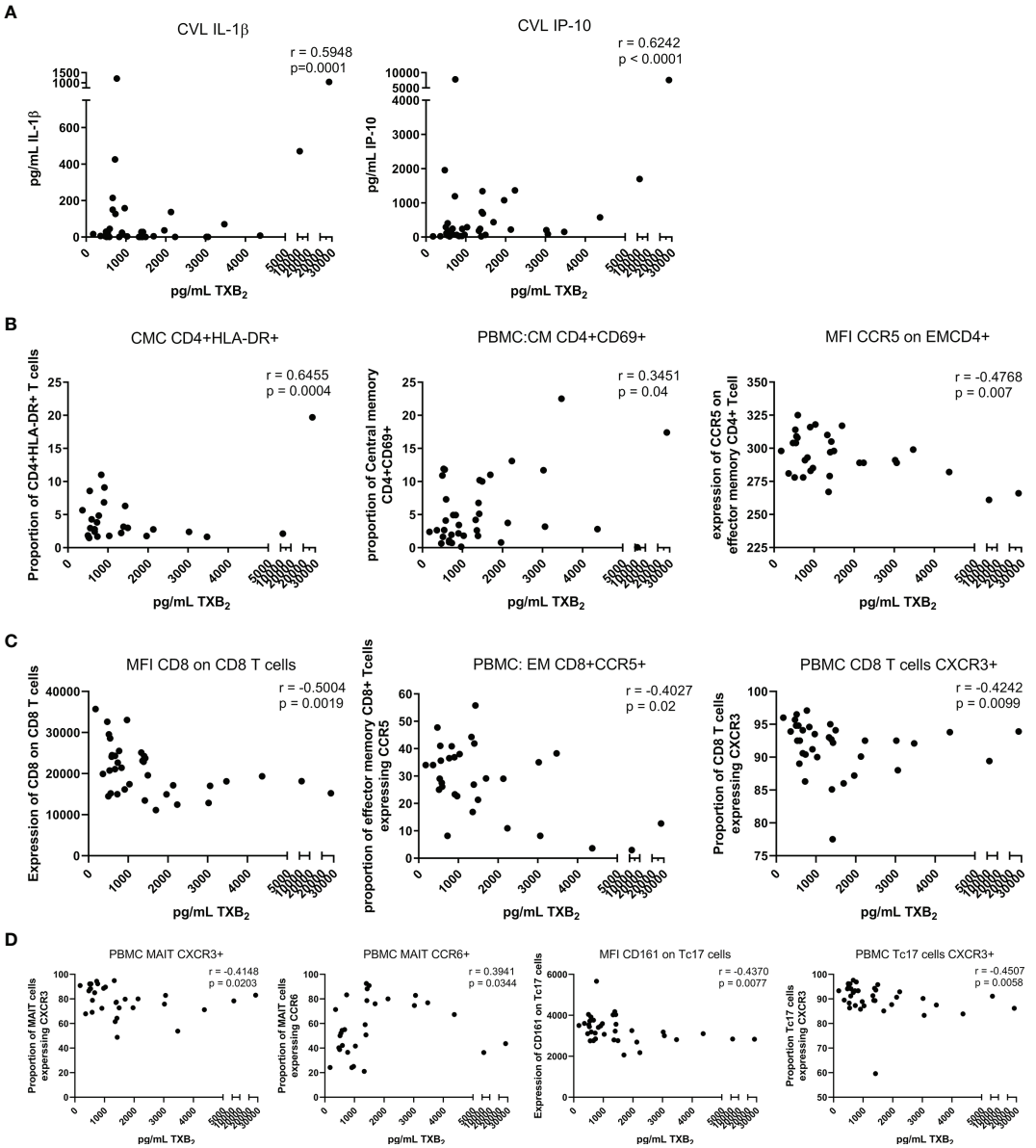

FIGURE 3 | Correlation between the level of TXB2 in the plasma and immune activation at the mucosal and systemic compartment at visit 3 (six weeks after starting daily ASA 81mg regimen). **(A)** correlations between cytokines and chemokine and TXB2. **(B)** correlations between CD4$^+$Tcell activation status and TXB2. **(C)** correlations between CD8$^+$Tcell activation status and TXB2. **(D)** correlations between MAIT and Tc17 activation status and TXB2. Data was analyzed using Pearson correlation or Spearman's rank test depending on normality of the data. p values<0.05 were considered significant. CVL, cervico-vaginal lavage; CMC, cervical mononuclear cells; PBMCs, peripheral blood mononuclear cells; CM, central memory cells; EM, effector memory cells; MFI, median fluorescent intensity indicates marker expression on a per cell bases.

(defined as CD8$^+$CD161$^+$) expressing CCR5 (p=0.02) was lower at V3 compared to the baseline. The proportion of Tc17 expressing HLA-DR$^+$ was increased after six weeks of ASA treatment (p=0.048). By measuring the expression of CD161 on CD8$^+$T cells, we were able to assess the proportion and immune activation state of MAIT cells (defined as CD8$^+$CD161^{++}). MAIT cell proportion was increased at V3 (p=0.04), however, among the MAIT population the intensity of expression of CCR5 and the proportion of MAIT cells expressing CD95 were reduced (p=0.003 and p=0.001 respectively) (**Figure 4B**). Neither age nor use of DMPA affected the outcome observed following multivariate analysis.

When assessing at the concentration effect of ASA on the immune response, we observed that the expression of CD161 on CD4$^+$T cells was positively correlated with the concentration of ASA measured in the blood(p=0.02). However, a negative

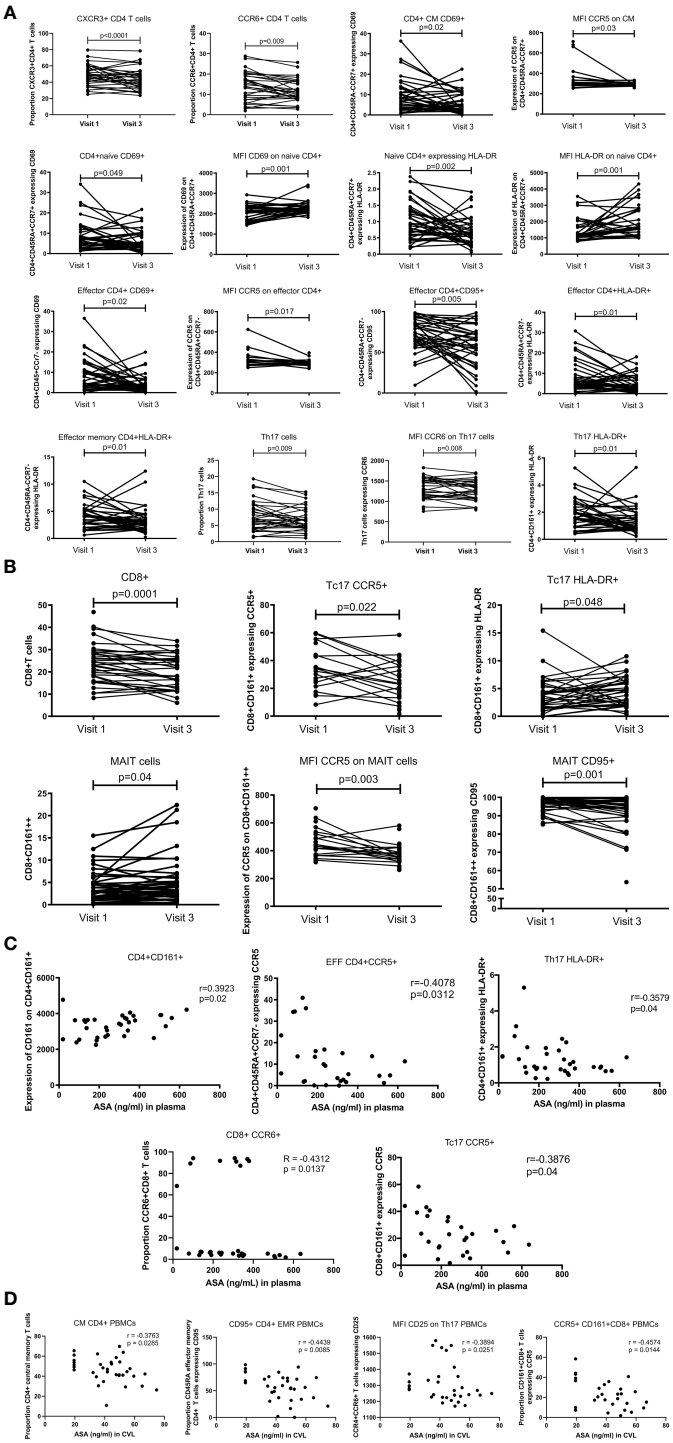

FIGURE 4 | T cell blood proportion and immune activation status measured by flow cytometry. **(A)** systemic $CD4^+$T cell activation changes between Visit 1 (baseline) and Visit 3 (after 6 weeks daily uptake of 81mg ASA). **(B)** systemic $CD8^+$T cell activation changes between Visit 1 and Visit 3. **(C)** correlation between systemic T cell activation and blood concentration of ASA (ng/mL) at Visit 3. **(D)** correlation between systemic T cell activation and CVL concentration of ASA (ng/mL) at Visit 3. Data for **(A, B)** was analyzed using Wilcoxon matched-pairs signed rank test, multivariate regression was performed to control for the effect of DMPA and age on immune activation changes. Median [IQR] values for visit 1 and visit 3 can be found in **Supplementary Table S1**. Data for **(C, D)** was analyzed using Pearson correlation or Spearman's rank test depending on normality of the data. p values<0.05 were considered significant. CM, central memory cells; MFI, median fluorescent intensity indicates marker expression on a per cell bases.

correlation between the concentration of ASA was also observed with the proportion of effector $CCR5^+CD4^+$Tcells (p=0.03) and with the proportion of long-term activated HLA-DR^+Th17 cells (p=0.04). The proportion of $CCR5^+$Tc17 (p=0.04), and the proportion of $CCR6^+$CD8 T cells (p=0.014) also exhibited a negative correlation with plasma ASA levels (**Figure 4C**). We also observed negative correlations between the CVL concentration of ASA and the proportion of $CCR5^+CD161^+CD8^+$T cells (p=0.014), $CD95^+CD4^+CD45RA^+$ effector memory T cells (p=0.008), the proportion of central memory $CD4^+$T cells (p=0.029), and the expression of CD25 on Th17 cells (p=0.025) (**Figure 4D**).

Effect of ASA on Mucosal Immune Activation in the FGT

Fresh cervico-mononuclear cells were also analysed by flow cytometry. We observed that at the female genital tract compartment, use of ASA led to a decrease in the proportion of $CD3^+$T cells (p=0.01). The proportion of $CD4^+$HLA-DR^+ increased between baseline and visit 3 (p=0.02). Activated double positive $CD4^+CCR5^+CD161^+$ (p=0.02) and $CD4^+CCR5^+CD95^+$ (p=0.001) decreased with ASA use while the proportion of the double negative $CD4^+CCR5^-CD161^-$ (p=0.0004) and $CD4^+CCR5^-CD95^-$ (p=0.0004) increased (**Figure 5A**). All these associations remained significant when controlled for age and DMPA use in the multivariate analysis (data not shown). $CD4^+CCR5^+$ HIV target cells were characterized in a previous paper (15).

For the $CD8^+$T cell population, we observed a reduced level of $CD8^+CCR5^+$T cells (p=0.02). The expression of CCR5 on $CD8^+$T cells and Tc17 was also decreased (p=0.001 and p=0.04 respectively). The density of CD69 on Tc17 was, however, increased from baseline to visit 3 (p=0.05). In the population of $CD8^+$T cells not expressing CD161, the proportion of those carrying CCR5 was slightly decreased (p=0.04). Furthermore, the expression of CCR5 on those cells ($CD8^+CD161^-$) was also lower after ASA use (p=0.0003). The proportion of $CD8^+CD161^-$HLA-DR^+ was increased between baseline and visit 3 (p=0.03). Finally, the proportion of double positive $CD8^+CCR5^+CD95^+$ and $CD8^+CD69^+$HLA-DR^+ was reduced between baseline and the end of ASA regimen (p=0.001 and p=0.03 respectively) (**Figure 5B**). None of those associations were affected by age or DMPA use.

Finally, the expression of CCR5 on $CD8^+$T cells positively correlated with the concentration of ASA measured in the blood (p=0.02) (**Figure 5C**). The concentration of ASA measured in the CVL did not correlate with any T cell populations. However, we did observe a negative correlation between the CVL concentration of ASA and IL-10 (p=0.018) (**Figure 5D**).

DISCUSSION

ASA is readily available worldwide. It has been used for decades for the treatment of pain and in more recent years to prevent heart diseases as well as pre-eclampsia (2, 21). In this study, we assessed how ASA use modifies the T cell immune response. We observed that six weeks of ASA treatment decreased T cell immune activation in HIV negative women.

Previous studies showed that about 50-70% of the initial dose of ASA passes into the systemic circulation (23). In our study, we observed that ASA can also pass the mucosal barrier and be detected at the female genital tract. To our knowledge, this is the first study showing that ASA can be measured in vaginal secretion. We also measured the level of TXB_2, which is inhibited by ASA and a direct measure of ASA activity. Herein, we observed a significant decrease in the level of TXB_2 after six weeks of ASA use. The level of ASA and TXB_2 measured indicates that the participants were highly adherent to the protocol and responded to the treatment.

In this study, we build upon our observations in HIV target cells (15) and observed that the proportion of chronically activated $CD4^+$T cells ($CD4^+$HLA-DR^+) was inversely correlated with the level of ASA measured in the blood. This was also the case for the relation between ASA level and the proportion of effector $CD4^+$T cells and Tc17 expressing HIV coreceptor CCR5. We previously reported that the mucosal level of ASA negatively correlated with the proportion of HIV target cells at the genital tract (15) and expand on our previous findings here demonstrating that the mucosal level of ASA negatively correlates with the proportion of $CD161^+CD8^+$T cells positive for CCR5 and the expression of activation marker CD25 on Th17 cells in the blood (24). Together, these results indicate that an increase concentration of ASA correlates with reduced inflammatory immune markers both in the blood and in the genital compartment.

It has been previously shown that ASA can impair T cell tissue recruitment by disrupting the integrin- and L-selectin-mediated binding of the T cells to the endothelium (25). In this study, we observed a lower proportion of $CD3^+$ lymphocytes at the genital tract after ASA regimen compared to the baseline. We also observed a lower proportion of systemic central memory, naïve and effector $CD4^+$T cells expressing CD69 as well as lower proportion of mucosal $CD8^+CD69^+$HLA-DR^+T cells during ASA treatment. CD69 is an acute activation marker and a marker of resident T cells (26). The reduced proportion of T cells expressing CD69 may indicate that there are more circulating T cells and a lower proportion of those T cells remain resident in the genital tract. In addition to lower levels of CD69, we found that following ASA treatment the proportion of $CD4^+$T cells expressing trafficking markers CCR6 and CXCR3 decreased as well as a decrease in the expression of CCR6 on Th17 cells. A decrease in CCR6 suggests ASA reduces the migration of these cells to mucosal tissues such as the intestine and colon (27), whereas decreases in CXCR3 indicate a reduction in lung and lymphoid tissue trafficking (28). We also found the concentration of ASA or TXB_2 in the blood had a predominantly inverse relationship with these same trafficking markers on several T cell subsets. Together, our data corroborates with the study conducted by Gerli et al. (25) and suggest ASA affects lymphocytes trafficking.

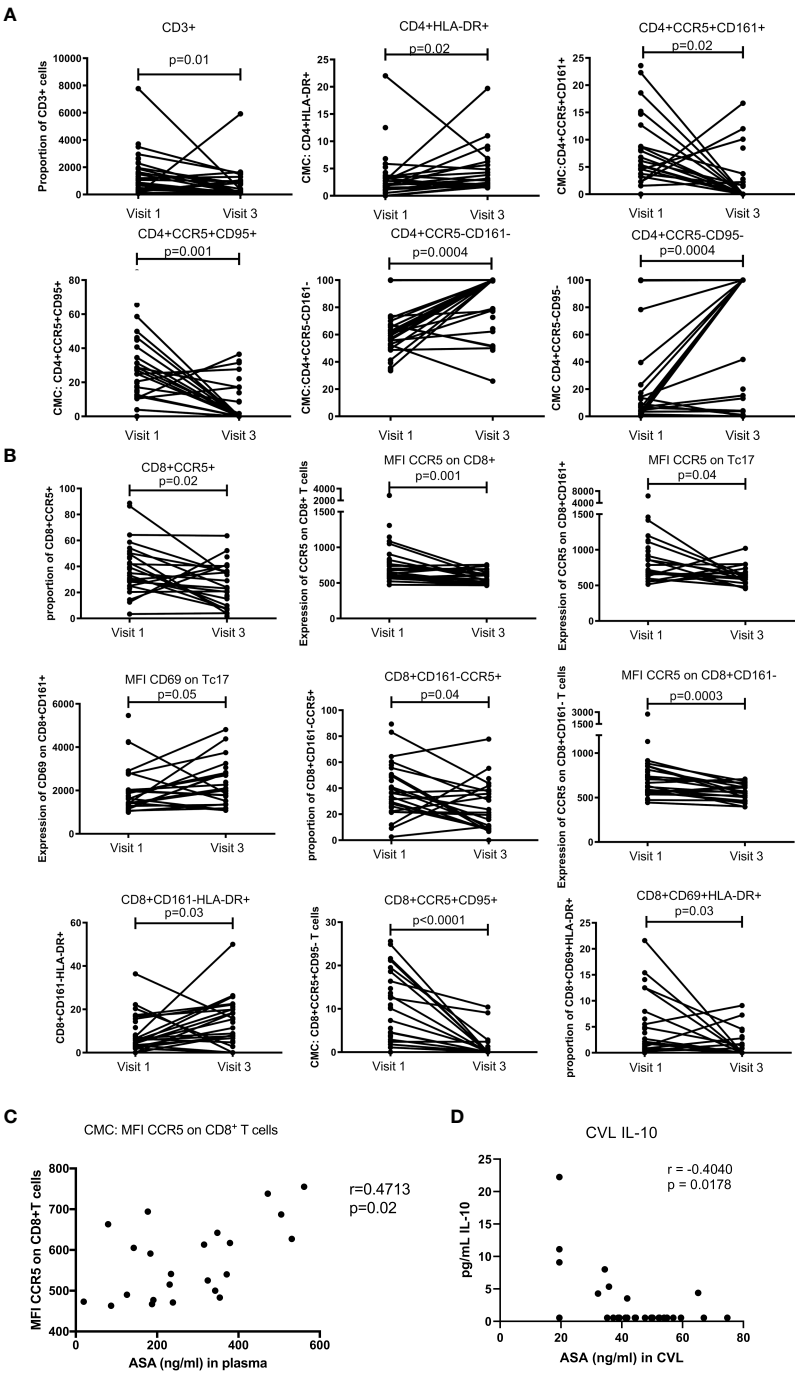

FIGURE 5 | T cell mucosal proportion and immune activation status measured by flow cytometry on cervical mononuclear cells. **(A)** mucosal CD4^{+}T cell activation changes between Visit 1 (baseline) and Visit 3 (after 6 weeks daily uptake of 81mg ASA). **(B)** mucosal CD8^{+}T cell activation changes between Visit 1 and Visit 3. **(C)** correlation between mucosal T cell activation and blood concentration of ASA (ng/mL) at Visit 3. **(C)** correlation between mucosal T cell activation and CVL concentration of ASA (ng/mL) at Visit 3. Data for **(A, B)** was analyzed using Wilcoxon matched-pairs signed rank test, multivariate regression was performed to control for the effect of DMPA and age on immune activation changes. Median [IQR] values for visit 1 and visit 3 can be found in **Supplementary Table S1**. Data for **(C, D)** was analyzed using Pearson correlation or Spearman's rank test depending on normality of the data. p values<0.05 were considered significant. MFI, median fluorescent intensity indicates marker expression on a per cell bases.

T lymphocytes play a major role in the regulation of the adaptive immune response against pathogens. In the context of HIV infection, they are the main target cells for the virus. It has been shown that HIV can infect activated T cells 1000 times more efficiently than quiescent T cells (29). While on bulk CD4 T cells we observed an increase in the proportion of cells positive for HLA-DR at the female genital tract, on HIV target cells at the female genital tract the proportion of activated T cells $CD4^+CCR5^+CD161^+$ and $CD4^+CCR5^+CD95^+$ reduced with ASA. treatment Decreasing baseline immune activation in high-risk individuals could help increase the efficiency of other biomedical preventive methods such as microbicides affected by local inflammation as seen in the CARPRISA004 study.

Limitations of this study include the difficulty of recovering a sufficient number of CMCs for robust analyses for all markers tested. Other limitations include the limited sample size of 38 participants, only 6 weeks on therapy, and a single dose of ASA tested. As this was a discovery and hypothesis generating study, we did not perform corrections for multiple comparisons. To confirm these initial findings, follow up studies should be performed which narrow the focus of cytokine analysis to only a core set of cytokines thereby minimizing the comparisons to only those factors that would be hypothesized to be altered. Strengths of this study include paired systemic and mucosal sample analysis, in depth phenotypic characterization of multiple immune phenotypes, and the ability to correlate findings with tissue and systemic drug levels.

This study offers new insights into the immunological effects of how ASA affects inflammation. It also suggests a new approach in preventing HIV infection that could be combined with other prevention approaches to provide a wider selection of HIV prevention tools (29). We showed that ASA decreases T cell immune activation both at the systemic and female genital tract compartment. This is the first study that looks into how ASA impacts the immune response at the genital tract immune environment. In the context of HIV, this study shows that it is possible to modify to the female genital tract environment toward a less pro-inflammatory more immune quiescent milieu thereby potentially reducing HIV risk.

DATA AVAILABILITY STATEMENT

The original contributions presented in the study are included in the article/**Supplementary Material**. Further inquiries can be directed to the corresponding author.

ETHICS STATEMENT

The studies involving human participants were reviewed and approved by the University of Nairobi/Kenyatta National Hospital and the University of Manitoba research ethic boards approved this study. The study was registered on ClinicalTrials.gov (NCT02079077). The patients/participants provided their written informed consent to participate in this study.

AUTHOR CONTRIBUTIONS

All authors participated in interpretation of data and critical review of the manuscript. JL participated in the study design, was the co-study coordinator, and wrote part of the article. MMK conducted the *in vitro* experiments and wrote part of the article. LM conducted many of the *ex vivo* experiments. GB-L was the field study coordinator and performed technical analyses. JO provided overall supervision of the Nairobi-based study. CY and EH performed ASA tissue concentrations. MK was the clinical officer and collected clinical samples. JK managed the clinical cohort. KF was the principal investigator of the study, obtained funding for the study and wrote the article.

FUNDING

Funding support was provided by the Canadian Institutes of Health Research (CIHR) OCH # 126275 (KF, JL), CIHR HB3-164065 (KF, JL, JO, JK), Grand Challenge Canada S5 386-01 (JL) and CIHR PJT166153 (EH).

ACKNOWLEDGMENTS

The authors wish to thank Julianna Cheruiyot for assistance with participant recruitment and specimen collection. They also thank all the participants of the IIQ study as well as the female sex workers from the Pumwani cohort in Nairobi, Kenya for their support.

SUPPLEMENTARY MATERIAL

The Supplementary Material for this article can be found online at: https://www.frontiersin.org/articles/10.3389/fimmu.2021.778455/full#supplementary-material

REFERENCES

1. Lanas A, McCarthy D, Voelker M, Brueckner A, Senn S, Baron JA. Short-Term Acetylsalicylic Acid (Aspirin) Use for Pain, Fever, or Colds - Gastrointestinal Adverse Effects: A Meta-Analysis of Randomized Clinical Trials. *Drugs R D* (2011) 11:277–88. doi: 10.2165/11593880-000000000-00000
2. Raber I, McCarthy CP, Vaduganathan M, Bhatt DL, Wood DA, Cleland JGF, et al. Review The Rise and Fall of Aspirin in the Primary Prevention of Cardiovascular Disease. *Lancet* (2019) 393:2155–67. doi: 10.1016/S0140-6736(19)30541-0
3. U.S. Preventive Services Task Force. *Low-Dose Aspirin Use for the Prevention of Morbidity and Mortality From Preeclampsia: Preventive Medication* (2017). Available at: https://www.uspreventiveservicestaskforce.org/Page/Document/RecommendationStatementFinal/low-dose-aspirin-use-for-the-prevention-of-morbidity-and-mortality-from-preeclampsia-preventive-medication (Accessed July 17, 2020).
4. Saxena A, Balaramnavar VM, Hohlfeld T, Saxena AK. Drug/drug Interaction of Common NSAIDs With Antiplatelet Effect of Aspirin in Human Platelets. *Eur J Pharmacol* (2013) 721:215–24. doi: 10.1016/j.ejphar.2013.09.032

5. Loprete L, Leuratti C, Scarsi C, Radicioni M. Pharmacodynamics and Pharmacokinetics of a Novel, Low-Dose, Soft-Gel Capsule of Acetylsalicylic Acid in Comparison With an Oral Solution After Single-Dose Administration to Healthy Volunteers: A Phase I, Two-Way Crossover Study. *Clin Drug Investig* (2014) 34:19–25. doi: 10.1007/s40261-013-0145-2
6. Esquivias P, Cebrián C, Morandeira A, Santander S, Ortego J, García-González MA, et al. Effect of Aspirin Treatment on the Prevention of Esophageal Adenocarcinoma in a Rat Experimental Model. *Oncol Rep* (2014) 31:2785–91. doi: 10.3892/or.2014.3137
7. Chan MM-Y, Moore AR. Resolution of Inflammation in Murine Autoimmune Arthritis Is Disrupted by Cyclooxygenase-2 Inhibition and Restored by Prostaglandin E2-Mediated Lipoxin A4 Production. *J Immunol* (2010) 184:6418–26. doi: 10.4049/jimmunol.0903816
8. Yin MJ, Yamamoto Y, Gaynor RB. The Anti-Inflammatory Agents Aspirin and Salicylate Inhibit the Activity of I(kappa)B Kinase-Beta. *Nature* (1998) 396:77–80. doi: 10.1038/23948
9. Moon H-G, Kang CS, Choi J-P, Choi DS, Choi HI, Choi YW, et al. Acetyl Salicylic Acid Inhibits Th17 Airway Inflammation *via* Blockade of IL-6 and IL-17 Positive Feedback. *Exp Mol Med* (2013) 45:e6. doi: 10.1038/emm.2013.10
10. Naranbhai V, Abdool Karim SS, Altfeld M, Samsunder N, Durgiah R, Sibeko S, et al. CAPRISA004 TRAPS Team. Innate Immune Activation Enhances Hiv Acquisition in Women, Diminishing the Effectiveness of Tenofovir Microbicide Gel. *J Infect Dis* (2012) 206:993–1001. doi: 10.1093/infdis/jis465
11. McKinnon LR, Liebenberg LJ, Yende-Zuma N, Archary D, Ngcapu S, Sivro A, et al. Genital Inflammation Undermines the Effectiveness of Tenofovir Gel in Preventing HIV Acquisition in Women. *Nat Med* (2018) 24:491–6. doi: 10.1038/nm.4506
12. Card CM, Ball TB, Fowke KR. Immune Quiescence: A Model of Protection Against HIV Infection. *Retrovirology* (2013) 10:141. doi: 10.1186/1742-4690-10-141
13. O'Brien M, Montenont E, Hu L, Nardi MA, Valdes V, Merolla M, et al. Aspirin Attenuates Platelet Activation and Immune Activation in HIV-1-Infected Subjects on Antiretroviral Therapy. *J Acquir Immune Defic Syndr* (2013) 63:280–8. doi: 10.1097/QAI.0b013e31828a292c
14. O'Brien MP, Hunt PW, Kitch DW, Klingman K, Stein JH, Funderburg NT, et al. A Randomized Placebo Controlled Trial of Aspirin Effects on Immune Activation in Chronically Human Immunodeficiency Virus-Infected Adults on Virologically Suppressive Antiretroviral Therapy. *Open Forum Infect Dis* (2017) 4:1–10. doi: 10.1093/ofid/ofw278
15. Lajoie J, Birse K, Mwangi L, Chen Y, Cheruiyot J, Akolo M, et al. Using Safe, Affordable and Accessible Non-Steroidal Anti-Inflammatory Drugs to Reduce the Number of HIV Target Cells in the Blood and at the Female Genital Tract. *J Int AIDS Soc* (2018) 21:e25150. doi: 10.1002/jia2.25150
16. Omollo K, Boily-Larouche G, lajoie J, Kimani M, Cheruiyot J, Kimani J, et al. The Impact of Sex Work Interruption on Blood-Derived T Cells in Sex Workers From Nairobi, Kenya. *AIDS Res Hum Retroviruses* (2016) 32:1072–8. doi: 10.1089/AID.2015.0332
17. Juno JA, Boily-Larouche G, lajoie J, Fowke KR. Collection, Isolation, and Flow Cytometric Analysis of Human Endocervical Samples. *J Vis Exp* (2014) 89: e51906–6. doi: 10.3791/51906
18. Kees F, Jehnich D, Grobecker H. Simultaneous Determination of Acetylsalicylic Acid and Salicylic Acid in Human Plasma by High-Performance Liquid Chromatography. *J Chromatogr B BioMed Appl* (1996) 677:172–7. doi: 10.1016/0378-4347(95)00464-5
19. Sivro A, lajoie J, Kimani J, Jaoko W, Plummer FA, Fowke K, et al. Age and Menopause Affect the Expression of Specific Cytokines/Chemokines in Plasma and Cervical Lavage Samples From Female Sex Workers in Nairobi, Kenya. *Immun Ageing* (2013) 10:42. doi: 10.1186/1742-4933-10-42
20. Lajoie J, Tjernlund A, Omollo K, Edfeldt G, Röhl M, Boily-Larouche G, et al. Increased Cervical CD4+CCR5+ T Cells Among Kenyan Sex Working Women Using Depot Medroxyprogesterone Acetate. *AIDS Res Hum Retroviruses* (2019) 35:236–46. doi: 10.1089/AID.2018.0188. aid.2018.0188.
21. Mckie J. Meds-QA-March-2016. (2019).
22. Saka B, Genc S, Eroglu H, Akpinar T, Karadag A, Kilic L, et al. Assessment of Platelet Aspirin Responsiveness in Turkish Population With PFA-100, Serum Thromboxane B2, Soluble CD40 Ligand and Soluble P-Selectin. *Turk J Bioch* (2013) 38:63–7. doi: 10.5505/tjb.2013.75437
23. Zhou G, Marathe GK, Willard B, McIntyre TM. Intracellular Erythrocyte Platelet-Activating Factor Acetylhydrolase I Inactivates Aspirin in Blood. *J Biol Chem* (2011) 286:34820–9. doi: 10.1074/jbc.M111.267161
24. Machura E, Mazur B, Pieniazek W, Karczewska K. Expression of Naive/Memory (CD45RA/CD45RO) Markers by Peripheral Blood CD4+ and CD8 + T Cells in Children With Asthma. *Arch Immunol Ther Exp (Warsz)* (2008) 56:55–62. doi: 10.1007/s00005-008-0005-6
25. Gerli R, Gresele P, Bistoni O, Paolucci C, Lanfrancone L, Fiorucci S, et al. Salicylates Inhibit T Cell Adhesion on Endothelium Under Nonstatic Conditions: Induction of L-Selectin Shedding by a Tyrosine Kinase-Dependent Mechanism. *J Immunol* (2001) 166:832–40. doi: 10.4049/jimmunol.166.2.832
26. Sathaliyawala T, Kubota M, Yudanin N, Turner D, Camp P, Thome JJC, et al. Distribution and Compartmentalization of Human Circulating and Tissue-Resident Memory T Cell Subsets. *Immunity* (2013) 38:187–97. doi: 10.1016/j.immuni.2012.09.020
27. Kondo T, Takata H, Takiguchi M. Functional Expression of Chemokine Receptor CCR6 on Human Effector Memory CD8+ T Cells. *Eur J Immunol* (2007) 37:54–65. doi: 10.1002/eji.200636251
28. Groom JR, Luster AD. CXCR3 in T Cell Function. *Exp Cell Res* (2011) 317:620–31. doi: 10.1016/j.yexcr.2010.12.017
29. Pan X, Baldauf H-M, Keppler OT, Fackler OT. Restrictions to HIV-1 Replication in Resting CD4+ T Lymphocytes. *Nat Publishing Group* (2013) 23:876–85. doi: 10.1038/cr.2013.74

Conflict of Interest: The authors declare that the research was conducted in the absence of any commercial or financial relationships that could be construed as a potential conflict of interest.

Publisher's Note: All claims expressed in this article are solely those of the authors and do not necessarily represent those of their affiliated organizations, or those of the publisher, the editors and the reviewers. Any product that may be evaluated in this article, or claim that may be made by its manufacturer, is not guaranteed or endorsed by the publisher.

frontiers in Immunology

ORIGINAL RESEARCH
published: 11 February 2022
doi: 10.3389/fimmu.2021.781923

HIV-Sheltering Platelets From Immunological Non-Responders Induce a Dysfunctional Glycolytic CD4$^+$ T-Cell Profile

Aiwei Zhu[1,2,3], *Fernando Real*[1,2,3], *Jaja Zhu*[4,5], *Ségolène Greffe*[4], *Pierre de Truchis*[5,6], *Elisabeth Rouveix*[4,5], *Morgane Bomsel*[1,2,3*†] *and Claude Capron*[4,5*†]

[1] Mucosal Entry of HIV and Mucosal Immunity, Institut Cochin, Université de Paris, Paris, France, [2] Institut National de la Santé et de la Recherche Médicale (INSERM) U1016, Paris, France, [3] Centre National de la Recherche Scientifique (CNRS) UMR8104, Paris, France, [4] Service d'Hématologie, Hôpital Ambroise Paré (AP-HP), Boulogne-Billancourt, France, [5] Université Versailles Saint Quentin-en-Yvelines (UVSQ), Université Paris Saclay, Versailles, France, [6] Service d'Infectiologie, Hôpital Raymond Poincaré (AP-HP), Garches, France

OPEN ACCESS

Edited by:
Constantinos Petrovas, Centre Hospitalier Universitaire Vaudois (CHUV), Switzerland

Reviewed by:
Sanjay B. Maggirwar, George Washington University, United States
Ashish A. Sharma, Emory University, United States

***Correspondence:**
Morgane Bomsel
morgane.bomsel@inserm.fr
Claude Capron
claude.capron@aphp.fr

[†]These authors have contributed equally to this work

Specialty section:
This article was submitted to Viral Immunology, a section of the journal Frontiers in Immunology

Received: 23 September 2021
Accepted: 13 December 2021
Published: 11 February 2022

Citation:
Zhu A, Real F, Zhu J, Greffe S, de Truchis P, Rouveix E, Bomsel M and Capron C (2022) HIV-Sheltering Platelets From Immunological Non-Responders Induce a Dysfunctional Glycolytic CD4$^+$ T-Cell Profile. Front. Immunol. 12:781923. doi: 10.3389/fimmu.2021.781923

Immunological non-responders (InRs) are HIV-infected individuals in whom the administration of combination antiretroviral therapy (cART), although successful in suppressing viral replication, cannot properly reconstitute patient circulating CD4$^+$ T-cell number to immunocompetent levels. The causes for this immunological failure remain elusive, and no therapeutic strategy is available to restore a proper CD4$^+$ T-cell immune response in these individuals. We have recently demonstrated that platelets harboring infectious HIV are a hallmark of InR, and we now report on a causal connection between HIV-containing platelets and T-cell dysfunctions. We show here that *in vivo*, platelet–T-cell conjugates are more frequent among CD4$^+$ T cells in InRs displaying HIV-containing platelets (<350 CD4$^+$ T cells/μl blood for >1 year) as compared with healthy donors or immunological responders (IRs; >350 CD4$^+$ T cells/μl). This contact between platelet containing HIV and T cell in the conjugates is not infectious for CD4$^+$ T cells, as coculture of platelets from InRs containing HIV with healthy donor CD4$^+$ T cells fails to propagate infection to CD4$^+$ T cells. In contrast, when macrophages are the target of platelets containing HIV from InRs, macrophages become infected. Differential transcriptomic analyses comparing InR and IR CD4$^+$ T cells reveal an upregulation of genes involved in both aerobic and anaerobic glycolysis in CD4$^+$ T cells from InR vs. IR individuals. Accordingly, InR platelets containing HIV induce a dysfunctional increase in glycolysis-mediated energy production in CD4$^+$ T cells as compared with T cells cocultured with IR platelets devoid of virus. In contrast, macrophage metabolism is not affected by platelet contact. Altogether, this brief report demonstrates a direct causal link between presence of HIV in platelets and T-cell dysfunctions typical of InR, contributing to devise a platelet-targeted therapy for improving immune reconstitution in these individuals.

Keywords: HIV-1, immunological failure, platelets, CD4$^+$ T-cell metabolism, glycolysis, virus-containing platelets

INTRODUCTION

Approximately 20% of the overall combination antiretroviral therapy (cART)-treated patients are immunological non-responders (InRs) who fail to reconstitute a competent immune status despite prolonged viral suppression as a result of proper treatment observance (1). The causes of this immunological failure remain unclear, and no treatment is available to improve $CD4^+$ T-cell count restoration and health of InRs (1), who are at higher risk of AIDS and non-AIDS morbidity and mortality (2–4).

Using blood obtained from virally suppressed HIV-infected patients under cART (viral load below detection limit for >1 year prior to sampling date, here referred to as cART-suppressed individuals), we have recently shown that platelets from InRs specifically carry infectious HIV *in vivo* (5). Hence, platelets from cART-suppressed individuals carry infectious HIV regardless of patient viremia and platelet numbers but are significantly correlated with $CD4^+$ T-cell nadir (<200 cells/µl) and sustained low blood $CD4^+$ T-cell counts (<350 $CD4^+$ T cells/µl) (5). Predictive statistical analyses indicated that the chance of remaining with $CD4^+$ T-cell count <350 $CD4^+$ T cells/µl in the next 18 months despite cART is >50-fold higher in individuals with platelets sheltering HIV than in individuals without HIV in platelets (5). These results indicate that the presence of HIV in platelets is a characteristic of InRs. However, a direct causal relationship between the presence of HIV in platelets and immunological failure remains elusive.

The poor immunological recovery in InR is mainly driven by a sustained low $CD4^+$ T-cell count that relies on persistent inflammation and immune activation affecting T-cell population profiles (6–10). Platelets may have a role in this process. Indeed, platelet–$CD4^+$ T-cell conjugates have been observed in the peripheral blood of patients with autoimmune disease, suggesting that platelets may be involved in regulating T-cell activation (11). Moreover, platelets form an increased proportion of conjugates with T cells in peripheral blood from HIV-infected patients compared to healthy controls (12). Platelets express adhesive proteins that not only promote platelet aggregation responsible for primary hemostasis (clotting) but also mediate interactions with leukocytes such as monocytes/macrophages or T cells. In particular, platelets can drive inhibition of proliferation and differentiation of either $CD4^+$ T cells into regulatory profiles ($FoxP3^+$ T_{reg}) (13) or Th17 in chronic inflammation (14). As platelet–T-cell conjugates form in the blood of HIV patients (12), we therefore speculate that HIV-containing platelets would directly act on $CD4^+$ T cells, causing T-cell dysfunction. Furthermore, polarization of T cells to activated or resting states requires changes in metabolism that might be implicated in InR immunological failure (15).

Here, in this brief report, we approached platelet-mediated T-cell dysfunction *in vitro* by characterizing comparatively the T-cell metabolic changes induced by HIV-containing platelets from InRs vs. immunological responders (IRs). In contrast with IR platelets, HIV-containing platelets from InR individuals induced an increased production of energy *via* glycolysis in $CD4^+$ T cells, not macrophages. This platelet-mediated glycolytic stimulus is not related to a platelet-mediated T cell infection, as HIV-containing platelets do not infect T cells upon *in vitro* interaction in contrast to macrophages. This is to our knowledge the first evidence of a direct causative action of HIV-containing platelets on T-cell dysfunctions.

MATERIALS AND METHODS

Ethics Statement

This non-interventional study was approved by the institutional review board of the "Comité de Protection des Personnes" (CPP) of Ile-de-France (VIH-PLAQUETTES, ID-RCB: 2020-A00307-32) and conforms to the principles outlined in the Declaration of Helsinki. Accordingly, all participants were informed in writing about the study and allowed not to participate.

Patient Sample Preparation

Platelet-rich plasma (PRP) and peripheral blood mononuclear cell (PBMC) samples were obtained during routine blood testing of 32 HIV-infected individuals on cART from the French Hospital Database on HIV receiving care at the Ambroise Paré (Boulogne-Billancourt, France) and Raymond Poincaré (Garches, France) Hospitals. The enrollment criterions for the French Hospital Database on HIV were confirmed HIV-1 and cART initiated for at least 1 year before the time of blood sampling. Human PBMC and PRP samples from healthy HIV-seronegative donors used as a negative control for all experiments were obtained from the French blood collection center [Etablissement Francais du Sang (EFS) Paris, France]. PRP and PBMCs were prepared as previously described (5).

InR subjects were defined as having sustained $CD4^+$ T-cell counts below 350 cells/µl for more than 6 months during viral suppression, i.e., plasma viral load copies below limit of detection (LOD) as detected by the Abbott RealTime HIV-1 assay on an automated m2000 system. IR subjects were defined as having sustained $CD4^+$ T-cell counts above 350 cells/µl during virological suppression during this time. Clinical information on InR and IR subjects is presented in **Table 1**.

Flow Cytometry

Peripheral Blood Mononuclear Cell

Multiparametric flow cytometry was performed using frozen PBMCs collected from InR, IR, and healthy donors. PBMCs were thawed, washed two times in phosphate buffered saline (PBS) with 2% fetal bovine serum (FBS), and resuspended in PBS supplemented with 2% FBS containing antibodies for surface marker staining at 1:20 v/v concentration each (CD4-PerCP and CD3-APC from BD Biosciences; CD41/61-PE A2A9/6 clone from BioLegend) for 15 min at room temperature. Next, cells were washed in PBS two times, fixed in 4% paraformaldehyde (PFA; EuroMedex) for 30 min, and washed three times before proceeding to flow cytometry data acquisition in a GUAVA 12HT system. The gating strategy for assessing $CD4^+$ T cell–platelet conjugates was performed by selecting cells and not debris based on forward (FSC) and side scatter (SSC), limited inclusion of doublets by FSC-area/FSC-height strategy, gating

TABLE 1 | Clinical data and HIV detection in platelets from InR and IR individuals included in the study.

Individuals information	InR	IR	Statistical test
Total of HIV-infected individuals on cART	n = 20	n = 12	-
Biological sex (male/female number)	15/5	10/2	ns, $p = 0.304$, chi-square
Age [mean years (IQR)]	51 (41–67)	46 (30–51)	ns, $p = 0.659$, Mann–Whitney
Years since HIV diagnosisis [mean years (IQR)]	14 (7–19)	13 (4–22)	ns, $p = 0.904$, Mann–Whitney
Months with confirmed status (responder or non-responder) [mean months (IQR)]	39 (10–56)	39 (31–82)	ns, $p = 0.794$, Mann–Whitney
Months with undetectable viral load [mean months (IQR)]	38 (16–56)	34 (24–78)	ns, $p = 0.754$, Mann–Whitney
Clinical parameters	**InR**	**IR**	**Statistical test**
Platelet count [mean million platelets per ml (IQR)]	209 (148–292)	218 (206–358)	ns, $p = 0.704$, Mann–Whitney
CD4+ T-cell count [mean cells per ml (IQR)]	221 (165–327)	923 (815–1,292)	*$p < 0.001$, Mann–Whitney
Total lymphocyte count [mean million cells per ml (IQR)]	1.54 (1.3–1.9)	2.5 (2.0–2.8)	*$p < 0.001$, Mann–Whitney
HIV+ platelets (FISH-flow) (positive/negative number)*	12/3	3/9	*$p = 0.004$, chi-square
HIV+ platelets (FISH-flow) [mean per million platelets in positive group (IQR)]**	1,113 (120–1,220)	150 (135–160)	*$p = 0.003$, Mann–Whitney

**number of individuals positive or negative for HIV in platelets as detected by FISH-flow method.*

***mean number with IQR of HIV+ platelets per million platelets in individuals detected positive for HIV in platelets.*

IQR: interquartile ranges showing 25th and 75th percentiles of data.

HIV, human immunodeficiency virus; InR, Immunological non-responders; IR, Immunological responders; cART, combination antiretroviral therapy; FISH-Flow, fluorescent in situ hybridation; IQR, Interquartile range.

$CD4^+$ T cells by CD4-$PerCP^+$ and CD3-APC^+ double-positive events, and finally gating CD41/61-PE^{high} cells among $CD4^+$ T-cell population (**Figure 1A**).

Platelet-Rich Plasma

InR and IR platelets were tested for the presence of HIV using the Fluorescence In Situ Hybridisation (FISH)-flow method we described earlier (5), which comprises double detection of HIV RNA and HIV p24 capsid protein in CD41/61-positive platelets quantified by flow cytometry. Briefly, platelets were fixed in PFA 4% for 30 min at room temperature and immunostained for CD41/61 and p24 before *in situ* hybridization with HIV Gag mRNA probes designed with the Stellaris Probe Designer program (https://www.biosearchtech.com/support/tools/design-software/stellaris-probe-designer) as we described (5). In our previous study (5), InR platelet samples in which HIV could not be detected by this methodology represent 22% of total InR samples, whereas IR platelets positive for HIV represent 14% of total IR samples. To be able to evaluate the role of the presence of HIV in platelets in both IRs and InRs, we thus selected for this study a set of 15 samples from InRs from which 12 were positive and 3 were negative for HIV and 12 samples from IRs from which 3 were positive and 9 were negative for HIV. HIV-containing platelets that we refer to below correspond to the population of platelets in which around 0.1% (5) of platelets do actually contain the virus and not to platelets that all individually contain HIV, unless otherwise stated.

Platelet–Leukocyte *In Vitro* Cocultures

Platelet–$CD4^+$ T-Cell Cocultures

$CD4^+$ T-cells from healthy donors were purified by negative selection from healthy donor's PBMCs using the EasySep Negative Human CD4 Kit (STEMCELL Technologies). A pool of cells from three independent donors were used for each experiment. $CD4^+$ T cells from healthy donors were cultivated in RPMI 1640 (Gibco) supplemented with 10% FBS, L-glutamine (2 mM, Gibco), and penicillin/streptomycin (100 U/ml, Gibco) at 10^6 cells/ml and activated by adding 2.5 µg/ml of phytohemagglutinin-L (PHA-L from *Phaseolus vulgaris*, Sigma-Aldrich) for 48 h. After two washes in RPMI 1640, $CD4^+$ T cells were resuspended in fresh medium without or with platelets from InRs, IRs, or healthy donors, respectively, and cultivated overnight at 37°C prior to processing for downstream experiments. The platelet:T cell ratio employed was 2:1.

Platelet–Macrophage Coculture

Monocytes from healthy donors were purified by negative selection from PBMCs from healthy donors using the EasySep Human Monocyte Enrichment Kit (STEMCELL Technologies). For each experiment, a pool of cells from three independent donors was used. Monocytes were differentiated into M2-like macrophages by cultivation in RPMI 1640 supplemented with 10% FBS in the presence of macrophage colony-stimulating factor (M-CSF; 25 µg/ml, Sigma-Aldrich) for 6 days, followed by M2-like macrophage polarization using interleukins IL-4 and IL-13 (20 ng/ml each) for 2 days as described (5). The macrophages were incubated with platelets from InRs, IRs, or healthy donors overnight prior to processing for downstream experiments. To account for the cell size differences between T cells and macrophages, the platelet:macrophage ratio employed was 5:1 (5).

Viral Outgrowth Assay

To measure comparatively infectious viral production from $CD4^+$ T cells and macrophages, we adapted our previously described VOA using $CD4^+$ T cells from healthy donors as reporter cells.

HIV Transfer From Platelet to $CD4^+$ T Cells

Healthy donor's $CD4^+$ T cells were activated by PHA-L (5 µg/ml) for 48 h and cultured in RPMI medium supplemented with 10% FBS and IL-2 at 20 U/ml (complete medium) for an additional 48 h before use in the VOA. To evaluate infectious viral production after platelet–$CD4^+$ T-cell interaction, HIV-containing platelets from InRs were added to 10^5 activated healthy donor's $CD4^+$

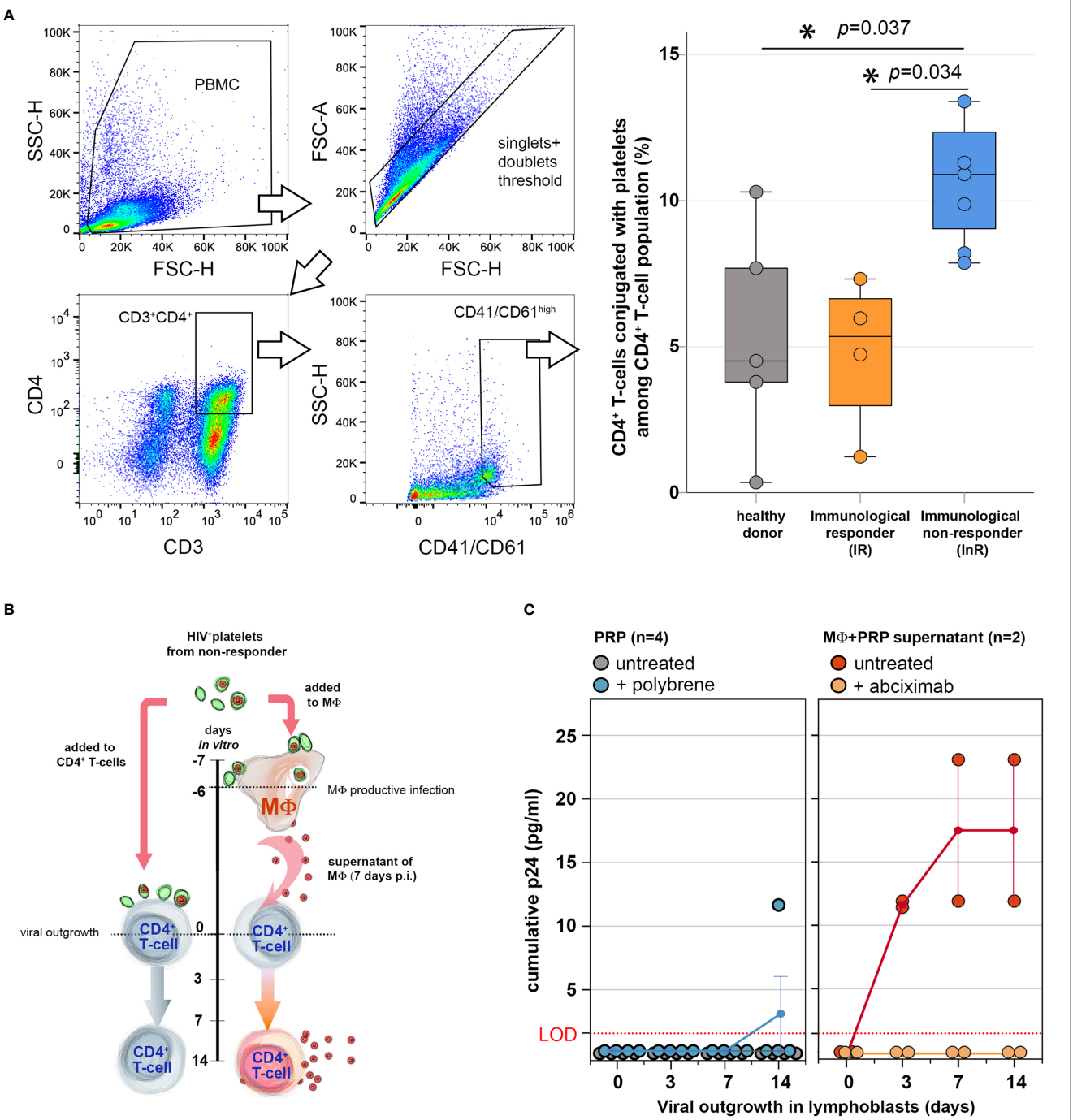

FIGURE 1 | Platelets from immunological non-responders (InRs) form more conjugates with CD4$^+$ T cells *in vivo* but do not transfer infectious virus to CD4$^+$ T cells *in vitro*. **(A)** Platelet–CD4$^+$ T-cell conjugates are more frequent in the circulation of InRs *in vivo*. Flow cytometry analysis of CD4$^+$ T cells (CD3$^+$CD4$^+$) conjugated with platelets (CD41/61^{high}) circulating in the blood of combination antiretroviral therapy (cART)-treated patients virally suppressed. Left: Gating strategy to assess platelet–T-cell conjugates. Right: Percentage of platelet–CD4$^+$ T cell (CD3$^+$CD4$^+$CD41/61^{high}) conjugates among CD4$^+$ T cells (CD3$^+$CD4$^+$) as detected in healthy donor (gray) and HIV-infected patient samples categorized as immunological responder (IR, orange) and InR (blue). Kruskal–Wallis, statistically relevant differences $p < 0.05$ (*). **(B, C)** Upon direct interaction, HIV-containing (HIV$^+$) platelets propagate infection to macrophages (MΦ), not to CD4$^+$ T cells. **(B)** *In vitro* experimental setup. Left: HIV$^+$ platelets are directly incubated with activated CD4$^+$ T cells from healthy donors for a 14-day viral outgrowth assay. Right: MΦ from heathy donors interacts overnight with HIV$^+$ platelets. At day 7, MΦ culture supernatants are collected and tested for their infectious replicative virus content by addition of the same activated CD4$^+$ T cells from healthy donors as in left for a 14-day viral outgrowth assay. **(C)** Viral production quantification: HIV-1 is quantified in coculture supernatants after 14 days of viral outgrowth in CD4$^+$ T cells that were incubated directly with HIV$^+$ platelets in the presence or absence of polybrene (left) or incubated with supernatants of MΦ infected upon interaction with HIV$^+$ platelets in the presence or absence of abciximab (right). LOD, limit of detection for the technique. *Statistically significant.

T cells cultured in complete medium with or without 20 μg/ml polybrene to facilitate fusion of viral envelope and host cell membrane (16). The platelet:T cell ratio employed was 2:1. After 7 days of coculture, medium was replaced and freshly prepared 10^5 healthy donor's activated $CD4^+$ T cells were added to the T cells that interacted with HIV-containing platelets to improve viral propagation for an additional 7 days. At days 0, 3, 7, and 14 of the VOA assay, culture medium was collected and replaced by fresh medium. Collected media were analyzed by HIV p24 capsid protein ELISA (Innotest HIV Antigen mAb, FUJIREBIO) to measure the cumulative viral production.

HIV Transfer From Platelets to Macrophages

In parallel experiments, to quantify viral outgrowth by macrophages upon interaction with InR platelets, macrophages were cocultured with HIV-containing platelets from InRs for 7 days in the presence or absence of the anti-platelet agent abciximab (ReoPro, Janssen Inc.) as described (5). Next, the macrophage–platelet coculture medium was collected and centrifuged, the supernatants were added for a 14-day period to the same pools of healthy donor's $CD4^+$ T cells used above for evaluating HIV transfer from platelets to $CD4^+$ T cells, and viral outgrowth was quantified as above.

Metabolic Profiling

Real-time cell metabolic analysis was carried out by Seahorse XFp Analyzer using the ATP Rate Assay Kit (Agilent) and following manufacturer's instructions. Platelets from InRs, IRs, or healthy donors were cultivated at 37°C overnight with healthy donor's $CD4^+$ T cells or macrophages (pool of three donors, 5×10^5 cells/well) in 48-well plates or in Seahorse XFp cell culture plates, respectively. After thorough wash out of unconjugated platelets, cell metabolism was further analyzed. The platelet: leukocyte ratio employed was 2:1 and 5:1 for $CD4^+$ T cells and macrophages, respectively. For $CD4^+$ T cells that had interacted with platelets, T cells were centrifuged at 300 g for 10 min, resuspended in Seahorse XF RPMI medium, and placed into Seahorse XFp cell culture plates pretreated with Cell-Tak (Corning, Fisher Scientific Inc.) following manufacturer's instructions. For macrophages that interacted with platelets directly in the Seahorse XFp cell culture plates, complete medium was replaced by Seahorse XF RPMI medium. The ATP Rate assay protocol established for the Seahorse XFp Analyzer by the manufacturer provides dynamic information on the total ATP energy production by mitochondrial respiration *via* oxidative phosphorylation (OXPHOS) and/or by glycolysis in living cells. Basic oxygen consumption rate (OCR), which indicates aerobic respiration by OXPHOS, and extracellular acidification rate (ECAR), which indicates glycolysis, were measured over 1 h at indicated time points before and after successive addition of OXPHOS inhibitor oligomycin and the mitochondrial respiratory inhibitors rotenone/antimycin. Results were analyzed by the Agilent Seahorse Analytics online software (seahorseanalytics.agilent.com) to assess the levels of OCR (pmol/min), ECAR (mpH/min), and ATP production rate (pmol/min). A metabolic cell energy map was built by correlating OCR vs. ECAR values, displaying data in a spectrum of metabolic profiles comprising aerobic (predominant ATP production *via* mitochondrial respiration), glycolytic (predominant ATP production *via* glycolysis), quiescent (low ATP production rate by both pathways), or energetic (high ATP production rate by both pathways). Results were displayed as mean with standard errors of values obtained from biological replicates of platelet samples (InR n = 6; IR n = 5; and healthy donors n = 6).

Microarray Data Analysis

The public microarray dataset GSE106792 from Gene Expression Omnibus (GEO) comparing the gene expression of $CD4^+$ T cells from InRs, IRs, and healthy donors (17) was reassessed using the GEO2R tool provided by the GEO website. Datasets were grouped in InRs, IRs, and healthy donors according to the Immune Non-Responders, Immune Responders, and Healthy Donors donor class metadata, respectively, but disregarding the source name metadata related to CD71 expression. Dimensional reduction was performed by Uniform Manifold Approximation and Projection (UMAP) of all individual datasets (from InRs, IRs, and healthy donors) as provided by GEO2R software. Confidence ellipses were plotted on UMAP in R software using UMAP coordinates. Volcano plots were generated in SPSS software (IBM) using the data output of the volcano plots comparing InR vs. IR gene expression generated by GEO2R software. The genes most significantly upregulated in InRs vs. IRs in the differentially expressed gene (DEG) analysis were selected based on Log_2 fold change >0.5 and the $-Log_{10}$ p value >3. The lists of DEG in InRs vs. IRs were used for biological pathway enrichment analysis and visualization of the biological processes enriched in InRs vs. IRs as described (18).

These lists were also submitted to g:Pprofiler (https://biit.cs.ut.ee/gprofiler/gost) (19). The statistical tests were performed by the g:GOSt functional profiling tool, and p values were calculated as described in https://biit.cs.ut.ee/gprofiler/page/docs, "section significance threshold". Briefly, the tool uses an in-house algorithm called g:SCS that performs multiple testing corrections outperforming the commonly used Bonferroni correction (BC) or Benjamini–Hochberg False Discovery Rate (FDR).

The graphical representation of the pathway enrichment analysis was performed by applying g:Profiler output into a Cytoscape Enrichment Map as described (18). Nodes represent gene sets that participate in a given function, and their size represents the number of genes composing this functional cluster. Lines connecting nodes indicate an overlap between gene sets composing both connected nodes. The line width represents the number of genes common to both nodes.

Next, the list of DEGs in InRs vs. IRs was submitted to HumanCyc metabolic map software (20) to visualize the contribution of DEGs on different metabolic pathways in InRs vs. IRs.

Statistical Analysis

All statistical analyses were performed using SPSS software (IBM) and parametric and non-parametric tests for normal and non-normal data distributions, respectively. Statistical significance is indicated by asterisks in figures and was established by p values <0.05.

RESULTS

In Vivo Platelets from Immunological Non-Responders (InRs) Form more Conjugates With CD4+ T Cells as Compared With Immunological Responder (IR) Ones

To address the immunomodulatory role of platelets on $CD4^+$ T cells in immunological failure, we first investigated the presence of platelet–$CD4^+$ T-cell conjugates in PBMCs from InRs, IRs, and healthy donors by flow cytometry. The median frequency of platelet–$CD4^+$ T-cell conjugates among $CD4^+$ T cells was 11% in InRs as compared with 6% in IRs and 3.5% in healthy controls (**Figure 1A**), indicating that platelets from InRs form more conjugates with $CD4^+$ T cells than platelets from IRs *in vivo* that could result in deleterious effects to T cell functions.

Platelets from InRs do not Transfer Infectious Virus to CD4+ T Cells

The InR subjects tested for platelet–$CD4^+$ T-cell conjugates harbor HIV in platelets as quantified by FISH-flow cytometry (see *Materials and Methods*), in contrast to IR subjects whose platelets were negative for viral components. A consequence of the intimate contact between HIV-containing platelets from InR and T cells when conjugates formed could be the transfer of HIV productive infection from platelet to T cells and in turn in their production of infectious viruses. To measure these infectious viruses, we established a viral outgrowth assay (VOA) in which HIV-containing platelets from InRs were allowed to interact directly with healthy donor $CD4^+$ T cells or macrophages. Resulting productive infection of $CD4^+$ T cells or macrophages was then quantified (**Figure 1B**). No outgrowth was detected in healthy donor's $CD4^+$ T cells (serving also as infection reporter cells) after interaction with HIV-containing platelets from InRs, even in the presence of polybrene, a facilitator of membrane fusion (**Figure 1C**, left). In contrast, we observed that the transfer of HIV sheltered in InR platelets to macrophages is productive, as infection spreads replication-competent virus to healthy donor's reporter $CD4^+$ T cells (**Figure 1C**, right). Adding the anti-GPIIbIIIa platelet drug abciximab to the platelet–macrophage coculture blocked this platelet-mediated HIV transfer to macrophages *in vitro*, as we demonstrated previously (5). Thus, unlike macrophages, infectious HIV enclosed in InR platelets does not target $CD4^+$ T cells, although HIV-containing platelets might immunomodulate $CD4^+$ T-cell functions, in turn triggering the immunological failure observed in non-responders.

CD4+ T Cells from InR are More Prone to Aerobic Glycolysis as Compared with IR Ones

Different studies have demonstrated the role of cellular metabolism in the innate and adaptive host responses to infection (21), especially in T-cell immunity (22, 23). To get insight on the $CD4^+$ T cell functional changes induced by InR platelets, we reassessed a transcriptome dataset obtained by Younes et al. (17), reporting on different transcriptome signatures presented by InR, IR, and healthy donor $CD4^+$ T cells. We now used an improved analytical pipeline comprising also metabolic pathway networks (18, 20). Our revised grouping of InR, IR, and healthy donor samples relied only on the provided metadata of clinical status but discarding the CD71 marker used to substratify InR samples as performed in the original analysis (17). Transcriptomic data of InR, IR, and healthy donor as we grouped and compared in a dimensional reduction strategy showed that differences between the three groups remained conserved (**Figure 2A**).

We then thus focused our differential analysis on two major metabolic pathways implicated in T-cell activated vs. resting states: OXPHOS and glycolysis (24). Among the genes upregulated in InR $CD4^+$ T cells as compared with IR counterparts in a DEG analysis, a significant number was implicated in glycolytic pathways (**Figure 2B**). Upregulated genes in InRs included Tyrosyl-DNA phosphodiesterase 1 (TDP1) that decreases phosphoglycolate formation, and phosphoglycolate is known to have an effect on two steps in glycolysis (25); Leucine Rich Repeat Neuronal 3 (LRRN3), a clinically relevant biomarker of immune status in HIV-1 infection whose upregulation correlates with a less senescent T-cell phenotype (26), that binds to LEDGF/p75 or LEDGF/p52 involved in HIV-1 integration (27) and associates with glycolysis canonical gene products ENO2, HK2, PFKFB3; Phosphofructokinase muscle type (PFKM) that is a subunit of phosphofructokinase enzyme, a central controller of the mammalian glycolytic pathway (28); Homeodomain-interacting protein kinase-2 (HIPK-2) that is a member of a family of proteins upregulated in highly proliferative tumors whose expression correlates with upregulation of genes involved in aerobic glycolysis (29); Progesterone Receptor Membrane Component protein-2 (PGRMC2) that is increased in glycolysis (30); and finally, STK36 that plays an important role in the Sonic hedgehog (SHH) pathway that regulates the activity of GLI transcription factors and drives glucose metabolism (31, 32). When analyzed together for functional enrichment using g:Profiler (19), genes specifically upregulated in InRs contributed to two main biological pathways about metabolism, namely, cellular metabolic processes (GO:0044237) and macromolecule metabolic pathways (GO:0043170), whereas those increased in IRs concern macromolecule catabolic processes (GO:0044265) and mRNA metabolic processes (GO:0016071) (**Figure 2C**).

Next, to get a better insight into how these biological pathways interact together, we built a network of biological processes most significantly enriched in $CD4^+$ T cells from InRs as compared with those from IRs. Three main networks of biological processes emerged: "vesicle mediated localization", "processing peptide antigen", and "regulation metabolic process" (**Figure 2D**). The "regulation metabolic process" cluster connects biological pathways enriched in both InR and IR $CD4^+$ T cells. However and in agreement with g:Profiler biological pathway analyses, whereas the nodes connecting biological pathway in IR $CD4^+$ T cells relate mainly to mRNA processing, those connecting biological pathways in InR $CD4^+$ T cells are mainly composed of macromolecule metabolic processes connected with pathways involved in ATP production. To better define the genes upregulated in InR $CD4^+$ T cells directly implicated in ATP production, we submitted the list of DEGs in InR vs. IR T cells to the HumanCyc database (20) to build a metabolic

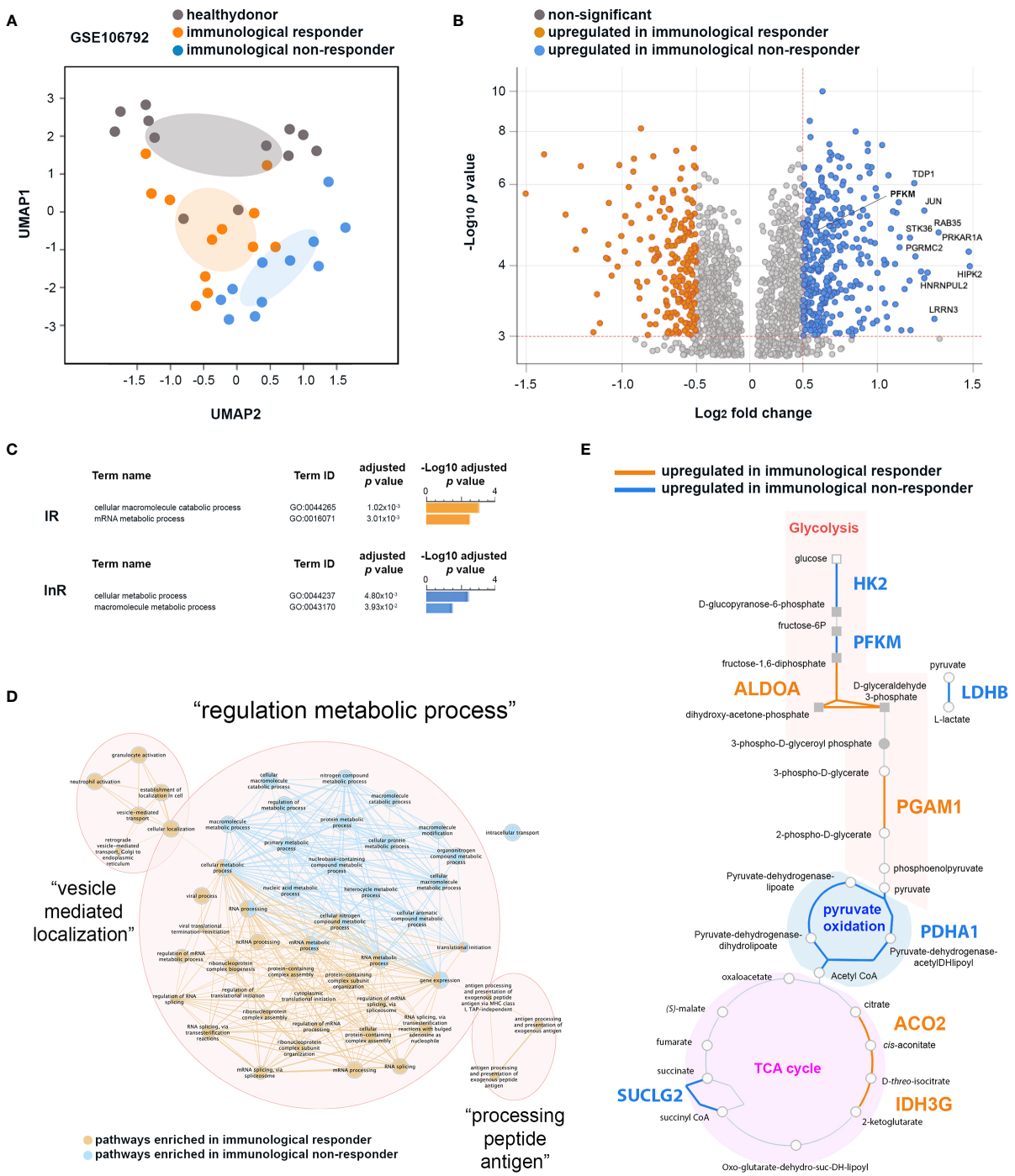

FIGURE 2 | Differential transcriptomic analyses of CD4$^+$ T cells from immunological non-responder (InR) and immunological responder (IR) patients focusing on genes associated with metabolic pathways. **(A)** InR, IR, and healthy donor transcriptomes have distinct profiles. Uniform Manifold Approximation and Projection (UMAP) of transcriptomic data from the GSE106792 dataset based on CD4$^+$ T cells InR, IR, and healthy donors grouping individuals according to blood CD4$^+$ T-cell counts and assessed by the Gene Expression Omnibus (GEO) constructed at a probability of 0.99. **(B)** Volcano plot from the differentially expressed gene (DEG) analysis between InR and IR CD4$^+$ T cells. In the *y* axis, significance is indicated by red dotted line threshold at -Log$_{10}$ *p* value >3 for both InR and IR datasets. In the *x* axis, significance is indicated by red dotted line thresholds at Log$_2$ fold change >0.5 for InR and <-0.5 for IR DEGs. **(C)** Differential biological pathway analysis activated in InR vs. IR CD4$^+$ T cells using g:Profiler. **(D)** Network of biological pathways enriched in CD4$^+$ T cells from InR (blue nodes and connectors) or from IR (orange nodes and connectors) **(E)** HumanCyC metabolic map showing genes upregulated in CD4$^+$ T cells from InR (blue font) and upregulated in CD4$^+$ T cells from IR (orange font) implicated in glycolysis, pyruvate oxidation, and TCA cycle biochemical reactions.

map. This map showed which enzymes that are implicated in biochemical reactions leading to ATP production would be differentially regulated in IR and InR $CD4^+$ T cells. Although both sets of cells harbor differentially upregulated genes for enzymes involved in glycolysis, pyruvate oxidation, and Tricarboxylic Acid TCA cycle, InR $CD4^+$ T cells show a remarkable upregulation of genes coding for enzymes involved in specific reactions of the glycolytic pathway (**Figure 2E**). Notably, Hexokinase 2 (HK2) is responsible for breaking glucose in D-glucopyranose-6-phosphate, ATP-dependent 6-phosphofructokinase muscle type (PFKM) is responsible for breaking fructose-6P in fructose-1,6-diphosphate, and, very importantly, Lactate Dehydrogenase B (LDHB) is responsible for breaking pyruvate (the end product of glycolysis) into L-lactate. This last reaction is a hallmark of aerobic glycolysis, a metabolic reaction performed by activated effector T cells (33). The upregulation of LDHB gene in InR as compared with IR $CD4^+$ T cells indicates that InR $CD4^+$ T cells have increased aerobic glycolysis or Warburg effect, a characteristic of T-cell activation states (34). Altogether, the analysis of $CD4^+$ T-cell transcriptomic data indicates that InR $CD4^+$ T cells are more prone to aerobic glycolysis than their IR counterparts, but the potential role of increased platelet–T-cell conjugates we observed in InRs in this process could not be assessed.

HIV-Containing Platelets from InRs Stimulate Energy Production in CD4+ T Cells via Glycolysis in CD4+ T Cells, not in Macrophages

To approach this question experimentally, we cocultured InR, IR, or healthy donor platelets with healthy donor $CD4^+$ T cells and evaluated the platelet-induced metabolic profile of these T cells. Accordingly, glycolysis and mitochondrial respiration in $CD4^+$ T cells after coculture with platelets were evaluated simultaneously and in live cells by measuring ECAR and OCR, respectively. $CD4^+$ T cells were sequentially treated with oligomycin (ATP synthase and OXPHOS inhibitor) and antimycin A/rotenone (mitochondrial complex III and complex I inhibitors) to functionally assess OXPHOS and mitochondrial respiration capacities. InR platelets positive for the presence of HIV in platelets induced in $CD4^+$ T cells a glycolysis baseline increase compared with InR lacking HIV in platelets, IR (positive or negative of HIV in platelets), or healthy donor platelets (**Figure 3A**, upper graph). No difference was observed in mitochondrial respiration baseline induced by platelets from the five studied conditions with the exception of InR platelets positive for the presence of HIV in platelets, capable of inducing an increased baseline mitochondrial respiration (**Figure 3A**, lower graph). As expected in this system, when the mitochondrial inhibitors were added sequentially, the mitochondrial respiration was drastically inhibited in all groups, and a compensatory increase in glycolysis was observed in $CD4^+$ T cells that was remarkable and more prominent after interaction with InR platelets positive for the presence of HIV as compared with all the other conditions (**Figure 3A**).

By correlating mitochondrial respiration capacities with the glycolytic compensatory increase, we built a bioenergetics phenotype map for $CD4^+$ T cells that interacted with InR or IR platelets, either positive or negative for HIV in platelets, or healthy donor platelets. In contrast with InR platelets without HIV, IR platelets positive or negative for HIV or healthy donor platelets, in which ATP production relies mostly on mitochondrial respiration (aerobic profile), InR platelets positive for HIV induce a more energetic phenotype in $CD4^+$ T cells, in which the ATP production is promoted by both mitochondrial respiration and glycolysis, indicating aerobic glycolysis (**Figure 3B**).

We then compared the contribution of mitochondrial respiration and glycolysis to ATP production in $CD4^+$ T cells vs. macrophages after interaction with InR platelets positive for HIV, IR platelets negative for HIV, or healthy donor platelets using the same dynamic metabolic measurements. Macrophages inherently produce more ATP than $CD4^+$ T cells upon interaction with all platelets tested, with macrophage ATP being produced mostly by mitochondrial respiration. In contrast, an augmented ATP production resulting mainly from an increase in ATP generated by glycolysis was observed in $CD4^+$ T cells that interacted with InR compared with IR or healthy donor platelets (**Figure 3C**).

We next compared specifically the ATP production *via* glycolysis induced in $CD4^+$ T cells after interaction with InR or IR platelets, positive or negative for HIV, or healthy donor platelets. In contrast to the other experimental conditions in which ATP production *via* glycolysis is similar whatever the type of platelets they had interacted with, interaction between InR platelets positive for HIV and $CD4^+$ T cells resulted in higher ATP production *via* glycolysis compared with interaction with IR platelets, independently of the presence of HIV, or healthy donor platelets (**Figure 3D**).

DISCUSSION

Although HIV infection is evolving into a chronic condition with comparable life expectancy to the uninfected population in patients treated with ART (35, 36), an increased risk remains in ART-treated individuals of developing serious non-AIDS complications despite viral suppression (37–41). However, these non-AIDS comorbidities are associated with low $CD4^+$ T-cell levels (42) and are thus frequent in InRs—unable to restore proper $CD4^+$ T-cell levels—that represent 20% of HIV-infected individuals (1, 3, 8, 43). There are currently no available treatments to improve InR immune recovery (8, 44). Chronic immune activation could be in part responsible of these non-AIDS comorbidities, but the exact mechanism of this phenomenon is not totally elucidated (11, 45, 46). It is thus important to define parameters associated with immunological failure in $CD4^+$ T cells from InRs at the cellular and molecular level.

We have recently shown that platelets from InRs can shelter HIV in direct correlation with immune failure (5), but the mechanism behind this correlation remains unclear. Accumulating evidence indicates that platelets can modulate lymphocyte functions (47). Indeed, besides hemostasis, human platelets also carry important immunological functions (48). Thus, platelets can participate in the pathology of the disease during chronic inflammatory conditions such as atherosclerosis, sepsis, and rheumatoid arthritis (49–51).

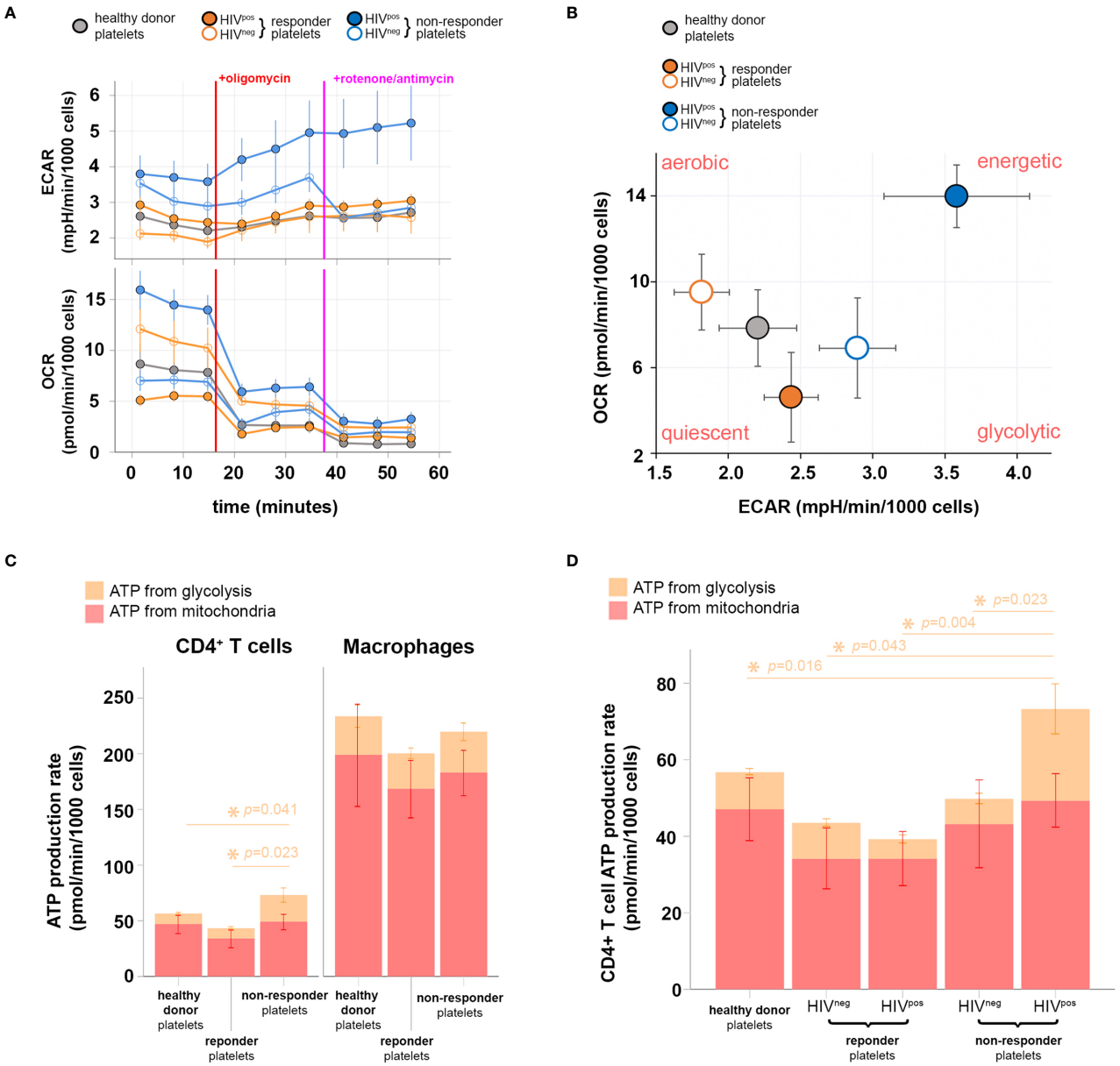

FIGURE 3 | Metabolic profiling of CD4$^+$ T cells after interaction with immunological non-responder (InR), immunological responder (IR), or healthy donor platelets, sheltering or not HIV in platelets. **(A)** Oxygen consumption rate (OCR; upper) and extracellular acidification rate (ECAR; lower) obtained throughout 1 h of data acquisition from live CD4$^+$ T cells that interacted with InR (blue), IR (orange), or healthy donor (gray) platelets. Filled or empty circles with the same color code indicate the presence (HIV^{pos}) or absence (HIV^{neg}) of HIV in platelets, respectively. During the time course of data acquisition, the oxidative phosphorylation (OXPHOS) inhibitor and mitochondrial respiratory chain blocker oligomycin and rotenone/antimycin were injected at time points indicated by red and purple lines, respectively. **(B)** Energy phenotype map of CD4$^+$ T cells that interacted with InR (blue), IR (orange), or healthy donor (gray) platelets. Filled or empty circles with the same color code indicate the presence (HIV^{pos}) or absence (HIV^{neg}) of HIV in platelets, respectively. **(C)** ATP production rate from CD4$^+$ T cells (left) or macrophages (right) that interacted with InR, IR, or healthy donor platelets. The contribution of either glycolysis or mitochondria respiration to ATP production is discriminated in the bar graph by orange and red, respectively. Asterisks indicate statistically relevant differences established using a threshold of $p < 0.05$ calculated with a Kruskal–Wallis test on glycolysis levels (orange). Mitochondrial ATP production does not differ between groups using the same statistical test and significance threshold. **(D)** ATP production rate from CD4$^+$ T cells that interacted with healthy donor platelets, IR platelets without HIV (HIV^{neg}) in platelets, IR platelets with HIV (HIV^{pos}) in platelets, InR HIV^{neg} platelets, and InR HIV^{pos} platelets. The contribution of either glycolysis or mitochondria respiration to ATP production is discriminated in the bar graph by orange and red, respectively. Asterisks indicate statistically relevant differences established by threshold of $p < 0.05$ using ANOVA on glycolysis levels (orange). Mitochondrial ATP production does not differ between groups using the same statistical test and significance threshold.

We now report that one of the mechanisms by which platelets contribute to immunological failure might rely on the capacity of platelets from InRs compared to IRs to form increased conjugate numbers with $CD4^+$ T cells *in vivo*, as also observed in the blood of HIV patients (12). HIV-containing platelet–T-cell conjugates do not result in HIV transfer to $CD4^+$ T cells, in contrast to macrophages in which HIV-containing platelets can propagate infection *in vitro* (5).

This result contrasts with another study by Simpson et al. (52) showing that $CD4^+$ T cells are permissive to HIV carried by platelets. However, the clinical status of patients studied in this publication differs from our own study, as samples were obtained from patients before cART administration that were thus viremic and from patients treated for 3 months by cART with a majority of patents remaining viremic. Consequently, platelets used in this publication had the capacity to bind and uptake circulating HIV and transfer infection to T cells *via* viruses attached to their surface. Furthermore, the mean patient $CD4^+$ T-cell counts was >460 cells/µl, indicating that the majority of samples studied by Simpson et al. (52) fall outside the group of individuals that most frequently have HIV in platelets [$CD4^+$ T-cell count of <350 cells/µl as described (5)].

In our study, by contrast, individuals were all cART-treated for more than 6 months before sampling, sustainedly aviremic (blood viral load below level of detection) and the InR group had sustained low CD4 counts of <350 cells/µl for >6 months, similar to our previous study (5). Accordingly, and as we have shown previously, the platelets studied here did not harbor cell-free HIV attached to their surface and the virus is only found inside platelet intracellular compartments. Furthermore, as no cell-free virus was circulating in the patients we have studied here, their platelets did not capture virus at their surface nor endocytosed it from the blood, as we already demonstrated (5), hampering for example a platelet-mediated T-cell infection by viruses carried on the surface of platelets. Thus, the mechanism of virus transfer from platelets to $CD4^+$ T cells likely occurs only by synaptic-like transfer during conjugate formation whereby the virus exits platelet internal compartments to reach and infect T cells.

We cannot exclude that increasing the platelet:T cell ratio in our *in vitro* coculture system would effectively promote platelet-mediated T-cell infection as observed by Simpson et al. (52) using platelets from viremic patients. However, our results demonstrate that HIV-containing platelets interacting with T cells at a low platelet:T cell ratio are sufficient to cause T-cell dysfunction even if this ratio does not promote $CD4^+$ T infection.

Accordingly, independent of infection, InR platelets containing HIV can induce a change in $CD4^+$ T-cell metabolism resulting in augmented glycolysis. This effect is specific to $CD4^+$ T cells interacting with InR platelets that contain HIV, as we found that $CD4^+$ T cells that interacted with platelets from InR lacking HIV, IR (containing or not HIV), or from healthy donors lack these capacities, and macrophages are insensitive to platelet-induced metabolic changes.

The energetic increase in T-cell metabolism induced by InR platelets we report could participate in chronic immune $CD4^+$ T-cell activation and in turn $CD4^+$ T-cell exhaustion as in other pathologies (11, 45, 46). Furthermore, the higher level of T-cell immune activation during chronic HIV infection (12) may enhance the formation of these conjugates and in turn maintain a state of chronic inflammation by increasing T-cell trafficking through inflamed tissues harboring HIV replication (12).

Increased glycolysis is a well-defined mark of T-cell activation (53). We show that platelets from InRs in which virus can be detected activate $CD4^+$ T cells by increasing $CD4^+$ T cell glycolysis in aerobic conditions. We hypothesize that the metabolic state of $CD4^+$ T cells activated upon conjugate formation with HIV-containing platelets has two main implications: 1) these $CD4^+$ T cells become exhausted, inducing an immunosenescence scenario related to immunological failure; and 2) these $CD4^+$ T cells might reverse pro-viral latency and stimulate the production of new viral particles despite the ART. This reactivation would in turn maintain an "active $CD4^+$ T-cell reservoir" (54) producing low-level, but constant, viral mRNA and potentially persistent viral particles despite ART. Validation of both scenarios will require further experiments.

The interaction of platelets with lymphocytes results in inhibition of T-cell proliferation and drives the differentiation of naive or memory $CD4^+$ T cells toward regulatory profiles (T_{reg} : $FoxP3^+$) or inflammatory ones like Th17 thus resulting in immunological failure (13, 55). It is still to be determined whether this pathway regulates *in situ* T-cell function, as suggested for patients with rheumatoid arthritis, leading to inefficient viral elimination and perpetuating inflammation (11). Along this line, the pro-inflammatory environment in InR individuals is linked to circulating T_{reg}/Th17 unbalance accompanied by their functional dysregulation (17, 56, 57).

Several mechanisms have been proposed to account for immunomodulation resulting from platelet interaction with $CD4^+$ T cells. Platelets can directly interact with lymphocytes by direct contact, inducing their polarization and/or secretion of cytokines/chemokines (58). Platelets can also shed microvesicles (ectosomes) that directly contact these lymphocytes (55) as well as myeloid and epithelial cells (47, 48, 58). Functionally, these platelet microvesicles could transfer active mRNA and microRNA (miRNA) to target cells (58, 59) and could promote T_{reg} differentiation (55).

The platelet–$CD4^+$ T-cell conjugates we quantified here rely on the identification of platelets by CD41/CD61. We cannot exclude the possibility that part of, or all of, $CD4^+$ T cells might have conjugated with platelet microvesicles. Additional morphological analyses would be required to solve this issue, at least qualitatively.

Platelet microvesicles can use multiple mechanisms to exert these effects such as extracellular signaling through receptors following transient interaction, transfer of surface molecules by trogocytosis-like mechanism, and delivery of their content including RNA and miRNA to the target cell cytoplasm (58, 59), thereby promoting platelet-derived mRNA by target T cells.

In particular, platelets contain a repertoire of mainly pro-inflammatory miRNAs such as miRNA-155 and miRNA-326, involved in nuclear factor (NF)-κB-mediated inflammatory macrophage responses (60) and Th17 cell polarization (61–63). These miRNAs could be differentially expressed in platelets

containing HIV, and their eventual transfer to target immune cells could participate in immune cell dysfunction as observed in InRs (64, 65). Furthermore, αIIb/β3 mRNA is a platelet-specific transcript conserved in circulating platelets throughout their life span (66) and can be exploited to track the process of transfer of mRNA/miRNA of HIV-containing platelets to leukocytes. Which of these mechanisms is at work in the metabolic immunomodulation of $CD4^+$ T cells by InR platelets we report remains to be determined.

Recent evidence indicates that the cellular metabolism controls both the activation and the differentiation of $CD4^+$ T cells (24). Cells use two major pathways for energy generation: glycolysis and OXPHOS. After activation, metabolically quiescent naive T cells switch from OXPHOS to glycolysis, providing energy and biosynthetic precursors for cell proliferation and effector functions. We have shown here that HIV-containing platelets increased the rates of glycolysis and the contribution of glycolysis in intracellular ATP production without affecting mitochondrial respiration in $CD4^+$ T cells from healthy donors. We thus suggest that platelets from InRs could impact $CD4^+$ T-cell metabolism thereby promoting immunological failure in HIV-infected ART-treated patients. Such metabolism modulation would affect uninfected bystander CD4+ T cells but also HIV-infected $CD4^+$ T-cell reservoirs in which viral replication is strongly impaired in $CD4^+$ T cells in glucose-deprived or glutamine-deprived conditions (67–69).

The metabolic environment that favors HIV-1 infection might also contribute to the persistence of the infected cells. Different reports have indicated that among infected cells, those cells that prevent aerobic glycolysis and preserve mitochondrial integrity and function may have a survival advantage and may better resist virus-induced cell death *in vitro* (69–71). Moreover, enhanced glycolytic activity in $CD4^+$ T cells was associated with T-cell activation in HIV-infected adults (72). Mitochondrial respiration is also impaired in $CD4^+$ T cells from individuals positive for HIV-1 (73) and associated with cell death, $CD4^+$ T-cell depletion (74), and dysfunctional T_{reg} (17).

Altogether, the data presented here advocate for a link between T cells and platelets in immunological failure. This interface may play an important role in host defense and in chronic inflammatory diseases associated with HIV infection. Agents that might inhibit this interaction, as anticipated with abciximab, may also block the formation of conjugates and inhibit oxidative metabolism in InR patients with HIV-containing platelets and thus provide a treatment for InRs, for whom no clinical treatment is available yet. Then, future immunotherapies may need to target the metabolic programs of T cells to enhance their antiviral potential.

In sum, our data demonstrate noticeable differences in the metabolic profile of T cells cocultured with HIV-containing platelets compared to T cells cocultured with HIV-negative platelets and healthy donor platelets, suggesting a shift in the bioenergetic profile of T lymphocytes toward glycolysis after contact with HIV-containing platelets and probably linked to chronic activation.

DATA AVAILABILITY STATEMENT

The datasets presented in this study can be found in online repositories. The names of the repository/repositories and accession number(s) can be found below: https://www.ncbi.nlm.nih.gov/geo/query/acc.cgi?acc=GSE106792.

ETHICS STATEMENT

The studies involving human participants were reviewed and approved by "Comité de Protection des Personnes" (CPP) of Ile-de-France. The patients/participants provided their written informed consent to participate in this study.

AUTHOR CONTRIBUTIONS

Study design: AZ, FR, CC, and MB. Methodology: AZ, FR, CC, and MB. Sample resources: CC, JZ, ER, PT, and SG. Investigation: AZ, FR, CC, and MB. Formal data analysis: AZ, FR, CC, and MB. Data interpretation: AZ, FR, CC, and MB. Funding acquisition: MB. Medical validation: CC. Writing, review, editing: AZ, FR, CC, and MB. All authors contributed to the article and approved the submitted version.

FUNDING

This work was supported by funds from Agence Nationale de la recherche sur le SIDA et les Hépatites (ANRS, Funding no.: AO2019-2-19401), from Fondation pour la Recherche Médicale (Équipe FRM EQU201903007830) and the fund Line Renaud-Loulou Gasté- Fondation pour la Recherche Médicale to MB, by funds from APHP 190574 IDRCB 2020-A00307-32 to CC and by funds from the DIM (Domaine d'Interet Majeur)-1-HEALTH (funding no.: 14-DIM1HEALTH-2017) to MB and CC. AZ was supported by the China Scholarship Council. Funders of the study had no role in the study design, data collection, data analysis, data interpretation, or writing of the article.

ACKNOWLEDGMENTS

The authors thank the patients for their participation in the study. They acknowledge Pr. E. Cramer-Bordé (Université St. Quentin en Yvelines) for helpful discussions.

SUPPLEMENTARY MATERIAL

The Supplementary Material for this article can be found online at: https://www.frontiersin.org/articles/10.3389/fimmu.2021.781923/full#supplementary-material

Supplementary Table 1 | List of Differentially Expressed Genes (DEG) comparing gene expression from Immunological Non-Responders (InR) versus Immunological Responders (IR) $CD4^+$ T cells, obtained by GEO2R software using the public microarray dataset GSE106792 from Gene Expression Omnibus (GEO). Table shows Illumina gene entries converted in ensemble entries, gene symbols and gene titles. Gene expression is shown as Log2 fold change and -Log10 *p* value.

REFERENCES

1. Kaufmann GR, Perrin L, Pantaleo G, Opravil M, Furrer H, Telenti A, et al. CD4 T-Lymphocyte Recovery in Individuals With Advanced HIV-1 Infection Receiving Potent Antiretroviral Therapy for 4 Years: The Swiss HIV Cohort Study. *Arch Intern Med* (2003) 163(18):2187–95. doi: 10.1001/archinte.163.18.2187
2. Baker JV, Peng G, Rapkin J, Krason D, Reilly C, Cavert WP, et al. Poor Initial CD4+ Recovery With Antiretroviral Therapy Prolongs Immune Depletion and Increases Risk for AIDS and Non-AIDS Diseases. *J Acquir Immune Defic Syndr* (2008) 48(5):541–6. doi: 10.1097/QAI.0b013e31817bebb3
3. Kelley CF, Kitchen CM, Hunt PW, Rodriguez B, Hecht FM, Kitahata M, et al. Incomplete Peripheral CD4+ Cell Count Restoration in HIV-Infected Patients Receiving Long-Term Antiretroviral Treatment. *Clin Infect Dis* (2009) 48(6):787–94. doi: 10.1086/597093
4. Chene G, Sterne JA, May M, Costagliola D, Ledergerber B, Phillips AN, et al. Prognostic Importance of Initial Response in HIV-1 Infected Patients Starting Potent Antiretroviral Therapy: Analysis of Prospective Studies. *Lancet* (2003) 362(9385):679–86. doi: 10.1016/s0140-6736(03)14229-8
5. Real F, Capron C, Sennepin A, Arrigucci R, Zhu A, Sannier G, et al. Platelets From HIV-Infected Individuals on Antiretroviral Drug Therapy With Poor CD4(+) T Cell Recovery can Harbor Replication-Competent HIV Despite Viral Suppression. *Sci Transl Med* (2020) 12(535):1–11. doi: 10.1126/scitranslmed.aat6263
6. Deeks SG, Kitchen CM, Liu L, Guo H, Gascon R, Narvaez AB, et al. Immune Activation Set Point During Early HIV Infection Predicts Subsequent CD4+ T-Cell Changes Independent of Viral Load. *Blood* (2004) 104(4):942–7. doi: 10.1182/blood-2003-09-3333
7. Hunt PW, Martin JN, Sinclair E, Bredt B, Hagos E, Lampiris H, et al. T Cell Activation is Associated With Lower CD4+ T Cell Gains in Human Immunodeficiency Virus-Infected Patients With Sustained Viral Suppression During Antiretroviral Therapy. *J Infect Dis* (2003) 187 (10):1534–43. doi: 10.1086/374786
8. Marziali M, De Santis W, Carello R, Leti W, Esposito A, Isgro A, et al. T-Cell Homeostasis Alteration in HIV-1 Infected Subjects With Low CD4 T-Cell Count Despite Undetectable Virus Load During HAART. *AIDS* (2006) 20 (16):2033–41. doi: 10.1097/01.aids.0000247588.69438.fd
9. Nunes-Alves C, Nobrega C, Behar SM, Correia-Neves M. Tolerance has Its Limits: How the Thymus Copes With Infection. *Trends Immunol* (2013) 34 (10):502–10. doi: 10.1016/j.it.2013.06.004
10. Wilson EM, Singh A, Hullsiek KH, Gibson D, Henry WK, Lichtenstein K, et al. Monocyte-Activation Phenotypes Are Associated With Biomarkers of Inflammation and Coagulation in Chronic HIV Infection. *J Infect Dis* (2014) 210(9):1396–406. doi: 10.1093/infdis/jiu275
11. Zamora C, Canto E, Nieto JC, Ortiz MA, Diaz-Torne C, Diaz-Lopez C, et al. Functional Consequences of Platelet Binding to T Lymphocytes in Inflammation. *J Leukoc Biol* (2013) 94(3):521–9. doi: 10.1189/jlb.0213074
12. Green SA, Smith M, Hasley RB, Stephany D, Harned A, Nagashima K, et al. Activated Platelet-T-Cell Conjugates in Peripheral Blood of Patients With HIV Infection: Coupling Coagulation/Inflammation and T Cells. *AIDS* (2015) 29(11):1297–308. doi: 10.1097/QAD.0000000000000701
13. Gerdes N, Zhu L, Ersoy M, Hermansson A, Hjemdahl P, Hu H, et al. Platelets Regulate CD4(+) T-Cell Differentiation *via* Multiple Chemokines in Humans. *Thromb Haemost* (2011) 106(2):353–62. doi: 10.1160/TH11-01-0020
14. Starossom SC, Veremeyko T, Yung AW, Dukhinova M, Au C, Lau AY, et al. Platelets Play Differential Role During the Initiation and Progression of Autoimmune Neuroinflammation. *Circ Res* (2015) 117(9):779–92. doi: 10.1161/CIRCRESAHA.115.306847
15. Shyer JA, Flavell RA, Bailis W. Metabolic Signaling in T Cells. *Cell Res* (2020) 30(8):649–59. doi: 10.1038/s41422-020-0379-5
16. Mohammadi P, di Iulio J, Munoz M, Martinez R, Bartha I, Cavassini M, et al. Dynamics of HIV Latency and Reactivation in a Primary CD4+ T Cell Model. *PLoS Pathog* (2014) 10(5):e1004156. doi: 10.1371/journal.ppat.1004156
17. Younes SA, Talla A, Pereira Ribeiro S, Saidakova EV, Korolevskaya LB, Shmagel KV, et al. Cycling CD4+ T Cells in HIV-Infected Immune Nonresponders Have Mitochondrial Dysfunction. *J Clin Invest* (2018) 128 (11):5083–94. doi: 10.1172/JCI120245
18. Reimand J, Isserlin R, Voisin V, Kucera M, Tannus-Lopes C, Rostamianfar A, et al. Pathway Enrichment Analysis and Visualization of Omics Data Using G: Profiler, GSEA, Cytoscape and EnrichmentMap. *Nat Protoc* (2019) 14(2):482–517. doi: 10.1038/s41596-018-0103-9
19. Raudvere U, Kolberg L, Kuzmin I, Arak T, Adler P, Peterson H, et al. G: Profiler: A Web Server for Functional Enrichment Analysis and Conversions of Gene Lists (2019 Update). *Nucleic Acids Res* (2019) 47(W1):W191–W8. doi: 10.1093/nar/gkz369
20. Romero P, Wagg J, Green ML, Kaiser D, Krummenacker M, Karp PD. Computational Prediction of Human Metabolic Pathways From the Complete Human Genome. *Genome Biol* (2005) 6(1):R2. doi: 10.1186/gb-2004-6-1-r2
21. Mathis D, Shoelson SE. Immunometabolism: An Emerging Frontier. *Nat Rev Immunol* (2011) 11(2):81. doi: 10.1038/nri2922
22. Pearce EL, Poffenberger MC, Chang CH, Jones RG. Fueling Immunity: Insights Into Metabolism and Lymphocyte Function. *Science* (2013) 342 (6155):1242454. doi: 10.1126/science.1242454
23. Waickman AT, Powell JD. mTOR, Metabolism, and the Regulation of T-Cell Differentiation and Function. *Immunol Rev* (2012) 249(1):43–58. doi: 10.1111/j.1600-065X.2012.01152.x
24. Palmer CS, Henstridge DC, Yu D, Singh A, Balderson B, Duette G, et al. Emerging Role and Characterization of Immunometabolism: Relevance to HIV Pathogenesis, Serious Non-AIDS Events, and a Cure. *J Immunol* (2016) 196(11):4437–44. doi: 10.4049/jimmunol.1600120
25. Gerin I, Bury M, Baldin F, Graff J, Van Schaftingen E, Bommer GT. Phosphoglycolate has Profound Metabolic Effects But Most Likely No Role in a Metabolic DNA Response in Cancer Cell Lines. *Biochem J* (2019) 476 (4):629–43. doi: 10.1042/BCJ20180435
26. Chou JP, Ramirez CM, Wu JE, Effros RB. Accelerated Aging in HIV/AIDS: Novel Biomarkers of Senescent Human CD8+ T Cells. *PLoS One* (2013) 8(5): e64702. doi: 10.1371/journal.pone.0064702
27. Singh PK, Plumb MR, Ferris AL, Iben JR, Wu X, Fadel HJ, et al. LEDGF/p75 Interacts With mRNA Splicing Factors and Targets HIV-1 Integration to Highly Spliced Genes. *Genes Dev* (2015) 29(21):2287–97. doi: 10.1101/gad.267609.115
28. Chesney J, Mitchell R, Benigni F, Bacher M, Spiegel L, Al-Abed Y, et al. An Inducible Gene Product for 6-Phosphofructo-2-Kinase With an AU-Rich Instability Element: Role in Tumor Cell Glycolysis and the Warburg Effect. *Proc Natl Acad Sci USA* (1999) 96(6):3047–52. doi: 10.1073/pnas.96.6.3047
29. Wong KKL, Liao JZ, Verheyen EM. A Positive Feedback Loop Between Myc and Aerobic Glycolysis Sustains Tumor Growth in a Drosophila Tumor Model. *Elife* (2019) 8:1–19. doi: 10.7554/eLife.46315
30. Thejer BM, Adhikary PP, Kaur A, Teakel SL, Van Oosterum A, Seth I, et al. PGRMC1 Phosphorylation Affects Cell Shape, Motility, Glycolysis, Mitochondrial Form and Function, and Tumor Growth. *BMC Mol Cell Biol* (2020) 21(1):24. doi: 10.1186/s12860-020-00256-3
31. Teperino R, Amann S, Bayer M, McGee SL, Loipetzberger A, Connor T, et al. Hedgehog Partial Agonism Drives Warburg-Like Metabolism in Muscle and Brown Fat. *Cell* (2012) 151(2):414–26. doi: 10.1016/j.cell.2012.09.021
32. Maloveryan A, Finta C, Osterlund T, Kogerman P. A Possible Role of Mouse Fused (STK36) in Hedgehog Signaling and Gli Transcription Factor Regulation. *J Cell Commun Signal* (2007) 1(3-4):165–73. doi: 10.1007/s12079-007-0014-y
33. Menk AV, Scharping NE, Moreci RS, Zeng X, Guy C, Salvatore S, et al. Early TCR Signaling Induces Rapid Aerobic Glycolysis Enabling Distinct Acute T Cell Effector Functions. *Cell Rep* (2018) 22(6):1509–21. doi: 10.1016/j.celrep.2018.01.040
34. Buck MD, O'Sullivan D, Pearce EL. T Cell Metabolism Drives Immunity. *J Exp Med* (2015) 212(9):1345–60. doi: 10.1084/jem.20151159

35. Dore GJ, Li Y, McDonald A, Ree H, Kaldor JM, National HIVSC. Impact of Highly Active Antiretroviral Therapy on Individual AIDS-Defining Illness Incidence and Survival in Australia. *J Acquir Immune Defic Syndr* (2002) 29 (4):388–95. doi: 10.1097/00126334-200204010-00010
36. Lewden C, Chene G, Morlat P, Raffi F, Dupon M, Dellamonica P, et al. HIV-Infected Adults With a CD4 Cell Count Greater Than 500 Cells/Mm3 on Long-Term Combination Antiretroviral Therapy Reach Same Mortality Rates as the General Population. *J Acquir Immune Defic Syndr* (2007) 46(1):72–7. doi: 10.1097/QAI.0b013e318134257a
37. Goehringer F, Bonnet F, Salmon D, Cacoub P, Paye A, Chene G, et al. Causes of Death in HIV-Infected Individuals With Immunovirologic Success in a National Prospective Survey. *AIDS Res Hum Retroviruses* (2017) 33(2):187–93. doi: 10.1089/aid.2016.0222
38. Grulich AE, van Leeuwen MT, Falster MO, Vajdic CM. Incidence of Cancers in People With HIV/AIDS Compared With Immunosuppressed Transplant Recipients: A Meta-Analysis. *Lancet* (2007) 370(9581):59–67. doi: 10.1016/S0140-6736(07)61050-2
39. Casper C. The Increasing Burden of HIV-Associated Malignancies in Resource-Limited Regions. *Annu Rev Med* (2011) 62:157–70. doi: 10.1146/annurev-med-050409-103711
40. Hasse B, Ledergerber B, Furrer H, Battegay M, Hirschel B, Cavassini M, et al. Morbidity and Aging in HIV-Infected Persons: The Swiss HIV Cohort Study. *Clin Infect Dis* (2011) 53(11):1130–9. doi: 10.1093/cid/cir626
41. Marin B, Thiebaut R, Bucher HC, Rondeau V, Costagliola D, Dorrucci M, et al. Non-AIDS-Defining Deaths and Immunodeficiency in the Era of Combination Antiretroviral Therapy. *AIDS* (2009) 23(13):1743–53. doi: 10.1097/QAD.0b013e32832e9b78
42. Lundgren JD, Baxter J, Deeks SG, Lane HC. Biomarkers in HIV Disease. *Curr Opin HIV AIDS* (2010) 5(6):459–62. doi: 10.1097/COH.0b013e32833f2ed6
43. Cenderello G, De Maria A. Discordant Responses to cART in HIV-1 Patients in the Era of High Potency Antiretroviral Drugs: Clinical Evaluation, Classification, Management Prospects. *Expert Rev Anti Infect Ther* (2016) 14(1):29–40. doi: 10.1586/14787210.2016.1106937
44. Carvalho-Silva WHV, Andrade-Santos JL, Souto FO, Coelho AVC, Crovella S, Guimaraes RL. Immunological Recovery Failure in cART-Treated HIV-Positive Patients is Associated With Reduced Thymic Output and RTE CD4+ T Cell Death by Pyroptosis. *J Leukoc Biol* (2020) 107(1):85–94. doi: 10.1002/JLB.4A0919-235R
45. Sarma J, Laan CA, Alam S, Jha A, Fox KA, Dransfield I. Increased Platelet Binding to Circulating Monocytes in Acute Coronary Syndromes. *Circulation* (2002) 105(18):2166–71. doi: 10.1161/01.CIR.0000015700.27754.6F
46. Li N, Ji Q, Hjemdahl P. Platelet-Lymphocyte Conjugation Differs Between Lymphocyte Subpopulations. *J Thromb Haemost* (2006) 4(4):874–81. doi: 10.1111/j.1538-7836.2006.01817.x
47. Hansson GK. Inflammation, Atherosclerosis, and Coronary Artery Disease. *N Engl J Med* (2005) 352(16):1685–95. doi: 10.1056/NEJMra043430
48. Semple JW, Italiano JE Jr, Freedman J. Platelets and the Immune Continuum. *Nat Rev Immunol* (2011) 11(4):264–74. doi: 10.1038/nri2956
49. Knijff-Dutmer EA, Koerts J, Nieuwland R, Kalsbeek-Batenburg EM, van de Laar MA. Elevated Levels of Platelet Microparticles are Associated With Disease Activity in Rheumatoid Arthritis. *Arthritis Rheum* (2002) 46(6):1498–503. doi: 10.1002/art.10312
50. Wagner DD, Burger PC. Platelets in Inflammation and Thrombosis. *Arterioscler Thromb Vasc Biol* (2003) 23(12):2131–7. doi: 10.1161/01.ATV.0000095974.95122.EC
51. Burger PC, Wagner DD. Platelet P-Selectin Facilitates Atherosclerotic Lesion Development. *Blood* (2003) 101(7):2661–6. doi: 10.1182/blood-2002-07-2209
52. Simpson SR, Singh MV, Dewhurst S, Schifitto G, Maggirwar SB. Platelets Function as an Acute Viral Reservoir During HIV-1 Infection by Harboring Virus and T-Cell Complex Formation. *Blood Adv* (2020) 4(18):4512–21. doi: 10.1182/bloodadvances.2020002420
53. Soto-Heredero G, Gomez de Las Heras MM, Gabande-Rodriguez E, Oller J, Mittelbrunn M. Glycolysis - a Key Player in the Inflammatory Response. *FEBS J* (2020) 287(16):3350–69. doi: 10.1111/febs.15327
54. Cohn LB, Chomont N, Deeks SG. The Biology of the HIV-1 Latent Reservoir and Implications for Cure Strategies. *Cell Host Microbe* (2020) 27(4):519–30. doi: 10.1016/j.chom.2020.03.014
55. Sadallah S, Amicarella F, Eken C, Iezzi G, Schifferli JA. Ectosomes Released by Platelets Induce Differentiation of CD4+T Cells Into T Regulatory Cells. *Thromb Haemost* (2014) 112(6):1219–29. doi: 10.1160/TH14-03-0281
56. Pandiyan P, Younes SA, Ribeiro SP, Talla A, McDonald D, Bhaskaran N, et al. Mucosal Regulatory T Cells and T Helper 17 Cells in HIV-Associated Immune Activation. *Front Immunol* (2016) 7:228. doi: 10.3389/fimmu.2016.00228
57. Piconi S, Trabattoni D, Gori A, Parisotto S, Magni C, Meraviglia P, et al. Immune Activation, Apoptosis, and Treg Activity are Associated With Persistently Reduced CD4+ T-Cell Counts During Antiretroviral Therapy. *AIDS* (2010) 24(13):1991–2000. doi: 10.1097/QAD.0b013e32833c93ce
58. D'Ambrosi S, Nilsson RJ, Wurdinger T. Platelets and Tumor-Associated RNA Transfer. *Blood* (2021) 137(23):3181–91. doi: 10.1182/blood.2019003978
59. Rowley JW, Schwertz H, Weyrich AS. Platelet mRNA: The Meaning Behind the Message. *Curr Opin Hematol* (2012) 19(5):385–91. doi: 10.1097/MOH.0b013e328357010e
60. Mann M, Mehta A, Zhao JL, Lee K, Marinov GK, Garcia-Flores Y, et al. An NF-kappaB-microRNA Regulatory Network Tunes Macrophage Inflammatory Responses. *Nat Commun* (2017) 8(1):851. doi: 10.1038/s41467-017-00972-z
61. Rodriguez-Munoz A, Martinez-Hernandez R, Ramos-Levi AM, Serrano-Somavilla A, Gonzalez-Amaro R, Sanchez-Madrid F, et al. Circulating Microvesicles Regulate Treg and Th17 Differentiation in Human Autoimmune Thyroid Disorders. *J Clin Endocrinol Metab* (2015) 100(12):E1531–9. doi: 10.1210/jc.2015-3146
62. Rowley JW, Chappaz S, Corduan A, Chong MM, Campbell R, Khoury A, et al. Dicer1-Mediated miRNA Processing Shapes the mRNA Profile and Function of Murine Platelets. *Blood* (2016) 127(14):1743–51. doi: 10.1182/blood-2015-07-661371
63. Du C, Liu C, Kang J, Zhao G, Ye Z, Huang S, et al. MicroRNA miR-326 Regulates TH-17 Differentiation and is Associated With the Pathogenesis of Multiple Sclerosis. *Nat Immunol* (2009) 10(12):1252–9. doi: 10.1038/ni.1798
64. Podshivalova K, Salomon DR. MicroRNA Regulation of T-Lymphocyte Immunity: Modulation of Molecular Networks Responsible for T-Cell Activation, Differentiation, and Development. *Crit Rev Immunol* (2013) 33 (5):435–76. doi: 10.1615/CritRevImmunol.2013006858
65. Ple H, Landry P, Benham A, Coarfa C, Gunaratne PH, Provost P. The Repertoire and Features of Human Platelet microRNAs. *PLoS One* (2012) 7 (12):e50746. doi: 10.1371/journal.pone.0050746
66. Fink L, Holschermann H, Kwapiszewska G, Muyal JP, Lengemann B, Bohle RM, et al. Characterization of Platelet-Specific mRNA by Real-Time PCR After Laser-Assisted Microdissection. *Thromb Haemost* (2003) 90(4):749–56. doi: 10.1160/TH03-02-0095
67. Valle-Casuso JC, Angin M, Volant S, Passaes C, Monceaux V, Mikhailova A, et al. Cellular Metabolism Is a Major Determinant of HIV-1 Reservoir Seeding in CD4(+) T Cells and Offers an Opportunity to Tackle Infection. *Cell Metab* (2019) 29(3):611–26.e5. doi: 10.1016/j.cmet.2018.11.015
68. Clerc I, Moussa DA, Vahlas Z, Tardito S, Oburoglu L, Hope TJ, et al. Entry of Glucose- and Glutamine-Derived Carbons Into the Citric Acid Cycle Supports Early Steps of HIV-1 Infection in CD4 T Cells. *Nat Metab* (2019) 1(7):717–30. doi: 10.1038/s42255-019-0084-1
69. Hegedus A, Kavanagh Williamson M, Huthoff H. HIV-1 Pathogenicity and Virion Production are Dependent on the Metabolic Phenotype of Activated CD4+ T Cells. *Retrovirology* (2014) 11:98. doi: 10.1186/s12977-014-0098-4
70. Sen S, Kaminiski R, Deshmane S, Langford D, Khalili K, Amini S, et al. Role of Hexokinase-1 in the Survival of HIV-1-Infected Macrophages. *Cell Cycle* (2015) 14(7):980–9. doi: 10.1080/15384101.2015.1006971
71. Castellano P, Prevedel L, Valdebenito S, Eugenin EA. HIV Infection and Latency Induce a Unique Metabolic Signature in Human Macrophages. *Sci Rep* (2019) 9(1):3941. doi: 10.1038/s41598-019-39898-5
72. Palmer CS, Ostrowski M, Gouillou M, Tsai L, Yu D, Zhou J, et al. Increased Glucose Metabolic Activity is Associated With CD4+ T-Cell Activation and Depletion During Chronic HIV Infection. *AIDS* (2014) 28(3):297–309. doi: 10.1097/QAD.0000000000000128
73. Korencak M, Byrne M, Richter E, Schultz BT, Juszczak P, Ake JA, et al. Effect of HIV Infection and Antiretroviral Therapy on Immune Cellular Functions. *JCI Insight* (2019) 4(12):1–14. doi: 10.1172/jci.insight.126675

74. Arnoult D, Petit F, Lelievre JD, Estaquier J. Mitochondria in HIV-1-Induced Apoptosis. *Biochem Biophys Res Commun* (2003) 304(3):561–74. doi: 10.1016/S0006-291X(03)00629-6

Conflict of Interest: The authors declare that the research was conducted in the absence of any commercial or financial relationships that could be construed as a potential conflict of interest.

Publisher's Note: All claims expressed in this article are solely those of the authors and do not necessarily represent those of their affiliated organizations, or those of the publisher, the editors and the reviewers. Any product that may be evaluated in this article, or claim that may be made by its manufacturer, is not guaranteed or endorsed by the publisher.

frontiers | Frontiers in Immunology

ORIGINAL RESEARCH
published: 16 June 2022
doi: 10.3389/fimmu.2022.883420

Subsets of Tissue CD4 T Cells Display Different Susceptibilities to HIV Infection and Death: Analysis by CyTOF and Single Cell RNA-seq

*Xiaoyu Luo[1], Julie Frouard[1,2], Gang Zhang[1], Jason Neidleman[1,2], Guorui Xie[1,2], Emma Sheedy[1], Nadia R. Roan[1,2] and Warner C. Greene[1,3,4]**

[1] Gladstone Institute of Virology, San Francisco, CA, United States, [2] Department of Urology, University of California, San Francisco, San Francisco, CA, United States, [3] Department of Medicine, University of California, San Francisco, San Francisco, CA, United States, [4] Department of Microbiology & Immunology, University of California, San Francisco, San Francisco, CA, United States

CD4 T lymphocytes belong to diverse cellular subsets whose sensitivity or resistance to HIV-associated killing remains to be defined. Working with lymphoid cells from human tonsils, we characterized the HIV-associated depletion of various CD4 T cell subsets using mass cytometry and single-cell RNA-seq. CD4 T cell subsets preferentially killed by HIV are phenotypically distinct from those resistant to HIV-associated cell death, in a manner not fully accounted for by their susceptibility to productive infection. Preferentially-killed subsets express CXCR5 and CXCR4 while preferentially-infected subsets exhibit an activated and exhausted effector memory cell phenotype. Single-cell RNA-seq analysis reveals that the subsets of preferentially-killed cells express genes favoring abortive infection and pyroptosis. These studies emphasize a complex interplay between HIV and distinct tissue-based CD4 T cell subsets, and the important contribution of abortive infection and inflammatory programmed cell death to the overall depletion of CD4 T cells that accompanies untreated HIV infection.

Keywords: human immunodeficiency virus (HIV), cell death, apoptosis, pyroptosis, lymphoid tissues, mass cytometry, flow cytometry, single-cell RNA-seq

OPEN ACCESS

Edited by:
Vijayakumar Velu, Emory University, United States

Reviewed by:
Namal P. M. Liyanage, The Ohio State University, United States
Prabhu S. Arunachalam, Stanford University, United States

***Correspondence:**
Warner C. Greene
warner.greene@gladstone.ucsf.edu

Specialty section:
This article was submitted to Viral Immunology, a section of the journal Frontiers in Immunology

Received: *25 February 2022*
Accepted: *11 May 2022*
Published: *16 June 2022*

Citation:
Luo X, Frouard J, Zhang G, Neidleman J, Xie G, Sheedy E, Roan NR and Greene WC (2022) Subsets of Tissue CD4 T Cells Display Different Susceptibilities to HIV Infection and Death: Analysis by CyTOF and Single Cell RNA-seq. Front. Immunol. 13:883420. doi: 10.3389/fimmu.2022.883420

INTRODUCTION

Massive depletion of CD4 T cells by HIV is a hallmark of untreated HIV infection (1–6). The pernicious depletion of these cells leads to AIDS, characterized by frequent opportunistic infections, emergence of various cancers, and death (6). Despite decades of study, the underlying mechanism of CD4 T cell depletion during HIV infection remains incompletely understood.

Multiple mechanisms have been reported to contribute to HIV-associated CD4 T cell depletion (7). These include autophagy of productively infected CD4 T cells, viral protein induced apoptosis (e.g. Env, Tat, Nef), and activation-induced cell death (8–13). These mechanisms were mainly demonstrated in blood-derived CD4 T cells experimentally infected with HIV. However *in vivo*, HIV-associated cell death predominantly occurs in lymphoid tissues (14–16). Our group has identified abortive infection and pyroptotic programmed cell death as a major driver of the cell

death occurring in lymphoid tissue-derived but not blood-derived CD4 T cells (17, 18). Abortive infection and pyroptotic cell death affect non-permissive CD4 T cells, also called "bystander" T cells, which die from HIV intrusion even though they do not sustain a productive infection. Pyroptosis is a highly inflammatory form of programmed cell death characterized by gasdermin D-induced pore formation in the plasma membrane followed by cellular swelling and rupture (19–21). This pyroptotic death was observed during *ex vivo* HIV infection of human lymphoid aggregated cultures (HLAC) formed with either human tonsil or spleen tissue (22). The signaling pathway leading to activation of this death pathway entails HIV entry into non-permissive bystander CD4 T cells, followed by stalling of the infective process during reverse transcription. The ensuing accumulation of viral DNAs is detected by the IFI16 sensor, which triggers inflammasome formation and cell death by caspase 1-mediated pyroptosis. Abortive infection followed by pyroptotic cell death is the fate of the majority of HLAC CD4 T cells. By comparison, only a small portion (~ 5%) of the CD4 T cells in HLAC are able to support productive infection by HIV (18, 23–25), However, these productively infected cells provide the source of virus driving abortive infection of bystander cells, which depends on cell-to-cell viral transmission (24). Ultimately the productively infected cells die chiefly by caspase 3-mediated apoptosis (18).

While these prior studies have revealed distinct mechanisms underlying HIV-associated CD4 T cell death in lymphoid tissues, certain details of the process remain unclear. In particular, it is unknown whether specific CD4 T cell subsets are preferentially depleted over others, and if so, what determines the different fates of these cells. Although preferential killing of memory versus naïve CD4 T has been reported (26), these studies involved blood-derived cells. No studies to date have examined whether HIV kills different CD4 subsets within lymphoid tissues. Furthermore, T cells subsets are far more complex than just memory and naïve subsets (27). Indeed, CD4 T cells are highly heterogeneous (27, 28), and with recent developments in high-parameter cellular phenotyping including mass cytometry (CyTOF), a more complete view of the diversity of CD4 T cell subsets has emerged (29). CyTOF, which involves the use of antibodies coupled to lanthanide metals instead of the fluorophores used in flow cytometry (FACS), enables simultaneous quantitation of ~ 40 different protein parameters uncompromised by spectral overlap (30). Recently, CyTOF has been used to interrogate the cellular subsets of CD4 T cells preferentially susceptible to productive infection by HIV (31–34).

CyTOF-mediated high-parameter phenotyping also enables the implementation of the Predicted Precursor as determined by SLIDE (PP-SLIDE), a bioinformatics approach that predicts the original state of cells prior to the remodeling that HIV infection induces (34). This viral remodeling, which causes the up- or down-regulation of various cellular proteins, is a prominent feature of HIV infection (35, 36). Viral remodeling raises a problem when trying to subset HIV-susceptible cells, because it may alter expression levels of the antigen used to define a subset. However, one can overcome this problem by simultaneous analysis of many antigens, since the collective information attained in this manner is sufficient to capture the subset identity of the original cell targeted by the virus. In this manner, the analysis of CyTOF datasets using PP-SLIDE allows prediction of the original phenotypes of preferentially-infected T cell subsets, and such predictions have been validated in multiple systems including within HIV-infected tonsil cells (31–34). To date, however, CyTOF and PP-SLIDE have not been implemented to understand HIV-associated cell death in subsets of human CD4 T cells present in lymphoid tissue.

In the current study, we combined the HLAC model of HIV-associated cell death in lymphoid tissues with high-dimensional single-cell phenotyping by CyTOF paired with PP-SLIDE analysis, to better understand the mechanisms underlying HIV-associated T cell depletion occurring in the CD4 T cell subsets residing in lymphoid tissue. We find that most cell death does not occur among productively-infected cells but rather among multiple subsets of bystander CD4 T cells in the infected cultures. We further identify specific surface markers of the subsets preferentially lost as bystanders and interrogate these subsets using single-cell transcriptomics to assess their mechanism of cell death.

RESULTS

HIV Differentially Depletes CD4 T Cell Subsets in the HLAC System

To assess whether HIV differentially depletes different subsets of tissue CD4 T cells, we measured HIV-associated cell depletion in several discrete T cell subsets using flow cytometry first (**Table S1**). Fresh HLAC were prepared as previously described (22), either mock infected or infected with an X4-tropic HIV.GFP reporter virus, and cultured for 6 days before analysis (**Figure 1A**). As previously reported, we observed a marked loss of CD4 T cells (defined as CD3+CD8-) in the infected culture (frequency of 6.89%) as compared to the uninfected control (frequency of 32.1%) (**Figure 1B**). In contrast and as expected, CD8 T cell numbers (defined as CD3+CD8+) did not decrease in infected cultures. Normalization of the leftover live CD4 T cell counts in the infected culture to the CD8 T cell counts (details described in Materials and Methods) confirmed significant depletion of the CD4 T cells (**Figure 1C**). Interestingly, HIV-associated CD4 T cell depletion was more pronounced in the CD4 T memory (Tm) relative to in the CD4 T naïve (Tn) cells. Furthermore, within the memory compartment, T follicular helper (Tfh) cells were preferentially killed over either effector memory (Tem) or central memory (Tcm) cells (**Figures 1C**; **S1**). These FACS results suggest that while HIV infection is associated with T cell depletion by HIV in multiple CD4 T subsets, and that the levels of depletion differ within these subsets.

Implementation of CyTOF and PP-SLIDE for Deep Phenotyping of the HIV-Depleted HLAC Cells

To study HIV-associated depletion in greater depth, and to take advantage of the PP-SLIDE bioinformatics approach that corrects for virus-induced remodeling of cellular phenotypes, we designed a new 38-parameter CyTOF panel able to distinguish a wide range of

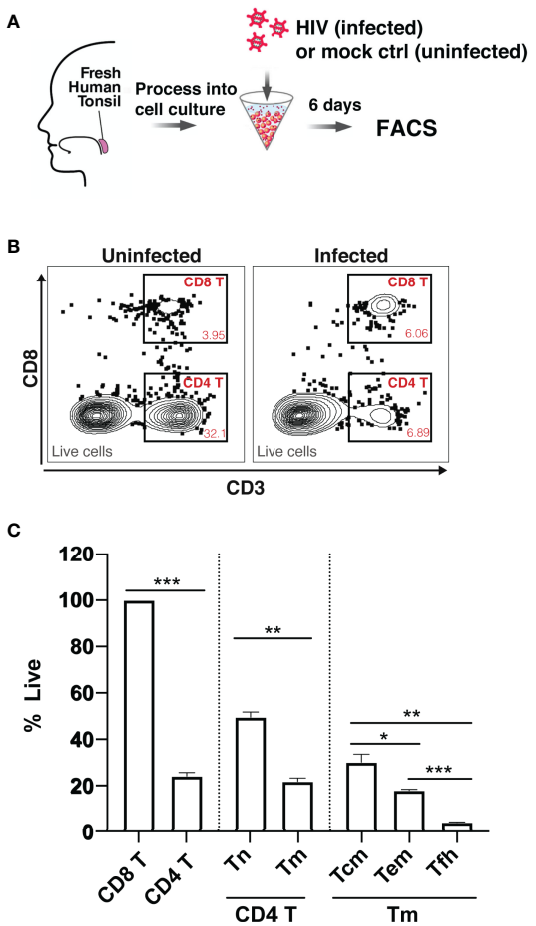

FIGURE 1 | Preferential death of CD4 T cells in tonsil HLAC specimens infected *ex vivo* with HIV. **(A)** Schematic of the HLAC collection and *ex vivo* infection. Fresh human tonsil cells were mock-treated or infected with HIV.GFP by spinoculation. Six days later samples were harvested for analysis by FACS. **(B)** Gating to identify CD8 T (CD8+CD3+), CD4 T (CD8-CD3+) in infected cultures (right) and uninfected control culture (left). Preceding parent gates are indicated at the lower left corner. Numbers correspond to percentages of cells in the indicated gate. Data for this one donor is representative of the 6 donors. **(C)** Quantification of CD4 T Naive (Tn), CD4 T memory (Tm), and CD4 T memory subsets including central memory (Tcm), effector memory (Tem), and T follicular helper (Tfh) cells, as identified by sequential gating (see **Figure S1**). For each subset, the percentage of live cells relative to uninfected control (% live) is shown. Data were normalized to CD8 T cell counts (details described in Materials and Methods). The data represent mean +SD of an experiment performed in triplicate. These data represent 6 donors studied in 3 independent experiments. *$p \le 0.05$; **$p \le 0.01$; ***$p \le 0.001$; *no label: not significant*, $p > 0.05$. Significance was measured by paired Student's T test.

T cell phenotypic subsets (**Table S2**). Even if some parameters are altered by infection, the high number of CyTOF parameters allows efficient backtracking to the original cell population *via* PP-SLIDE. As recently described (34), PP-SLIDE uses the 40 CyTOF parameters to match each cell in the infected culture to its "k-nearest neighbor" (kNN) cell in the uninfected control population (**Figure 2A**, and Materials and Methods). HIV infection is known to remodel productively-infected cells ("infected"), but non-productively-infected ("bystander") cells could also be remodeled by the inflammatory environment of infected cells. To examine killing, we infected HLAC cells with HIV-GFP for 6 days followed by CyTOF and PP-SLIDE analysis. Using CD4 T cell markers and HIV reporter (GFP) expression, we selected infected (GFP+) and bystander (GFP-) CD4 T cells in the infected HLAC population, as well as the CD4 T cells present in the uninfected control (**Figures 2B**; **S3**). We then visualized the phenotypes of CD4 T cells using t-distributed stochastic neighbor embedding (tSNE), a dimension reduction visualization method (37) (**Figure 2C**). Remodeling of both infected (pink dots) and bystander (purple dots) CD4 T cells from the infected culture was suggested by the fact that many of these cells did not map to regions of the tSNE plot occupied by CD4 T cells from the uninfected sample (gray dots) (**Figure 2C**, left panels). In contrast, after application of PP-SLIDE, their "nearest neighbors" ("kNN infected" and "kNN bystander") localized within the regions occupied by the uninfected CD4 T cells in the tSNE plot (**Figure 2C**, right panels, aqua, blue and gray dots). As the kNN infected and kNN bystander cells harbor the predicted features of the original infected and bystander CD4 T cells, prior to remodeling, for the remainder of the study we simply refer to these cells as "infected" and "bystander" cells.

Tissue Memory CD4 T Cells Are Preferentially Killed and Infected Compared to Naïve CD4 T Cells

Although our flow cytometry data suggested that HIV-associated killing occurred preferentially among memory CD4 T cells (Tm cells), this might have been an artifact due to the remodeling of the surviving bystander cells into naïve-like CD4 T cells (Tn cells). To address this possibility, we classified the HLAC cells into the main immune subsets (B, CD8 T, Tn, and Tm cells) by applying the FlowSOM clustering approach (38) to the PP-SLIDE corrected CyTOF data (**Figures 3A**; **S4**). We found that both Tm and Tn cells were killed by HIV but at different levels. Compared to the uninfected culture, the infected culture had lost 84% of its Tm cells and 68% of its Tn cells (**Figure 3A**, red and aqua). The higher loss of Tm over Tn cells was statistically significant (n=6 donors, **Figure 3B**), confirming preferential depletion of memory over naïve CD4 T cells.

Preferential killing of the Tm subset could result from higher permissivity to productive infection leading to higher viral-induced cytotoxicity. To test if Tm cells were also preferentially infected by HIV, we measured the level of productive infection (% productively infected) in Tm and Tn cells (**Figure 3C**). We found a higher proportion of productively-infected cells among Tm than Tn cells; in fact, the majority of the Tn cells (> 95%) were resistant to HIV infection. Our observation that Tn cells are depleted but poorly infected suggests that many Tn cells die as bystander cells.

Preferentially-Killed and Preferentially-Infected Tm Subsets Do Not Fully Overlap

As Tm cells were preferentially killed compared to Tn cells, we focused the rest of our analysis on Tm cells. We characterized killing within different Tm subsets and investigated whether the higher

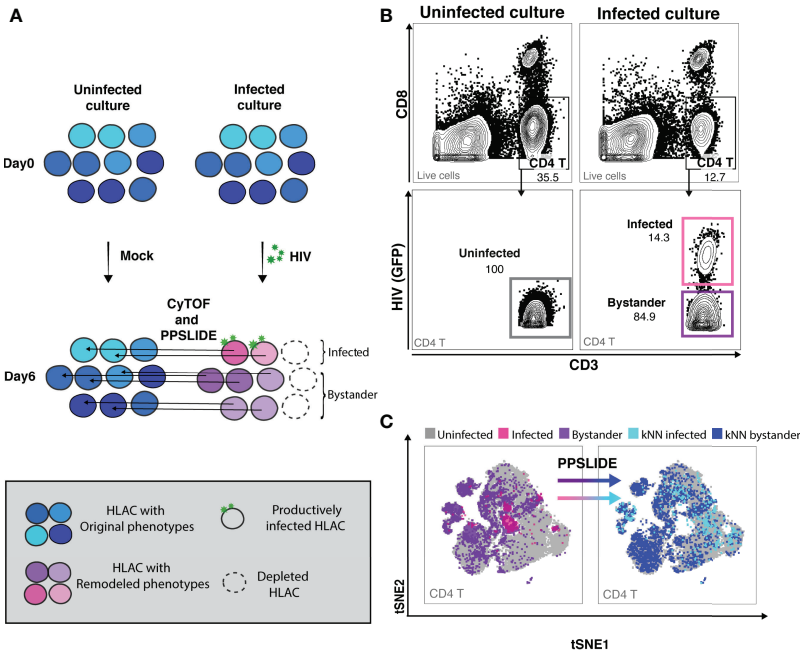

FIGURE 2 | CyTOF and PP-SLIDE analysis of HIV-associated killing in HLAC system. **(A)** Schematic of CyTOF and PP-SLIDE experimental strategy. HLAC cells were mock-treated or infected with HIV.GFP for 6 days and then processed for CyTOF analysis. Only cells that are productively infected express GFP. For every infected cell (in pink), we employed PP-SLIDE to trace it back to the most phenotypically similar cell in the uninfected culture using a k-nearest neighbor (kNN) approach. This kNN infected cell harbors the predicted phenotype of the infected cell prior to HIV-induced cell remodeling. Similarly, bystander cells in the HIV-exposed culture (purple) were also mapped to their predicted state prior to infection using PP-SLIDE. The key is shown in the grey inset. **(B)** Example of manual gating strategies to identify the following CD4 T subsets: uninfected (CD3+CD8-, uninfected culture, gray gate), infected (CD3+CD8-HIV+, infected culture, pink gate) and bystander (CD3+CD8-HIV-, infected culture, purple gate). Preceding parent gates are indicated at the lower left corner. Numbers correspond to percentages for each gate. **(C)** tSNE plots showing infected (pink dots) and bystander (purple dots) CD4 T cells overlayed onto uninfected CD4 T cells (gray dots). Both infected and bystander CD4 T cells were remodeled as suggested by their presence in regions of the tSNE not occupied by uninfected CD4 T cells. Using PP-SLIDE, infected and bystander CD4 T cells were converted to their predicted original states, kNN infected (aqua dots) and kNN bystander (blue dots) respectively. Preceding parent gates are indicated at the lower left corner.

HIV-associated killing of Tm subsets correlated with their permissivity to productive infection. First, the Tm cells were subjected to FlowSOM clustering (**Figure 4A**). Tm subsets that were preferentially killed (red) and -infected (aqua) were identified by their higher level of death or infection, respectively, as compared to those found in total Tm cells (details described in Materials and Methods, **Figure S5**). Interestingly, although there was overlap, cells preferentially killed resided in distinct areas of the tSNE relative to those preferentially infected, suggesting they represent different subsets (**Figure 4B**, dotted circles). Next, we looked into each of the preferentially-killed Tm subsets (clusters 1, 2, and 3), and quantitatively assessed their levels of HIV-associated depletion and infection (**Figures 4C–E**). Among these three preferentially-killed clusters, cluster 1 was preferentially depleted but was highly resistant to productive infection, suggesting that these cells likely died as bystander cells (**Figures 4D, E**). In contrast, clusters 2 and 3 were preferentially depleted and were highly permissive to productive infection, suggesting death in these two clusters might be attributed at least in part to apoptosis triggered by a productive infection. In addition to clusters 2 and 3, cluster 4 was also preferentially infected (**Figures 4E, F, H**). However, unlike cluster 2 and 3, cluster 4 was not preferentially killed (**Figure 4G**). Taken together, these findings suggest that Tm subsets are differentially depleted by HIV. Among the preferentially-killed Tm subsets, some are resistant to productive infection (cluster 1) while others are highly permissive to productive infection (cluster 2, 3). Moreover, high permissivity to infection is not always associated with high killing of Tm cells, as exemplified by cluster 4 (Table S3).

Phenotypic Features Associated With Preferentially-Killed Subsets

To further characterize the phenotypic features of preferentially-killed and preferentially-infected Tm subsets, we assessed expression levels of various antigens within our CyTOF panel (**Figure 5**). We found that all preferentially-killed subsets (clusters 1, 2, and 3) expressed high levels of the two chemokine receptors CXCR5 and CXCR4 (**Figure 5A**). While CXCR5 defines Tfh-like cells, CXCR4 is the co-receptor used by our reporter virus, suggesting that efficient entry of HIV into cells may underlie preferential HIV-associated cell death. In contrast, unique features of the preferentially-infected subsets (clusters 2, 3, and 4) included low expression levels of CCR7 and CD62L, markers of Tcm cells (**Figure 5B**). These results suggest that Tm cells with a Tem phenotype (CCR7-CD62L-) (33) are

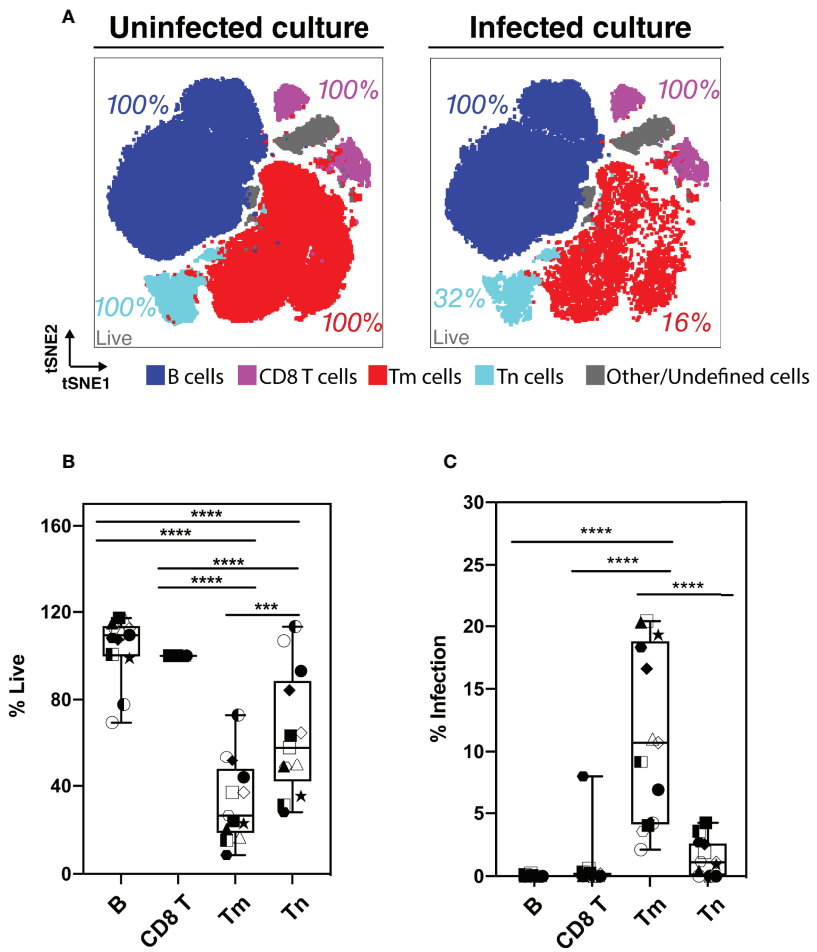

FIGURE 3 | Assessment of preferential killing and infection of main subsets of HLAC cells (B, CD8T, CD4 T memory, and CD4 T naïve cells). **(A)** tSNE plots of total HLAC cells from uninfected culture (left panel), and HIV infected culture (right panel). HLAC cells were classified and colored by main subsets including B (CD19+) (dark blue), CD8 T (CD3+CD8+) (purple), Tm (CD3+CD4+CD45RO+CD45RA-) (red), Tn (CD3+CD4+CD45RO-CD45RA+) (light blue), and Other/Undefined (CD19-CD3-, gray). These subsets were defined using FlowSOM and cell surface marker expression (**Figure S4**). Live cell percentage (% live) in each subset were calculated as described in the Materials and Methods, and are labeled beside each cell subset. Preceding parent gates are indicated at the lower left corner. **(B, C)** Proportions of live **(B)** and infected **(C)** cells among B, CD8 T, Tm, and Tn cells from 6 donors, calculated as described in Materials and Methods. Symbols represents technical repeats from 6 donors. Each donor is represented as a shape with technical repeats represented with different type of fill (details described in Materials and Methods). ****p ≤ 0.001; ****p ≤ 0.0001; no label: not significant, p > 0.05*. Significance was measured by one-way ANOVA with repeated measurements followed by *post-hoc* tests (n = total paired-wise comparisons). Paired effect between Tm and Tn is shown by estimation plots in **Figure S8**.

preferentially infected. The preferentially-infected clusters also expressed high levels of the exhaustion markers PD1 and CTLA4 (**Figure 5C**). As these antigens are also markers of activated cells (39, 40), we assessed the activation status of the preferentially-infected subsets. We observed that the early activation marker CD69 was high on all the preferentially-infected clusters, while CD25 and HLADR, which are upregulated at later stages of T cell activation, were preferentially expressed only in cluster 4 (**Figure 5D**).

Interestingly, cluster 4 was the only subset that was preferentially infected but spared from HIV-associated killing. This suggests that preferentially-infected cells resistant to HIV-induced killing exhibit the following features: 1) low expression of the CXCR4 co-receptor, 2) a Tem phenotype (CCR7-CD62L-), and 3) high expression of activation markers (PD1, CTLA4, CD69, CD25, and HLADR) (**Figures 5A–D**). In contrast, among the four analyzed Tm clusters, cluster 1 was the only one preferentially susceptible to HIV-associated killing but not productive HIV infection, suggesting its propensity to be killed by bystander mechanisms (**Figures 4D, E**). The phenotypes associated with cluster 1 were: 1) high CXCR4 expression, and 2) a Tcm phenotype (CCR7+CD62L+), 3) low expression of exhaustion markers (PD1-CTLA4-), and 4) low expression of activation markers (CD69-CD25-HLADR-) (**Figures 5A–D**).

Further mining of the phenotyping data revealed that various combinations of CD127, CD25, PD1, CD57, and CXCR5 could be

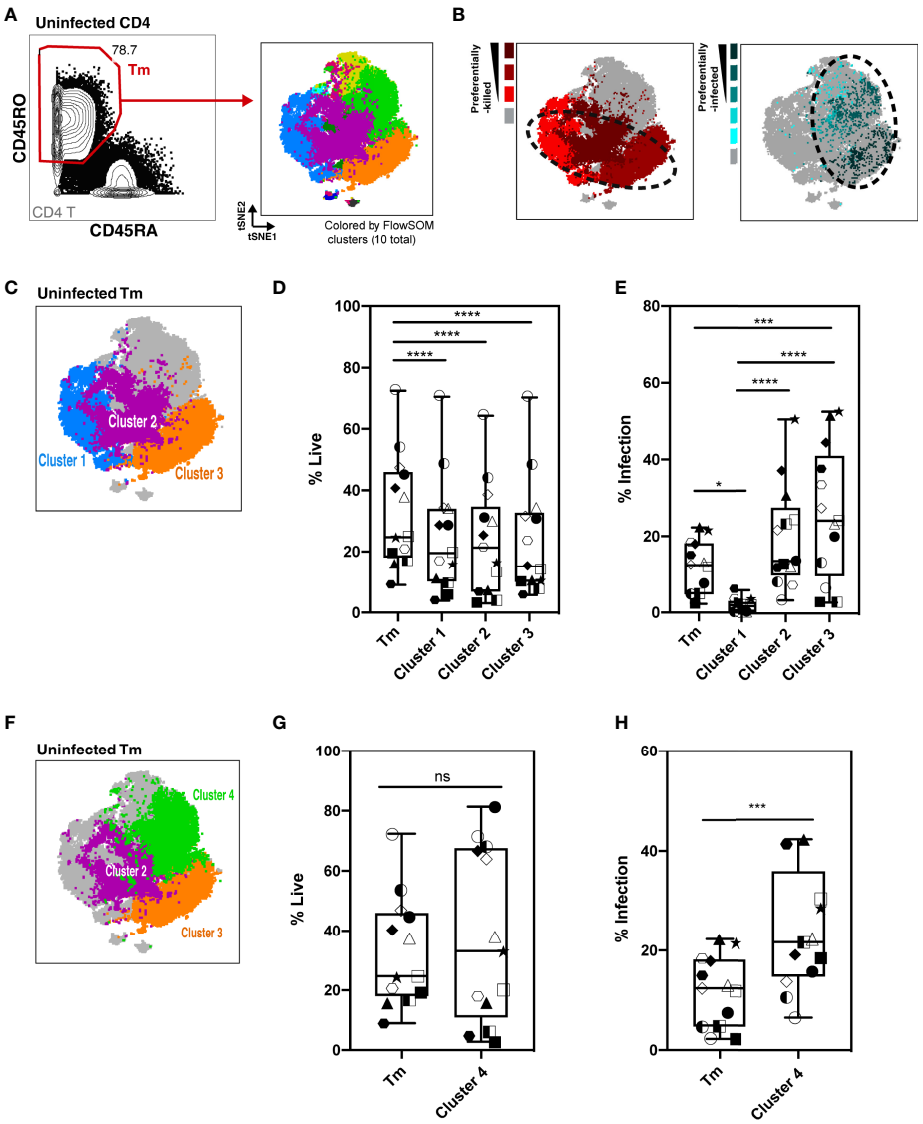

FIGURE 4 | Characterization of HIV-associated killing and infection in FlowSOM-defined Tm subsets. **(A)** Visualization of HLAC Tm cell clusters by FlowSOM, an algorithm based on a self-organizing map. *Left panel:* Example of Tm gating strategy (CD45RO+CD45RA-) (left). *Right panel:* Example of a tSNE plot colored by FlowSOM clusters (10 total). Preceding parent gates are indicated at the lower left corner. Numbers correspond to percentages for each gate. **(B)** *Left panel:* Preferentially-killed clusters colored in different shades of red (darker red represents a higher level of killing). *Right panel:* Preferentially-infected clusters colored in different shades of aqua (darker aqua represents a higher infection rate). Other clusters were colored in gray. Dotted circles on the tSNE plot shows that the preferentially-killed (left) and preferentially-infected (right) subsets do not completely overlap phenotypically. **(C)** Location of three preferentially-killed subsets shown on a tSNE plot: cluster 1 (blue), cluster 2 (purple), and cluster 3 (orange). Other clusters were colored as gray. **(D, E)** Proportion of live cells **(D)** and infection rate **(E)** of each of the 3 preferentially-killed subsets from 6 donors, plotted as box plots. Symbols represents technical repeats from 6 donors. Each donor is represented as a shape with technical repeats represented with different type of fill (details described in Materials and Methods). ****p ≤ 0.001; ****p ≤ 0.0001; no label: not significant, p > 0.05.* Significance was measured by one-way ANOVA with repeated measurements followed by *post-hoc* tests for multiple comparisons correction. (n = total paired-wise comparisons). **(F)** Location of the three preferentially-infected subsets of Tm cells on the tSNE plot: cluster 2 (purple), cluster 3 (orange) and cluster 4 (green). Other Tm clusters are colored as gray. Tm (**G, H)** Proportion of live cells **(G)** and infection rate **(H)** in Tm and in cluster 4 from 6 donors, plotted as box plots. Symbols represents technical repeats from 6 donors. Each donor is represented as a shape with technical repeats represented with different type of fill (details described in Materials and Methods). ****p ≤ 0.001; n.s., not significant, p > 0.05.* Significance was measured by paired Student's T test. Paired effect between Tm and each of the 4 clusters was shown by estimation plots in **Figure S9**.

used to uniquely define the four subsets (**Figure S7**; **Table S3**). In particular, we found cluster 1, the only cluster preferentially killed by bystander mechanisms, could be defined as CD127+CD25- Tm cells. Cluster 4, which was highly permissive but not preferentially killed, could be defined as CD25+PD1+CD57- Tm cells. Clusters 2 and 3 were characterized by CD57+PD1+ Tm cells and CXCR5+PD1+CD25-CD57-CD127- Tm cells, respectively, and both of these subsets were both preferentially

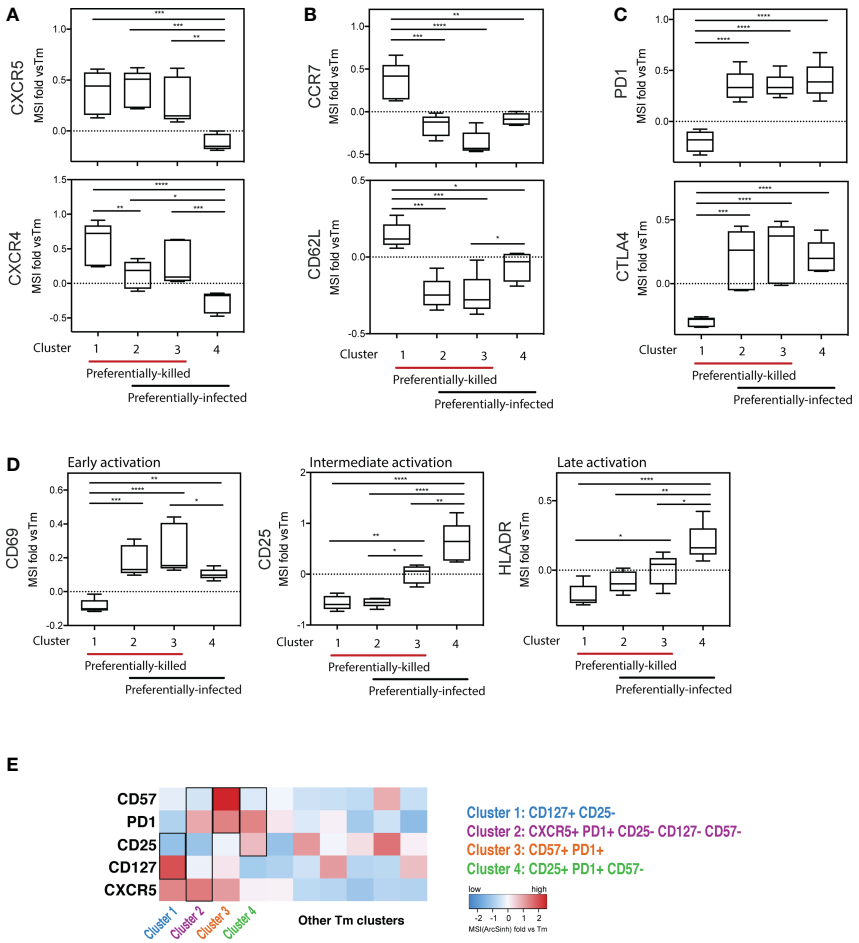

FIGURE 5 | Deep phenotyping of the preferentially-killed versus preferentially-infected CD4 Tm subsets. **(A–D)** Expression levels of selected cell markers in clusters 1-4 (identified in **Figure 4**) relative to the CD4 Tm population (MSI fold vs Tm). For each marker, the mean expression intensity (MSI) of the cluster is compared to the MSI of the Tm population, according to the following equation: ($MSI_{Cluster}$ / MSI_{Tm}) -1. If this value is > 0, the cluster cells expressed a higher level of the selected cell marker on average than did the total Tm cells. On the x-axes, clusters 1-4 were grouped into 2 categories including preferentially-killed (red line) and preferentially-infected (black line). The plots combine data from 6 donors. *$p \leq 0.05$; **$p \leq 0.01$; ***$p \leq 0.001$; ****$p \leq 0.0001$; no label: not significant, $p > 0.05$. Significance was measured by one-way ANOVA with repeated measurements followed by *post-hoc* tests for multiple comparisons correction. (n = total paired-wise comparisons). **(E)** Heatmap of the 5 cell markers that can be used to distinguish cells belonging to clusters 1-4 from other Tm cells. The marker combinations corresponding to the 4 clusters is listed on the right. All MSI values used in **Figure 5** were arcsinh transformed.

killed and infected. These identified markers enable characterization of preferentially killed/infected subsets without a need for 40 parameter clustering.

Expression of Viral Restriction Factors and Cell Death Pathways Distinguish Tm Cells That Die as Bystander Cells From Tm Cells That Survive Productive Infection

To refine our understanding of what distinguishes the different Tm cell subsets, we analyzed their transcriptional profiles. Taking advantage of our ability to identify preferentially killed/infected subsets using only a limited number of surface markers, we then implemented Antibody-Seq, which isolates cells with DNA oligo-barcoded antibodies directed as their surface antigens and subjects them to single-cell RNA-seq (41, 42). We focused this analysis on the two extreme categories: the preferentially-killed but not infected subset (cluster 1-like), which could be defined as CD127+CD25- Tm cells; and the preferentially-infected but not killed subset (cluster 4-like), which could be defined as CD25+PD1+CD57- Tm cells. Consistent with our CyTOF data (**Figure 5A**), the cluster 1-like cells expressed high levels of CXCR4 protein (**Figure 6A**). In contrast, the cluster 4-like cells expressed lower levels of CXCR4; this level is presumably sufficient to support productive infection but not viral-induced killing, as previously suggested (24). In addition, similar to our CyTOF result (**Figure 5D**, right), we found cluster 1-like cells expressed lower levels of HLADR, while cluster 4-like cells expressed high levels (**Figure 6B**, left). In addition, the mRNA levels of OX40, another activation marker, was expressed in a similar pattern of low expression in cluster 1-like cells and high expression in cluster 4-like cells (**Figure 6B**, right).

We next delved into transcriptomic features pertinent to HIV permissivity and cell death. Cluster 1-like cells preferentially expressed genes for the HIV restriction factors SERINC5, SAMHD1, APOBEC3G, MX2, TRIM32, ISG15 (43–48), which may explain their low permissivity to productive infection (**Figure 6C**). In contrast, cluster 4-like cells expressed lower level of these restriction factor genes, which may explain why these cells allow the virus to complete its life cycle.

Interestingly, cluster 1-like cells highly expressed the genes for caspase 1, caspase 4, and gasdermin D, which are involved in inflammatory pyroptosis. The gene for caspase 3, classically associated with apoptosis but more recently also shown to be linked to pyroptotic death (49, 50), was also upregulated in these cells (**Figure 6D**). The preferential expression of these cell death-associated genes in cluster 1-like cells over cluster 4-like cells suggests that these cells are primed for pyroptotic death (**Table S3**).

In summary, these transcriptomics data demonstrate that the killing of bystander Tm cells is associated with high expression of intracellular restriction factors and cell death factors. In contrast, cells expressing low levels of viral restriction factors and cell death factors were more highly permissive to HIV infection but relatively spared from virus-induced cell death.

DISCUSSION

HIV induces death of tissue CD4 T cells through two principal mechanisms:1) productive infection of activated cells followed by non-inflammatory apoptosis and 2) abortive infection of nonpermissive cells leading to inflammatory pyroptosis (18). However, little is known about the use of these death pathways within different subsets of tissue memory T cells. In this study, we have used a tissue-based HLAC system combined with extensive phenotyping by CyTOF and single-cell RNA-seq to examine which subsets of CD4 T cells die in the presence of HIV. We find that specific subsets of memory CD4 T cells are highly susceptible to productive viral infection and direct killing. In contrast, other subsets of memory CD4 T cells, along with naïve CD4 T cells, appear refractory to productive infection and die as bystander cells.

One of our most surprising findings is that susceptibility to productive infection and to death do not necessarily go hand in hand. For instance, we identified a Tm subset (cluster 4) that is highly infected but quite resistant to cell death following productive HIV infection. It is not clear why these cells survive so well, although it is intriguing that these cells express high levels of OX40. OX40 is a member of the TNF receptor superfamily and is implicated in protecting the long-term viability of memory T cells, particularly cells underdoing clonal expansion (51). Kuo and colleagues have described how OX40 signaling in HIV-infected cells leads to upregulation of BIRC5 (survivin) (52), a member of the inhibitor of apoptosis (IAP) family and may act by binding to and inhibiting caspase 3 and caspase 7 (53). Furthermore, in mucosal tissues, HIV appears to both preferentially infect cells expressing high BIRC5, and to further upregulate its expression, perhaps to promote survival and dissemination of the infected cells (33). However, BIRC5

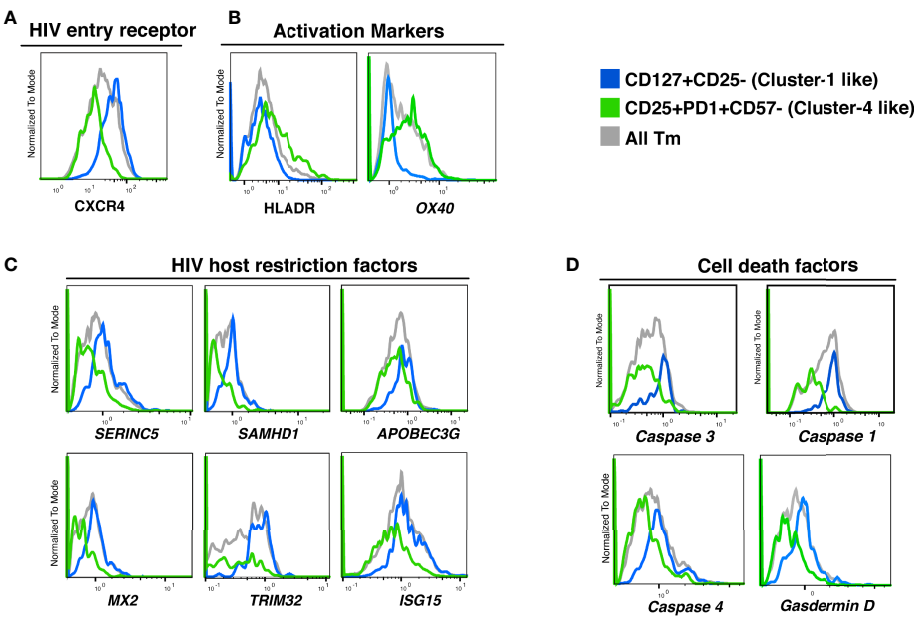

FIGURE 6 | Proteins and transcripts distinguishing CD4 Tm cells preferentially killed as bystander cells from CD4 Tm cells able to survive productive infection. **(A–D)** Histograms of the expression of **(A)** HIV entry receptors, **(B)** activation markers, **(C)** HIV host restriction factors, and **(D)** cell death related factors in CD127 +CD25- Tm (cluster 1-like, blue), CD25+PD1+CD57- Tm (cluster 4-like, green), and total Tm cells (grey). Names in italics indicate markers identified as transcripts. The data represented were collected from 2 donors in 2 independent experiments.

mRNA levels were not convincingly upregulated in cluster 4 Tm cells relative to Tm cells (data not shown). It will be of interest to study BIRC5 expression at the protein level in these cells and to test the effects of a BIRC5 inhibitor such as YM155 on their ability to survive HIV-induced abortive infection (54).

Reciprocally, being non-permissive to infection does not protect cells from dying, as previously shown (23). Our analysis shows that the main subset of memory CD4 T cells in this category (cluster 1) display a CD127+CD25- phenotype. The high susceptibility of CD127+CD25- Tm cells to HIV-associated depletion is consistent with *in vivo* observations that CD127+ cells are lost in HIV-infected individuals (55–57). Our studies suggest that this may be primarily due to bystander mechanisms, since cluster 1 cells were rarely infected productively. As CD127 encodes the alpha chain of the IL7 receptor, and is important for T cell homeostasis and survival, depletion of the CD127+ subset could further enhance T cell loss *in vivo* by reducing T cell restoration capacity.

Interestingly, we recently reported that CD127-expressing memory CD4 T cells are resistant to productive infection by HIV (58), consistent with our current study. However, those cells were not preferentially depleted by HIV, but instead became latently infected. One important difference between this prior study and the current one is the tropism of the virus employed: a CCR5-tropic virus was used in the prior study while a CXCR4-tropic virus was used in the current investigation. We chose to work with a CXCR4-tropic virus because this viral type is associated with extensive T cell depletion (59), and is an established system for assessing bystander killing in lymphoid tissue cells (18, 23). A second difference is how the virus is delivered to the target cell. The studies involving R5-tropic virus infection entailed primarily cell-free viral infection whereas the infection in our study is primarily driven by cell-to-cell transmission, which is critically important for effective bystander cell killing (24). Indeed, when cells producing R5-tropic HIV are mixed with CCR5 expressing cells purified from tonsils, pyroptotic bystander cell death is detectable (18).

We observe that preferentially killed cells express especially high levels of CXCR4. These results, coupled with our prior finding that increased levels of viral entry are required for bystander death (24), suggest that the quantity of X4-HIV entering into CD127-expressing CD4 Tm cells shapes the outcome. While the high expressors preferentially undergo bystander cell death, presumably because high CXCR4 levels facilitate transfer of virus from productively infected cells, the low CXCR4 expressors are potentially more prone to undergo productive infection.

Besides CXCR4, other cellular factors also seem to affect cell fate after HIV entry. For example, the CD127+CD25- Tm cells (similar to cluster 1 cells preferentially undergoing bystander cell death) exhibit an overall resting-like phenotype defined by low expression of activation markers. In addition, these cells are distinguished by increased expression of several HIV restriction factors, which further reinforces their nonpermissive state, encouraging abortive infection and caspase-1 dependent pyroptosis (18, 23). Furthermore, these cells appear primed for bystander cell death as evidenced by increased expression of the genes for caspase-1, caspase-4 and gasdermin D. Each of these proteins are important effectors in the pyroptotic pathway, and their synchronized upregulation may promote this rapid death mechanism.

The features we describe of Tm subsets preferentially prone to undergo productive infection vs. abortive cell death likely will not hold true in blood. Unstimulated blood CD4 T cells are highly resistant to abortive infection and pyroptosis unless first cultured with lymphoid tissue cells under conditions where cell-to-cell interactions occur (17). These findings underscore the importance of studying HIV pathogenesis in cells from lymphoid tissues rather than from PBMCs, because at least some biological responses are strikingly different.

Of note, the cluster 1 cells also expressed caspase-3 mRNA. Caspase 3 is generally regarded as an important inducer of apoptosis rather than pyroptosis. However, recent studies suggest cross-talk between the apoptotic and pyroptotic pathways of programmed cell death. For example, activation of caspase-3 by chemotherapeutic drugs can stimulate pyroptosis. In this case, caspase-3 cleaves gasdermin E, liberating an active N-terminal fragment that promotes membrane pore formation (49). In another example of caspase cross-talk, activated caspase 1 can activate caspase 3 and 7, inducing an apoptotic form of cell death as a safeguard to ensure the death of cells that initiate but do not complete pyroptotic pathway of programmed cell death (50).

In summary, our studies highlight how the response to HIV infection can sharply differ within different subsets of CD4 memory T cells. Some cell subsets readily undergo productive infection and survive, while others die after productive infection. Other subsets mainly die as bystanders as a consequence of abortive infection and pyroptotic cell death. Bystander death is favored when infection involves X4-tropic viruses, under such conditions is associated with higher levels of expression of CXCR4. Additionally, susceptible bystander cells appear primed for death by pyroptosis based on increased mRNA expression of the inflammatory caspases (caspase 1 and caspase 4) as well as the pyroptotic executioner, gasdermin D. The nature of the signals underlying this priming remains unclear but likely results from the unique environment provided by lymphoid tissues. Effective interdiction of such signaling could prevent both bystander cell death and the inflammation it engenders.

MATERIALS AND METHODS

Cells and Media Supplements

Human tonsils were obtained from the Cooperative Human Tissue Network (CHTN) during routine tonsillectomies, mainly for sleep disorders. These tissues were processed as previously described (18). Briefly, HLAC single-cell suspensions were created by dissection and then by pressing the Tonsil tissue through a 40-μm mesh. Live lymphocytes were then isolated from the single cell suspensions by Ficoll density gradient centrifugation. HLAC cells were cultured in tonsil culture media that consisted of RPMI 1640 supplemented with 15% fetal bovine serum (FBS) (Corning), 100 mg/mL gentamicin (Gibco), 200 mg/mL ampicillin (Sigma-Aldrich), 1 mM sodium pyruvate (Sigma-Aldrich), 1% non-

essential amino acids (Mediatech), 1% Glutamax (ThermoFisher), and 1% Fungizone (Invitrogen).

Antibodies and Reagents

Details about the antibodies used in flow cytometry staining are listed in supplemental table 1 and for CyTOF in supplemental table 2. All CyTOF antibodies were purchased from Fluidigm. HLADR Qdot(112Cd) was purchased pre-conjugated. All other CyTOF antibodies were purchased unconjugated and then conjugated with elemental isotopes in house using MAXPAR® X8 Ab Label Kits from Fluidigm.

Virus Preparation

The pNLENG1-IRES-GFP clone was derived from NL4-3 as previously described (59). The pro-viral expression vector DNA encoding the pNLENG1-IRES-GFP reporter virus was transfected into 293T cells using the Promega Fugene HD transfection reagent (catalog no. E2311) and cultured at 37°C. Media was replaced after 16 hours. Culture supernatants were collected 24 and 48 hours post-transfection. Virions were concentrated by ultracentrifugation at 20,000 rpm (32198 g) for 2 hours on a Beckman Coulter Optima XE-90. Gag-p24 levels of the HIV.GFP viral stocks were quantitated by enzyme-linked immunosorbent assay (ELISA) using the Lenti-X™ p24 Rapid Titer Kit from Clontech (catalog no. 632200).

HLAC Killing Assay by Spinoculation

One million HLAC cells were mixed with HIV-1.GFP (NLENG1-IRES-GFP) or mock control (culture media) in 100 µl total volume and cultured in V-bottom wells of a 96-well plate. To achieve different levels of T cell depletion, we applied 3 different HIV amounts (25, 50, and 100 ng p24 gag of HIV) and treated them as technical repeats in the current study. Cells were centrifuged at 25° C at 1200 x g for 2 hours and then cultured at 37°C as a pellet (23). Both infected and uninfected (mock) HLAC cells were collected and processed for FACS or CyTOF staining followed by calculation of % live and % infection as described in the following sections. A total of 6 donors were included in the current study and technical repeats from each donor with more than of 10% CD4 T cell depletion were analyzed.

FACS Analysis and Gating Strategy

Cells collected from HLAC cultures were processed for fluorescence-activated cell sorting (FACS) staining using a live-dead cell discriminator dye (Zombie Aqua) and stained with fluorescently labeled antibodies specific for the cell markers in supplemental table 1. Data were collected on a BD LSRFortessa™ X-20 Cell Analyzer flow cytometer and analyzed with FlowJo software from BD bioscience. At least 100,000 events per sample were collected, and at least 50,000 live cells were included in the subsequent data analysis. Gating strategies for each cell subset are shown in **Supplementary Figure S1** (Cells, Singlet, Live, CD8 T, CD4 T, Tn, Tm, Tem, Tcm, and Tfh).

CyTOF Staining and Data Processing

CyTOF staining was conducted as previously described (32). Briefly, cells collected from HLAC cultures were first stained for cell surface markers using antibodies conjugated with elemental isotopes listed in supplemental table 2. For live-dead staining, cells were treated with 139In-loaded-maleimide-DOTA (Macrocyclics) at 5 µg/ml on ice for 30 minutes, and cisplatin (Sigma-Aldrich) at 25 µM at room temperature for 60 seconds. Cells were then immediately fixed with 2% paraformaldehyde overnight at 4°C. Cells from multiple samples were barcoded using a Cell-ID™ 20-Plex Pd Barcoding Kit from Fluidigm, and combined before being permeabilized using the eBioscience™ Foxp3/Transcription Factor Staining Buffer Set. Cells were then stained for intracellular antigens including GFP, Gag, Foxp3, cleaved caspase-3, CTLA4, SAMHD1, and IFI16. CyTOF data were collected from a Fluidigm CyTOF2 Helios Mass Cytometer, normalized, and de-barcoded by CyTOF® Software from Fluidigm. Expression data for all parameters in each cell were next analyzed in the form of Flow Cytometry Standard (FCS) files in FlowJo™ software from BD bioscience. Data were pre-gated on Cells, Intact cells, Singlets, and Live cells before further analysis (**Figure S2**). A range of 10,000-130,000 cells (Live singlets post-CD8 normalization) per sample were included in the CyTOF analyses. tSNE and FlowSOM analysis were conducted in the Cytobank platform from Cytobank, Inc.

PP-SLIDE Analysis

PP-SLIDE was previously introduced and validated as an approach to trace HIV-remodeled cells back to their original pre-infected state (31–34). The detailed description and R script were made available in our previous publication [Neidleman et al. eLife 2020 (32)]. In the current study, we implemented PP-SLIDE to predict the pre-infection cell marker expression of all cells in the HIV-exposed HLAC culture. As an example of the single-cell analysis using PP-SLIDE, for Infe-cell #1, we calculated the Euclidian distances between Infe-cell #1 and each cell from the uninfected culture. The cell in the uninfected culture found to have the shortest Euclidian distance with Infe-cell #1 is identified as the predicted precursor of Infe-cell #1 ($kNN_{Infe\text{-}cell\ \#1}$). The cell marker expression of the kNN cells was used for phenotyping the infected and bystander cells in all our CyTOF data.

Measuring the Level of HIV-Productive Infection

To evaluate the level of productive infection in specific cell subsets, we first gated on the subset of interest in FlowJo and then measured the cell number in this subset in uninfected and infected samples. The level of HIV-productive infection in a selected subset, for example, subset S1, is calculated by the equation below:

% infection (S1): percent of productively infected cells in subset S1

% infection (S1) = number of S1 cells in infected sample/ number of S1 cells in uninfected sample x 100

Similarly, the level of productive HIV infection in the Tm population is calculated as: number of productively infected cells in the infected sample/number of Tm cells in the uninfected sample.

Tm subsets with a higher proportion of productively infected cells (% infection) than total Tm cells are referred to as "preferentially-infected subsets".

Measuring the Level of HIV-Associated Killing

To evaluate the level of HIV-associated killing in specific cell subsets, we first gated on the subset of interest in FlowJo and then measured the following cell numbers (for example, subset S1):

$cNum_{UnS1}$: Cell number of S1 subset from uninfected sample

$cNum_{InfeS1}$: Cell number of S1 subset from infected sample

$cNum_{UnCD8}$: Cell number of CD8 T cells from uninfected sample

$cNum_{InfeCD8}$: Cell number of CD8 T cells from infected sample

The level of HIV-associated killing is indicated by % killing and is calculated using the following equation:

% killing (S1): percent of HIV-associated killing of cells in subsets of interest S1 compared to uninfected sample and normalized with CD8 T cell number.

% killing (S1) = ($cNum_{InfeS1} \div cNum_{UnS1}$) X ($cNum_{UnCD8} \div cNum_{InfeCD8}$) X100

Tm subsets with a higher level of HIV-associated killing than that of total Tm cells are defined as "preferentially-killed subsets".

Single-cell RNA sequencing

T cells were isolated from HLAC using Immunomagnetic negative selection (StemCell Technologies), and dead cells were removed using a dead cells removal kit (Miltenyi Biotec). The cells were stained with a panel of TotalSeq-A human antibodies (BioLegend) according to manufacturer's protocol. Stained cells were then loaded onto a Chromium Next GEM chip G and both ADT (Antibody Derived Tag) and GEX (Gene Expression) libraries were generated using Chromium Next GEM Single Cell 3' Reagent Kits v3.1 (10X genomics) for next generation sequencing. A range of 11,000-13,000 events per sample were collected for the subsequent single-cell RNAseq analysis. The data was preprocessed in Cell Ranger for alignment against the human genome and further analyzed in SeqGeq ®.

DATA AVAILABILITY STATEMENT

The datasets presented in this study can be found in online repositories. The names of the repository/repositories and accession number(s) can be found below: https://datadryad.org/stash, https://datadryad.org/stash/share/rGPu0kf279Om-HMWZmFnL-elCzILgnb2KVfppH3McxU.

AUTHOR CONTRIBUTIONS

All authors listed have made a substantial, direct, and intellectual contribution to the work and approved it for publication.

FUNDING

This research was supported by the National Institutes of Health (R01 DA044605, P01 10018714, P01 AI124912, P30 DK063720, R01 AI127219, R01 AI147777, P01 AI131374, UM1 AI164559, S10 OD018040). We also gratefully acknowledge funding support from the James B. Pendleton Charitable Trust. This publication was made possible with help from the UCSF-Gladstone Center for AIDS Research (CFAR), an NIH-funded program (P30 AI027763). We also acknowledge the funding from the HOPE Collaboratory (UM1 AI164559).

ACKNOWLEDGMENTS

The authors acknowledge David N. Levy of NYU for the multiple-round NLENG1-IRES HIV reporter clones and Oliver T. Keppler for HIV-1*.GFP proviral DNA. We acknowledge technical support from the Gladstone Flow Cytometry Core, including assistance from Jane Srivastava and Nandhini Rahman. We thank Stanley Tamaki and Claudia Bispo for CyTOF assistance at the Parnassus Flow Core. We thank Francoise Chanut for editorial assistance and Robin Givens for administrative assistance.

SUPPLEMENTARY MATERIAL

The Supplementary Material for this article can be found online at: https://www.frontiersin.org/articles/10.3389/fimmu.2022.883420/full#supplementary-material

REFERENCES

1. Grossman Z, Meier-Schellersheim M, Sousa AE, Victorino RM, Paul WE. CD4+ T-Cell Depletion in HIV Infection: Are We Closer to Understanding the Cause? *Nat Med* (2002) 8:319–23. doi: 10.1038/nm0402-319
2. Haase AT. Population Biology of HIV-1 Infection: Viral and CD4+ T Cell Demographics and Dynamics in Lymphatic Tissues. *Annu Rev Immunol* (1999) 17:625–56. doi: 10.1146/annurev.immunol.17.1.625
3. Hazenberg MD, Hamann D, Schuitemaker H, Miedema F. T Cell Depletion in HIV-1 Infection: How CD4+ T Cells Go Out of Stock. *Nat Immunol* (2000) 1:285–9. doi: 10.1038/79724
4. McCune JM. The Dynamics of CD4+ T-Cell Depletion in HIV Disease. *Nature* (2001) 410:974–9. doi: 10.1038/35073648
5. Klatzmann D, Barre-Sinoussi F, Nugeyre MT, Danquet C, Vilmer E, Griscelli C, et al. Selective Tropism of Lymphadenopathy Associated Virus (LAV) for Helper-Inducer T Lymphocytes. *Science* (1984) 225:59–63. doi: 10.1126/science.6328660
6. Masur H, Ognibene FP, Yarchoan R, Shelhamer JH, Baird BF, Travis W, et al. CD4 Counts as Predictors of Opportunistic Pneumonias in Human Immunodeficiency Virus (HIV) Infection. *Ann Intern Med* (1989) 111:223–31. doi: 10.7326/0003-4819-111-3-223
7. Paim AC, Badley AD, Cummins NW. Mechanisms of Human Immunodeficiency Virus-Associated Lymphocyte Regulated Cell Death. *AIDS Res Hum Retroviruses* (2020) 36:101–15. doi: 10.1089/aid.2019.0213
8. Garg H, Blumenthal R. Role of HIV Gp41 Mediated Fusion/Hemifusion in Bystander Apoptosis. *Cell Mol Life Sci* (2008) 65:3134–44. doi: 10.1007/s00018-008-8147-6

9. Espert L, Biard-Piechaczyk M. Autophagy in HIV-Induced T Cell Death. *Curr Top Microbiol Immunol* (2009) 335:307–21. doi: 10.1007/978-3-642-00302-8_15
10. Leng Q, Borkow G, Weisman Z, Stein M, Kalinkovich A, Bentwich Z. Immune Activation Correlates Better Than HIV Plasma Viral Load With CD4 T-Cell Decline During HIV Infection. *J Acquir Immune Defic Syndr* (2001) 27:389–97. doi: 10.1097/00126334-200108010-00010
11. Li CJ, Friedman DJ, Wang C, Metelev V, Pardee AB. Induction of Apoptosis in Uninfected Lymphocytes by HIV-1 Tat Protein. *Science* (1995) 268:429–31. doi: 10.1126/science.7716549
12. Lenassi M, Cagney G, Liao M, Vaupotic T, Bartholomeeusen K, Cheng Y, et al. HIV Nef is Secreted in Exosomes and Triggers Apoptosis in Bystander CD4+ T Cells. *Traffic* (2010) 11:110–22. doi: 10.1111/j.1600-0854.2009.01006.x
13. Garg H, Mohl J, Joshi A. HIV-1 Induced Bystander Apoptosis. *Viruses* (2012) 4:3020–43. doi: 10.3390/v4113020
14. Finkel TH, Tudor-Williams G, Banda NK, Cotton MF, Curiel T, Monks C, et al. Apoptosis Occurs Predominantly in Bystander Cells and Not in Productively Infected Cells of HIV- and SIV-Infected Lymph Nodes. *Nat Med* (1995) 1:129–34. doi: 10.1038/nm0295-129
15. Brenchley JM, Schacker TW, Ruff LE, Price DA, Taylor JH, Beilman GJ, et al. CD4+ T Cell Depletion During All Stages of HIV Disease Occurs Predominantly in the Gastrointestinal Tract. *J Exp Med* (2004) 200:749–59. doi: 10.1084/jem.20040874
16. Pantaleo G, Graziosi C, Demarest JF, Butini L, Montroni M, Fox CH, et al. HIV Infection is Active and Progressive in Lymphoid Tissue During the Clinically Latent Stage of Disease. *Nature* (1993) 362:355–8. doi: 10.1038/362355a0
17. Munoz-Arias I, Doitsh G, Yang Z, Sowinski S, Ruelas D, Greene WC. Blood-Derived CD4 T Cells Naturally Resist Pyroptosis During Abortive HIV-1 Infection. *Cell Host Microbe* (2015) 18:463–70. doi: 10.1016/j.chom.2015.09.010
18. Doitsh G, Galloway NL, Geng X, Yang Z, Monroe KM, Zepeda O, et al. Cell Death by Pyroptosis Drives CD4 T-Cell Depletion in HIV-1 Infection. *Nature* (2014) 505:509–14. doi: 10.1038/nature12940
19. Bergsbaken T, Fink SL, Cookson BT. Pyroptosis: Host Cell Death and Inflammation. *Nat Rev Microbiol* (2009) 7:99–109. doi: 10.1038/nrmicro2070
20. Liu X, Zhang Z, Ruan J, Pan Y, Magupalli VG, Wu H, et al. Inflammasome-Activated Gasdermin D Causes Pyroptosis by Forming Membrane Pores. *Nature* (2016) 535:153–8. doi: 10.1038/nature18629
21. He WT, Wan H, Hu L, Chen P, Wang X, Huang Z, et al. Gasdermin D is an Executor of Pyroptosis and Required for Interleukin-1beta Secretion. *Cell Res* (2015) 25:1285–98. doi: 10.1038/cr.2015.139
22. Eckstein DA, Penn ML, Korin YD, Scripture-Adams DD, Zack JA, Kreisberg JF, et al. HIV-1 Actively Replicates in Naive CD4(+) T Cells Residing Within Human Lymphoid Tissues. *Immunity* (2001) 15:671–82. doi: 10.1016/S1074-7613(01)00217-5
23. Doitsh G, Cavrois M, Lassen KG, Zepeda O, Yang Z, Santiago ML, et al. Abortive HIV Infection Mediates CD4 T Cell Depletion and Inflammation in Human Lymphoid Tissue. *Cell* (2010) 143:789–801. doi: 10.1016/j.cell.2010.11.001
24. Galloway NL, Doitsh G, Monroe KM, Yang Z, Munoz-Arias I, Levy DN, et al. Cell-To-Cell Transmission of HIV-1 Is Required to Trigger Pyroptotic Death of Lymphoid-Tissue-Derived CD4 T Cells. *Cell Rep* (2015) 12:1555–63. doi: 10.1016/j.celrep.2015.08.011
25. Monroe KM, Yang Z, Johnson JR, Geng X, Doitsh G, Krogan NJ, et al. IFI16 DNA Sensor is Required for Death of Lymphoid CD4 T Cells Abortively Infected With HIV. *Science* (2014) 343:428–32. doi: 10.1126/science.1243640
26. Zhou Y, Shen L, Yang HC, Siliciano RF. Preferential Cytolysis of Peripheral Memory CD4+ T Cells by *In Vitro* X4-Tropic Human Immunodeficiency Virus Type 1 Infection Before the Completion of Reverse Transcription. *J Virol* (2008) 82:9154–63. doi: 10.1128/JVI.00773-08
27. Sallusto F, Lanzavecchia A. Heterogeneity of CD4+ Memory T Cells: Functional Modules for Tailored Immunity. *Eur J Immunol* (2009) 39:2076–82. doi: 10.1002/eji.200939722
28. Woodland DL, Dutton RW. Heterogeneity of CD4(+) and CD8(+) T Cells. *Curr Opin Immunol* (2003) 15:336–42. doi: 10.1016/S0952-7915(03)00037-2
29. Wang L, Abbasi F, Ornatsky O, Cole KD, Misakian M, Gaigalas AK, et al. Human CD4+ Lymphocytes for Antigen Quantification: Characterization Using Conventional Flow Cytometry and Mass Cytometry. *Cytometry A* (2012) 81:567–75. doi: 10.1002/cyto.a.22060
30. Bendall SC, Simonds EF, Qiu P, Amir el AD, Krutzik PO, Finck R, et al. Single-Cell Mass Cytometry of Differential Immune and Drug Responses Across a Human Hematopoietic Continuum. *Science* (2011) 332:687–96. doi: 10.1126/science.1198704
31. Xie G, Luo X, Ma T, Frouard J, Neidleman J, Hoh R, et al. Characterization of HIV-Induced Remodeling Reveals Differences in Infection Susceptibility of Memory CD4(+) T Cell Subsets *In Vivo*. *Cell Rep* (2021) 35:109038. doi: 10.1016/j.celrep.2021.109038
32. Neidleman J, Luo X, Frouard J, Xie G, Hsiao F, Ma T, et al. Phenotypic Analysis of the Unstimulated *In Vivo* HIV CD4 T Cell Reservoir. *Elife* (2020) 9:60933. doi: 10.7554/eLife.60933
33. Ma T, Luo X, George AF, Mukherjee G, Sen N, Spitzer TL, et al. HIV Efficiently Infects T Cells From the Endometrium and Remodels Them to Promote Systemic Viral Spread. *Elife* (2020) 9. doi: 10.7554/eLife.55487
34. Cavrois M, Banerjee T, Mukherjee G, Raman N, Hussien R, Rodriguez BA, et al. Mass Cytometric Analysis of HIV Entry, Replication, and Remodeling in Tissue CD4+ T Cells. *Cell Rep* (2017) 20:984–98. doi: 10.1016/j.celrep.2017.06.087
35. Matheson NJ, Sumner J, Wals K, Rapiteanu R, Weekes MP, Vigan R, et al. Cell Surface Proteomic Map of HIV Infection Reveals Antagonism of Amino Acid Metabolism by Vpu and Nef. *Cell Host Microbe* (2015) 18:409–23. doi: 10.1016/j.chom.2015.09.003
36. Haller C, Muller B, Fritz JV, Lamas-Murua M, Stolp B, Pujol FM, et al. HIV-1 Nef and Vpu are Functionally Redundant Broad-Spectrum Modulators of Cell Surface Receptors, Including Tetraspanins. *J Virol* (2014) 88:14241–57. doi: 10.1128/JVI.02333-14
37. van der Maaten L, Hinton G. Visualizing Data Using T-SNE. *J Mach Learn Res* (2008) 9:2579–605.
38. Van Gassen S, Callebaut B, Van Helden MJ, Lambrecht BN, Demeester P, Dhaene T, et al. FlowSOM: Using Self-Organizing Maps for Visualization and Interpretation of Cytometry Data. *Cytometry A* (2015) 87:636–45. doi: 10.1002/cyto.a.22625
39. Walunas TL, Lenschow DJ, Bakker CY, Linsley PS, Freeman GJ, Green JM, et al. CTLA-4 can Function as a Negative Regulator of T Cell Activation. *Immunity* (1994) 1:405–13. doi: 10.1016/1074-7613(94)90071-X
40. Agata Y, Kawasaki A, Nishimura H, Ishida Y, Tsubata T, Yagita H, et al. Expression of the PD-1 Antigen on the Surface of Stimulated Mouse T and B Lymphocytes. *Int Immunol* (1996) 8:765–72. doi: 10.1093/intimm/8.5.765
41. Stoeckius M, Hafemeister C, Stephenson W, Houck-Loomis B, Chattopadhyay PK, Swerdlow H, et al. Simultaneous Epitope and Transcriptome Measurement in Single Cells. *Nat Methods* (2017) 14:865–8. doi: 10.1038/nmeth.4380
42. Peterson VM, Zhang KX, Kumar N, Wong J, Li L, Wilson DC, et al. Multiplexed Quantification of Proteins and Transcripts in Single Cells. *Nat Biotechnol* (2017) 35:936–9. doi: 10.1038/nbt.3973
43. Sun L, Wang X, Zhou Y, Zhou RH, Ho WZ, Li JL. Exosomes Contribute to the Transmission of Anti-HIV Activity From TLR3-Activated Brain Microvascular Endothelial Cells to Macrophages. *Antiviral Res* (2016) 134:167–71. doi: 10.1016/j.antiviral.2016.07.013
44. Sheehy AM, Gaddis NC, Choi JD, Malim MH. Isolation of a Human Gene That Inhibits HIV-1 Infection and Is Suppressed by the Viral Vif Protein. *Nature* (2002) 418:646–50. doi: 10.1038/nature00939
45. Ozato K, Shin DM, Chang TH, Morse HC3rd. TRIM Family Proteins and Their Emerging Roles in Innate Immunity. *Nat Rev Immunol* (2008) 8:849–60. doi: 10.1038/nri2413
46. Neil SJ, Zang T, Bieniasz PD. Tetherin Inhibits Retrovirus Release and is Antagonized by HIV-1 Vpu. *Nature* (2008) 451:425–30. doi: 10.1038/nature06553
47. Kane M, Yadav SS, Bitzegeio J, Kutluay SB, Zang T, Wilson SJ, et al. MX2 is an Interferon-Induced Inhibitor of HIV-1 Infection. *Nature* (2013) 502:563–6. doi: 10.1038/nature12653
48. Hrecka K, Hao C, Gierszewska M, Swanson SK, Kesik-Brodacka M, Srivastava S, et al. Vpx Relieves Inhibition of HIV-1 Infection of Macrophages Mediated by the SAMHD1 Protein. *Nature* (2011) 474:658–61. doi: 10.1038/nature10195

49. Wang Y, Gao W, Shi X, Ding J, Liu W, He H, et al. Chemotherapy Drugs Induce Pyroptosis Through Caspase-3 Cleavage of a Gasdermin. *Nature* (2017) 547:99–103. doi: 10.1038/nature22393
50. de Vasconcelos NM, Van Opdenbosch N, Van Gorp H, Martin-Perez R, Zecchin A, Vandenabeele P, et al. An Apoptotic Caspase Network Safeguards Cell Death Induction in Pyroptotic Macrophages. *Cell Rep* (2020) 32:107959. doi: 10.1016/j.celrep.2020.107959
51. Song J, So T, Cheng M, Tang X, Croft M. Sustained Survivin Expression From OX40 Costimulatory Signals Drives T Cell Clonal Expansion. *Immunity* (2005) 22:621–31. doi: 10.1016/j.immuni.2005.03.012
52. Kuo HH, Ahmad R, Lee GQ, Gao C, Chen HR, Ouyang Z, et al. Anti-Apoptotic Protein BIRC5 Maintains Survival of HIV-1-Infected CD4(+) T Cells. *Immunity* (2018) 48:1183–1194 e5. doi: 10.1016/j.immuni.2018.04.004
53. Tamm I, Wang Y, Sausville E, Scudiero DA, Vigna N, Oltersdorf T, et al. IAP-Family Protein Survivin Inhibits Caspase Activity and Apoptosis Induced by Fas (CD95), Bax, Caspases, and Anticancer Drugs. *Cancer Res* (1998) 58:5315–20.
54. Clemens MR, Gladkov OA, Gartner E, Vladimirov V, Crown J, Steinberg J, et al. Multicenter, Open-Label, Randomized Study of YM155 Plus Docetaxel as First-Line Treatment in Patients With HER2-Negative Metastatic Breast Cancer. *Breast Cancer Res Treat* (2015) 149:171–9. doi: 10.1007/s10549-014-3238-6
55. Mojumdar K, Vajpayee M, Chauhan NK, Singh A, Singh R, Kurapati S. Loss of CD127 & Increased Immunosenescence of T Cell Subsets in HIV Infected Individuals. *Indian J Med Res* (2011) 134:972–81. doi: 10.4103/0971-5916.92645
56. Kiazyk SA, Fowke KR. Loss of CD127 Expression Links Immune Activation and CD4(+) T Cell Loss in HIV Infection. *Trends Microbiol* (2008) 16:567–73. doi: 10.1016/j.tim.2008.08.011
57. Dunham RM, Cervasi B, Brenchley JM, Albrecht H, Weintrob A, Sumpter B, et al. CD127 and CD25 Expression Defines CD4+ T Cell Subsets That are Differentially Depleted During HIV Infection. *J Immunol* (2008) 180:5582–92. doi: 10.4049/jimmunol.180.8.5582
58. Hsiao F, Frouard J, Gramatica A, Xie G, Telwatte S, Lee GQ, et al. Tissue Memory CD4+ T Cells Expressing IL-7 Receptor-Alpha (CD127) Preferentially Support Latent HIV-1 Infection. *PloS Pathog* (2020) 16: e1008450. doi: 10.1371/journal.ppat.1008450
59. Trinite B, Chan CN, Lee CS, Mahajan S, Luo Y, Muesing MA, et al. Suppression of Foxo1 Activity and Down-Modulation of CD62L (L-Selectin) in HIV-1 Infected Resting CD4 T Cells. *PloS One* (2014) 9: e110719. doi: 10.1371/journal.pone.0110719

Conflict of Interest: The authors declare that the research was conducted in the absence of any commercial or financial relationships that could be construed as a potential conflict of interest.

frontiers | Frontiers in Immunology

TYPE Systematic Review
PUBLISHED 26 August 2022
DOI 10.3389/fimmu.2022.915805

OPEN ACCESS

EDITED BY
Constantinos Petrovas,
Centre Hospitalier Universitaire Vaudois (CHUV), Switzerland

REVIEWED BY
Yvonne Mueller,
Erasmus Medical Center, Netherlands
Cecilia Graziosi,
Centre Hospitalier Universitaire Vaudois (CHUV), Switzerland

*CORRESPONDENCE
Karin J. Metzner
Karin.Metzner@usz.ch

†These authors have contributed equally to this work

SPECIALTY SECTION
This article was submitted to Viral Immunology, a section of the journal Frontiers in Immunology

RECEIVED 08 April 2022
ACCEPTED 13 July 2022
PUBLISHED 26 August 2022

CITATION
Inderbitzin A, Loosli T, Opitz L, Rusert P and Metzner KJ (2022) Transcriptome profiles of latently- and reactivated HIV-1 infected primary CD4$^+$ T cells: A pooled data-analysis. *Front. Immunol.* 13:915805. doi: 10.3389/fimmu.2022.915805

Transcriptome profiles of latently- and reactivated HIV-1 infected primary CD4$^+$ T cells: A pooled data-analysis

Anne Inderbitzin[1,2,3†], Tom Loosli[1,2,3†], Lennart Opitz[4], Peter Rusert[2] and Karin J. Metzner[1,2*]

[1]Department of Infectious Diseases and Hospital Epidemiology, University Hospital Zurich, Zurich, Switzerland, [2]Institute of Medical Virology, University of Zurich, Zurich, Switzerland, [3]Life Science Zurich Graduate School, University of Zurich, Zurich, Switzerland, [4]Functional Genomics Center Zurich, Eidgenössische Technische Hochschule (ETH) Zürich/University of Zurich, Zurich, Switzerland

The main obstacle to cure HIV-1 is the latent reservoir. Antiretroviral therapy effectively controls viral replication, however, it does not eradicate the latent reservoir. Latent CD4$^+$ T cells are extremely rare in HIV-1 infected patients, making primary CD4$^+$ T cell models of HIV-1 latency key to understanding latency and thus finding a cure. In recent years several primary CD4$^+$ T cell models of HIV-1 latency were developed to study the underlying mechanism of establishing, maintaining and reversing HIV-1 latency. In the search of biomarkers, primary CD4$^+$ T cell models of HIV-1 latency were used for bulk and single-cell transcriptomics. A wealth of information was generated from transcriptome analyses of different primary CD4$^+$ T cell models of HIV-1 latency using latently- and reactivated HIV-1 infected primary CD4$^+$ T cells. Here, we performed a pooled data-analysis comparing the transcriptome profiles of latently- and reactivated HIV-1 infected cells of 5 *in vitro* primary CD4$^+$ T cell models of HIV-1 latency and 2 *ex vivo* studies of reactivated HIV-1 infected primary CD4$^+$ T cells from HIV-1 infected individuals. Identifying genes that are differentially expressed between latently- and reactivated HIV-1 infected primary CD4$^+$ T cells could be a more successful strategy to better understand and characterize HIV-1 latency and reactivation. We observed that natural ligands and coreceptors were predominantly downregulated in latently HIV-1 infected primary CD4$^+$ T cells, whereas genes associated with apoptosis, cell cycle and HLA class II were upregulated in reactivated HIV-1 infected primary CD4$^+$ T cells. In addition, we observed 5 differentially expressed genes that co-occurred in latently- and reactivated HIV-1 infected primary CD4$^+$ T cells, one of which, MSRB2, was found to be differentially expressed between latently- and reactivated HIV-1 infected cells. Investigation of primary CD4$^+$ T cell models of HIV-1 latency that mimic the *in vivo* state remains essential for the study of HIV-1 latency and thus providing the opportunity to compare the

transcriptome profile of latently- and reactivated HIV-1 infected cells to gain insights into differentially expressed genes, which might contribute to HIV-1 latency.

KEYWORDS

latently HIV-1 infected primary CD4+ T cells, reactivated HIV-1 infected primary CD4+ T cells, HIV-1 latency reversal agents, transcriptome profile, primary CD4+ T cell models of HIV-1 latency, pooled data-analysis, pooled data-analysis differentially expressed genes (pdaDEGs)

Introduction

The human immunodeficiency virus type 1 (HIV-1) remains a global health problem, while ART efficiently blocks viral replication it does not cure HIV-1 infection owing to persistent proviruses (1). These proviruses are quiescent and mainly found in resting memory $CD4^+$ T cells, known as the latent reservoir (2, 3). The latent reservoir is defined as replication-competent but transcriptionally silent viruses. The latent reservoir is established within the first weeks of infection (4, 5) but the exact mechanisms of its establishment is still being investigated. Potential mechanisms leading HIV-1 into latency include transcriptional interference, chromatin remodelling, epigenetic silencing, and transcription factor sequestration (6). Nevertheless, to date the driving forces for HIV-1 latency are not fully understood. It is still unknown which factors distinguish between latently- and reactivated HIV-1 infected $CD4^+$ T cells on a molecular level. Numerous studies searched for cellular markers identifying latently HIV-1 infected cells and several cellular markers were described, however, these cellular markers could only rarely be confirmed and are controversially discussed (7).

Therefore, primary $CD4^+$ T cell models of HIV-1 latency that mimic the *in vivo* state remain a necessity for the study of HIV-1 latency. A wealth of information has been generated from the transcriptome profiles of primary $CD4^+$ T cell models of HIV-1 latency. To obtain a comprehensive understanding of drivers that might maintain HIV-1 in latency, we performed a pooled data-analysis comparing the transcriptome profiles of latently- and reactivated HIV-1 infected cells from 5 *in vitro* primary $CD4^+$ T cell models of HIV-1 latency and 2 *ex vivo* studies of reactivated HIV-1 infected primary $CD4^+$ T cells from HIV-1 infected individuals (detailed description of the models/studies in Supplementary Figure 1 and Supplementary Material). By conducting a pooled data-analysis, high-throughput data from multiple independent primary $CD4^+$ T cell models of HIV-1 latency are included, resulting in 1. larger sample size, 2. overcoming donor variability bias and 3. allowing for a comprehensive assessment of transcriptome profiles, thus providing more insights into HIV-1 pathogenesis and latency. In our pooled data-analysis, we identified 247 differentially expressed genes (DEGs) that were present in at least 3 of 4-5 datasets of latently- and reactivated HIV-1-infected primary $CD4^+$ T cells, respectively. These DEGs were called pooled data-analysis differentially expressed genes (pdaDEGs). This may be a successful strategy to better understand and characterize HIV-1 latency and reactivation. This could provide insights into the mechanisms leading to HIV-1 latency and reactivation.

Results

Quantitative assessment of gene expression from data sets of *in vitro* primary $CD4^+$ T cell models of HIV-1 latency and *ex vivo* studies of reactivated HIV-1 infected primary $CD4^+$ T cells from HIV-1 infected individuals

To gain a comprehensive understanding of differentially expressed genes (DEGs) between latently- and reactivated HIV-1 infected cells, we analysed DEGs in 5 *in vitro* primary $CD4^+$ T cell models of HIV-1 latency and 2 *ex vivo* studies of reactivated HIV-1 infected primary $CD4^+$ T cells from HIV-1 infected individuals, in particular latently- (8–11) and reactivated (10–13) HIV-1 infected cells. Applying our search parameters resulted in 47 full text publications. We excluded studies using ChIP assays, non-primary $CD4^+$ T cells data, cell line studies, and studies which did not contain transcriptome data and resulted in 4 *in vitro* primary $CD4^+$ T cell models of HIV-1 latency (8–11) (Figure 1). By including 2 *ex vivo* studies of reactivated HIV-1 infected primary $CD4^+$ T cells from suppressed HIV-1 infected individuals and our own model (14), a total of 50 unique transcriptome samples (26 HIV-1 infected cells and 24 uninfected cells) were included in our pooled data-analysis. We obtained 1'297-21'886 HGNC annotated genes per dataset (Table 1). We determined the

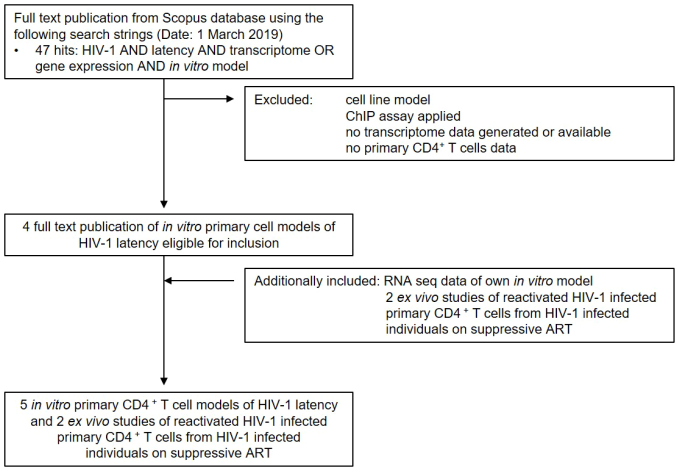

FIGURE 1
Summary of study search and selection procedure from the Scopus database.

mean standardised expression of all genes in all primary $CD4^+$ T cell models of HIV-1 latency by averaging the fold changes standardized by the study-specific standard error. To account for the differences in the datasets, we refrained from identifying the DEGs by |fold change| >2 and false discovery rate (FDR) <0.05, but employed a custom filtering score method based on: 1. FDR <0.1 increasing the score by 1, 2. absolute fold change greater than the study-specific 50% absolute fold change quantile,

TABLE 1 Cross-reference of 5 *in vitro* primary $CD4^+$ T cell models of HIV-1 latency and 2 *ex vivo* studies of reactivated HIV-1 infected primary $CD4^+$ T cells from HIV-1 infected individuals, of latently- and reactivated HIV-1 infected cells.

Study	Dataset	Gene IDs of dataset*	Gene IDs after filtering**	HGNC annotated genes	pdaDEGs***	Up and downregulated pdaDEGs***
Iglesias-Ussel et al. (9)	latent	1297	1297	1297	104 of 130	up: 45 down: 59
White et al. (11)	latent	50312	15781	13907	121 of 130	up: 52 down: 69
	reactivated	50312	16452	14720	112 of 117	up: 71 down: 41
Mohammadi et al. (10)	latent	50249	21972	21886	129 of 130	up: 62 down: 67
	reactivated	50249	21051	20972	114 of 117	up: 70 down: 44
Bradley et al. (8)	latent	21386	17029	16141	128 of 130	up: 51 down: 77
Inderbitzin et al. (14)	reactivated	21505	14664	13946	109 of 117	up: 65 down: 44
Cohn et al. (12)	reactivated	28079	11903	11869	116 of 117	up: 82 down: 34
Kulpa et al. (13)	reactivated	35797	19245	19206	98 of 117	up: 70 down: 28

* Includes: Ensembl Gene IDs, Hugo Gene Nomenclature Committee (HGNC) symbols, transcript names.
** Removal of non-informative reads and low read count. Includes: Ensembl Gene IDs, Hugo Gene Nomenclature Committee (HGNC) symbols, transcript names.
*** Defined as passing the filter score; 130 and 117 pdaDEGs obtained from datasets of latently- and reactivated HIV-1 infected primary $CD4^+$ T cells, respectively.
Depicted Gene IDs of dataset, prior and after filtering by score, and up and downregulated pooled data-analysis differentially expressed genes (pdaDEGs).

increasing the score by 1, and 3. up- or downregulation, resulting in either a positive or negative score, respectively. A gene can get a score of maximally 2 per dataset, i.e., maximum score of 8 for latently and 10 for reactivated HIV-1 infected cells (Table 1). For each gene the scores are summed up across datasets and normalized to 1. Pooled data-analysis DEGs (pdaDEGs) were then identified by applying a filtering score ≥0.5. This resulted in 130 pdaDEGs for latently- and 117 pdaDEGs for reactivated HIV-1 infected primary $CD4^+$ T cells (Table 1). The 130 pdaDEGs obtained from the latently HIV-1 infected cells were present in at least 3 out of the 4 primary $CD4^+$ T cell models of HIV-1 latency. Whereas in the reactivated HIV-1 infected cells 117 pdaDEGs were present in at least 3 out of 5 datasets. In general, pdaDEGs were more frequently downregulated in latently HIV-1 infected primary $CD4^+$ T cells and more frequently upregulated in reactivated HIV-1 infected primary $CD4^+$ T cells (Table 1).

pdaDEGs identified in latently HIV-1 infected cells from 4 *in vitro* primary $CD4^+$ T cell models of HIV-1 latency

A comprehensive understanding of how latently HIV-1 infected primary $CD4^+$ T cells are altered to allow HIV-1 persistence would be an important step towards developing cures for HIV-1-infected individuals. Therefore, it is important to determine whether the observed transcriptional heterogeneity in latently HIV-1 infected primary $CD4^+$ T cells, which suggests that latent HIV-1 infection can persist in very different host cell environments, indeed masks common core motifs that would be responsible for controlling HIV-1 latency (12, 15, 16). To address this goal, we analysed and compared the 130 identified pdaDEGs in latently HIV-1 infected cells of 4 *in vitro* primary $CD4^+$ T cell models of HIV-1 latency (8–11) (Table 1 and Supplementary Figure 1A). Of those 130 pdaDEGs, 75 were down- and 55 upregulated. 48 pdaDEGs showed associations with HIV-1 based on the Database for Annotation, Visualization and Integrated Discovery (DAVID), of which 29/48 were downregulated (Figure 2). 9 pdaDEGs with known HIV-1 associations were observed across all 4 *in vitro* primary $CD4^+$ T cell models of HIV-1 latency. Out of which, 5 were downregulated (CCL4, CCL5, CXCR6, LYZ and RRBP1) and 4 upregulated (PLAU, LMNA, LY96 and CD69) (Supplementary Table 1). Downregulated pdaDEGs were predominantly natural ligands or coreceptor: CCL4 (chemokine (C-C motif) ligands 4), CCL5 (RANTES, regulated on activation, normal T cell expressed and secreted), and CXCR6 (C-X-C chemokine receptor type 6). CCL4 is known to activate and enhance the cytotoxicity in natural killer cells (17). CCL5 has been shown to interfere with the spread of HIV-1 by 1. binding to the CCR5 receptor and thereby blocking the binding of the HIV-1 envelope or 2. inducing the internalisation of the bound receptor and thereby reducing the surface amounts of CCR5 (18–21). CXCR6 was found to be downregulated across primary cell models of HIV-1 latency; it is known as a minor coreceptor of HIV-1 and might play a role in disease progression through its role as mediator of inflammation (22). The main HIV-1 co-receptor CCR5 was also found to be downregulated in 3/4 *in vitro* primary cell models of HIV-1 latency, which is in line with the study from Shan et al., showing that CCR5 is downregulated in resting $CD4^+$ T cells (23). In summary, we found that natural ligands and coreceptors were predominantly downregulated in all investigated models for latently HIV-1 infected primary $CD4^+$ T cells.

pdaDEGs identified in reactivated HIV-1 infected cells from 3 *in vitro* primary $CD4^+$ T cell models of HIV-1 latency and 2 *ex vivo* studies of reactivated HIV-1 infected primary $CD4^+$ T cells from HIV-1 infected individuals

In *in vivo* and *in vitro* settings, a large number of latently HIV-1 infected primary $CD4^+$ T cells remain unresponsive to strong latency reversal agents (24–35). To investigate transcriptional heterogeneity in HIV-1 latency reversal and to find common core motifs responsible for controlling HIV-1 latency reactivation, we analysed and compared pdaDEGs in reactivated HIV-1 infected cells of 3 *in vitro* (10, 11, 14) primary $CD4^+$ T cell models of HIV-1 latency and 2 *ex vivo* studies of reactivated HIV-1 infected primary $CD4^+$ T cells from HIV-1 infected individuals (Supplementary Figure 1) (12, 13).

In the reactivated HIV-1 infected primary $CD4^+$ T cells, 117 pdaDEGs were identified, of which 35 pdaDEGs were down-, and 82 upregulated. 24 pdaDEGs have known HIV-1 associations based on DAVID, of which 16/24 were upregulated (Figure 3). 6 of those upregulated pdaDEGs with known HIV-1 associations were observed in all 5 datasets, namely ACTA2, LAMP3, HLA-DOA, CXCL10, SLC7A11 and SPTBN5 (Supplementary Table 2).

The upregulated pdaDEGs were predominantly genes associated with 1. the p53 pathway, such as ACTA2 (actin alpha 2) which is known to be induced by p53 (11), 2. the PI3K/Akt pathway, such as LAMP3 (lysosome-associated membrane glycoprotein 3) which is involved in cell cycle and apoptosis (36) or 3. the human leukocyte antigen (HLA) class II such as HLA-DOA and HLA-DQB1, which was found in 4/5 *in vitro* and *ex vivo* HIV-1 studies, the latter is associated with increased risk of susceptibility to HIV-1 infection and for a rapid HIV-1 disease progression (37). CXCL10 (C-X-C motif chemokine ligand 10) is a pro-inflammatory cytokine involved in processes such as differentiation, regulation of cell growth, activation of peripheral immune cells and apoptosis (38). In addition, CXCL10 was suggested as a biomarker in the clinic for

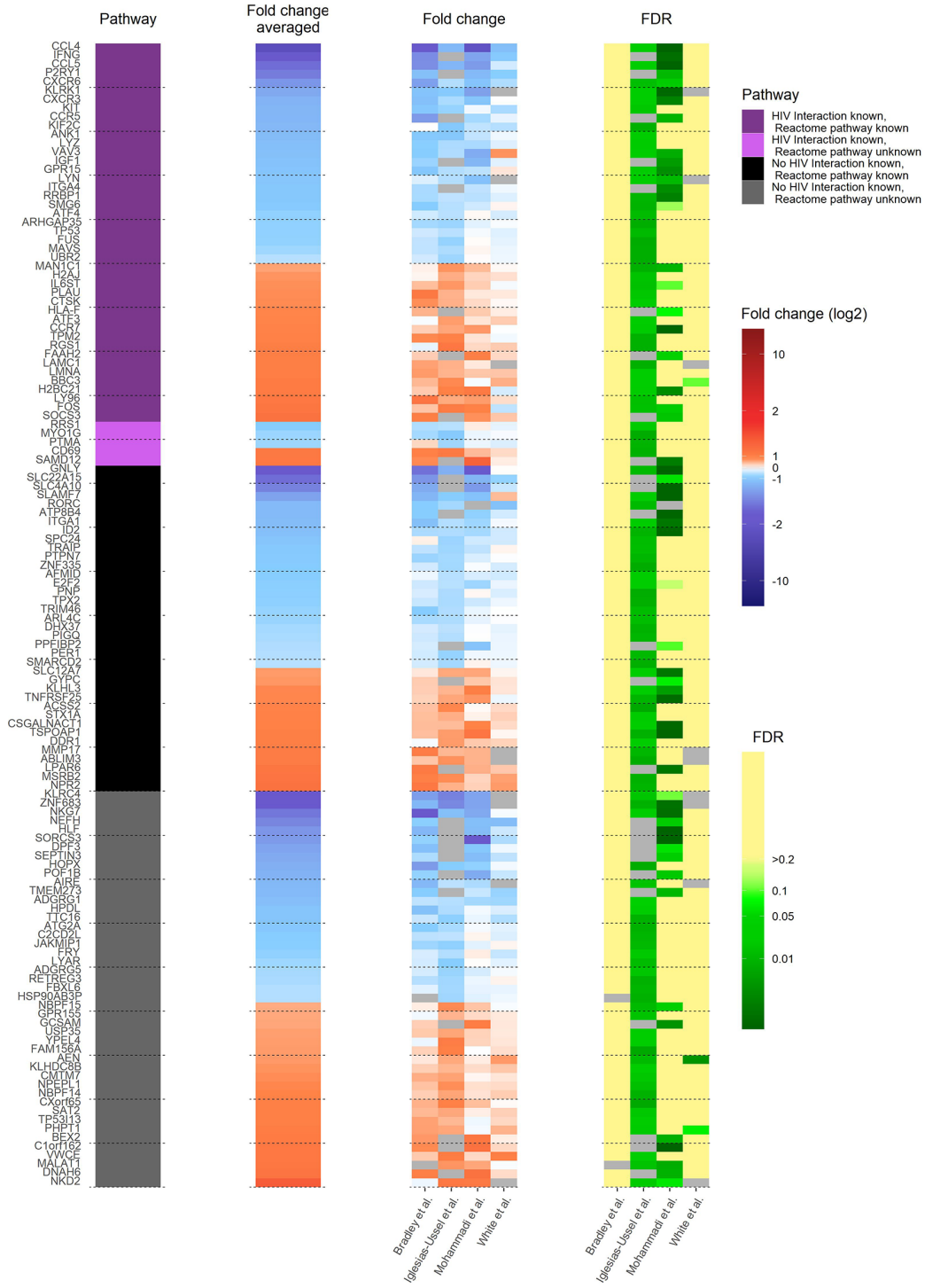

FIGURE 2
Heat map of transcriptome profile of latently HIV-1 infected cells of 4 *in vitro* primary CD4$^+$ T cell models of HIV-1 latency. The 130 pdaDEGs depicted in the heat map are co-occurring in the latently HIV-1 infected cells of the at least 3 of 4 primary CD4$^+$ T models of HIV-1 latency. For each gene the available information on pathways, mean standardized fold change, and study-specific fold change and false discovery rates (FDR) are illustrated. The pathway describes whether an HIV-1 interaction/association and/or the reactome pathway is known or not. Fold change and FDR in grey indicates no gene expression reported in the according dataset [Bradley et al. (8) Iglesias-Ussel et al. (9), Mohammadi et al. (10) and White et al. (11)].

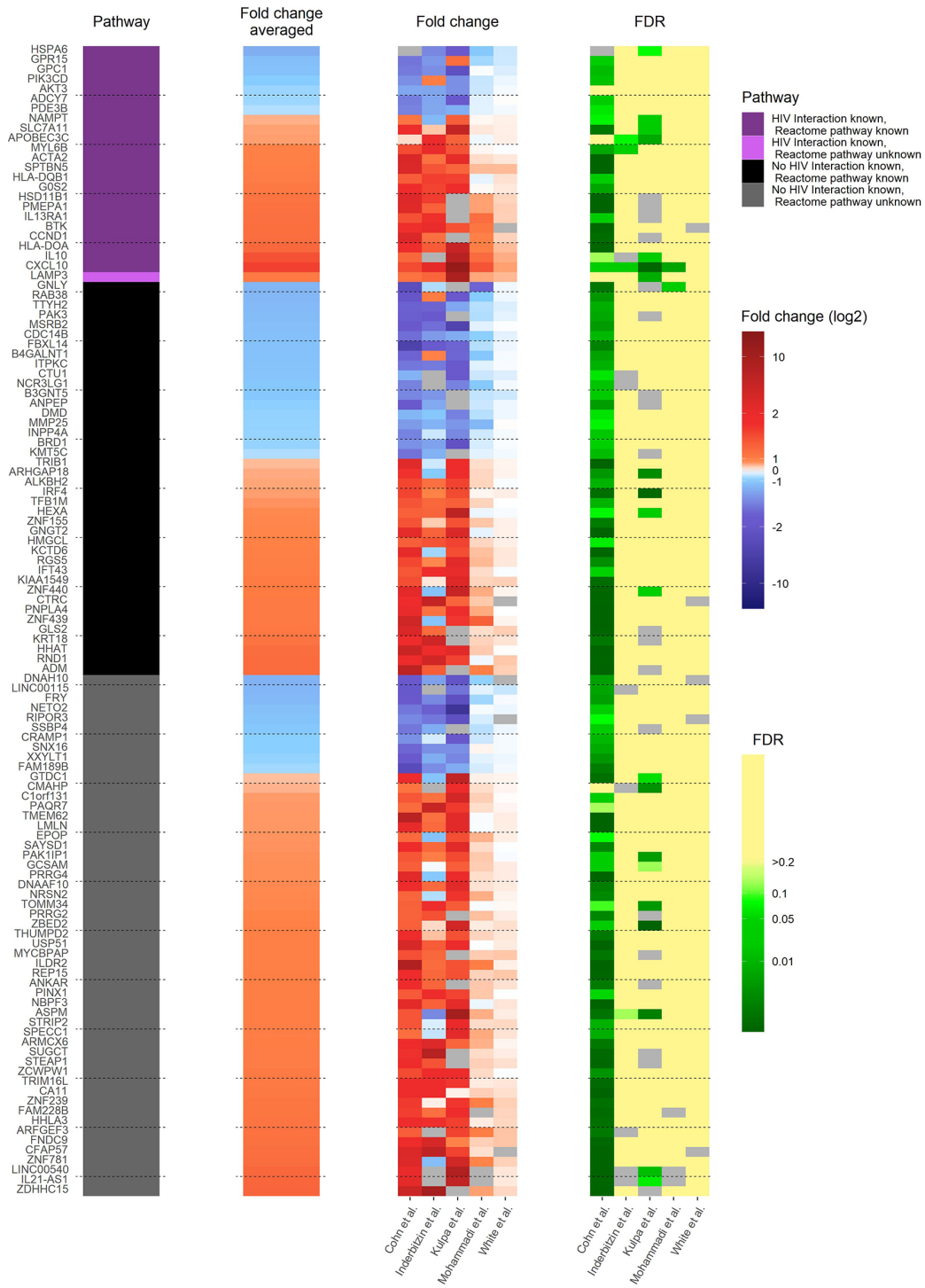

FIGURE 3
Heat map of gene expression profile of reactivated HIV-1 infected cells of 3 *in vitro* primary CD4$^+$ T cell models of HIV-1 latency and 2 *ex vivo* studies of reactivated HIV-1 infected primary CD4$^+$ T cells from HIV-1 infected individuals. The 117 pdaDEGs depicted in the heat map co-occurring in the reactivated HIV-1 infected cells of at least 3 out of 5 primary CD4$^+$ T cell models of HIV-1 latency. For each gene the available information on pathways, mean standardized fold change, and study-specific fold change and false discovery rates (FDR) are illustrated. The pathway describes whether an HIV-1 interaction/association and/or the reactome pathway is known or not. Fold change and FDR in grey indicates no gene expression reported in the according dataset [Cohn et al. (12), Inderbitzin et al. (14), Kulpa et al. (13), Mohammadi et al. (10) and White et al. (11)].

long-term HIV disease prognosis (39). SLC7A11 (solute carrier family 7 member 11), also named xCT, is a cytoplasmic membrane antiporter that exports one glutamate molecule for each imported cystine molecule (40–43). SLC7A11 has shown to inhibit HIV-1 infection (44).

In summary, we found genes associated with apoptosis, cell cycle and HLA class II were predominantly upregulated in all investigated models for reactivated HIV-1 infected primary CD4$^+$ T cells.

Comparison of transcriptome profiles of latently- and reactivated HIV-1 infected CD4$^+$ T cells

Next, we analysed the overlaps of the 130 and 117 pdaDEGs in latently- and reactivated HIV-1 infected primary CD4$^+$ T cells, respectively. 5 pdaDEGs were observed in latently- and reactivated HIV-1 infected primary CD4$^+$ T cells: FRY, GCSAM, GNLY, GPR15 and MSRB2 (Figure 4). Of those pdaDEGs, FRY, GNLY and GPR15 were downregulated and GCSM was upregulated in both groups. Only methionine sulfoxide reductase B2 (MSRB2) was regulated differentially between the latently- and reactivated HIV-1 infected CD4$^+$ T cells, namely, upregulated in latently HIV-1 infected primary CD4$^+$ T cells and downregulated in reactivated HIV-1 infected primary CD4$^+$ T cells. Based on DAVID there is only an HIV-1 interaction known for GPR15, namely an interaction with HIV-1 Env gp120. GPR15 has been found to be the co-receptor of SIV and HIV-2 (45). According to the reactome, FRY and GCSAM could not be assigned to any pathway (Figures 2, 3). All those genes might be interesting in further studies, in particular MSRB2.

Enriched biological processes of pdaDEGs

Gene ontology (GO) enrichment analysis was performed for functional investigation of pdaDEGs. In the GO enrichment analysis we observed predominantly downregulation of the T cell activation and STAT, JAK pathways in latently HIV-1 infected cells of the 4 *in vitro* primary CD4$^+$ T cell models of HIV-1 latency (Figure 5). In addition, *bona fide* markers for IFN related genes were identified to be downregulated in 3/4 *in vitro* primary CD4$^+$ T cell models of HIV-1 latency, such as MAVS, IFNG, TRIM46. In parallel, genes associated with the p53 signalling pathways were found to be upregulated in particular pathways related to apoptosis and DNA damage repair (11), such as BBC3 and TNFRSF25. For the reactivated HIV-1 infected primary CD4$^+$ T cells, we could not observe any enriched biological processes in the pdaDEGs.

Discussion

Current single-cell RNAseq studies of latently HIV-1 infected primary CD4$^+$ T cells revealed a high degree of heterogeneity between individual latently HIV-1-infected cells, suggesting that HIV-1 latency can persist in very different host cell environments (12, 15, 16). Host cell heterogeneity may explain, at least in part, the differential responsiveness of latently infected primary CD4$^+$ T cells to reactivation. Identifying genes that drive and maintain HIV-1 latency is important to improve current curative strategies. In this study, we performed a pooled data-analysis of transcriptome datasets of latently- and reactivated HIV-1 infected cells from 5 *in vitro*

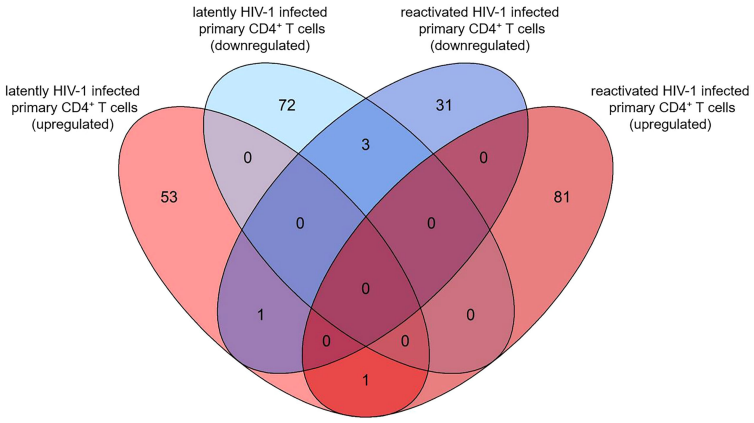

FIGURE 4
Overlap of pdaDEGs identified in latently- and reactivated HIV-1 infected cells from 5 *in vitro* primary CD4$^+$ T cell models of HIV-1 latency and 2 *ex vivo* studies of reactivated HIV-1 infected primary CD4$^+$ T cells from HIV-1 infected individuals. Of the 130 and 117 pdaDEGs identified in latently- and reactivated HIV-1 infected cells, respectively, 5 co-occurred in both groups. Of those, 3 pdaDEGs were downregulated, one pdaDEGs upregulated and one pdaDEGs was differentially expressed in latently- and reactivated HIV-1 infected primary CD4$^+$ T cells.

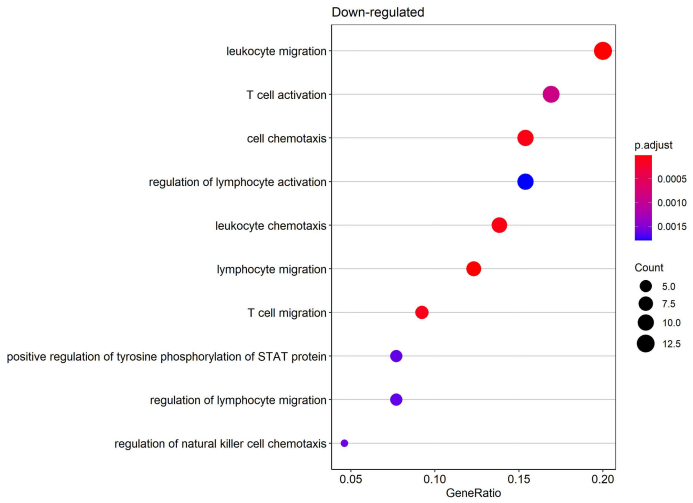

FIGURE 5
Enriched biological processes by gene ontology (GO) enrichment analysis of downregulated pdaDEGs in latently HIV-1 infected primary CD4$^+$ T cells. Depicted are overrepresented biological processes of downregulated pdaDEGs shown by the gene count in circle size and color coded by adjusted p-value.

primary CD4$^+$ T cell models of HIV-1 latency and 2 *ex vivo* studies of reactivated HIV-1 infected primary CD4$^+$ T cells from HIV-1 infected individuals. Although the experimental settings are unique for each *in vitro* primary CD4$^+$ T cell models of HIV-1 latency and *ex vivo* studies of reactivated HIV-1 infected primary CD4$^+$ T cells from HIV-1 infected individuals, regarding 1. how long cells are maintained in culture prior to infection 2. how CD4$^+$ T cell survival is ensured, 3. how reactivation was achieved and 4. using replication competent or incompetent HIV-1, we observed pdaDEGs across *in vitro* primary CD4$^+$ T cell models of HIV-1 latency and *ex vivo* studies of reactivated HIV-1 infected primary CD4$^+$ T cells from HIV-1 infected individuals. In latently- and reactivated HIV-1 infected primary CD4$^+$ T cells we could observe five co-occurring pdaDEGs, one of which MSRB2 was differentially expressed. We observed that natural ligands and coreceptors were predominantly downregulated in latently HIV-1 infected primary CD4$^+$ T cells, whereas genes associated with apoptosis, cell cycle and HLA class II were upregulated in reactivated HIV-1 infected CD4$^+$ T cells.

Latently HIV-1 infected primary CD4$^+$ T cells are rare and to this day no unique markers for their identification is known (46, 47). There are numerous RNAseq/microarrays datasets of HIV-1 infected primary CD4$^+$ T cells, which either apply strict fold change >2 and FDR <0.05 filters or select a single candidate to propose as newly discovered HIV-1 latency marker, yet the respective results have rarely been confirmed by others. In this study we combined RNAseq datasets from published primary CD4$^+$ T cell models of HIV-1 latency and *ex vivo* studies of reactivated HIV-1 infected primary CD4$^+$ T cells from HIV-1 infected individuals, to get a more comprehensive picture. By considering the expression patterns of different datasets, we can identify genes with small effects that would otherwise be missed. Furthermore, we argue that if genes, even if the effect is small, are similarly differentially expressed in different datasets, the effect of HIV-1 infection on dysregulation is even more likely to be.

Among the 130 pdaDEGs in latently- and 117 pdaDEGs in reactivated HIV-1 infected primary CD4$^+$ T cells we identified 5 pdaDEGs which co-occurred in both groups. One of which, MSRB2, was differentially expressed, namely upregulated in latently HIV-1 infected primary CD4$^+$ T cells and downregulated in reactivated HIV-1 infected primary CD4$^+$ T cells. To date, there is no HIV-1 interaction with MSRB2 reported. MSRB2 has been associated with diabetes mellitus (48), Parkinsons' disease (48) and Alzheimer (49) and MSRB2 has shown to reside in the mitochondrial matrix (50–52). In Parkinson's disease it was observed to be necessary for induction of mitophagy, a process in which damaged, toxic mitochondria are removed to protect a cell from apoptosis (53, 54). In the absence of MSRB2 it was observed that mitochondria undergo oxidative stress, leading to reduced mitophagy (48). Other studies also made similar observations: MSRB2 protects cell damage from oxidative stress in various cells such as lymphoblast and leukemia cells (55, 56). Therefore, upregulation of MSRB2 in latently HIV-1 infected primary CD4$^+$ T cells could inhibit apoptosis, while downregulation in reactivated HIV-1 infected genes leads to apoptosis due to the cytotoxic response of LRA or infectious virus particle release. However, this process has not yet been documented in CD4$^+$ T cells and therefore needs further investigation.

Many identified pdaDEGs in latently HIV-1 infected primary CD4$^+$ T cells have been reported as *bona fide* markers for antiviral defense and apoptosis, such as IFN related genes or genes associated with the p53 pathway. In reactivated HIV-1 infected primary CD4$^+$ T cells we observed upregulation of genes associated with apoptosis, cell cycle and HLA class II, particularly in association with the p53 pathway and the PI3K/Akt pathway. The observed genes can be used in future primary CD4$^+$ T cell models of HIV-1 latency to clarify the functional and physiological significance in primary CD4$^+$ T cells.

Different LRA were used for reactivation in the *in vitro* primary CD4$^+$ T cell models of HIV-1 latency compared to the *ex vivo* studies of reactivated HIV-1 infected primary CD4$^+$ T cells from HIV-1 infected individuals, nevertheless we could observe genes to be similarly differentially expressed across studies. However, the impact of differences in clonality of the reservoir exposed to different antiretroviral drugs and LRA treatments could bias transcriptome profiles. We have tried not to become too speculative when comparing latently- and reactivated HIV-1 infected primary CD4$^+$ T cells, and have therefore selected genes and pathways already known to play a role in the life cycle and pathogenesis of HIV-1 to get as close as possible to biological significance. We believe that our pooled data-analysis can help estimate the relative contribution of some key genes and pathways of HIV-1 latency and reactivation.

Concluding remarks and future perspective

To summarize, our pooled data-analysis of different primary CD4$^+$ T cell models of HIV-1 latency gave insights into transcriptome profile signatures in latently- and reactivated HIV-1 infected primary CD4$^+$ T cells. We identified 130 pdaDEGs in latently- and 117 pdaDEGs in reactivated HIV-1 infected cells from 5 *in vitro* primary CD4$^+$ T cell models of HIV-1 latency and 2 *ex vivo* studies of reactivated HIV-1 infected primary CD4$^+$ T cells. We observed that in pdaDEGs natural ligands and coreceptors were predominantly downregulated in latently HIV-1 infected primary CD4$^+$ T cells, whereas pdaDEGs associated with apoptosis, cell cycle and HLA class II were upregulated in reactivated HIV-1 infected primary CD4$^+$ T cells. In addition, we observed 5 pdaDEGs that co-occurred in latently- and reactivated HIV-1 infected primary CD4$^+$ T cells, one of which, MSRB2, was found to be differentially expressed between latently- and reactivated HIV-1 infected primary CD4$^+$ T cells. This pooled data-analysis is unique in that it analyzes differentially expressed genes of latently- and reactivated HIV-1 infected cells from different *in vitro* primary CD4$^+$ T cell models of HIV-1 latency and *ex vivo* studies of reactivated HIV-1 infected primary CD4$^+$ T cells from HIV-1 infected individuals, providing insight into differentially expressed genes that might contribute to HIV-1 latency.

Material and methods

Study selection for the pooled data-analysis

On the 1st of March 2019 we searched for *in vitro* primary CD4$^+$ T cell models of HIV-1 latency on Scopus database. We searched for ((TITLE (HIV OR HIV-1)) AND (TITLE (latent OR latently OR latency)) AND TITLE-ABS-KEY ((transcriptome OR transcriptomics OR "gene expression"))) AND (ALL ("primary cell")) AND (ALL ("*in vitro* model" OR "cell model")) AND (LIMIT-TO (DOCTYPE, "ar")). Each study was independently reviewed and included based on the criterion that each study contained transcriptome data and its methodology derived from an *in vitro* primary CD4$^+$ T cell model of HIV-1 latency. In addition, we included two *ex vivo* studies of reactivated HIV-1 infected primary CD4$^+$ T cells from HIV-1 infected individuals and our own primary CD4$^+$ T cell model of HIV-1 latency.

Primary CD4$^+$ T cells isolation of own model

Detailed description of isolation, transfection and RNAseq data preparation of primary CD4$^+$ T cells of own model is given in Supplementary Material.

RNAseq data collection

Raw read counts of Bradley et al. (8), White et al. (11) and Cohn et al. (12). were downloaded from Gene Expression Omnibus (GEO) Database (57). Differentially expressed genes (DEGs) as fold-change were obtained from Kulpa et al. (13) through personal communication. DEGs for Mohammadi et al. (10) were downloaded from the open access interactive web resource http://litchi.labtelenti.org.

Differential expression testing

All analyses were performed using R software version 4.0.5 (58). We identified DEGs in data sets where raw read counts were available [(8, 10, 12, 13) and our data] using the Bioconductor package EdgeR (59, 60) in a study-by-study basis. Hereby, ambiguous and low-quality reads were removed and genes with low read counts (more than 10 reads in 70% of replicates per group were required) were filtered out. Read counts were normalized *via* trimmed mean of M values (TMM) method. Common dispersion was estimated across all genes by maximizing the negative binomial conditional common likelihood, and tagwise dispersion by an empirical Bayes method based on weighted conditional maximum likelihood. Differential

expression testing was performed assuming negative-binomially distributed read counts and computing genewise exact tests for differences in the means between groups. Eventually, fold changes were log2-transformed and p-values adjusted for false discovery rate (FDR) by the Benjamini-Hochberg method.

From Kulpa et al. (13) we selected the RNAseq data for the TCM cell subset, choosing the LRA Bryostatin, as we have seen the least impact on cell viability compared to the other LRAs IL-15 and PMA. As raw read counts were not available and fold changes were given per transcript ID, we filtered for the transcript ID per gene name with the highest CPM. FDR values were estimated using the available p-values with the Bioconductor package qvalue (61).

The microarray data from Iglesias et al. (9) was available only as fold change per gene name, lacking p-values, FDR or raw signals. White et al. (11) previously worked with this dataset and kindly provided us with a dataset comprised of 1297 genes, selected by filtering for adjusted p-value smaller than 0.05.

Gene annotation and data analysis

Datasets were combined and genes annotations obtained and unified across primary $CD4^+$ T cell models of HIV-1 latency using the Bioconductor package bioMart (62, 63) to download annotation Ensembl data (64). HGNC symbol duplications were checked on https://www.genenames.org/tools/multi-symbol-checker/. Known HIV interactions per gene were retrieved from DAVID (Database for Annotation, Visualization and Integrated Discovery) (65, 66) using the HGNC gene symbol and Entrez gene IDs. Functional pathways of genes were obtained from Reactome (67). We calculated the mean standardized expression of genes across all primary $CD4^+$ T cell models of HIV-1 latency by averaging over fold changes standardized by study-specific standard error. To account for the differences in the datasets, we refrained from identifying the genes of interest by |fold change| > 2 and FDR < 0.05, but employed a custom filtering method. Hereby a filter score is calculated for every gene based on FDR being smaller than 0.1 and the absolute fold change being greater than the study-specific 50% absolute fold change quantile. Downregulated genes obtain a negative score. Meeting these conditions, a gene can get a score of maximally 2 per study, i.e., maximum score of 8 for latently and 10 for reactivated HIV-1 infected primary $CD4^+$ T cells. For each gene the scores are summed up across studies and normalized to 1. Genes of interest were then identified by having a score ≥ 0.5.

GO enrichment analysis

GO enrichment analysis of genes of interest were performed using the Bioconductor package clusterProfiler (68) using the org.Hs.eg.db Bioconductor annotation package (69) with default settings, apart from setting the minimal size of genes to 3 and choosing a more stringent q-value cutoff of 0.05. Data management and wrangling, as well as visualizations were performed using the R package tidyverse (70). With the parameters set, we could not detect any upregulated biological processes in latently HIV-1 infected $CD4^+$ T cells from 4 *in vitro* primary $CD4^+$ T cell models of HIV-1 latency.

Data availability statement

Publicly available datasets were analyzed in this study. This data can be found here (GEO accession number): Bradley et al: SSAMN08685499, SAMN08685500, SAMN08685501, SAMN08685502. White et al: GSE81810; Iglesias-Ussel et al: GSM996242, GSM996243, GSM996244, GSM996245; Mohammadi et al.: http://litchi.labtelenti.org; Kulpa et al. were received upon request.; Cohn et al.: GSM2801437. Inderbitzin et. al. data is available on the European Nucleotide Archive (ENA) of the EMBL's European Bioinformatics Institute (EMBL-EBI) - Project accession PRJEB53230.

Author contributions

AI designed the study, performed the literature search, cultured the cells, isolated the RNA for the RNAseq analysis. LO cleaned and performed analysis of the RNAseq datasets. TL downloaded, cleaned and performed analyses of the data sets. PR supported the experiments and analysis of the data. KM supported the analysis of the data, and edited the manuscript. All authors approved the manuscript.

Funding

This study was funded by the Swiss National Science Foundation, grant No. 310030_141067 and 310030_204404 to KM and from the Forschungskredit Candoc, grant No. FK-19-032 to AI. The funders had no role in study design, data collection and analysis, decision to publish, or preparation of the manuscript.

Acknowledgments

We want to thank Yik Lim Kok and Roger Kouyos for the fruitful discussion, Catharine Aquino and Andreia Cabral de Gouvea from the Functional Genomics Center Zurich for the RNAseq service.

Conflict of interest

The authors declare that the research was conducted in the absence of any commercial or financial relationships that could be construed as a potential conflict of interest.

Publisher's note

All claims expressed in this article are solely those of the authors and do not necessarily represent those of their affiliated organizations, or those of the publisher, the editors and the reviewers. Any product that may be evaluated in this article, or claim that may be made by its manufacturer, is not guaranteed or endorsed by the publisher.

Supplementary material

The Supplementary Material for this article can be found online at: https://www.frontiersin.org/articles/10.3389/fimmu.2022.915805/full#supplementary-material

References

1. Vanhamel J, Bruggemans A, Debyser Z. Establishment of latent HIV-1 reservoirs: What do we really know? *J Virus Eradication* (2019) 5(1):3–9. doi: 10.1016/S2055-6640(20)30275-2

2. Finzi D, Hermankova M, Pierson T, Carruth LM, Buck C, Chaisson RE, et al. Identification of a reservoir for HIV-1 in patients on highly active antiretroviral therapy. *Science* (1997) 278(5341):1295–300. doi: 10.1126/science.278.5341.1295

3. Wong JK, Hezareh M, Gunthard HF, Havlir DV, Ignacio CC, Spina CA, et al. Recovery of replication-competent HIV despite prolonged suppression of plasma viremia. *Science* (1997) 278(5341):1291–5. doi: 10.1126/science.278.5341.1291

4. Chun TW, Finzi D, Margolick J, Chadwick K, Schwartz D, Siliciano RF. *In vivo* fate of HIV-1-Infected T cells: Quantitative analysis of the transition to stable latency. *Nat Med* (1995) 1(12):1284–90. doi: 10.1038/nm1295-1284

5. Stellbrink HJ, van Lunzen J, Hufert FT, Froschle G, Wolf-Vorbeck G, Zollner B, et al. Asymptomatic HIV infection is characterized by rapid turnover of HIV rna in plasma and lymph nodes but not of latently infected lymph-node CD4+ T cells. *AIDS* (1997) 11(9):1103–10. doi: 10.1097/00002030-199709000-00004

6. Verdikt R, Hernalsteens O, Van Lint C. Epigenetic mechanisms of HIV-1 persistence. *Vaccines* (2021) 9(5):514. doi: 10.3390/vaccines9050514

7. Bruel T, Schwartz O. Markers of the HIV-1 reservoir: Facts and controversies. *Curr Opin HIV AIDS* (2018) 13(5):383–8. doi: 10.1097/coh.0000000000000482

8. Bradley T, Ferrari G, Haynes BF, Margolis DM, Browne EP. Single-cell analysis of quiescent HIV infection reveals host transcriptional profiles that regulate proviral latency. *Cell Rep* (2018) 25(1):107–17.e3. doi: 10.1016/j.celrep.2018.09.020

9. Iglesias-Ussel M, Vandergeeten C, Marchionni L, Chomont N, Romerio F. High levels of CD2 expression identify HIV-1 latently infected resting memory CD4+ T cells in virally suppressed subjects. *J Virol* (2013) 87(16):9148–58. doi: 10.1128/jvi.01297-13

10. Mohammadi P, di Iulio J, Munoz M, Martinez R, Bartha I, Cavassini M, et al. Dynamics of HIV latency and reactivation in a primary CD4+ T cell model. *PLoS Pathog* (2014) 10(5):e1004156. doi: 10.1371/journal.ppat.1004156

11. White CH, Moesker B, Beliakova-Bethell N, Martins LJ, Spina CA, Margolis DM, et al. Transcriptomic analysis implicates the p53 signaling pathway in the establishment of HIV-1 latency in central memory CD4 T cells in an in vitro model. *PLoS Pathog* (2016) 12(11):e1006026. doi: 10.1371/journal.ppat.1006026

12. Cohn LB, da Silva IT, Valieris R, Huang AS, Lorenzi JCC, Cohen YZ, et al. Clonal CD4(+) T cells in the HIV-1 latent reservoir display a distinct gene profile upon reactivation. *Nat Med* (2018) 24(5):604–9. doi: 10.1038/s41591-018-0017-7

13. Kulpa DA, Talla A, Brehm JH, Ribeiro SP, Yuan S, Bebin-Blackwell AG, et al. Differentiation into an effector memory phenotype potentiates HIV-1 latency reversal in Cd4(+) T cells. *J Virol* (2019) 93(24):e00969–19. doi: 10.1128/jvi.00969-19

14. Inderbitzin A, Loosli T, Opitz L, Rusert P, Metzner KJ. Transcriptomic analysis showed upregulation of genes associated with p53- and Pi3k/Akt pathway in primary CD4+ T cells after CRISPR/Cas9-mediated insertion of replication-competent HIV-1 into three target sites (Unpublished data), project accession PRJEB53230. *EMBL's Eur Bioinf Institute (EMBL-EBI)* (2022).

15. Matsuda Y, Kobayashi-Ishihara M, Fujikawa D, Ishida T, Watanabe T, Yamagishi M. Epigenetic heterogeneity in HIV-1 latency establishment. *Sci Rep* (2015) 5:7701. doi: 10.1038/srep07701

16. Golumbeanu M, Cristinelli S, Rato S, Munoz M, Cavassini M, Beerenwinkel N, et al. Single-cell rna-seq reveals transcriptional heterogeneity in latent and reactivated HIV-infected cells. *Cell Rep* (2018) 23(4):942–50. doi: 10.1016/j.celrep.2018.03.102

17. Kim BO, Liu Y, Zhou BY, He JJ. Induction of C chemokine XCL1 (lymphotactin/single C motif-1 alpha/activation-induced, T cell-derived and chemokine-related cytokine) expression by HIV-1 Tat protein. *J Immunol* (2004) 172(3):1888–95. doi: 10.4049/jimmunol.172.3.1888

18. Secchi M, Grampa V, Vangelista L. Rational CCL5 mutagenesis integration in a lactobacilli platform generates extremely potent HIV-1 blockers. *Sci Rep* (2018) 8(1):1890. doi: 10.1038/s41598-018-20300-9

19. Vangelista L, Secchi M, Lusso P. Rational design of novel HIV-1 entry inhibitors by Rantes engineering. *Vaccine* (2008) 26(24):3008–15. doi: 10.1016/j.vaccine.2007.12.023

20. Hartley O, Offord RE. Engineering chemokines to develop optimized HIV inhibitors. *Curr Protein Pept Sci* (2005) 6(3):207–19. doi: 10.2174/1389203054065400

21. Cocchi F, DeVico AL, Garzino-Demo A, Arya SK, Gallo RC, Lusso P. Identification of RANTES, MIP-1 alpha, and MIP-1 beta as the major HIV-suppressive factors produced by CD8+ T cells. *Science* (1995) 270(5243):1811–5. doi: 10.1126/science.270.5243.1811

22. Limou S, Coulonges C, Herbeck JT, van Manen D, An P, Le Clerc S, et al. Multiple-cohort genetic association study reveals CXCR6 as a new chemokine receptor involved in long-term nonprogression to aids. *J Infect Dis* (2010) 202 (6):908–15. doi: 10.1086/655782

23. Shan L, Deng K, Gao H, Xing S, Capoferri AA, Durand CM, et al. Transcriptional reprogramming during effector-to-Memory transition renders CD4(+) T cells permissive for latent HIV-1 infection. *Immunity* (2017) 47 (4):766–75.e3. doi: 10.1016/j.immuni.2017.09.014

24. Reuse S, Calao M, Kabeya K, Guiguen A, Gatot JS, Quivy V, et al. Synergistic activation of HIV-1 expression by deacetylase inhibitors and prostratin: Implications for treatment of latent infection. *PLoS One* (2009) 4(6):e6093. doi: 10.1371/journal.pone.0006093

25. Darcis G, Kula A, Bouchat S, Fujinaga K, Corazza F, Ait-Ammar A, et al. An in-depth comparison of latency-reversing agent combinations in various in vitro and ex vivo HIV-1 latency models identified Bryostatin-1+JQ1 and Ingenol-B+JQ1 to potently reactivate viral gene expression. *PLoS Pathog* (2015) 11(7):e1005063. doi: 10.1371/journal.ppat.1005063

26. Bouchat S, Delacourt N, Kula A, Darcis G, Van Driessche B, Corazza F, et al. Sequential treatment with 5-Aza-2'-Deoxycytidine and deacetylase inhibitors reactivates HIV-1. *EMBO Mol Med* (2016) 8(2):117–38. doi: 10.15252/emmm.201505557

27. Bouchat S, Gatot JS, Kabeya K, Cardona C, Colin L, Herbein G, et al. Histone methyltransferase inhibitors induce HIV-1 recovery in resting CD4(+) T cells from HIV-1-Infected haart-treated patients. *Aids* (2012) 26(12):1473–82. doi: 10.1097/QAD.0b013e32835535f5

28. Jiang G, Mendes EA, Kaiser P, Wong DP, Tang Y, Cai I, et al. Synergistic reactivation of latent HIV expression by ingenol-3-Angelate, Pep005, targeted nf-kb signaling in combination with JQ1 induced p-tefb activation. *PLoS Pathog* (2015) 11(7):e1005066. doi: 10.1371/journal.ppat.1005066

29. Laird GM, Bullen CK, Rosenbloom DI, Martin AR, Hill AL, Durand CM, et al. Ex vivo analysis identifies effective HIV-1 latency-reversing drug combinations. *J Clin Invest* (2015) 125(5):1901–12. doi: 10.1172/jci80142

30. Pache L, Dutra MS, Spivak AM, Marlett JM, Murry JP, Hwang Y, et al. BIRC2/cIAP1 is a negative regulator of HIV-1 transcription and can be targeted by

smac mimetics to promote reversal of viral latency. *Cell Host Microbe* (2015) 18 (3):345–53. doi: 10.1016/j.chom.2015.08.009

31. Tripathy MK, McManamy ME, Burch BD, Archin NM, Margolis DM. H3k27 demethylation at the proviral promoter sensitizes latent HIV to the effects of vorinostat in ex vivo cultures of resting CD4+ T cells. *J Virol* (2015) 89(16):8392–405. doi: 10.1128/jvi.00572-15

32. Abdel-Mohsen M, Chavez L, Tandon R, Chew GM, Deng X, Danesh A, et al. Human Galectin-9 is a potent mediator of HIV transcription and reactivation. *PloS Pathog* (2016) 12(6):e1005677. doi: 10.1371/journal.ppat.1005677

33. Chen HC, Martinez JP, Zorita E, Meyerhans A, Filion GJ. Position effects influence HIV latency reversal. *Nat Struct Mol Biol* (2017) 24(1):47–54. doi: 10.1038/nsmb.3328

34. Rochat MA, ScHLAepfer E, Speck RF. Promising role of toll-like receptor 8 agonist in concert with prostratin for activation of silent HIV. *J Virol* (2017) 91(4): e0208416–16. doi: 10.1128/jvi.02084-16

35. Das B, Dobrowolski C, Luttge B, Valadkhan S, Chomont N, Johnston R, et al. Estrogen receptor-1 is a key regulator of HIV-1 latency that imparts gender-specific restrictions on the latent reservoir. *Proc Natl Acad Sci U.S.A.* (2018) 115 (33):E7795–e804. doi: 10.1073/pnas.1803468115

36. Liao X, Song L, Zhang L, Wang H, Tong Q, Xu J, et al. LAMP3 regulates hepatic lipid metabolism through activating PI3K/Akt pathway. *Mol Cell Endocrinol* (2018) 470:160–7. doi: 10.1016/j.mce.2017.10.010

37. Achord AP, Lewis RE, Brackin MN, Cruse JM. HLA-DQB1 markers associated with human immunodeficiency virus type I disease progression. *Pathobiology* (1997) 65(4):210–5. doi: 10.1159/000164125

38. Liu M, Guo S, Hibbert JM, Jain V, Singh N, Wilson NO, et al. CXCL10/IP-10 in infectious diseases pathogenesis and potential therapeutic implications. *Cytokine Growth factor Rev* (2011) 22(3):121–30. doi: 10.1016/j.cytogfr.2011.06.001

39. Yin X, Wang Z, Wu T, Ma M, Zhang Z, Chu Z, et al. The combination of CXCL9, CXCL10 and CXCL11 levels during primary HIV infection predicts HIV disease progression. *J Transl Med* (2019) 17(1):417. doi: 10.1186/s12967-019-02172-3

40. Bannai S. Exchange of cystine and glutamate across plasma membrane of human fibroblasts. *J Biol Chem* (1986) 261(5):2256–63. doi: 10.1016/S0021-9258(17)35926-4

41. Sato H, Tamba M, Ishii T, Bannai S. Cloning and expression of a plasma membrane Cystine/Glutamate exchange transporter composed of two distinct proteins*. *J Biol Chem* (1999) 274(17):11455–8. doi: 10.1074/jbc.274.17.11455

42. Sasaki H, Sato H, Kuriyama-Matsumura K, Sato K, Maebara K, Wang H, et al. Electrophile response element-mediated induction of the Cystine/Glutamate exchange transporter gene expression*. *J Biol Chem* (2002) 277(47):44765–71. doi: 10.1074/jbc.M208704200

43. Habib E, Linher-Melville K, Lin H-X, Singh G. Expression of xCT and activity of system xc− are regulated by NRF2 in human breast cancer cells in response to oxidative stress. *Redox Biol* (2015) 5:33–42. doi: 10.1016/j.redox.2015.03.003

44. Rabinowitz J, Sharifi HJ, Martin H, Marchese A, Robek M, Shi B, et al. xCT/SLC7A11 antiporter function inhibits HIV-1 infection. *Virology* (2021) 556:149–60. doi: 10.1016/j.virol.2021.01.008

45. Sauter D, Kirchhoff F. *Natural hosts of SIV, chapter 4 - properties of human and simian immunodeficiency viruses*. AA Ansari, G Silvestri, editors. Amsterdam: Elsevier (2014) p. 69–84 p.

46. Crooks AM, Bateson R, Cope AB, Dahl NP, Griggs MK, Kuruc JD, et al. Precise quantitation of the latent HIV-1 reservoir: Implications for eradication strategies. *J Infect Dis* (2015) 212(9):1361–5. doi: 10.1093/infdis/jiv218

47. Siliciano JD, Kajdas J, Finzi D, Quinn TC, Chadwick K, Margolick JB, et al. Long-term follow-up studies confirm the stability of the latent reservoir for HIV-1 in resting CD4+ T cells. *Nat Med* (2003) 9(6):727–8. doi: 10.1038/nm880

48. Lee SH, Lee S, Du J, Jain K, Ding M, Kadado AJ, et al. Mitochondrial MSRB2 serves as a switch and transducer for mitophagy. *EMBO Mol Med* (2019) 11(8): e10409–e. doi: 10.15252/emmm.201910409

49. Xiang XJ, Song L, Deng XJ, Tang Y, Min Z, Luo B, et al. Mitochondrial methionine sulfoxide reductase B2 links oxidative stress to Alzheimer's disease-like pathology. *Exp Neurol* (2019) 318:145–56. doi: 10.1016/j.expneurol.2019.05.006

50. Pascual I, Larrayoz IM, Campos MM, Rodriguez IR. Methionine sulfoxide reductase B2 is highly expressed in the retina and protects retinal pigmented epithelium cells from oxidative damage. *Exp Eye Res* (2010) 90(3):420–8. doi: 10.1016/j.exer.2009.12.003

51. Ugarte N, Petropoulos I, Friguet B. Oxidized mitochondrial protein degradation and repair in aging and oxidative stress. *Antioxid Redox Signal* (2010) 13(4):539–49. doi: 10.1089/ars.2009.2998

52. Fischer F, Hamann A, Osiewacz HD. Mitochondrial quality control: An integrated network of pathways. *Trends Biochem Sci* (2012) 37(7):284–92. doi: 10.1016/j.tibs.2012.02.004

53. Palikaras K, Lionaki E, Tavernarakis N. Coordination of mitophagy and mitochondrial biogenesis during ageing in c. *Elegans*. *Nat* (2015) 521(7553):525–8. doi: 10.1038/nature14300

54. García-Prat L, Martínez-Vicente M, Perdiguero E, Ortet L, Rodríguez-Ubreva J, Rebollo E, et al. Autophagy maintains stemness by preventing senescence. *Nature* (2016) 529(7584):37–42. doi: 10.1038/nature16187

55. Cabreiro F, Picot CR, Perichon M, Castel J, Friguet B, Petropoulos I. Overexpression of mitochondrial methionine sulfoxide reductase B2 protects leukemia cells from oxidative stress-induced cell death and protein damage. *J Biol Chem* (2008) 283(24):16673–81. doi: 10.1074/jbc.M708580200

56. Cabreiro F, Picot CR, Perichon M, Friguet B, Petropoulos I. Overexpression of methionine sulfoxide reductases A and B2 protects MOLT-4 cells against zinc-induced oxidative stress. *Antioxid Redox Signal* (2009) 11(2):215–25. doi: 10.1089/ars.2008.2102

57. Clough E, Barrett T. The gene expression omnibus database. *Methods Mol Biol (Clifton NJ)* (2016) 1418:93–110. doi: 10.1007/978-1-4939-3578-9_5

58. Core Team R R. A language and environment for statistical computing. In: *R foundation for statistical computing*. Vienna, Austria (2021). Available at: https://www.R-project.org/.

59. Robinson MD, McCarthy DJ, Smyth GK. Edger: A bioconductor package for differential expression analysis of digital gene expression data. *Bioinformatics* (2010) 26(1):139–40. doi: 10.1093/bioinformatics/btp616

60. McCarthy DJ, Chen Y, Smyth GK. Differential expression analysis of multifactor RNA-seq experiments with respect to biological variation. *Nucleic Acids Res* (2012) 40(10):4288–97. doi: 10.1093/nar/gks042

61. Storey JD, Bass JB, Dabney D, Robinson D. Qvalue: Q-value estimation for false discovery rate control. (2020). Available at: https://www.ncbi.nlm.nih.gov/pmc/articles/PMC7132874/

62. Durinck S, Spellman PT, Birney E, Huber W. Mapping identifiers for the integration of genomic datasets with the R/Bioconductor package biomart. *Nat Protoc* (2009) 4(8):1184–91. doi: 10.1038/nprot.2009.97

63. Durinck S, Moreau Y, Kasprzyk A, Davis S, De Moor B, Brazma A, et al. Biomart and bioconductor: A powerful link between biological databases and microarray data analysis. *Bioinformatics* (2005) 21(16):3439–40. doi: 10.1093/bioinformatics/bti525

64. Howe KL, Achuthan P, Allen J, Allen J, Alvarez-Jarreta J, Amode MR, et al. Ensembl 2021. *Nucleic Acids Res* (2021) 49(D1):D884–D91. doi: 10.1093/nar/gkaa942

65. Huang da W, Sherman BT, Lempicki RA. Systematic and integrative analysis of Large gene lists using David bioinformatics resources. *Nat Protoc* (2009) 4(1):44–57. doi: 10.1038/nprot.2008.211

66. Huang DW, Sherman BT, Lempicki RA. Bioinformatics enrichment tools: Paths toward the comprehensive functional analysis of Large gene lists. *Nucleic Acids Res* (2009) 37(1):1–13. doi: 10.1093/nar/gkn923

67. Sidiropoulos K, Viteri G, Sevilla C, Jupe S, Webber M, Orlic-Milacic M, et al. Reactome enhanced pathway visualization. *Bioinformatics* (2017) 33(21):3461–7. doi: 10.1093/bioinformatics/btx441

68. Yu G, Wang LG, Han Y, He QY. Clusterprofiler: An r package for comparing biological themes among gene clusters. *Omics* (2012) 16(5):284–7. doi: 10.1089/omi.2011.0118

69. Carlson MOrg.Hs.Eg.Db. Genome wide annotation for human. In: *R package version 3.11.4* (2020).

70. Wickham H, Averick M, Bryan J, Chang W, D'Agostino McGowan L, François R, et al. Welcome to the tidyverse. *J Open Source Software* (2019) 4(43):1686.

Frontiers in Immunology

Explores novel approaches and diagnoses to treat immune disorders.

The official journal of the International Union of Immunological Societies (IUIS) and the most cited in its field, leading the way for research across basic, translational and clinical immunology.

Discover the latest Research Topics

See more →

Frontiers

Avenue du Tribunal-Fédéral 34
1005 Lausanne, Switzerland
frontiersin.org

Contact us

+41 (0)21 510 17 00
frontiersin.org/about/contact